

# TECHNICAL NOTE

ADB TN-29-62

## RESEARCH AND INVESTIGATIVE ANALYSIS USING KRON'S METHOD OF ANALYZING REDUNDANT STRUCTURES

Prepared for

GEORGE C. MARSHALL SPACE FLIGHT CENTER  
HUNTSVILLE, ALABAMA

Contract No. NAS8-5000

Control No. TP 2-81080  
(CPB 16-610-62) (IF)

GPO PRICE \$ \_\_\_\_\_

CFSTI PRICE(S) \$ \_\_\_\_\_

Hard copy (HC) 7.00

Microfiche (MF) 1.75

# 853 July 85

N66-17094

FACILITY FORM 602

(ACCESSION NUMBER)  
339  
(PAGES)  
CP 70332  
(NASA CR OR TMX OR AD NUMBER)

(THRU)  
1  
(CODE)  
30  
(CATEGORY)



CHRYSLER CORPORATION MISSILE DIVISION

Sgt 29332

ADB-TN-29-62

RESEARCH AND INVESTIGATIVE ANALYSIS USING KRON'S  
METHOD OF ANALYZING REDUNDANT STRUCTURES

by

J.D. O'Rourke

and

C. Rydz

Mechanics Department

1 November 1962

CWO 10002357

Approved: R.A. Horvath  
R.A. Horvath, Manager, Mechanics

Approved: R.P. Erickson  
R.P. Erickson, Chief Engineer, Advanced Development Branch

## ABSTRACT

A complete description of the analysis technique first proposed by Gabriel Kron is provided. This description describes the underlying theory of the analysis and the solution of the governing equations as programed on the digital computer. In addition, the mathematical model of the Saturn SA-D1 is discussed. The subsequent computer runs involving this mathematical model are used to establish seven predominant frequencies and five of these are compared to the results of a test program conducted on this vehicle.

## TABLE OF CONTENTS

	Page
OBJECT	1
CONCLUSIONS	1
RECOMMENDATIONS	1
INTRODUCTION	3
DISCUSSION	4
Mathematical Analysis	4
<u>Introduction</u>	4
<u>Part One - Analysis</u>	6
Primitive Elements:	6
Tensor Transformation Laws:	19
Orientation of Primitive Beams:	21
Interconnection:	25
Interconnection of "Torn" System:	28
<u>Part Two - Solution</u>	36
Mathematical Model	50
RESULTS	54
REFERENCES	63
APPENDIX A	64
Directional Cosine Matrix	64
APPENDIX B - INPUT PREPARATION AND COMPUTER PROGRAM	
Input Preparation	
Description of Program	70

## LIST OF TABLES

Table		Page
I	Summary of Support Outrigger Deflection Analysis	84
II	Summary of Thrust Outrigger Deflection Analysis	85
III	Summary of Vehicle Response	86

## LIST OF FIGURES

Figure		Page
1	Coordinate System	7
2	Cantilever Beam - Forces Acting at End 1	8
3	Cantilever Beam - Restraint Forces at End 2	11
4	Definition of Directional Cosines	22
5	Beam - Mass System	25
6	Free-Body Diagrams	28
7	(a) Interconnected Network	29
	(b) Torn Network	29
8	Saturn SA-D1	90
9	Section Properties - Payload Body and S-V Dummy Stage	91
10	Section Properties - S-IV Dummy Stage	92
11	Section Properties - 105 Inch Diameter Fuel Tank	93
12	Section Properties - 70 Inch Diameter Liquid Oxygen Tanks	94
13	Section Properties - 70 Inch Diameter Fuel Tank	95
14	Transition Section	96
15	Spider Assembly	97
16	Outer Tank Attachment Points	98
17	Saturn Outriggers	99
18	Mathematical Model - Saturn SA-D1	100
19	Displacement vs. Length Saturn SA-D1 - Frequency=1.90 cps, Main Tank and Upper Stages	101
20	Displacement vs. Length Saturn SA-D1 - Frequency=1.90 cps, L-1 and L-2	102
21	Displacement vs. Length Saturn SA-D1 - Frequency=1.90 cps, L-3 and L-4	103
22	Displacement vs. Length Saturn SA-D1 - Frequency=1.90 cps, F-1 and F-2	104

## LIST OF FIGURES (Cont)

Figure		Page
23	Displacement vs. Length Saturn SA-D1 - Frequency=1.90 cps, F-3 and F-4	105
24	Displacement vs. Length Saturn SA-D1 - Frequency=2.00 cps, Main Tank and Upper Stages	106
25	Displacement vs. Length Saturn SA-D1 - Frequency=2.00 cps, L-1 and L-2	107
26	Displacement vs. Length Saturn SA-D1 - Frequency=2.00 cps, L-3 and L-4	108
27	Displacement vs. Length Saturn SA-D1 - Frequency=2.00 cps, F-1 and F-2	109
28	Displacement vs. Length Saturn SA-D1 - Frequency=2.00 cps, F-3 and F-4	110
29	Displacement vs. Length Saturn SA-D1 - Frequency=2.10 cps, Main Tank and Upper Stages	111
30	Displacement vs. Length Saturn SA-D1 - Frequency=2.10 cps, L-1 and L-2	112
31	Displacement vs. Length Saturn SA-D1 - Frequency=2.10 cps, L-3 and L-4	113
32	Displacement vs. Length Saturn SA-D1 - Frequency=2.10 cps, F-1 and F-2	114
33	Displacement vs. Length Saturn SA-D1 - Frequency=2.10 cps, F-3 and F-4	115
34	Displacement vs. Length Saturn SA-D1 - Frequency=2.20 cps, Main Tank and Upper Stages	116
35	Displacement vs. Length Saturn SA-D1 - Frequency=2.20 cps, L-1 and L-2	117
36	Displacement vs. Length Saturn SA-D1 - Frequency=2.20 cps, L-3 and L-4	118
37	Displacement vs. Length Saturn SA-D1 - Frequency=2.20 cps, F-1 and F-2	119
38	Displacement vs. Length Saturn SA-D1 - Frequency=2.20 cps, F-3 and F-4	120

v

LIST OF FIGURES (Cont)

Figure		Page
39	Displacement vs. Length Saturn SA-D1 - Frequency=2.30 cps, Main Tank and Upper Stages	121
40	Displacement vs. Length Saturn SA-D1 - Frequency=2.30 cps, L-1 and L-2	122
41	Displacement vs. Length Saturn SA-D1 - Frequency=2.30 cps, L-3 and L-4	123
42	Displacement vs. Length Saturn SA-D1 - Frequency=2.30 cps, F-1 and F-2	124
43	Displacement vs. Length Saturn SA-D1 - Frequency=2.30 cps, F-3 and F-4	125
44	Displacement vs. Length Saturn SA-D1 - Frequency=2.34 cps, Main Tank and Upper Stages	126
45	Displacement vs. Length Saturn SA-D1 - Frequency=2.34 cps, L-1 and L-2	127
46	Displacement vs. Length Saturn SA-D1 - Frequency=2.34 cps, L-3 and L-4	128
47	Displacement vs. Length Saturn SA-D1 - Frequency=2.34 cps, F-1 and F-2	129
48	Displacement vs. Length Saturn SA-D1 - Frequency=2.34 cps, F-3 and F-4	130
49	Displacement vs. Length Saturn SA-D1 - Frequency=2.37 cps, Main Tank and Upper Stages	131
50	Displacement vs. Length Saturn SA-D1 - Frequency=2.37 cps, L-1 and L-2	132
51	Displacement vs. Length Saturn SA-D1 - Frequency=2.37 cps, L-3 and L-4	133
52	Displacement vs. Length Saturn SA-D1 - Frequency=2.37 cps, F-1 and F-2	134
53	Displacement vs. Length Saturn SA-D1 - Frequency=2.37 cps, F-3 and F-4	135
54	Displacement vs. Length Saturn SA-D1 - Frequency=2.40 cps, Main Tank and Upper Stages	136

## LIST OF FIGURES (Cont)

Figure		Page
55	Displacement vs. Length Saturn SA-D1 - Frequency=2.40 cps, L-1 and L-2	137
56	Displacement vs. Length Saturn SA-D1 - Frequency=2.40 cps, L-3 and L-4	138
57	Displacement vs. Length Saturn SA-D1 - Frequency=2.40 cps, F-1 and F-2	139
58	Displacement vs. Length Saturn SA-D1 - Frequency=2.40 cps, F-3 and F-4	140
59	Displacement vs. Length Saturn SA-D1 - Frequency=2.50 cps, Main Tank and Upper Stages	141
60	Displacement vs. Length Saturn SA-D1 - Frequency=2.50 cps, L-1 and L-2	142
61	Displacement vs. Length Saturn SA-D1 - Frequency=2.50 cps, L-3 and L-4	143
62	Displacement vs. Length Saturn SA-D1 - Frequency=2.50 cps, F-1 and F-2	144
63	Displacement vs. Length Saturn SA-D1 - Frequency=2.50 cps, F-3 and F-4	145
64	Displacement vs. Length Saturn SA-D1 - Frequency=2.54 cps, Main Tank and Upper Stages	146
65	Displacement vs. Length Saturn SA-D1 - Frequency=2.54 cps, L-1 and L-2	147
66	Displacement vs. Length Saturn SA-D1 - Frequency=2.54 cps, L-3 and L-4	148
67	Displacement vs. Length Saturn SA-D1 - Frequency=2.54 cps, F-1 and F-2	149
68	Displacement vs. Length Saturn SA-D1 - Frequency=2.54 cps, F-3 and F-4	150
69	Displacement vs. Length Saturn SA-D1 - Frequency=2.57 cps, Main Tank and Upper Stages	151
70	Displacement vs. Length Saturn SA-D1 - Frequency=2.57 cps, L-1 and L-2	152

## LIST OF FIGURES (Cont)

Figure		Page
71	Displacement vs. Length Saturn SA-D1 - Frequency=2.57 cps, L-3 and L-4	153
72	Displacement vs. Length Saturn SA-D1 - Frequency=2.57 cps, F-1 and F-2	154
73	Displacement vs. Length Saturn SA-D1 - Frequency=2.57 cps, F-3 and F-4	155
74	Displacement vs. Length Saturn SA-D1 - Frequency=2.60 cps, Main Tank and Upper Stages	156
75	Displacement vs. Length Saturn SA-D1 - Frequency=2.60 cps, L-1 and L-2	157
76	Displacement vs. Length Saturn SA-D1 - Frequency=2.60 cps, L-3 and L-4	158
77	Displacement vs. Length Saturn SA-D1 - Frequency=2.60 cps, F-1 and F-2	159
78	Displacement vs. Length Saturn SA-D1 - Frequency=2.60 cps, F-3 and F-4	160
79	Displacement vs. Length Saturn SA-D1 - Frequency=2.70 cps, Main Tank and Upper Stages	161
80	Displacement vs. Length Saturn SA-D1 - Frequency=2.70 cps, L-1 and L-2	162
81	Displacement vs. Length Saturn SA-D1 - Frequency=2.70 cps, L-3 and L-4	163
82	Displacement vs. Length Saturn SA-D1 - Frequency=2.70 cps, F-1 and F-2	164
83	Displacement vs. Length Saturn SA-D1 - Frequency=2.70 cps, F-3 and F-4	165
84	Displacement vs. Length Saturn SA-D1 - Frequency=2.80 cps, Main Tank and Upper Stages	166
85	Displacement vs. Length Saturn SA-D1 - Frequency=2.80 cps, L-1 and L-2	167
86	Displacement vs. Length Saturn SA-D1 - Frequency=2.80 cps, L-3 and L-4	168

## LIST OF FIGURES (Cont)

Figure		Page
87	Displacement vs. Length Saturn SA-D1 - Frequency=2.80 cps, F-1 and F-2	169
88	Displacement vs. Length Saturn SA-D1 - Frequency=2.80 cps, F-3 and F-4	170
89	Displacement vs. Length Saturn SA-D1 - Frequency=2.90 cps, Main Tank and Upper Stages	171
90	Displacement vs. Length Saturn SA-D1 - Frequency=2.90 cps, L-1 and L-2	172
91	Displacement vs. Length Saturn SA-D1 - Frequency=2.90 cps, L-3 and L-4	173
92	Displacement vs. Length Saturn SA-D1 - Frequency=2.90 cps, F-1 and F-2	174
93	Displacement vs. Length Saturn SA-D1 - Frequency=2.90 cps, F-3 and F-4	175
94	Displacement vs. Length Saturn SA-D1 - Frequency=3.00 cps, Main Tank and Upper Stages	176
95	Displacement vs. Length Saturn SA-D1 - Frequency=3.00 cps, L-1 and L-2	177
96	Displacement vs. Length Saturn SA-D1 - Frequency=3.00 cps, L-3 and L-4	178
97	Displacement vs. Length Saturn SA-D1 - Frequency=3.00 cps, F-1 and F-2	179
98	Displacement vs. Length Saturn SA-D1 - Frequency=3.00 cps, F-3 and F-4	180
99	Displacement vs. Length Saturn SA-D1 - Frequency=3.20 cps, Main Tank and Upper Stages	181
100	Displacement vs. Length Saturn SA-D1 - Frequency=3.20 cps, L-1 and L-2	182
101	Displacement vs. Length Saturn SA-D1 - Frequency=3.20 cps, L-3 and L-4	183
102	Displacement vs. Length Saturn SA-D1 - Frequency=3.20 cps, F-1 and F-2	184

## LIST OF FIGURES (Cont)

Figure		Page
103	Displacement vs. Length Saturn SA-D1 - Frequency=3.20 cps, F-3 and F-4	185
104	Displacement vs. Length Saturn SA-D1 - Frequency=3.25 cps, Main Tank and Upper Stages	186
105	Displacement vs. Length Saturn SA-D1 - Frequency=3.25 cps, L-1 and L-2	187
106	Displacement vs. Length Saturn SA-D1 - Frequency=3.25 cps, L-3 and L-4	188
107	Displacement vs. Length Saturn SA-D1 - Frequency=3.25 cps, F-1 and F-2	189
108	Displacement vs. Length Saturn SA-D1 - Frequency=3.25 cps, F-3 and F-4	190
109	Displacement vs. Length Saturn SA-D1 - Frequency=3.30 cps, Main Tank and Upper Stages	191
110	Displacement vs. Length Saturn SA-D1 - Frequency=3.30 cps, L-1 and L-2	192
111	Displacement vs. Length Saturn SA-D1 - Frequency=3.30 cps, L-3 and L-4	193
112	Displacement vs. Length Saturn SA-D1 - Frequency=3.30 cps, F-1 and F-2	194
113	Displacement vs. Length Saturn SA-D1 - Frequency=3.30 cps, F-3 and F-4	195
114	Displacement vs. Length Saturn SA-D1 - Frequency=3.35 cps, Main Tank and Upper Stages	196
115	Displacement vs. Length Saturn SA-D1 - Frequency=3.35 cps, L-1 and L-2	197
116	Displacement vs. Length Saturn SA-D1 - Frequency=3.35 cps, L-3 and L-4	198
117	Displacement vs. Length Saturn SA-D1 - Frequency=3.35 cps, F-1 and F-2	199
118	Displacement vs. Length Saturn SA-D1 - Frequency=3.35 cps, F-3 and F-4	200

## LIST OF FIGURES (Cont)

Figure		Page
119	Displacement vs. Length Saturn SA-D1 - Frequency=3.40 cps, Main Tank and Upper Stages	201
120	Displacement vs. Length Saturn SA-D1 - Frequency=3.40 cps, L-1 and L-2	202
121	Displacement vs. Length Saturn SA-D1 - Frequency=3.40 cps, L-3 and L-4	203
122	Displacement vs. Length Saturn SA-D1 - Frequency=3.40 cps, F-1 and F-2	204
123	Displacement vs. Length Saturn SA-D1 - Frequency=3.40 cps, F-3 and F-4	205
124	Displacement vs. Length Saturn SA-D1 - Frequency=3.80 cps, Main Tank and Upper Stages	206
125	Displacement vs. Length Saturn SA-D1 - Frequency=3.80 cps, L-1 and L-2	207
126	Displacement vs. Length Saturn SA-D1 - Frequency=3.80 cps, L-3 and L-4	208
127	Displacement vs. Length Saturn SA-D1 - Frequency=3.80 cps, F-1 and F-2	209
128	Displacement vs. Length Saturn SA-D1 - Frequency=3.80 cps, F-3 and F-4	210
129	Displacement vs. Length Saturn SA-D1 - Frequency=4.00 cps, Main Tank and Upper Stages	211
130	Displacement vs. Length Saturn SA-D1 - Frequency=4.00 cps, L-1 and L-2	212
131	Displacement vs. Length Saturn SA-D1 - Frequency=4.00 cps, L-3 and L-4	213
132	Displacement vs. Length Saturn SA-D1 - Frequency=4.00 cps, F-1 and F-2	214
133	Displacement vs. Length Saturn SA-D1 - Frequency=4.00 cps, F-3 and F-4	215
134	Displacement vs. Length Saturn SA-D1 - Frequency=4.20 cps, Main Tank and Upper Stages	216

## LIST OF FIGURES (Cont)

Figure		Page
135	Displacement vs. Length Saturn SA-D1 - Frequency=4.20 cps, L-1 and L-2	217
136	Displacement vs. Length Saturn SA-D1 - Frequency=4.20 cps, L-3 and L-4	218
137	Displacement vs. Length Saturn SA-D1 - Frequency=4.20 cps, F-1 and F-2	219
138	Displacement vs. Length Saturn SA-D1 - Frequency=4.20 cps, F-3 and F-4	220
139	Displacement vs. Length Saturn SA-D1 - Frequency=4.30 cps, Main Tank and Upper Stages	221
140	Displacement vs. Length Saturn SA-D1 - Frequency=4.30 cps, L-1 and L-2	222
141	Displacement vs. Length Saturn SA-D1 - Frequency=4.30 cps, L-3 and L-4	223
142	Displacement vs. Length Saturn SA-D1 - Frequency=4.30 cps, F-1 and F-2	224
143	Displacement vs. Length Saturn SA-D1 - Frequency=4.30 cps, F-3 and F-4	225
144	Displacement vs. Length Saturn SA-D1 - Frequency=4.40 cps, Main Tank and Upper Stages	226
145	Displacement vs. Length Saturn SA-D1 - Frequency=4.40 cps, L-1 and L-2	227
146	Displacement vs. Length Saturn SA-D1 - Frequency=4.40 cps, L-3 and L-4	228
147	Displacement vs. Length Saturn SA-D1 - Frequency=4.40 cps, F-1 and F-2	229
148	Displacement vs. Length Saturn SA-D1 - Frequency=4.40 cps, F-3 and F-4	230
149	Displacement vs. Length Saturn SA-D1 - Frequency=4.50 cps, Main Tank and Upper Stages	231
150	Displacement vs. Length Saturn SA-D1 - Frequency=4.50 cps, L-1 and L-2	232

## LIST OF FIGURES (Cont)

Figure		Page
151	Displacement vs. Length Saturn SA-D1 - Frequency=4.50 cps, L-3 and L-4	233
152	Displacement vs. Length Saturn SA-D1 - Frequency=4.50 cps, F-1 and F-2	234
153	Displacement vs. Length Saturn SA-D1 - Frequency=4.50 cps, F-3 and F-4	235
154	Displacement vs. Length Saturn SA-D1 - Frequency=4.60 cps, Main Tank and Upper Stages	236
155	Displacement vs. Length Saturn SA-D1 - Frequency=4.60 cps, L-1 and L-2	237
156	Displacement vs. Length Saturn SA-D1 - Frequency=4.60 cps, L-3 and L-4	238
157	Displacement vs. Length Saturn SA-D1 - Frequency=4.60 cps, F-1 and F-2	239
158	Displacement vs. Length Saturn SA-D1 - Frequency=4.60 cps, F-3 and F-4	240
159	Displacement vs. Length Saturn SA-D1 - Frequency=4.70 cps, Main Tank and Upper Stages	241
160	Displacement vs. Length Saturn SA-D1 - Frequency=4.70 cps, L-1 and L-2	242
161	Displacement vs. Length Saturn SA-D1 - Frequency=4.70 cps, L-3 and L-4	243
162	Displacement vs. Length Saturn SA-D1 - Frequency=4.70 cps, F-1 and F-2	244
163	Displacement vs. Length Saturn SA-D1 - Frequency=4.70 cps, F-3 and F-4	245
164	Displacement vs. Length Saturn SA-D1 - Frequency=4.80 cps, Main Tank and Upper Stages	246
165	Displacement vs. Length Saturn SA-D1 - Frequency=4.80 cps, L-1 and L-2	247
166	Displacement vs. Length Saturn SA-D1 - Frequency=4.80 cps, L-3 and L-4	248

## LIST OF FIGURES (Cont)

Figure		Page
167	Displacement vs. Length Saturn SA-D1 - Frequency=4.80 cps, F-1 and F-2	249
168	Displacement vs. Length Saturn SA-D1 - Frequency=4.80 cps, F-3 and F-4	250
169	Displacement vs. Length Saturn SA-D1 - Frequency=5.00 cps, Main Tank and Upper Stages	251
170	Displacement vs. Length Saturn SA-D1 - Frequency=5.00 cps, L-1 and L-2	252
171	Displacement vs. Length Saturn SA-D1 - Frequency=5.00 cps, L-3 and L-4	253
172	Displacement vs. Length Saturn SA-D1 - Frequency=5.00 cps, F-1 and F-2	254
173	Displacement vs. Length Saturn SA-D1 - Frequency=5.00 cps, F-3 and F-4	255
174	Displacement vs. Length Saturn SA-D1 - Frequency=5.40 cps, Main Tank and Upper Stages	256
175	Displacement vs. Length Saturn SA-D1 - Frequency=5.40 cps, L-1 and L-2	257
176	Displacement vs. Length Saturn SA-D1 - Frequency=5.40 cps, L-3 and L-4	258
177	Displacement vs. Length Saturn SA-D1 - Frequency=5.40 cps, F-1 and F-2	259
178	Displacement vs. Length Saturn SA-D1 - Frequency=5.40 cps, F-3 and F-4	260
179	Displacement vs. Length Saturn SA-D1 - Frequency=5.80 cps, Main Tank and Upper Stages	261
180	Displacement vs. Length Saturn SA-D1 - Frequency=5.80 cps, L-1 and L-2	262
181	Displacement vs. Length Saturn SA-D1 - Frequency=5.80 cps, L-3 and L-4	263
182	Displacement vs. Length Saturn SA-D1 - Frequency=5.80 cps, F-1 and F-2	264

## LIST OF FIGURES (Cont)

Figure		Page
183	Displacement vs. Length Saturn SA-D1 - Frequency=5.80 cps, F-3 and F-4	265
184	Displacement vs. Length Saturn SA-D1 - Frequency=6.10 cps, Main Tank and Upper Stages	266
185	Displacement vs. Length Saturn SA-D1 - Frequency=6.10 cps, L-1 and L-2	267
186	Displacement vs. Length Saturn SA-D1 - Frequency=6.10 cps, L-3 and L-4	268
187	Displacement vs. Length Saturn SA-D1 - Frequency=6.10 cps, F-1 and F-2	269
188	Displacement vs. Length Saturn SA-D1 - Frequency=6.10 cps, F-3 and F-4	270
189	Displacement vs. Length Saturn SA-D1 - Frequency=6.40 cps, Main Tank and Upper Stages	271
190	Displacement vs. Length Saturn SA-D1 - Frequency=6.40 cps, L-1 and L-2	272
191	Displacement vs. Length Saturn SA-D1 - Frequency=6.40 cps, L-3 and L-4	273
192	Displacement vs. Length Saturn SA-D1 - Frequency=6.40 cps, F-1 and F-2	274
193	Displacement vs. Length Saturn SA-D1 - Frequency=6.40 cps, F-3 and F-4	275
194	Displacement vs. Length Saturn SA-D1 - Frequency=6.65 cps, Main Tank and Upper Stages	276
195	Displacement vs. Length Saturn SA-D1 - Frequency=6.65 cps, L-1 and L-2	277
196	Displacement vs. Length Saturn SA-D1 - Frequency=6.65 cps, L-3 and L-4	278
197	Displacement vs. Length Saturn SA-D1 - Frequency=6.65 cps, F-1 and F-2	279
198	Displacement vs. Length Saturn SA-D1 - Frequency=6.65 cps, F-3 and F-4	280

## LIST OF FIGURES (Cont)

Figure		Page
199	Displacement vs. Length Saturn SA-D1 - Frequency=6.75 cps, Main Tank and Upper Stages	281
200	Displacement vs. Length Saturn SA-D1 - Frequency=6.75 cps, L-1 and L-2	282
201	Displacement vs. Length Saturn SA-D1 - Frequency=6.75 cps, L-3 and L-4	283
202	Displacement vs. Length Saturn SA-D1 - Frequency=6.75 cps, F-1 and F-2	284
203	Displacement vs. Length Saturn SA-D1 - Frequency=6.75 cps, F-3 and F-4	285
204	Displacement vs. Length Saturn SA-D1 - Frequency=6.80 cps, Main Tank and Upper Stages	286
205	Displacement vs. Length Saturn SA-D1 - Frequency=7.20 cps, Main Tank and Upper Stages	287
206	Displacement vs. Length Saturn SA-D1 - Frequency=7.60 cps, Main Tank and Upper Stages	288
207	Displacement vs. Length Saturn SA-D1 - Frequency=8.00 cps, Main Tank and Upper Stages	289
208	Frequency vs. Response - Payload Pt. No.1	290
209	Angular Response vs. Frequency - Payload Pt. No.1	291
210	Frequency vs. Response - Lox Tank No. 1 Pt.77	292
211	Frequency vs. Response - Lox Tank No. 2 Pt.79	293
212	Frequency vs. Response - Lox Tank No. 3 Pt.81	294
213	Frequency vs. Response - Lox Tank No. 4 Pt.83	295
214	Frequency vs. Response - Fuel Tank No. 1 Pt.78	296
215	Frequency vs. Response - Fuel Tank No. 2 Pt.80	297
216	Frequency vs. Response - Fuel Tank No. 3 Pt.82	298
217	Frequency vs. Response - Fuel Tank No. 4 Pt.76	299

## LIST OF FIGURES (Cont)

Figure		Page
218	Qualitative Vector Response of the Saturn SA-D1 - 1st Cluster Mode and 1st Bending Mode	300
219	Qualitative Vector Response of the Saturn SA-D1 - Fuel Tank Mode (F-2 & F-4) and Second Cluster Mode	301
220	Qualitative Vector Response of the Saturn SA-D1 - Lox Tank Mode and Second Bending Mode	302

## OBJECT

The object of this analysis is to determine the response characteristics, frequency, and mode shape of the Saturn SA-D1 vehicle with particular emphasis on the booster section.

## CONCLUSIONS

1. The analysis results compare favorably with the five similar frequencies obtained in the test results of Reference 5.
2. The largest source of error occurring in the comparisons could be attributed to the damping and sloshing fluid mass effects on the test program results.
3. Due to the lack of damping or dissipation terms in the analysis, the resonant points were of very narrow band width and required small frequency intervals for identification.
4. The frequencies appear to occur in pairs throughout the frequency range investigated.
5. The outer tank motions are such that the analyst can often envision individual torsion modes on the separate tanks. To ascertain such effects the various angular motions would require plotting which is far beyond the scope of the present analysis.
6. The analysis provided explicit identification of seven frequencies and mode shapes.

## RECOMMENDATIONS

The recommendations in this report are entirely concerned with future developments of Kron's analysis technique. Although the present program

is capable of determining the response characteristics of highly redundant three dimensional structures, the analysis technique is far from being exploited to its full potential in its present role. Several modifications and extensions to the existing program would greatly increase its scope of usefulness. These extensions may be broken down into modifications of the present program which are within present capabilities and extensions requiring long range research to ascertain their feasibility and incorporation.

The extensions needed on the present program are:

1. Addition of a provision to obtain stresses and strains directly.
- \*2. Addition of a provision for transmitting a load from one point to another without deflections.
- \*3. Addition of a provision for the use of pin joints in the analysis.
4. Addition of a provision allowing shear panels to be analyzed.

The extensions requiring additional research to ascertain their feasibility are:

1. The inclusion of damping or dissipation terms.
2. The extension of the analysis to allow the use of transient forcing functions.
3. The extension of the program to allow large problems to be subdivided into small problems, solutions arrived at, and the sub-solutions interconnected to obtain the solution of the original problem. This

\* These properties may be artificially induced in the present program by proper specification of the beam properties.

is very advantageous from an efficiency and accuracy standpoint.

A complete description of this extension is provided in Reference 9.

The goals described above would be most efficiently approached if they were the primary objective of the investigation. That is, the extensions should be approached with the sole intent of obtaining the desired extension rather than stipulating that a specific piece of hardware be analyzed with the desired extension.

#### INTRODUCTION

The analysis of a highly redundant three-dimensional structure, such as the Saturn SA-D1 vehicle, poses a formidable problem for which a solution may be attempted by only a limited number of analysis techniques. The analysis technique utilized by Chrysler Missile Division is based on the method first proposed by Gabriel Kron. While the primary objective of this analysis is to predict the natural frequencies and mode shapes of the SA-D1 vehicle, this report will also fulfill the twofold purpose of: (1) providing a complete detailed description of Kron's analysis technique, and (2) establishing the merit of the analysis technique through correlation with the results of the test program.

The analysis was conducted only for the lift-off or fully fueled condition with a suspension system having a lateral spring rate of 626#/in. and a vertical spring rate of 625,500#/in. The outer tank identification system and excitation load were consistent with the test program to aid in comparing results.

## DISCUSSION

### Mathematical Analysis

#### Introduction

The engineering literature is overabundantly supplied with models that replace special types of elastic and dynamic structures by a network of mass points and simple springs. In that type of topological representation the ultimate building blocks, namely the masses and springs, each have only one degree of freedom. The emphasis in this method of analysis is on building blocks with more than one degree of freedom.

The method of analysis which was used in this report is an application of G. Kron's treatise called "Diakoptics." From his voluminous works (Reference 1) the necessary principles for solving network type problems were extracted, modified and applied to the solution of redundant-type elastic structures. The resultant method which has been developed is capable of solving the eigenvalue problems - associated with mechanical vibration as well as the deflections problem of redundant structures under static loading conditions.

In the most general sense, this treatise is an attempt to combine the resources of point set topology with those of combinatorial topology into one engineering tool for the analysis and solution of complex systems having a large number of variables. This is accomplished by utilizing the disciplines of tensor and matrix analysis, and the concepts of tearing and interconnecting topological models. The latter has the advantage of subdividing the processes of both analysis and solution into manageable small pieces.

The use of combinatorial topology in the solution of network problems such as elastic structures is also characterized by the important fact that in the interconnection of the ultimate building blocks, i.e., beams and masses, the various energy principles and complimentary energy principles of the theory of

elasticity are not required. These functions are taken over by the law of transformation of tensors derived from the geometry or topology of the structure. Obviously, in the derivation of the stiffness matrices of the ultimate building blocks themselves, the energy principles reappear since the role of topology is again taken over by physics. Thus it appears that topology and physics are interchangeable concepts in the study of interconnection.

Although the tensor concept is the underlying idea behind this treatise, it would be presumptuous to try and explain both tensor analysis and its application in this limited space. The interested reader without a background in tensor analysis is referred to the first few chapters of Reference 3 or to any of the many textbooks available on tensor analysis. It is suggested that the casual reader replace the word tensor by the word matrix and think of the symbols as matrices instead of tensors.

One of the most important properties of tensor equations is that they are invariant under a coordinate transformation. If a tensor equation is valid in one coordinate system, it is valid in every coordinate system of the same type. This property permits one to derive the equations of state of ultimate building blocks in one coordinate system, then the laws of tensor transformations will automatically take care of all the details if it is desired to apply the equations in a different coordinate system. This is precisely the application which is utilized in this method of analyzing redundant structures.

The procedure for obtaining a solution will consist of two phases; namely, the "Analysis" and the "Solution." In the analysis, the complex structure is first torn into its two types of building blocks which are simple beams and concentrated masses. Then, the equations of state are formulated only once for each building block in the simplest coordinate system. For example, cartesian coordinates would be used for straight beams whereas cylindrical coordinates would

be used for curved beams. These equations of state are the relationships between force and displacement. The equations of state for the entire interconnected structure in a new coordinate system then follow in a routine manner from the laws of tensor transformation and from connection tensors which are derived from the topological model.

- Once the equations of state are obtained for the entire interconnected model, it is then necessary to perform a solution. Conventional means of finding a solution, that is by either matrix iteration or matrix inversion, are not practical for systems which are as large as implied in this report. A method of finding the solution which is utilized in this method of analysis is called "Factorizing the Inverse."

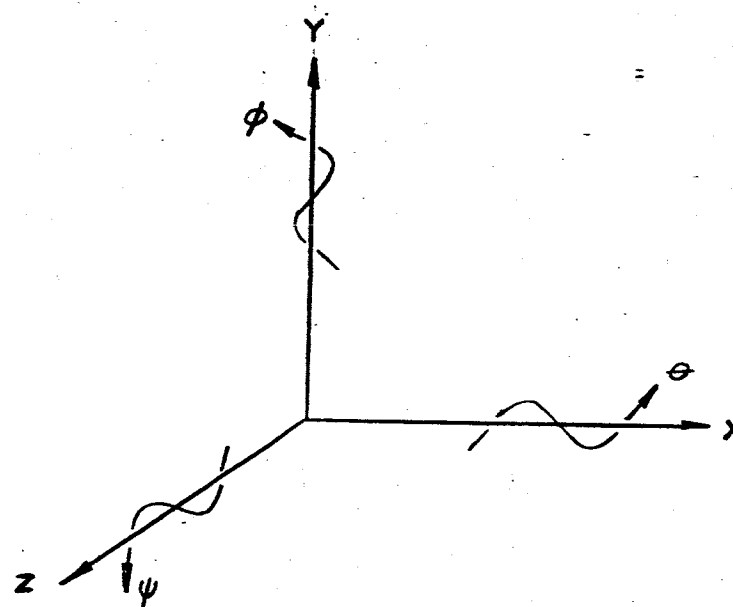
The remainder of this discussion will be consisted of two parts: , the analysis and the solution. In Part One, the equations of state which describe the system are developed. The solution of these equations is explained in Part Two.

#### Part One - Analysis

##### Primitive Elements:

The primitive elements or building blocks which are considered in this analysis consist of an elastic beam whose masses and mass moments of inertia are concentrated at the two end points of the generalized spring. In other words, a beam consists of two rigid bodies whose centers of gravity are connected by an elastic spring of length  $l$ . The ultimate beam therefore is a generalized straight beam having six degrees of freedom at each end, plus two rigid bodies - one connected to each of its end points. Since a rigid body has six degrees of freedom (three rotations and three translations) an ultimate beam has twelve degrees of freedom. The simplest coordinate system which can be

used for deriving the equations of state for these primitive elements is a right-handed orthogonal cartesian coordinate system which is illustrated in Figure 1.



Coordinate System

Figure 1

In a system such as this each end of the beam will be acted upon by three forces and three moments. Corresponding to these forces and moments there will be three linear and three angular displacements. These will be denoted as follows:

- $f^x$  = Force in  $x$  direction
  - $f^y$  = Force in  $y$  direction
  - $f^z$  = Force in  $z$  direction
  - $f^\theta$  = Moment about  $x$  direction
  - $f^\phi$  = Moment about  $y$  direction
  - $f^\psi$  = Moment about  $z$  direction
  - $D_x$  = Linear deflection due to  $f^x$
  - $D_y$  = Linear deflection due to  $f^y$
  - $D_z$  = Linear deflection due to  $f^z$
- (1)

$D_\theta$  = Angular deflection due to  $f^\theta$

$D_\phi$  = Angular deflection due to  $f^\phi$

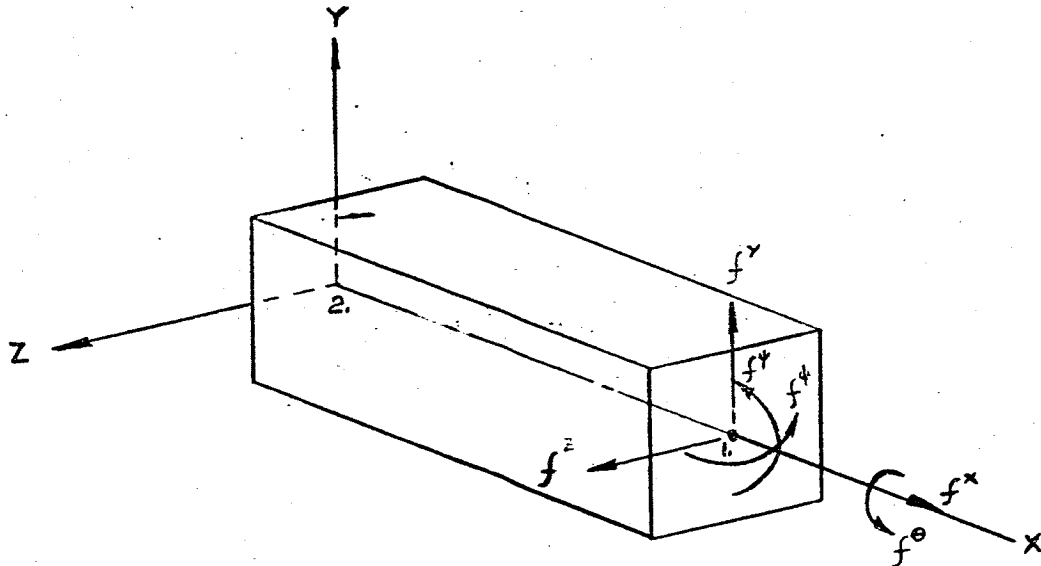
$D_\psi$  = Angular deflection due to  $f^\psi$

(1) cont'd.

It is an accepted convention in tensor calculus to use subscripts and superscripts to denote covariant and contravariant tensors, respectively.

The reason for this is that in generalized coordinates the law of transformation for covariant tensors is not the same as the law of transformation for contravariant tensors. However, for cartesian coordinates and cartesian tensors there is no difference between covariant and contravariance and all the suffixes can legitimately be written as subscripts. We shall use both subscripts and superscripts to be consistent with Reference 3.

In Figure 2, consider a simple beam cantilevered at the origin and oriented so that its elastic axis lies along the  $x$  axis and that the principal axes of its cross section lie along the  $y$  and  $z$  axis of the reference axes. Let the free end of this beam be acted upon by the forces and moments as given by Equation (1).



Cantilever Beam - Forces Acting at End 1

Figure 2

Southwell, in Reference 2, has shown that the total strain energy stored in this beam can be expressed as:

$$U = \frac{1}{2} \int_0^L \left[ \frac{(f_x)^2}{EA} + \frac{(f_\theta + \xi f_z^2)^2}{EI_y} + \frac{(f_\theta - \xi f_z)^2}{EI_z} + \frac{(f_\theta)^2}{GJ} \right] d\xi \quad (2)$$

where

$U$  = total strain energy

$E$  = Young's Modulus

$GJ$  = torsional rigidity

$A$  = cross sectional area

$L$  = length of beam

$I_y$  = area moment of inertia about  $y$  axis

$I_z$  = area moment of inertia about  $z$  axis

$\xi$  = variable of integration

and the  $f^i$ 's,  $i = x, y, z, \theta, \phi, \psi$  are defined by (1). The deflection of the free end of the beam due to these forces can be determined by utilizing Castigliano's Second Theorem; namely, the deflection of a beam at a point of load application and in the direction of this load can be obtained by differentiating the expression for the total strain energy with respect to the applied load.

$$\frac{\partial U}{\partial f^i} = D_i \quad (3)$$

Applying Equation (3) to Equation (2) for  $i = x, y, z, \theta, \phi, \psi$ , and then performing the integration, we have;

$$D_{ix} = \left( \frac{L}{AE} \right) f'^x$$

$$D_{iy} = \left( \frac{L^3}{3EI_y} \right) f''y - \left( \frac{L^2}{2EI_z} \right) f'^\phi$$

$$D_{iz} = \left( \frac{L^3}{3EI_y} \right) f''z + \left( \frac{L^2}{2EI_y} \right) f'^\theta$$

$$D_{i\theta} = \left( \frac{L}{GJ} \right) f'^\theta$$

$$D_{i\phi} = \left( \frac{L^2}{2EI_y} \right) f''z + \left( \frac{L}{EI_y} \right) f'^\phi$$

$$D_{i\psi} = - \left( \frac{L^2}{2EI_z} \right) f''y + \left( \frac{L}{EI_z} \right) f'^\psi$$

These equations can be written in matrix form as follows:

$$\begin{bmatrix} D_{1x} \\ D_{1y} \\ D_{1z} \\ D_{1\theta} \\ D_{1\phi} \\ D_{1\psi} \end{bmatrix} = \begin{bmatrix} \frac{EA}{L} & 0 & 0 & 0 & 0 & -\frac{L^2}{2EI_z} \\ 0 & \frac{L^3}{3EI_z} & 0 & 0 & 0 & -\frac{L^2}{2EI_z} \\ 0 & 0 & \frac{3EI_y}{L^3} & 0 & \frac{L^2}{2EI_y} & 0 \\ 0 & 0 & 0 & \frac{GJ}{L} & 0 & 0 \\ 0 & 0 & \frac{L^2}{2EI_y} & 0 & \frac{L}{EI_y} & 0 \\ 0 & -\frac{L^2}{2EI_z} & 0 & 0 & 0 & \frac{L}{EI_z} \end{bmatrix} \begin{bmatrix} f'^x \\ f'^y \\ f'^z \\ f'^\theta \\ f'^\phi \\ f'^\psi \end{bmatrix}$$

or more briefly,

$$[D_1] = [Z_{11}] [f'] \quad (5)$$

where  $[D_1]$  and  $[f']$  are column matrices and  $[Z_{11}]$  is a square matrix of flexibility influence coefficients. Its inverse is a stiffness matrix and it will be denoted by

$$[Y''] = [Z_{11}]^{-1} \quad (6)$$

Pre-multiplying both sides of Equation (5) by  $[Y^{11}]$  and using Equation (6), we have:

$$[f'] = [Y''] [D_1] \quad (7)$$

where

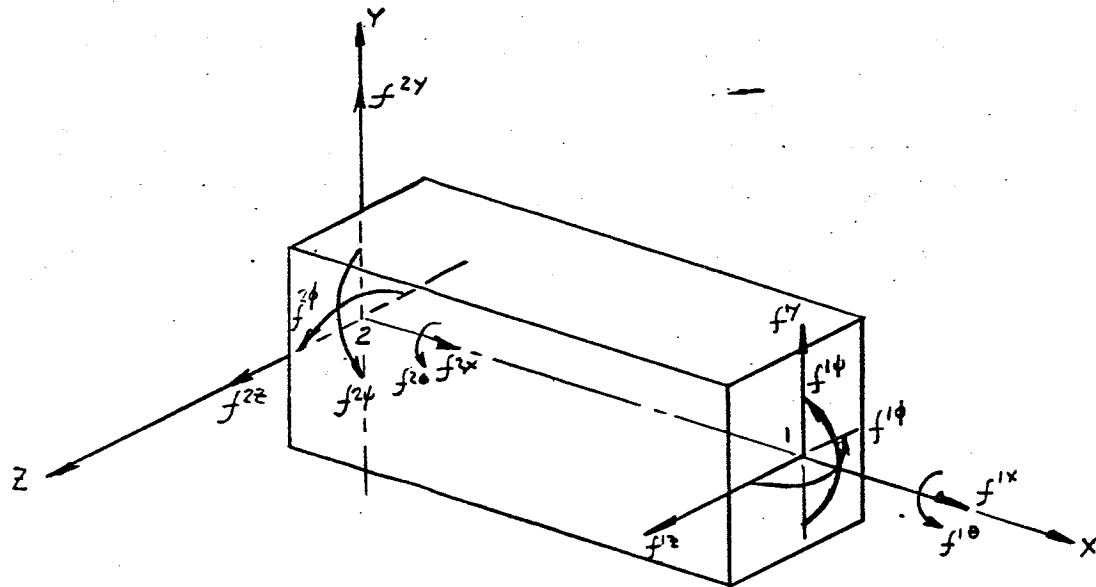
$$[Y''] = \begin{bmatrix} \frac{EA}{L} & 0 & 0 & 0 & 0 & 0 \\ 0 & \frac{12EI_z}{L^3} & 0 & 0 & 0 & \frac{6EI_z}{L} \\ 0 & 0 & \frac{12EI_y}{L^3} & 0 & -\frac{6EI_y}{L^2} & 0 \\ 0 & 0 & 0 & \frac{GJ}{L} & 0 & 0 \\ 0 & 0 & -\frac{6EI_y}{L^2} & 0 & \frac{4EI_y}{L} & 0 \\ 0 & \frac{6EI_z}{L^2} & 0 & 0 & 0 & \frac{4EI_z}{L} \end{bmatrix} \quad (8)$$

At this point it is necessary to explicitly define what has been done and more important, to establish what is yet to be done. Equation (7) is the relationship

between the forces at point 1 due to a deflection of point 1 for a beam which is constrained at point 2 as shown in Figure 2. The ultimate goal of this analysis is to obtain a relationship or equations of state for this beam such that this beam is not constrained or equivalently, not orientated. The object is to allow both ends of the beam to deflect such that its stored strain energy is only a function of the relative deflections of its ends. A non-isolated beam such as this has the important property that it is accessible from both ends, therefore, it can be connected to other similar beams at both ends to form the entire complex structure.

To obtain the equations of state for a beam which is not orientated, it will now be necessary to solve for the constraint forces at point 2 in terms of the applied forces at point 1. Next, the free and constrained ends will be reversed and the relationship between forces and deflections at point 2 and similarly, the constraint forces at point 1 will be determined. These relationships will then be combined to obtain the correspondence between all of the forces and deflections of this generalized spring.

The constraint forces (see Figure 3) at point 2 can be established from the conditions of equilibrium. Solving the equilibrium conditions we have



Cantilever Beam - Restraint Forces at End 2

Figure 3

$$\begin{aligned}
 f^{2x} &= -f^{1x} \\
 f^{2y} &= -f^{1y} \\
 f^{2z} &= -f^{1z} \\
 f^{2\theta} &= -f^{1\theta} \\
 f^{2\phi} &= -f^{1\phi} + L f^{1z} \\
 f^{2\psi} &= -f^{1\psi} - L f^{1y}
 \end{aligned} \tag{9}$$

or in matrix form,

$$[f^2] = [\lambda_1^2][f'] \tag{10}$$

where  $\lambda_1^2$  is the matrix of coefficients in Equation (9)

$$[\lambda_1^2] = \begin{bmatrix} -1 & 0 & 0 & 0 & 0 & 0 \\ 0 & -1 & 0 & 0 & 0 & 0 \\ 0 & 0 & -1 & 0 & 0 & 0 \\ 0 & 0 & 0 & -1 & 0 & 0 \\ 0 & 0 & L & 0 & -1 & 0 \\ 0 & -L & 0 & 0 & 0 & -1 \end{bmatrix} \tag{11}$$

$[\lambda_1^2]$  may be considered a force transfer tensor which transfers the forces from point one to point two.

The above procedure is now repeated for the conditions that point one is constrained and point two is free and acted upon by the forces and moments. The only change that is required is that the dummy variable of integration in Equation (2) is changed from  $\xi$  to  $-\xi$ . This results in the following flexibility influence coefficients  $[Z_{22}]$  for end 2.

$$[Z_{22}] = \begin{bmatrix} \frac{L}{RE} & 0 & 0 & 0 & 0 & 0 \\ 0 & \frac{L^3}{3EI_x} & 0 & 0 & 0 & \frac{L^2}{2EI_x} \\ 0 & 0 & \frac{L^3}{3EI_y} & 0 & -\frac{L^2}{2EI_y} & 0 \\ 0 & 0 & 0 & \frac{L}{GJ} & 0 & 0 \\ 0 & 0 & -\frac{L^2}{2EI_y} & 0 & \frac{L}{EI_y} & 0 \\ 0 & \frac{L^2}{2EI_x} & 0 & 0 & 0 & \frac{L}{EI_x} \end{bmatrix} \tag{12}$$

By inverting Equation (12) the following equation, relating the forces and deflections at end 2 in terms of a stiffness matrix, can be written as

$$[f^2] = [Y^{22}] [D_2] \quad (13)$$

where

$$[Y^{22}] = [Z_{22}]^{-1} \quad (14)$$

and is given by

$$[Y^{22}] = \begin{bmatrix} \frac{EA}{L} & 0 & 0 & 0 & 0 & 0 \\ 0 & \frac{12EI_z}{L^3} & 0 & 0 & 0 & -\frac{6EI_z}{L} \\ 0 & 0 & \frac{12EI_y}{L^3} & 0 & \frac{CEI_y}{L} & 0 \\ 0 & 0 & 0 & \frac{GJ}{L} & 0 & 0 \\ 0 & 0 & 0 & \frac{6EI_y}{L} & 0 & \frac{4EI_y}{L} \\ 0 & -\frac{6EJ_z}{L} & 0 & 0 & 0 & \frac{4EI_z}{L} \end{bmatrix} \quad (15)$$

The force transfer tensor can be derived as before. It is:

$$[\lambda'_2] = \begin{bmatrix} -1 & 0 & 0 & 0 & 0 & 0 \\ 0 & -1 & 0 & 0 & 0 & 0 \\ 0 & 0 & -1 & 0 & 0 & 0 \\ 0 & 0 & 0 & -1 & 0 & 0 \\ 0 & 0 & -1 & 0 & -1 & 0 \\ 0 & 1 & 0 & 0 & 0 & -1 \end{bmatrix} \quad (16)$$

where

$$[f'] = [\lambda'_2] [f^2] \quad (17)$$

and

$$[\lambda'_2] = [\lambda'_1]^{-1} \quad (17a)$$

It is now necessary to combine the above results to establish the equations of state for non-orientated beam; that is, for a beam which is not constrained. The resultant force at end one is the sum of the forces acting at end one and the transfer forces at end one due to the forces at end two. In matrix form this is expressed as:

$$[F'] = [f'] + [\lambda'_2] [f^2] \quad (18)$$

Similarly, for end two;

$$[F^2] = [f^2] + [\lambda^2_1] [f'] \quad (19)$$

where  $[F^1]$  and  $[F^2]$  are column matrices.

Applying Equations (7) and (13) to Equations (18) and (19) we have:

$$\begin{aligned} [F'] &= [Y''] [D_1] + [\lambda'_2] [Y^{22}] [D_2] \\ [F^2] &= [Y^{22}] [D_2] + [\lambda^2_1] [Y''] [D_1] \end{aligned} \quad (20)$$

Letting

$$\begin{aligned} [\lambda'_2] [Y^{22}] &= [Y'^2] \\ [\lambda^2_1] [Y''] &= [Y^{21}] \end{aligned} \quad (21)$$

and for convenience, dropping the bracket notation to denote matrices, we have:

$$\begin{aligned} F' &= Y'' D_1 + Y'^2 D_2 \\ F^2 &= Y^{21} D_1 + Y^{22} D_2 \end{aligned} \quad (21)$$

or

$$F = Y D \quad (21a)$$

where

$$Y = \begin{bmatrix} Y'' & Y'^2 \\ Y^{21} & Y^{22} \end{bmatrix}$$

Equations (21) are the final equations of state for an unconstrained generalized spring that is orientated in its own "primitive" coordinate system as illustrated in Figure 2, where  $y^{11}$  and  $y^{22}$  are defined by Equations (8) and (15), respectively, and where

$$[Y^{21}] = [Y^{12}]^T \quad (22)$$

that is  $y^{21}$  is equal to the transpose of  $y^{12}$  and where:

$$Y^{12} = \lambda_2 Y^{22} = \begin{bmatrix} -\frac{EA}{L} & 0 & 0 & 0 & 0 & 0 \\ 0 & -\frac{12EI_2}{L^3} & 0 & 0 & 0 & -\frac{6EI_2}{L^2} \\ 0 & 0 & -\frac{12EI_2}{L^3} & 0 & \frac{6EI_2}{L^2} & 0 \\ 0 & 0 & 0 & \frac{GJ}{L} & 0 & 0 \\ 0 & 0 & \frac{6EI_2}{L^2} & 0 & \frac{2EI_2}{L^2} & 0 \\ 0 & -\frac{6EI_2}{L^2} & 0 & 0 & 0 & \frac{2EI_2}{L^2} \end{bmatrix} \quad (23)$$

A few comments about the system of Equations (21) is in order.

Each of the  $Y$  matrices are non-singular six x six matrices whereas the system matrix,

$$Y = \begin{bmatrix} Y^{11} & Y^{12} \\ Y^{21} & Y^{22} \end{bmatrix}$$

which is a twelve x twelve matrix, is singular. This can be shown as follows:

Consider the matrix  $Y$ . Multiply the second row of matrices by  $-\lambda_2'$  and add it to the first. This is a valid matrix operation which does not alter the original matrix. We have

$$Y = \begin{bmatrix} (Y^{11} - \lambda_2' Y^{21}) & (Y^{12} - \lambda_2' Y^{22}) \\ Y^{21} & Y^{22} \end{bmatrix}$$

but  $\lambda_2' F^2 = F^1$  by (17)

$\lambda_2' Y^{22} = Y^{12}$  by (20a)

$\lambda_2' Y^{21} = \lambda_2' (\lambda_1^2 Y^{11}) = Y^{11}$  by (20a) and (17a)

therefore,

$$Y = \begin{bmatrix} 0 & 0 \\ Y^{21} & Y^{22} \end{bmatrix}$$

Since  $Y^{21}$  and  $Y^{22}$  are non-singular it can be concluded that, in the general case, Equations (21) have a degeneracy of six. A discrete solution exists if six constraints or boundary conditions are applied at one end or if several boundary conditions are applied at each such that their sum is at least six.

Having established the equations of state for the beam, it is now necessary to determine the equations of state for a concentrated mass. A concentrated mass will be considered as having no linear dimensions and allowed to have six degrees of freedom; namely, three linear displacements and three angular displacements. Associated with these displacements will be three forces and three moments, respectively. The coordinate system which will be used is illustrated in Figure 1. The deflections of the mass will be denoted as follows:

$D_x$  = linear deflection due to  $F^x$  acting on the mass

$D_y$  = linear deflection due to  $F^y$  acting on the mass

$D_z$  = linear deflection due to  $F^z$  acting on the mass

$D_\theta$  = angular deflection due to  $F^\theta$  acting on the mass

$D_\phi$  = angular deflection due to  $F^\phi$  acting on the mass

$D_\psi$  = angular deflection due to  $F^\psi$  acting on the mass

Assuming simple harmonic motion, then the instantaneous displacement of the mass in any of the six directions can be expressed as

$$D_i = D_{0i} e^{i\omega t} \quad (24)$$

where  $D_{0i}$  is the maximum deflection of the mass and  $\omega$  = frequency of oscillation.

Differentiating Equation (24) twice with respect to time we have

$$\frac{\partial^2 D_i}{\partial t^2} = -\omega^2 D_{0i} e^{i\omega t} = -\omega^3 D_i \quad (25)$$

For dynamic equilibrium, the forces acting on the body in each direction must equal the product of the mass times the linear acceleration, and the moment about each axis must equal the mass moment of inertia times the angular acceleration about their respective axes. Thus, there are six equations of dynamic equilibrium for each concentrated mass which are,

$$\begin{aligned} F^x &= -\omega^2 M^{xx} D_x \\ F^y &= -\omega^2 M^{yy} D_y \\ F^z &= -\omega^2 M^{zz} D_z \\ F^\theta &= -\omega^2 M^{\theta\theta} D_\theta \\ F^\phi &= -\omega^2 M^{\phi\phi} D_\phi \\ F^\psi &= -\omega^2 M^{\psi\psi} D_\psi \end{aligned} \quad (26)$$

where

$$M^{xx} = M^{yy} = M^{zz} = \text{concentrated mass}$$

$M^{\theta\theta}$  = mass moment of inertia about the x axis

$M^{\phi\phi}$  = mass moment of inertia about the y axis

$M^{\psi\psi}$  = mass moment of inertia about the z axis

Referring to the definition of the primitive element, we see that the continuous mass properties of an actual beam are simulated in the primitive element by two concentrated masses, one at each end of the generalized spring. The concentrated masses are defined as equal and are computed on the basis of the mass properties about the center of gravity of a uniform beam of length L. Thus associated with each primitive element there are twelve additional mass equations of state, six at each end of the generalized spring, which can be written as

$$\begin{aligned} F^1 &= M^{\theta\theta} D_1 \\ F^2 &= M^{zz} D_z \end{aligned} \quad (27)$$

where

$$M'' = M^{22} = \begin{bmatrix} -\omega^2 M^{xx} & 0 & 0 & 0 & 0 & 0 \\ 0 & -\omega^2 M^{yy} & 0 & 0 & 0 & 0 \\ 0 & 0 & -\omega^2 M^{zz} & 0 & 0 & 0 \\ 0 & 0 & 0 & -\omega^2 I^{yy} & 0 & 0 \\ 0 & 0 & 0 & 0 & -\omega^2 I^{zz} & 0 \\ 0 & 0 & 0 & 0 & 0 & -\omega^2 I^{yy} \end{bmatrix} \quad (28)$$

where;

$\mu$  = mass density

$A$  = cross sectional area of beam

$L$  = length of beam

$\omega$  = frequency of oscillation

$$M^{xx} = M^{yy} = M^{zz} = \frac{\mu AL}{2} \quad (29)$$

$$I^{yy} = M^{xx} (I_{max} + I_{min}) / A$$

$$I^{zz} = M^{yy} \left( \frac{L^2}{12} + I_{min} / A \right)$$

$$I^{yy} = M^{zz} \left( \frac{L^2}{12} + I_{max} / A \right)$$

Before continuing, let us briefly summarize our results up to this stage and then postulate the succeeding stages of the analysis. We now have available the fundamental equations of state for an isolated primitive element which consists of two concentrated masses connected by a generalized spring. These equations were developed for a beam orientated in the primitive coordinate system as shown in Figure 2 and are given by equations (21) and (27).

Having summarized the analysis to this point, let us consider a complex, three dimensional, redundant structure which is composed of simple uniform beams which are connected to one another to form a structural network. It is

obvious that relative to some particular coordinate system for the entire structure the individual beams will have different orientations. Conceivably, no two beams necessarily must have the same orientation. In addition, the equations of state which have been developed for the primitive beams are tensor equations or, equivalently, vectors. Based on the above discussion it can be readily postulated that before the primitive beams can be connected one to another to form the final structure, the equations of state for each of the primitive elements must be transformed such that they are applicable to a common coordinate system. The procedure which is utilized in obtaining the equations of state for the entire structure consists of (1) "tearing" this structure into its smallest basic building blocks which are the primitive elements, (2) establishing the equations of state for the primitive elements only once, which is in the primitive coordinate system, (3) transform these equations of state such that all of the primitive elements are orientated properly with respect to each other, and finally (4) fuse all of these elements together by a connection tensor or, equivalently, by a transformation.

Having set the stage, we will embark first on developing the tensor transformation laws which are applicable to this analysis and finally, two transformation tensors; one which will orientate the primitive elements and the second which will satisfy the equilibrium and continuity conditions at each point where beams are joined.

#### Tensor Transformation Laws:

Consider the following tensor equation:

$$F^\alpha = Y^{\alpha\beta} D_\beta \quad (30)$$

and assume the following coordinate transformations:

$$D_\beta = A_\beta^\alpha D_\alpha \quad (31)$$

$$F^\alpha = A_\alpha^\beta F^\beta \quad (32)$$

where  $A_\beta^b$  maps the range of  $D_b$  into the domain  $D_\beta$ , and similarly  $A_\alpha^a$  maps the range of  $F^\alpha$  into the domain  $F^a$ . Substituting Equation (31) into (30) we have

$$F^\alpha = Y^{\alpha\beta} A_\beta^b D_b \quad (33)$$

Multiplying both sides of Equation (33) by  $A_\alpha^a$  we have

$$F^a = A_\alpha^a F^\alpha = A_\alpha^a Y^{\alpha\beta} A_\beta^b D_b \quad (34)$$

Since we postulate that Equation (30) is a tensor equation, then Equation (34) can be written as

$$F^a = Y^{ab} D_b \quad (35)$$

since tensor equations have the property that they are invariant under a coordinate transformation. Comparing Equations (34) and (35) we can conclude that the transformation law for  $Y^{ab}$  is as follows

$$Y^{ab} = A_\alpha^a Y^{\alpha\beta} A_\beta^b \quad (36)$$

where  $A_\alpha^a$  and  $A_\beta^b$  are defined by Equations (31) and (32). The tensor transformation laws under a change of coordinates can be derived in another manner which may appeal to ones physical senses. Consider an elastic structure which is acted upon by a force system which will be expressed as the column matrix  $F^a$  and the corresponding system of deflections  $D_a$  of the structure.  $D_a$  is also a column matrix. We postulate that the work done on the structure is independent of the reference frame or coordinate system which describes the system. Assume a change of coordinate systems that can be expressed by the following relation:

$$D_a = A D_b \quad (37)$$

where  $D_a$  = deflections under the original coordinate system

$D_b$  = deflections under the new coordinate system.

The above postulate can be expressed in equation form as,

$$(F^a)_T D_a = (F^b)_T D_b \quad (38)$$

Substituting Equation (37) into (38), we have

$$(F^a)_T A D_b = (F^b)_T D_b \quad (39)$$

Comparing both sides of Equation (39), we can conclude that

$$(F^a)_T A = (F^b)_T \quad (40)$$

And, finally, taking the transpose of both sides of Equation (40) we have

$$[(F^a)_T A]_T = A_T [(F^a)_T]_T = A_T F^a = [(F^b)_T]_T = F^b$$

therefore,

$$F^b = A_T F^a \quad (41)$$

Rewriting Equation (2la)

$$F^a = Y^{aa} D_a$$

and substituting Equation (37) into (2la) we obtain

$$F^a = Y^{aa} A D_b$$

and multiplying both sides by  $A_T$ , we obtain

$$A_T F^a = A_T Y^{aa} A D_b$$

where  $A_T F^a = F^b$  by Equation (41).

Finally,

$$F^b = Y^{bb} D_b$$

where

$$Y^{bb} = A_T Y^{aa} A \quad (42)$$

Equations (37), (41) and (42) are the tensor transformation laws which are necessary in the following analysis.

#### Orientation of Primitive Beams:

The equations of state for each of the primitive beams are derived in terms of their own coordinate axes; namely, along the principal axes of each

primitive element. Since each primitive element is orientated differently in space, so also are their coordinate systems. In order to analyze the system of primitive elements as one interconnected structure, it is necessary to establish a direction cosine matrix whereby each primitive coordinate system is referenced to one coordinate system which is chosen as a basis for the interconnected structure. If a primitive beam denoted by its end indices  $(i, j)$  lies along an arbitrary direction relative to the basic coordinate system as shown in Figure 4, the positions of its three principal axes are defined in terms of nine directional cosines for a straight beam.

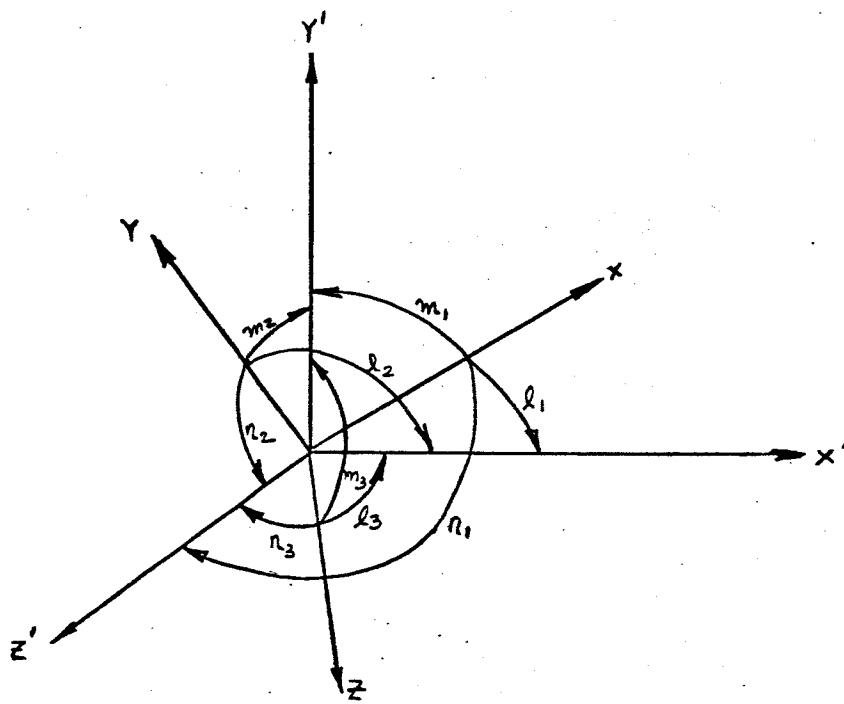


Figure 4 - Definition of Directional Cosines

They express at either end of the beam the six linear and angular displacements  $D$  along the principal axes (primitive axes) in terms of the six displacements  $D'$  along the basic coordinate system. The equations relating these two sets of axis at one end of the beam by the direction cosines can be written as

$$\begin{aligned}
 x &= l_1 x' + m_1 y' + n_1 z' \\
 y &= l_2 x' + m_2 y' + n_2 z' \\
 z &= l_3 x' + m_3 y' + n_3 z' \\
 \theta &= l_1 x' + m_1 y' + n_1 z' \\
 \phi &= l_2 x' + m_2 y' + n_2 z' \\
 \psi &= l_3 x' + m_3 y' + n_3 z'
 \end{aligned} \tag{43}$$

where  $l_1$  is the cosine of the angle between  $X$  and  $X'$ ;  $m_1$ , the cosine of the angle between  $X$  and  $Y'$ ;  $n_1$ , the cosine of the angle between  $X$  and  $Z'$ , etc. These quantities are derived in Appendix A. Rewriting these equations in matrix form for end  $i$  we have

$$D_i = A_i D'_i \tag{44}$$

where

$$A_i = \begin{bmatrix} A_{ii} & 0 \\ 0 & A_{ii} \end{bmatrix}$$

and

$$A_{ii} = \begin{bmatrix} l_1 & m_1 & n_1 \\ l_2 & m_2 & n_2 \\ l_3 & m_3 & n_3 \end{bmatrix} \tag{45}$$

For a generalized spring which has twelve degrees of freedom, six at each end, this transformation matrix has the form,

$$\begin{bmatrix} D_i \\ D_j \end{bmatrix} = \begin{bmatrix} A_i & 0 \\ 0 & A_j \end{bmatrix} \begin{bmatrix} D'_i \\ D'_j \end{bmatrix}$$

where  $D_i$  = deflection matrix at end  $i$  in the primitive coordinate system  
 $D_j$  = deflection matrix at end  $j$  in the primitive coordinate system  
 $D'_i$  = deflection matrix at end  $i$  in the basic coordinate system  
 $D'_j$  = deflection matrix at end  $j$  in the basic coordinate system

For a straight beam

$$A_i = A_j$$

therefore

$$\begin{bmatrix} D_i \\ D_j \end{bmatrix} = \begin{bmatrix} A_i & 0 \\ 0 & A_i \end{bmatrix} \begin{bmatrix} D'_i \\ D'_j \end{bmatrix} \quad (46)$$

The tensor transformation matrix which orientates the masses for the interconnected structure is given by Equation (45) whereas the orientation of the generalized straight spring is accomplished by Equation (46).

Consider a primitive beam which is defined by its end points (i, j).

The equations of state for the generalized spring are expressed as:

$$\begin{bmatrix} F_s^i \\ F_s^j \end{bmatrix} = \begin{bmatrix} Y^{ii} & Y^{ij} \\ Y^{ji} & Y^{jj} \end{bmatrix} \begin{bmatrix} D_s^i \\ D_s^j \end{bmatrix} \quad (47)$$

where  $F_s^i$ ,  $D_s^i$  are the forces and deflections respectively on  $i^{\text{th}}$  end, and similarly,  $F_s^j$ ,  $D_s^j$  are the forces and deflections at the  $j^{\text{th}}$  end, and the index s denotes association with the generalized spring. Utilizing the transformation laws which were derived previously, the equations of state for this generalized spring in the basic coordinate system are

$$\begin{bmatrix} F_s^i \\ F_s^j \end{bmatrix} = \begin{bmatrix} (A_i)_T F_s^i \\ (A_i)_T F_s^j \end{bmatrix} = \begin{bmatrix} (A_i)_T & 0 \\ 0 & (A_i)_T \end{bmatrix} \begin{bmatrix} Y^{ii} & Y^{ij} \\ Y^{ji} & Y^{jj} \end{bmatrix} \begin{bmatrix} A_i & 0 \\ 0 & A_i \end{bmatrix} \begin{bmatrix} D'_s^i \\ D'_s^j \end{bmatrix}$$

and after performing the above indicated matrix multiplications we have

$$\begin{bmatrix} F_s^i \\ F_s^j \end{bmatrix} = \begin{bmatrix} (A_i)_T Y^{ii} A_i & (A_i)_T Y^{ij} A_i \\ (A_i)_T Y^{ji} A_i & (A_i)_T Y^{jj} A_i \end{bmatrix} \begin{bmatrix} D'_s^i \\ D'_s^j \end{bmatrix} \quad (48)$$

Similarly, the equations of state for the mass elements are transformed to

$$\begin{bmatrix} F_m^i \\ F_m^j \end{bmatrix} = \begin{bmatrix} (A_i)_T M^{ii} A_i & 0 \\ 0 & (A_i)_T M^{jj} A_i \end{bmatrix} \begin{bmatrix} D'^m_i \\ D'^m_j \end{bmatrix} \quad (49)$$

where the index m denotes association with the masses. The same directional cosine matrices are used to transform both the generalized spring and masses since

it has been postulated that the principal axes of the mass element lie along the principal axes of the generalized spring.

#### Interconnection:

The equations of state for the complete primitive element consisting of a generalized spring with two concentrated masses, one at each end, will now be formed by the use of a connection tensor. This tensor is established by applying the principle of continuity at the junction points of the masses and generalized spring.

Consider the system shown in Figure 5 whose equations of state are governed by Equations (48) and (49)

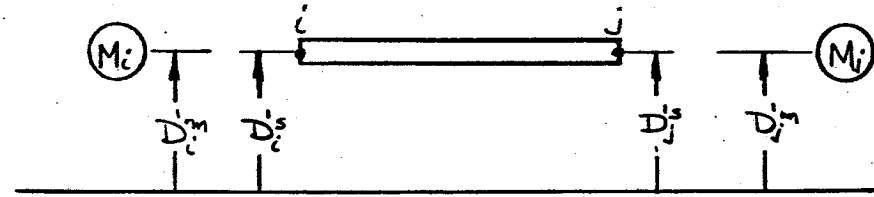


Figure 5 - Beam - Mass System

Combining these equations in matrix form we have:

$$\begin{bmatrix} F_s^{i,i} \\ F_s^{i,j} \\ F_m^{i,i} \\ F_m^{i,j} \end{bmatrix} = \begin{bmatrix} (A_i)_T Y^{ii} A_i & (A_i)_T Y^{ij} A_i & 0 & 0 \\ (A_i)_T Y^{ji} A_i & (A_i)_T Y^{jj} A_i & 0 & 0 \\ 0 & 0 & (A_i)_T M^{ii} A_i & 0 \\ 0 & 0 & 0 & (A_i)_T M^{jj} A_i \end{bmatrix} \begin{bmatrix} D_i^s \\ D_j^s \\ D_i^m \\ D_j^m \end{bmatrix} \quad (50)$$

or

$$[F'_{S,m}] = [Y_{S,m}] [D'_{S,m}] \quad (50a)$$

Equation (50) is actually twenty-four scalar equations representing the twelve degrees of freedom of the generalized spring and six degrees of freedom associated with each mass. Using the continuity principle, the following relations can be established

$$D'_i = D_i^m = \bar{D}'_i$$

$$D'_j = D_j^m = \bar{D}'_j$$

The above identities can be written in matrix form as

$$\begin{bmatrix} D'_i \\ D'_j \\ D_i^m \\ D_j^m \end{bmatrix} = \begin{bmatrix} 1 & 0 \\ 0 & 1 \\ 1 & 0 \\ 0 & 1 \end{bmatrix} \begin{bmatrix} D'_i \\ D'_j \end{bmatrix}$$

or more briefly,

$$[D'_{s,m}] = [C][D'] \quad (51)$$

where  $C =$

$$\begin{bmatrix} 1 & 0 \\ 0 & 1 \\ 1 & 0 \\ 0 & 1 \end{bmatrix} \quad (51a)$$

Equation (51a) is the connection tensor which interconnects the two end masses to the generalized spring. Applying this connection tensor to Equation (50) according to the tensor transformation laws, we obtain the following equations:

$$\begin{bmatrix} F'^i \\ F'^j \\ F'_s \\ F'_m \end{bmatrix} = [C]_T \begin{bmatrix} F_s^i \\ F_s^j \\ F_m^i \\ F_m^j \end{bmatrix} = \begin{bmatrix} 1 & 0 & 1 & 0 \\ 0 & 1 & 0 & 1 \end{bmatrix} \begin{bmatrix} F_s^i \\ F_s^j \\ F_m^i \\ F_m^j \end{bmatrix} = \begin{bmatrix} F_s^i + F_m^i \\ F_s^j + F_m^j \end{bmatrix} \quad (52)$$

$$\begin{aligned} C_T Y_{s,m} C &= \begin{bmatrix} 1 & 0 & 1 & 0 \\ 0 & 1 & 0 & 1 \end{bmatrix} \begin{bmatrix} (A_i)_T Y^{ii} A_i & (A_i)_T Y^{ij} A_i & 0 & 0 \\ (A_i)_T Y^{ji} A_i & (A_i)_T Y^{jj} A_i & 0 & 0 \\ 0 & 0 & (A_i)_T M^{ii} A_i & 0 \\ 0 & 0 & 0 & (A_i)_T M^{jj} A_i \end{bmatrix} \\ &= \begin{bmatrix} (A_i)_T Y^{ii} A_i - (A_i)_T M^{ii} A_i & (A_i)_T Y^{ij} A_i \\ (A_i)_T Y^{ji} A_i & (A_i)_T Y^{jj} A_i - (A_i)_T M^{jj} A_i \end{bmatrix} \quad (52a) \end{aligned}$$

Combining and factorizing terms, the equations of state for the complete primitive element becomes

$$\begin{bmatrix} F'_i \\ F'_j \end{bmatrix} = \begin{bmatrix} A_{iT}(Y^{ii} + M^{ii})A_i & A_{iT}Y^{ij}A_i \\ A_{iT}Y^{ji}A_i & A_{iT}(Y^{jj} + M^{jj})A_i \end{bmatrix} \begin{bmatrix} D'_i \\ D'_j \end{bmatrix} \quad (53)$$

where  $\begin{bmatrix} F'^i \\ F'^j \end{bmatrix}$  and  $\begin{bmatrix} D'^i \\ D'^j \end{bmatrix}$  are defined by Equations (52) and (51), respectively.

Equation (53) is now twelve scalar equations representing the twelve degrees of freedom of a complete primitive element. These equations of state (53) are developed for each primitive element of the "torn" system and with the use of a connection tensor which is developed using identically the same procedure as developed for connecting the masses to the ends of the generalized spring, they are joined to form the equations of state for the "untorn" or interconnected systems.

To conclude the discussion of the primitive elements, it is interesting to note that Equation (52) satisfies the force equilibrium condition at the intersection of the masses and spring. Consider the forces defined by the left side of Equation (50) as internal beam forces or stresses and similarly, consider the forces defined by the left side of Equation (52) as externally applied loads to the beam. It can be seen from the free body diagrams of Figure 6a that if no external forces act at a joint, then  $[f_1] = -[f_2]$  where  $[f]$  denotes a general force system consisting of three forces and three moments, whereas for the condition shown in Figure 6b, the equilibrium conditions yield

$$[F_{ext.}] + [f_1] + [f_2] = 0$$

therefore

$$[F_{ext.}] = -[f_1 + f_2]$$

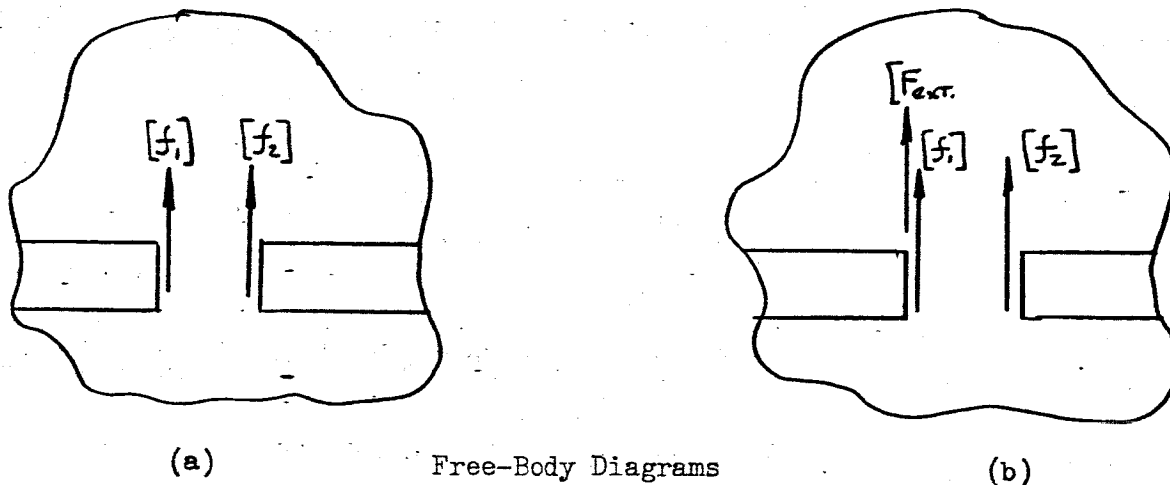


Figure 6

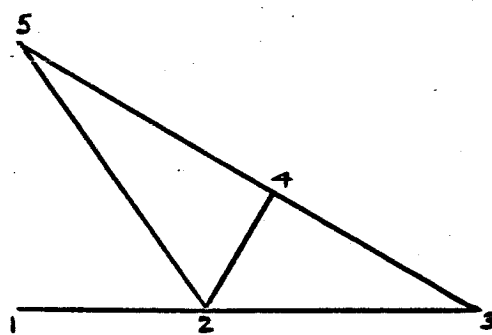
In defining the basic building blocks, it could have been assumed that the primitive element was only composed of a generalized spring. In this case, the equations of state are developed as before, with the exception that the masses are not considered. Then, in the process of interconnecting these primitive elements, one must consider the inertia forces as externally applied loads and include them in the left side of, say, Equation (52). It then follows, once harmonic motion is assumed, that the equations can be rearranged to produce identically the relationship which is shown in Equation (53). This is just another point of view of the same problem.

#### Interconnection of "Torn" System:

It is difficult to discuss the concept of interconnecting from a theoretical point of view since many of the engineering concepts which appeal to common sense and/or intuition become obscure. Therefore, the interconnection of primitive elements is best illustrated by an example problem.

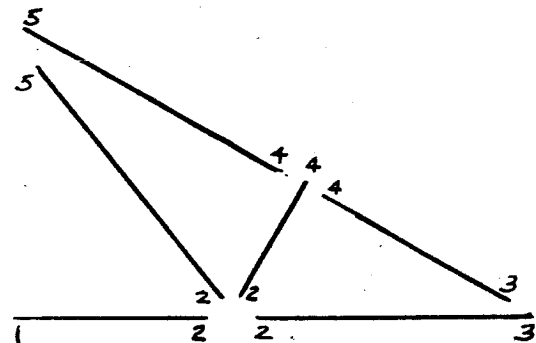
Consider a structure as shown in Figure 7a which is, from the topological point of view, a network of beams. This network is composed of interconnected branches or, in the terminology of this report, an interconnection of

primitive elements. Assign to each branch end point of this network an index number as shown in the same figure. Next, "tear" this network into its primitive elements and assign an index number to each end of every branch of this torn system. This is illustrated in Figure 7b.



Interconnected Network

(a)



Torn Network

(b)

Figure 7

A specific indexing system is used for the torn model. That is, there exists a correspondence between the branch point index numbers of the interconnected network and of the branch points of the torn network. In the general case, this correspondence is not necessary. A somewhat random numbering scheme can be used for the torn network but it would have the disadvantage of losing the physical identity of each primitive element relative to the interconnected system.

For each primitive element shown in Figure 7b, there exists equations of state of the form which is given by Equation (53). As stated previously, the equations of state for each beam is actually twelve scalar equations which represent its twelve degrees of freedom. Since each element is uniquely defined by the numbers assigned to its end points, a very convenient coding scheme can be

adapted for defining the matrix elements in the equations of state. Let each primitive element twelve by twelve matrix be partitioned into four six by six matrices as shown in Equation (53). Using the identification numbers assigned to the end points, say  $(i, j)$ , we identify each six by six matrix with two subscripts and two superscripts as follows:

$$\begin{bmatrix} Y_{ii}^{ij} & | & Y_{ij}^{ij} \\ \hline Y_{ji}^{ij} & + & Y_{jj}^{ij} \end{bmatrix} \quad (54)$$

The superscripts indicate which beam element the matrix came from and the subscripts identify the influence coefficient matrix relative to the beam.

In addition, let the forces be defined as follows:

$$F'^i = F_{ij}^i, D'_i = D_{ij}^{ij}, \text{ etc. where}$$

$F_{ij}^i$  = force acting at end  $i$  of the  $(i, j)$  primitive element

$D_{ij}^{ij}$  = deflection of end  $i$  of the  $(i, j)$  primitive element

A comparison of Equation (53) with (54) yields the following identities:

$$\begin{aligned} Y_{ii}^{ij} &= A_{it} (Y_{ii}^{ij} + M_{ii}^{ij}) A_i \\ Y_{ij}^{ij} &= A_{it} (Y_{ij}^{ij}) A_i \\ Y_{ji}^{ij} &= A_{it} (Y_{ji}^{ij}) A_i \\ Y_{jj}^{ij} &= A_{it} (Y_{jj}^{ij} + M_{jj}^{ij}) A_i \end{aligned} \quad (56)$$

Rewriting Equation (53) in this new notation, we have

$$\begin{bmatrix} F_{ij}^i \\ F_{ij}^j \end{bmatrix} = \begin{bmatrix} Y_{ii}^{ij} & Y_{ij}^{ij} \\ Y_{ji}^{ij} & Y_{jj}^{ij} \end{bmatrix} \begin{bmatrix} D_i^{ij} \\ D_j^{ij} \end{bmatrix} \quad (57)$$

This is the form which will be used in writing the equations of state for this example problem. For the torn system, given in Figure 7b, these equations are expressed as:

element 1-2

$$\begin{bmatrix} F_{12}^1 \\ F_{12}^2 \end{bmatrix} = \begin{bmatrix} Y_{11}^{12} & Y_{12}^{12} \\ Y_{21}^{12} & Y_{22}^{12} \end{bmatrix} \begin{bmatrix} D_1^2 \\ D_2^2 \end{bmatrix}$$

element 2-3

$$\begin{bmatrix} F_{23}^2 \\ F_{23}^3 \end{bmatrix} = \begin{bmatrix} Y_{22}^{23} & Y_{23}^{23} \\ Y_{32}^{23} & Y_{33}^{23} \end{bmatrix} \begin{bmatrix} D_2^{23} \\ D_3^{23} \end{bmatrix}$$

element 2-4

$$\begin{bmatrix} F_{24}^2 \\ F_{24}^4 \end{bmatrix} = \begin{bmatrix} Y_{22}^{24} & Y_{24}^{24} \\ Y_{42}^{24} & Y_{44}^{24} \end{bmatrix} \begin{bmatrix} D_2^{24} \\ D_4^{24} \end{bmatrix}$$

(58)

element 2-5

$$\begin{bmatrix} F_{25}^2 \\ F_{25}^5 \end{bmatrix} = \begin{bmatrix} Y_{22}^{25} & Y_{25}^{25} \\ Y_{52}^{25} & Y_{55}^{25} \end{bmatrix} \begin{bmatrix} D_2^{25} \\ D_5^{25} \end{bmatrix}$$

element 3-4

$$\begin{bmatrix} F_{34}^3 \\ F_{34}^4 \end{bmatrix} = \begin{bmatrix} Y_{33}^{34} & Y_{34}^{34} \\ Y_{43}^{34} & Y_{44}^{34} \end{bmatrix} \begin{bmatrix} D_3^{34} \\ D_4^{34} \end{bmatrix}$$

—

element 4-5

$$\begin{bmatrix} F_{45}^4 \\ F_{45}^5 \end{bmatrix} = \begin{bmatrix} Y_{44}^{45} & Y_{45}^{45} \\ Y_{54}^{45} & Y_{55}^{45} \end{bmatrix} \begin{bmatrix} D_4^{45} \\ D_5^{45} \end{bmatrix}$$

These equations are now combined to form one system matrix composed of disconnected primitive elements. This yields:

$$\begin{bmatrix}
 F_1 \\
 F_{12} \\
 F_{12}^2 \\
 F_{23}^2 \\
 F_{23}^3 \\
 F_{23}^4 \\
 F_{24}^2 \\
 F_{24}^4 \\
 F_{25}^2 \\
 F_{25}^5 \\
 F_{34}^3 \\
 F_{34}^4 \\
 F_{45}^4 \\
 F_{45}^5
 \end{bmatrix}
 \begin{bmatrix}
 Y_{11}^{12} & Y_{11}^{12} \\
 Y_{21}^{12} & Y_{21}^{12} \\
 Y_{22}^{23} & Y_{22}^{23} \\
 Y_{32}^{23} & Y_{32}^{23} \\
 Y_{22}^{24} & Y_{22}^{24} \\
 Y_{32}^{24} & Y_{32}^{24} \\
 Y_{22}^{25} & Y_{22}^{25} \\
 Y_{52}^{25} & Y_{52}^{25} \\
 Y_{33}^{34} & Y_{33}^{34} \\
 Y_{43}^{34} & Y_{43}^{34} \\
 Y_{44}^{45} & Y_{44}^{45} \\
 Y_{54}^{45} & Y_{54}^{45}
 \end{bmatrix}
 \begin{bmatrix}
 D_1^{12} \\
 D_2^{12} \\
 D_2^{23} \\
 D_3^{23} \\
 D_2^{24} \\
 D_3^{24} \\
 D_2^{25} \\
 D_5^{25} \\
 D_3^{34} \\
 D_4^{34} \\
 F_{44}^{45} \\
 D_4^{45} \\
 D_5^{45}
 \end{bmatrix}$$
(59)

This system matrix in an abbreviated form is:

$$F^P = Y^{PP} D_P \quad (60)$$

where  $F^P$  = forces in the primitive system

$D_P$  = deflections in the primitive system.

It is now necessary to derive the connection tensor to obtain the equations of state for the interconnected system. Using the continuity principle we can say that the deflections of the elements at each joint in the interconnected system must necessarily be equal. Thus the following continuity relationships can be formulated:

$$\begin{aligned}
 D_1^{12} &= D_1 \\
 D_2^{12} &= D_2^{23} = D_2^{24} = D_2 \\
 D_3^{23} &= D_3^{34} = D_3 \\
 D_4^{24} &= D_4^{34} = D_4^{45} = D_4 \\
 D_5^{25} &= D_5^{45} = D_5
 \end{aligned}
 \quad (61)$$

In matrix form, Equations (61) become

$$\begin{bmatrix} D_1^{12} \\ D_2^{12} \\ D_2^{23} \\ D_3^{23} \\ D_2^{24} \\ D_2^{24} \\ D_4^{24} \\ D_2^{25} \\ D_5^{25} \\ D_3^{34} \\ D_4^{34} \\ D_4^{45} \\ D_5^{45} \end{bmatrix} = \begin{bmatrix} 1 & 0 & 0 & 0 & 0 \\ 0 & 1 & 0 & 0 & 0 \\ 0 & 1 & 0 & 0 & 0 \\ 0 & 0 & 1 & 0 & 0 \\ 0 & 1 & 0 & 0 & 0 \\ 0 & 0 & 0 & 1 & 0 \\ 0 & 1 & 0 & 0 & 0 \\ 0 & 0 & 0 & 0 & 1 \\ 0 & 0 & 1 & 0 & 0 \\ 0 & 0 & 0 & 1 & 0 \\ 0 & 0 & 0 & 1 & 0 \\ 0 & 0 & 0 & 0 & 1 \end{bmatrix} \begin{bmatrix} D_1 \\ D_2 \\ D_3 \\ D_4 \\ D_5 \end{bmatrix} \quad (61a)$$

or more briefly

$$[D_P] = [C][D_I] \quad (62)$$

where  $[D_P]$  is a column matrix defined by Equation (61)

$[D_I]$  is a column matrix defined as the deflections in the interconnected system and,

$[C]$  is the connection tensor which relates the primitive beam deflections with the junction point deflections of the interconnected system. This connection tensor is defined by Equation (61a).

It is this derived connection tensor that will transform the equations of states (59) of the torn or disconnected primitive system to the equations of state for the interconnected system. This transformation is performed using the tensor transformation laws which were derived previously.

Let

$$F^I = Y^{II} D_I \quad (63)$$

be the equations of state for the interconnected system.

Then,

$$F^I = C_T F^P$$

$$Y^{II} = C_T Y^{PP} C$$

and  $D_I$  is defined by Equation (61).

Performing these transformations we have:

$$\begin{bmatrix} F^1 \\ F^2 \\ F^3 \\ F^4 \\ F^5 \end{bmatrix} = \begin{bmatrix} F_1^1 \\ F_1^2 + F_{23}^2 + F_{24}^2 + F_{25}^2 \\ F_{23}^3 + F_{24}^3 \\ F_{24}^4 + F_{34}^4 + F_{45}^4 \\ F_{25}^5 + F_{45}^5 \end{bmatrix} \quad (64)$$

and

$$Y^{II} = C_T Y^{PP} C = \begin{bmatrix} Y_{11}^{12} & Y_{12}^{12} & 0 & 0 & 0 \\ Y_{21}^{12} & (Y_{22}^{12} + Y_{22}^{23} + Y_{22}^{24} + Y_{22}^{25}) & Y_{23}^{23} & Y_{24}^{24} & Y_{25}^{25} \\ 0 & Y_{32}^{23} & (Y_{33}^{23} + Y_{33}^{34}) & Y_{34}^{34} & 0 \\ 0 & Y_{42}^{24} & Y_{43}^{34} & (Y_{44}^{24} + Y_{44}^{34} + Y_{44}^{45}) & Y_{45}^{45} \\ 0 & Y_{52}^{25} & 0 & Y_{54}^{45} & (Y_{55}^{25} + Y_{55}^{45}) \end{bmatrix} \quad (65)$$

Rewriting Equation (63) in expanded form, we have

$$\begin{bmatrix} F^1 \\ F^2 \\ F^3 \\ F^4 \\ F^5 \end{bmatrix} = \begin{bmatrix} Y_{11}^{12} & Y_{12}^{12} & 0 & 0 & 0 \\ Y_{21}^{12} & (Y_{22}^{12} + Y_{22}^{23} + Y_{22}^{24} + Y_{22}^{25}) & Y_{23}^{23} & Y_{24}^{24} & Y_{25}^{25} \\ Y_{32}^{23} & (Y_{33}^{23} + Y_{33}^{34}) & Y_{34}^{34} & 0 & 0 \\ Y_{42}^{24} & Y_{43}^{34} & (Y_{44}^{24} + Y_{44}^{34} + Y_{44}^{45}) & Y_{45}^{45} & 0 \\ Y_{52}^{25} & 0 & Y_{54}^{45} & (Y_{55}^{25} + Y_{55}^{45}) & D_5 \end{bmatrix} \quad (66)$$

This equation (66) is the equation of state for the simple example problem which was considered to illustrate the concept of interconnecting a torn primitive system. A number of general comments about this system of equations is now in order. Equation (66) represents thirty scalar equations. Therefore, the order of the influence coefficient matrix  $y^{II}$  is equal to thirty. The rank of this matrix is less than thirty and therefore it is also singular. To obtain a solution, adequate boundary conditions or, equivalently, constraint must be specified. This condition requires that in the general case at least six deflections be given as known and that for a deflection analysis the order of the  $y^{II}$  matrix reduced. An alternate procedure is to consider that the constraint forces corresponding to the given boundary conditions are unknown, and after transposing these forces to the right side of say Equation (63) solve for the unknown deflections and constraint forces.

Another comment should be made with regards to the identification scheme which was selected for the submatrices and to the indexing scheme of the primitive or torn system. Observing Equations (58) and (66), it can be concluded that under this proposed system, the equations of state for the interconnected system can be formed directly by summing all of the submatrices of the disconnected system which have identical subscripts, say  $(i j)$ , and assigning this sum to the  $i j$  location of the interconnected matrix. This indexing scheme automatically "satisfies" the continuity relationships or, equivalently, interconnects the primitive elements.

Now that we have completed the analysis, i.e., established the equations of state, we are ready to start the second part or solution. It should be pointed out that Equation (65) represents only an example and a rather simple one at that. An actual structure or missile requires a much larger number of elements and points for an adequate representation. Consequently, the order of the stiffness matrix representing the system can become extremely large.

Part Two - Solution

Specifically, the solution required is to find the deflections, D, for a given set of external forces, F, and a given frequency,  $\omega$ . Since the complete inversion of the stiffness matrix  $Y^{II}$  by conventional methods is prohibited by the order of magnitude of the rank of  $Y^{II}$  which is implied in this report, we use a method which (in Reference 1) is called "Factorizing the Inverse." This method results in what is called the "Factorizing Inverse Table" and, as the name implies, it is a table of matrices which contains all of the factors necessary to compute the required deflections in easy stages. The foundation behind this table is presented in Reference 4. Among its various titles, it has been called the "Craut's Elimination Process." It can be looked upon as follows: Consider the equations of state for an interconnected system as given by Equation (63) and further, for the purposes of operation or manipulation, consider the quantities  $F^i$ 's and  $D_i$ 's which are six by one column matrices and  $Y_{ij}$ 's which are six by six matrices, as scalars. Therefore, for the purposes of operation Equation (63) may be considered as n scalar equations where n equals the number of junction points and where F and  $D_1$  and Y represent  $n \times 1$  column matrices and an  $n \times n$  square matrix, respectively. Once having established this concept of n linear equations and n unknowns, the process of eliminating the unknowns and finding the solution in an orderly manner can be presented.

Let the equations of state for the interconnected system be expressed as

$$\begin{aligned}
 a_{11}D_1 + a_{12}D_2 + \dots + a_{1n}D_n &= F^1 \\
 a_{21}D_1 + a_{22}D_2 + \dots + a_{2n}D_n &= F^2 \\
 \vdots &\quad \vdots \\
 a_{i1}D_1 + a_{i2}D_2 + \dots + a_{in}D_n &= F^i \\
 \vdots &\quad \vdots \\
 a_{n1}D_1 + a_{n2}D_2 + \dots + a_{nn}D_n &= F^n
 \end{aligned} \tag{67}$$

where the above developed concept is utilized. Any other set of  $n$  equations which are linear combinations of these equation (called an equivalent set) clearly has the same solution. Since only the coefficients  $a_{ij}$  and those of the quantities  $F^1, \dots, F^n$  are significant in the formation of such linear combinations, it is expedient to carry out the contemplated manipulations upon the matrix

$$\left[ \begin{array}{cccccc} a'_{11} & a'_{12} & a'_{13} & \dots & a'_{1n} & F^1 \\ a'_{21} & a'_{22} & a'_{23} & \dots & a'_{2n} & F^2 \\ \vdots & \vdots & \vdots & & \vdots & \vdots \\ \vdots & \vdots & \vdots & & \vdots & \vdots \\ \vdots & \vdots & \vdots & & \vdots & \vdots \\ a'_{n1} & a'_{n2} & \dots & \dots & a'_{nn} & F^n \end{array} \right] \quad (68)$$

which is the matrix of coefficients from equation (67) with the quantities  $F^1, \dots, F^n$  added as an additional column and the superscript added to the coefficients to keep an account of the manipulations. This resultant matrix involving  $n$  rows and  $n + 1$  columns is referred to as the augmented matrix corresponding to Equation (67). The series of manipulations which are described presently, have for their objective the derivation of an equivalent set of equations having an augmented matrix in which all of the elements of the principal diagonal are unity and all those below this diagonal are zero. A word of caution must be injected at this time. Although the identity of the matrices has been lost in the representation of the elements in Equation (67), it must be kept in mind that they are, in reality, matrices; thus the laws of matrix multiplication must be adhered to and it must be recognized that the commutative law is not valid. The first step is to pre-multiply the first row in matrix (68) by the inverse of the leading coefficient so to obtain,

$$\begin{bmatrix} 1 & (a'_{11})^{-1}a'_{12} & (a'_{11})^{-1}a'_{13} & \cdots & (a'_{11})^{-1}a'_{1n} & (a'_{11})^{-1}F' \\ a'_{21} & a'_{22} & a'_{23} & \cdots & a'_{2n} & F^2 \\ \vdots & & & & \vdots & \vdots \\ a'_{n1} & a'_{n2} & a'_{n3} & \cdots & a'_{nn} & F^n \end{bmatrix} \quad (69)$$

The inverse of this always exists since it was established in Part One that it is a non-singular matrix. The  $a'_{21}$  pre-multiplied elements of the first row are now subtracted from the corresponding elements of the second row giving,

$$\begin{bmatrix} 1 & (a'_{11})^{-1}a'_{12} & (a'_{11})^{-1}a'_{13} & \cdots & (a'_{11})^{-1}a'_{1n} & (a'_{11})^{-1}F' \\ 0 & a'^2_{22} & a'^2_{23} & \cdots & a'^2_{2n} & F^2 - a'_{21}(a'_{11})^{-1}F' \\ a'_{31} & a'_{32} & a'_{33} & \cdots & a'_{3n} & F^3 \\ \vdots & & & & & \vdots \\ a'_{n1} & a'_{n2} & a'_{n3} & \cdots & a'_{nn} & F^n \end{bmatrix} \quad (70)$$

in which

$$\begin{aligned} a'^2_{22} &= a'_{22} - a'_{21}(a'_{11})^{-1}a'_{12} \\ a'^2_{23} &= a'_{23} - a'_{21}(a'_{11})^{-1}a'_{13} \\ &\vdots &&\vdots &&\vdots \\ a'^2_{2n} &= a'_{2n} - a'_{21}(a'_{11})^{-1}a'_{1n} \end{aligned} \quad (71)$$

Next, the  $a'_{31}$  pre-multiplied elements of the first row are subtracted from the corresponding elements of the third row. This leaves the augmented matrix in the form

$$\begin{bmatrix} 1 & (a'_{11})^{-1}a'_{12} & (a'_{11})^{-1}a'_{13} & \dots & (a'_{11})^{-1}a'_{1n} & (a'_{11})^{-1}F' \\ 0 & a^2_{22} & a^2_{23} & \dots & a^2_{2n} & F^2 - a'_1(a'_{11})^{-1}F' \\ 0 & a^2_{32} & a^2_{33} & \dots & a^2_{3n} & F^3 - a'_3(a'_{11})^{-1}F' \\ \vdots & \vdots & \vdots & \ddots & \vdots & \vdots \\ 0 & a^2_{n2} & a^2_{n3} & \dots & a^2_{nn} & F^n \end{bmatrix} \quad (72)$$

where

$$\begin{aligned} a^2_{32} &= a'_3 a'_{32} - a'_3 (a'_{11})^{-1} a'_{12} \\ a^2_{33} &= a'_3 a'_{33} - a'_3 (a'_{11})^{-1} a'_{13} \\ &\vdots &&\vdots \\ a^2_{3n} &= a'_3 a'_{3n} - a'_3 (a'_{11})^{-1} a'_{1n} \end{aligned} \quad (73)$$

This procedure is continued until the matrix assumes the form

$$\begin{bmatrix} 1 & (a'_{11})^{-1}a'_{12} & (a'_{11})^{-1}a'_{13} & \dots & (a'_{11})^{-1}a'_{1n} & (a'_{11})^{-1}F' \\ 0 & a^2_{22} & a^2_{23} & \dots & a^2_{2n} & F^2 - a'_2(a'_{11})^{-1}F' \\ 0 & a^2_{32} & a^2_{33} & \dots & a^2_{3n} & F^3 - a'_3(a'_{11})^{-1}F' \\ 0 & \vdots & \vdots & \ddots & \vdots & \vdots \\ 0 & \vdots & \vdots & \vdots & \vdots & \vdots \\ 0 & a^2_{n2} & a^2_{n3} & \dots & a^2_{nn} & F^n - a'_n(a'_{11})^{-1}F' \end{bmatrix} \quad (74)$$

A single formula for the coefficients  $b_{ij}$  is recognized to be

$$a^2_{ij} = a'_{ij} - a'_{ii} (a'_{11})^{-1} a'_{ij} \quad \begin{matrix} i = 2, 3, \dots, n \\ j = 2, 3, \dots, n \end{matrix} \quad (75)$$

In addition, let

$$(a'_{11})^{-1} a'_{12} = C_{12}$$

$$(a'_{11})^{-1} a'_{13} = C_{13}$$

and in general,

$$(a'_{11})^{-1} a'_{1j} = c_{1j} \quad j = 2, 3, \dots, n \quad (76)$$

Further, let

$$F' = f'$$

and

$$(a'_{11})^{-1} F' = (a'_{11})^{-1} f' = d_1 \quad (77)$$

Substituting Equations (76) and (77) into Equations (74) we have

$$\begin{bmatrix} 1 & c_{12} & c_{13} & \dots & c_{1n} & d_1 \\ 0 & a_{22}^2 & a_{23}^2 & \dots & a_{2n}^2 & F^2 - a'_{21}d_1 \\ 0 & a_{32}^2 & a_{33}^2 & \dots & a_{3n}^2 & F^3 - a'_{31}d_1 \\ 0 & \vdots & \vdots & \ddots & \vdots & \vdots \\ 0 & \vdots & \vdots & \ddots & \vdots & \vdots \\ 0 & a_{n2}^2 & a_{n3}^2 & \dots & a_{nn}^2 & F^n - a'_{n1}d_1 \end{bmatrix} \quad (78)$$

Now the elements of the second row are pre-multiplied by  $a_{22}^2$ . One then has

$$\begin{bmatrix} 1 & c_{12} & c_{13} & \dots & c_{1n} & d_1 \\ 0 & 1 & (a_{22}^2)^{-1} a_{23}^2 & \dots & (a_{22}^2)^{-1} a_{2n}^2 & (a_{22}^2)^{-1} f^2 \\ 0 & a_{32}^2 & a_{33}^2 & \dots & a_{3n}^2 & F^3 - a'_{31}d_1 \\ 0 & \vdots & \vdots & \ddots & \vdots & \vdots \\ 0 & a_{n2}^2 & a_{n3}^2 & \dots & a_{nn}^2 & F^n - a'_{n1}d_1 \end{bmatrix} \quad (79)$$

where the following substitution was made:

$$f^2 = F^2 - a'_{21}d_1 \quad (80)$$

The portion of this matrix exclusive of the first row and column is now dealt with in a manner which is identical with that just described for the transformation of

the matrix (69) into (78). In the first step the  $a_{32}^2$  pre-multiplied elements of the second row are subtracted from the corresponding ones of the third row.

Next, the  $a_{42}^2$  pre-multiplied elements of the second row are subtracted from the corresponding elements of the fourth row, and so on. This set of operations finally yields the matrix in the form

$$\left[ \begin{array}{cccc|c} 1 & C_{12} & C_{13} & \dots & C_{1n} & d_1 \\ 0 & 1 & (a_{22}^2)^{-1}a_{23}^2 & \dots & (a_{22}^2)^{-1}a_{2n}^2 & (a_{22}^2)^{-1}f^2 \\ 0 & 0 & a_{33}^3 & \dots & a_{3n}^3 & F^3 - a_{31}^1 d_1 - a_{32}^2 (a_{22}^2)^{-1} f^2 \\ \vdots & \vdots & \vdots & \ddots & \vdots & \vdots \\ 0 & 0 & a_{i3}^3 & \dots & a_{in}^3 & F^i - a_{i1}^1 d_1 - a_{i2}^2 (a_{22}^2)^{-1} f^2 \\ 0 & 0 & a_{n3}^3 & \dots & a_{nn}^3 & F^n - a_{n1}^1 d_1 - a_{n2}^2 (a_{22}^2)^{-1} f^2 \end{array} \right] \quad (81)$$

in which the elements  $a_{ij}^3$  are given by the formula

$$a_{ij}^3 = a_{ij}^2 - a_{i2}^2 (a_{22}^2)^{-1} a_{2j}^2 \quad i = 3, 4, \dots, n \quad j = 3, 4, \dots, n \quad (82)$$

The following substitutions which are similar to Equations (76) and (77) are made into Equation (81).

Let

$$C_{2j} = (a_{22}^2)^{-1} a_{2j}^2 \quad j = 3, 4, \dots, n$$

and

$$d_2 = (a_{22}^2)^{-1} f^2 \quad (83)$$

Then, Equation (81) takes the form

$$\left[ \begin{array}{cccc|c} 1 & C_{12} & C_{13} & \dots & C_{1n} & d_1 \\ 0 & 1 & C_{23} & \dots & C_{2n} & d_2 \\ 0 & 0 & a_{33}^3 & \dots & a_{3n}^3 & F^3 - a_{31}^1 d_1 - a_{32}^2 d_2 \\ \vdots & \vdots & \vdots & \ddots & \vdots & \vdots \\ 0 & 0 & a_{i3}^3 & \dots & a_{in}^3 & F^i - a_{i1}^1 d_1 - a_{i2}^2 d_2 \\ 0 & 0 & a_{n3}^3 & \dots & a_{nn}^3 & F^n - a_{n1}^1 d_1 - a_{n2}^2 d_2 \end{array} \right] \quad (84)$$

The portion of this matrix involving the coefficients  $a_{ij}^3$  is now treated as described for the original matrix (68) and as repeated in the manipulation of that portion of the matrix (78) involving the elements  $a_{ij}^2$ . The resulting matrix then assumes the form

$$\begin{bmatrix} 1 & C_{12} & C_{13} & \dots & C_{1n} & d_1 \\ 0 & 1 & C_{23} & \dots & C_{2n} & d_2 \\ 0 & 0 & 1 & C_{34} & \dots & C_{3n} & d_3 \\ \vdots & \vdots & \vdots & C_{44} & \dots & C_{4n} & F^4 - \alpha_{41}^1 d_1 - \alpha_{42}^2 d_2 - \alpha_{43}^3 d_3 \\ \vdots & \vdots & \vdots & C_{i4} & \dots & C_{in} & F^i - \alpha_{i1}^1 d_1 - \alpha_{i2}^2 d_2 - \alpha_{i3}^3 d_3 \\ 0 & 0 & 0 & C_{n4} & \dots & C_{nn} & F^n - \alpha_{n1}^1 d_1 - \alpha_{n2}^2 d_2 - \alpha_{n3}^3 d_3 \end{bmatrix} \quad (85)$$

where the substitutions

$$\begin{aligned} C_{3j} &= (\alpha_{33}^3)^{-1} \alpha_{3j}^3 \quad j = 4, 5, \dots, n \\ f^3 &= F^3 - \alpha_{31}^1 d_1 - \alpha_{32}^2 d_2 \\ d^3 &= (\alpha_{33}^3)^{-1} f^3 \\ \alpha_{ij}^4 &= \alpha_{ij}^3 - \alpha_{i3}^3 (\alpha_{33}^3)^{-1} \alpha_{3j}^3 \quad i = 4, 5, \dots, n \\ &\quad j = 4, 5, \dots, n \end{aligned} \tag{86}$$

have been made. The continuation of this process is obvious. For the case where  $s$  operations have been performed, where  $s < n$ , we have the following form of the augmented matrix:

$$\begin{array}{ccccccccc}
 1 & C_{12} & C_{13} & \cdots & \cdots & C_{ij} & \cdots & C_{in} & d_1 \\
 0 & 1 & C_{23} & \cdots & \cdots & C_{2j} & \cdots & C_{2n} & d_2 \\
 0 & 0 & 1 & C_{34} & \cdots & C_{3j} & \cdots & C_{3n} & d_3 \\
 0 & 0 & 0 & 1 & C_{45} & \cdots & C_{4j} & \cdots & C_{4n} & d_4 \\
 0 & 0 & 0 & 0 & \ddots & \ddots & \ddots & \ddots & \ddots \\
 \vdots & \vdots \\
 0 & 0 & 0 & 0 & 1 & C_{sj} & \cdots & C_{sn} & d_s \\
 0 & 0 & 0 & 0 & 0 & \overset{(s+1)}{C_{(s+1)1}} & \cdots & \overset{(s+1)}{C_{(s+1,n}}} & F^{s+1} - a_{(s+1),1}^2 d_1 - a_{(s+1),2}^2 d_2 - \cdots - a_{(s+1,s}^2 d_s \\
 \vdots & \vdots \\
 0 & 0 & 0 & 0 & 0 & \overset{(s+1)}{a_{n,1}} & \cdots & \overset{(s+1)}{a_{n,n}} & F^n - a_{n,1}^2 d_1 - a_{n,2}^2 d_2 - \cdots - a_{n,s}^2 d_s
 \end{array} \tag{87}$$

and after  $n$  operations we have

$$\left[ \begin{array}{cccc|c} 1 & C_{12} & C_{13} & C_{14} & \dots & C_{1n} & d_1 \\ 0 & 1 & C_{23} & C_{24} & \dots & C_{2n} & d_2 \\ 0 & 0 & 1 & C_{34} & \dots & C_{3n} & d_3 \\ 0 & 0 & 0 & 1 & \dots & C_{4n} & d_4 \\ \vdots & \vdots & \vdots & \vdots & \ddots & \vdots & \vdots \\ 0 & 0 & 0 & 0 & \dots & C_{n-1n} & d_{n-1} \\ 0 & 0 & 0 & 0 & 0 & 1 & d_n \end{array} \right] \quad (88)$$

The solution to the equivalent equations having this augmented matrix (88) are easily found. They are given by

$$D_n = d_n$$

$$D_{n-1} = d_{n-1} - C_{n-1, n} D_n$$

$$D_{n-2} = d_{n-2} - C_{n-2, n-1} D_{n-1} - C_{n-2, n} D_n$$

and in general

$$D_i = d_i - \sum_{j=i+1}^n C_{ij} D_j \quad i=1, 2, \dots, n \quad (89)$$

Consider the last column in the augmented matrices (68), (74), (81), (85), (87), and (88).

The computational procedure has the following order:

Let  $f' = F'$  where  $F'$  is given

then,

$$d_1 = (a_{11}')^{-1} f'$$

$$f^2 = F^2 - a_{11}' d_1$$

$$d_2 = (a_{22}')^{-1} f^2$$

$$f^3 = F^3 - (a_{21}') d_1 - (a_{32}') d_2$$

$$d_3 = (a_{33}')^{-1} f^3$$

and in general,

$$f^i = F^i - \sum_{s=1}^{i-1} (\alpha_{is}^s) ds \quad (90)$$

and

$$d^i = (\alpha_{ii}^i)^{-1} f^i$$

therefore, to obtain a solution, the little f's and little d's are computed, in turn, with the appropriate coefficients and then, after setting little  $d_n$  equal to  $D_n$ , the remaining unknowns are obtained by Equation (89). The computation of the little d's and little f's is called the forward solution and the computation of the  $D_i$ 's,  $i = n-1, n-2, \dots, 1$  is called the backwards solution.

Associated with the forward solution are two arrays of coefficients which correspond to the calculation of the little f's and little d's. These are,

$$\begin{bmatrix} 0 & 0 & 0 & \cdots & 0 \\ \alpha_{11}^1 & 0 & 0 & \cdots & 0 \\ \alpha_{21}^1 & \alpha_{22}^2 & 0 & \cdots & 0 \\ \alpha_{31}^1 & \alpha_{32}^2 & \alpha_{33}^3 & \cdots & \vdots \\ \vdots & \vdots & \vdots & \ddots & \vdots \\ \alpha_{n1}^1 & \alpha_{n2}^2 & \alpha_{n3}^3 & \cdots & d_{n,(n-1)}^{n-1} 0 \end{bmatrix} \quad (91)$$

and

$$\begin{bmatrix} (\alpha_{11}^1)^{-1} 0 & & & & 0 \\ 0 & (\alpha_{22}^2)^{-1} & & & 0 \\ & & (\alpha_{33}^3)^{-1} & & \vdots \\ & & & \ddots & \vdots \\ & & & & (\alpha_{nn}^n)^{-1} \end{bmatrix} \quad (92)$$

where (91) are the coefficients that are used in computing the little f's and are defined by

$$\alpha_{ij}^v = \alpha_{ij}' - \sum_{s=1}^{j-1} \alpha_{is}^s (\alpha_{ss}^s)^{-1} \alpha_{sj}^s \quad (93)$$

and (92) are the coefficients used in determining the little d's as defined by Equation (90). Similarly, associated with the backward solution there is an array of coefficients given by

$$\begin{bmatrix} 0 & C_{12} & C_{13} & \dots & C_{1n} \\ 0 & 0 & C_{23} & \dots & C_{2n} \\ \vdots & & \vdots & \ddots & C_{3n} \\ \vdots & & \vdots & \ddots & \vdots \\ \vdots & & \vdots & \ddots & \vdots \\ \vdots & & \vdots & \ddots & C_{(n-1),n} \\ 0 & 0 & 0 & 0 & \dots & 0 \end{bmatrix} \quad (94)$$

where

$$C_{ij} = (\alpha_{ii}^i)^{-1} \alpha_{ij}^i \quad (95)$$

and the  $D_i$ 's are computed using Equation (89).

In order to systematize the computational procedure it is expedient to form the following "auxiliary matrix."

$$\begin{bmatrix} (\alpha_{11}^1)^{-1} & C_{12} & C_{13} & \dots & C_{1n} \\ \alpha_{21}^1 & (\alpha_{22}^2)^{-1} & C_{23} & \dots & C_{2n} \\ \alpha_{31}^1 & \alpha_{32}^2 & (\alpha_{33}^3)^{-1} & \dots & C_{3n} \\ \vdots & \alpha_{42}^2 & \alpha_{43}^3 & \dots & C_{4n} \\ \vdots & & \vdots & \ddots & \vdots \\ \vdots & & \vdots & \ddots & C_{(n-1),n} \\ \alpha_{n1}^1 & \alpha_{n2}^2 & \alpha_{n3}^3 & \dots & \alpha_{n(n-1)}^{(n-1)} (\alpha_{nn}^n)^{-1} \end{bmatrix} \quad (96)$$

It can readily be seen by inspection that (96) is formed by merging the coefficients of (91), (92) and (94). This is not a matrix. It is only three arrays of coefficients which have been merged into one table to systematize the computational procedure and it is called the "Factorized Inverse Table."

The advantages to this method of finding the solution are numerous and the most important ones are listed below:

1. At most, the largest matrix that must be inverted is a six by six.
2. Given a full  $n \times n$  matrix  $\mathbf{Y}^{II}$ , that is, a matrix whose elements are all non-zero, it requires  $n^3$  arithmetic operations to obtain its inverse; whereas, the "factorized inverse" process requires only  $n^2$  arithmetic operations.
3. The structural stiffness matrix  $\mathbf{Y}^{II}$ , in general, tends to be strongly diagonal, therefore many of the  $a_{ij}^j$  matrices are empty. This further reduces the number of arithmetic operations and, as a consequence, it also reduces computer rounding errors. Further, the true inverse of such a structural stiffness matrix is nearly full, whereas, the factorized inverse table is again strongly diagonal.
4. Physical meaning is associated with the little d's and little f's. These are the internal strains and internal forces, respectively. Therefore, in addition to a deflection analysis, this method of solution can be used for a stress analysis for both, static and dynamic loading conditions.

To further describe this method of solution, the factorized inverse table for the example problem given in Figure 7 will be obtained.

Consider the stiffness matrix given by (66) and which is reproduced below where, for convenience, the superscripts have been dropped and the indicated matrix additions performed.

$$\begin{bmatrix} Y_{11} & Y_{12} & 0 & 0 & 0 \\ Y_{21} & Y_{22} & Y_{23} & Y_{24} & Y_{25} \\ 0 & Y_{32} & Y_{33} & Y_{34} & 0 \\ 0 & Y_{42} & Y_{43} & Y_{44} & Y_{45} \\ 0 & Y_{52} & 0 & Y_{54} & Y_{55} \end{bmatrix} \quad (97)$$

The factorized inverse table is formed by first inverting the  $Y_{11}$  element, multiplying the first row by this inverse and then subtracting the  $Y_i$ ,  $i = 2, 3, 4, 5$  pre-multiplied first row from the second row. The result of these operations is:

$$\begin{bmatrix} Z_{11} & C_{12} & 0 & 0 & 0 \\ Y_{21} (Y_{22} - Y_{21} C_{12}) & Y_{23} & Y_{24} & Y_{25} \\ 0 & Y_{32} & Y_{33} & Y_{34} & 0 \\ 0 & Y_{42} & Y_{43} & Y_{44} & Y_{45} \\ 0 & Y_{52} & 0 & Y_{54} & Y_{55} \end{bmatrix} \quad (98)$$

$$\text{where } C_{12} = Z_{11} Y_{12}$$

The inverse  $Z_{22} = [Y_{22} - Y_{21} C_{12}]^{-1}$  is formed and the procedure is repeated until finally, the complete factorized inverse table is formed.

$$\begin{bmatrix} Z_{11} & C_{12} & 0 & 0 & 0 \\ Y_{21} & Z_{22} & C_{23} & C_{24} & C_{25} \\ 0 & Y_{32} & Z_{33} & C_{34} & C_{35} \\ 0 & Y_{42} & Y_{43} & Z_{44} & C_{45} \\ 0 & Y_{52} & Y_{53} & Y_{54} & Z_{55} \end{bmatrix} \quad (99)$$

$$\text{where}$$

$$z_{11} = [y_{11}]^{-1}$$

$$c_{12} = z_{11} y_{12}$$

$$y_{21} = y_{21}$$

$$z_{22} = [y_{22} - y_{21} c_{12}]^{-1}$$

$$c_{23} = z_{22} y_{23}$$

$$c_{24} = z_{22} y_{24}$$

$$c_{25} = z_{22} y_{25}$$

$$y_{32} = y_{32}$$

$$y_{42} = y_{42}$$

$$y_{52} = y_{52}$$

$$z_{33} = [y_{33} - y_{32} c_{23}]^{-1}$$

$$c_{34} = z_{33} [y_{34} - y_{32} c_{24}]$$

$$c_{35} = z_{33} [-y_{32} c_{25}]$$

$$\overset{2}{y}_{43} = [y_{43} - y_{42} c_{23}]$$

$$\overset{2}{y}_{53} = [-y_{52} c_{23}]$$

$$z_{44} = [y_{44} - y_{42} c_{24} - \overset{2}{y}_{43} c_{34}]^{-1}$$

$$c_{45} = z_{44} [y_{45} - y_{42} c_{25} - \overset{2}{y}_{43} c_{35}]$$

$$\overset{3}{y}_{54} = [y_{54} - y_{52} c_{24} - \overset{2}{y}_{53} c_{34}]$$

$$z_{55} = [y_{55} - y_{52} c_{25} - \overset{2}{y}_{53} c_{35} - \overset{3}{y}_{51} c_{45}]^{-1}$$

The expressions for the general element in the factorized inverse table are given by the following recursion formulæ:

$$\begin{aligned} A_{ij} &= Y_{ij} - \sum_{k=1}^{j-1} A_{ik} A_{kj} \quad i > j \\ A_{ii} &= \left[ Y_{ii} - \sum_{k=1}^{i-1} A_{ik} A_{ki} \right]^{-1} \quad i = j \\ A_{ij} &= A_{ii} \left[ Y_{ij} - \sum_{k=1}^{i-1} A_{ik} A_{kj} \right] \quad i < j \end{aligned} \quad (100)$$

The continuation of the computation procedure is as previously stated in Equations (90) and (89) where Equations (90) are called the forward solution and Equations (89) the backward solution. Rewriting these equations in the notation of the example problem, we have, for the forward solutions,

$$\begin{aligned} f' &= F' \\ d' &= Z_{ii} f' \end{aligned}$$

and in general

$$f^i = F^i - \sum_{j=1}^{i-1} Y_{ij} d_j'$$

$$d_i = Z_{ii} f^i$$

and, finally, the backwards solution

$$D_n = d_n$$

and in general

$$D_i = d_i - \sum_{j=i+1}^n C_{ij} D_j$$

This method of analysis adapts itself very strongly to computer techniques. The present program proceeds to calculate the elements of the factorized inverse table eliminating one row and corresponding column at a time. A general description of the program is included in Appendix B. In addition, the above discussed example problem has been analyzed by this program and the complete

definition of the problem including a complete print-out of the results is included in Appendix C.

#### Mathematical Model

To perform an analysis of a complicated highly redundant structure, such as the Saturn SA-D1, the analyst must establish a mathematical model which will accurately represent the actual structure. The mathematical model utilized in Kron's analysis is composed of elements which have constant mass and section properties and whose deflections may be described by elementary beam theory. The variable properties of a typical structure are approximated in the mathematical model by linking several beams of constant property. This provides a step function approximation which can be made as accurately as desired by increasing the number of beams. The properties of the beams are input into the program in the following parameters: Young's Modulus (E), the shear modulus (G), the density ( $\mu$ ), the cross-sectional area (A), the torsional rigidity (K), and the maximum and minimum moments of inertia. The location of the end points of the beams are input as x, y and z coordinates. A summary of the input for the mathematical model of the Saturn SA-D1 is given in the Appendix B.

Since the objective of this analysis is to determine the natural vibration frequencies and mode shapes of the Saturn SA-D1, the mathematical model will not attempt to provide elaborate detail in areas which will not contribute to the overall response of the vehicle. That is, areas which do not have a large mass and are relatively unimportant in response characteristics will be described by a minimum of beams, while areas which play a predominant role in the response will contain a large number of beams. The reduction of the total number of beams used in the analysis is desirable because the computation time in the digital computer will be reduced and roundoff error minimized. However, the reduction

of beams may be done only after a careful analysis of the structure involved and is often accomplished by using an equivalent beam in the model. This technique is used in preparing the mathematical model of the Saturn SA-D1 and is discussed in detail below.

The Saturn SA-D1 is divided into the upper stages consisting of the payload, dummy S-V and dummy S-IV, and the booster or S-I stage as shown in Figure 8. The upper stages are single tank structures of semimonocoque construction, while the S-I stage consists of nine tanks of semimonocoque construction coupled together by a system of beams at the top and bottom. The interconnection of the S-I stage and the upper stages is accomplished by a system of beams identified as the transition section. The mathematical model of the upper stages and tank structures of the lower stages are represented by simple beams. The computed properties and mathematical model of these sections are shown in Figures 9, 10, 11, 12, and 13. The use of a simple beam to represent a tank structure is consistent with most available analysis techniques and provides good overall response characteristics for large length to diameter tank ratios such as exist on the Saturn. The remainder of the Saturn SA-D1 is constructed primarily of beams and therefore may be represented in a straightforward manner.

The transition section of the Saturn consists of eight outer tension and compression members which connect the S-IV base to the S-I spider and sixteen inner members which transfer the load from the S-IV to the S-I through an intermediate shell. In order to accurately represent this section, an analysis was conducted which determined the design concept and established an equivalent beam structure. The actual structure and mathematical model are shown in Figure 14. The design concept of the transition section is to carry the bulk of the bending loads (about two-thirds) through the eight outer tension compression members, while the shear loads are transferred to the center shell by the sixteen inner

tension compression members as a torsion load. The points of attachment of the outer beams and the shell are so designed that the 105" diameter center tank receives about 70% of the load and the remainder is transferred to the four outer 70" diameter LOX tanks. The 70" diameter fuel tanks have a slip joint at the upper attachment point to the spider to allow for contraction of the LOX tanks and will not take an axial load from the upper stages. The mathematical model was prepared in such a manner that the design concept was preserved although a fewer number of beams were used. This was accomplished by fixing the beams so they could take a bending load as well as a tension compression loading. The transition from a single beam representation to a multiple beam representation at the S-IV base was accomplished by the use of stiff beams from the center to the eight outer points, point 13 to 14 through 21, to provide the illusion of depth in the y - z plane, i.e., a disk about point 13.

The multiple beam structure or spider which links the eight outer 70" diameter tanks is represented in the model by 32 beams as shown in Figure 15. The LOX tanks are attached to the spider by means of ball joints, while the fuel tanks are attached by slip joints as shown in Figure 16a. Since the tanks are attached at two points the LOX tank will have a large bending stiffness along one axis and very little along an axis perpendicular to this. This is accounted for in the mathematical model by orienting the maximum and minimum moment of inertia axes of the beam in such a manner that the properties of the attachment are duplicated. The slip joints of the fuel tank are represented as beams having a very small cross-sectional area thus being incapable of transferring an axial load. The attachment points at the lower ends of the tanks consist of ball joints (see Figure 16b) for both type tanks and these are represented in the mathematical model in a manner similar to the upper LOX tank attachment.

The outriggers serve to link the eight outer tanks to the center tank, provide support for the outer tanks, and to support the entire vehicle prior to launch. The outriggers are divided into two categories, the support outrigger and the thrust outrigger. The four thrust outriggers provide the added duty of supporting the four outer rocket engines and transferring the rockets thrust to the vehicle. If the outriggers were represented by a beam structure as it is actually constructed, a large number of beams would be required. Since this area will not contribute much to the overall dynamic response of the vehicle due to its low mass it is desirable to utilize a simplified representation in the mathematical model. This was accomplished by conducting a deflection analysis of the outriggers and replacing them by an equivalent cantilever beam. The deflection analysis was conducted using Kron's method. The model of the outriggers used is shown in Figure 17 along with a table of the physical properties. Loads were applied in the six degrees of freedom at the attachment points of the tanks. A summary of the deflections obtained is shown in Tables I and II.

During the test program, the Saturn SA-D1 was suspended in launch position by eight cables. Reference 5 provides the vertical and horizontal spring constants of this suspension system. The mathematical model of the Saturn SA-D1 used four beams of suitable cross-sectional areas and inertias to duplicate the spring constants of the cable suspension system. These were attached at the support outriggers at one end and fixed in space at the other end. The direction of the exciting force used during the test was used in the excitation of the mathematical model.

The density of the beams were prepared from References 6, 7, and 8. The total weight of the mathematical model was within 1% of the total vehicle weight as provided in Reference 5 and within .15% of the weight given in Reference 7, which was used in the preparation of the model.

## RESULTS

The discussion of the results of this analysis will be all inclusive, that is, a brief discussion of the problems encountered during the analysis will be included along with a summary of the final results and a comparison with the SA-D1 test results. Although the discussion of the problems encountered does not aid in the evaluation of the accuracy of Kron's Method, it will contribute to the overall purpose of this analysis by providing an insight into the problems that may occur and the techniques used to eliminate these problems.

The first computer run conducted on any large complex problem is the static case. This is a special case (0 frequency) of the dynamic response and through proper specification of the boundary conditions, it may be easily checked by the use of a desk calculator. This enables the analyst to determine if: (1) the mathematical model of the problem has been correctly input to the computer, and (2) if the mathematical model is a reasonable facsimile of the actual structure. The importance of this procedure cannot be over emphasized since the program is such that the computer operations are identical for the static and dynamic case and, if the static case provides correct results, correct dynamic results will follow.

The preliminary computer runs on the mathematical model of the Saturn SA-D1 included the static loading case and the results could not be correlated with a hand computation. The error was characterized by a buildup in the magnitude of the "x" deflections from the tip to the base until they were of the same order of magnitude as the "y" and "z" deflections. This is not possible for the points lying along the "x" axis since the load is applied in a "y-z" plane. The appearance is similar to that of round-off error, but this was known to be impossible since test problems of as many as 220 points have been

successfully run with four digit accuracy. In order to determine the source of the error in a systematic manner, the mathematical model was divided at the spider and two models formed. Computer runs of models were then conducted for cantilevered boundary conditions. The results were then compared to their respective hand computations to isolate the error. The error was located in the upper stage model, where the error was traced to several beams emanating radially from a single point at the junction of the S-IV stage and the S-I transition section (point 13). A critical look at the input data in this area revealed that the beams (13 to 14-21) were several orders of magnitude stiffer than the beams to which they were connected. The philosophy behind the use of such stiff members was to provide the illusion of a common point, i.e., an "infinitely" stiff disc, which would transfer the loading of the upper stages to the outer members by rotation and translation of the center point with no relative deflection between the center point and the eight outer points. Since it was previously thought that an "infinitely" stiff beam could be utilized in Kron's Method, a test problem was formulated and a complete printout obtained. The error was located in the factorized inverse portion of the program, where the accuracy was lost in the subtraction of very large terms. Corrections were made in the program by reducing the stiffness to a reasonable level although a large stiffness ratio to the connecting members was maintained. The above approach accomplished the desired goal, but is considered only as a quick fix and provision for transfer from one point to another without deflection must be made. Computer runs were correct and the corrected model was used in the final analysis.

The computer program for Kron's Method contains a very elaborate system of checks to detect errors if they should occur and will immediately dump the problem if a check is not completed properly. This system of checks, combined

with the requirements of long time durations and a large number of computer operations, sometimes triggers a computer malfunction. This occurred on the SA-D1 problem and caused approximately a two week delay during the analysis. The malfunction that occurred was the dropping of a "bit" in the ninth chain, which was diagnosed as a machine error, i.e., electrical circuit error. These problems were corrected by using new system tapes on Kron's program and correcting the machine circuit.

Since the purpose of this analysis is to duplicate the results of the SA-D1 test program, all of the test conditions which could influence the response were duplicated. For instance, the external excitation force was applied in the same manner, directed radially inward through the location of F-3, in order to more closely duplicate the test results. Theoretically, the exciting force location would not be important on a symmetrical vehicle such as the SA-D1 at a resonant condition, but the comparison of results between the two analyses would become more difficult. The particular choice of force direction in the test program required the external force to be input in two components along the "y" and "z" axes, since the coordinate system did not coincide with the force. This tends to complicate the results of the analytical study since two responses, "y" and "z", will be of the same order of magnitude and must be shown in the final plots. Had this analyst been more farsighted the axes could have been rotated to coincide with the external force and simplified the results.

Contractual obligations call for the identification of six frequencies and their mode shapes and this report will follow these guidelines. That is, although additional frequencies are recognized to exist, only the required six frequencies will be sought since the underlying purpose of this investigation will have been fulfilled. To add completeness to this discussion a few of

the more obvious comparisons between the test results and analysis results will be made. To aid in this comparison the identification system for the outer tanks was made identical to that used in the test program.

The frequency range investigated was 1.9 cps to 8.0 cps as suggested by Reference 5. The runs conducted in this area established seven significant frequencies of which five can be compared to the test results. The seven significant frequencies are identified as follows:

- |                                 |             |
|---------------------------------|-------------|
| (1) Fuel Tank No. 1 Mode        | - 1.936 cps |
| (2) First Cluster Mode          | - 2.325 cps |
| (3) First Bending Mode          | - 2.512 cps |
| (4) Fuel Tanks No. 2 and 4 Mode | - 3.285 cps |
| (5) Second Cluster Mode         | - 4.40 cps  |
| (6) Lox Tank Mode               | - 4.60 cps  |
| (7) Second Bending Mode         | - 6.711 cps |

The terminology used in identifying the various modes will be based on both the relative magnitude of the response and the phase relationships. The modes are defined as follows: (1) the first and second bending modes will identify the frequency where the main tank and outer tanks are in phase, (2) the cluster modes will describe the frequency where the main tank and outer tanks are out of phase, (3) fuel or lox tank mode will describe the motion of a particularly active tank or tanks. The above definitions are considered all inclusive, but a detailed description as well as figures provided for each mode. The analysis results are presented in displacement versus length plots shown in Figures 19 through 207, and frequency response curves are shown in Figures 208 through 217. The displacement versus length results are summarized in Table III and qualitative vector plots of several modes are provided (Figures 218-220) to aid in evaluating the results.

The criteria used for determining a resonance condition is the 180 degree phase shift of the response curve. This is merely an extention of the phenomena occurring in simple systems which may be found in any elementary vibration textbook. The existence of this phase shift is very evident in the results summarized in Table III and will be pointed out in the discussion of each frequency.

The first frequency identified is the F-1 (Fuel Tank Number 1) bending mode at 1.936 cps. The existence of this mode is clearly shown in Figure 210 and is also indicated by the phase shift in Table III. The response of the vehicle at this frequency is completely dominated by the response of the F-1 tank. The remaining outer tanks show an increase in response at this frequency, but do not participate in the resonance condition. This particular frequency was not indicated in the test results but may have been considered unimportant due to the magnitude of the response on the overall vehicle.

The second frequency identified is designated as a cluster mode in keeping with the above definition. This mode is characterized by a large response of the outer tanks, which causes the phase shift in the main tank between 2.30 cps and 2.34 cps as indicated in Table III. This conclusion is evident since the main tank mode shape returns to its previous form after the outer tank resonance point is passed. The motion of the outer tanks F-2 and F-4 is tangential and in phase with the main tank, while the remaining outer tanks have a radial motion out of phase with the main tank. The motion is best described in the qualitative vector plot of Figure 218a. The nodal points of the main tank occur at 670 inches and 1445 inches from the tip. The motion of the outer tanks at this frequency concur with those indicated in the test results for the first bending mode at 2.20 cps (Figure 16 of

Reference 5). A comparison of these results will show the analysis frequency high by 5.69 percent and the nodal points having a maximum deviation of 8.93 percent.

The third frequency identified is the vehicle first bending mode at 2.512 cps. This mode again shows the 180 degree phase shift of the main tank, but subsequent runs show that the mode shape does not return to its original shape as before. Fuel tanks F-2 and F-4 have a tangential motion opposing the main tank motion while the remaining tanks have a radial motion in phase with the main tank as shown in Figure 218b. The outer tank individual response is much less than the main tank response substantiating the identification of this mode as the first bending mode. The tank motions concur with those indicated by the test results of Fuel Tank No. 1 Mode at 2.31 cps (Figure 17 of Reference 5), although the phase relationships differ. In comparing these frequencies the analysis frequency is high by 8.71 percent, while the nodal points of 670 inches and 1450 inches from the tip differ by a maximum of 8.21 percent.

The fourth frequency identified is the Fuel Tanks No. 2 and 4 Mode. This nomenclature does not completely describe the mode, but serves to indicate that the response of the F-2 and F-4 tanks is greater than the other tanks. Table III shows that there are actually two resonant points in this area, one occurring between 3.25 cps and 3.35 cps and the other between 3.35 cps and 3.40 cps. Only the first one is positively identified on the frequency curves and is the only one discussed here. A qualitative indication of the tank responses is shown in Figure 219a. The motion of all of the outer tanks is tangential with the tanks opposing each other in such a manner that the overall vehicle response is not large. In referring to Figure 219a this out of phase force component is seen to be provided primarily by fuel tanks F-2 and

F-4. It appears reasonable to compare this mode to the test results of Fuel Tank No. 4 mode at 2.915 cps (Figure 18 of Reference 5). If this is done the analysis frequency is high by 12.7 percent and the maximum nodal point deviation is 9.28 percent. In passing it may be noted, particularly in Figure 104, that the main tank response implies the existence of an outer tank resonance at this frequency. That is, for the unrestrained case the summation of forces and moments in the referenced coordinate system must equate to zero and to reach this condition the outer tanks must be out of phase with the main tank.

The fifth mode identified is the Second Cluster Mode at 4.40 cps. The motion of the outer tanks is approximately along the line of the forcing function and 180 degrees out of phase with the main tank. This is shown qualitatively in the vector response plot of Figure 219b. This mode may be compared favorably with the first cluster mode of the test results at 4.02 cps (Figure 19 of Reference 5). The correlation of the single nodal point location on the main tank is quite close, with both results indicating the nodal point location at about 425 inches from the tip. The frequency of the analysis result is high by 9.52 percent.

The sixth frequency identified is at 4.60 cps. The existence of this mode is indicated by comparing the main tank mode shape for frequencies 4.60 and 4.70 (see Table III). The main tank returned to its previous shape after the tank resonance at 4.40 cps and again indicated the characteristic phase shift between 4.60 cps and 4.70 cps. This is very similar to the first cluster mode and first bending mode discussed previously. It is also noted that the resonant points appear to occur in pairs as shown in the frequency response curves, Figures 208 through 217. A qualitative vector plot of the vehicle response is shown in Figure 220a. The response is predominately in line with the forcing function which gives L-2, L-4, F-2 and F-4 a tangential

motion and F-1, F-3, L-1 and L-3 a radial motion. The outer tanks are out of phase with the main tank.

The last frequency identified in this analysis is the second bending mode. The outer tanks are in phase with the main tank and their mode shape is seen to be greatly influenced by the main tank mode shape. The main tank mode shape has nodal points at 420, 1200, and 1725 inches from the tip. This mode compares very favorably with the second bending mode of the test results (Figure 21 of Reference 5). The mode shape of the main tank is very similar with both results exhibiting the unusual flattening of the response of the S-IV section. The nodal points show a maximum deviation of 8 percent while the frequency is low by only 0.43 percent.

Since the above discussion has drawn some comparisons between the analytical results and the test results of the SA-D1 vibration study, a brief discussion of the various sources of inaccuracies is felt to be in order. The sources of inaccuracies may be divided into two categories: (1) restrictions of the analytical technique, and (2) deviations of the mathematical model from the actual vehicle.

The primary restriction in the analytical technique that would affect the accuracy is the lack of damping. This causes the frequencies to be very narrow in band width and would tend to predict a higher frequency than the test program. Damping would also have a significant effect on the mode shapes at resonance.

The deviations of the mathematical model from the actual vehicle may be caused by inherent inaccuracies due to beam representation and discrepancies in the representation of the structural properties. One major contribution to this area is the sloshing mass of the fluids. This represents a considerable

amount of weight and was not considered in this analysis. This could be considered if the sloshing mass and frequency of each tank were known, by adding a simple spring mass system at the proper point in each tank.

## REFERENCES

1. Kron, G.: Diakoptics. (A series of 20 articles appearing in the Electrical Journal, 5 July 1957 through 13 February 1959.)
2. Southwell, R.V.: Relaxation Methods in Engineering. Oxford University Press, 1940.
3. Kron, G.: Tensor Analysis of Networks. John Wiley and Sons, New York, 1939.
4. Scanlan, R.H. and Rosenbaum, R.: Introduction to the Study of Aircraft Vibration and Flutter. The MacMillan Company, 1951, pp. 30-31.
5. Appendix B, Saturn Quarterly Progress Report. Experimental Vibration Program on a Full Scale Saturn Space Vehicle.
6. Weight Distribution and Unit Load Deflections for the Saturn Booster Assembly (SA-1). CCMD Huntsville Operations S&M Branch Report No. 1029, 1 November 1960.
7. Geiger, M.H.: Final Mass Characteristics of Saturn SA-1 Vehicle. George C. Marshall Space Flight Center Report No. IN-M-S&M-E-61-2, 30 June 1961, (Confidential)
8. Analytical Weight Analysis of Saturn Vehicle SA-1. ABMA Report No. DSL-TM-17-60, 18 April 1960, (Confidential)
9. Zoldos, A.J.: On Kron's Method of Tearing Mechanical Structures. Internal Document, Chrysler Corporation Missile Division

## APPENDIX A

## Directional Cosine Matrix

Consider a straight primitive beam element which is defined by its end points ( $i, j$ ) and which has a general orientation in a basic coordinate system as shown in Figure A-1. The basic coordinate system which is associated with the interconnected structure is a right-handed cartesian coordinate system whose axes are denoted by the primed quantities ( $x', y', z'$ ). The coordinate system associated with the primitive element is also a right-handed cartesian coordinate system whose axes, denoted by the unprimed quantities ( $x, y, z$ ), are orientated relative to the beam element as follows: The origin is at end  $j$ . The  $x$ -axis lies along the elastic axis of the beam and it is positive when directed towards end  $i$ . The  $y$ -axis lies along the principal axis of the beam where the area moment of inertia is a minimum and the  $z$ -axis lies along the principal axis where the area moment of inertia is a maximum.

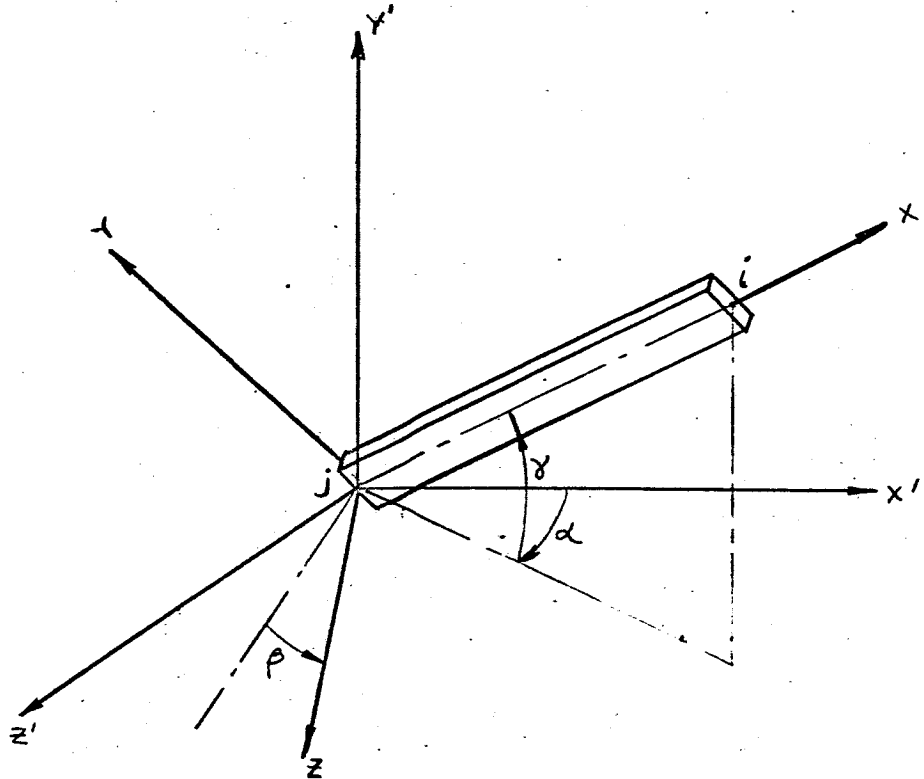


Figure A-1. Coordinate System

A study of Figure A-1 yields three angles which define the orientation of the primitive beam element relative to the basic coordinate system. These are angles  $\alpha$ ,  $\gamma$ ,  $\beta$ , the rotation of the  $x$ -axis from the  $x'$  axis measured in the  $x'-z'$  plane, the angular displacement of the  $x$ -axis above the  $x'-z'$  plane which is measured from the projection of the  $x$ -axis on the  $x'-z'$  plane and the rotation of the beam about the  $x$ -axis, respectively. Angle  $\beta$  is measured from the intersection of planes  $y-z$  and  $x'-z'$  and the  $z$ -axis of the beam. The positive direction of these angular deflections is specified in the figure.

In establishing the direction cosine matrix for each primitive element, the computer first calculates angles  $\alpha$  and  $\gamma$  using the junction coordinates of ends  $i$  ( $x'_i, y'_i, z'_i$ ) and  $j$  ( $x'_j, y'_j, z'_j$ ) which are part of the input. These angles are defined by the following relationships:

$$\alpha_{j,i} = \tan^{-1} \left( \frac{z'_i - z'_j}{x'_i - x'_j} \right) \quad (A-1)$$

$$\gamma_{j,i} = \tan^{-1} \left[ \frac{y'_i - y'_j}{\sqrt{(x'_i - x'_j)^2 + (z'_i - z'_j)^2}} \right] \quad (A-2)$$

For the case where the  $x$ -axis lies along the  $y'$  axis,  $\alpha_{j,i}$  becomes indeterminate. To calculate the direction cosines for this case, angle  $\beta$  is specified as zero and angle  $\alpha_{j,i}$  is given as input into the program. Having computed these angles, the directional cosine is then formed using the following equations:

$$l_1 = \cos \alpha \cos \gamma$$

$$m_1 = \sin \gamma$$

$$n_1 = \sin \alpha \cos \gamma$$

$$l_2 = -\cos \alpha \cos \beta \sin \gamma - \sin \alpha \sin \beta$$

$$m_2 = \cos \beta \cos \gamma$$

$$n_2 = -\sin \alpha \cos \beta \sin \gamma + \cos \alpha \sin \beta$$

$$l_3 = \cos \alpha \sin \beta \sin \gamma - \sin \alpha \cos \beta$$

$$m_3 = -\sin \beta \cos \gamma$$

$$n_3 = \sin \alpha \sin \beta \sin \gamma + \cos \alpha \cos \beta$$

## APPENDIX B - INPUT PREPARATION AND COMPUTER PROGRAM

### Input Preparation

A primary objective in establishing the computer program for this method of analysis was to minimize the amount of work that an engineer or analyst must perform in preparing the required input data and to simplify data preparation to an extent that an engineer aide with minimum supervision of an engineer could competently prepare the input. To arrive at these goals, it was decided that the computation of input data be limited to finding cross section areas, equivalent densities and torsional rigidities, and principal moments of inertia of the beam elements.

The following is an outline of the procedure which is used in data preparation:

1. Given a structure to be analyzed, select a basic coordinate system which for this program is a right-handed cartesian coordinate system. The choice of this coordinate is arbitrary but it is recommended that it be orientated along a plane of symmetry of the structure if such a plane exists.
2. From the actual structure, determine the following properties:
  - a) E Young's Modulus ( $\text{#/in}^2$ )
  - b) G Shear Modulus ( $\text{#/in}^2$ )
  - c)  $I_{\max}$  Maximum Area Moment of Inertia ( $\text{in}^4$ )
  - d)  $I_{\min}$  Minimum Area Moment of Inertia ( $\text{in}^4$ )
  - e) A Cross sectional area ( $\text{in}^2$ )
  - f)  $w$  Weight distribution ( $\text{#/in}^3$ )

The above information must be determined for every element in the system.

3. At this stage it is necessary to establish the junction or control points. This is accomplished by studying the entire structure and the

beam properties which were determined under (2) above. Junction points are first assigned to each point where two or more beams of different orientation are interconnected to each other. Next, the beam properties are studied to determine discontinuities of stiffness and mass characteristics. At these points of discontinuities additional junction points are assigned. Further, for a structural dynamics study, it may be required to assign additional junction points on a uniform beam to better approximate its mass distribution.

The only limitation to the number of junction points is computer capacity and round-off error. To this date, successful computer runs have been made on three dimensional structures having 150 junction points. The results were accurate to three significant figures. Successful runs of planes and grid type problems yielded five significant figure accuracy when 225 junction points were used.

4. Index numbers must be assigned to the junction points. The order in which these numbers are assigned follows certain rules that are the result of the programming technique. These are:
  - a) Point 1 cannot have all six boundary conditions specified (cantilevered case).
  - b) For a system with  $n$  junction points, point  $n$  must have at least one pertinent boundary condition.
  - c) Given a junction point, say  $j$ , it must be connected through a beam to some junction point  $i$ , where  $i < j$ .

To minimize computer round-off error, it is desirable to minimize the "bandwidth" of the factorized inverse table. This is accomplished as follows: Given a beam element which is described by its end point

indices, say (i, j), then number the system such that the quantity (j - i) is a minimum.

5. Once the indexed junction points are established, it is necessary to determine their ( $x'$ ,  $y'$ ,  $z'$ ) coordinates relative to the basic coordinate system. These dimensions can be computed from the assembly and detail drawings of the structure. In addition, the  $\beta$  angles must be found, where  $\beta$  is the angle that the  $I_{max}$  or  $z$  axis of the primitive beam elements makes with the intersection of the  $y$ - $z$  and  $x'$ - $z'$  planes. (See Appendix A) In most cases, it will be given on the drawings. For the more general orientations of the primitive beams, it can be computed from information given by the drawings.
6. The data compiled in 1 through 5 defines the mathematical model of the actual structure. It is summarized on data cards for the computer as follows:

Junction Coordinates:

J	X-Coordinate	Y-Coordinate	Z-Coordinate
1			
⋮			
n			

Beam Properties:

i	j	l	E	G	w	A
i	J	2	$\beta$	K	$I_{max}$	$I_{min}$

There are two cards of beam properties for each primitive beam. The first two entries of each card identify the beam element, say (i, j). The third entry identifies the card as being the first or the second of the beam property cards. On card one, the following information is given in the following sequence: E, Young's modulus; G, shear modulus;  $\omega$ , weight density; and A, cross section area. On card two, we have, in sequence,  $\beta$ , z-axis orientation angle;  $K = K_1 J$ , torsional rigidity, where  $K_1$  is the shape factor;  $I_{\max}$ , maximum area moment of inertia; and  $I_{\min}$ , the minimum area moment of inertia.

#### Boundary Conditions:

Junction Pt.	x	y	z	$\theta$	$\phi$	$\psi$
i						

Restrictions associated with the boundary conditions are, boundary conditions cannot be specified at more than 100 junction points, and only zero deflection can be specified. This limitation is due to the programming technique.

#### Externally Applied Forces:

Junction Pt.	$F^x$	$F^y$	$F^z$	$F^\theta$	$F^\phi$	$F^\psi$
i						

A restriction which is imposed on the externally applied forces is that a force cannot be specified at a boundary condition. That is, if

a boundary condition say,  $D_z$ , is specified at junction point j, then  $F^z$  cannot be specified at that same junction point.

#### Excitation Frequency:

$$\omega_1, \omega_2, \dots, \omega_n \text{ (cps)}$$

One or more excitation frequencies can be specified for each computer run. The program takes these in sequence and computes the response of the structure. If a static deflection study is being performed then  $\omega$  is set equal to zero.

#### Description of Program

The program is divided into ten segments called "chains." A brief description of each chain follows:

##### Chain I:

Chain I first reads in all of the junction coordinates,  $(x_i, y_i, z_i)$ , and then, one at a time, it reads in the given beam properties for each primitive element (i, j) and computes the following:

###### 1. Stiffness Coefficients

$$\frac{E A}{L}, \frac{12 E I_z}{L^3}, \frac{12 E I_y}{L^3}, \frac{K_l G J}{L}, \frac{4 E I_y}{L}, \frac{4 E I_z}{L}$$

$$\frac{2 E I_y}{L}, \frac{2 E I_z}{L}, \frac{G E I_z}{L^2}, \frac{G E I_y}{L^2}$$

The above computed quantities are the elements of the stiffness matrices.

###### 2. Mass Coefficients

$$M^{xx} = M^{yy} = M^{zz} = \frac{\omega^2 A L}{2 g}$$

$$M^{ee} = \frac{M^{xx}}{A} (I_{MAX.} + I_{MIN.})$$

$$M^{ff} = M^{yy} \left( \frac{L^2}{12} + \frac{I_{MIN.}}{A} \right)$$

$$M^{\psi\psi} = M^{zz} \left( \frac{L^2}{12} + \frac{I_{MAX.}}{A} \right)$$

3. The direction cosine matrix,  $A_i$ , is formed

where

$$A_i = \begin{bmatrix} l_1 & m_1 & n_1 \\ l_2 & m_2 & n_2 \\ l_3 & m_3 & n_3 \end{bmatrix} \quad (\text{see Appendix A})$$

The above computed quantities are now used to form the transformed stiffness and mass matrices as follows:

$$Y_{ii}^{ij} = A_{iT} Y^{ii} A_i$$

$$Y_{ij}^{ij} = A_{iT} Y^{ij} A_i$$

$$Y_{ji}^{ij} = A_{iT} Y^{ji} A_i$$

$$Y_{jj}^{ij} = A_{iT} Y^{jj} A_i$$

$$M_{ii}^{ij} = A_{iT} M^{ii} A_i$$

$$M_{jj}^{ij} = A_{iT} M^{jj} A_i$$

The results of the above operations are stored on tape 10 as they are computed.

#### Chain II:

This chain reads in the given external forces and boundary conditions and leaves them in the core.

#### Chain III: (Elimination of Deflections)

This chain reviews the given boundary conditions and proceeds to eliminate the row and column of every stiffness and mass matrix corresponding to boundary conditions which have been specified.

#### Chain IV: (Sort Variable Length Stiffness Matrices)

This chain examines the subscripts of all the stiffness matrices and then sums the matrices of like indices and writes them on tape 11 in an increasing order of indices.

Chain V: (Sort Variable Length Mass Matrices)

In this chain mass matrices are sorted exactly like Chain IV, and are written on tape 4.

Chain VI: (Merge Stiffness and Mass Matrices)

This chain forms the interconnected structure. At this point of the program, we have formed the interconnected stiffness matrix and interconnected mass matrix. In equation form, we have assembles:

$$A_T Y A \text{ and } A_T M A,$$

which are the interconnected stiffness and mass matrices, respectively.

Chain VII:

The complete equations of state are formed in this chain. The excitation frequency is read in and it multiplies each of the mass matrix coefficients. Finally, the mass and stiffness matrices are merged to form

$$(A_T Y A - \omega^2 A_T M A)$$

Chain VII: (Factorized Inverse Table)

The factorized inverse table is computed in this chain. A detailed description of the operations which are used in forming this table is given in part two of the mathematical analysis.

Chain IX: (Forward Solution)

The forward solution computes little f's and little d's. This is performed according to the following formulas:

$$f' = F'$$

$$d_1 = Z_{11} f'$$

$$f^2 = F^2 - Y^{21} d_1$$

$$d_2 = Z_{22} f^2$$

and in general,  $f^i = F^i - \sum_{j=1}^{i-1} Y^{ij} d_j$

$$d^i = Z_{ii} f^i$$

Chain X: (Backward Solution)

The backward solution computes the final absolute deflections according to the following process:

$$D_n = d_n$$

$$D_{n-1} = d_{n-1} - C_{(n-1)} \cdot n D_n$$

$$D_{n-2} = d_{n-2} - C_{(n-2)} \cdot (n-1) D_{(n-1)} - C_{(n-2)} \cdot (n) D_n$$

and in general

$$D_i = d_i - \sum_{j=i+1}^n C_{ij} D_j$$

At the conclusion of solving for the absolute deflections, a check is made to determine if another frequency is specified. If there is, then the program proceeds to Chain VII and repeats the succeeding computations.

## APPENDIX B - SUMMARY OF INPUT DATA

Junction Point Coordinates

<u>Junction Point No.</u>	<u>X</u>	<u>Y</u>	<u>Z</u>
1	0	0	0
2	158.0	0	0
3	232.00	0	0
4	275.0	0	0
5	363.5	0	0
6	452.0	0	0
7	496.0	0	0
8	619.0	0	0
9	656.0	0	0
10	760.5	0	0
11	865.0	0	0
12	918.0	0	0
13	978.7	0	0
14	978.7	110.0	0
15	978.7	77.7	77.7
16	978.7	0	110.0
17	978.7	-77.7	77.7
18	978.7	-110.0	0
19	978.7	-77.7	-77.7
20	978.7	0	-110.0
21	978.7	77.7	-77.7
22	1041.2	0	0
23	1078.7	0	0
24	1078.7	52.65	0
25	1078.7	37.2	37.2
26	1078.7	0	52.65
27	1078.7	-37.2	37.2
28	1078.7	-52.65	0
29	1078.7	-37.2	-37.2
30	1078.7	0	-52.65
31	1078.7	37.2	-37.2
32	1078.7	101.2	0
33	1078.7	86.385	35.782
34	1078.7	66.114	66.114
35	1078.7	35.782	86.385
36	1078.7	0	101.2
37	1078.7	-35.782	86.385
38	1078.7	-66.114	66.114
39	1078.7	-86.385	35.782
40	1078.7	-101.2	0
41	1078.7	-86.385	-35.782
42	1078.7	-66.114	-66.114
43	1078.7	-35.782	-86.385
44	1078.7	0	-101.2
45	1078.7	35.782	-86.385

## APPENDIX B - SUMMARY OF INPUT DATA

Junction Point Coordinates (Cont)

<u>Junction Point No.</u>	<u>X</u>	<u>Y</u>	<u>Z</u>
46	1078.7	66.114	-66.114
47	1078.7	86.385	-35.782
48	1091.4	0	0
49	1095.1	86.385	-35.782
50	1091.4	86.385	35.782
51	1095.1	35.782	86.385
52	1091.4	-35.782	86.385
53	1095.1	-86.385	35.782
54	1091.4	-86.385	-35.782
55	1095.1	-35.782	-86.385
56	1091.5	35.782	-86.385
57	1168.802	0	0
58	1168.214	86.385	-35.782
59	1158.9	86.385	35.782
60	1168.214	35.782	86.385
61	1158.9	-35.782	86.385
62	1168.214	-86.385	35.782
63	1158.9	-86.385	-35.782
64	1168.214	-35.782	-86.385
65	1158.9	35.782	-86.385
66	1223.502	0	0
67	1335.9	86.385	-35.782
68	1219.9	86.385	35.782
69	1335.9	35.782	86.385
70	1219.9	-35.782	86.385
71	1335.9	-86.385	35.782
72	1219.9	-86.385	-35.782
73	1335.9	-35.782	-86.385
74	1219.9	35.782	-86.385
75	1362.402	0	0
76	1458.2	86.385	-35.782
77	1448.9	86.385	35.782
78	1458.2	35.782	86.385
79	1448.9	-35.782	86.385
80	1458.2	-86.385	35.782
81	1448.9	-86.385	-35.782
82	1458.2	-35.782	-86.385
83	1448.9	35.782	-86.385
84	1501.302	0	0
85	1574.2	86.385	-35.782
86	1564.9	86.385	35.782
87	1574.2	35.782	86.385
88	1564.9	-35.782	86.385
89	1574.2	-86.385	35.782
90	1564.9	-86.385	-35.782

## APPENDIX B - SUMMARY OF INPUT DATA

Junction Point Coordinates (Cont)

<u>Junction Point No.</u>	<u>X</u>	<u>Y</u>	<u>Z</u>
91	1574.2	-35.782	-86.385
92	1564.9	35.782	-86.385
93	1607.907	0	0
94	1705.8	86.385	-35.782
95	1704.8	86.385	35.782
96	1705.8	35.782	86.385
97	1704.8	-35.782	86.385
98	1705.8	-86.385	35.782
99	1704.9	-86.385	-35.782
100	1705.8	-35.782	-86.385
101	1704.9	35.782	-86.385
102	1714.512	0	0
103	1769.0	86.385	-35.782
104	1769.0	86.385	35.782
105	1769.0	35.782	86.385
106	1769.0	-35.782	86.385
107	1769.0	-86.385	35.782
108	1769.0	-86.385	-35.782
109	1769.0	-35.782	-86.385
110	1769.0	35.782	-86.385
111	1773.452	0	0
112	1773.452	71.562	-71.562
113	1773.452	86.385	-35.782
114	1773.452	101.204	0
115	1773.452	86.385	35.782
116	1773.452	71.562	71.562
117	1773.452	35.782	86.385
118	1773.452	0	101.204
119	1773.452	-35.782	86.385
120	1773.452	-71.562	71.562
121	1773.452	-86.385	35.782
122	1773.452	-101.204	0
123	1773.452	-86.385	-35.782
124	1773.452	-71.562	-71.562
125	1773.452	-35.782	-86.385
126	1773.452	0	-101.204
127	1773.452	35.782	-86.385
128	1793.452	0	0
129	1813.452	0	0
130	1833.452	0	0
131	1855.702	0	0
132	1773.452	142.273	-142.273
133	1773.452	142.273	142.273
134	1773.452	-142.273	142.273
135	1773.452	-142.273	-142.273

## APPENDIX B - SUMMARY OF INPUT DATA

Beam Element Section Properties

<u>Beam Element</u>	<u>A</u>	<u>K</u>	<u>I(max)</u>	<u>I(min)</u>
1-2 *	9.75	$13.34 \times 10^3$	$6.67 \times 10^3$	$6.67 \times 10^3$
2-3 *	19.5	$56.6 \times 10^3$	$28.3 \times 10^3$	$28.3 \times 10^3$
3-4 *	22.6	$81.6 \times 10^3$	$40.8 \times 10^3$	$40.8 \times 10^3$
4-5 *	22.6	$81.6 \times 10^3$	$40.8 \times 10^3$	$40.8 \times 10^3$
5-6 *	22.6	$81.6 \times 10^3$	$40.8 \times 10^3$	$40.8 \times 10^3$
6-7	104.5	$812.0 \times 10^3$	$406 \times 10^3$	$406 \times 10^3$
7-8	139.5	$1870 \times 10^3$	$935 \times 10^3$	$935 \times 10^3$
8-9	171	$2642 \times 10^3$	$1321 \times 10^3$	$1321 \times 10^3$
9-10	362.5	$2852 \times 10^3$	$1426 \times 10^3$	$1426 \times 10^3$
10-11	362.5	$2852 \times 10^3$	$1426 \times 10^3$	$1426 \times 10^3$
11-12	362.5	$2852 \times 10^3$	$1426 \times 10^3$	$1426 \times 10^3$
12-13	362.5	$2852 \times 10^3$	$1426 \times 10^3$	$1426 \times 10^3$
13-14 *	$10 \times 10^9$	$1 \times 10^{20}$	$1 \times 10^{20}$	$1 \times 10^{20}$
13-15 *	$10 \times 10^9$	$1 \times 10^{20}$	$1 \times 10^{20}$	$1 \times 10^{20}$
13-16 *	$10 \times 10^9$	$1 \times 10^{20}$	$1 \times 10^{20}$	$1 \times 10^{20}$
13-17 *	$10 \times 10^9$	$1 \times 10^{20}$	$1 \times 10^{20}$	$1 \times 10^{20}$
13-18 *	$10 \times 10^9$	$1 \times 10^{20}$	$1 \times 10^{20}$	$1 \times 10^{20}$
13-19 *	$10 \times 10^9$	$1 \times 10^{20}$	$1 \times 10^{20}$	$1 \times 10^{20}$
13-20 *	$10 \times 10^9$	$1 \times 10^{20}$	$1 \times 10^{20}$	$1 \times 10^{20}$
13-21 *	$10 \times 10^9$	$1 \times 10^{20}$	$1 \times 10^{20}$	$1 \times 10^{20}$
13-22	8.8	130.9	65.46	65.46
14-22	2.02	2.34	1.17	1.17
14-24	8.8	130.9	65.46	65.46
15-22	2.02	2.34	1.17	1.17
15-25	8.8	130.9	65.46	65.46

## APPENDIX B - SUMMARY OF INPUT DATA

Beam Element Section Properties (Cont)

<u>Beam Element</u>	<u>A</u>	<u>K</u>	<u>I(max)</u>	<u>I(min)</u>
16-22	2.02	2.34	1.17	1.17
16-26	8.8	130.9	65.46	65.46
17-22	2.02	2.34	1.17	1.17
17-27	8.8	130.9	65.46	65.46
18-22	2.02	2.34	1.17	1.17
18-28	8.8	130.9	65.46	65.46
19-22	2.02	2.34	1.17	1.17
19-29	8.8	130.9	65.46	65.46
20-22	2.02	2.34	1.17	1.17
20-30	8.8	130.9	65.46	65.46
21-22	2.02	2.34	1.17	1.17
21-31	8.8	130.9	65.46	65.46
22-23	102.2	$436 \times 10^3$	$218 \times 10^3$	$218 \times 10^3$
23-24	13.928	1.545	939	42.7
23-25	13.928	1.545	939	42.7
23-26	13.928	1.545	939	42.7
23-27	13.928	1.545	939	42.7
23-28	13.928	1.545	939	42.7
23-29	13.928	1.545	939	42.7
23-30	13.928	1.545	939	42.7
23-31	13.928	1.545	939	42.7
24-32	13.928	1.545	939	42.7
25-34	13.928	1.545	939	42.7
26-36	13.928	1.545	939	42.7
27-38	13.928	1.545	939	42.7

## APPENDIX B - SUMMARY OF INPUT DATA

Beam Element Section Properties (Cont)

<u>Beam Element</u>	<u>A</u>	<u>K</u>	<u>I<sub>(max)</sub></u>	<u>I<sub>(min)</sub></u>
28-40	13.928	1.545	939	42.7
29-42	13.928	1.545	939	42.7
30-44	13.928	1.545	939	42.7
31-46	13.928	1.545	939	42.7
32-33	13.928	1.545	939	42.7
32-47	13.928	1.545	939	42.7
33-34	13.928	1.545	939	42.7
33-50 *	18.78	$2.1963 \times 10^3$	$2.149 \times 10^3$	47.3
34-35	13.928	1.545	939	42.7
35-36	13.928	1.545	939	42.7
35-51 *	$1 \times 10^{-4}$	$1.0193 \times 10^3$	$1.014 \times 10^3$	5.30
36-37	13.928	1.545	939	42.7
37-38	13.928	1.545	939	42.7
37-52 *	18.78	$2.1963 \times 10^3$	$2.149 \times 10^3$	47.3
38-39	13.928	1.545	939	42.7
39-40	13.928	1.545	939	42.7
39-53 *	$1 \times 10^{-4}$	$1.0193 \times 10^3$	$1.014 \times 10^3$	5.30
40-41	13.928	1.545	939	42.7
41-42	13.928	1.545	939	42.7
41-54 *	18.78	$2.1963 \times 10^3$	$2.149 \times 10^3$	47.3
42-43	13.928	1.545	939	42.7
43-44	13.928	1.545	939	42.7
43-55 *	$1 \times 10^{-4}$	$1.0193 \times 10^3$	$1.014 \times 10^3$	5.30
44-55	13.928	1.545	939	42.7
45-46	13.928	1.545	939	42.7

## APPENDIX B - SUMMARY OF INPUT DATA

Beam Element Section Properties (Cont)

<u>Beam Element</u>	<u>A</u>	<u>K</u>	<u>I(max)</u>	<u>I(min)</u>
45-56 *	18.78	$2.1963 \times 10^3$	$2.149 \times 10^3$	47.3
46-47	13.928	1.545	939	42.7
47-49 *	$1 \times 10^{-4}$	$1.0193 \times 10^3$	$1.014 \times 10^3$	5.30
48-57	100.9	279.728	$139.864 \times 10^3$	$139.864 \times 10^3$
49-58	19.807	$24.336 \times 10^3$	$12.168 \times 10^3$	$12.168 \times 10^3$
50-59	41.903	$51.592 \times 10^3$	$25.796 \times 10^3$	$25.796 \times 10^3$
51-60	19.807	$2.4336 \times 10^4$	$1.2168 \times 10^4$	$1.2168 \times 10^4$
52-61	41.903	$5.1592 \times 10^4$	$2.5796 \times 10^4$	$2.5796 \times 10^4$
53-62	19.807	$24.336 \times 10^3$	$12.168 \times 10^3$	$12.168 \times 10^3$
54-63	41.903	$5.1592 \times 10^4$	$2.5796 \times 10^4$	$2.5796 \times 10^4$
55-64	19.807	$24.336 \times 10^3$	$12.168 \times 10^3$	$12.168 \times 10^3$
56-65	41.903	$5.1592 \times 10^4$	$2.5796 \times 10^4$	$2.5796 \times 10^4$
57-66	68.09	1.545	$94.19 \times 10^3$	$94.19 \times 10^3$
58-67	13.2	16.32	$8.16 \times 10^3$	$8.16 \times 10^3$
59-68	22.682	$2.798 \times 10^4$	$1.399 \times 10^4$	$1.399 \times 10^4$
60-69	13.20	$16.32 \times 10^3$	$8.16 \times 10^3$	$8.16 \times 10^3$
61-70	22.682	$27.98 \times 10^3$	$13.99 \times 10^3$	$13.99 \times 10^3$
62-71	13.2	$16.32 \times 10^3$	$8.16 \times 10^3$	$8.16 \times 10^3$
63-72	22.682	27.98	$13.99 \times 10^3$	$13.99 \times 10^3$
64-73	13.20	16.32	$8.16 \times 10^3$	$8.16 \times 10^3$
65-74	22.682	$27.98 \times 10^3$	$13.99 \times 10^3$	$13.99 \times 10^3$
66-75	67.42	1.545	$93.279 \times 10^3$	$93.279 \times 10^3$
67-76	14.02	$17.316 \times 10^3$	$8.658 \times 10^3$	$8.658 \times 10^3$
68-77	22.682	$27.98 \times 10^3$	$13.99 \times 10^3$	$13.99 \times 10^3$
69-78	14.02	$17.316 \times 10^3$	$8.658 \times 10^3$	$8.658 \times 10^3$

## APPENDIX B - SUMMARY OF INPUT DATA

Beam Element Section Properties (Cont)

<u>Beam Element</u>	<u>A</u>	<u>K</u>	<u>I<sub>(max)</sub></u>	<u>I<sub>(min)</sub></u>
70-79	22.682	$27.98 \times 10^3$	$13.99 \times 10^3$	$13.99 \times 10^3$
71-80	14.02	$17.316 \times 10^3$	$8.658 \times 10^3$	$8.658 \times 10^3$
72-81	22.682	$2.798 \times 10^4$	$13.99 \times 10^3$	$13.99 \times 10^3$
73-82	14.02	$17.316 \times 10^3$	$8.658 \times 10^3$	$8.658 \times 10^3$
74-83	22.682	$2.798 \times 10^4$	$13.99 \times 10^3$	$13.99 \times 10^3$
75-84	67.42	1.545	$93.279 \times 10^3$	$93.279 \times 10^3$
76-85	14.80	$18.172 \times 10^3$	$9.086 \times 10^3$	$9.086 \times 10^3$
77-86	26.49	$3.2612 \times 10^4$	$1.6306 \times 10^4$	$1.6306 \times 10^4$
78-87	14.80	$18.172 \times 10^3$	$9.086 \times 10^3$	$9.086 \times 10^3$
79-88	26.49	$3.2612 \times 10^4$	$1.6306 \times 10^4$	$1.6306 \times 10^4$
80-89	14.8	$18.172 \times 10^3$	$9.086 \times 10^3$	$9.086 \times 10^3$
81-90	26.49	$3.2612 \times 10^4$	$1.6306 \times 10^4$	$1.6306 \times 10^4$
82-91	14.80	$18.162 \times 10^3$	$9.086 \times 10^3$	$9.086 \times 10^3$
83-92	26.49	$3.2612 \times 10^4$	$1.6306 \times 10^4$	$1.6306 \times 10^4$
84-93	82.66	1.545	$114.263 \times 10^3$	$114.263 \times 10^3$
85-94	16.78	$21.26 \times 10^6$	$10.63 \times 10^3$	$10.63 \times 10^3$
86-95	30.9	$3.864 \times 10^4$	$1.932 \times 10^4$	$1.932 \times 10^4$
87-96	16.78	$2.126 \times 10^4$	$1.063 \times 10^4$	$1.063 \times 10^4$
88-97	26.49	$3.2612 \times 10^4$	$1.932 \times 10^4$	$1.932 \times 10^4$
89-98	16.78	$2.126 \times 10^4$	$1.063 \times 10^4$	$1.063 \times 10^4$
90-99	30.9	$3.864 \times 10^4$	$1.932 \times 10^4$	$1.932 \times 10^4$
91-100	16.78	$2.126 \times 10^4$	$1.063 \times 10^4$	$1.063 \times 10^4$
92-101	30.9	$3.864 \times 10^4$	$1.932 \times 10^4$	$1.932 \times 10^4$
93-102	94.0	1.545	$136 \times 10^3$	$136 \times 10^3$
94-103	25.74	1.545	1.6613	1.6613

## APPENDIX B - SUMMARY OF INPUT DATA

Beam Element Section Properties (Cont)

<u>Beam Element</u>	<u>A</u>	<u>K</u>	<u>I(max)</u>	<u>I(min)</u>
95-104	23.408	$6.0912 \times 10^4$	$3.0456 \times 10^4$	$3.0456 \times 10^4$
96-105	25.74	1.0	$16.613 \times 10^3$	$16.613 \times 10^3$
97-106	23.408	1.0	$30.456 \times 10^3$	$30.456 \times 10^3$
98-107	25.74	1.0	$16.613 \times 10^3$	$16.613 \times 10^3$
99-108	23.408	1.0	$30.456 \times 10^3$	$30.456 \times 10^3$
100-109	25.74	1.0	$16.613 \times 10^3$	$16.613 \times 10^3$
101-110	23.408	1.0	$30.456 \times 10^3$	$30.456 \times 10^3$
102-111	44.74	1.0	$61.696 \times 10^3$	$61.696 \times 10^3$
103-113 *	7.92	$2.102 \times 10^3$	$1.051 \times 10^3$	$1.051 \times 10^3$
104-115 *	7.92	$5.176 \times 10^3$	$2.538 \times 10^3$	$2.538 \times 10^3$
105-117 *	7.92	$2.102 \times 10^3$	$1.051 \times 10^3$	$1.051 \times 10^3$
106-119 *	7.92	$5.176 \times 10^3$	$2.538 \times 10^3$	$2.538 \times 10^3$
107-121 *	7.92	$2.102 \times 10^3$	$1.051 \times 10^3$	$1.051 \times 10^3$
108-123 *	7.92	$5.176 \times 10^3$	$2.538 \times 10^3$	$2.538 \times 10^3$
109-125 *	7.92	$2.102 \times 10^3$	$1.051 \times 10^3$	$1.051 \times 10^3$
110-127 *	7.92	$5.176 \times 10^3$	$2.538 \times 10^3$	$2.538 \times 10^3$
111-112	7.552	$7.38 \times 10^2$	$380.67 \times 10^3$	$7.05 \times 10^2$
111-114	7.269	$1.181 \times 10^3$	$34.41 \times 10^3$	$7 \times 10^2$
111-116	7.552	$7.38 \times 10^2$	$380.67 \times 10^3$	$7.05 \times 10^2$
111-118	7.269	$1.181 \times 10^3$	$34.41 \times 10^3$	$7 \times 10^2$
111-120	7.552	$7.38 \times 10^3$	$380.67 \times 10^3$	$7.05 \times 10^2$
111-122	7.269	$1.181 \times 10^3$	$34.41 \times 10^3$	$7 \times 10^2$
111-124	7.552	$7.38 \times 10^2$	$380.67 \times 10^3$	$7.05 \times 10^2$
111-126	7.269	$1.181 \times 10^3$	$34.41 \times 10^3$	$7 \times 10^2$
111-128	108.49	$260.034 \times 10^3$	130.017	130.017

## APPENDIX B - SUMMARY OF INPUT DATA

Beam Element Section Properties (Cont)

<u>Beam Element</u>	<u>A</u>	<u>K</u>	<u>I(max)</u>	<u>I(min)</u>
112-113	.5	1.0	$95.150 \times 10^3$	6.048
112-127	.5	1.0	$95.150 \times 10^3$	6.048
112-132	$3.0 \times 10^{-2}$	1.0	$13.041 \times 10^3$	1.08
113-114	.5	1.0	$8.6 \times 10^3$	6.048
114-115	.5	1.0	$8.6 \times 10^3$	6.048
115-116	.5	1.0	$95.15 \times 10^3$	6.048
116-117	.5	1.0	$95.15 \times 10^3$	6.048
116-133	$3 \times 10^{-2}$	1.0	$13.041 \times 10^3$	1.08
117-118	.5	1.0	$8.6 \times 10^3$	6.048
118-119	.5	1.0	$8.6 \times 10^3$	6.048
119-120	.5	1.0	$95.15 \times 10^3$	6.048
120-121	.5	1.0	$95.15 \times 10^3$	6.048
120-134	$3 \times 10^{-2}$	1.0	$13.041 \times 10^3$	1.08
121-122	.5	1.0	$8.6 \times 10^3$	6.048
122-123	.5	1.0	$8.6 \times 10^3$	6.048
123-124	.5	1.0	$95.15 \times 10^3$	6.048
124-125	.5	1.0	$95.15 \times 10^3$	6.048
124-135	$3.0 \times 10^{-2}$	1.0	$13.041 \times 10^3$	1.08
125-126	.5	1.0	$8.6 \times 10^3$	6.048
126-127	.5	1.0	$8.6 \times 10^3$	6.048
128-129	108.49	$260.034 \times 10^3$	$130.017 \times 10^3$	$130.017 \times 10^3$
129-130	108.49	$260.034 \times 10^3$	$130.017 \times 10^3$	$130.017 \times 10^3$
130-131	108.49	$260.034 \times 10^3$	$130.017 \times 10^3$	$130.017 \times 10^3$

\*- E =  $30 \times 10^6$ All Others - E =  $10.3 \times 10^6$ G =  $11.5 \times 10^6$ G =  $3.9 \times 10^6$

TABLE I

## SUMMARY OF SUPPORT OUTRIGGER DEFLECTION ANALYSIS

	$\Delta x$	$\Delta y$	$\Delta z$	$\theta$	$\phi$	$\psi$
$F_x = 1000 \#$	$-11787 \times 10^{-5}$	0	$.11816 \times 10^{-3}$	0	$.68642 \times 10^{-6}$	0
	$.66637 \times 10^{-4}$	0	$.37301 \times 10^{-4}$	0	$-.13632 \times 10^{-4}$	0
	$.13010 \times 10^{-2}$	0	$.38047 \times 10^{-4}$	0	$-.39679 \times 10^{-4}$	0
$F_y = 1000 \#$	0	$.73471 \times 10^{-2}$	0	$.44456 \times 10^{-3}$	0	$.74834 \times 10^{-4}$
	0	$.15459 \times 10^{-1}$	0	$.57058 \times 10^{-3}$	0	$.34548 \times 10^{-3}$
	0	$.47143 \times 10^{-1}$	0	$.91698 \times 10^{-3}$	0	$.14933 \times 10^{-2}$
$F_z = 1000 \#$	$.79260 \times 10^{-4}$	0	$.59647 \times 10^{-4}$	0	$-.25452 \times 10^{-5}$	0
	$.52950 \times 10^{-4}$	0	$.62160 \times 10^{-4}$	0	$-.41932 \times 10^{-5}$	0
	$.38047 \times 10^{-4}$	0	$.87309 \times 10^{-4}$	0	$.23923 \times 10^{-5}$	0
$F_\theta = 1000 " / \#$	0	$-.22300 \times 10^{-3}$	0	$.23299 \times 10^{-5}$	0	$-.48593 \times 10^{-5}$
	0	$.12426 \times 10^{-4}$	0	$.11826 \times 10^{-4}$	0	$-.46357 \times 10^{-6}$
	0	$.91698 \times 10^{-3}$	0	$.35154 \times 10^{-4}$	0	$.29014 \times 10^{-4}$
$F_\phi = 1000 " / \#$	$.21021 \times 10^{-5}$	0	$.13668 \times 10^{-4}$	0	$-.30664 \times 10^{-6}$	0
	$.12636 \times 10^{-4}$	0	$.25094 \times 10^{-5}$	0	$-.56506 \times 10^{-6}$	0
	$-.39679 \times 10^{-4}$	0	$.23923 \times 10^{-5}$	0	$.58764 \times 10^{-5}$	0
$F_\psi = 1000 " / \#$	0	$.23530 \times 10^{-3}$	0	$.14094 \times 10^{-4}$	0	$.24201 \times 10^{-5}$
	0	$.49073 \times 10^{-3}$	0	$.18059 \times 10^{-4}$	0	$.11020 \times 10^{-4}$
	0	$.14933 \times 10^{-2}$	0	$.29014 \times 10^{-4}$	0	$.92912 \times 10^{-4}$

Note: See Figure 5 for numbering and loading scheme. Points 5 and 6 are fixed.

TABLE II

## SUMMARY OF THRUST OUTRIGGER DEFLECTION ANALYSIS

	$\Delta x$	$\Delta y$	$\Delta z$	$\theta$	$\phi$	$\psi$
$F_x = 1000 \#$						
Point 1	.79612x10 <sup>-5</sup>	0	.73274x10 <sup>-4</sup>	0	-.30727x10 <sup>-5</sup>	0
2	-.68108x10 <sup>-5</sup>	0	-.29691x10 <sup>-4</sup>	0	-.63785x10 <sup>-6</sup>	0
3	.10948x10 <sup>-3</sup>	0	-.36307x10 <sup>-4</sup>	0	-.99891x10 <sup>-5</sup>	0
4	.13517x10 <sup>-2</sup>	0	.34516x10 <sup>-4</sup>	0	-.41485x10 <sup>-4</sup>	0
$F_y = 1000 \#$						
Point 1	0	.13918x10 <sup>-1</sup>	0	.62820x10 <sup>-3</sup>	0	.20538x10 <sup>-3</sup>
2	0	.47724x10 <sup>-2</sup>	0	.32435x10 <sup>-3</sup>	0	.19757x10 <sup>-3</sup>
3	0	.18732x10 <sup>-1</sup>	0	.54662x10 <sup>-3</sup>	0	.68524x10 <sup>-3</sup>
4	0	.47458x10 <sup>-1</sup>	0	.71251x10 <sup>-3</sup>	0	.15050x10 <sup>-2</sup>
$F_z = 1000 \#$						
Point 1	-.72083x10 <sup>-4</sup>	0	.41166x10 <sup>-3</sup>	0	.10458x10 <sup>-4</sup>	0
2	-.36495x10 <sup>-4</sup>	0	.55762x10 <sup>-3</sup>	0	-.34839x10 <sup>-5</sup>	0
3	-.34035x10 <sup>-3</sup>	0	.69218x10 <sup>-3</sup>	0	.33073x10 <sup>-5</sup>	0
4	.34516x10 <sup>-4</sup>	0	.96551x10 <sup>-3</sup>	0	-.16692x10 <sup>-4</sup>	0
$F_\theta = 1000''/\#$						
Point 1	0	-.97697x10 <sup>-4</sup>	0	.79049x10 <sup>-5</sup>	0	-.19856x10 <sup>-5</sup>
2	0	-.69154x10 <sup>-4</sup>	0	.33404x10 <sup>-5</sup>	0	-.19604x10 <sup>-5</sup>
3	0	.98359x10 <sup>-4</sup>	0	.84771x10 <sup>-5</sup>	0	.54502x10 <sup>-5</sup>
4	0	.71251x10 <sup>-3</sup>	0	.21964x10 <sup>-4</sup>	0	.19976x10 <sup>-4</sup>
$F_\phi = 1000''/\#$						
Point 1	.55980x10 <sup>-5</sup>	0	.16979x10 <sup>-4</sup>	0	-.10174x10 <sup>-5</sup>	0
2	.91915x10 <sup>-6</sup>	0	-.98477x10 <sup>-5</sup>	0	-.31356x10 <sup>-6</sup>	0
3	.32318x10 <sup>-4</sup>	0	-.11871x10 <sup>-4</sup>	0	-.12978x10 <sup>-5</sup>	0
4	-.41485x10 <sup>-4</sup>	0	-.16692x10 <sup>-4</sup>	0	.10579x10 <sup>-4</sup>	0
$F_\psi = 1000''/\#$						
Point 1	0	.44320x10 <sup>-3</sup>	0	.19942x10 <sup>-4</sup>	0	.65485x10 <sup>-5</sup>
2	0	.15203x10 <sup>-3</sup>	0	.10278x10 <sup>-4</sup>	0	.62972x10 <sup>-5</sup>
3	0	.59454x10 <sup>-3</sup>	0	.17328x10 <sup>-4</sup>	0	.21822x10 <sup>-4</sup>
4	0	.15050x10 <sup>-2</sup>	0	.19976x10 <sup>-4</sup>	0	.93336x10 <sup>-4</sup>

Note: See Figure 5 for numbering and loading scheme. Points 5 and 6 are fixed.

TABLE III SUMMARY OF VEHICLE RESPONSE

TABLE III SUMMARY OF VEHICLE RESPONSE (CONT.)

FREQ MAINTANK & UPPER STAGES	L-1	L-2	L-3	L-4	F-1	F-2	F-3	F-4
2.60								
2.70								
2.80								
2.90								
3.00								
3.20								
3.25								
3.30								
3.40								
3.80								
4.00								

\* FREQUENCY 3.35 CPS OUT OF SEQUENCE, SEE END OF TABLE

TABLE III SUMMARY OF VEHICLE RESPONSE (CONT.)

FREQ.	MAIN TANK & UPPER STAGES	L-1	L-2	L-3	L-4	F-1	F-2	F-3	F-4
4.20									
4.30									
4.40									
4.50									
4.60									
4.70									
4.80									
5.00									
5.40									
5.80									
6.10									

TABLE III SUMMARY OF VEHICLE RESPONSE (CONT.)

FREQ.	MAIN TANK & UPPER STAGES	L-1	L-2	L-3	L-4	F-1	F-2	F-3	F-4
6.40									
6.65									
6.75									
3.35									

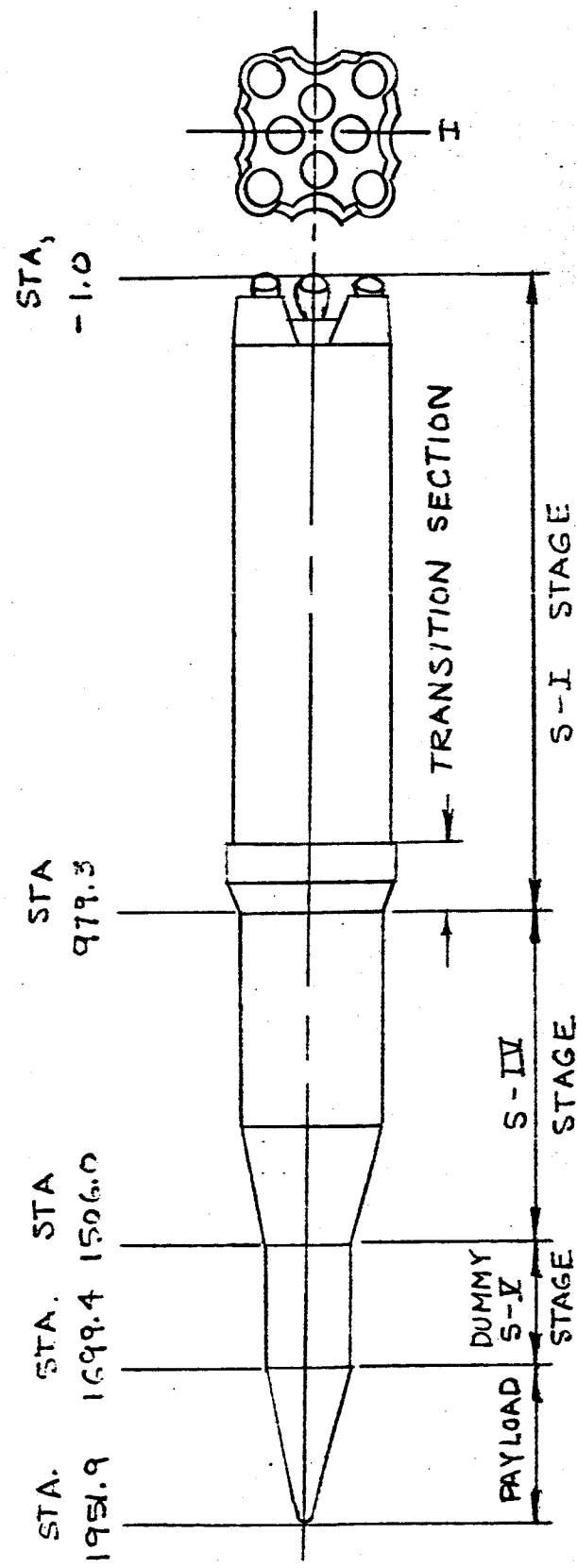


FIG 8 SATURN SA-D1

FIG. 9 SECTION PROPERTIES

PAYOUT BODY AND SV DUMMY STAGE

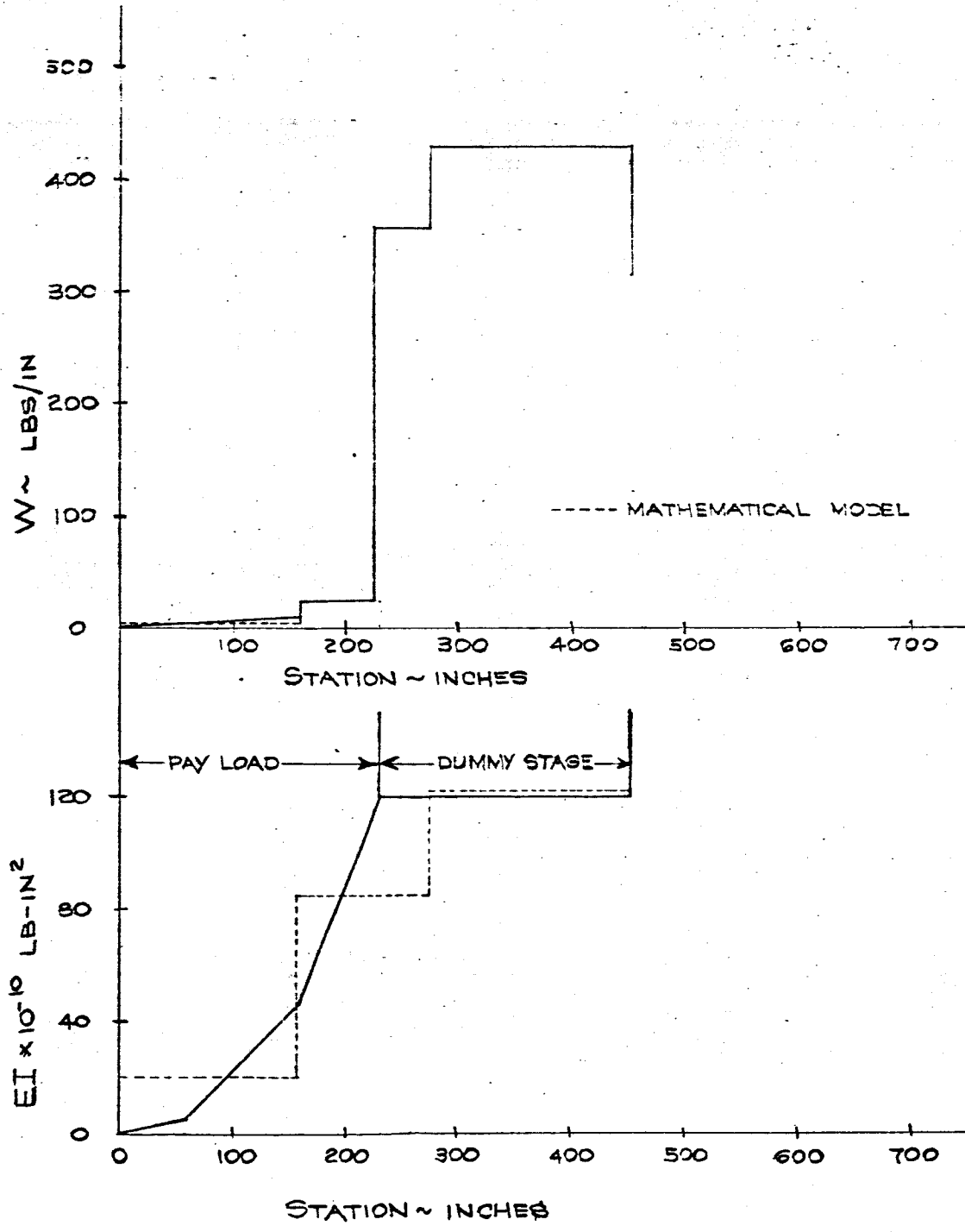


FIG. 10 SECTION PROPERTIES

SIV DUMMY STAGE

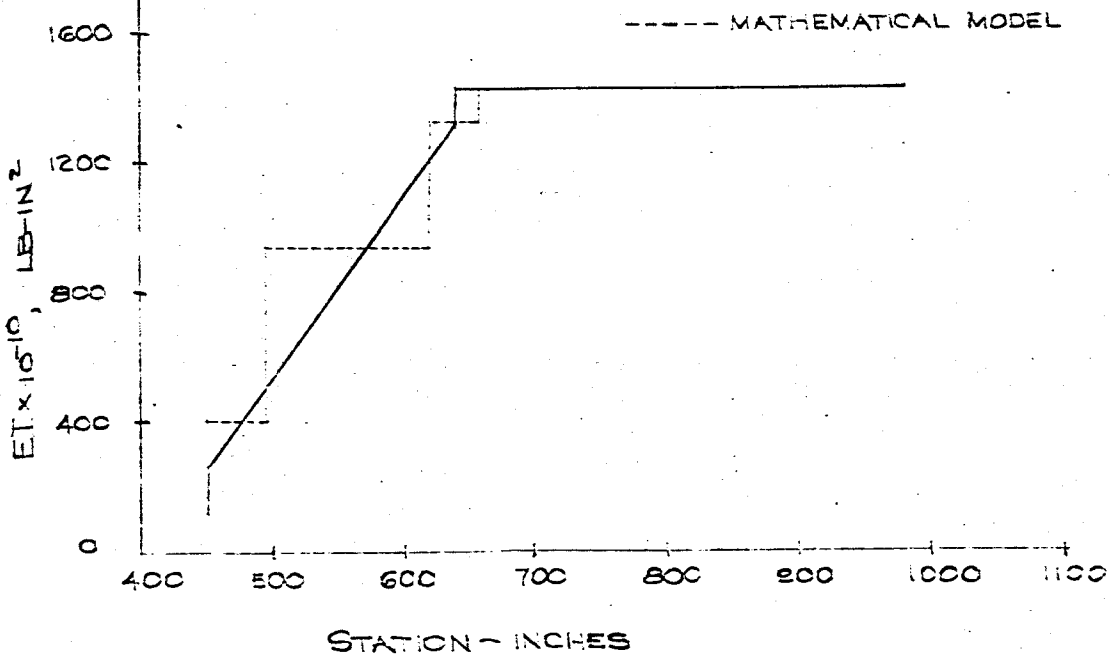
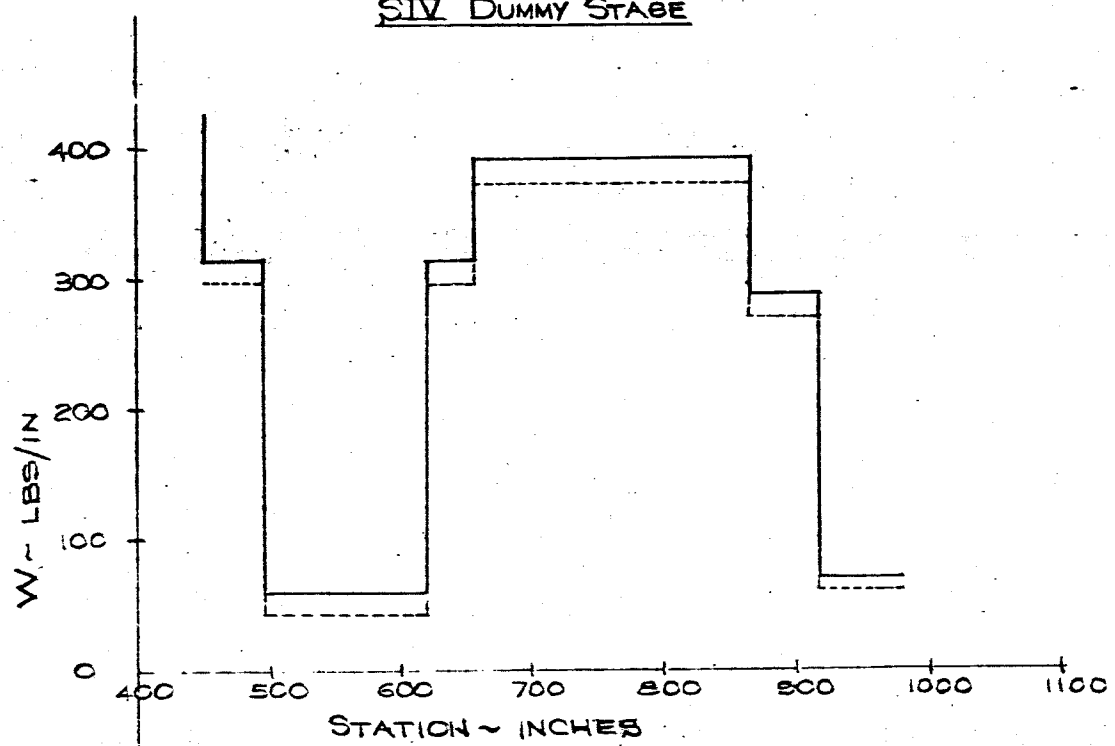


FIG. 11 SECTION PROPERTIES  
105 INCH DIAMETER FUEL TANK

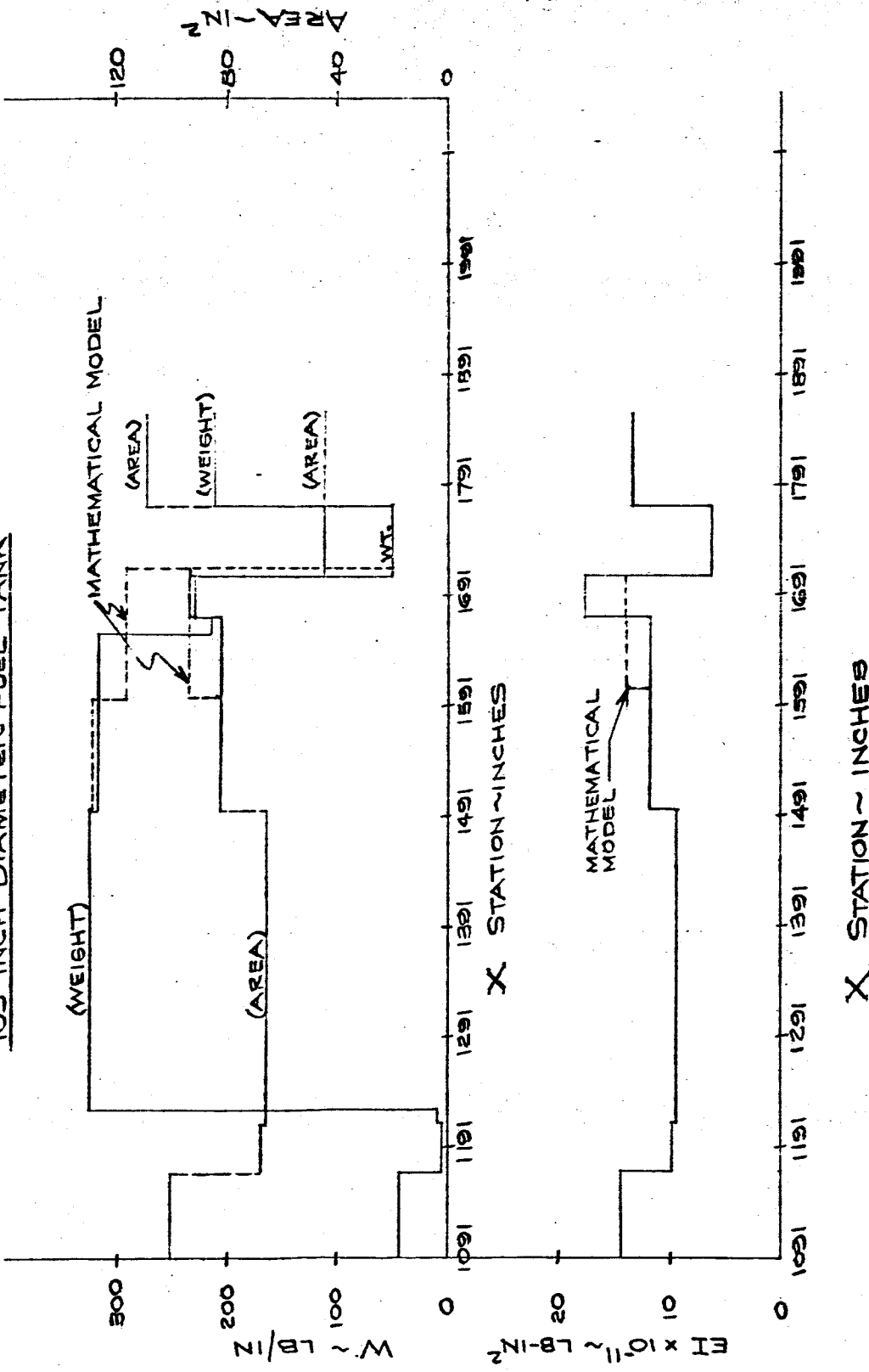


FIG. 12 SECTION PROPERTIES  
70-INCH DIAMETER LIQUID OXYGEN TANKS

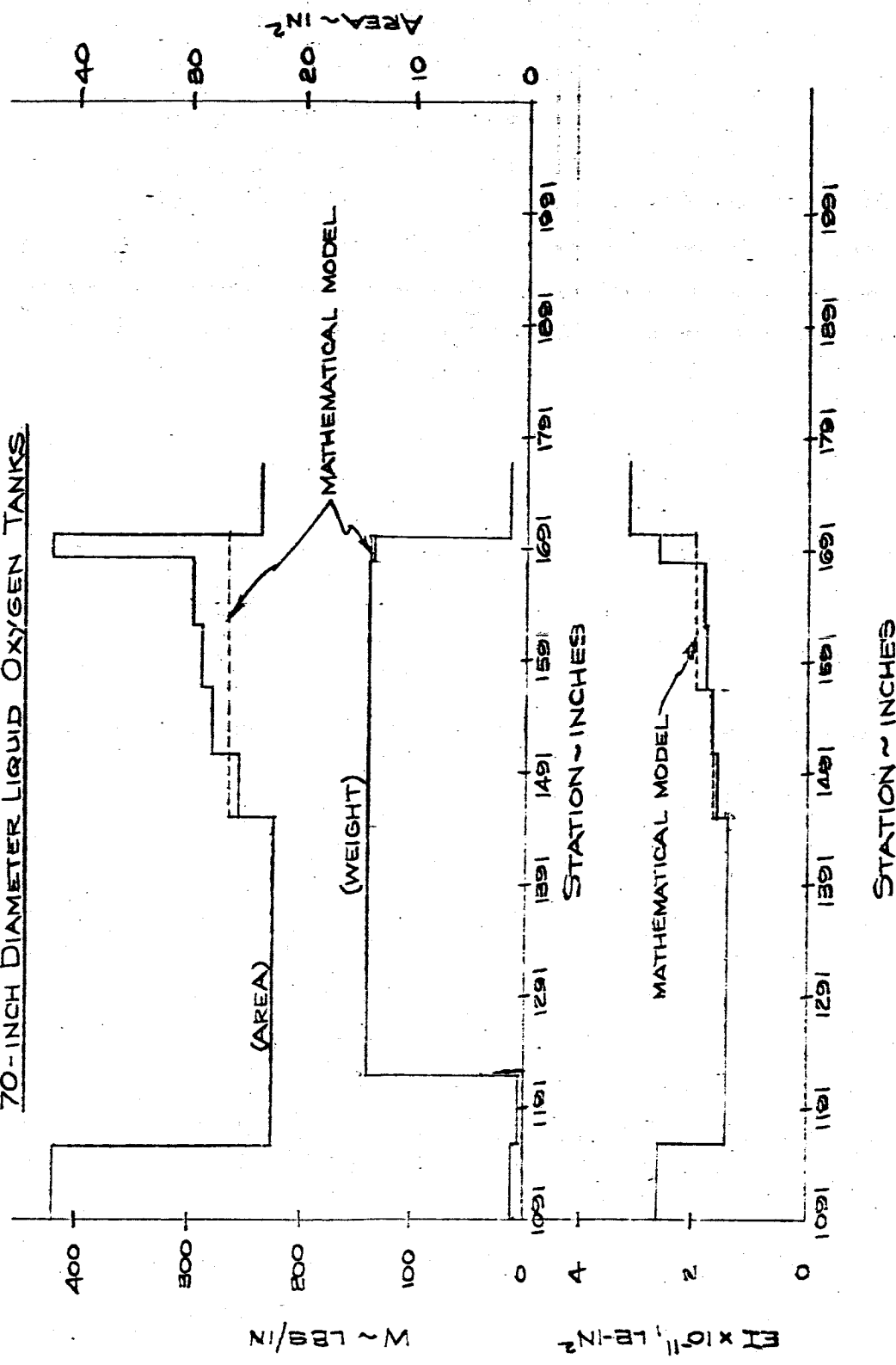
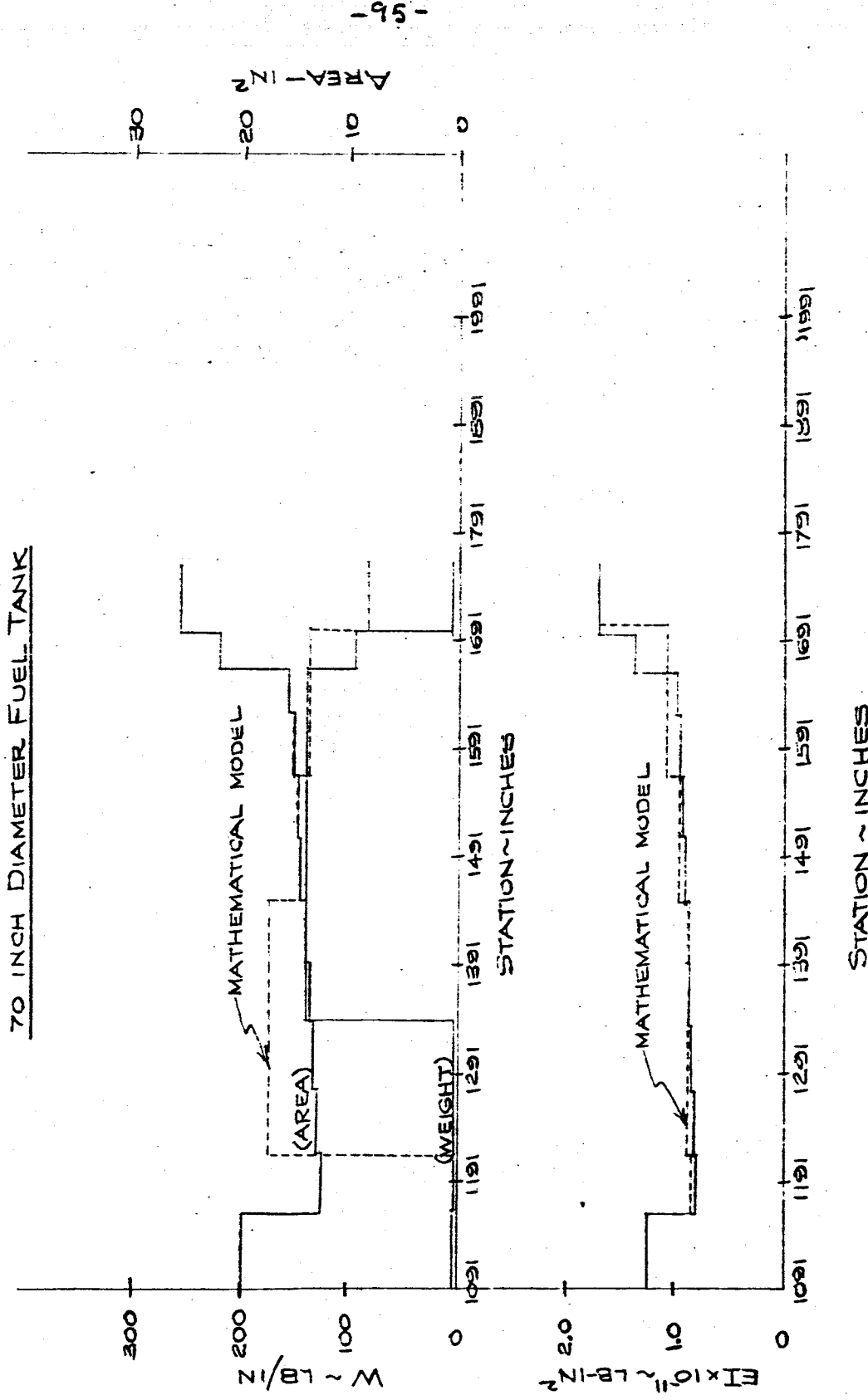


FIG. 13 SECTION PROPERTIES  
70 INCH DIAMETER FUEL TANK



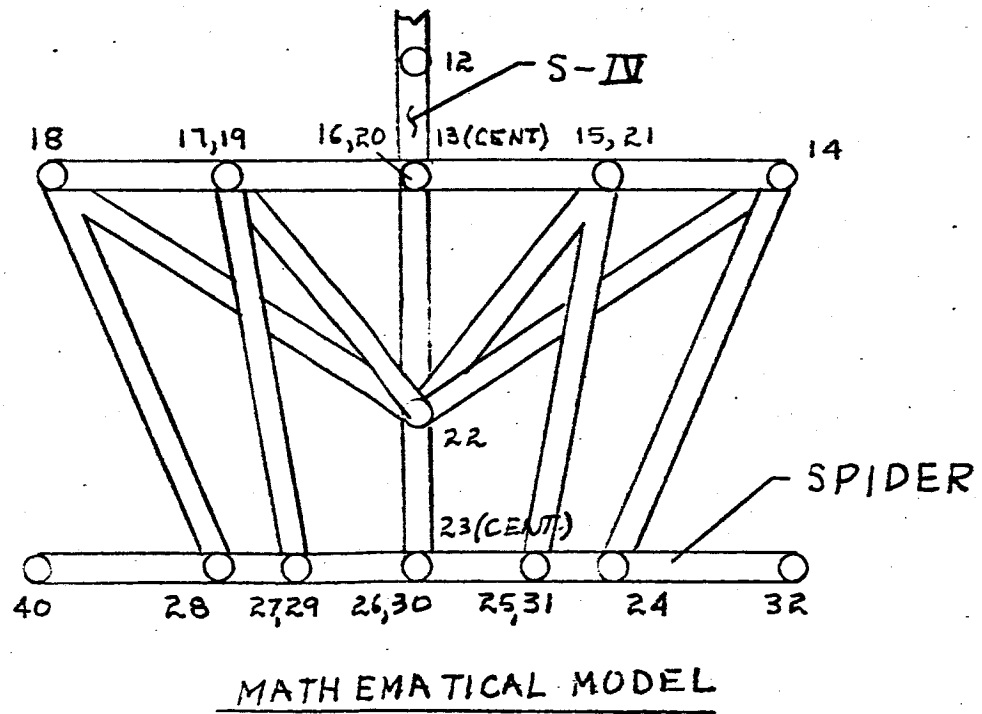
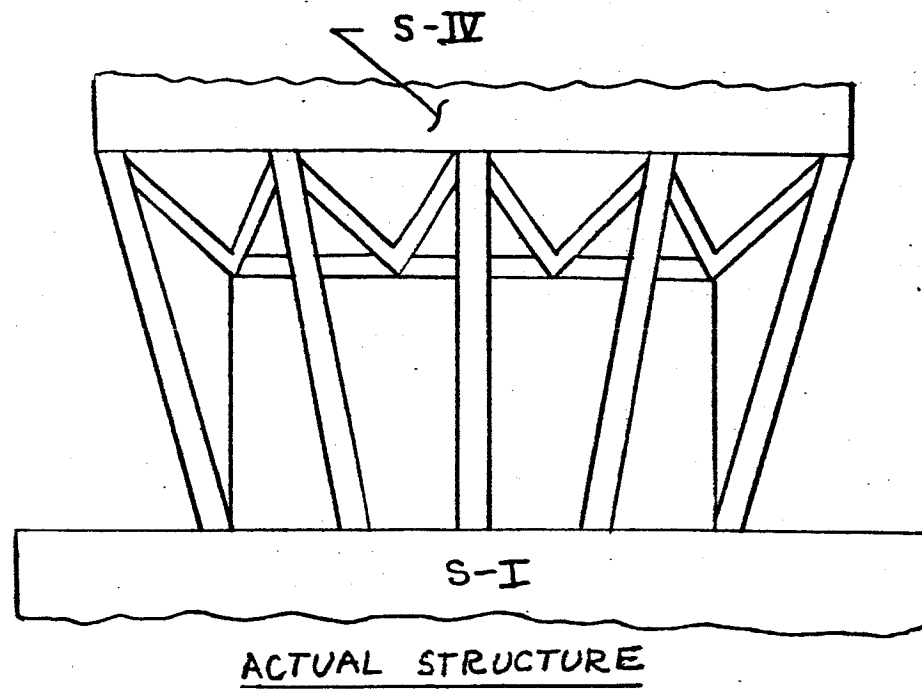
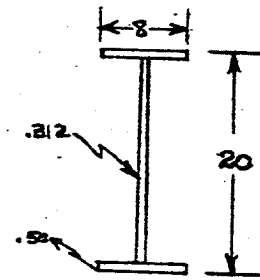
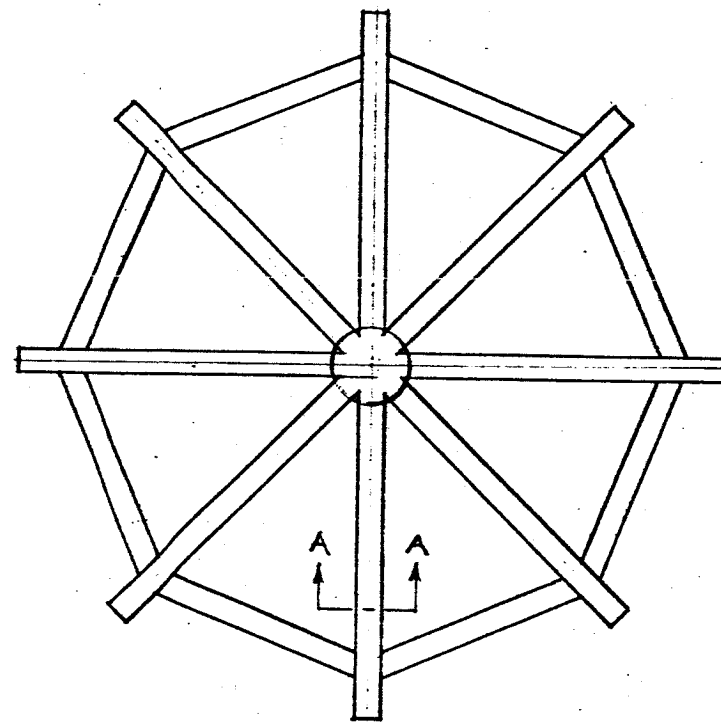


FIG. 14 TRANSITION SECTION

FIG 15 SPIDER ASSEMBLY



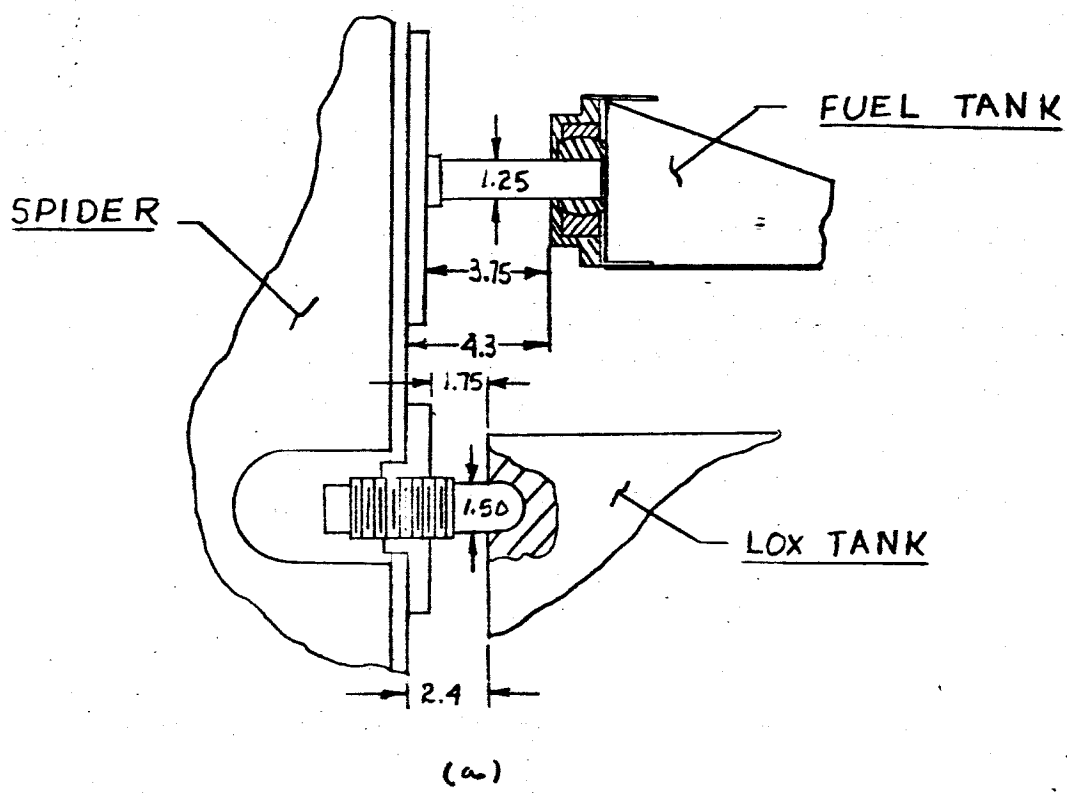
A-A  
(TYPICAL)

$$I_{MAX} = 939 \text{ IN}^4$$

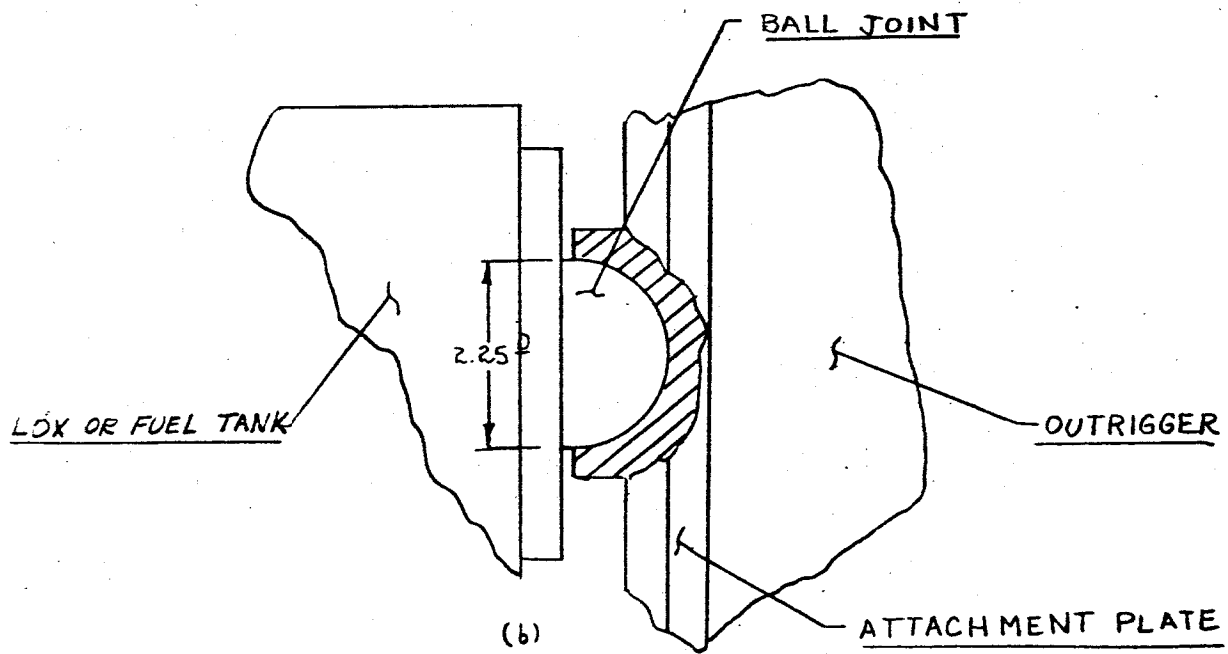
$$I_{MIN} = 42.7 \text{ IN}^4$$

$$E = 10.3 \times 10^6$$

$$G = 3.9 \times 10^6$$

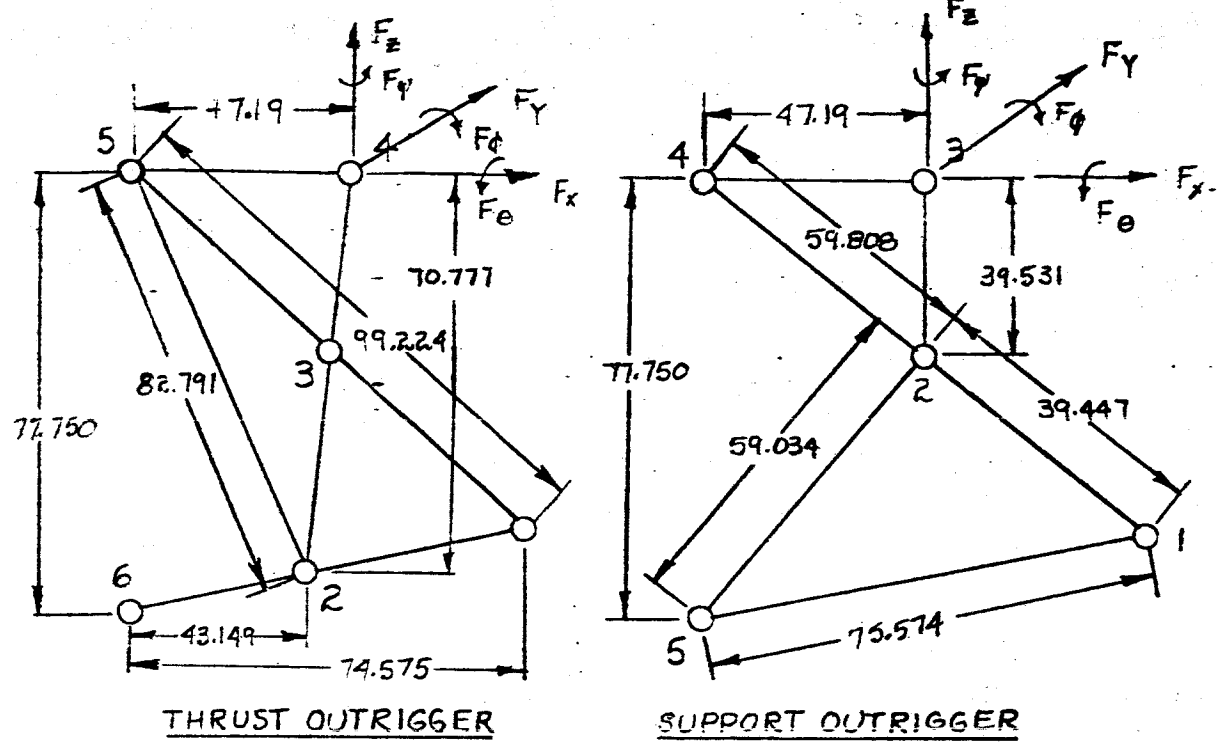


(a)



(b)

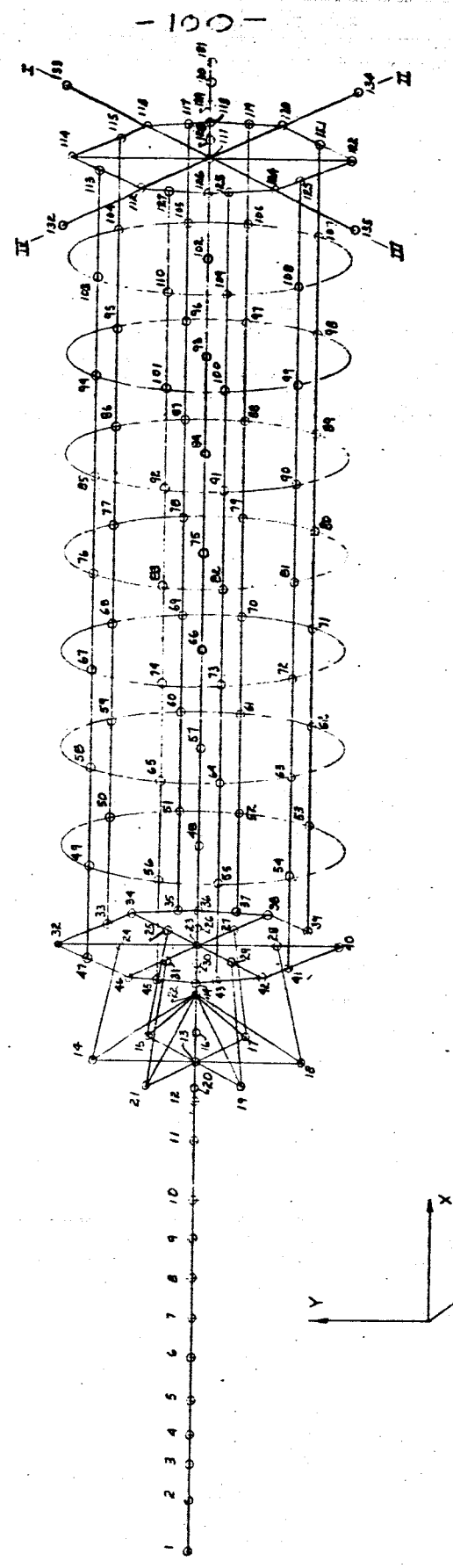
FIG. 16 OUTER TANK ATTACHMENT POINTS

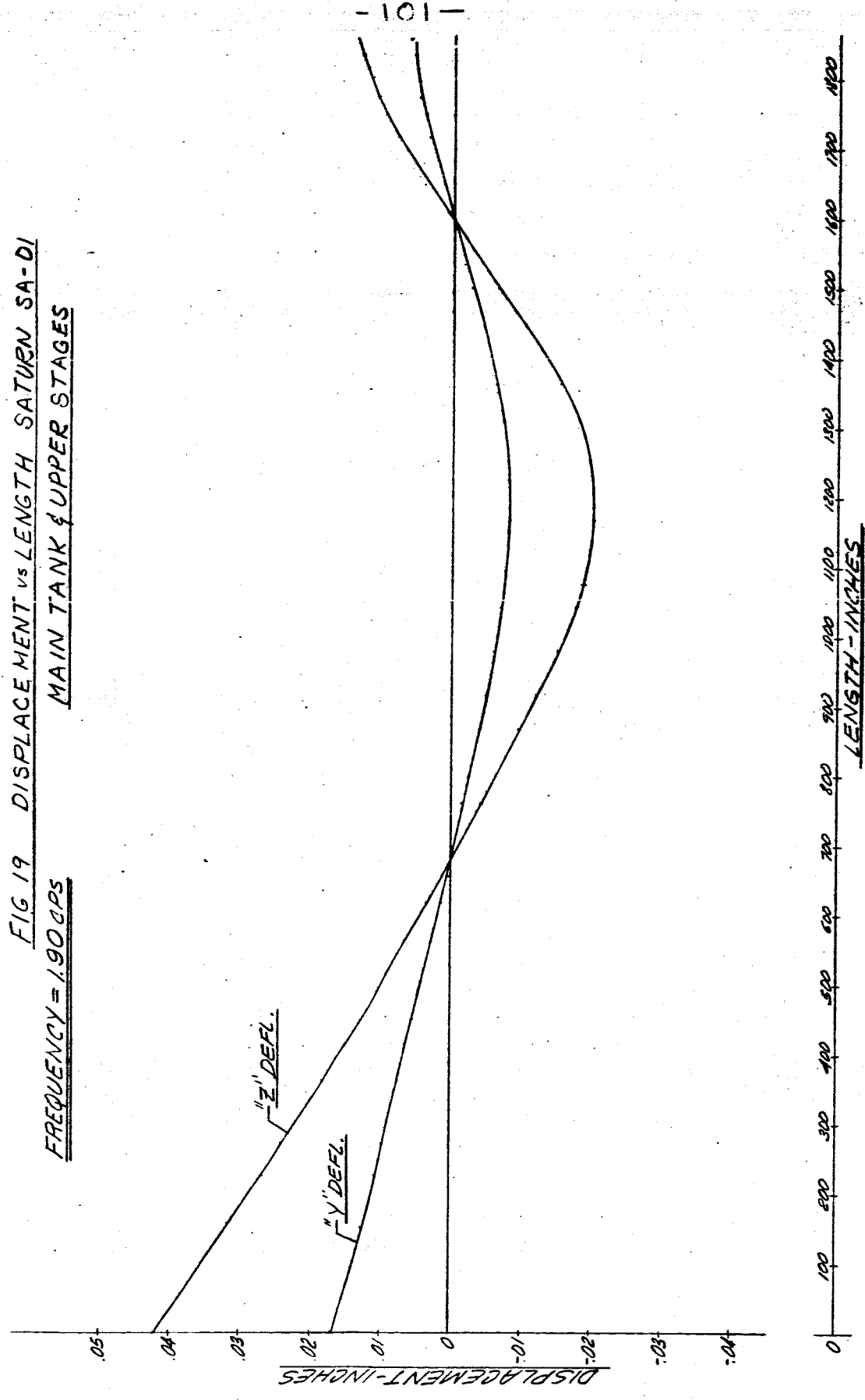


BEAM	THRUST OUTRIGGER						SUPPORT OUTRIGGER					
	$E \times 10^6$ #/ $\text{IN}^2$	$G \times 10^6$ #/ $\text{IN}^2$	AREA $\text{IN}^2$	$I_{\text{MAX}}$ $\text{IN}^4$	$I_{\text{MIN}}$ $\text{IN}^4$	$\mu$ #/ $\text{IN}^3$	$E \times 10^6$ #/ $\text{IN}^2$	$G \times 10^6$ #/ $\text{IN}^2$	AREA $\text{IN}^2$	$I_{\text{MAX}}$ $\text{IN}^4$	$I_{\text{MIN}}$ $\text{IN}^4$	$\mu$ #/ $\text{IN}^3$
1-2	10.3	3.9	12.54	365.9	124.8	.101	10.3	3.9	9.75	96.7	61.3	.101
1-3			9.8	97.3	78.0					12.676	236.8	126.3
1-5										15.214	262.0	142.0
2-3			14.40	230.9	131.4					9.75	96.7	61.3
2-4										12.352	220.0	122.1
2-5			9.84	101.7	83.9							
2-6			19.33	272.8	245.8							
3-4			14.40	230.9	131.4					3.188	25.0	2.76
3-5			9.80	97.3	78.0							
4-5			3.188	25.0	2.76							

FIG. 17 SATURN OUTRIGGERS

FIG. 18 MATHEMATICAL MODEL - SATURN SA-01





- 192 -

FIG 20 DISPLACEMENT VS LENGTH SATURN SA-D1  
FREQUENCY = 1.90 CPS.

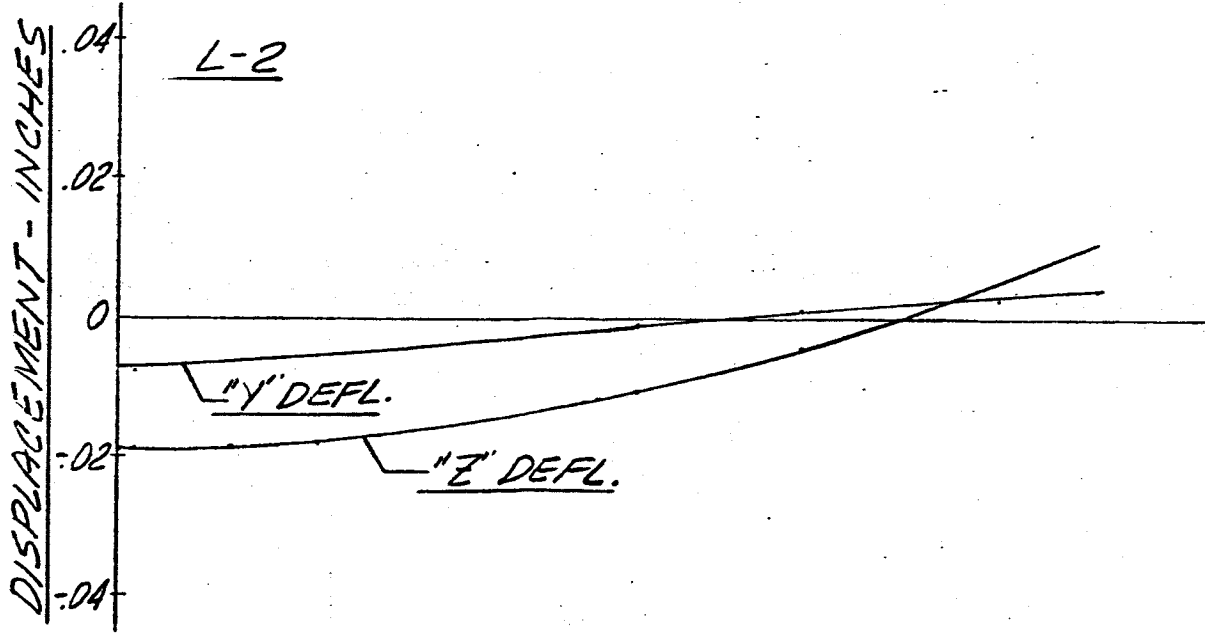
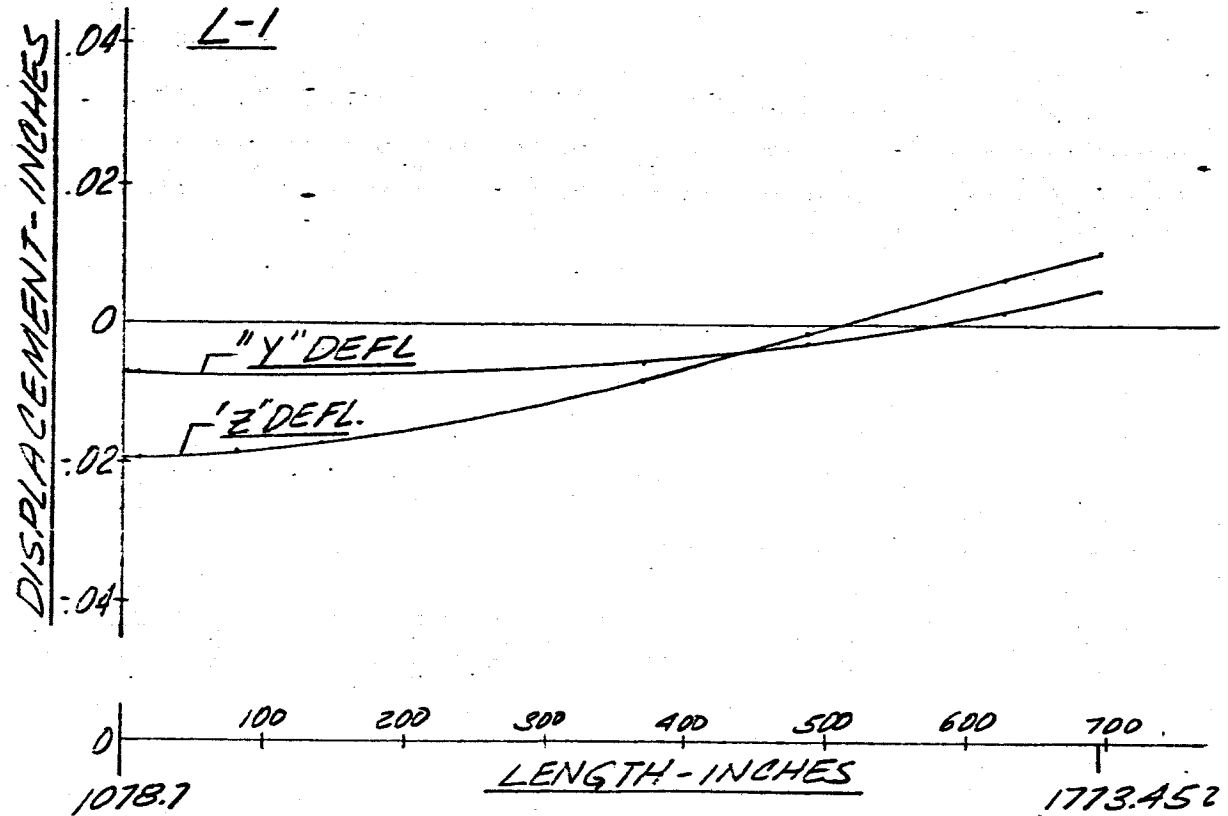
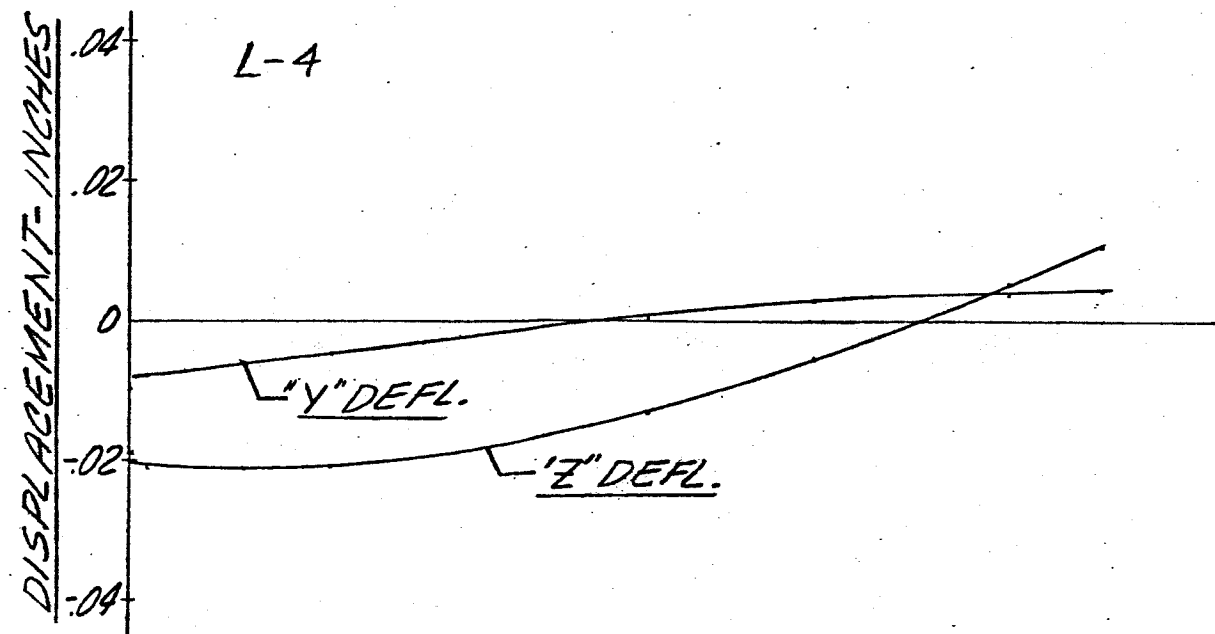
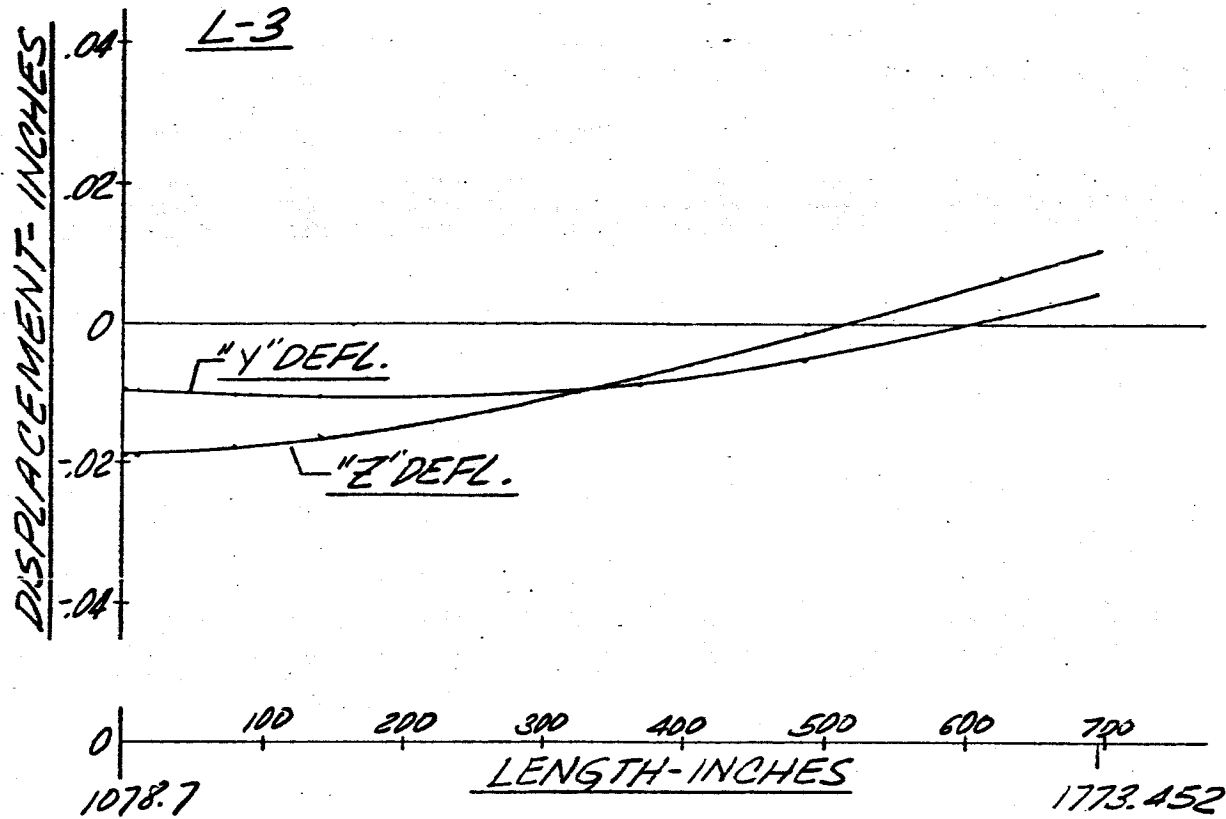


FIG 21 DISPLACEMENT VS LENGTH SATURN SA-D1

FREQUENCY = 1.90 CPS



- 109 -

FIG 22 DISPLACEMENT VS LENGTH SATURN SA-D1

FREQUENCY = 1.90 CPS

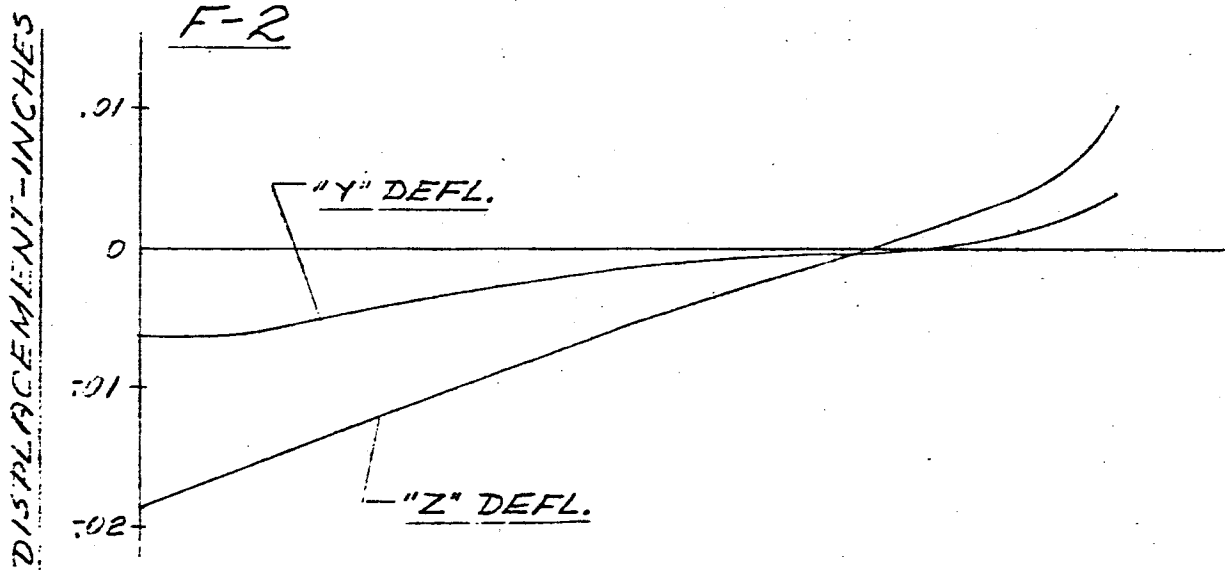
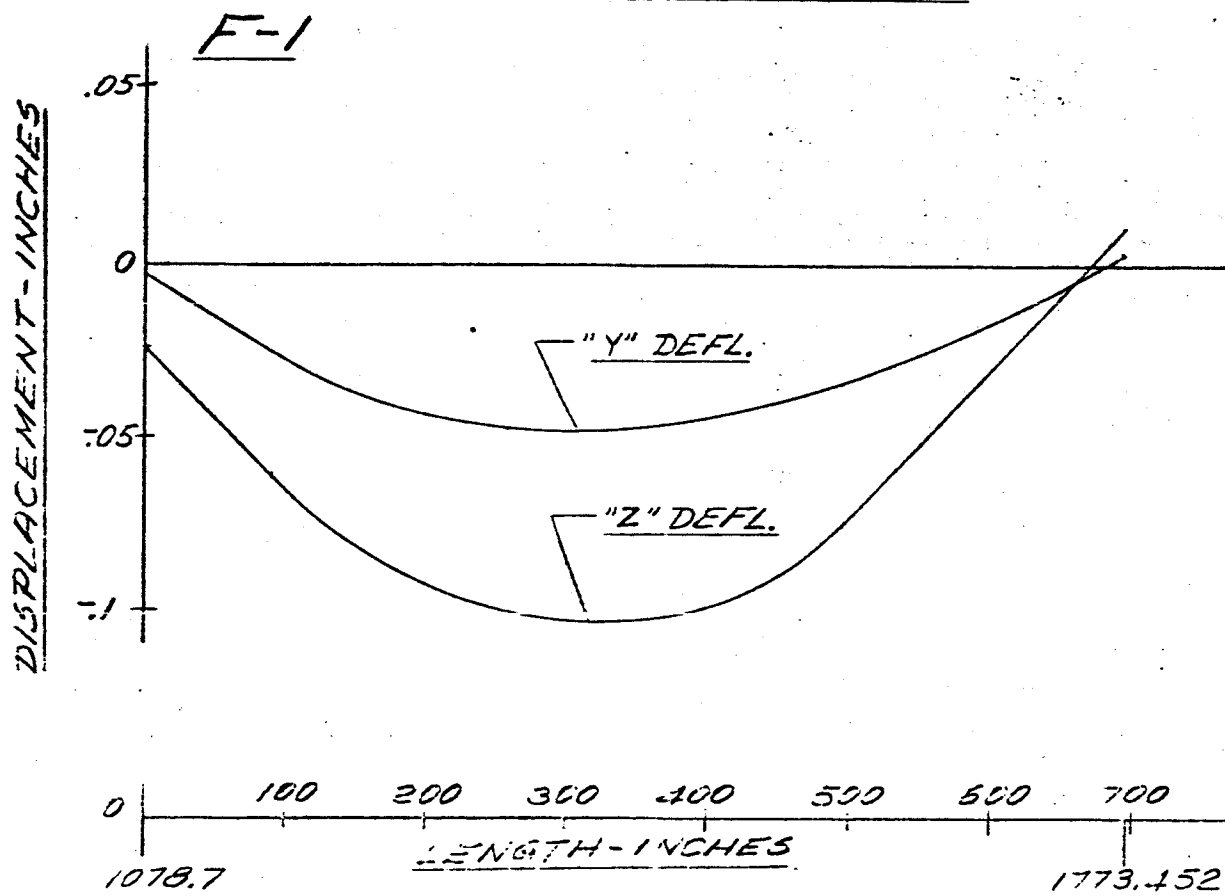


FIG. 23 DISPLACEMENT VS LENGTH SATURN SA-D1

FREQUENCY = 1.90 CPS

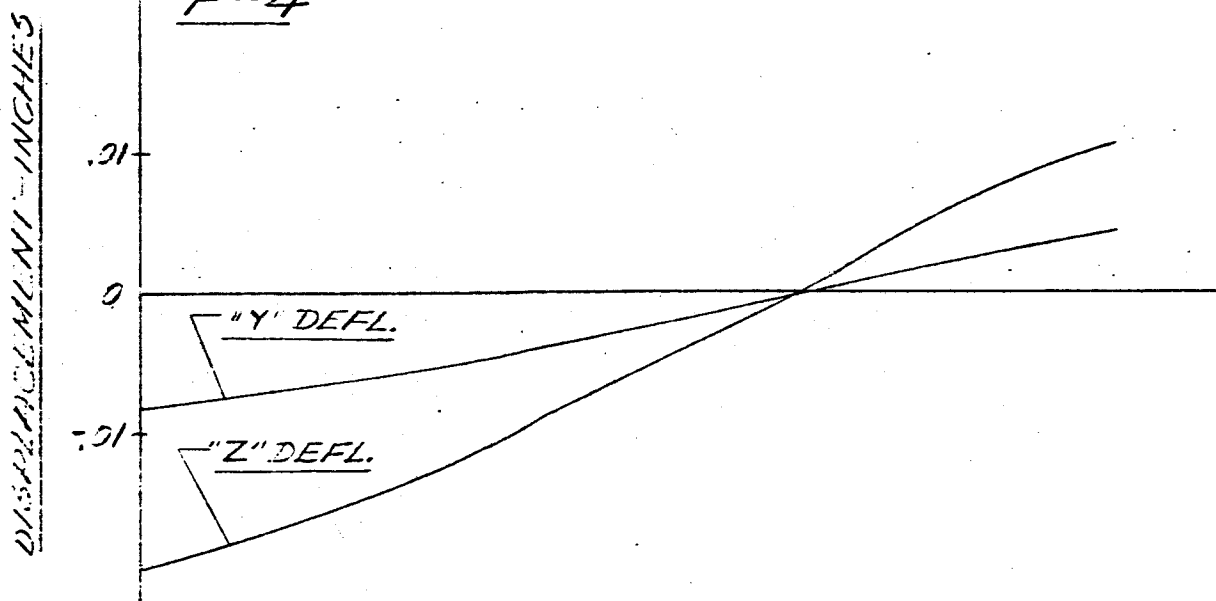
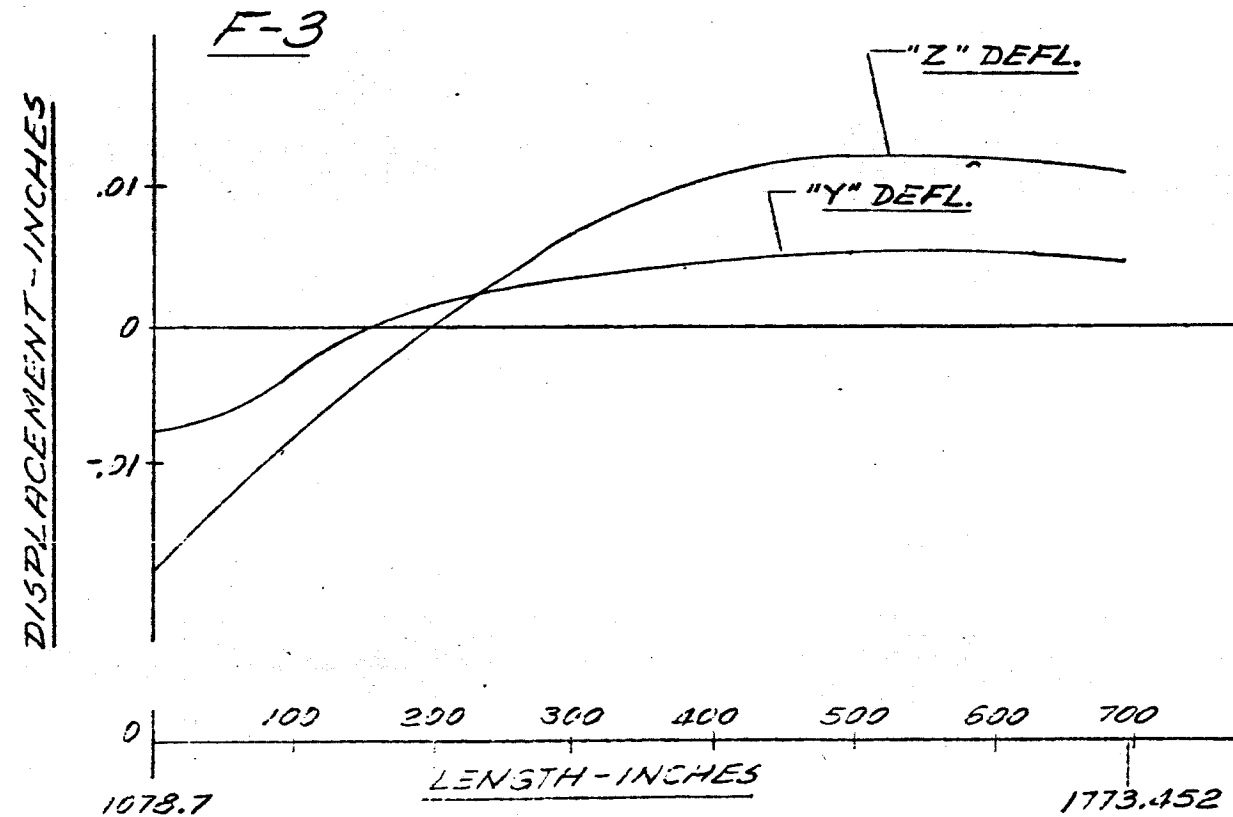
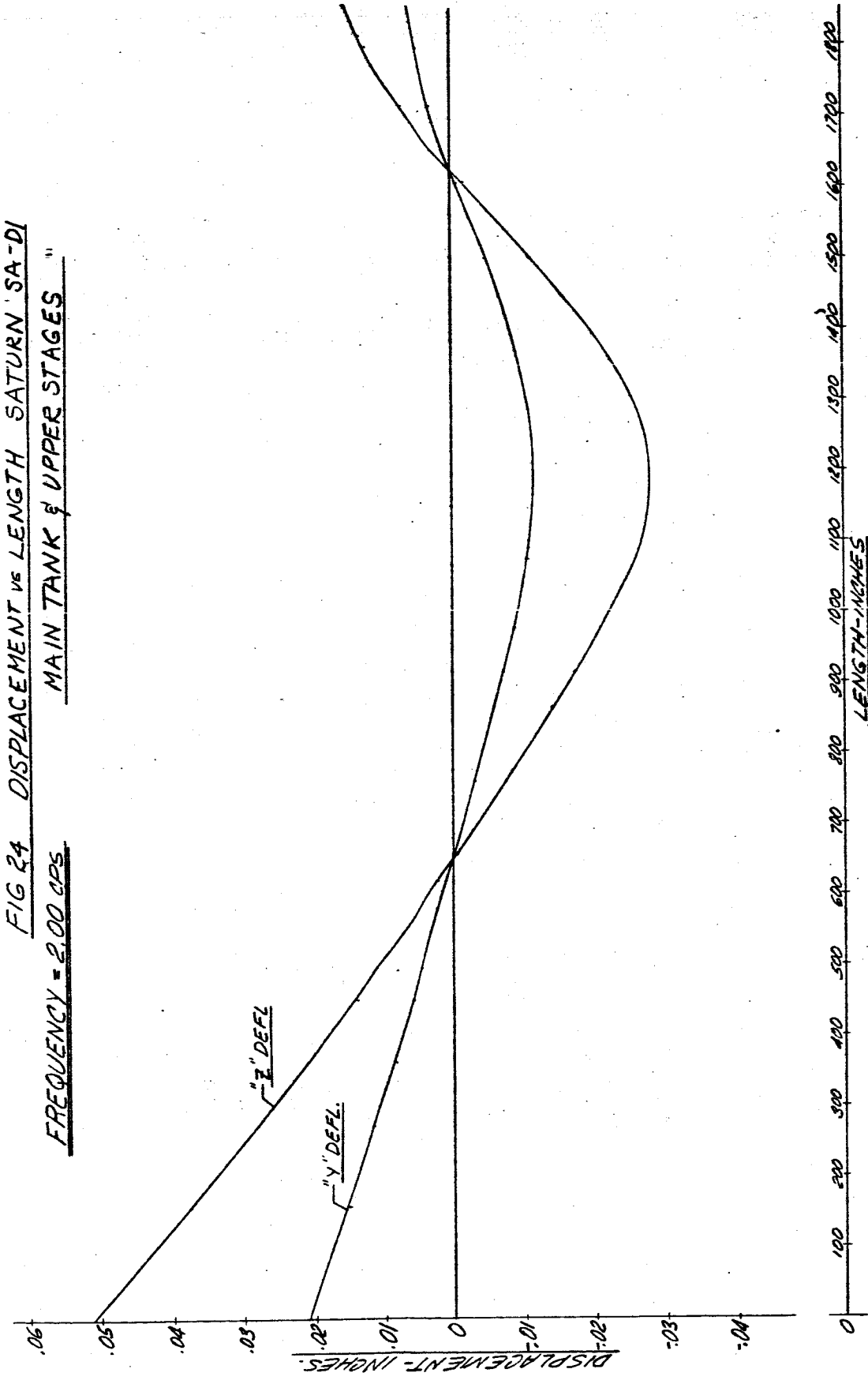


FIG 24 DISPLACEMENT vs LENGTH SATURN 'SA-DI  
MAIN TANK & UPPER STAGES"

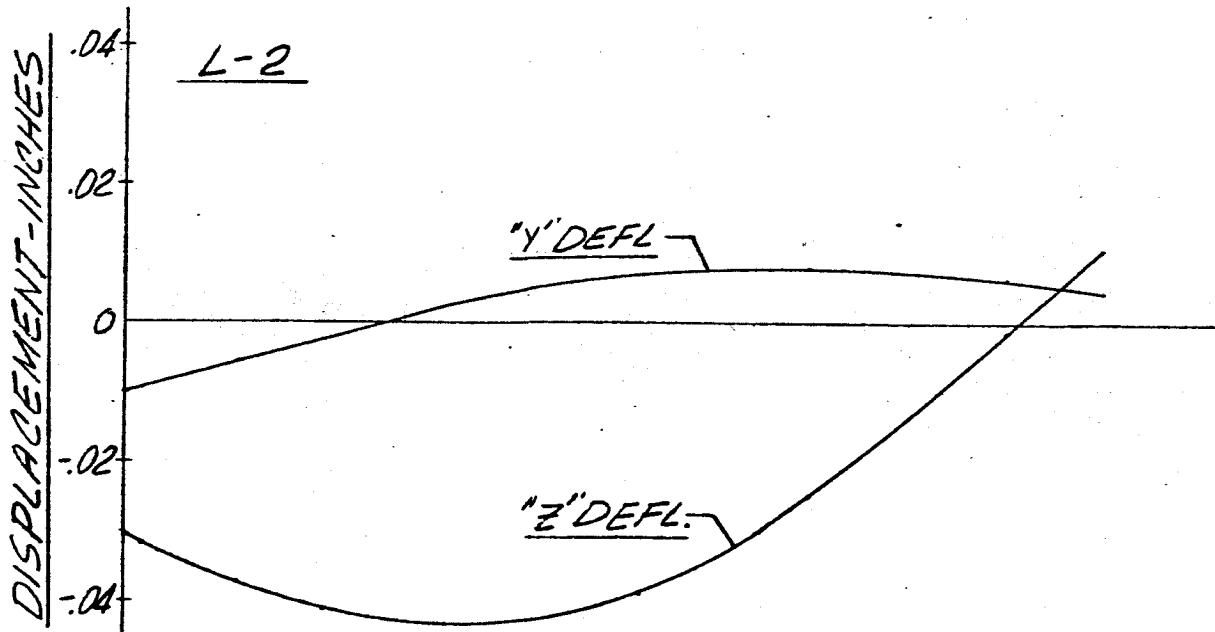
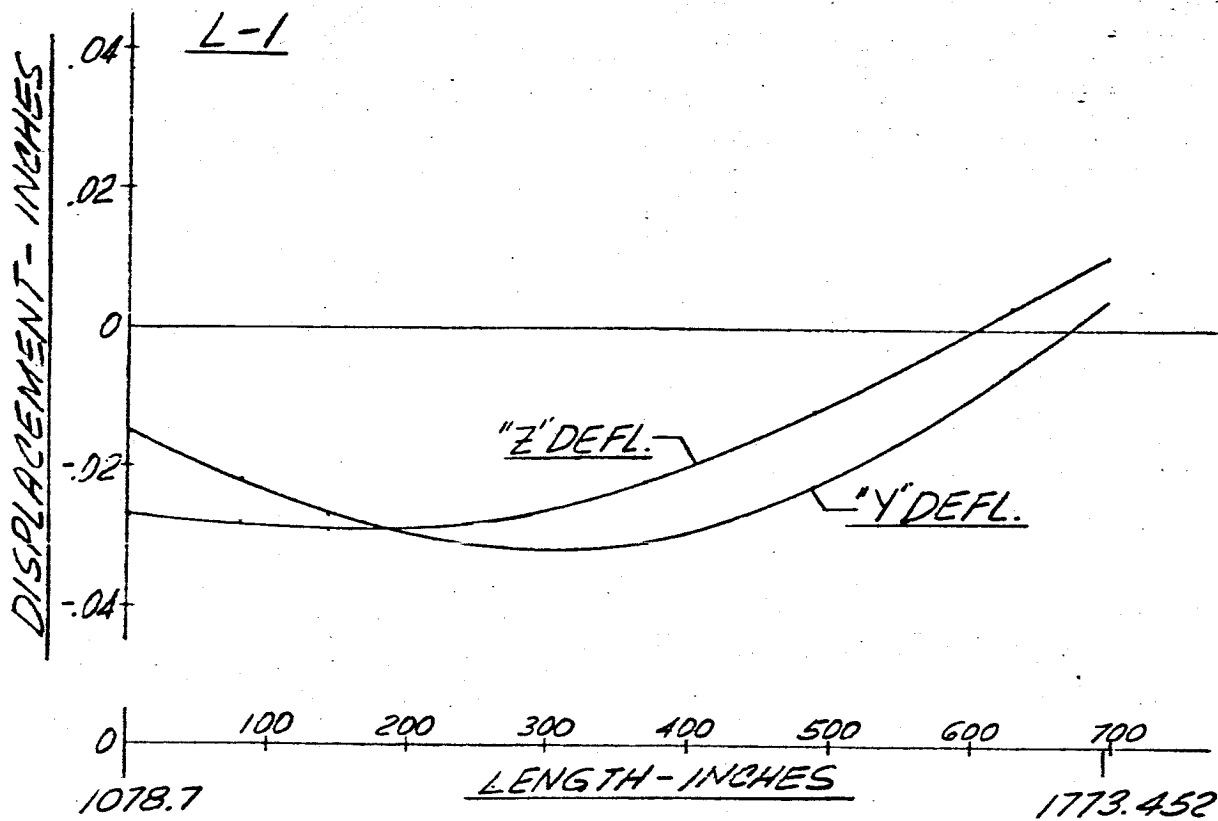
FREQUENCY = 2.00 cps



-107-

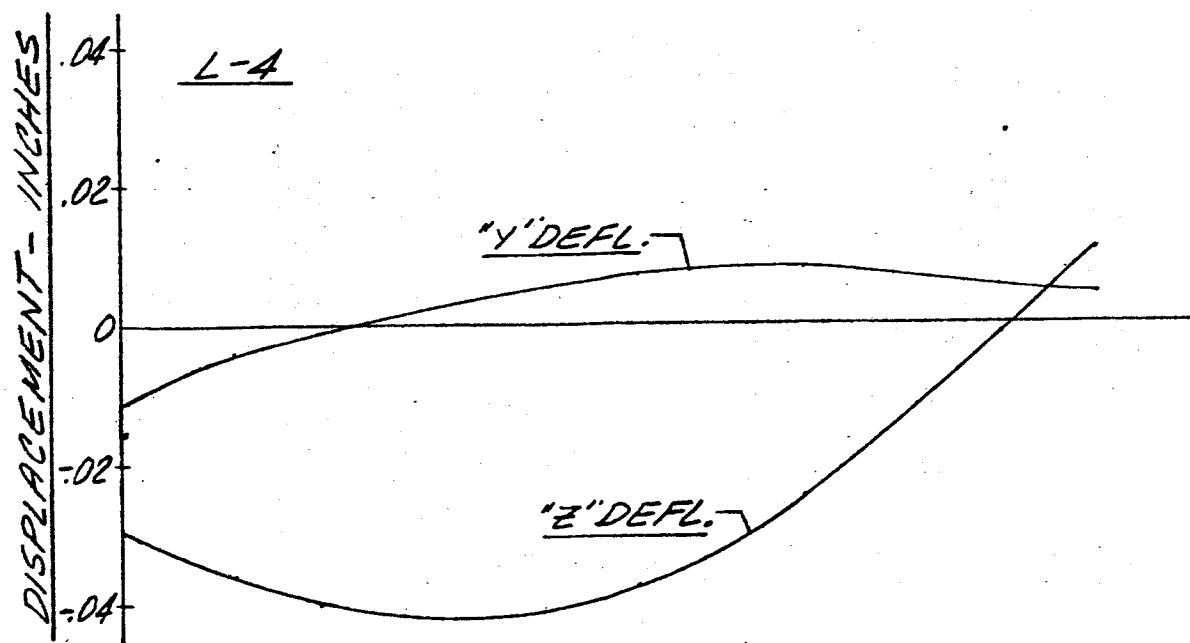
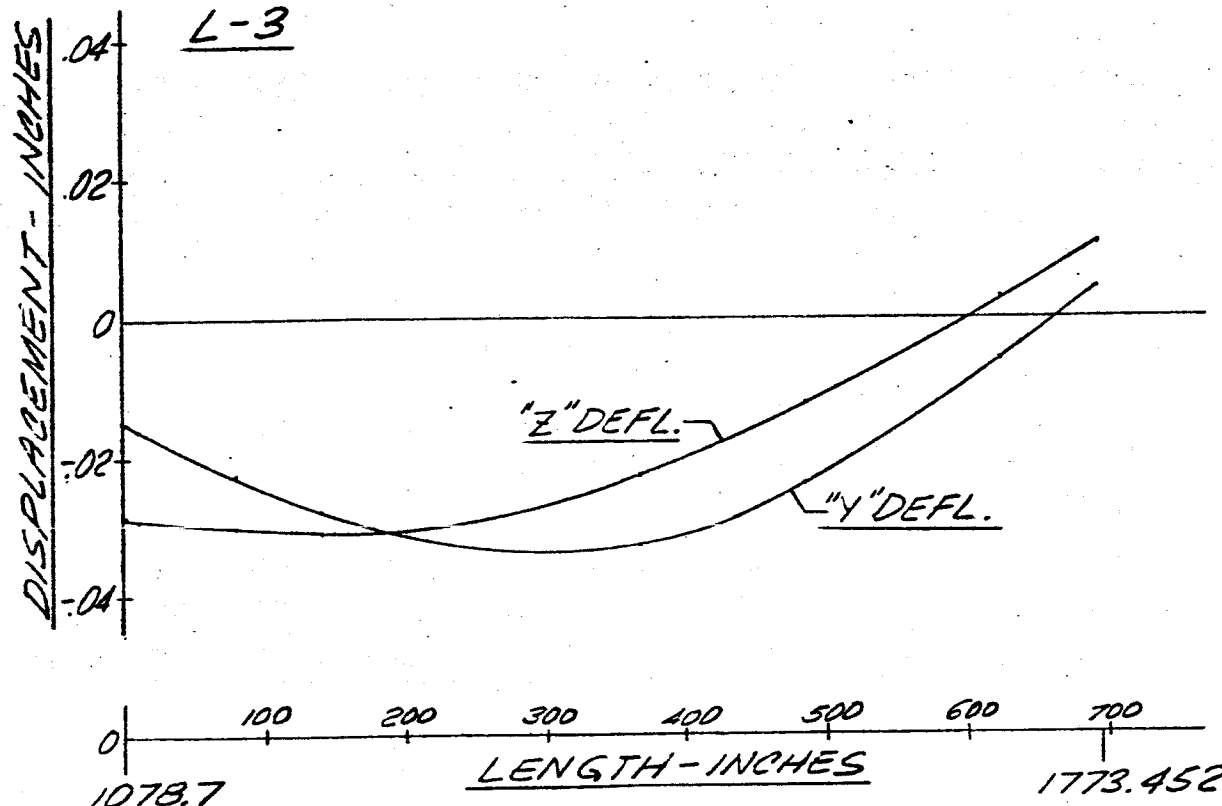
FIG 25 DISPLACEMENT VS LENGTH SATURN SA-DI

FREQUENCY = 2.00 CPS.



-108-

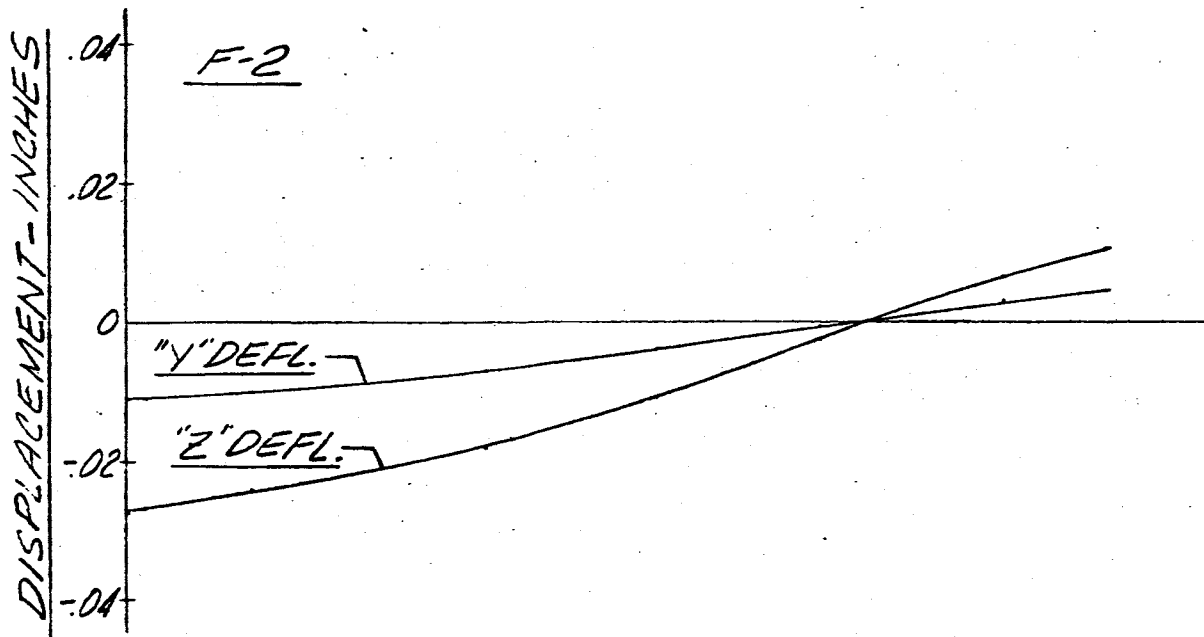
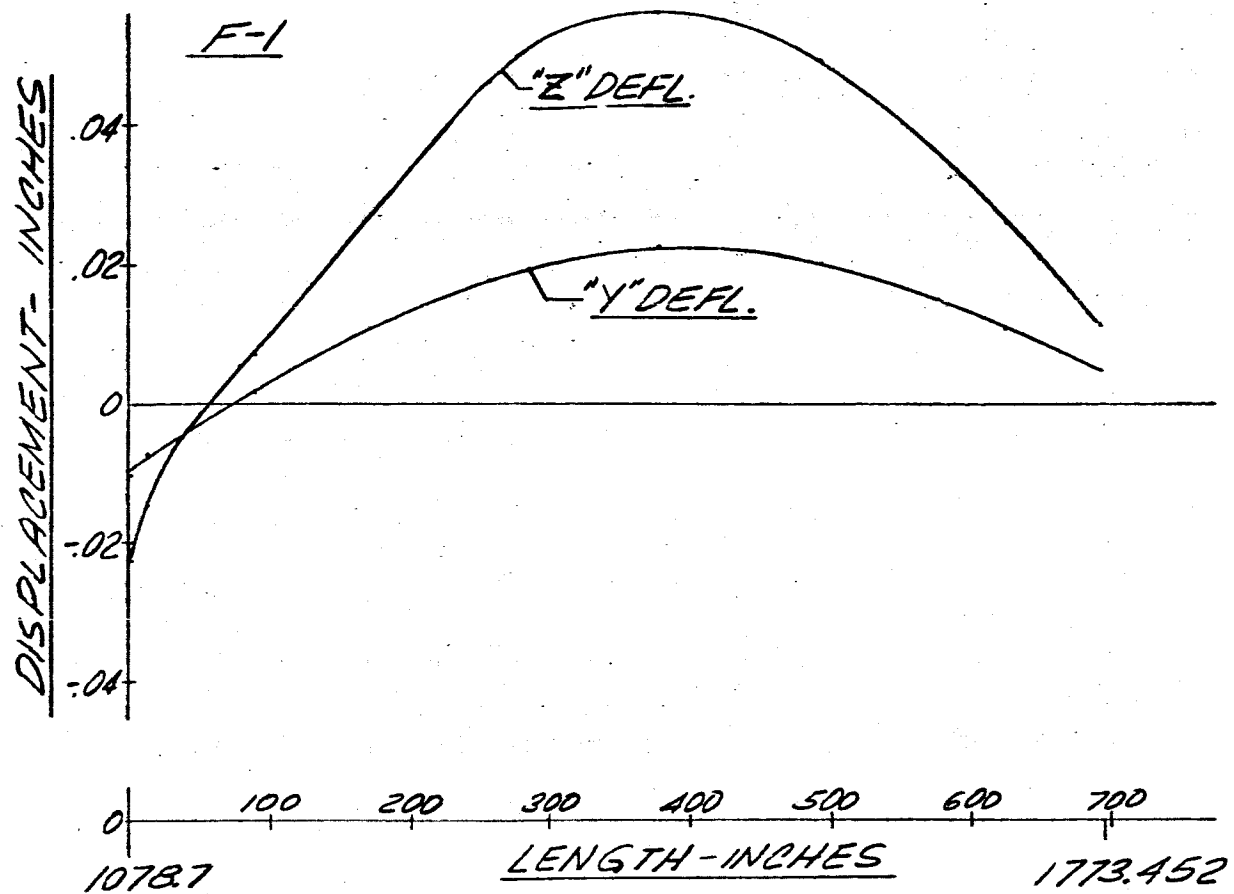
FIG 2.6 DISPLACEMENT VS LENGTH SATURN SA-D1  
FREQUENCY = 2.00 CPS



-109-

FIG 27 DISPLACEMENT VS LENGTH SATURN SA-D1

FREQUENCY = 2.00 CPS



-110-

FIG 2E DISPLACEMENT VS LENGTH SATURN SA-DI  
FREQUENCY = 2.00 CPS

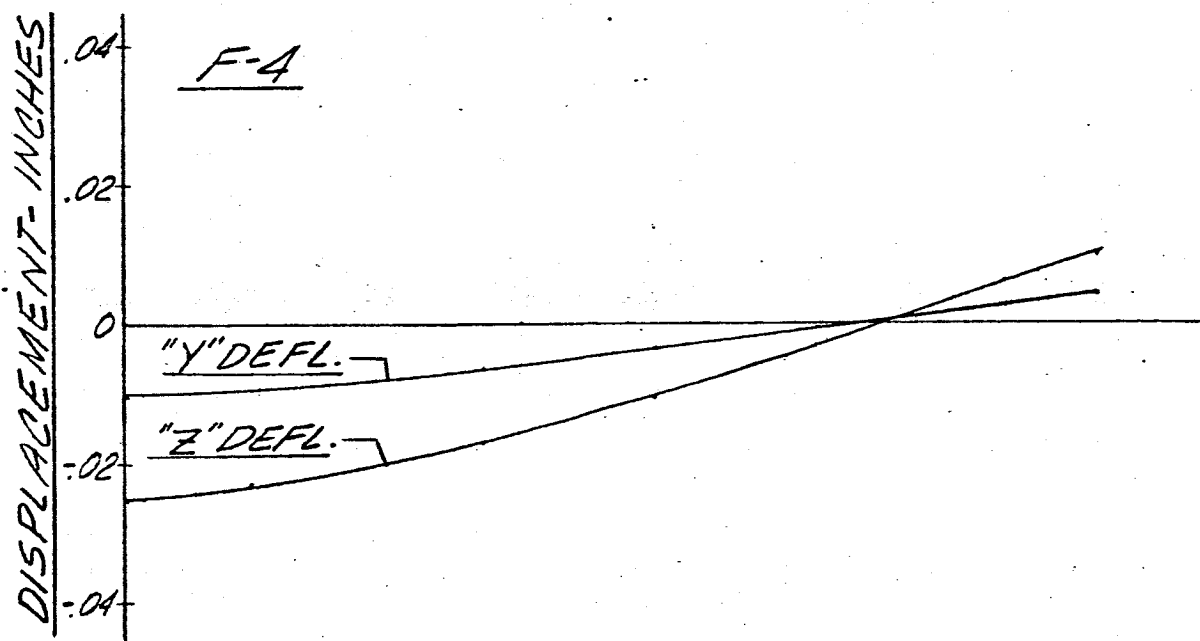
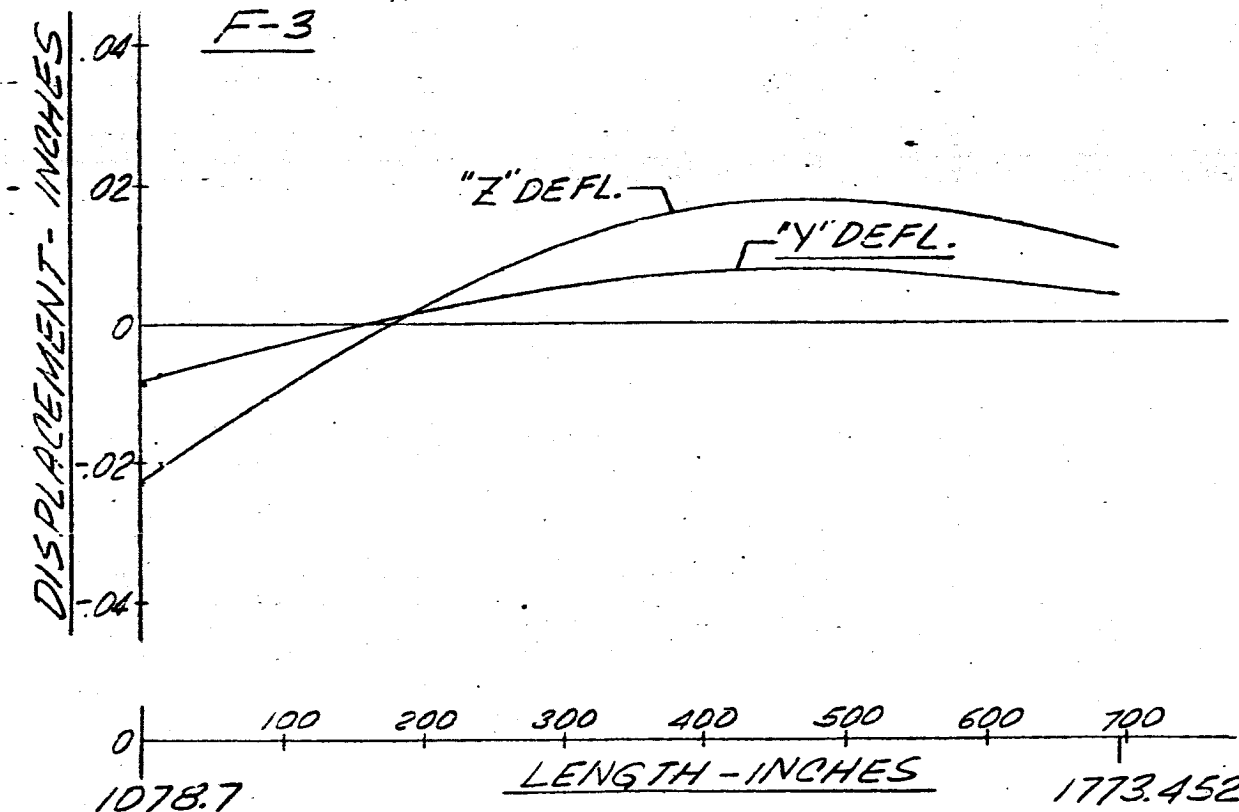
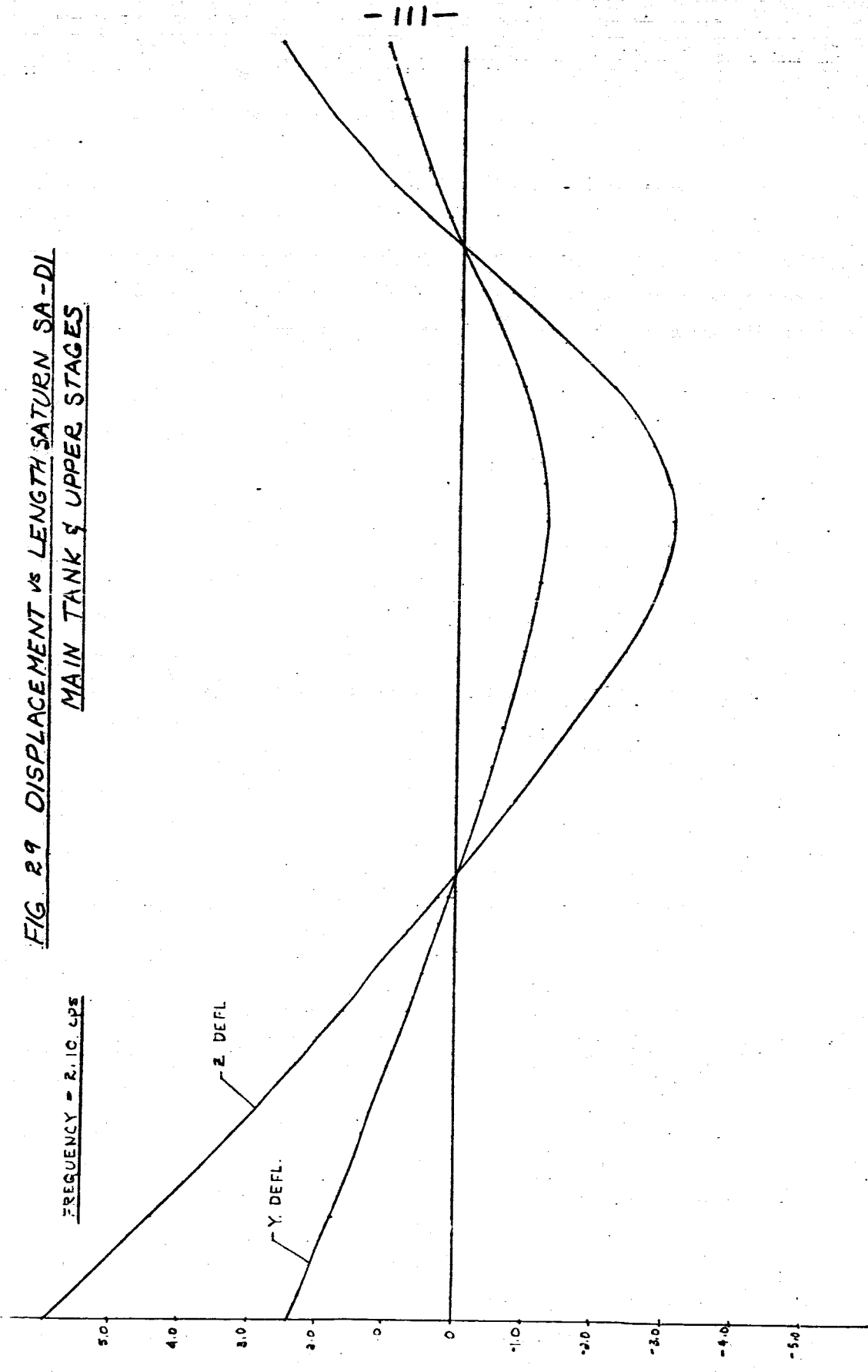


FIG. 29 DISPLACEMENT vs LENGTH SATURN SA-DL  
MAIN TANK & UPPER STAGES

FREQUENCY = 2.10 cps



-112-

FIG 30 DISPLACEMENT VS LENGTH SATURN SA-D1

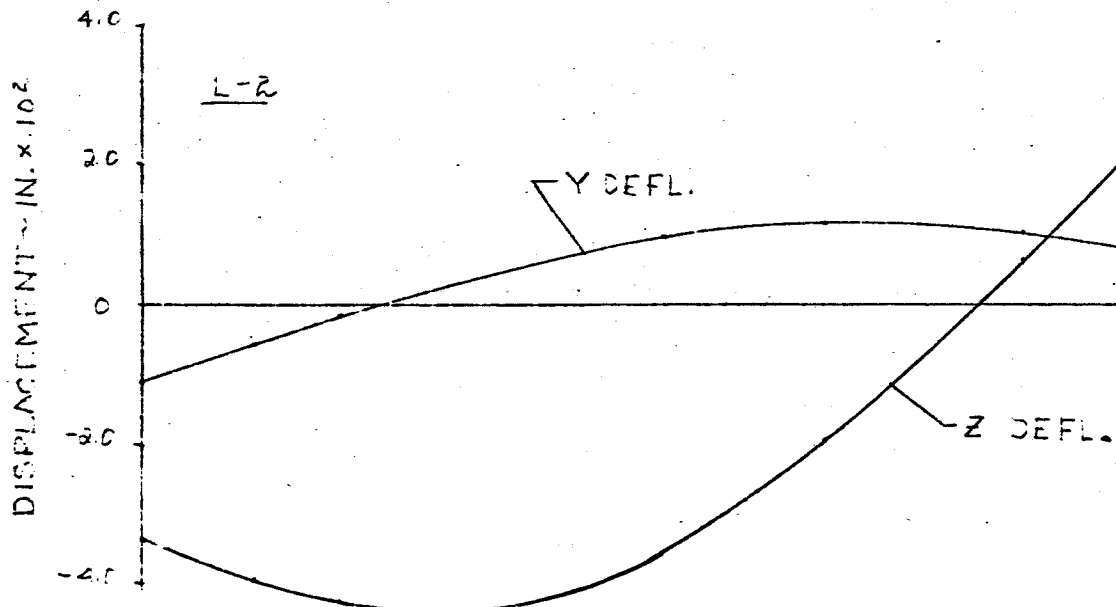
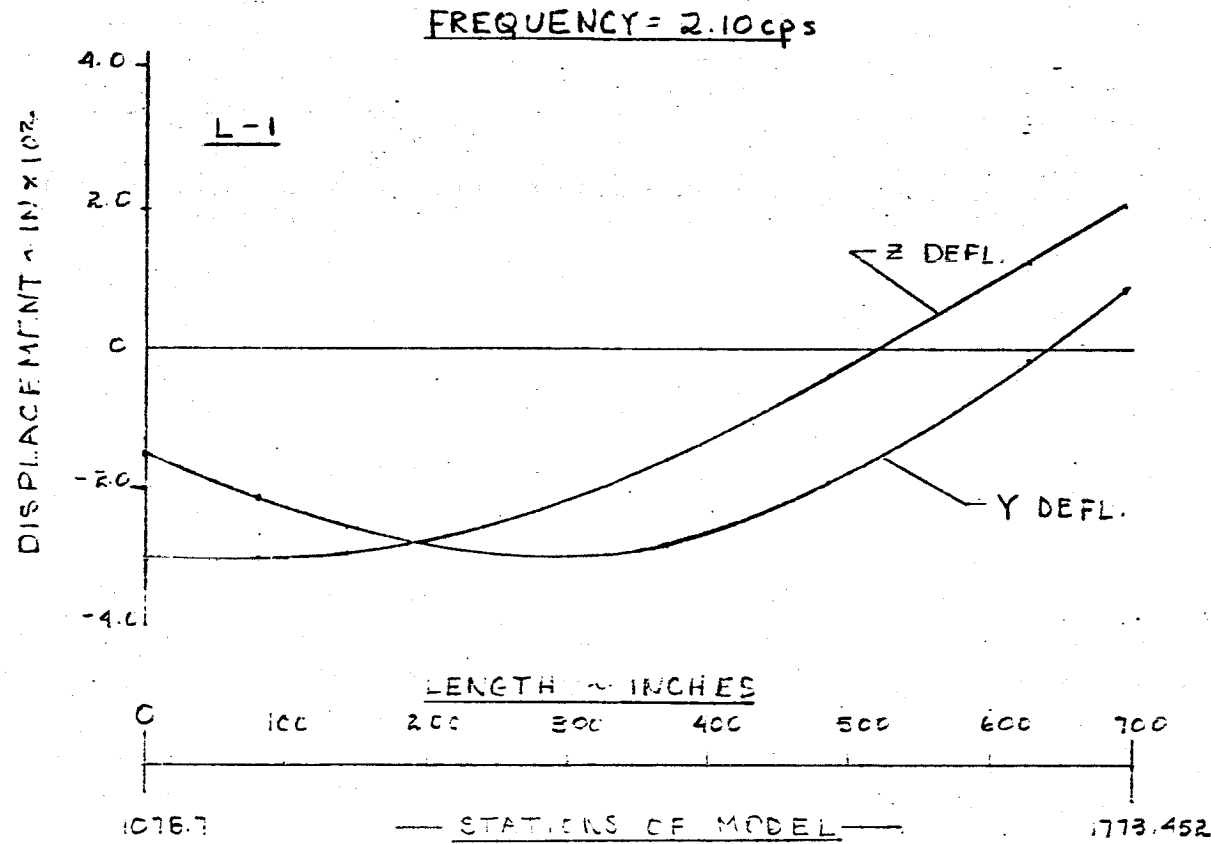


FIG 31 DISPLACEMENT VS LENGTH SATURN SA-D1

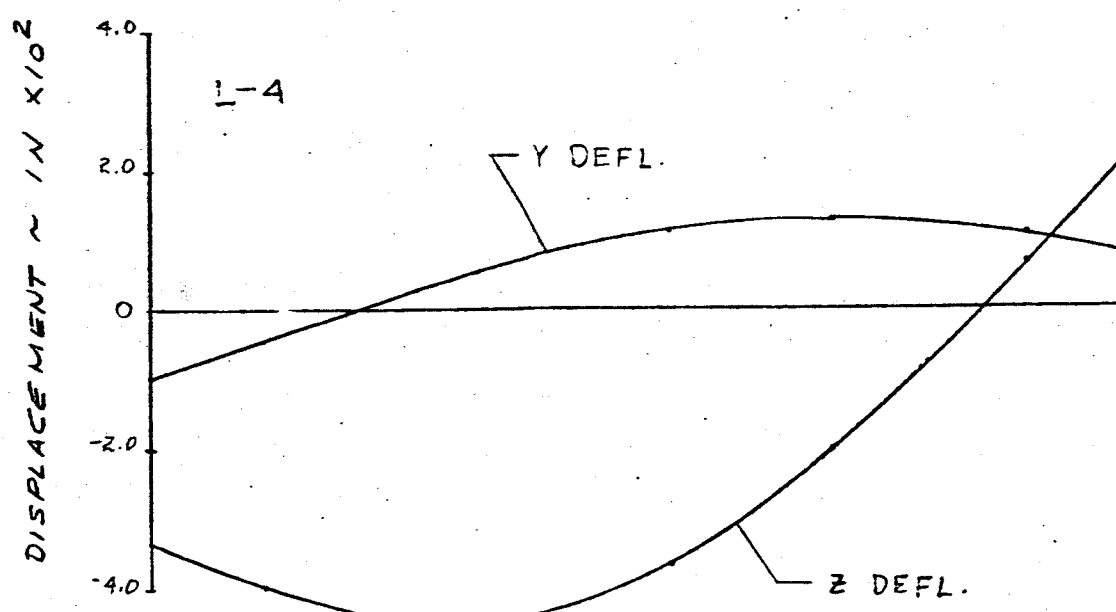
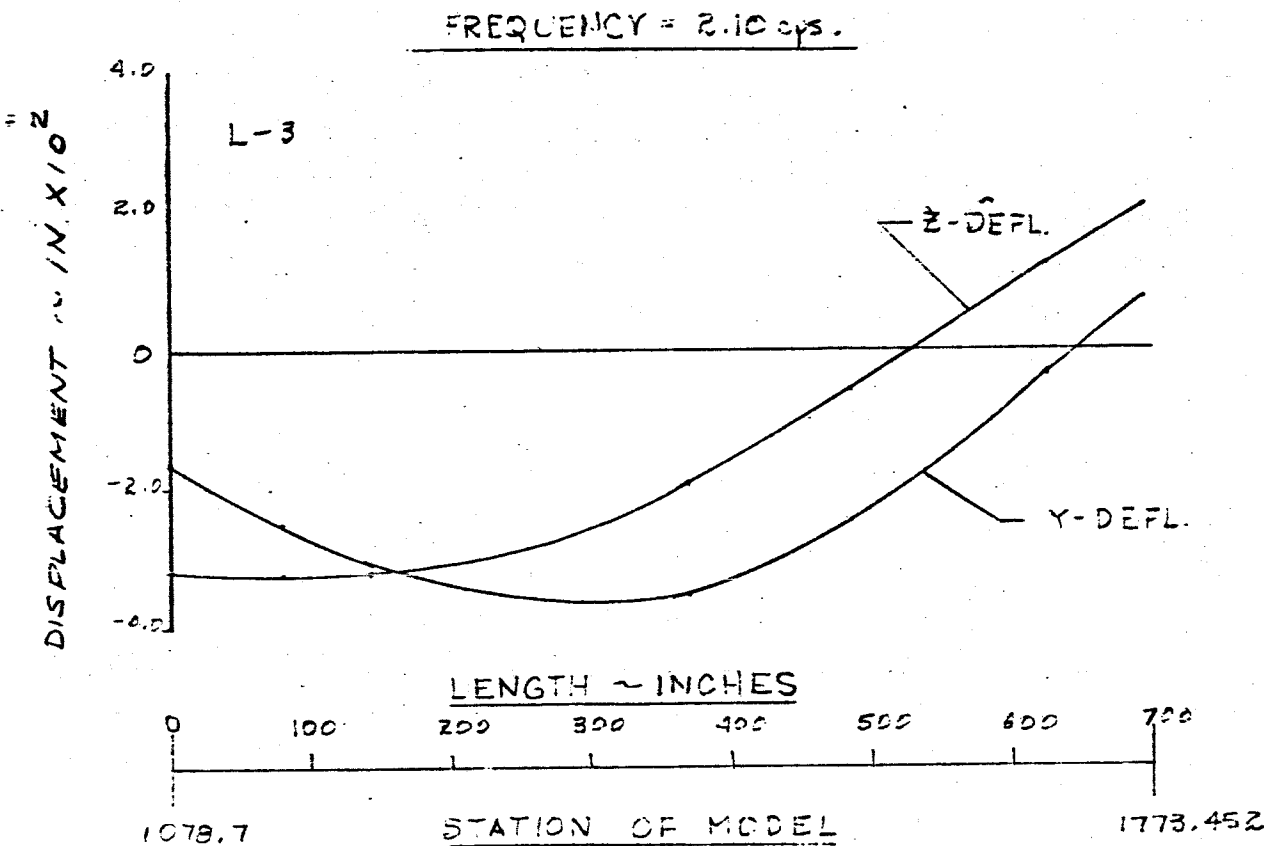
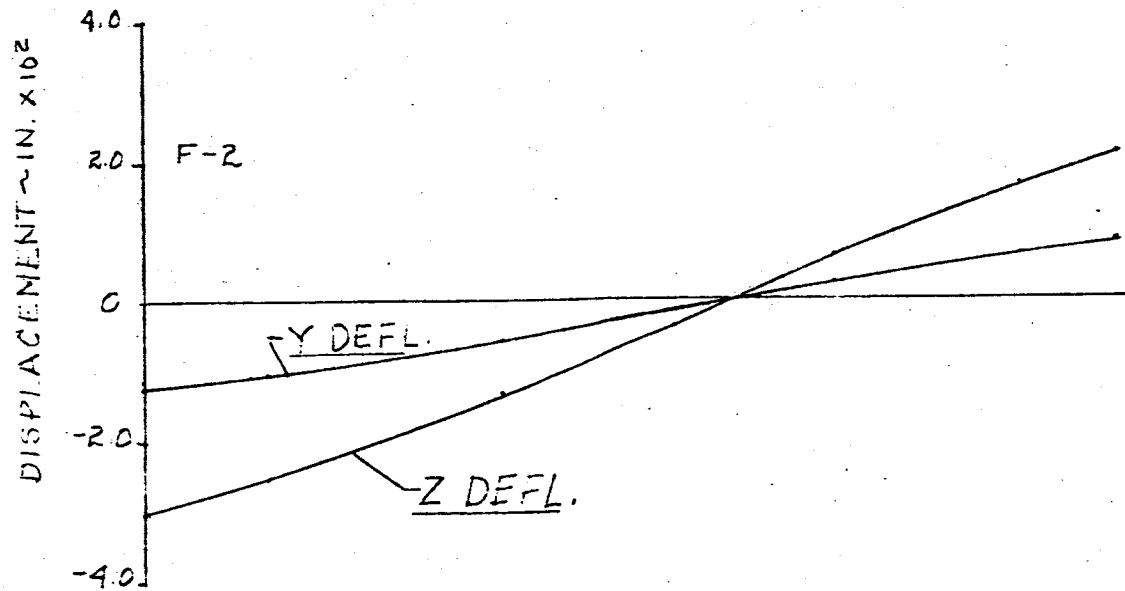
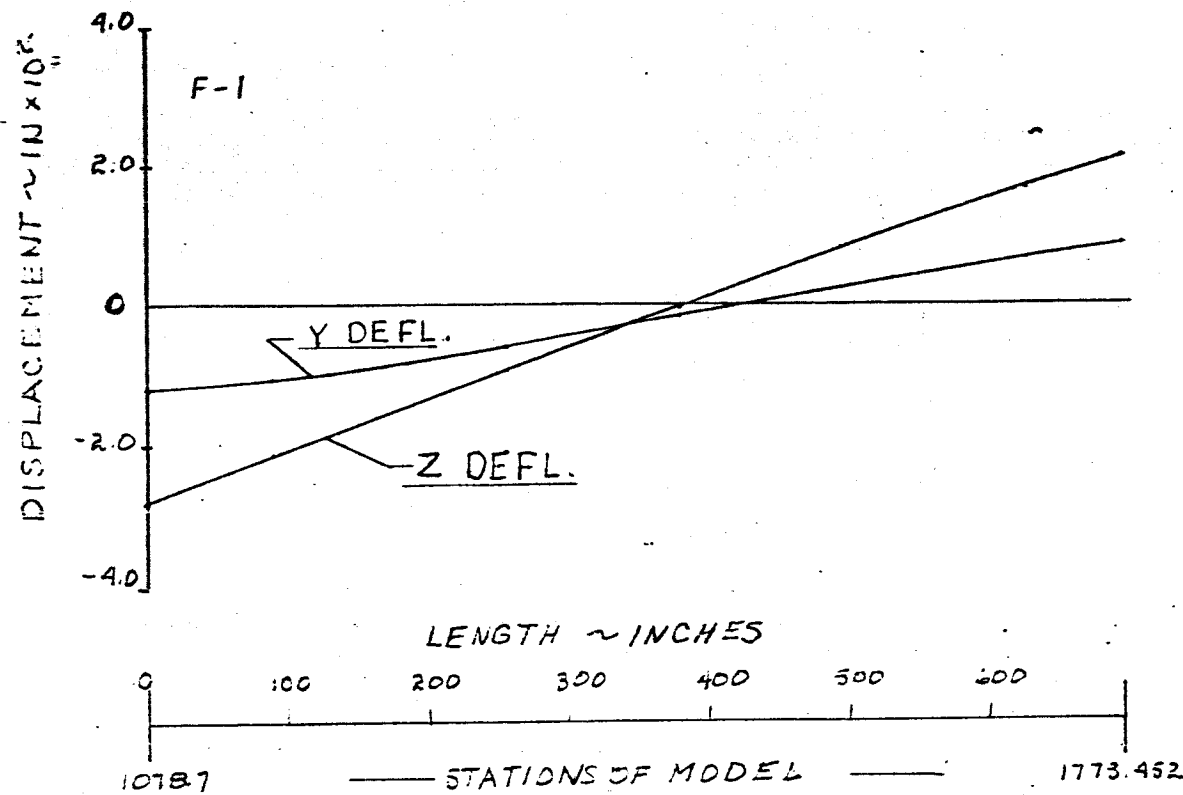


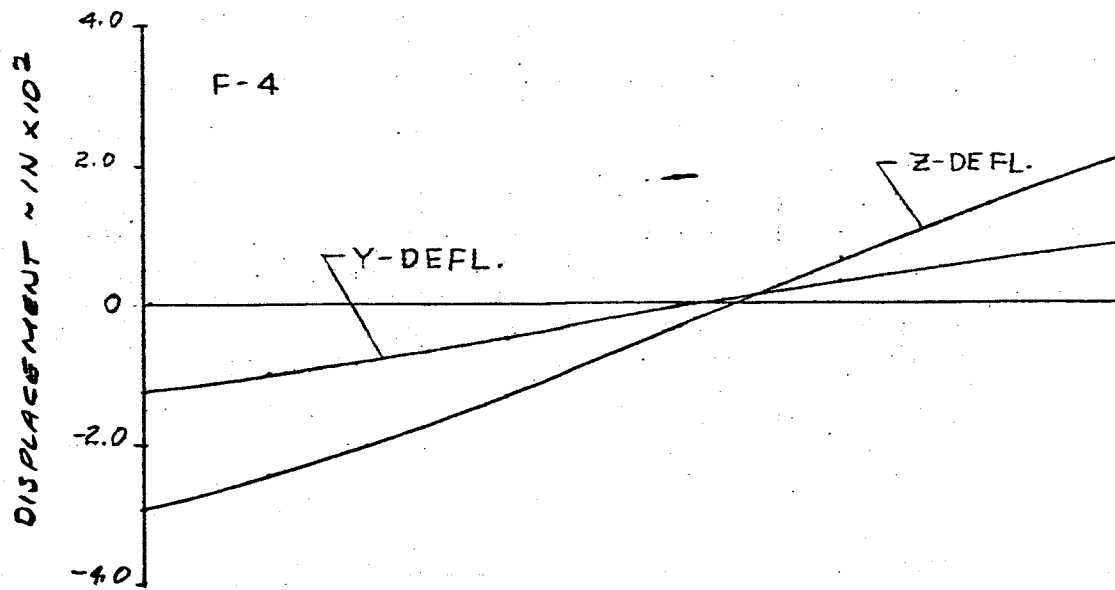
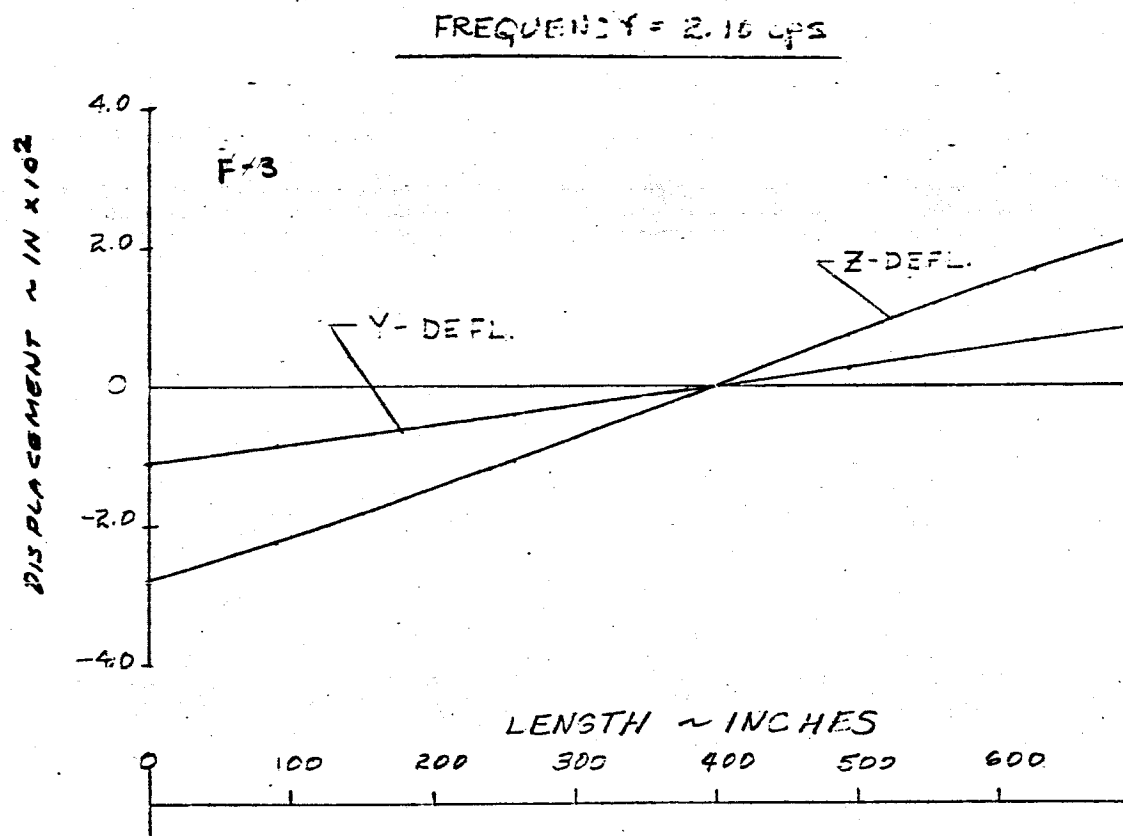
FIG 32 DISPLACEMENT VS LENGTH SATURN SA-DI

FREQUENCY = 2.10 cps



-115-

FIG 38. DISPLACEMENT VS LENGTH SATURN SA-D1



-116-

FIG. 34 DISPLACEMENT vs LENGTH SATURN SA-DI  
MAIN TANK & UPPER STAGES

FREQUENCY = 2.20 cps.

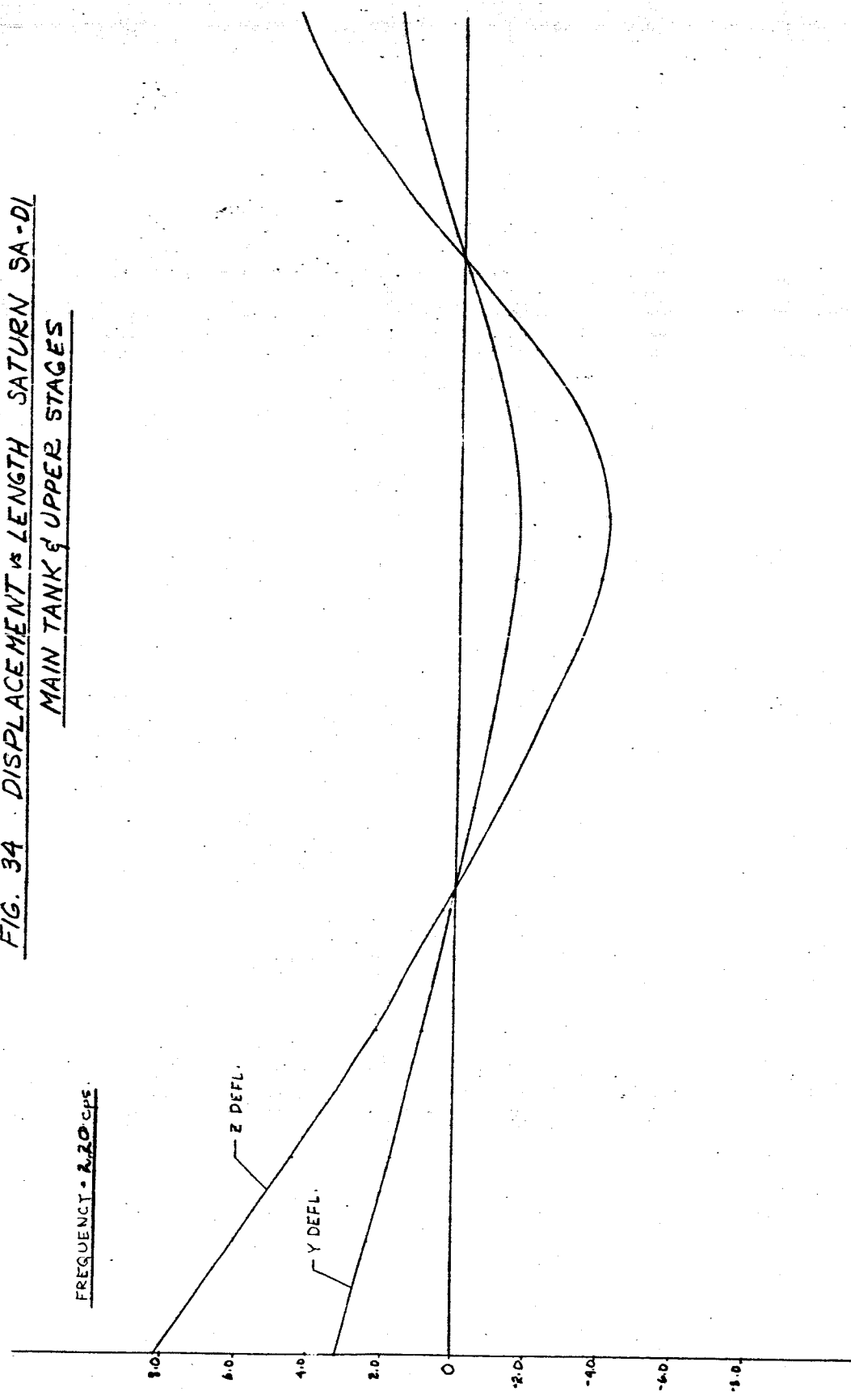
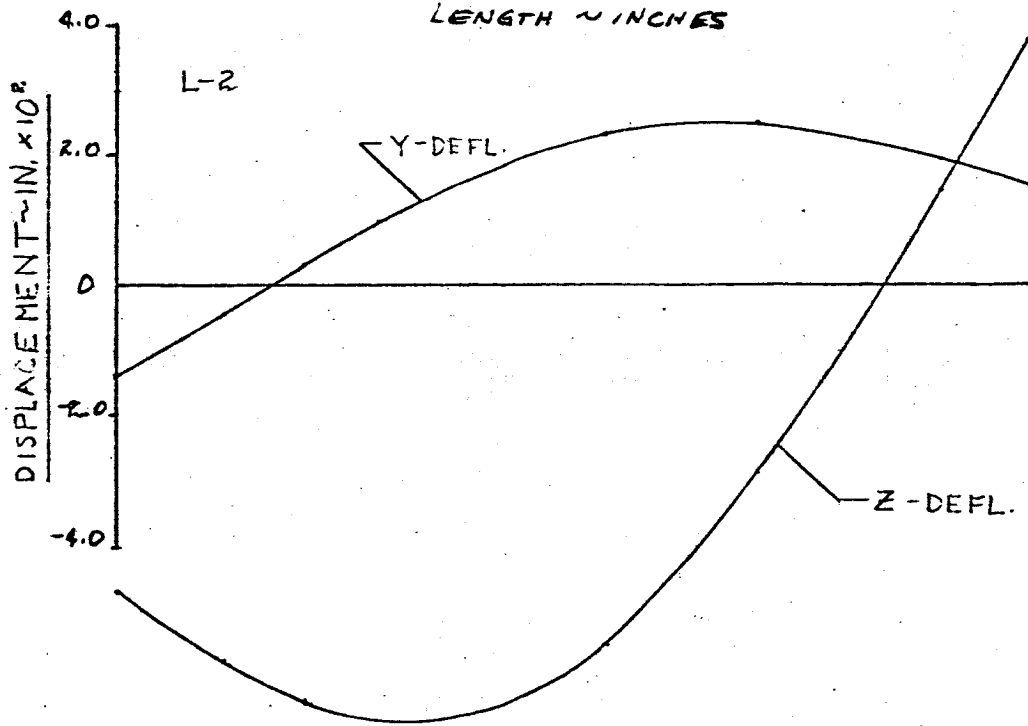
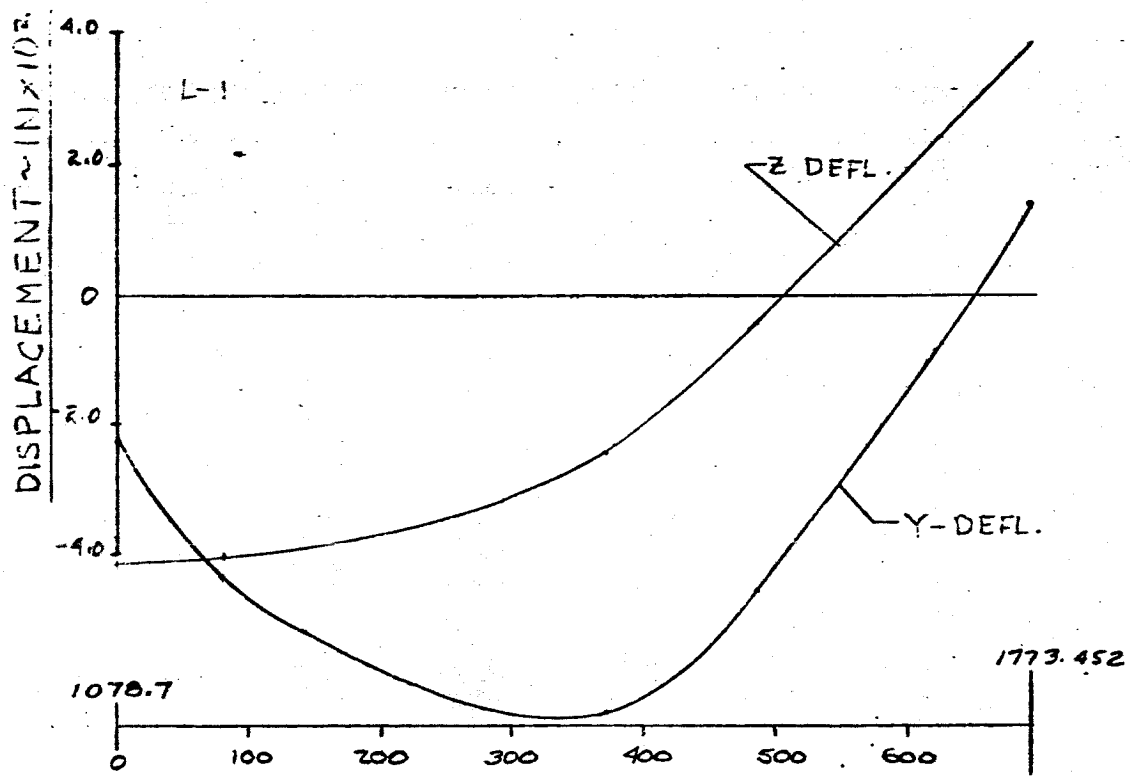


FIG 35. DISPLACEMENT VS LENGTH SATURN SA-DI

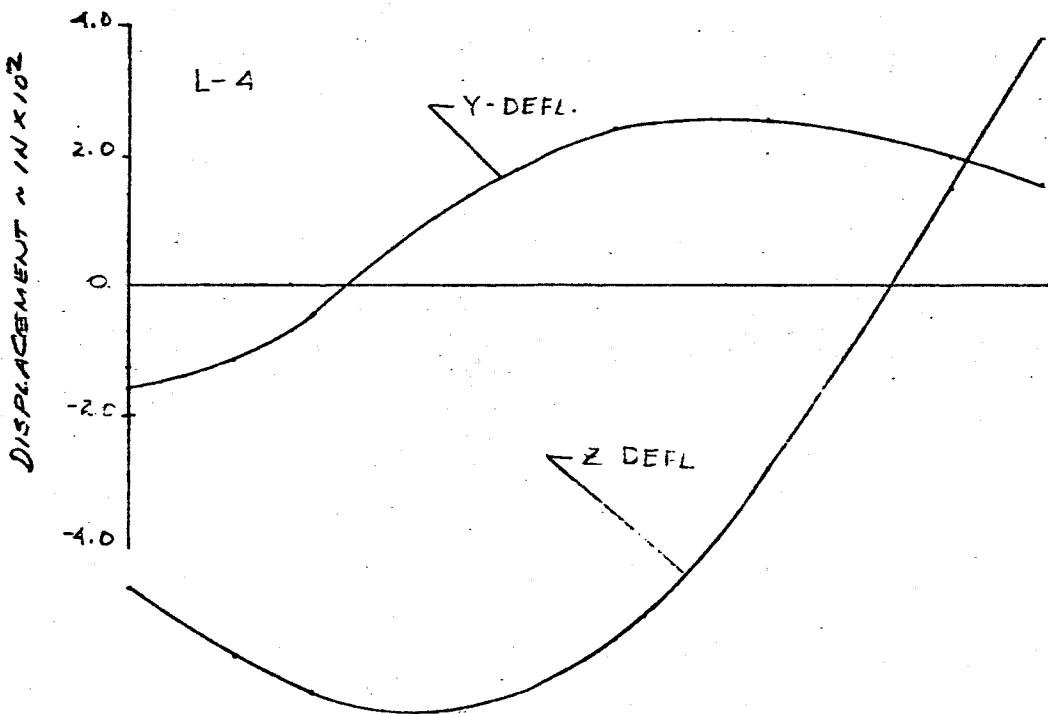
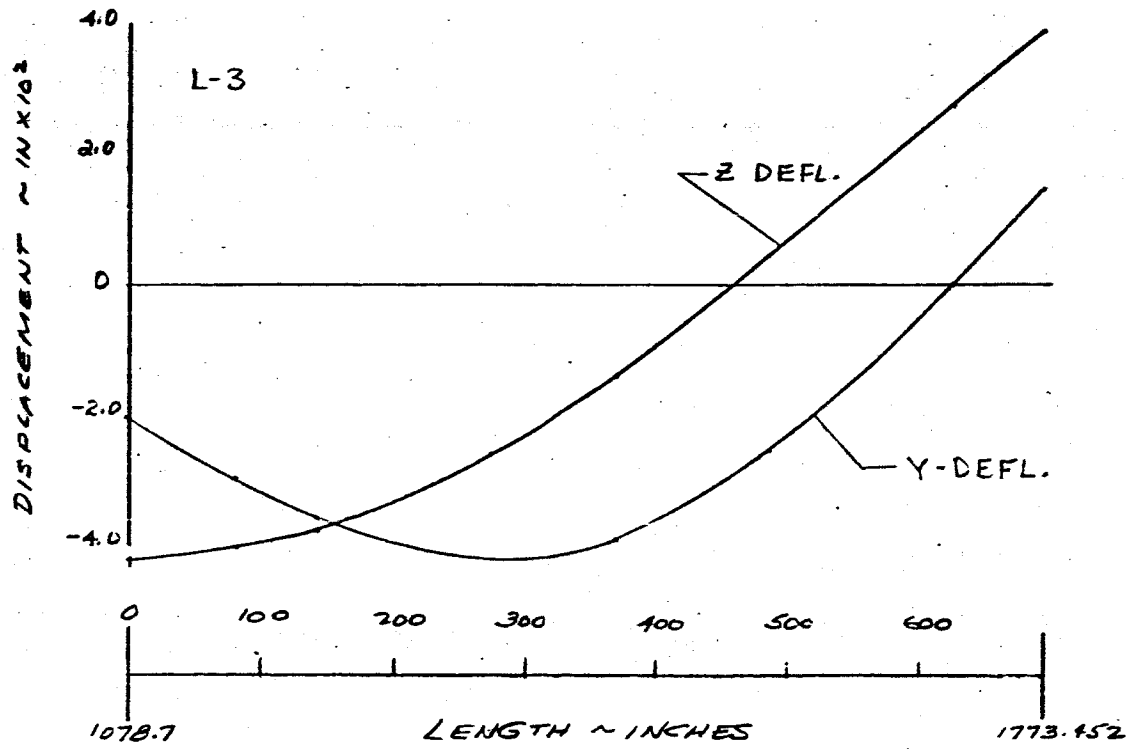
FREQUENCY = 2.20 CPS.



-118-

FIG 3.6 DISPLACEMENT VS LENGTH SATURN SA-D1

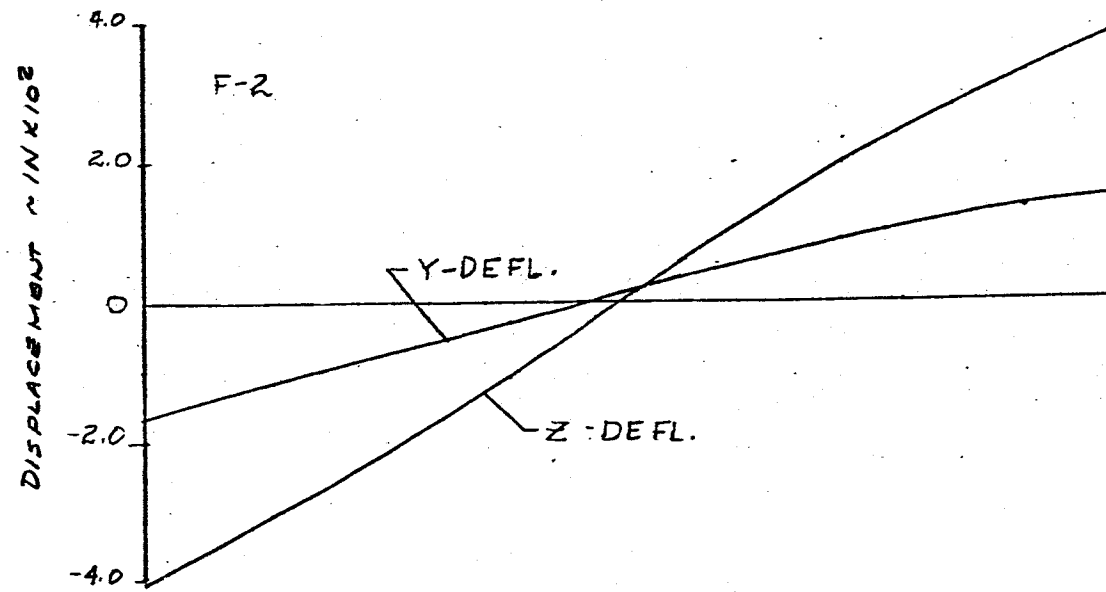
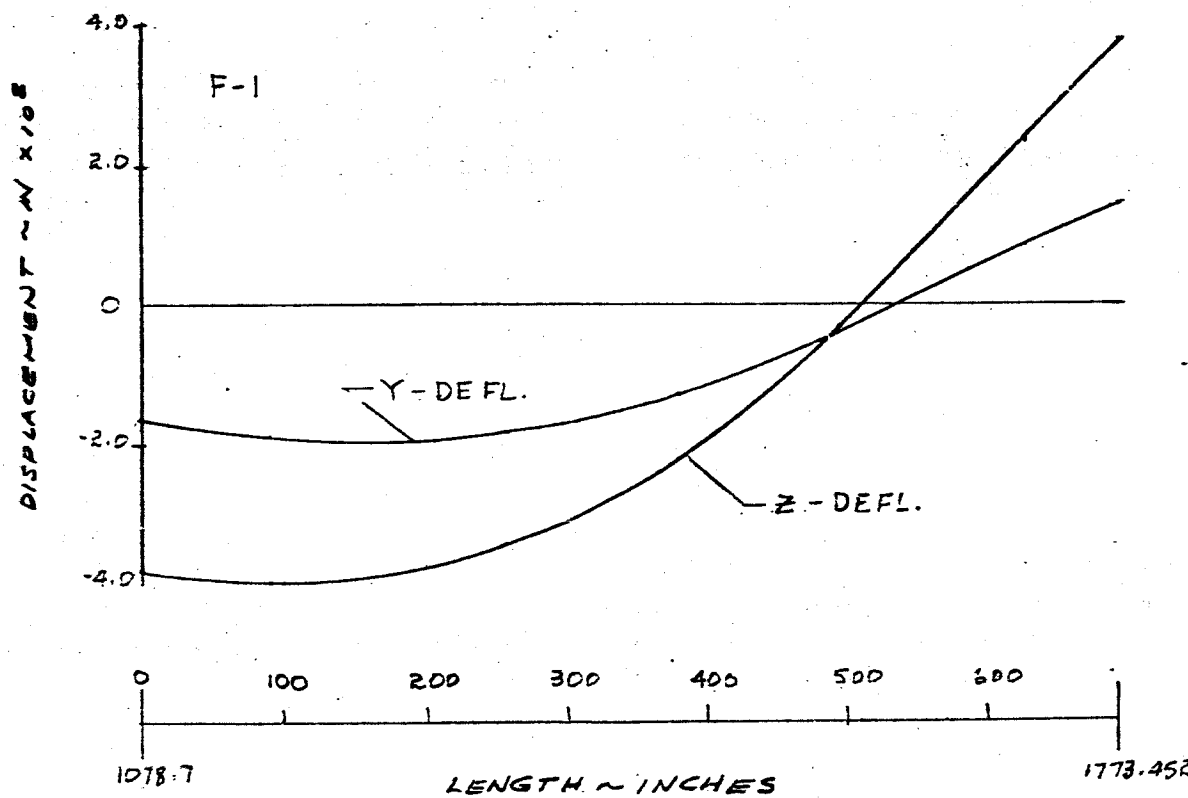
FREQUENCY = 2.20 CPS.



-119-

FIG 37 DISPLACEMENT VS LENGTH SATURN SA-DI

FREQUENCY = 2.27 cps



-120-

FIG 3B DISPLACEMENT VS LENGTH SATURN SA-DI

FREQUENCY = 2.20 cps.

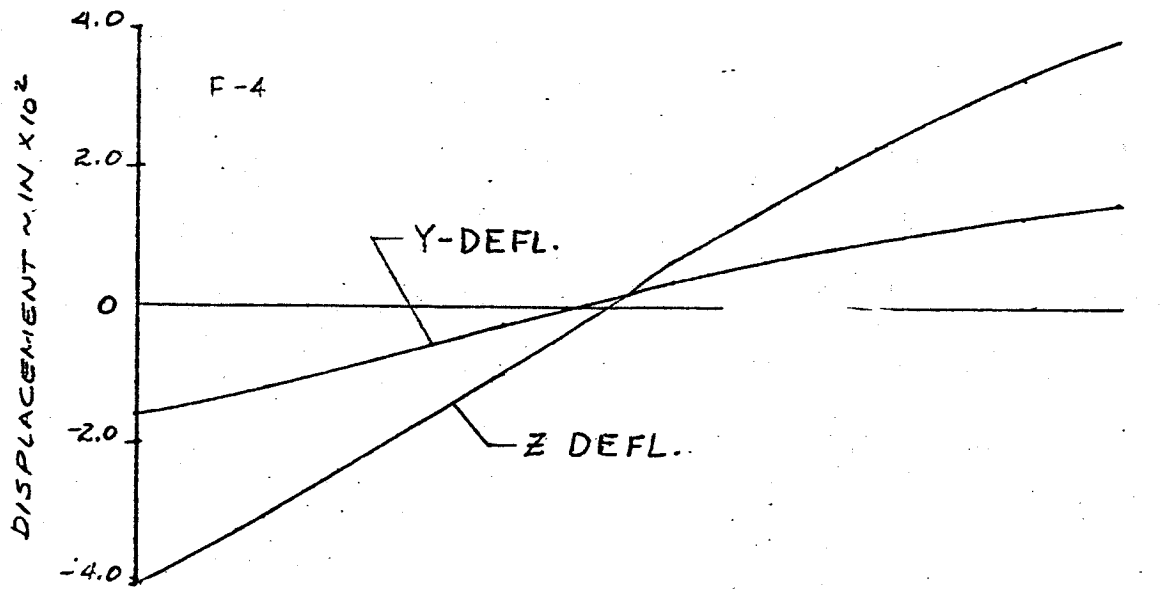
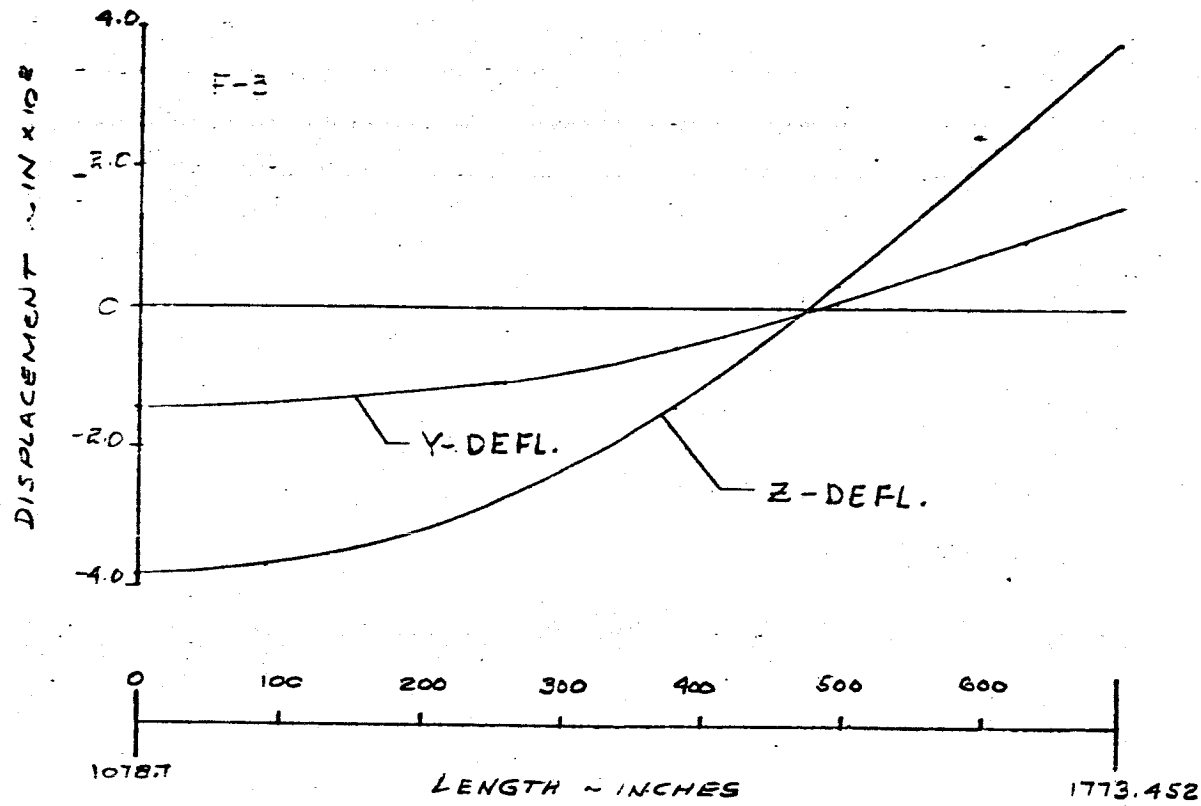
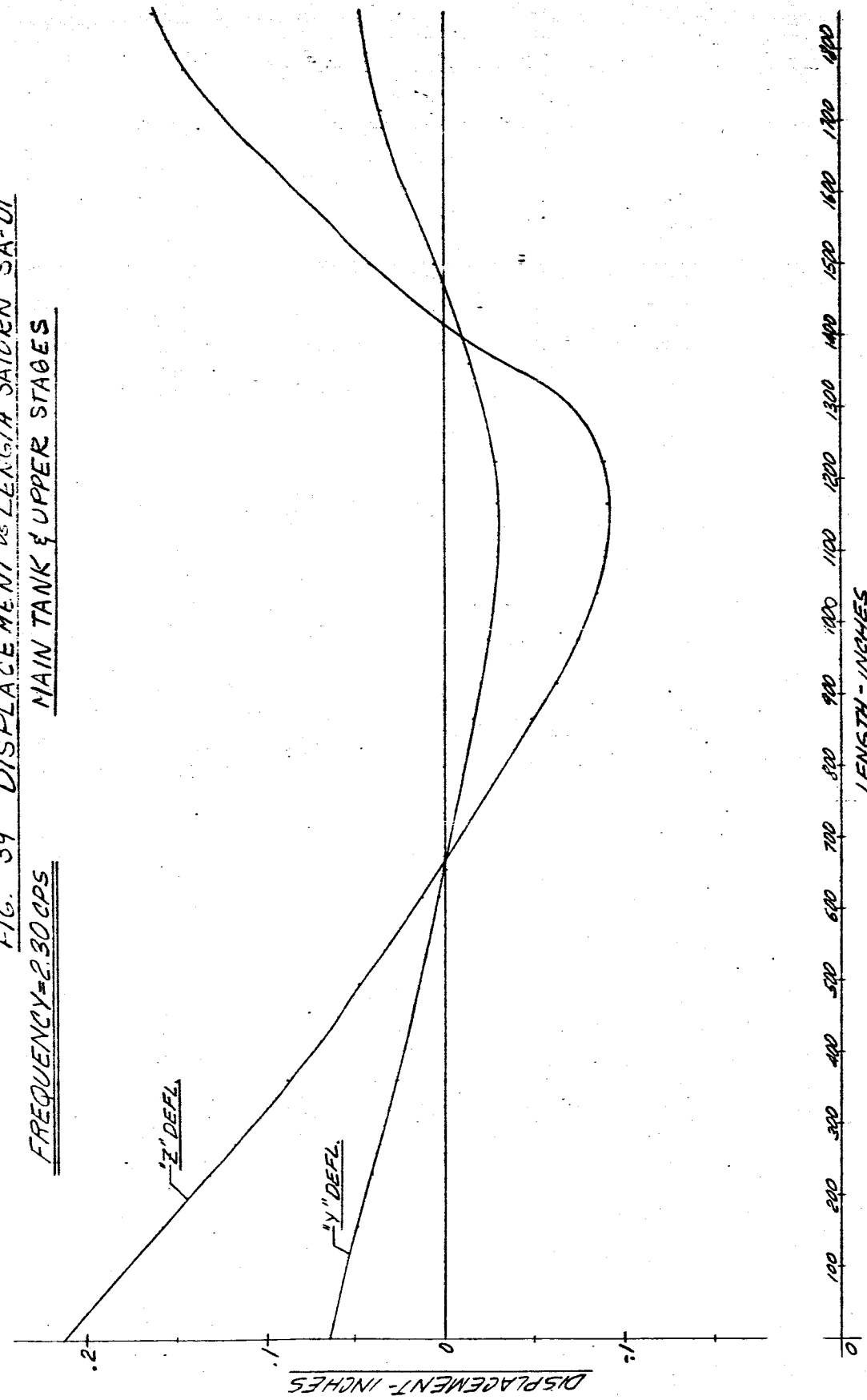


FIG. 39 DISPLACEMENT vs LENGTH SATURN SA-01  
MAIN TANK & UPPER STAGES

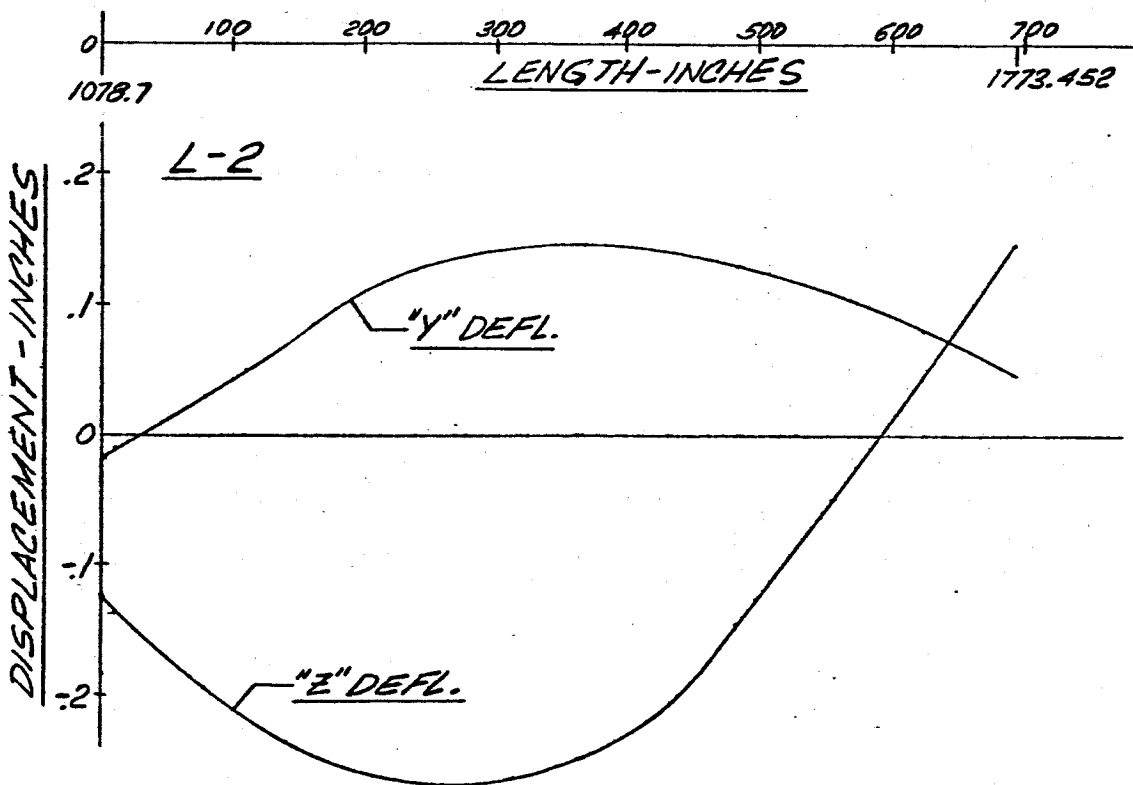
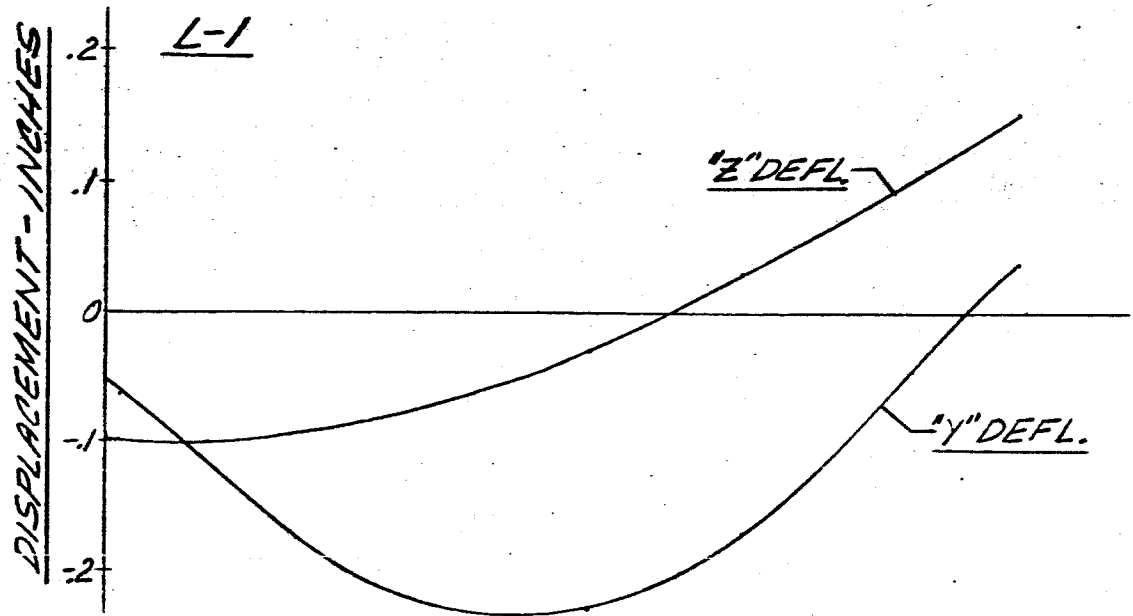
FREQUENCY=2.30 cps

- 121 -



-122-

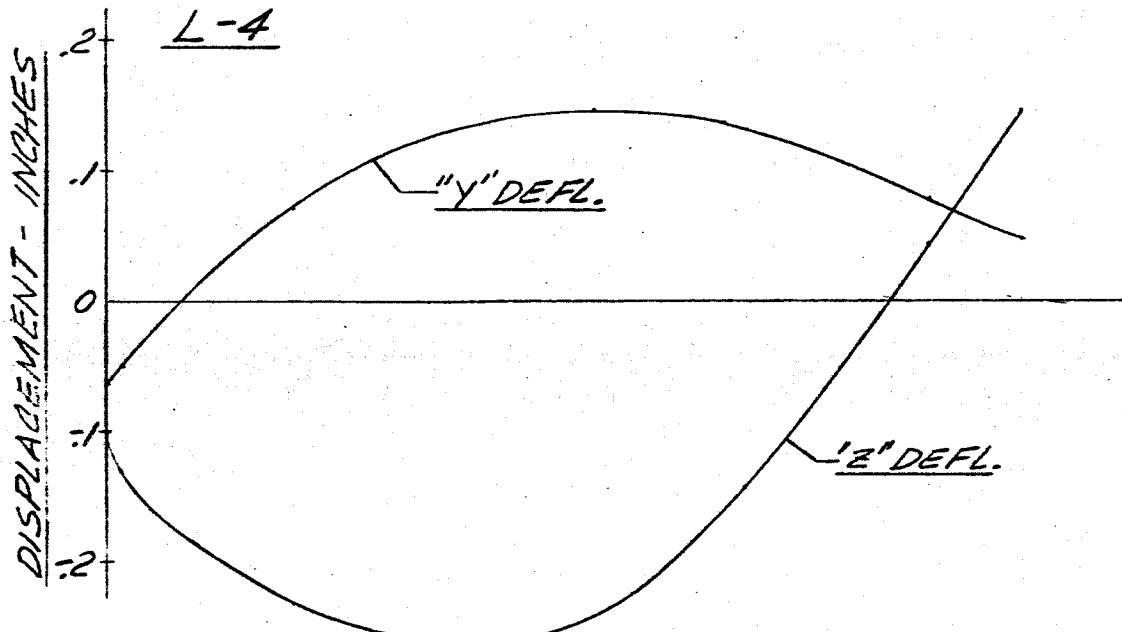
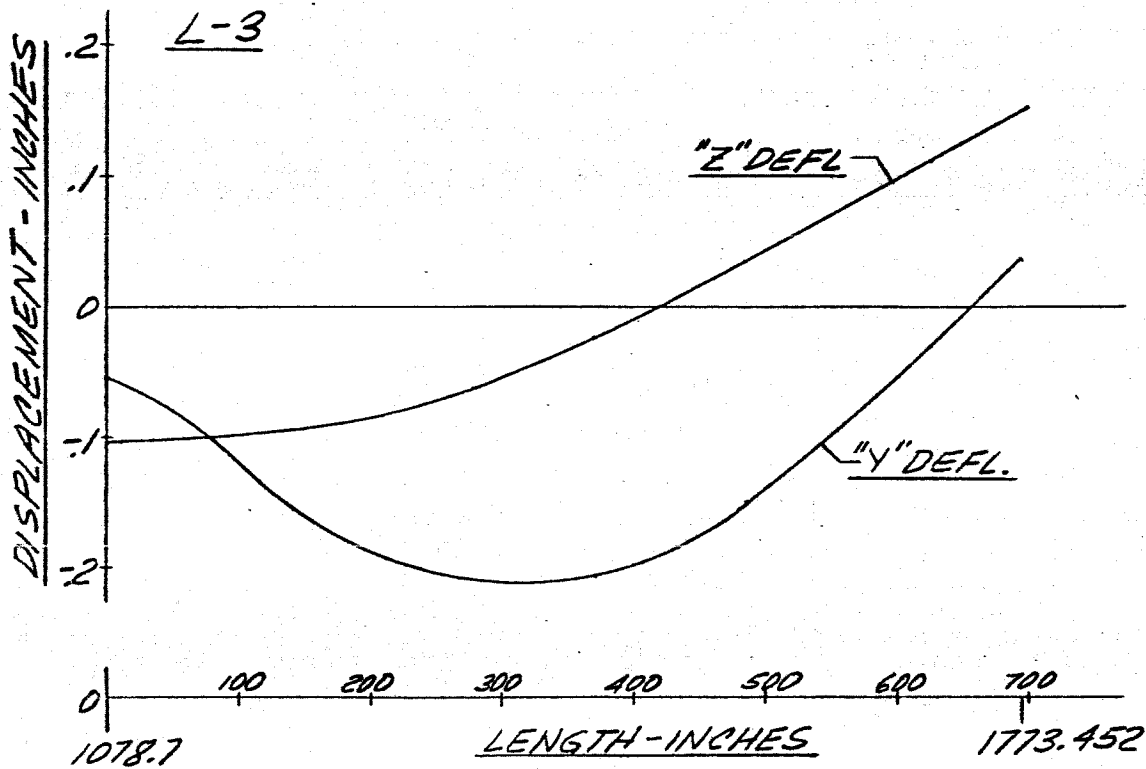
FIG 40 DISPLACEMENT VS LENGTH SATURN SA-D1  
FREQUENCY = 2.30 CPS



-123-

FIG 41 DISPLACEMENT VS LENGTH SATURN SA-01

FREQUENCY = 2.30 CPS



-124-

FIG 42. DISPLACEMENT VS LENGTH SATURN SA-D1  
FREQUENCY=2.30CPS

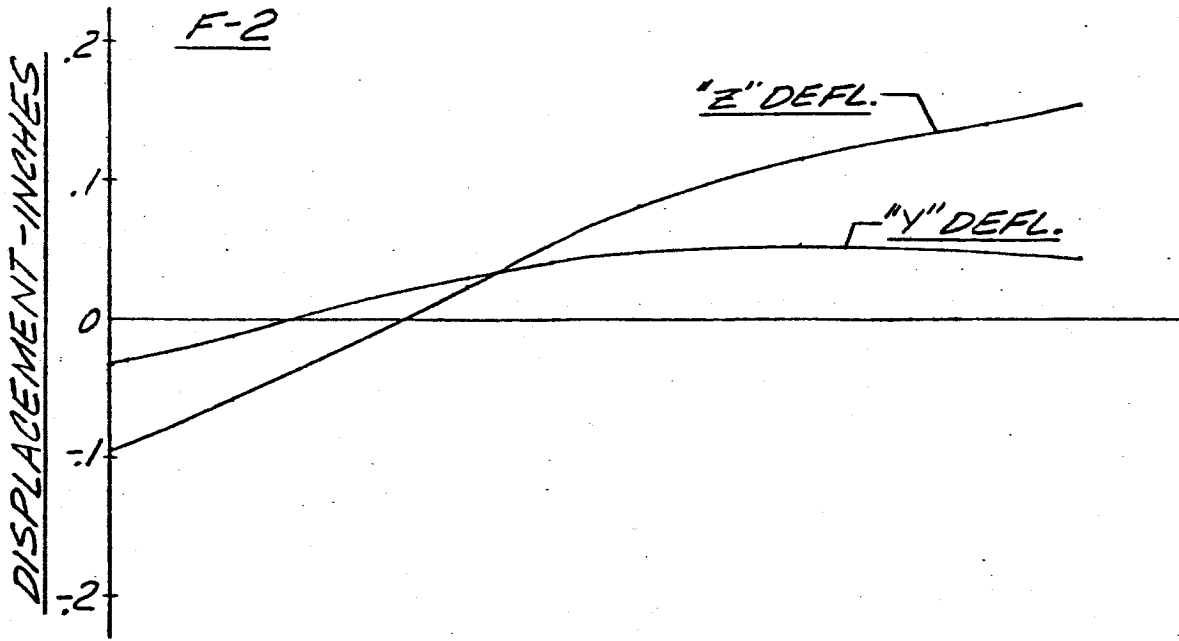
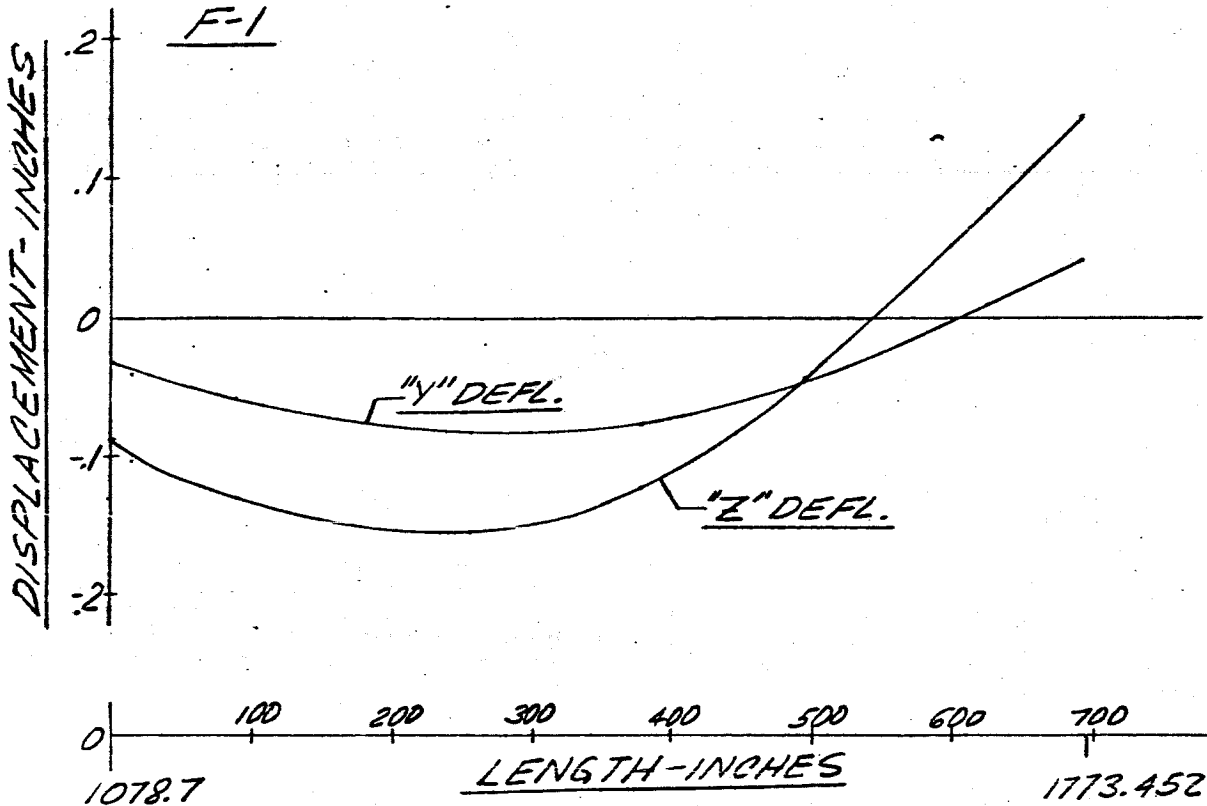


FIG 43 DISPLACEMENT VS LENGTH SATURN SA-D1

FREQUENCY = 2.30 CPS

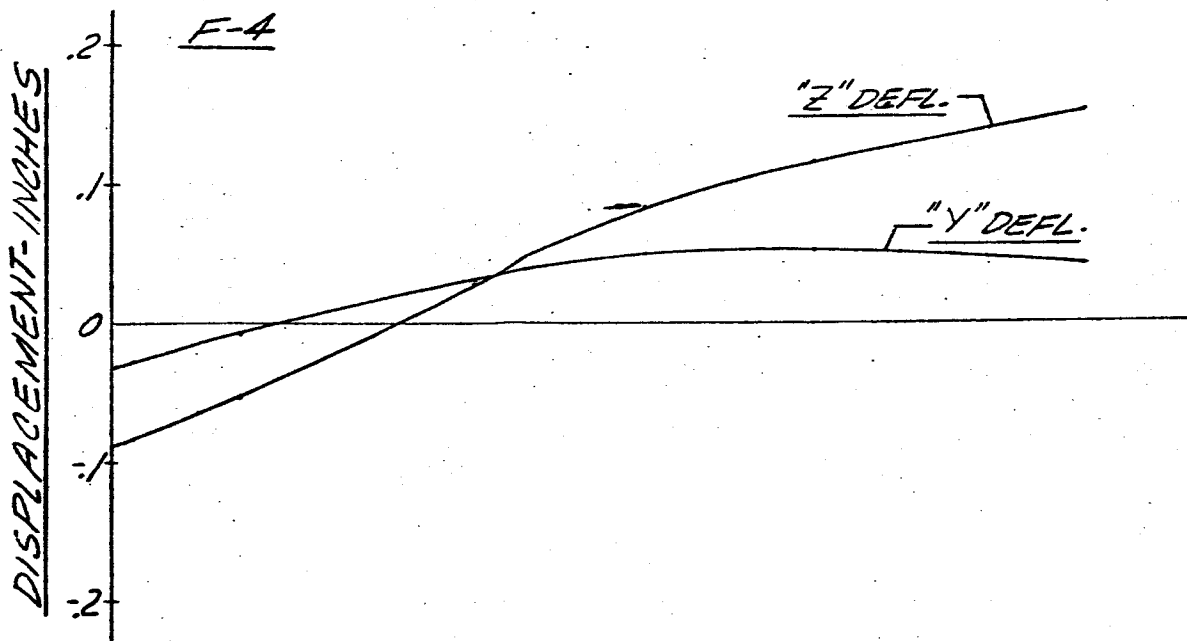
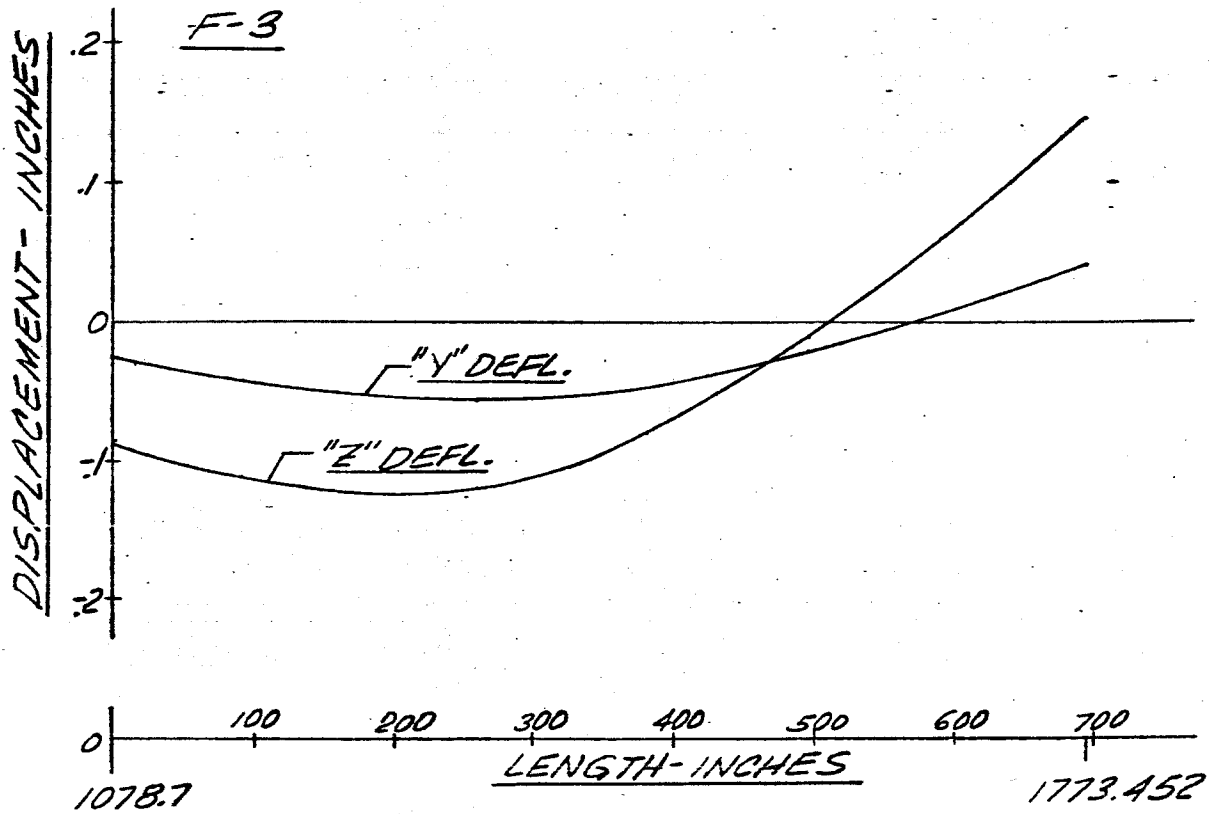


FIG 44. DISPLACEMENT vs LENGTH SATURN SA-DI  
MAIN TANK SUPER STAGES.

FREQUENCY = 2.34 cps

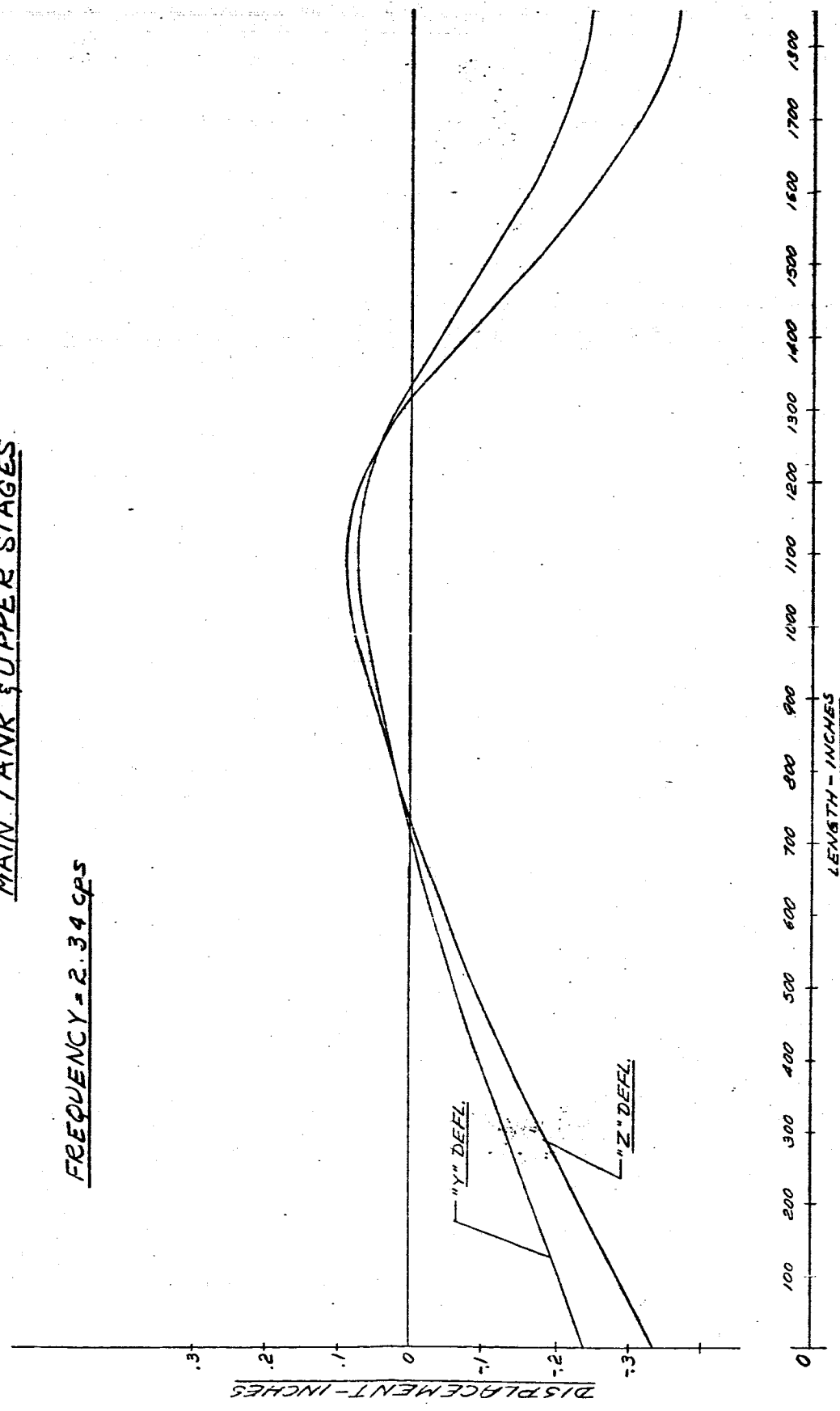
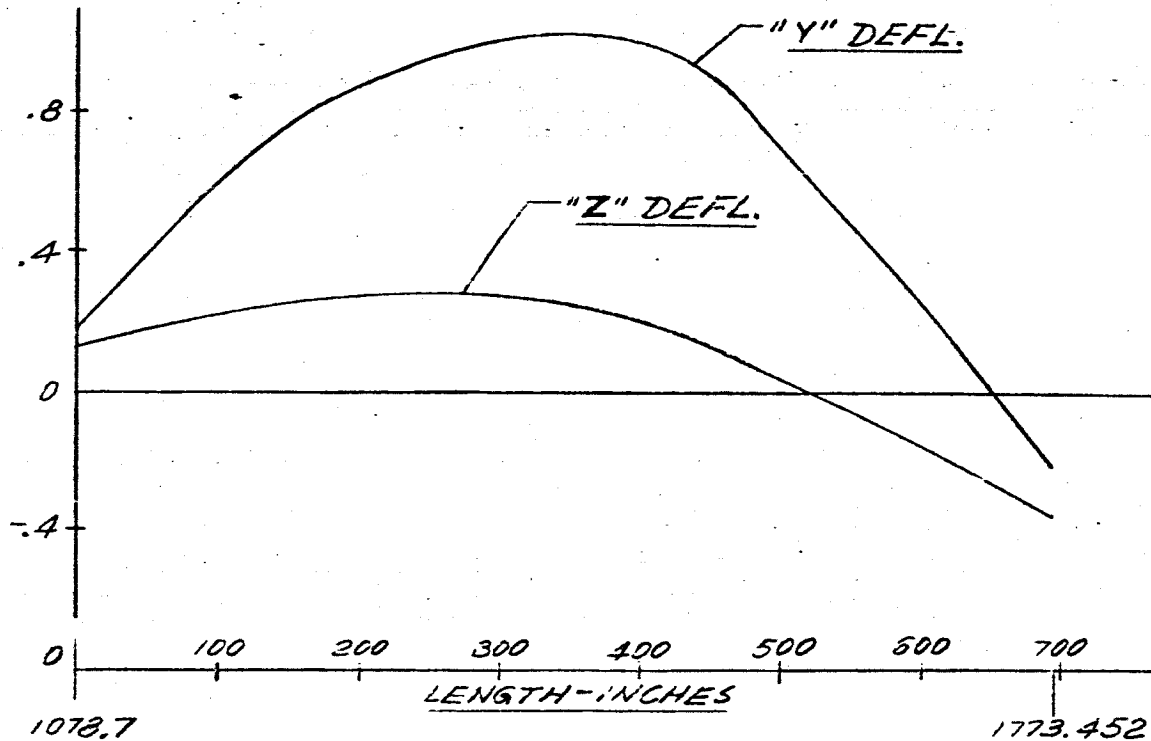


FIG A5 DISPLACEMENT VS LENGTH SATURN SA-DI

FREQUENCY = 2.34 CPS

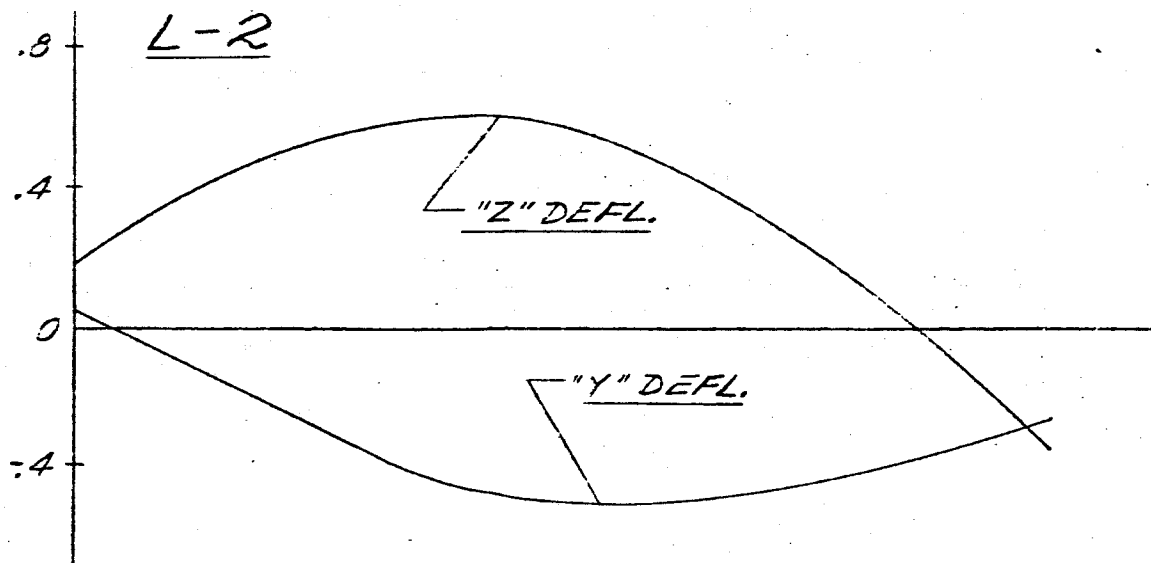
L-1

DISPLACEMENT-INCHES



L-2

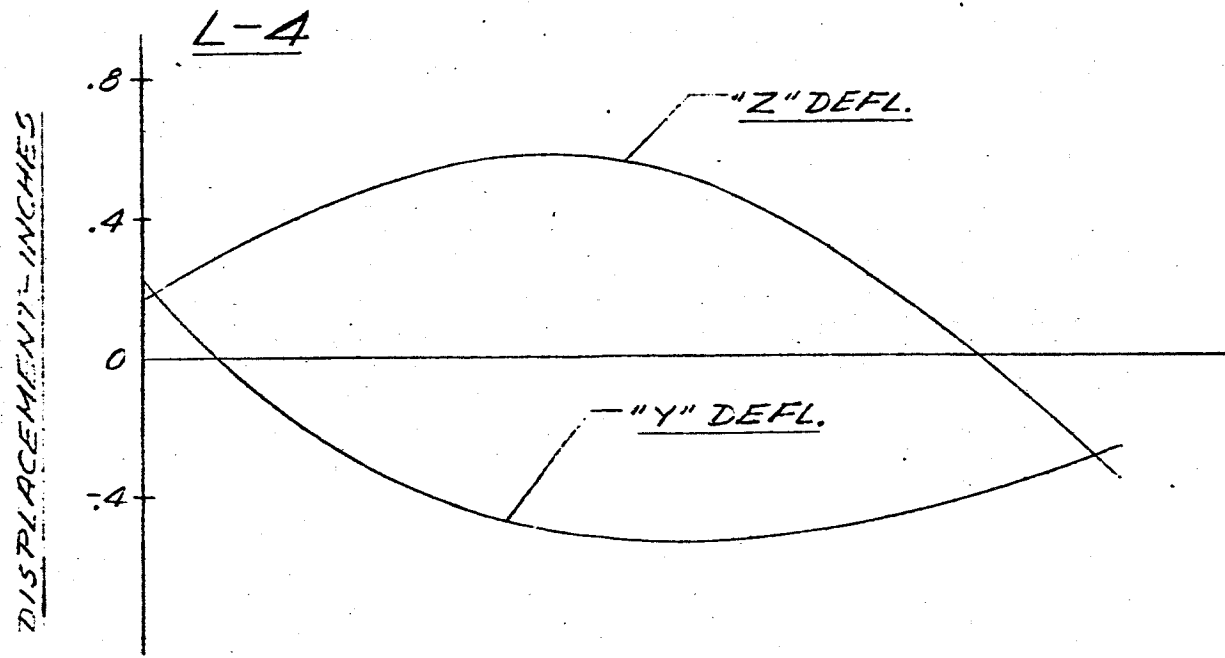
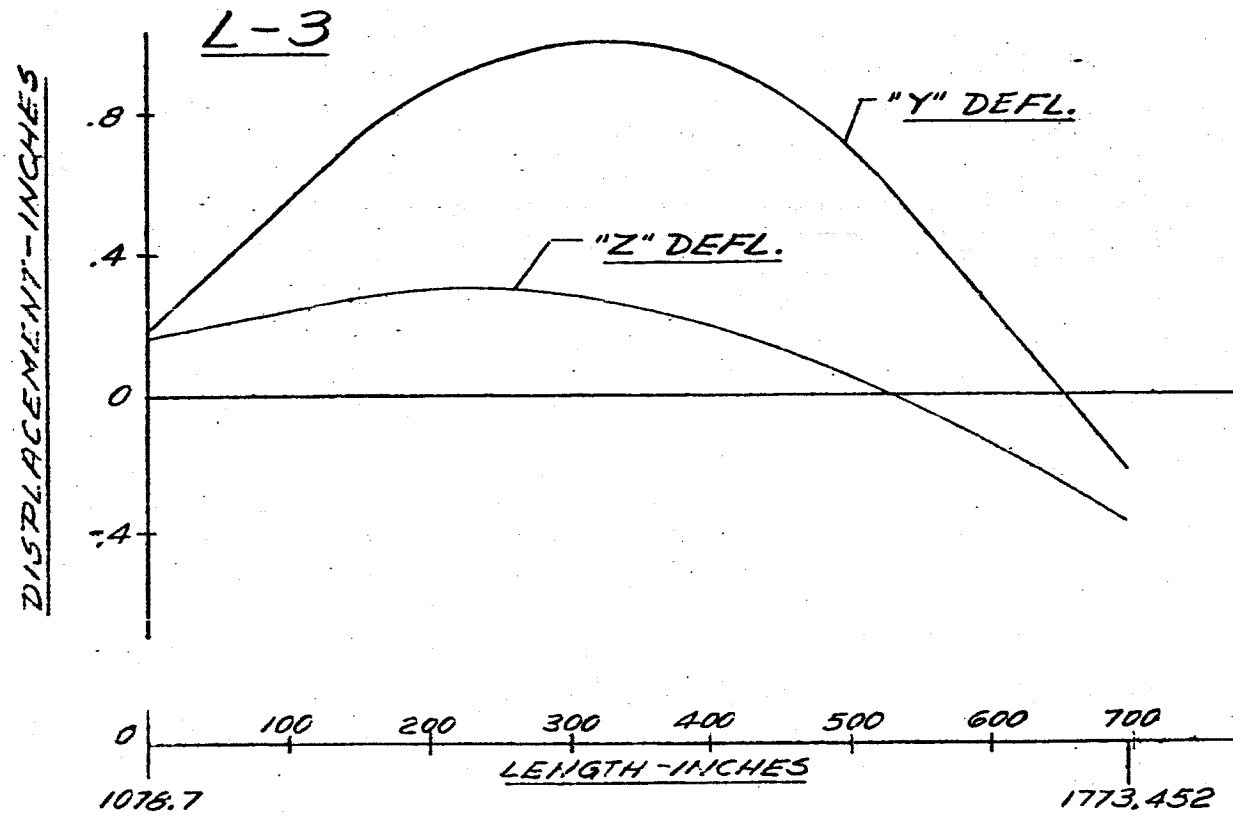
DISPLACEMENT-INCHES



-128-

FIG 46 DISPLACEMENT VS LENGTH SATURN SA-DI

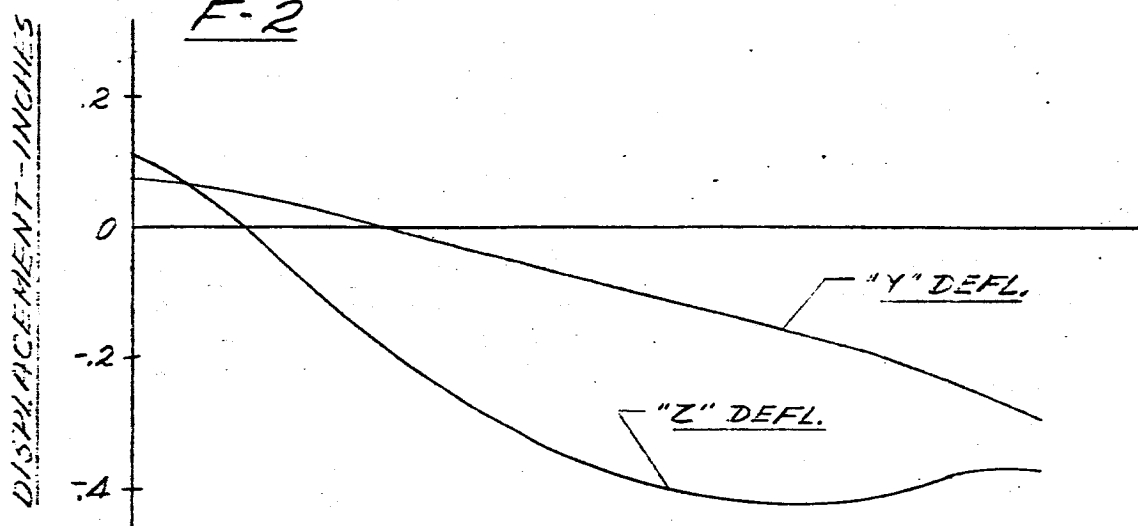
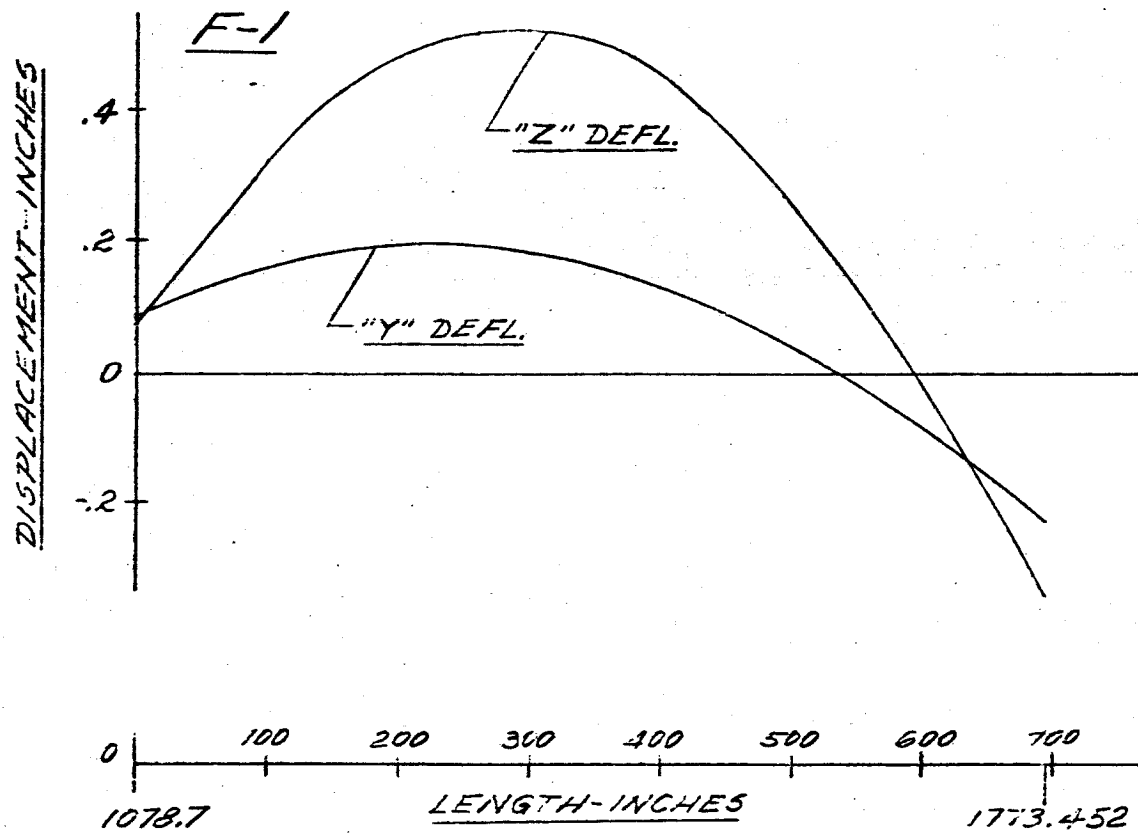
FREQUENCY = 2.34 CPS



-129-

FIG 47 DISPLACEMENT VS LENGTH SATURN SA-D1

FREQUENCY = 2.34 CPS

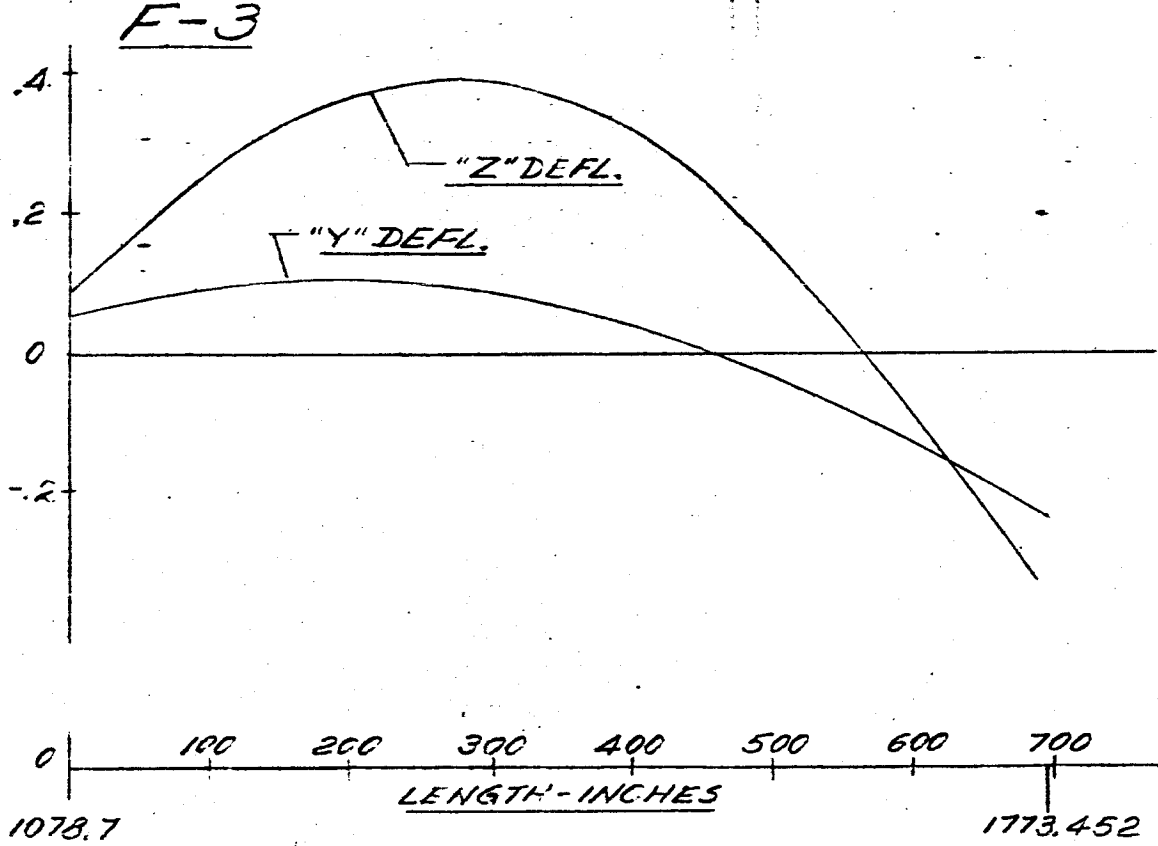


-130-

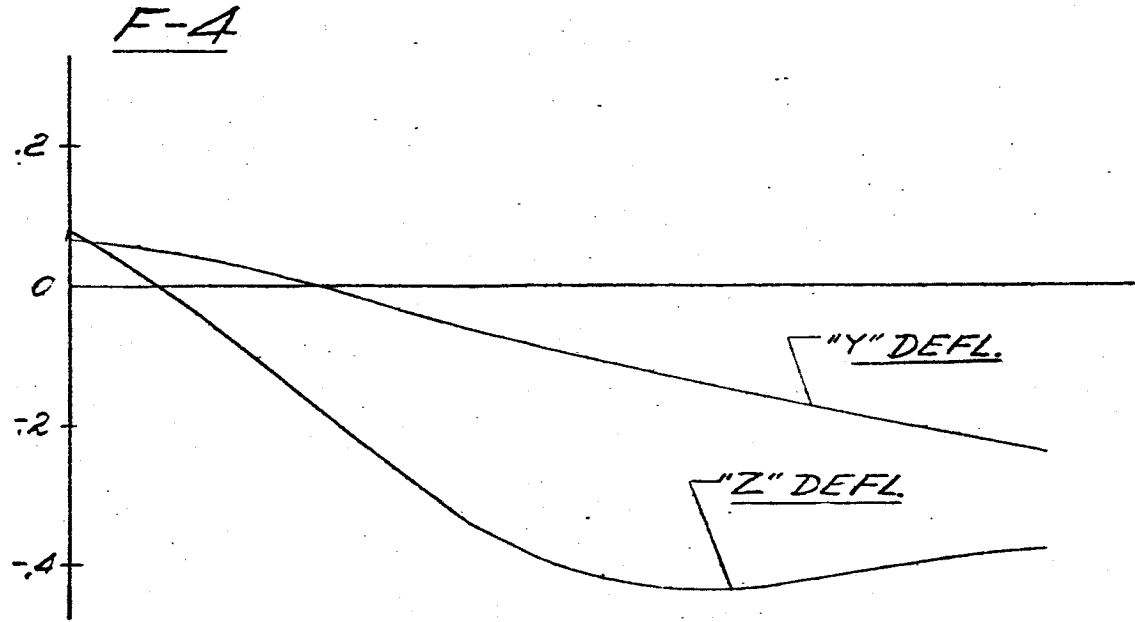
FIG 4 E DISPLACEMENT VS LENGTH SATURN SA-DI

FREQUENCY = 2.34 CPS

DISPLACEMENT - INCHES:



DISPLACEMENT - INCHES



-131-

EIG 49 DISPLACEMENT VS LENGTH SATURN SA-DI  
MAIN TANK & UPPER STAGES  
FREQUENCY = 2.37 CPS

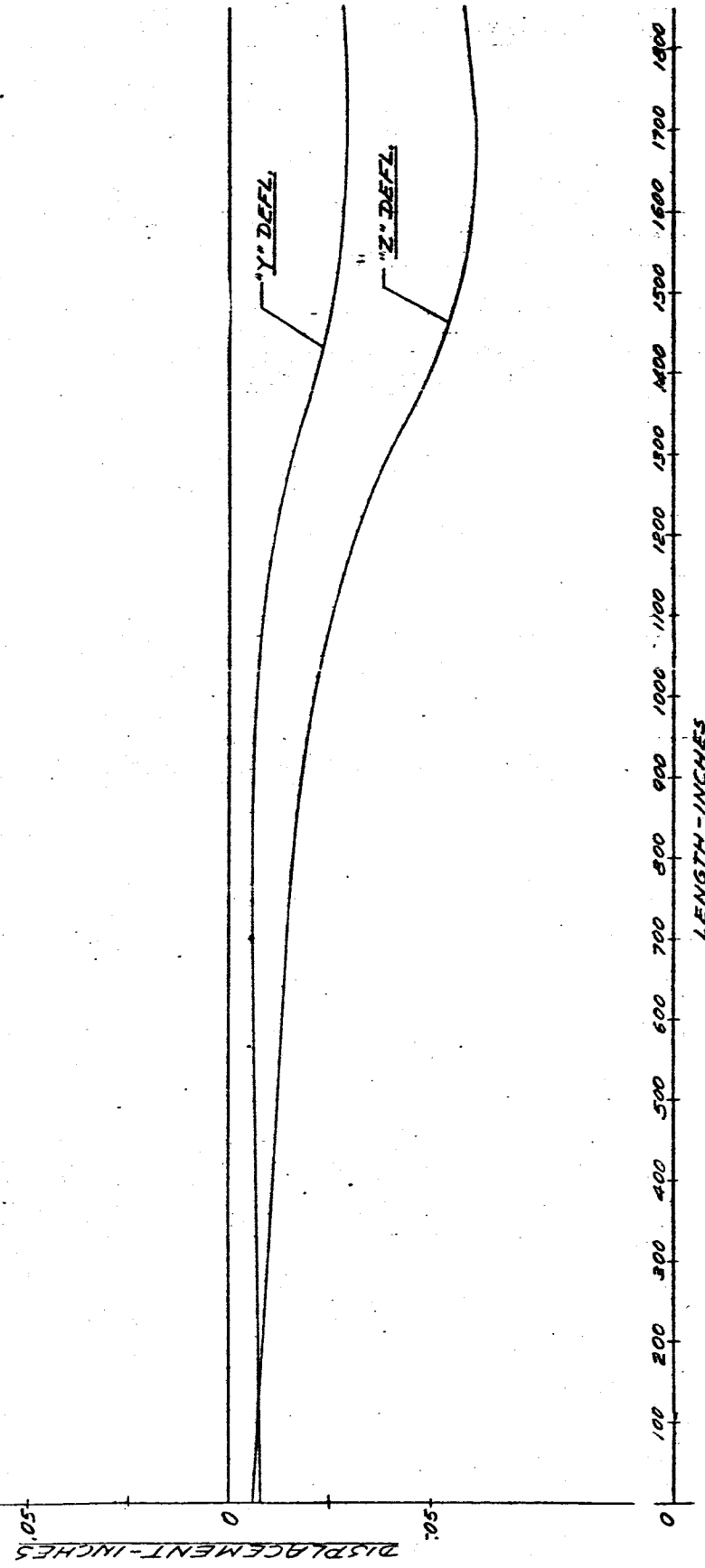


FIG 50 DISPLACEMENT VS LENGTH SATURN SA-D1

FREQUENCY = 2.37 CPS

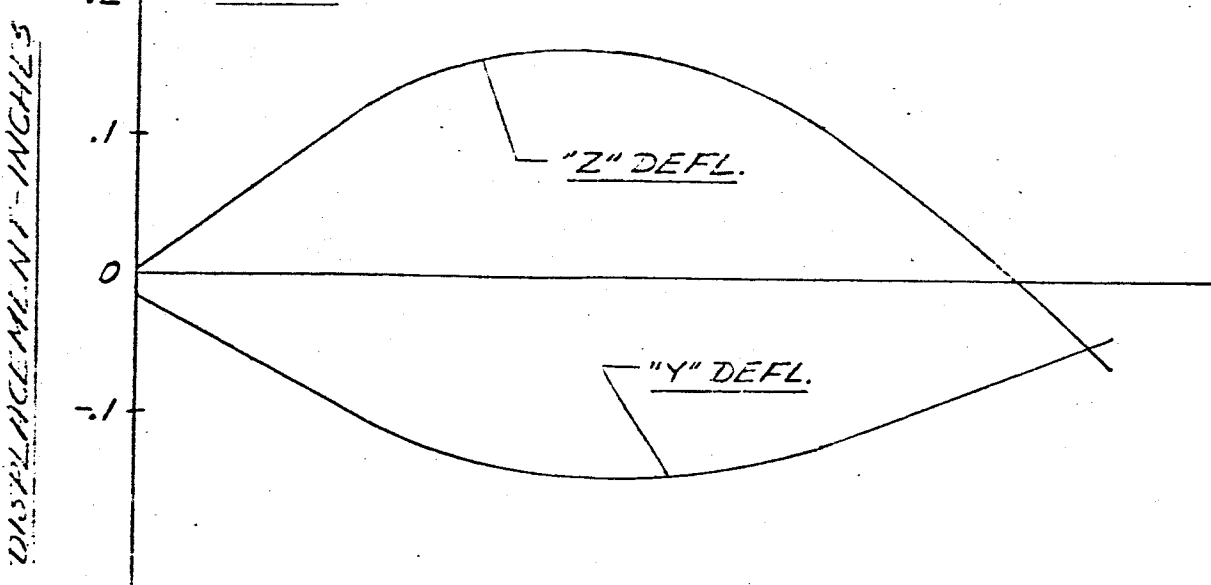
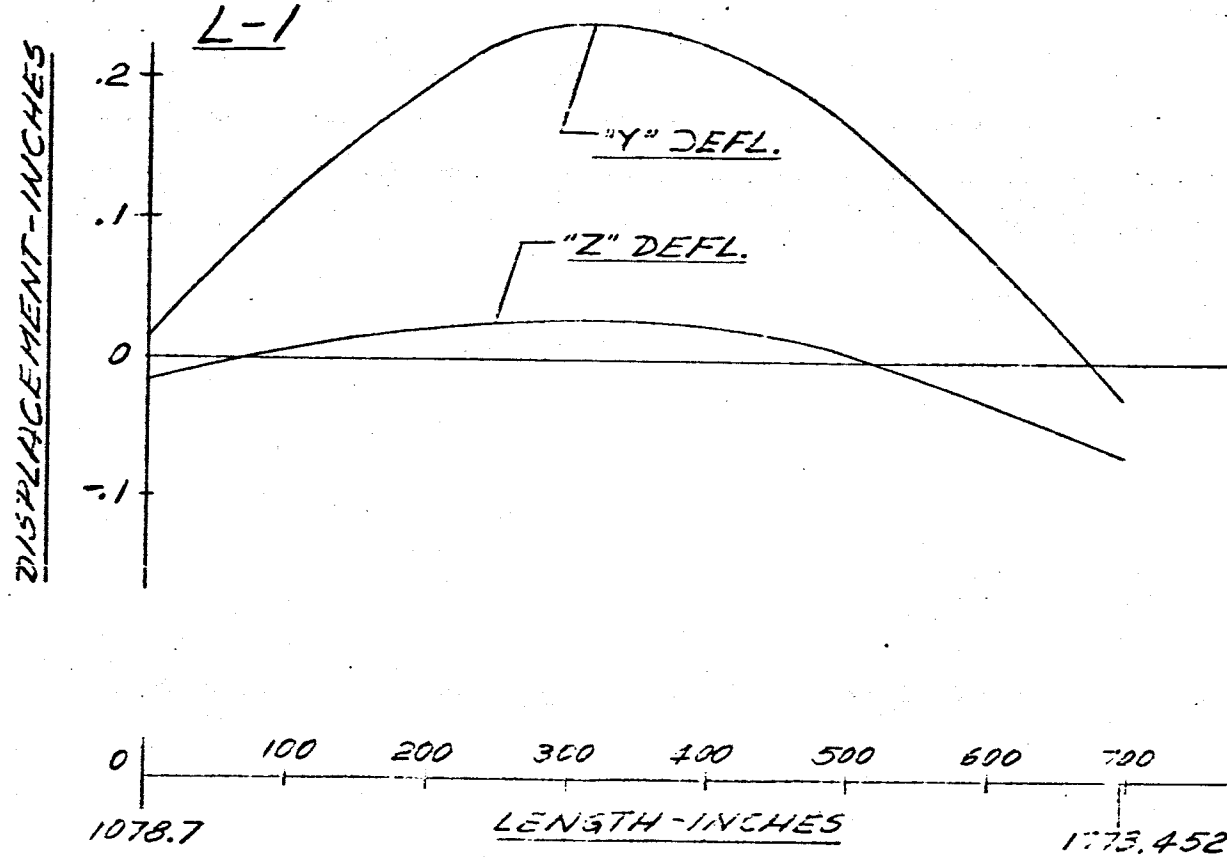
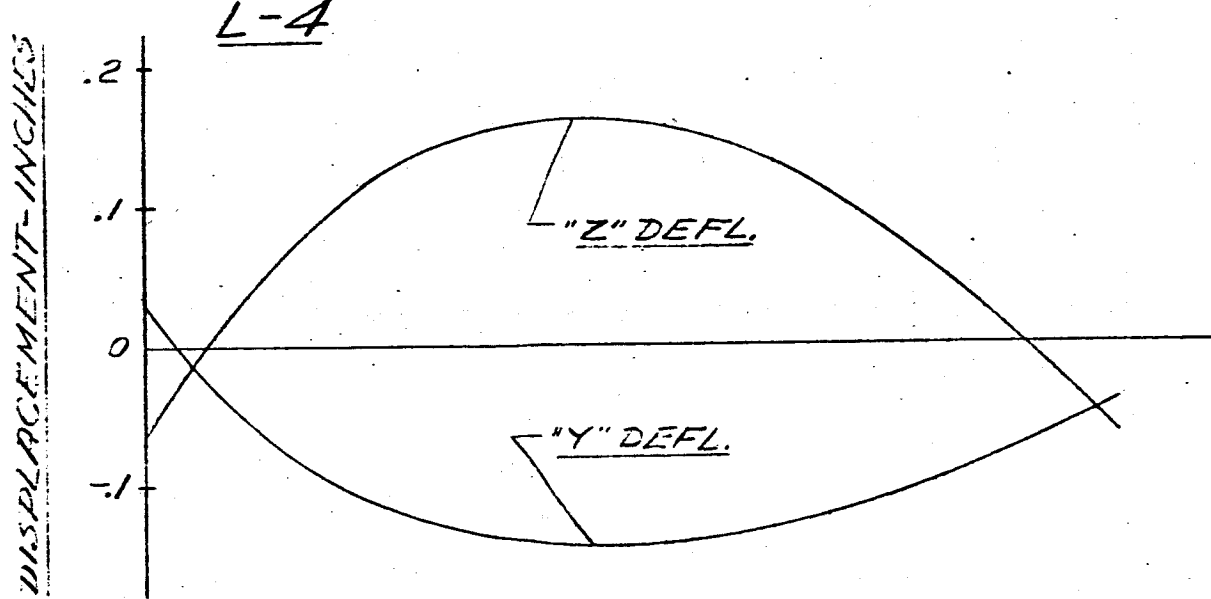
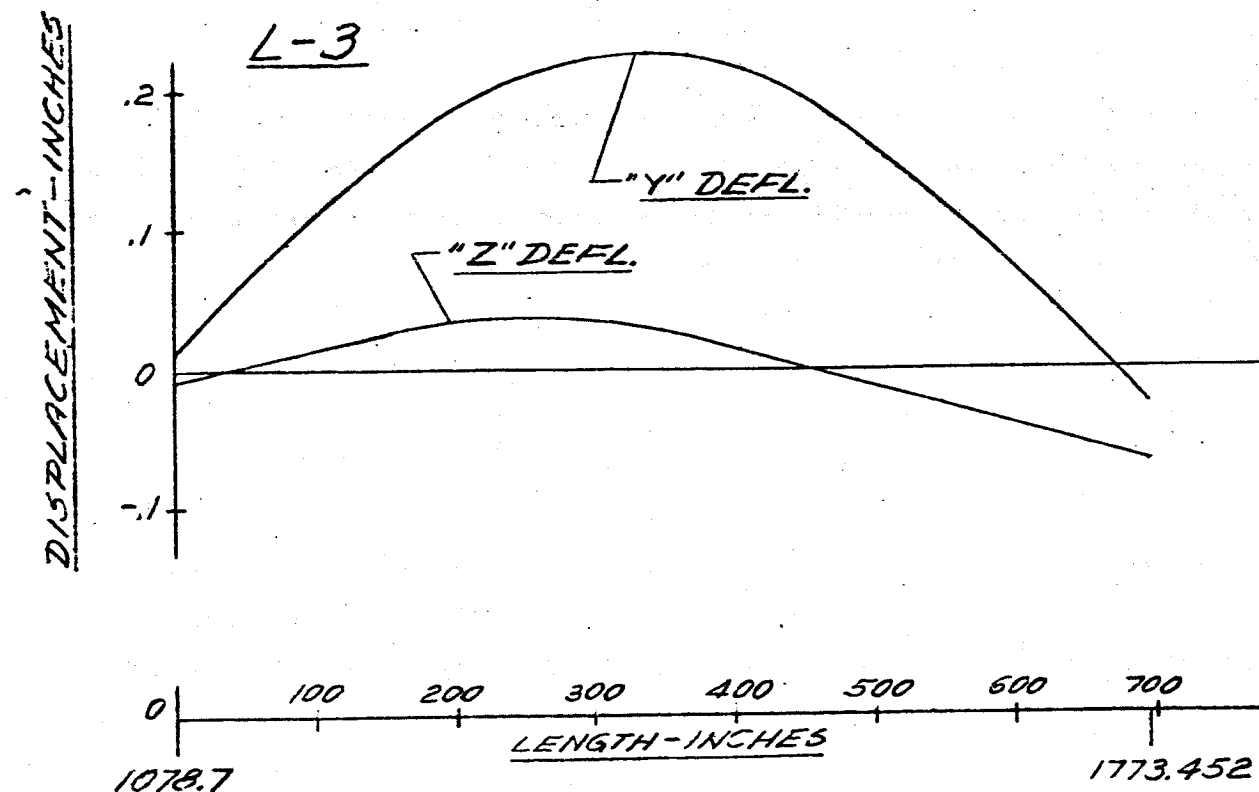


FIG 51 DISPLACEMENT VS LENGTH SATURN SA-01

FREQUENCY = 2.37 CPS



-134-

FIG 52 DISPLACEMENT VS LENGTH SATURN SA-01

FREQUENCY = 2.37 CPS.

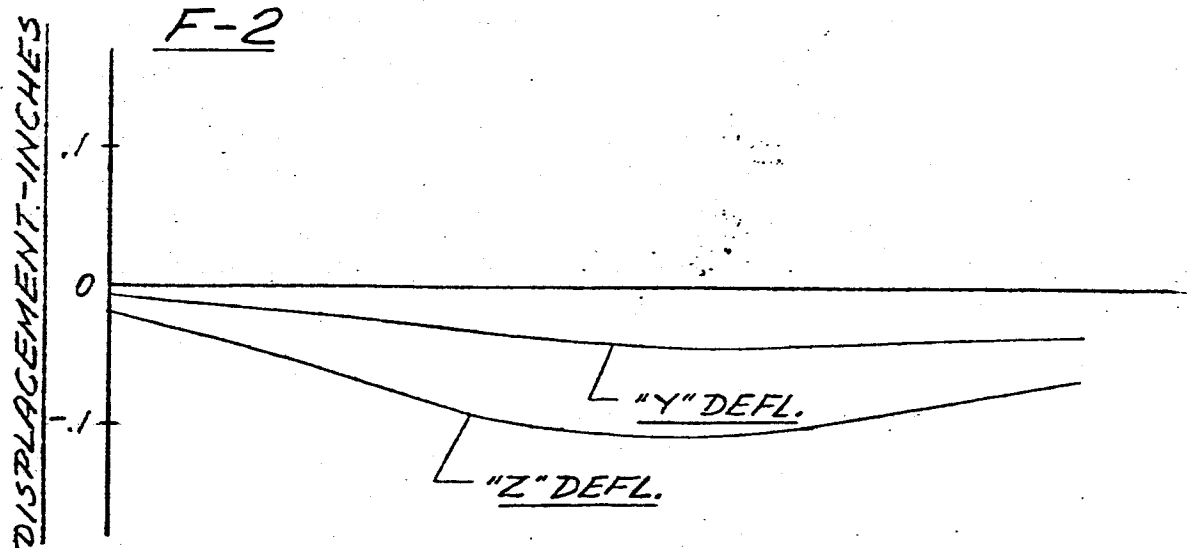
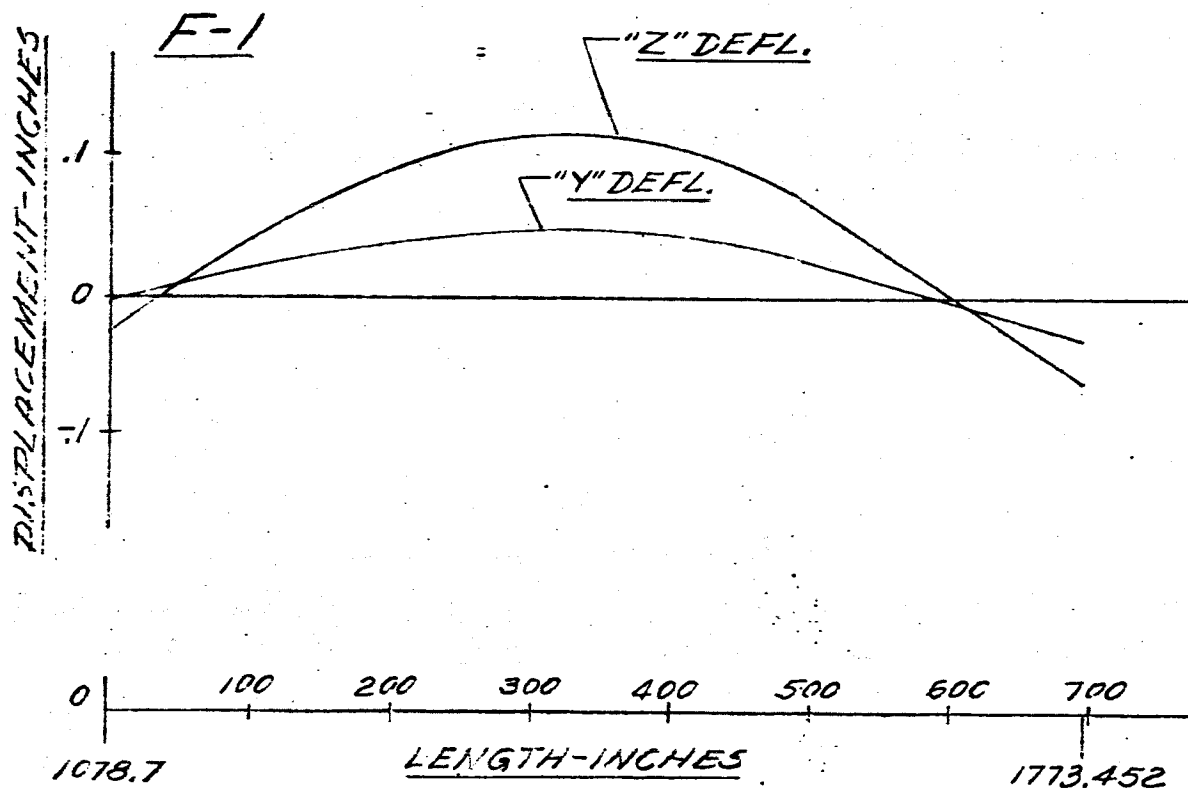
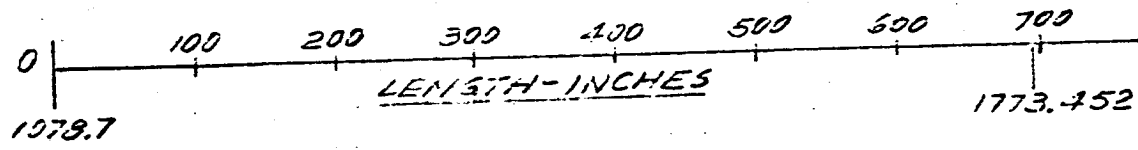
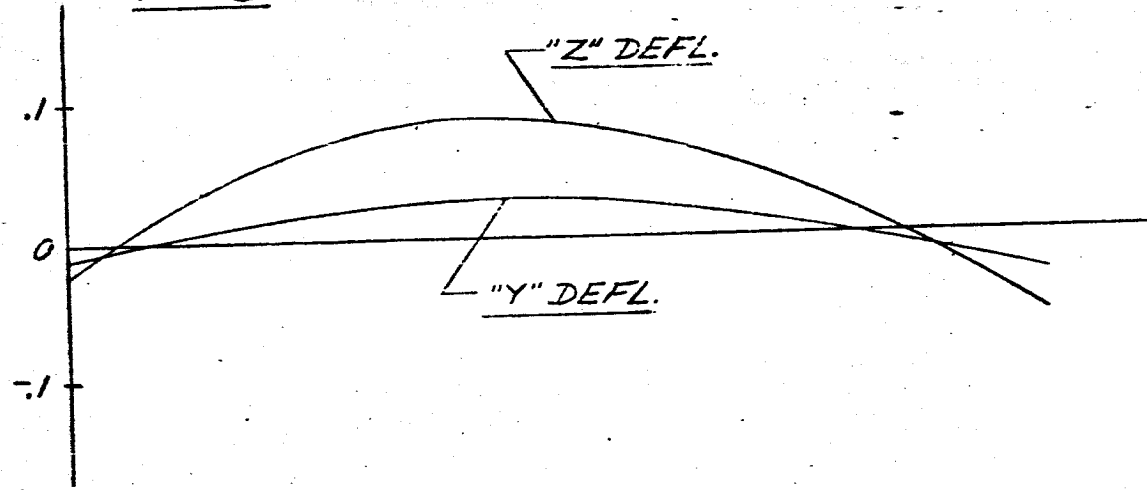


FIG 53 DISPLACEMENT VS LENGTH SATURN SA-DI

FREQUENCY = 2.37 CPS

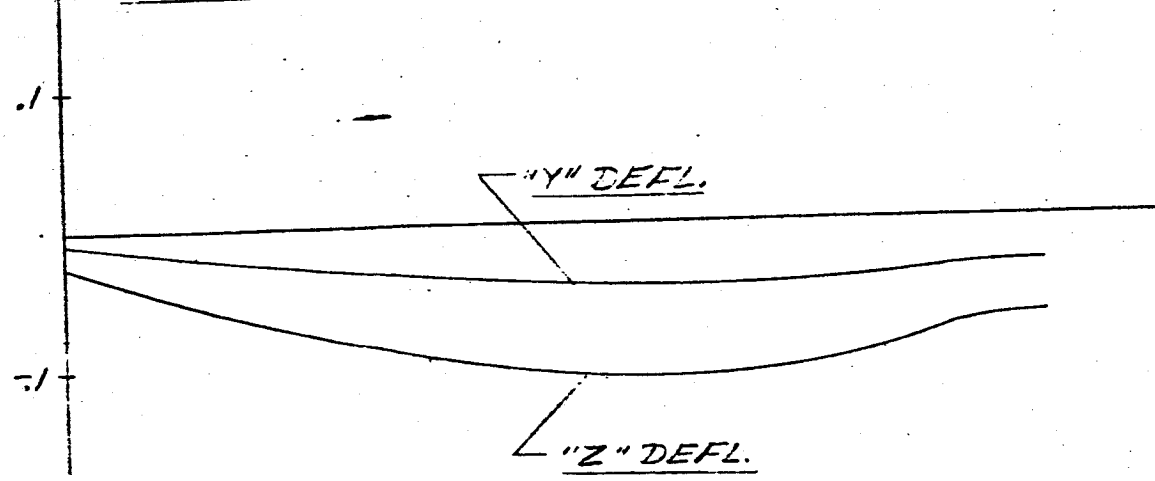
DISPLACEMENT-INCHES

F-3



DISPLACEMENT-INCHES

F-4



FREQUENCY = 2.40 CPS

FIG. 54 DISPLACEMENT vs LENGTH SATURN SA-DI  
MAIN TANK & UPPER STAGES

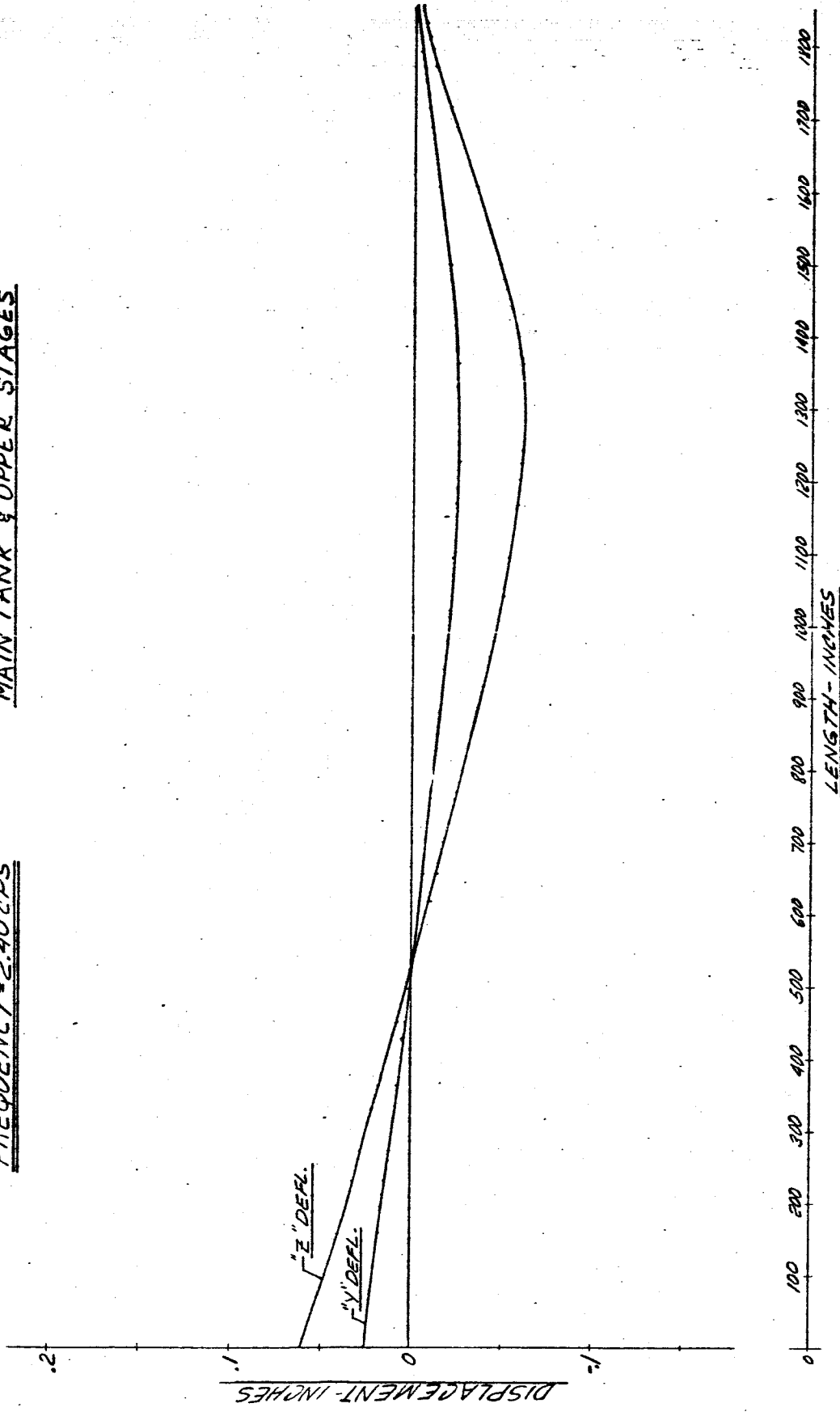


FIG 55 DISPLACEMENT VS LENGTH SATURN SA-DI.

FREQUENCY=2.40CPS

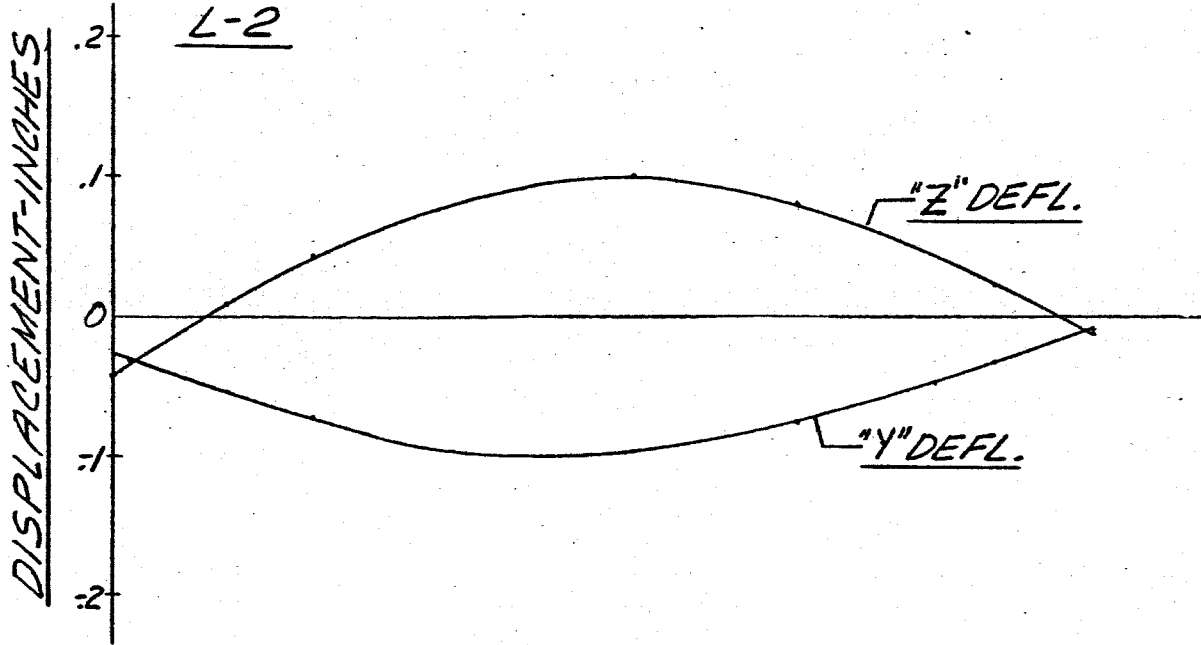
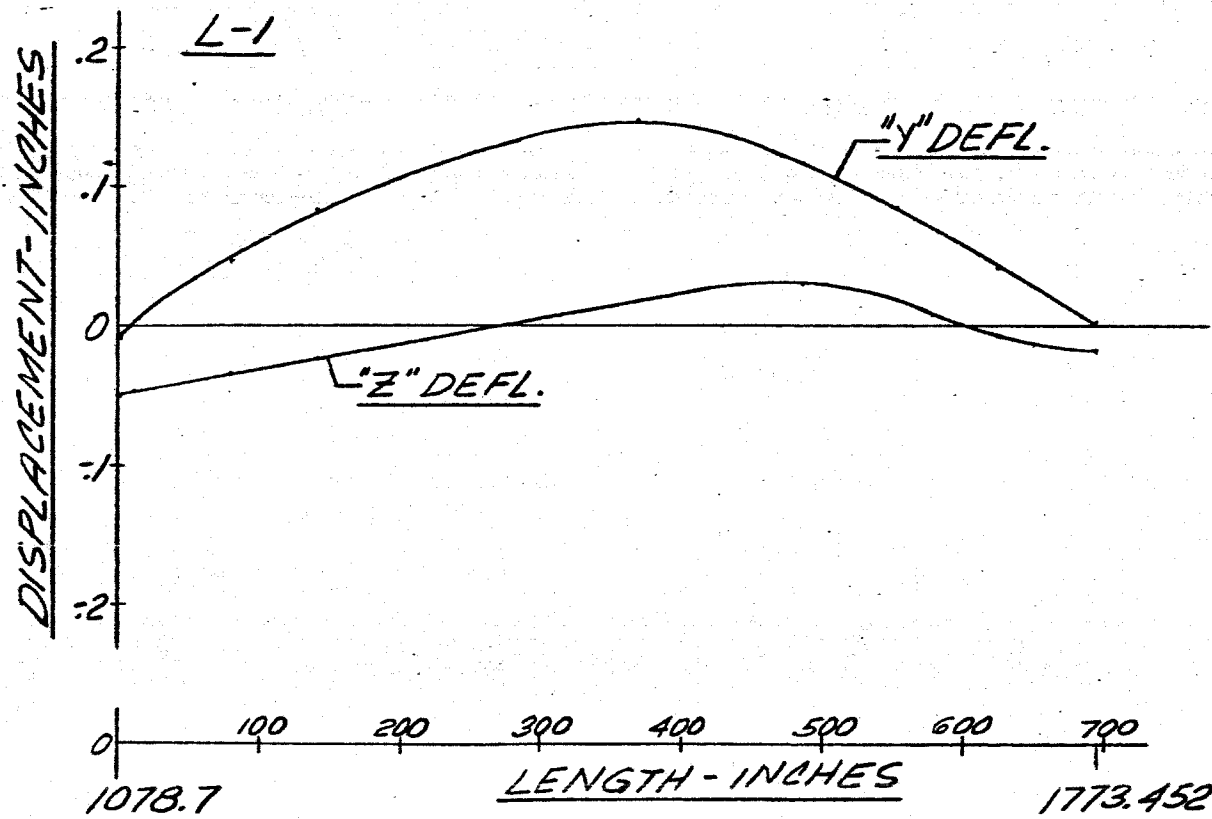


FIG. E6 DISPLACEMENT VS LENGTH SATURN SA-DI  
FREQUENCY = 2.40 CPS

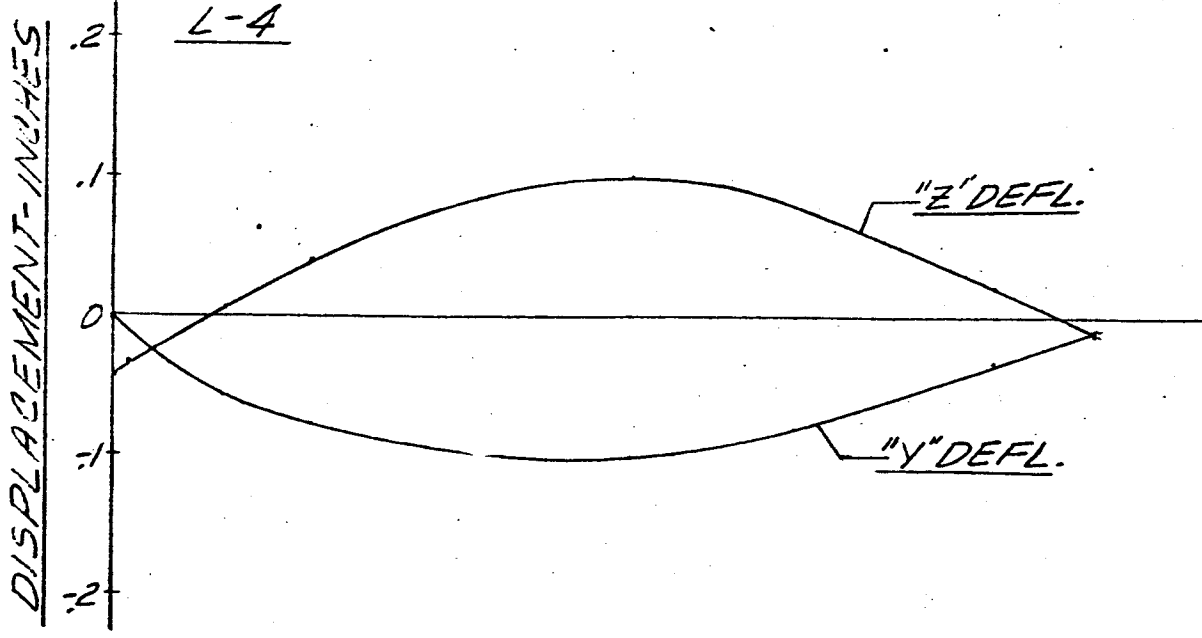
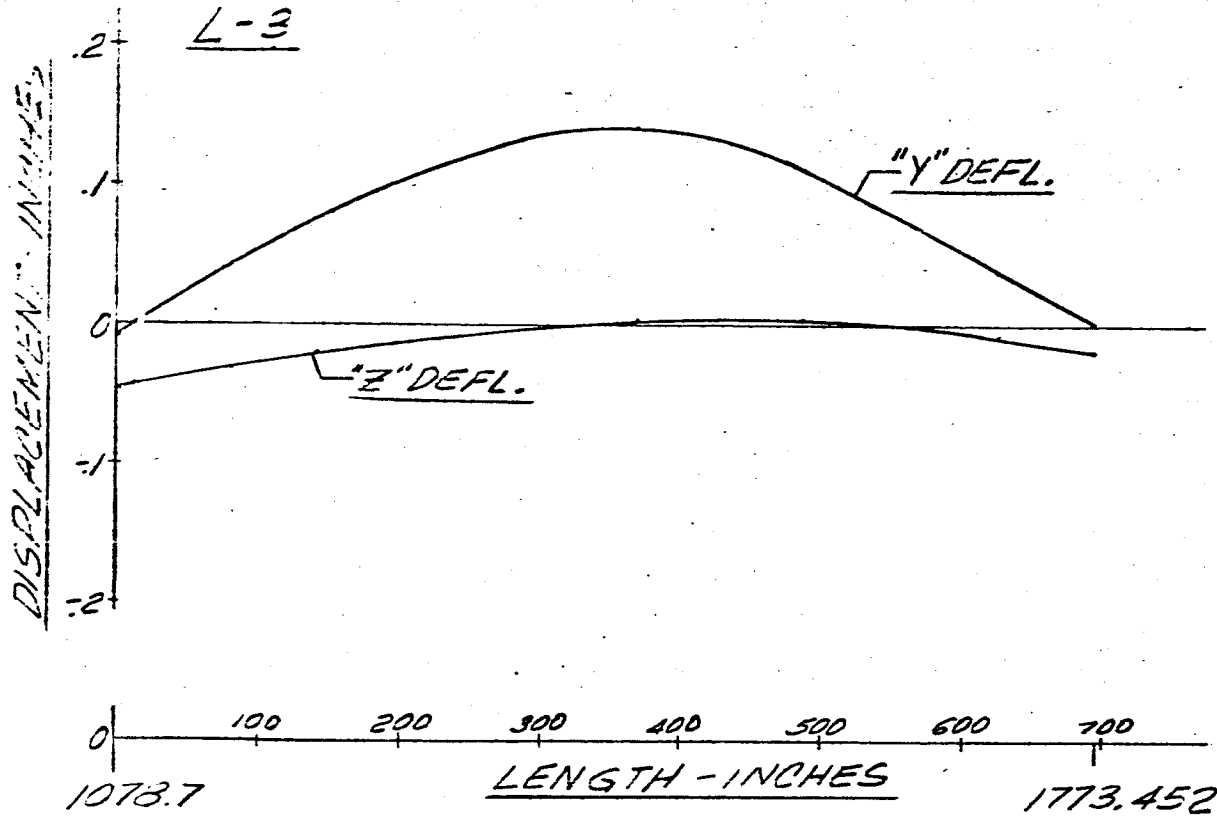
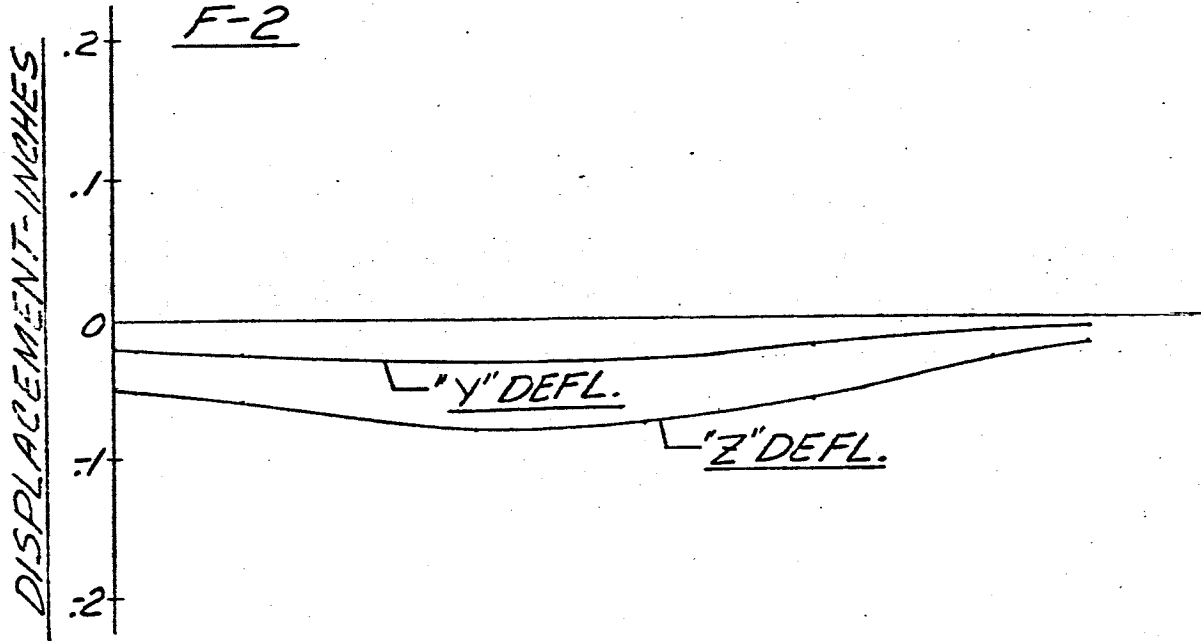
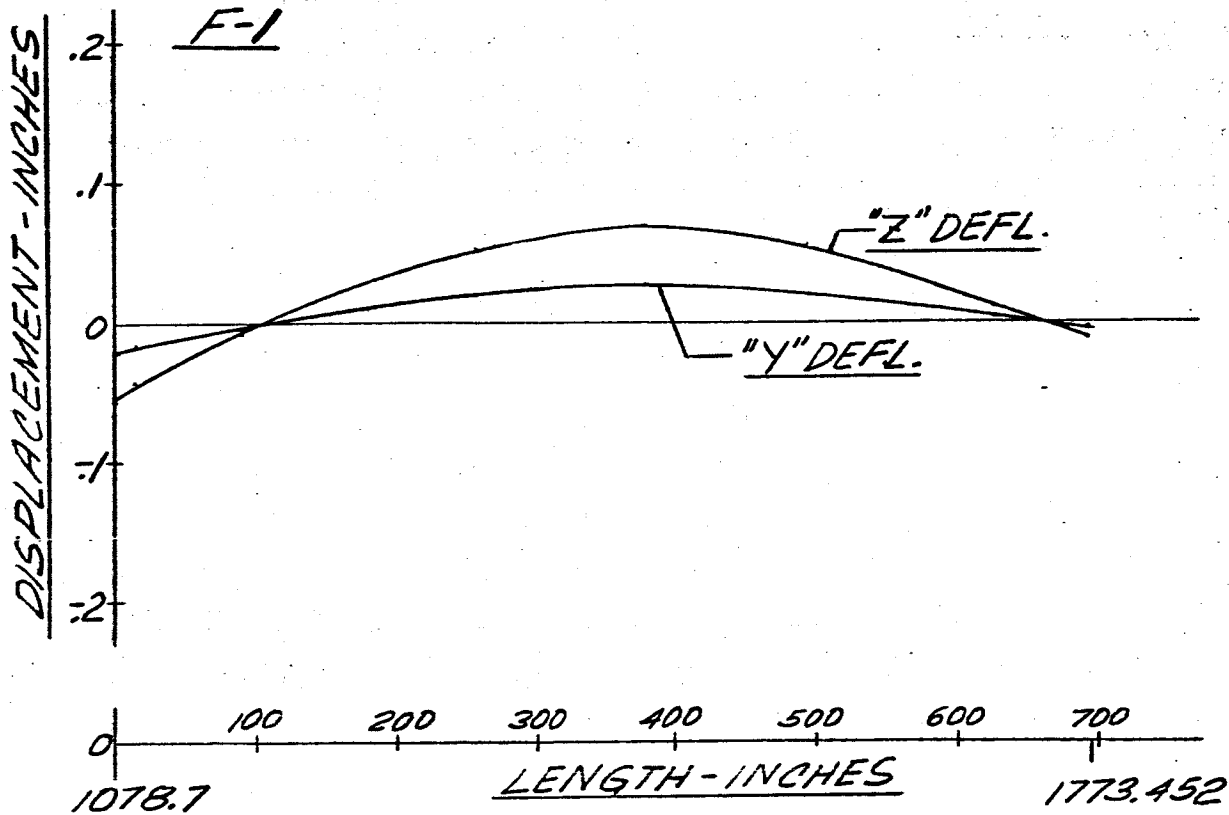


FIG 57 DISPLACEMENT VS LENGTH SATURN SA-DI

FREQUENCY = 2.40 CPS



-140-

FIG 5B DISPLACEMENT VS LENGTH SATURN SA-DI  
FREQUENCY = 2.40 CPS.

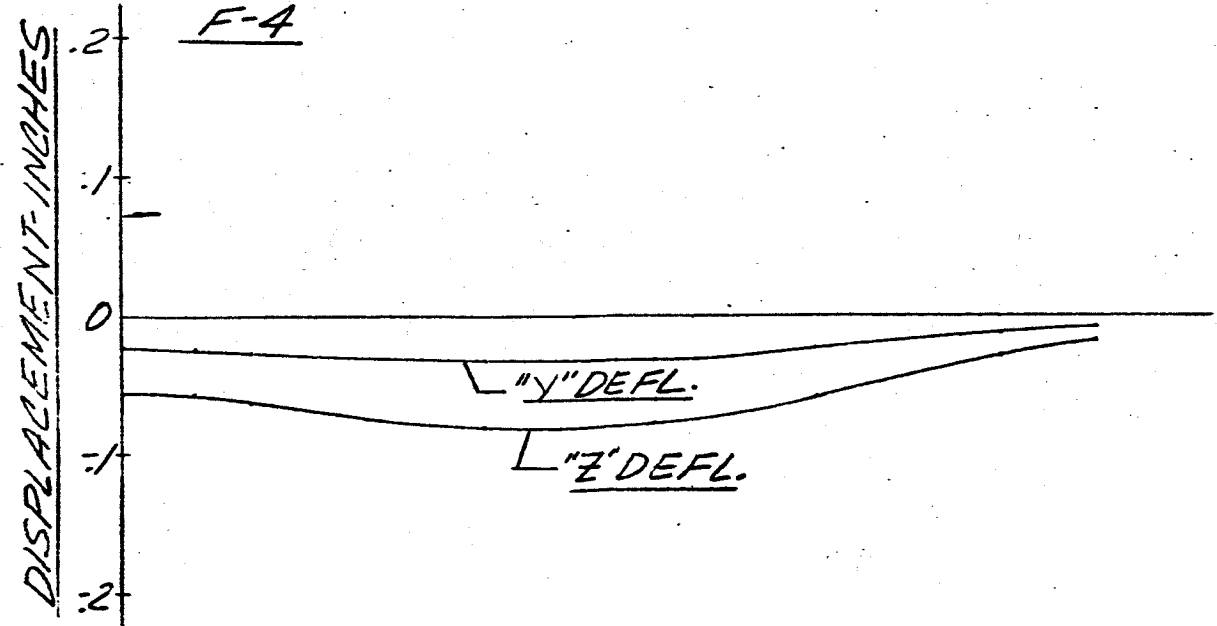
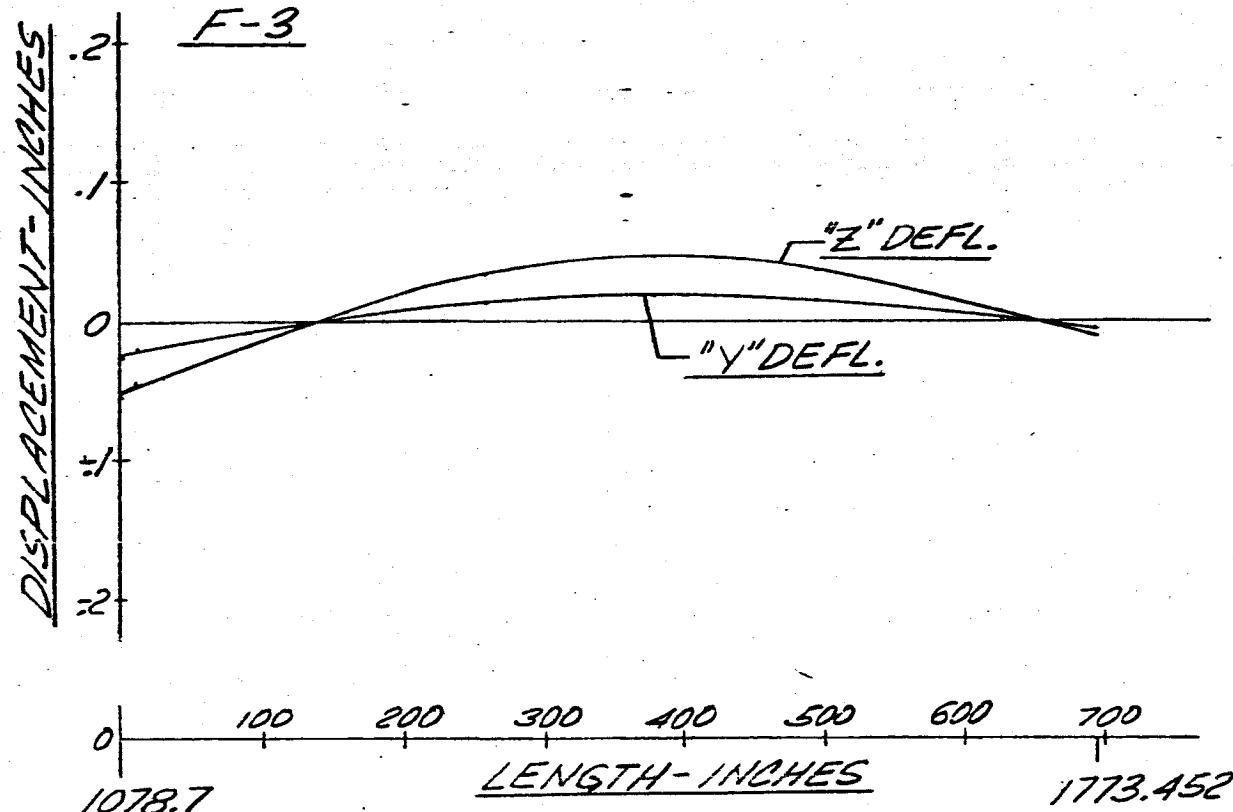
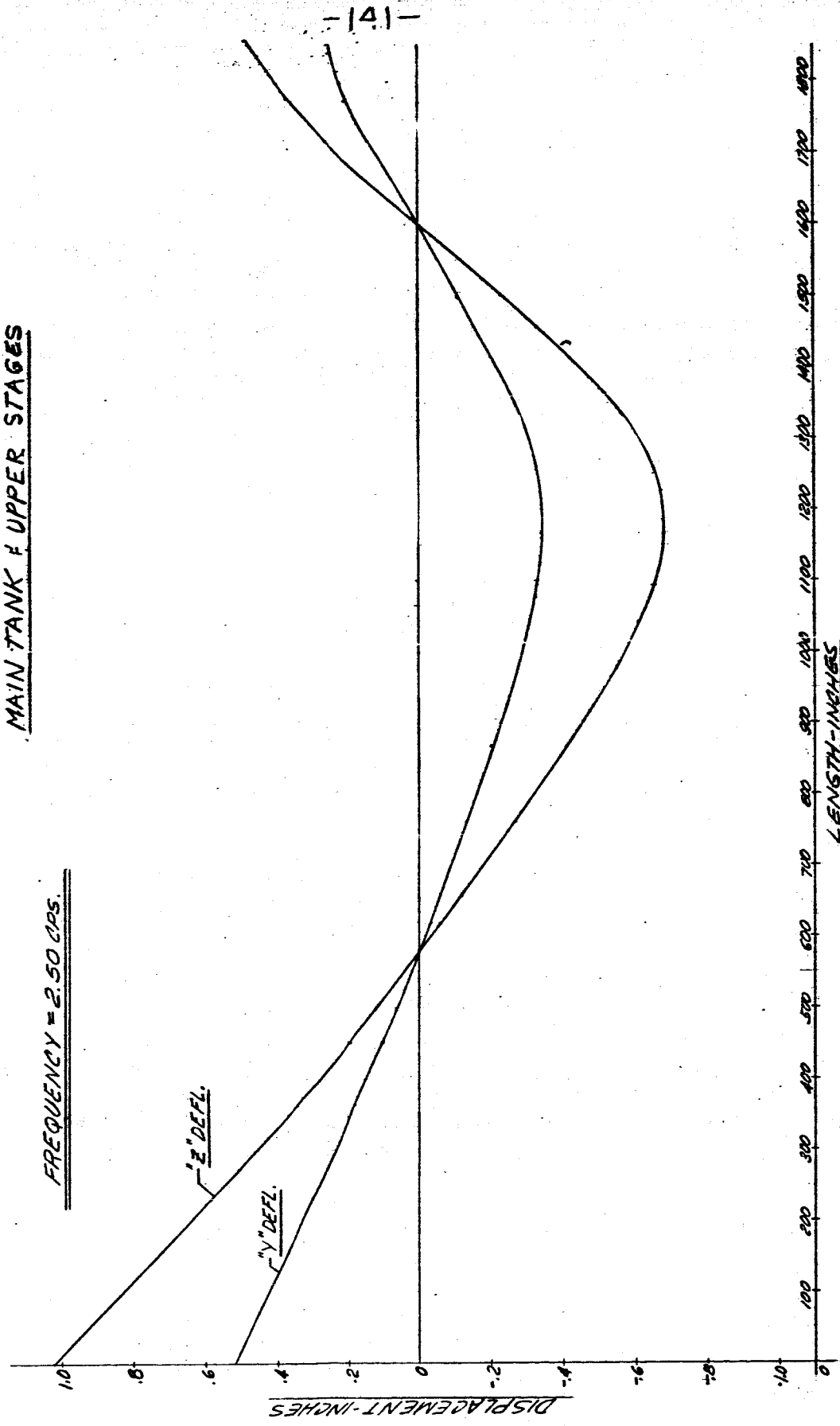


FIG. 59 DISPLACEMENT vs LENGTH SATURN SA-01  
MAIN TANK & UPPER STAGES

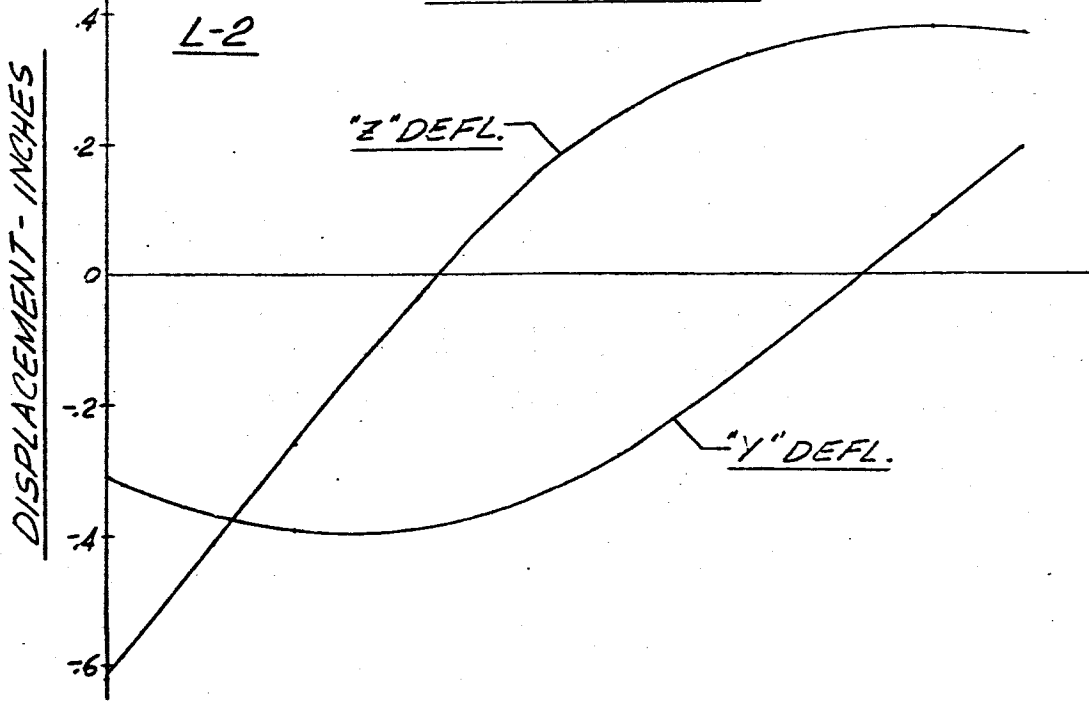
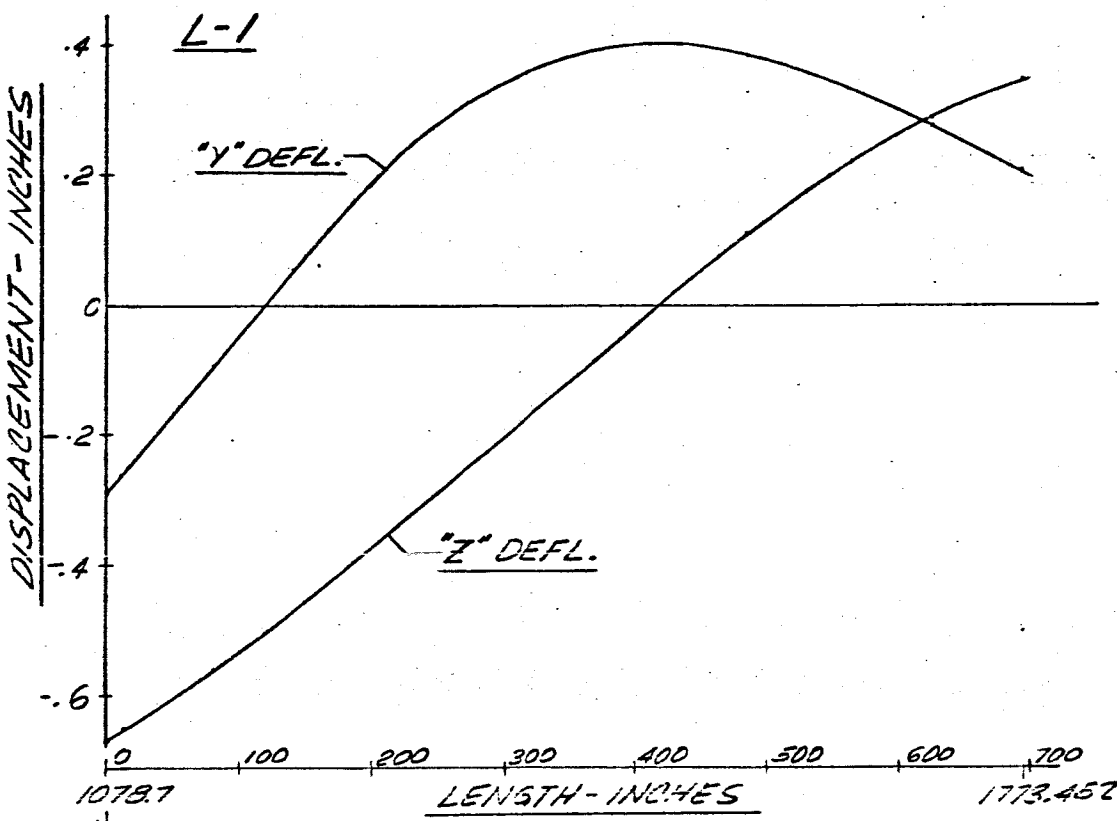
FREQUENCY = 2.50 CPS.



-192-

FIG 60 DISPLACEMENT VS LENGTH SATURN SA-D1

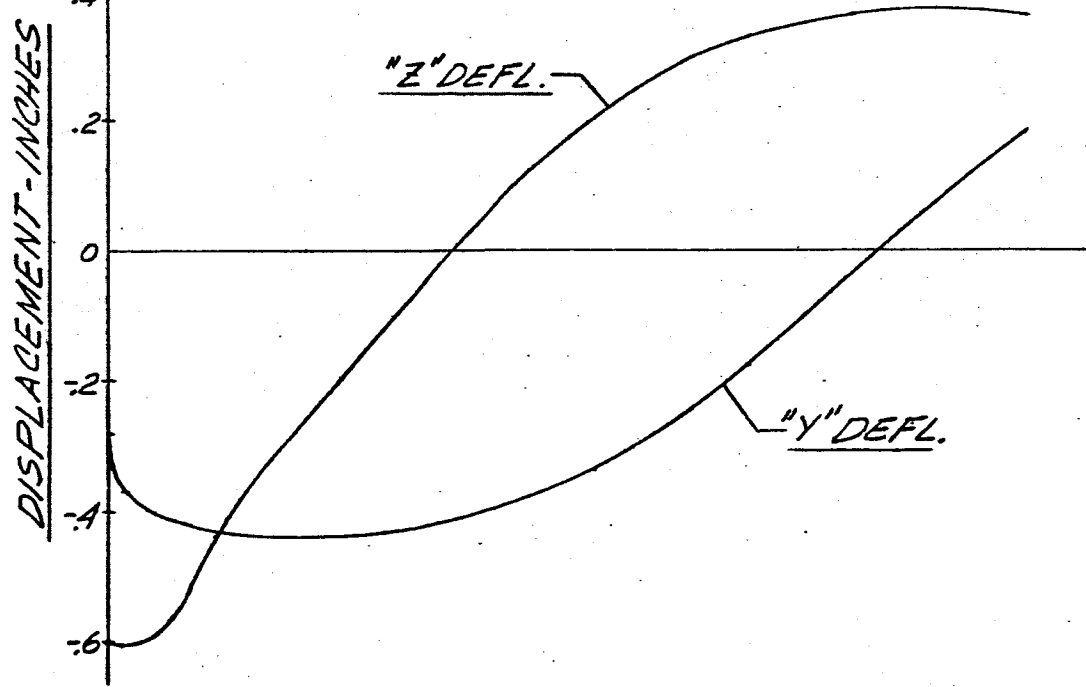
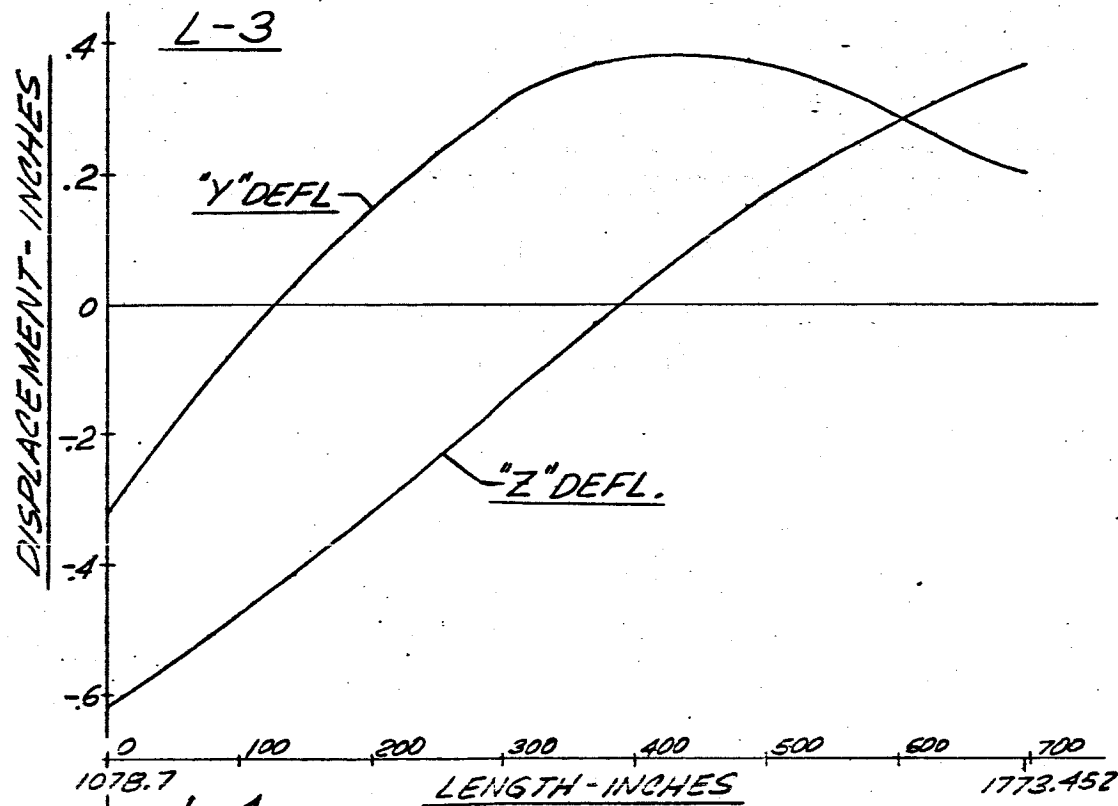
FREQUENCY=2.50 CPS.



-143-

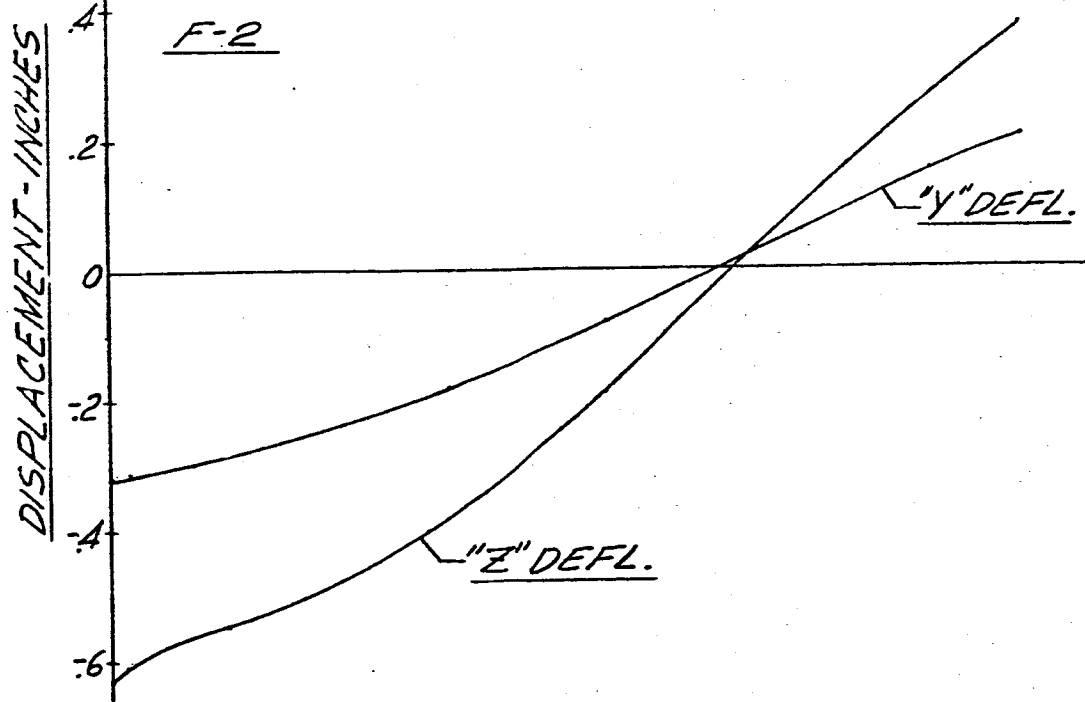
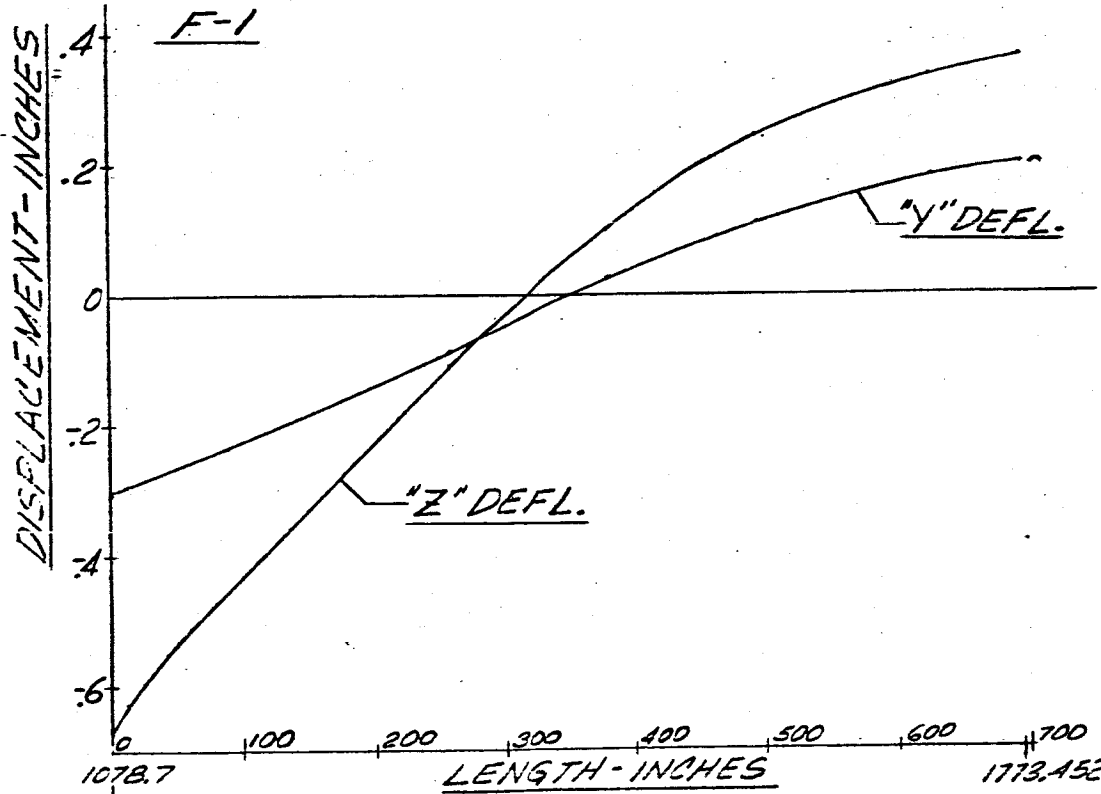
FIG 61 DISPLACEMENT VS LENGTH SATURN SA-D1

FREQUENCY = 2.50 CPS



-144-

FIG GR DISPLACEMENT VS LENGTH SATURN SA-D1  
FREQUENCY=2.50 CPS.



-145-

FIG 63 DISPLACEMENT VS LENGTH SATURN SA-DI

FREQUENCY = 2.50 CPS

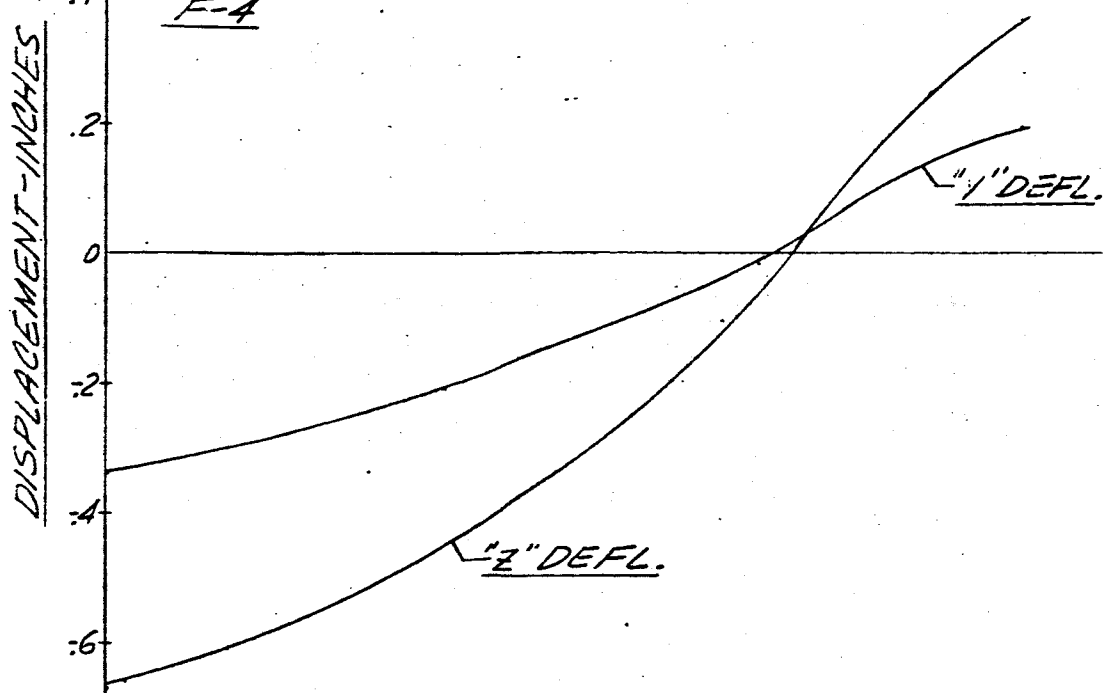
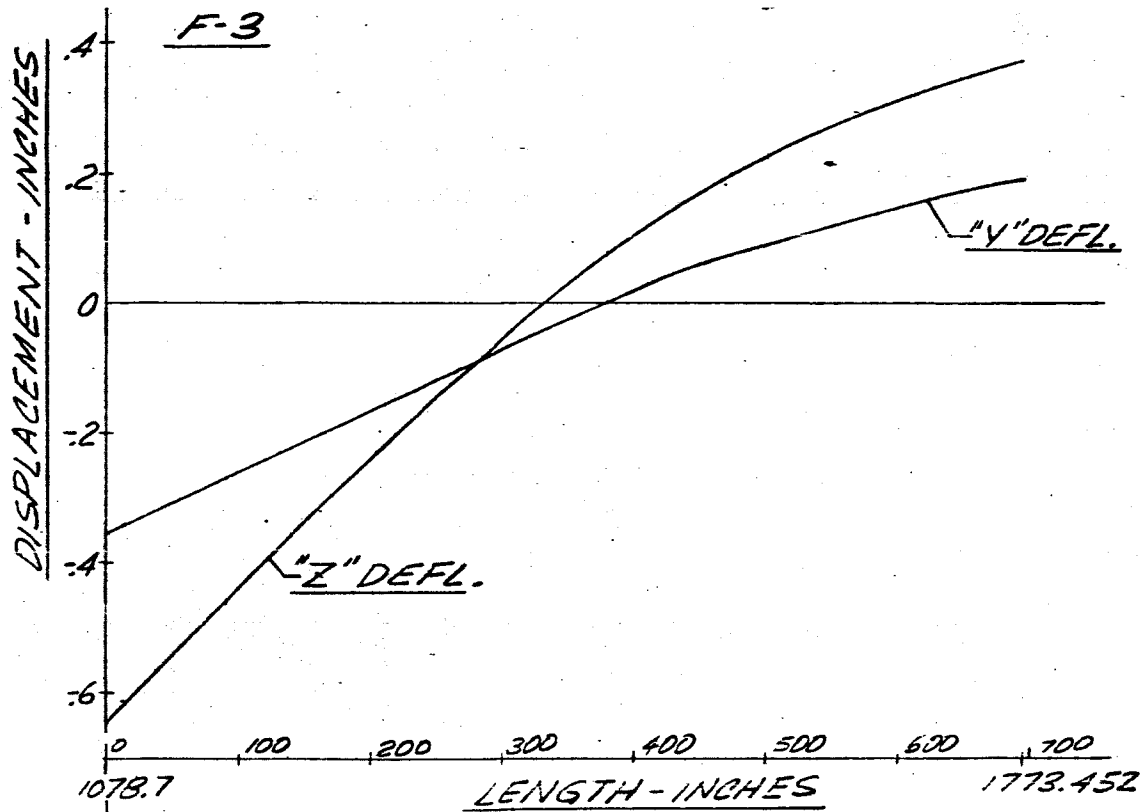


FIG G4 DISPLACEMENT vs LENGTH SATURN SA-DI  
FREQUENCY = 2.54 CPS MAIN TANK & UPPER STAGES

-146-

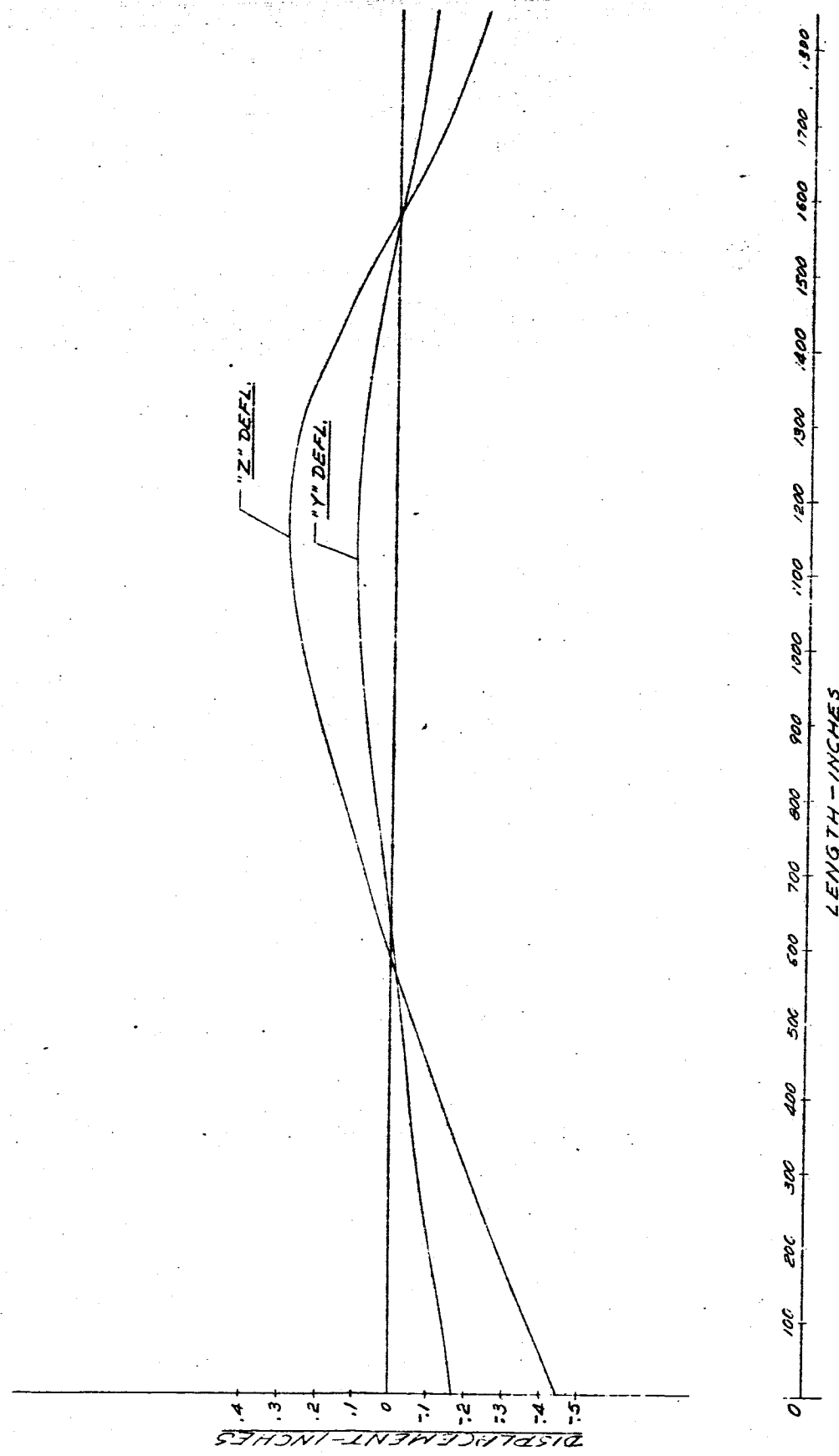
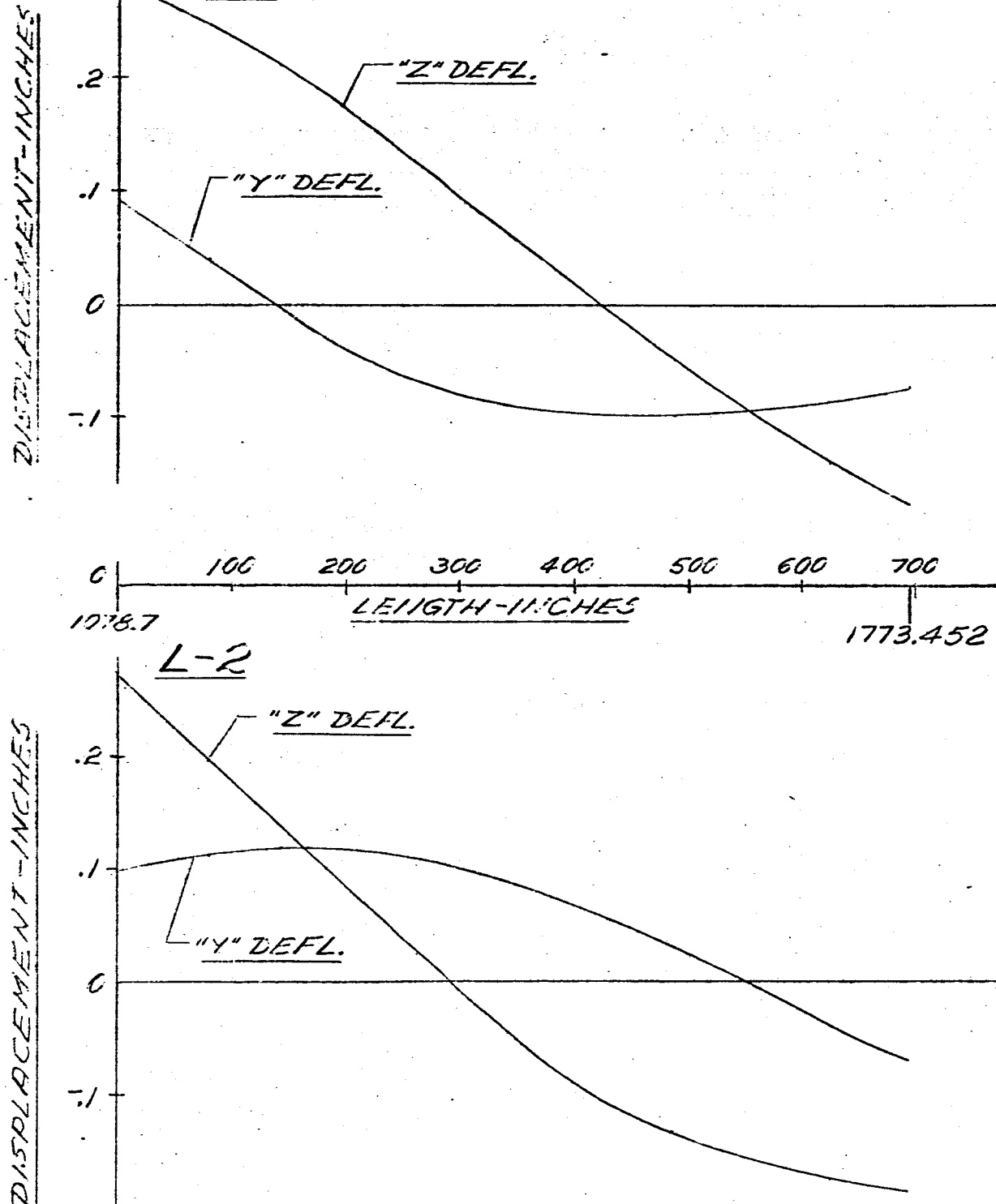


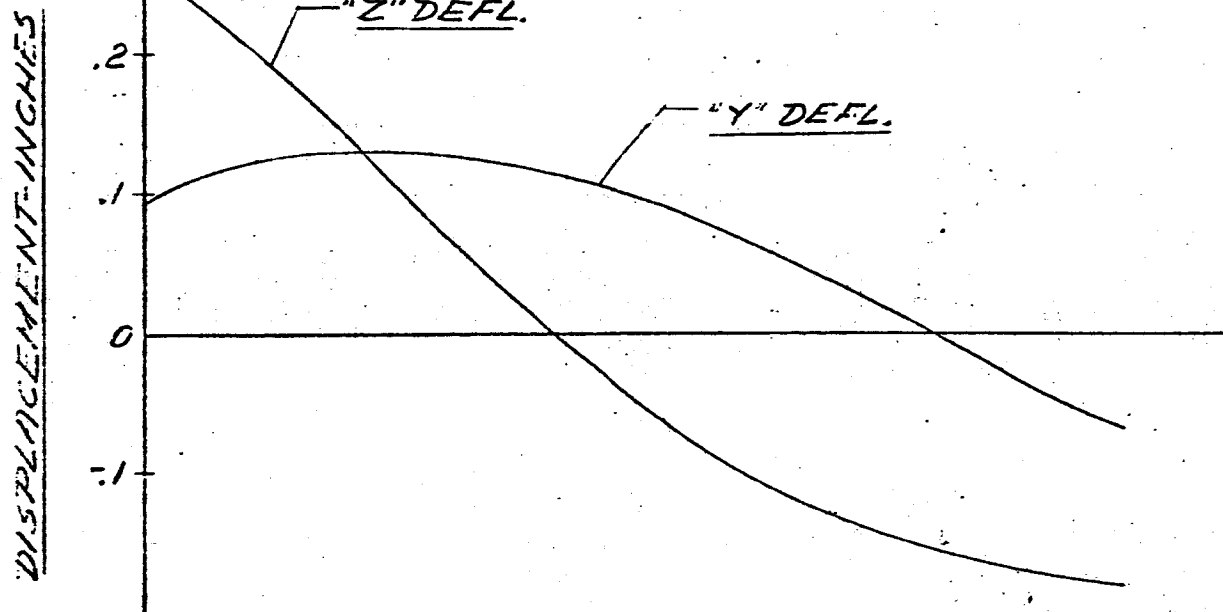
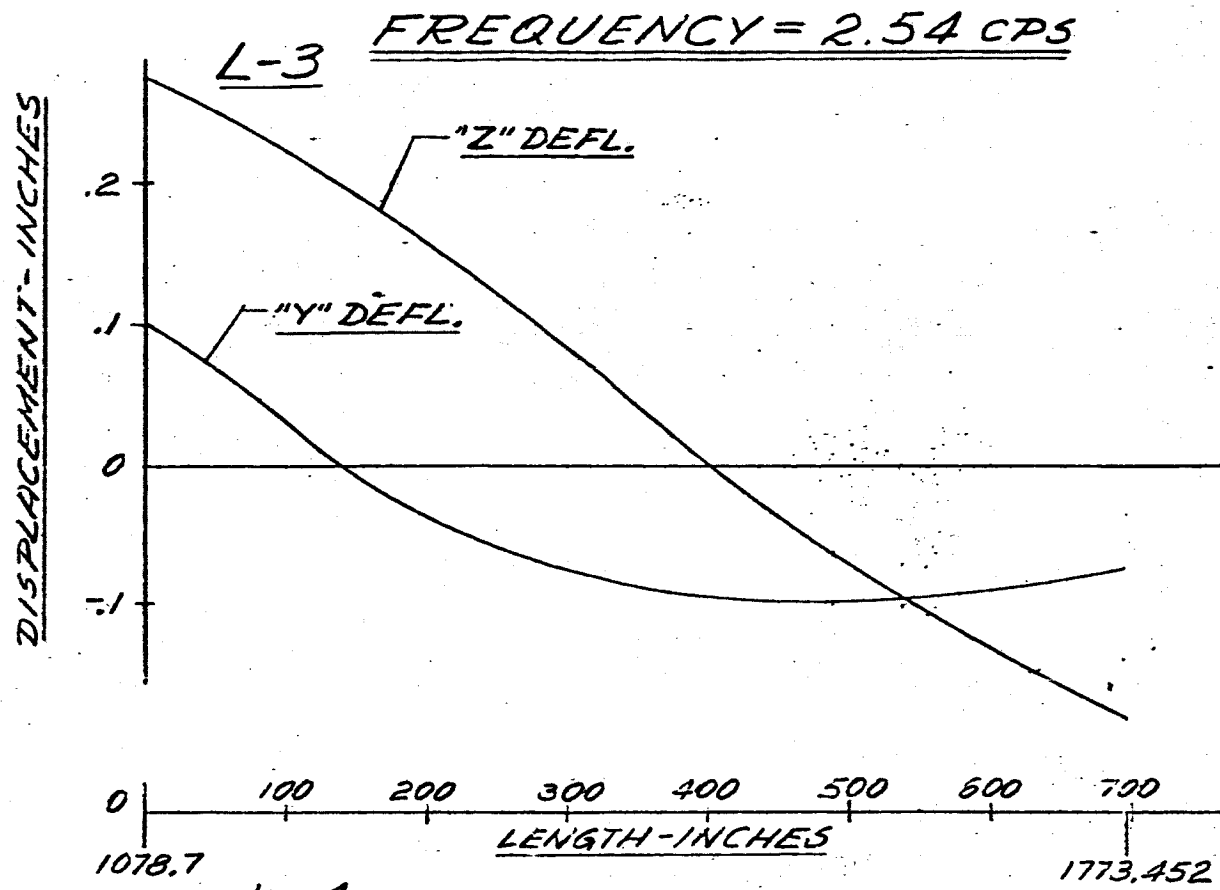
FIG 65 DISPLACEMENT VS LENGTH SATURN SA-DI

FREQUENCY = 2.54 CPS



-148-

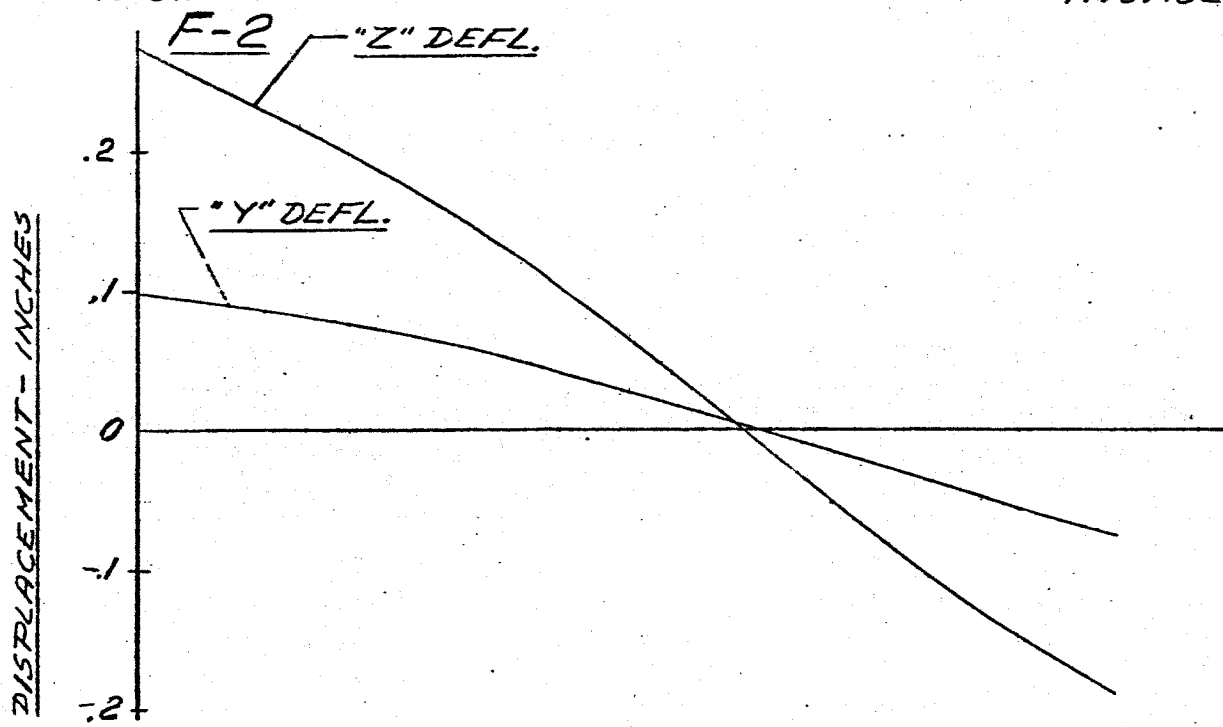
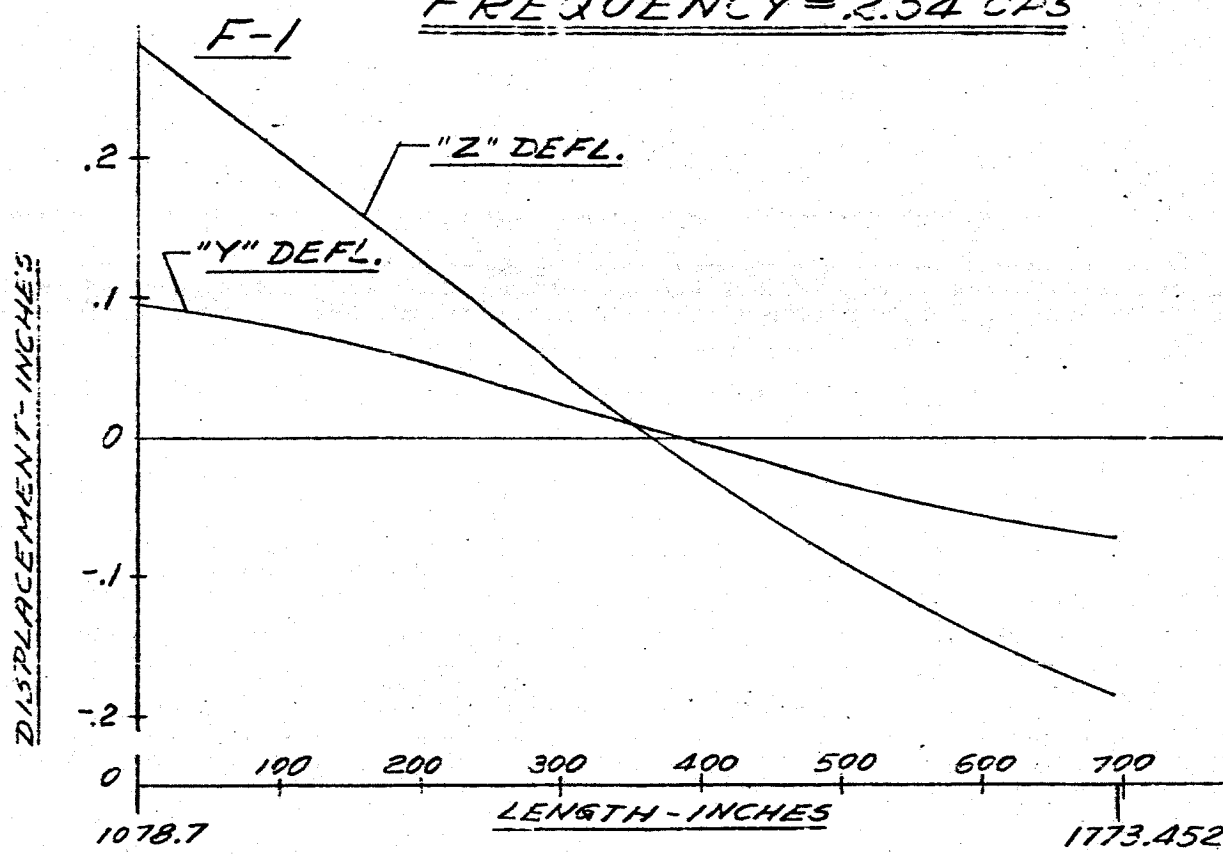
FIG 66 DISPLACEMENT VS LENGTH SATURN SA-D1



-149-

FIG 67 DISPLACEMENT VS LENGTH SATURN SA-DI

FREQUENCY = 2.54 CPS



-150-

FIG 6B DISPLACEMENT VS LENGTH SATURN SA-DI

FREQUENCY = 2.54 CPS

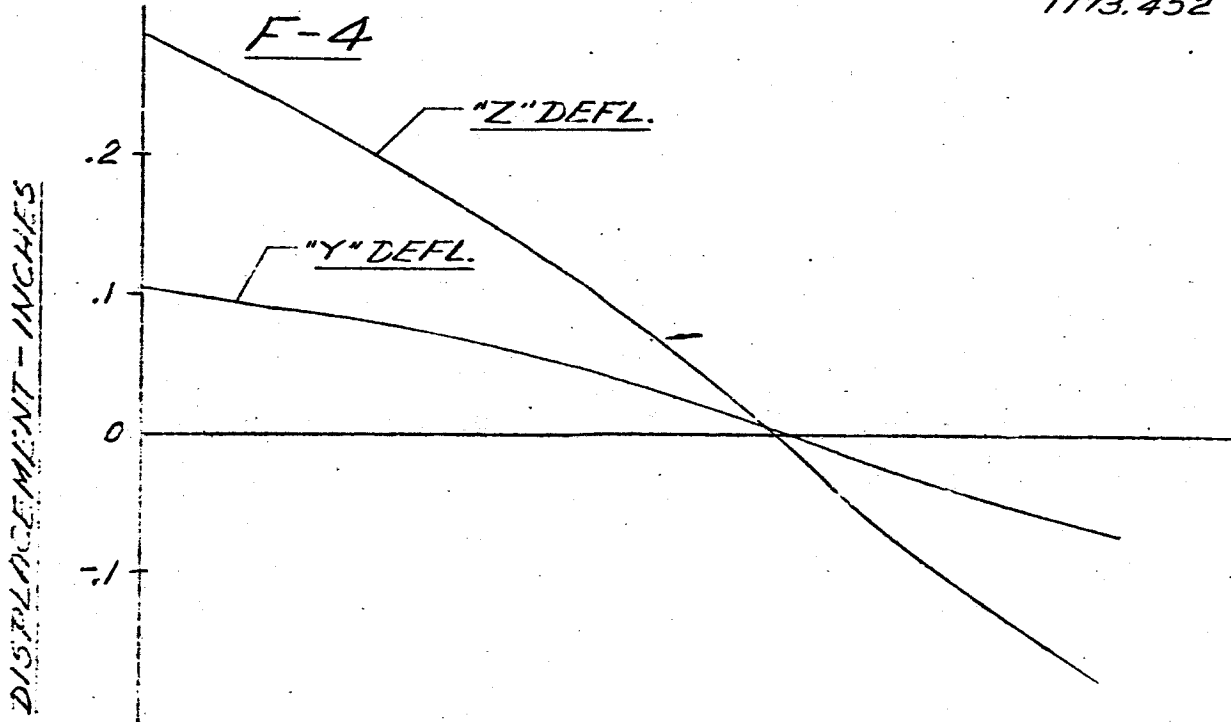
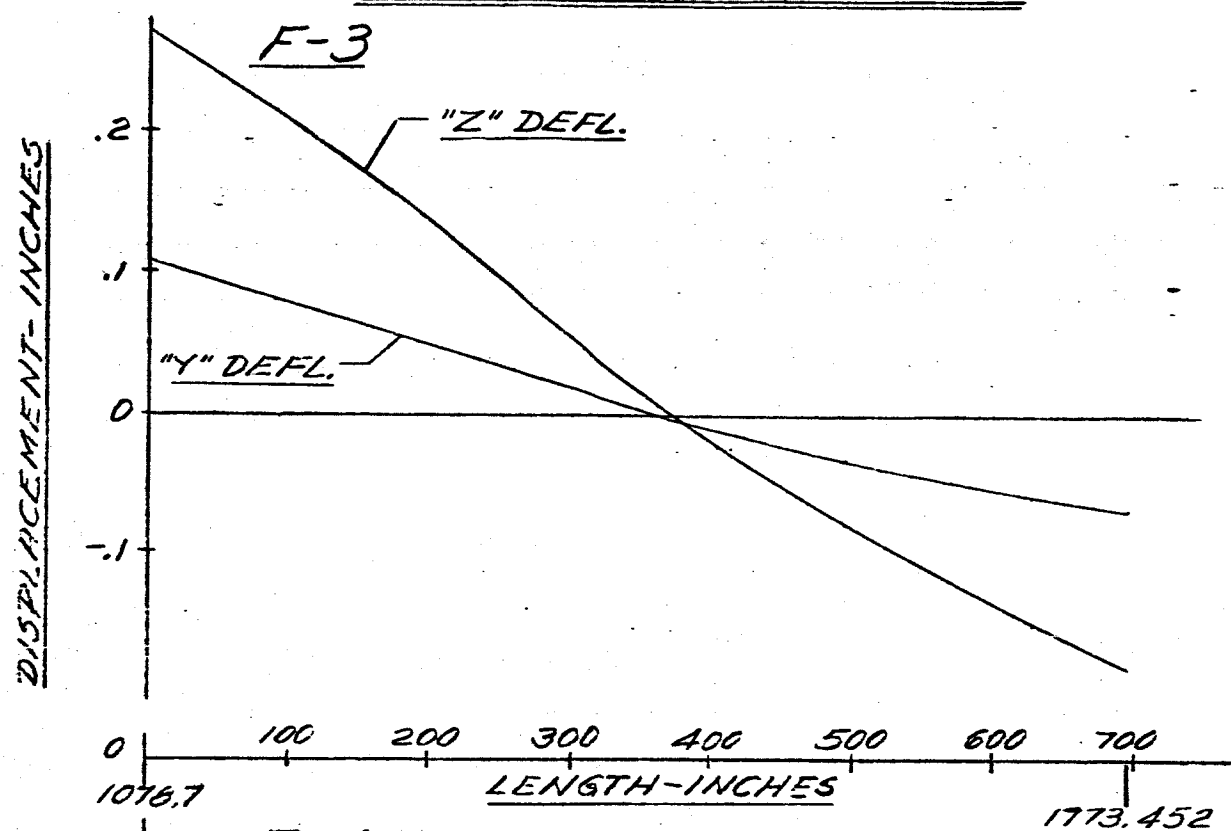
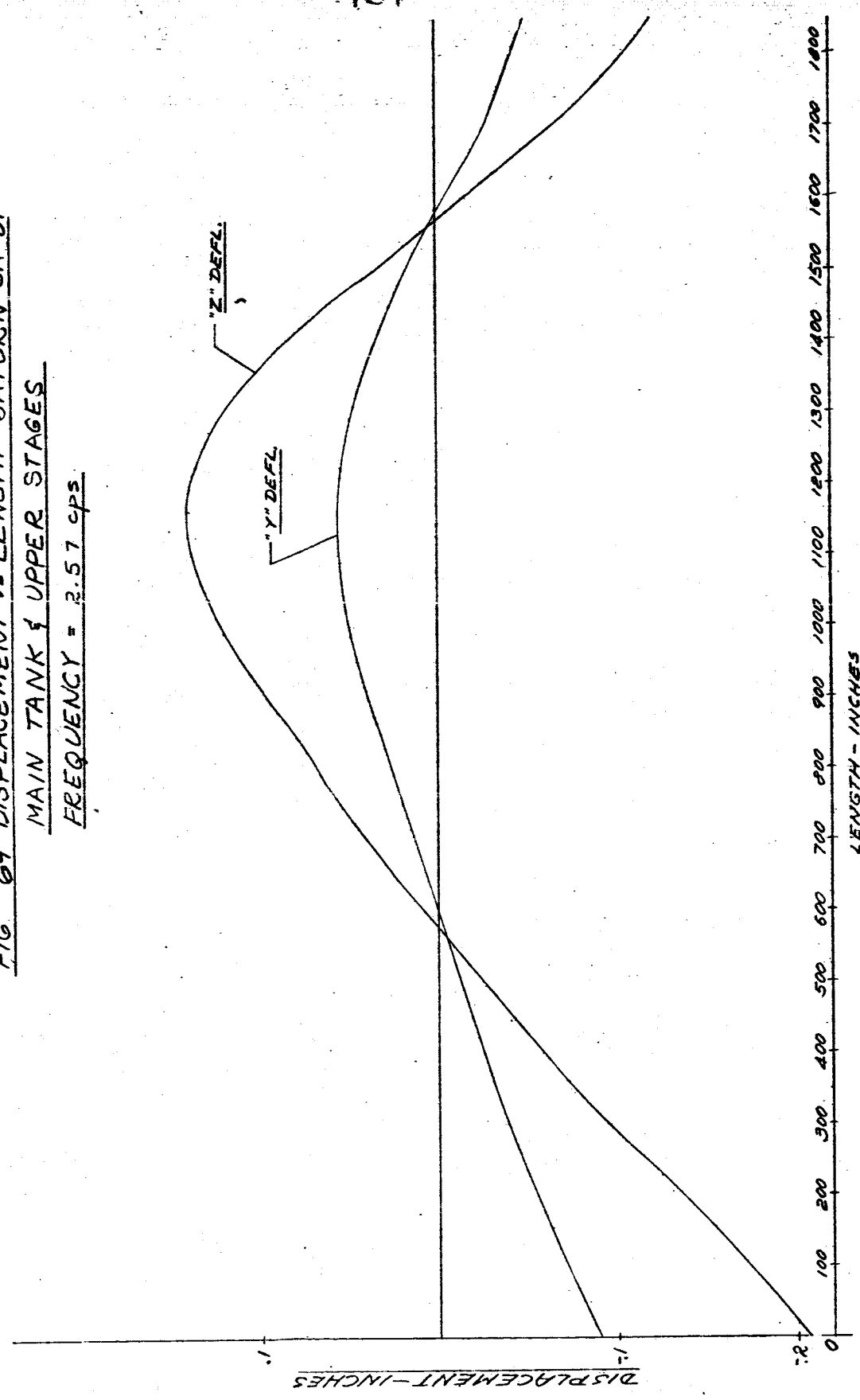


FIG. 69 DISPLACEMENT VS LENGTH SATURN SA-DI

MAIN TANK & UPPER STAGES

FREQUENCY = 2.57 cps.



- 152 -

FIG 7D DISPLACEMENT VS LENGTH SATURN SA-D1

FREQUENCY = 2.57 CPS

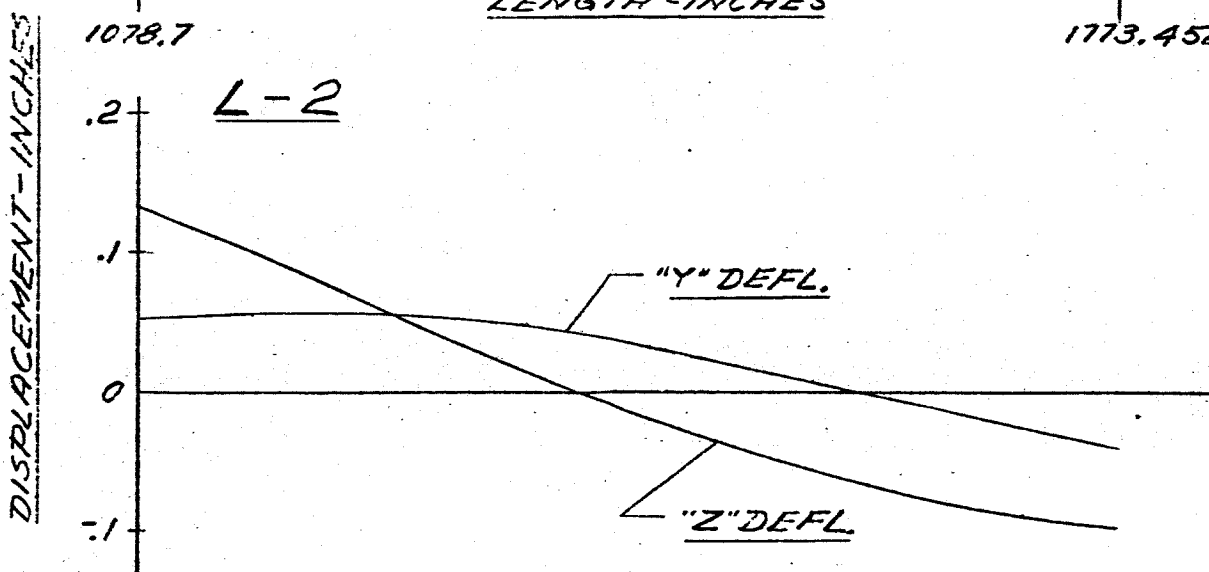
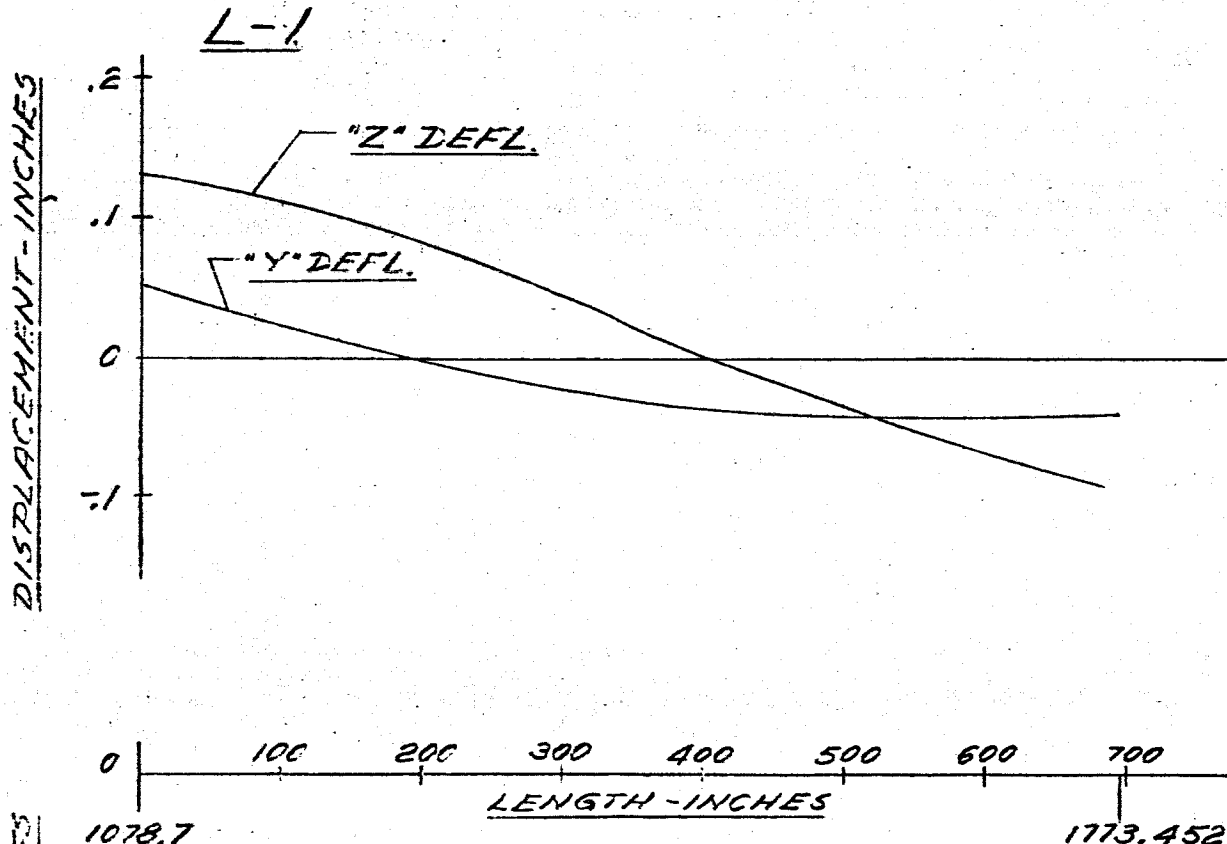
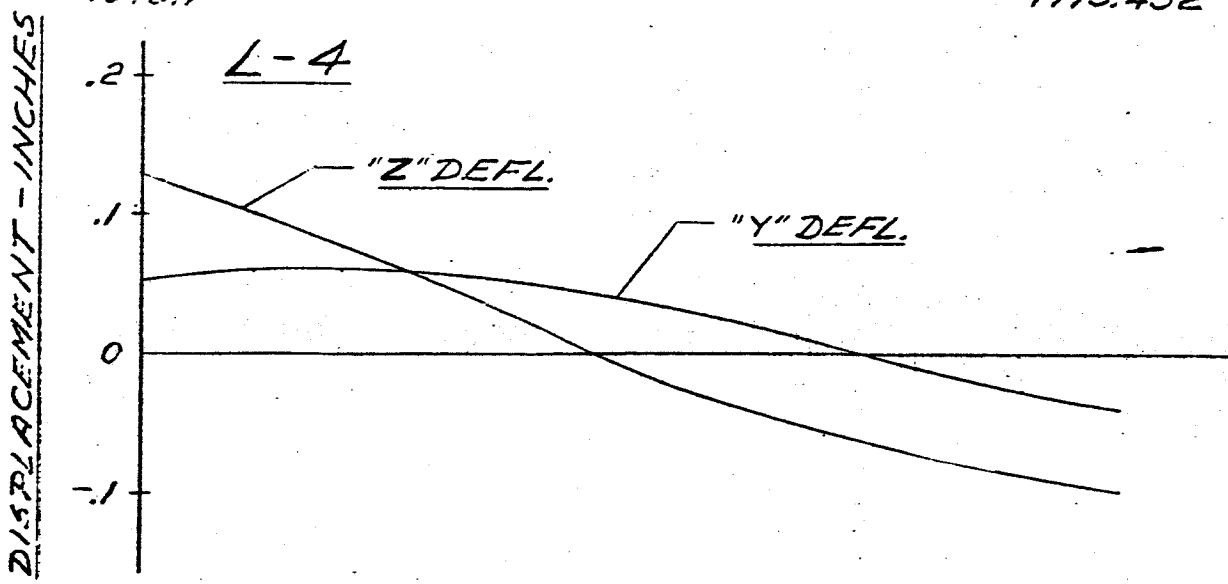
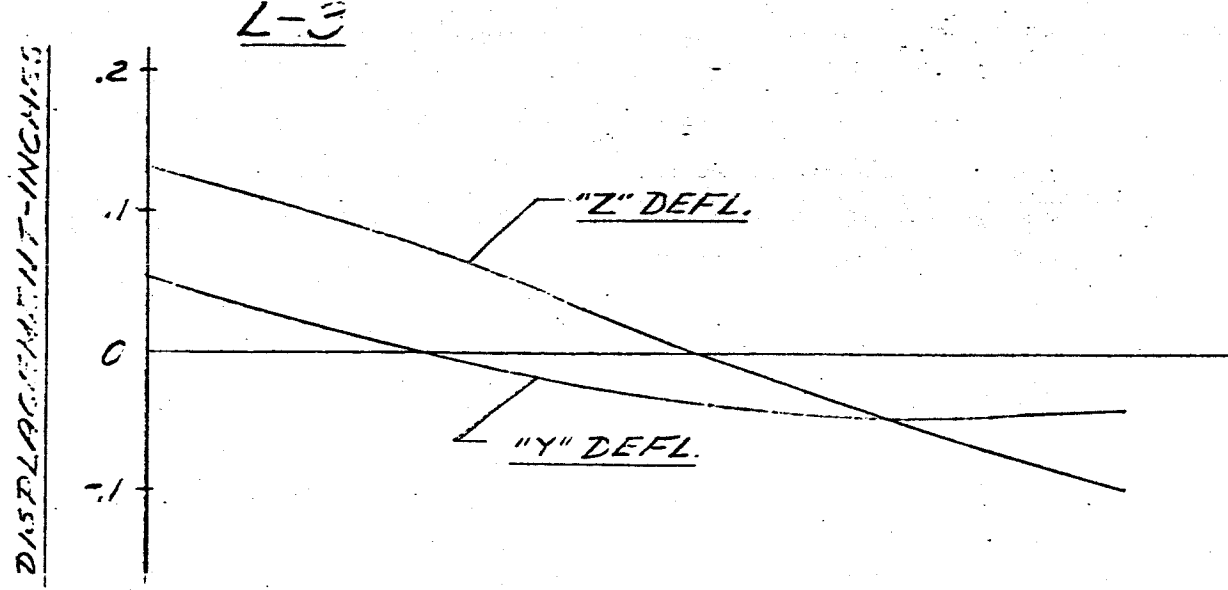


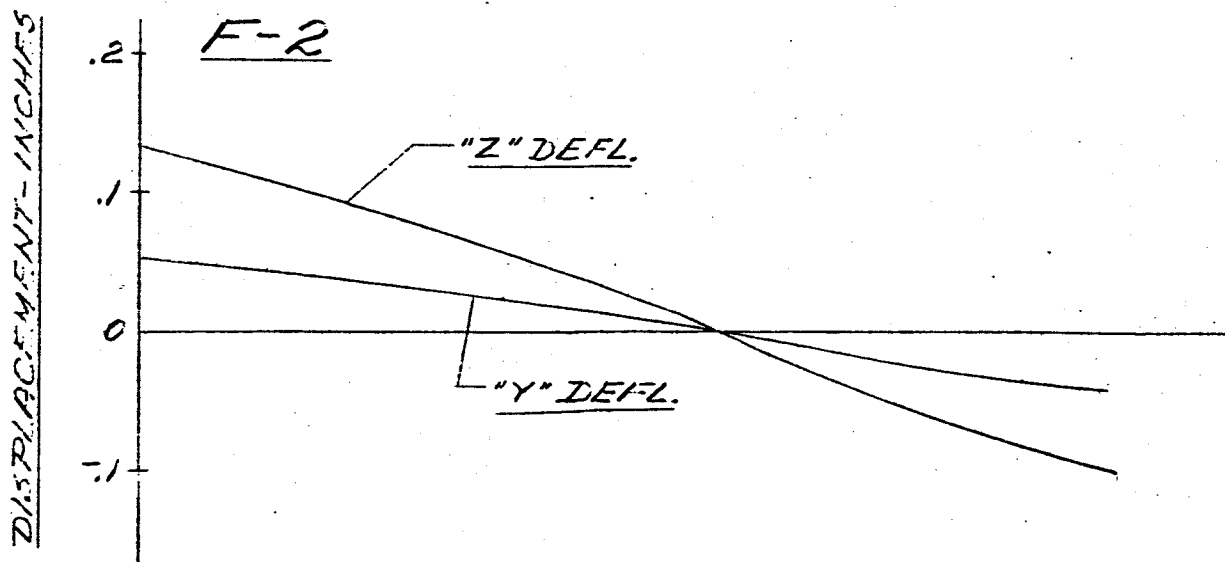
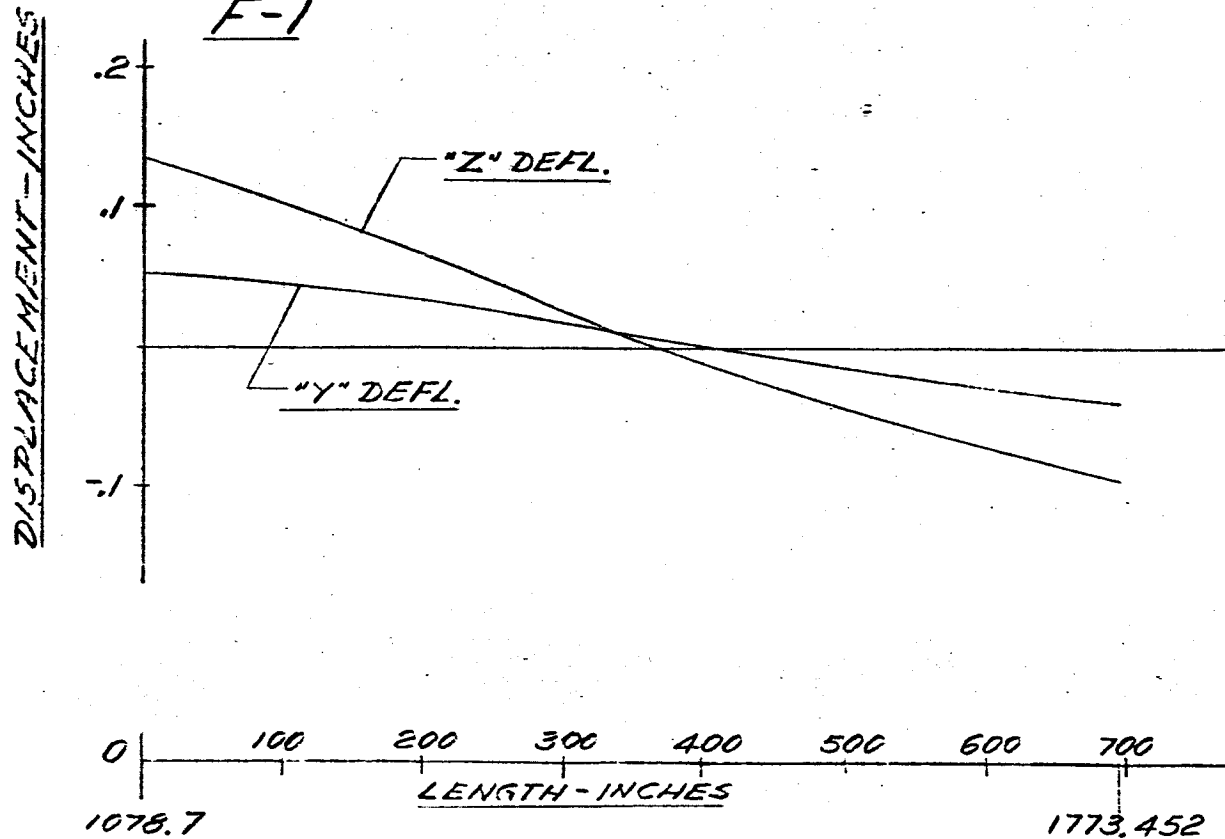
FIG 71 DISPLACEMENT VS LENGTH SATURN SA-D1

FREQUENCY = 2.57 CPS



-154-

FIG 72 DISPLACEMENT VS LENGTH SATURN SA-DI  
FREQUENCY = 2.57 CPS



-155-

FIG 73 DISPLACEMENT VS LENGTH SATURN SA-D1  
FREQUENCY = 2.57 CPS

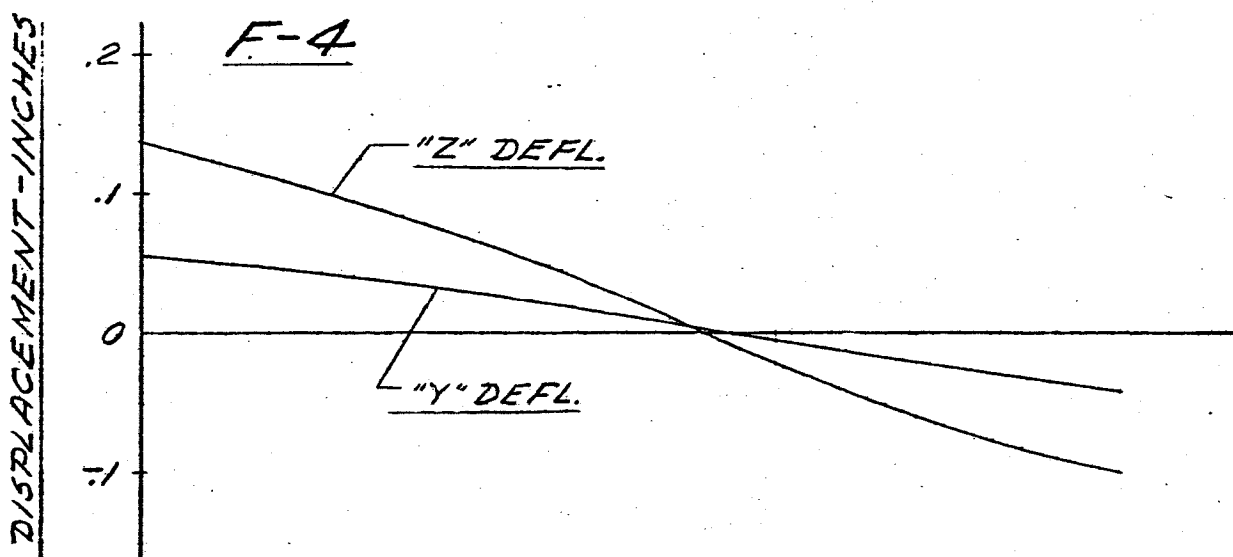
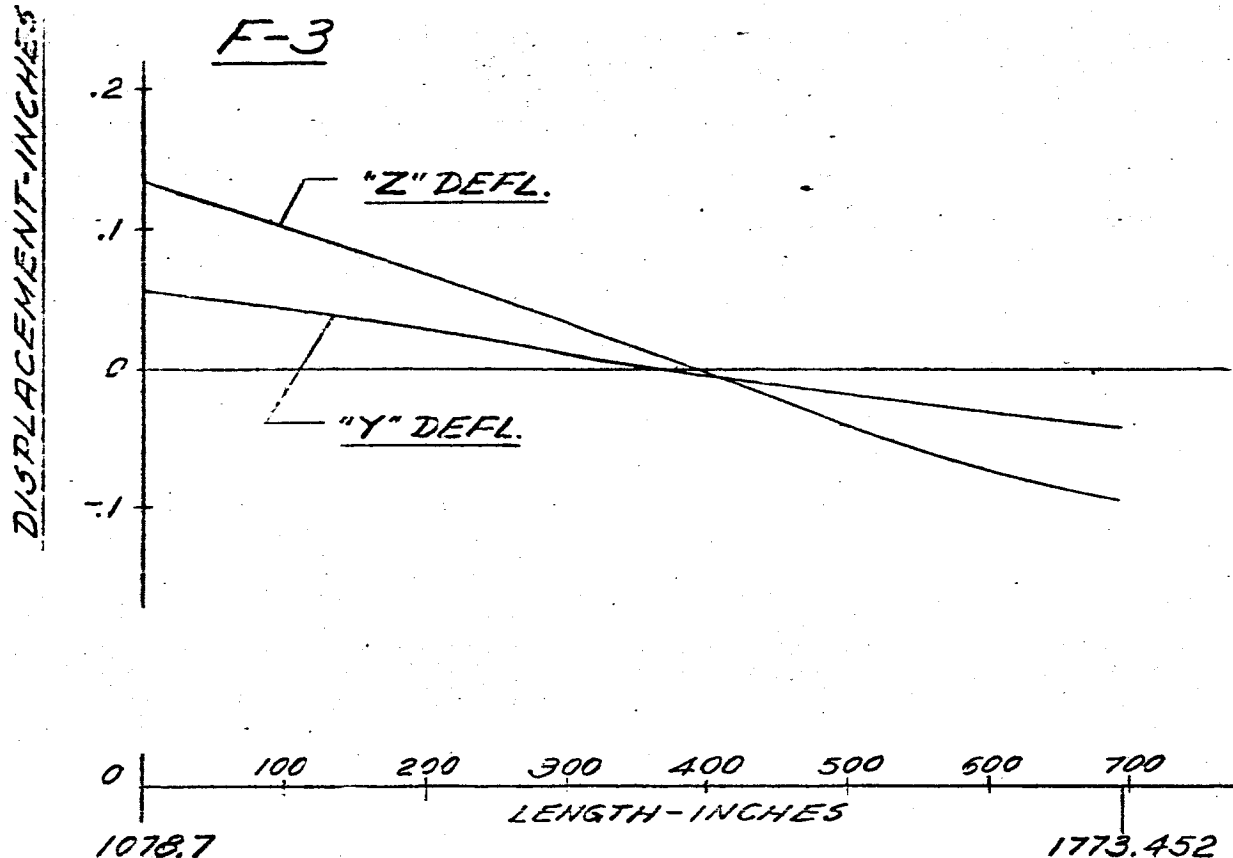


FIG. 7A DISPLACEMENT vs LENGTH SATURN SA-DI  
FREQUENCY = 2.60 CPS. MAIN TANK & UPPER STAGES

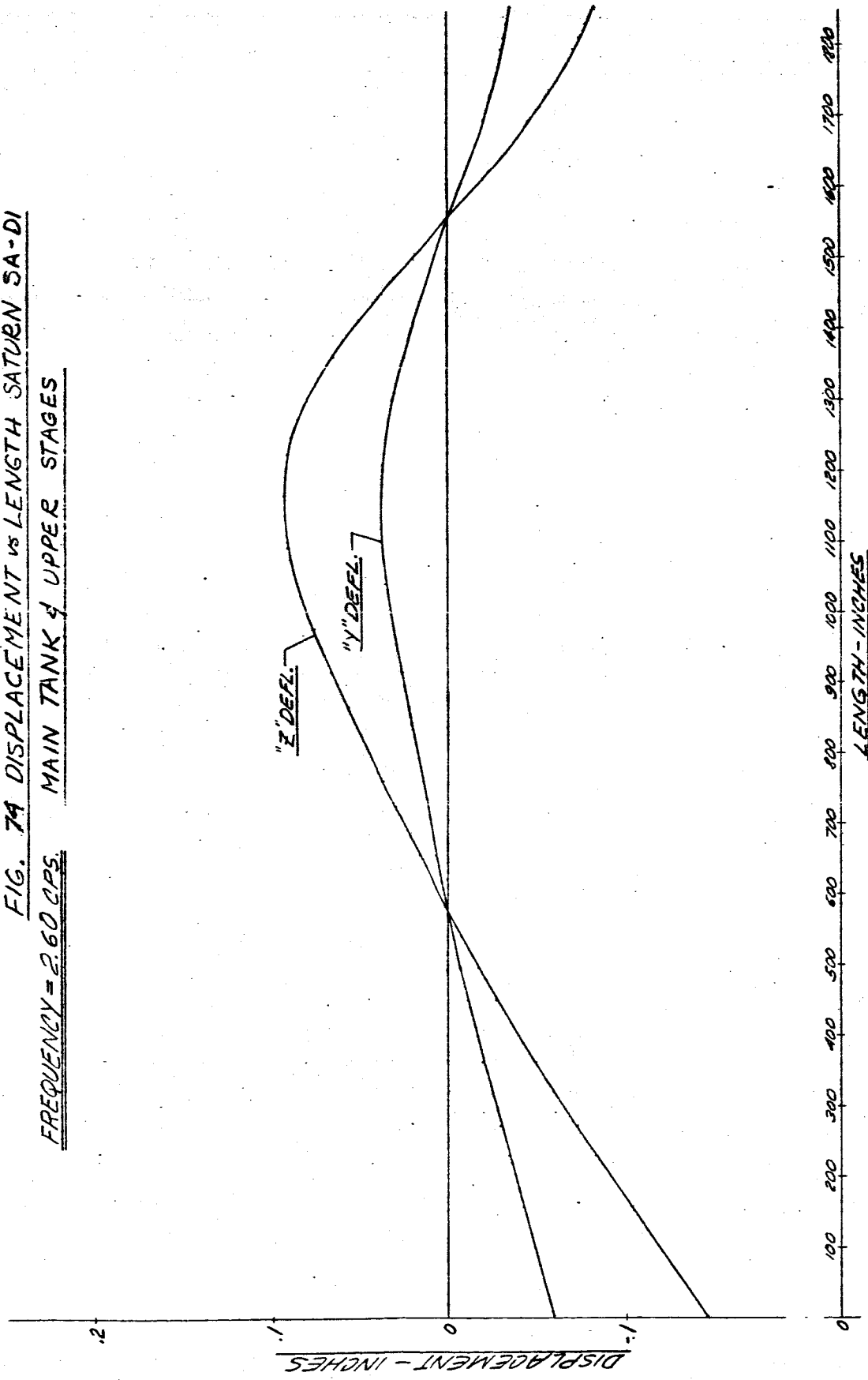
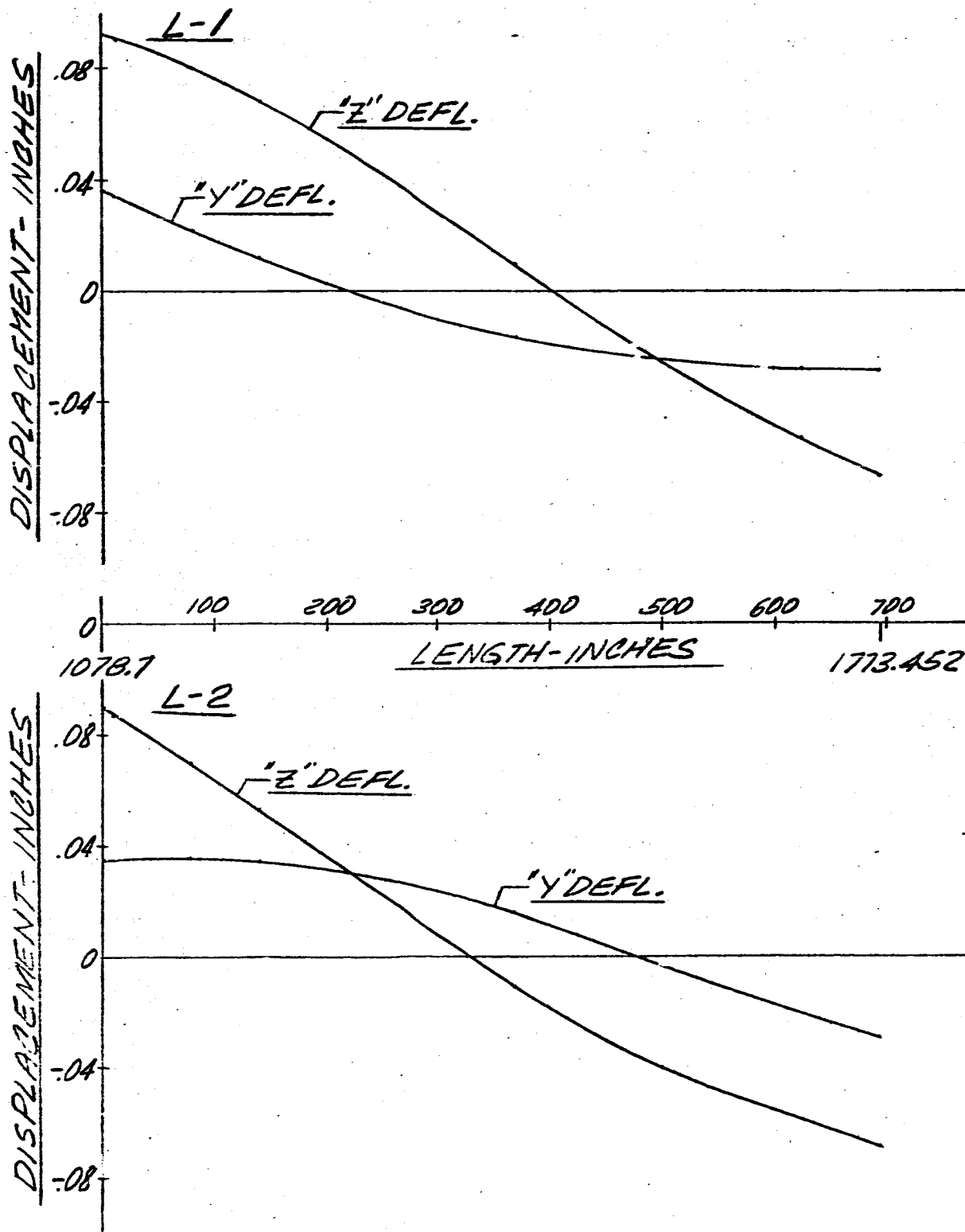


FIG 75 DISPLACEMENT VS LENGTH SATURN SA-01  
FREQUENCY = 2.60 CPS.



-158-

FIG 76 DISPLACEMENT VS LENGTH SATURN SA-D1

FREQUENCY = 2.60 CPS.

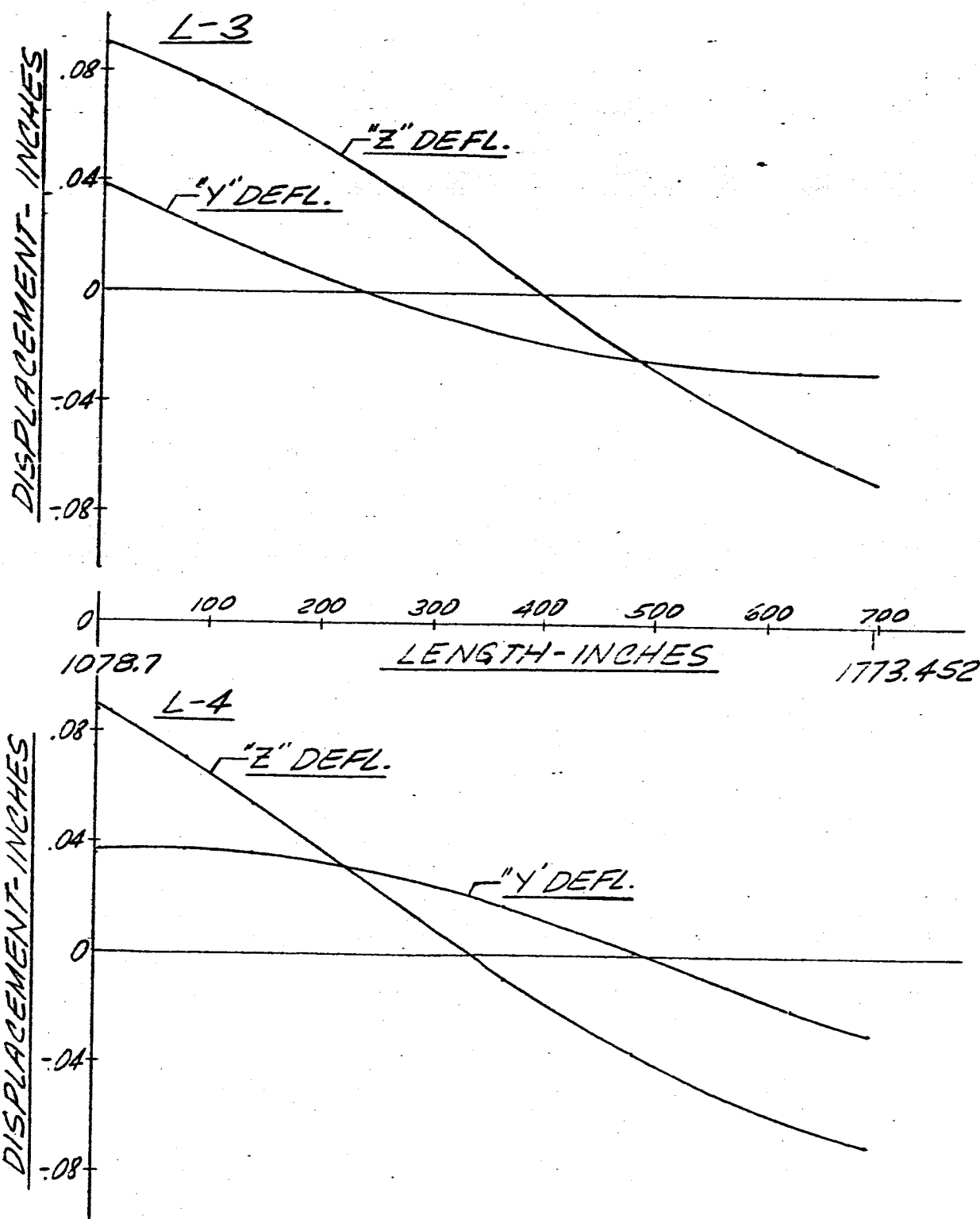
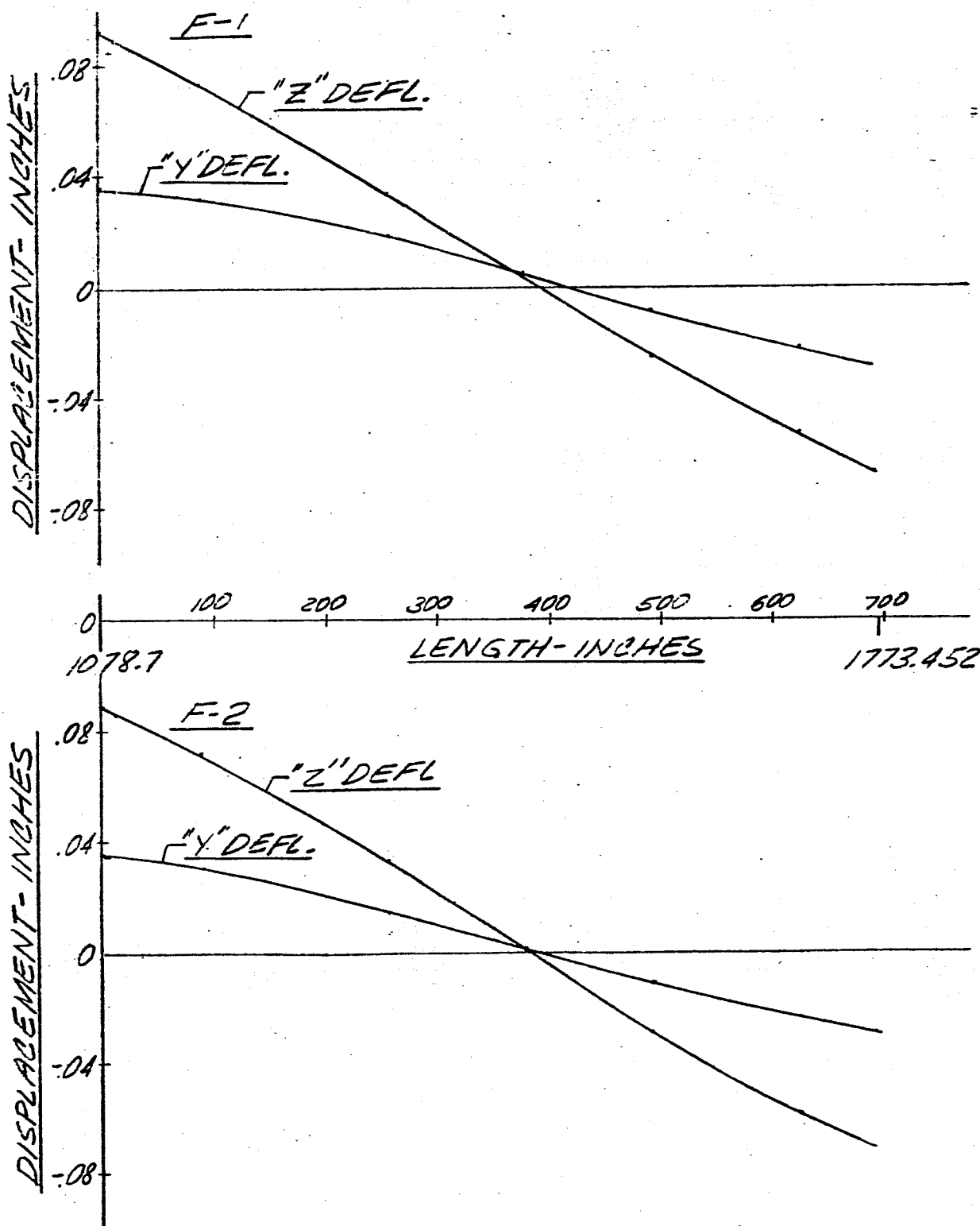


FIG 71 DISPLACEMENT IS LENGTH SATURN SA-DI  
FREQUENCY=2.60 CPS.



-160-

FIG 7B DISPLACEMENT VS LENGTH SATURN SA-DI

FREQUENCY = 2.60 CPS.

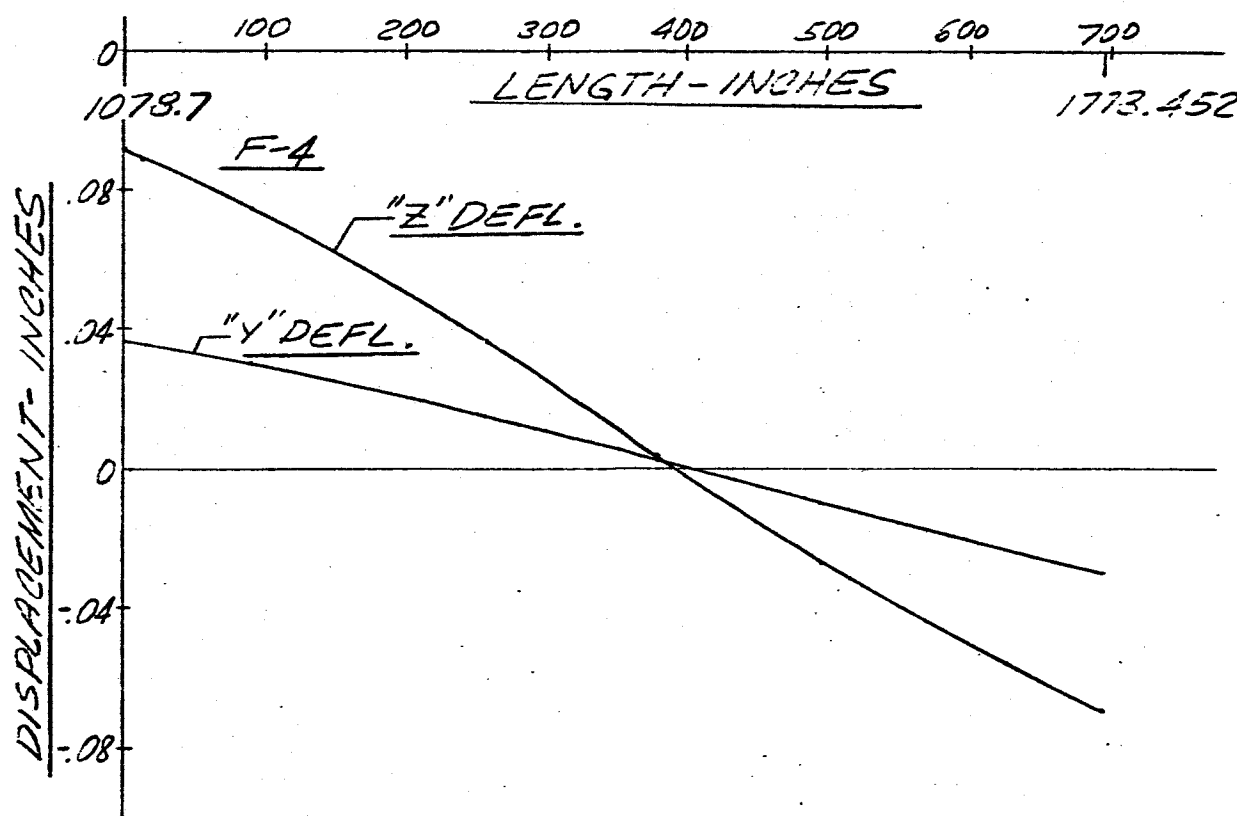
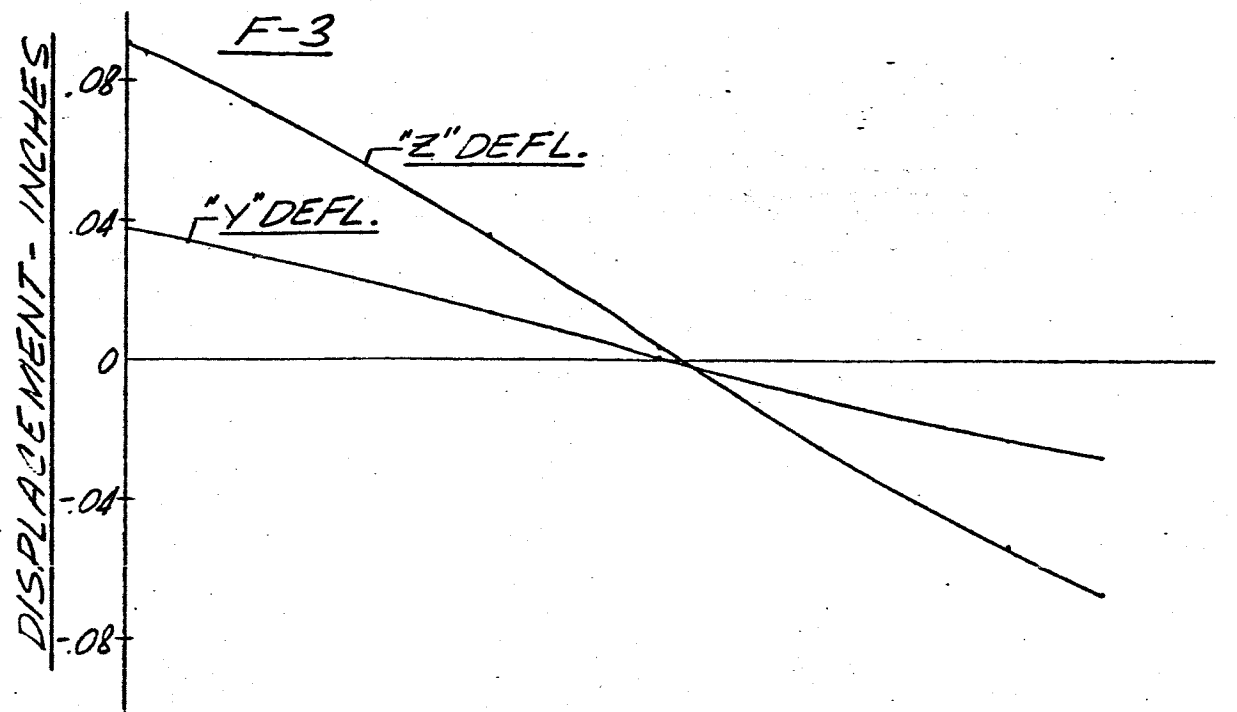
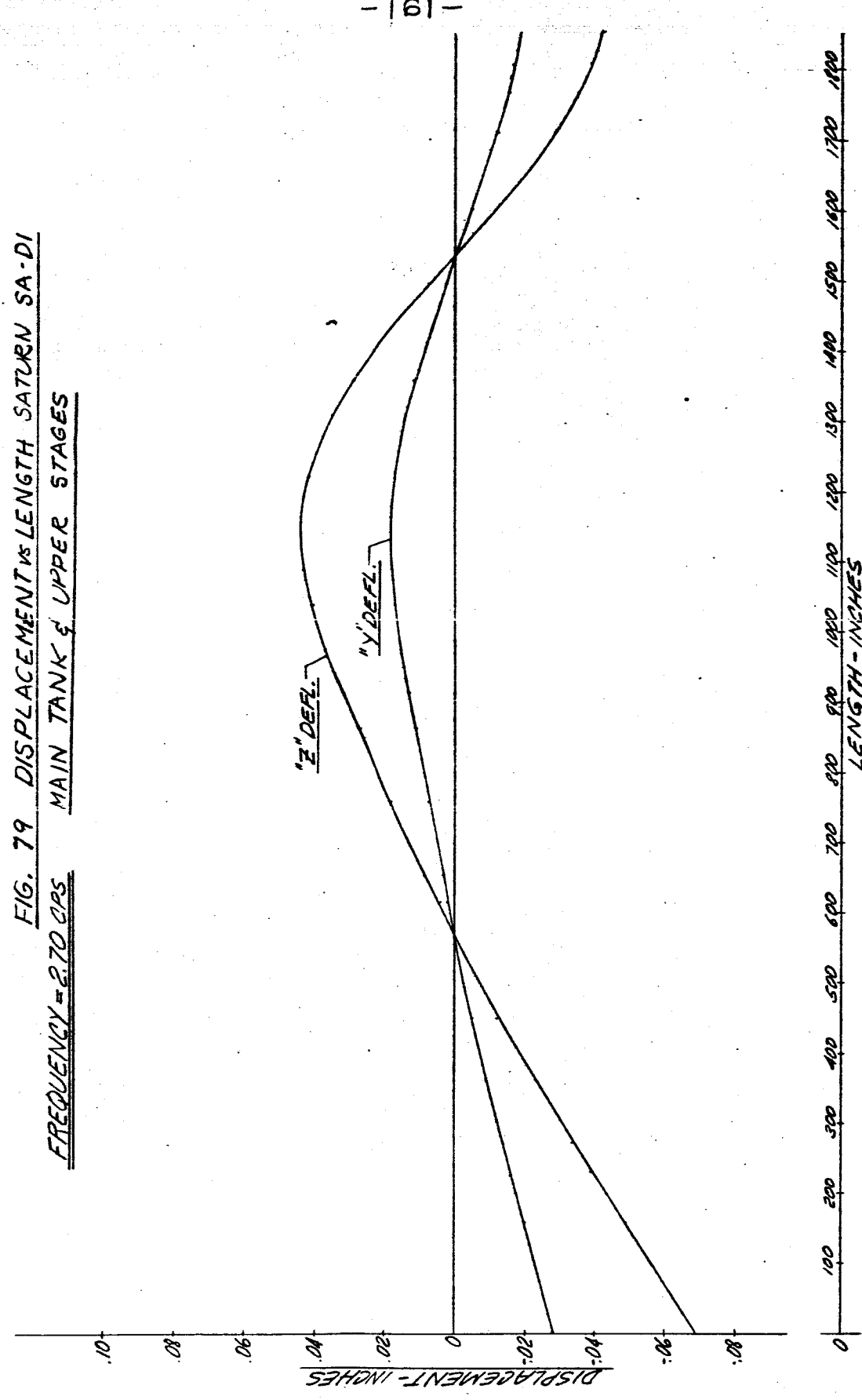


FIG. 79 DISPLACEMENT VS LENGTH SATURN SA-DI  
FREQUENCY = 2.70 CPS MAIN TANK & UPPER STAGES



-162-

FIG 80 DISPLACEMENT VS LENGTH SATURN SA-DI

FREQUENCY = 2.70 CPS

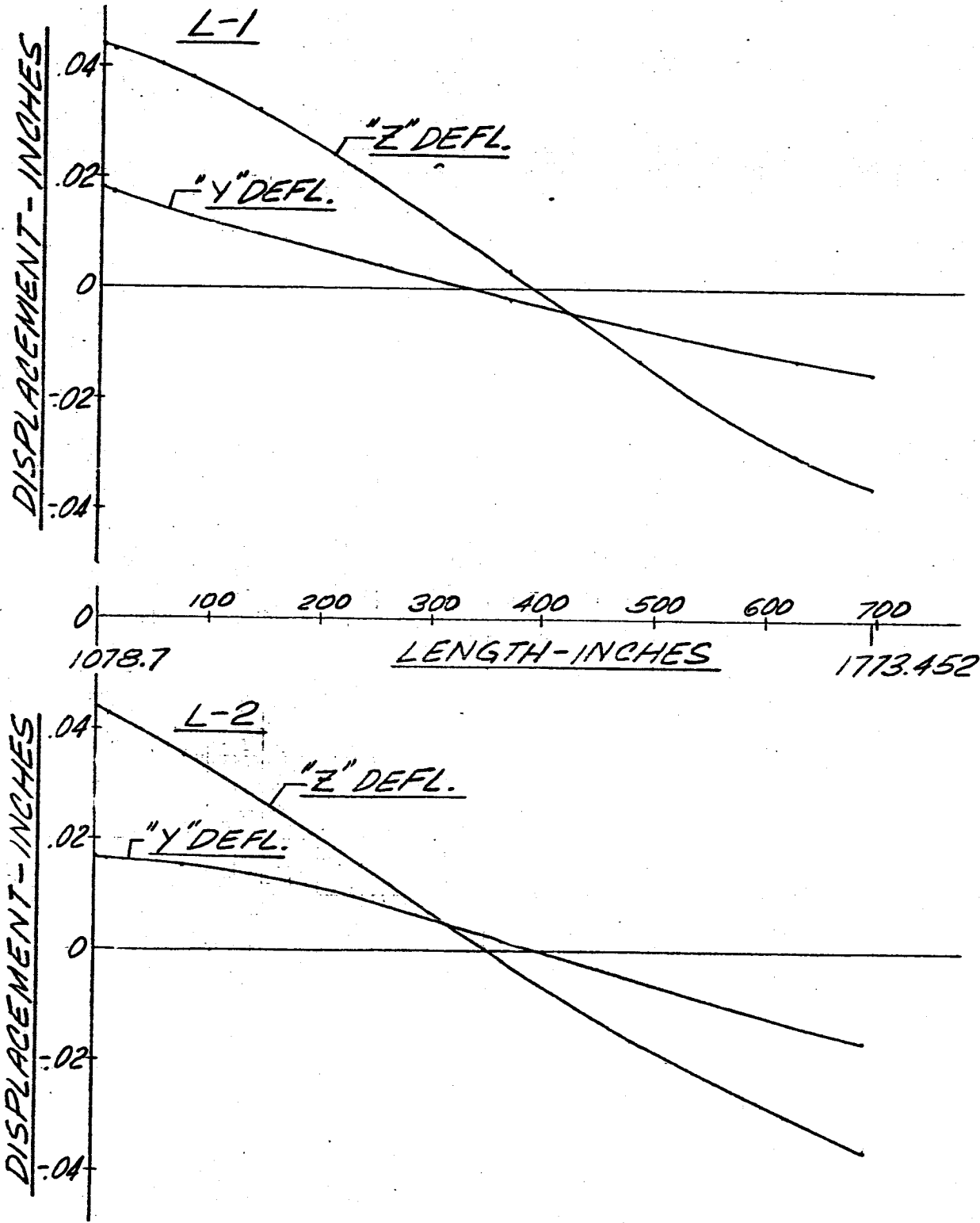
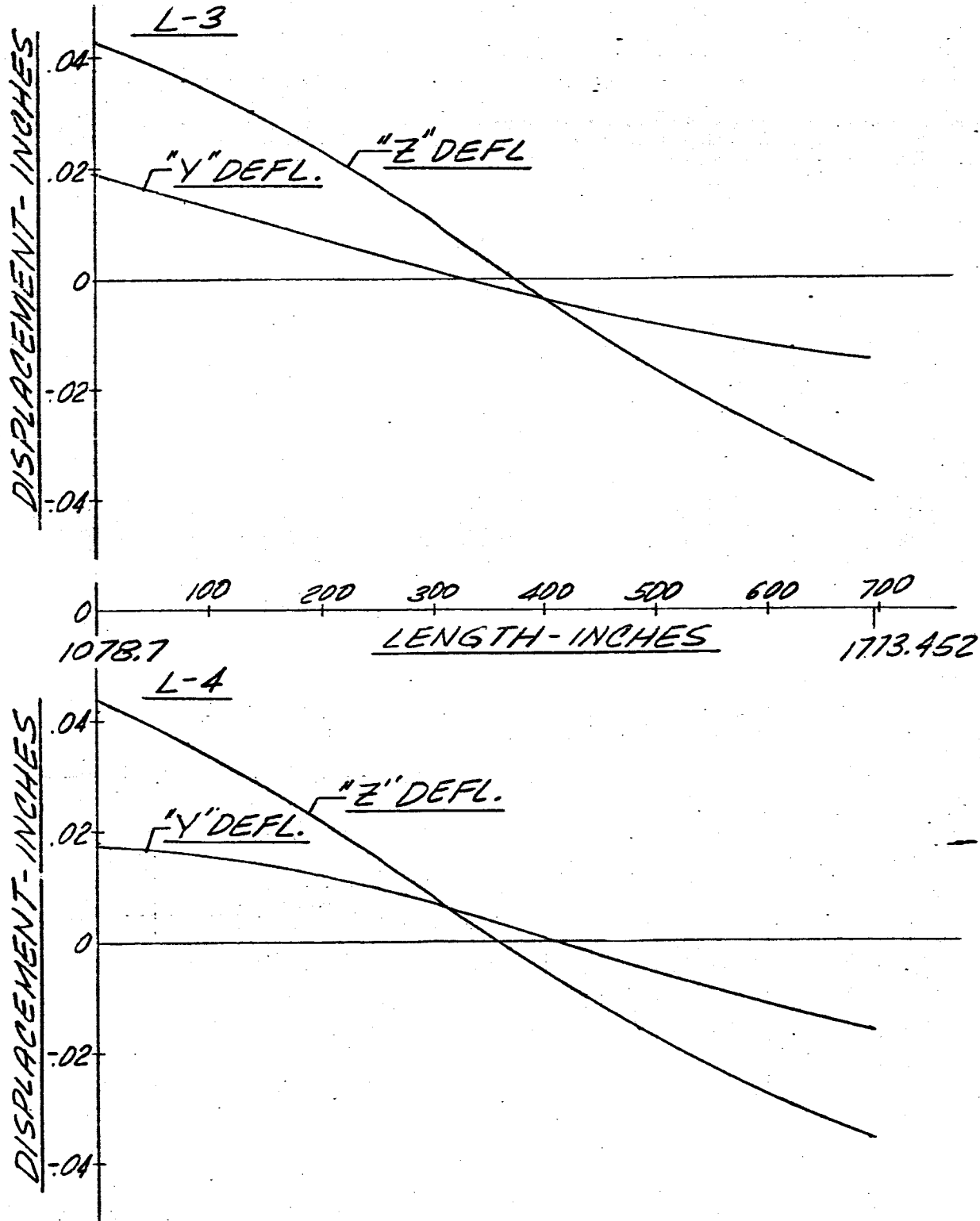


FIG E1 DISPLACEMENT VS LENGTH SATURN SA-D1

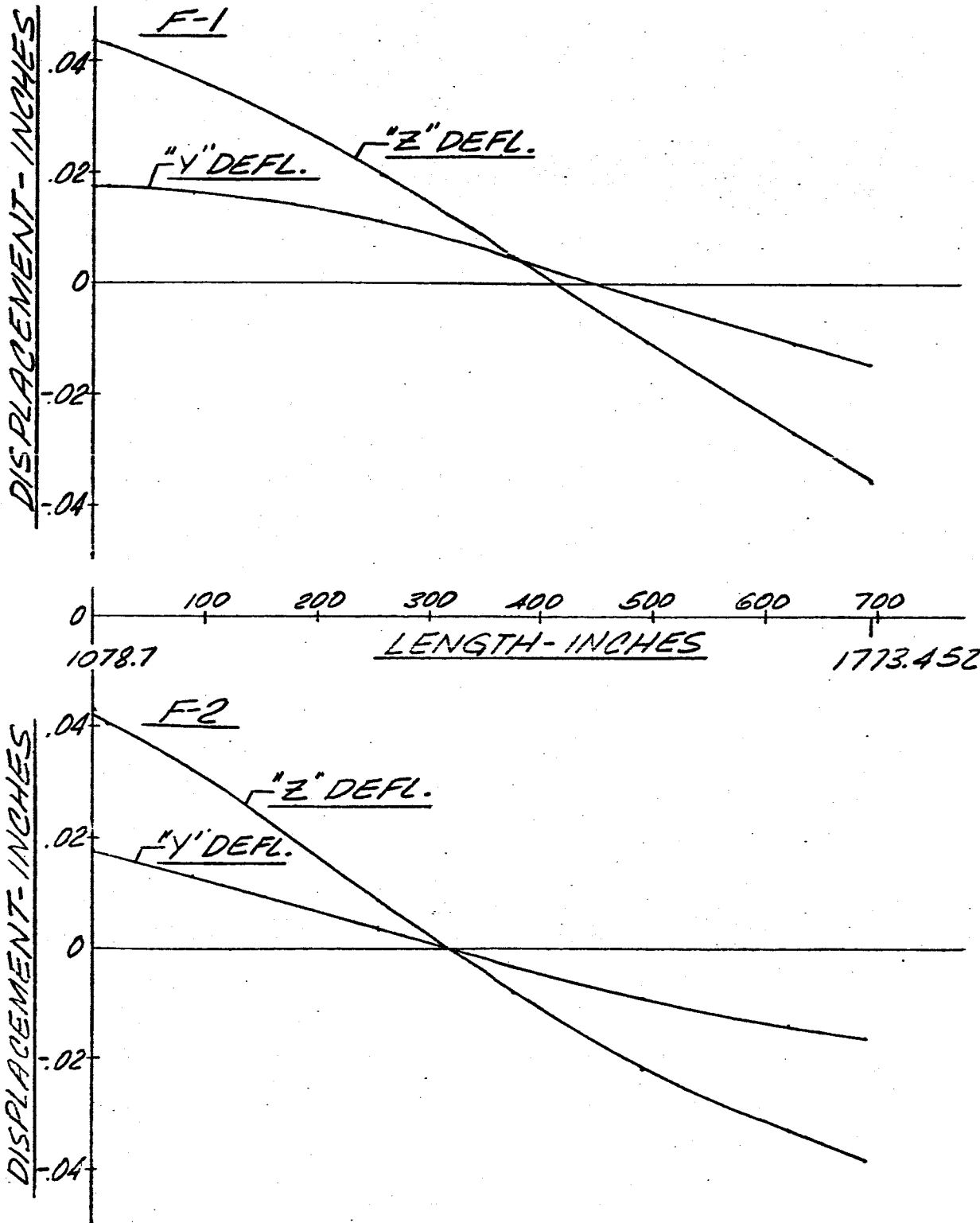
FREQUENCY = 2.70 CPS



-164-

FIG 82 DISPLACEMENT VS LENGTH SATURN SA-D1

FREQUENCY=2.70 CPS



-165-

FIG 83 DISPLACEMENT VS LENGTH SATURN SA-D1

FREQUENCY=2.70 CPS

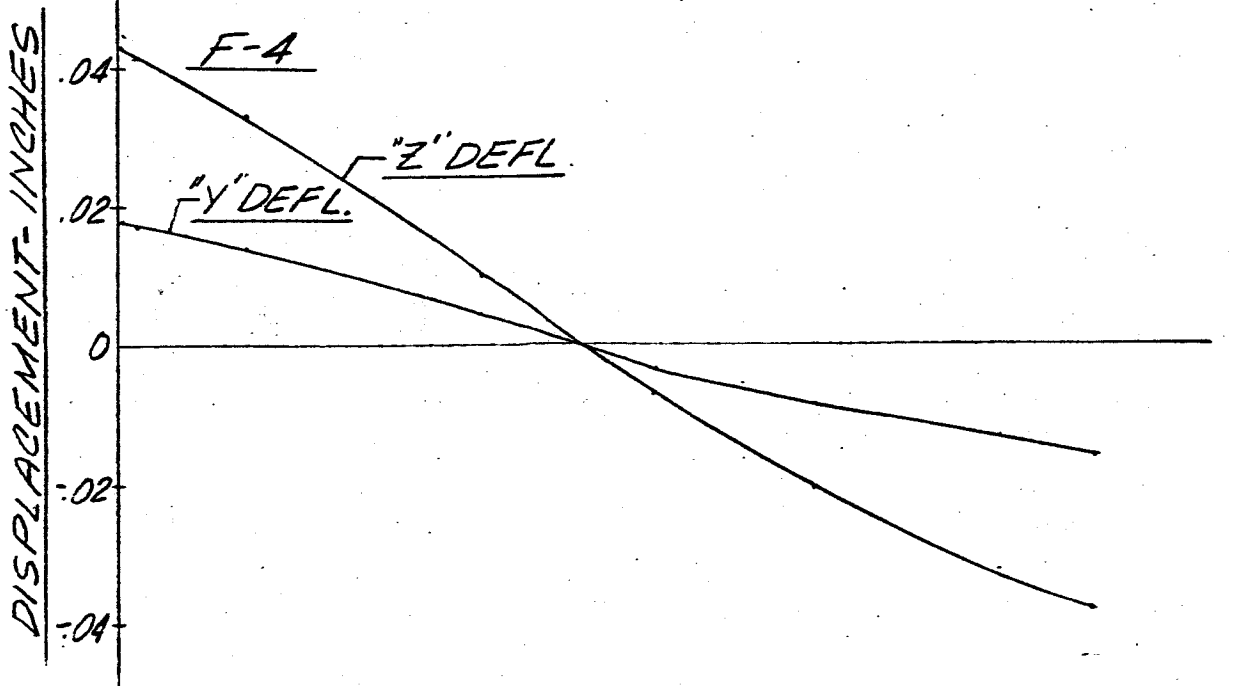
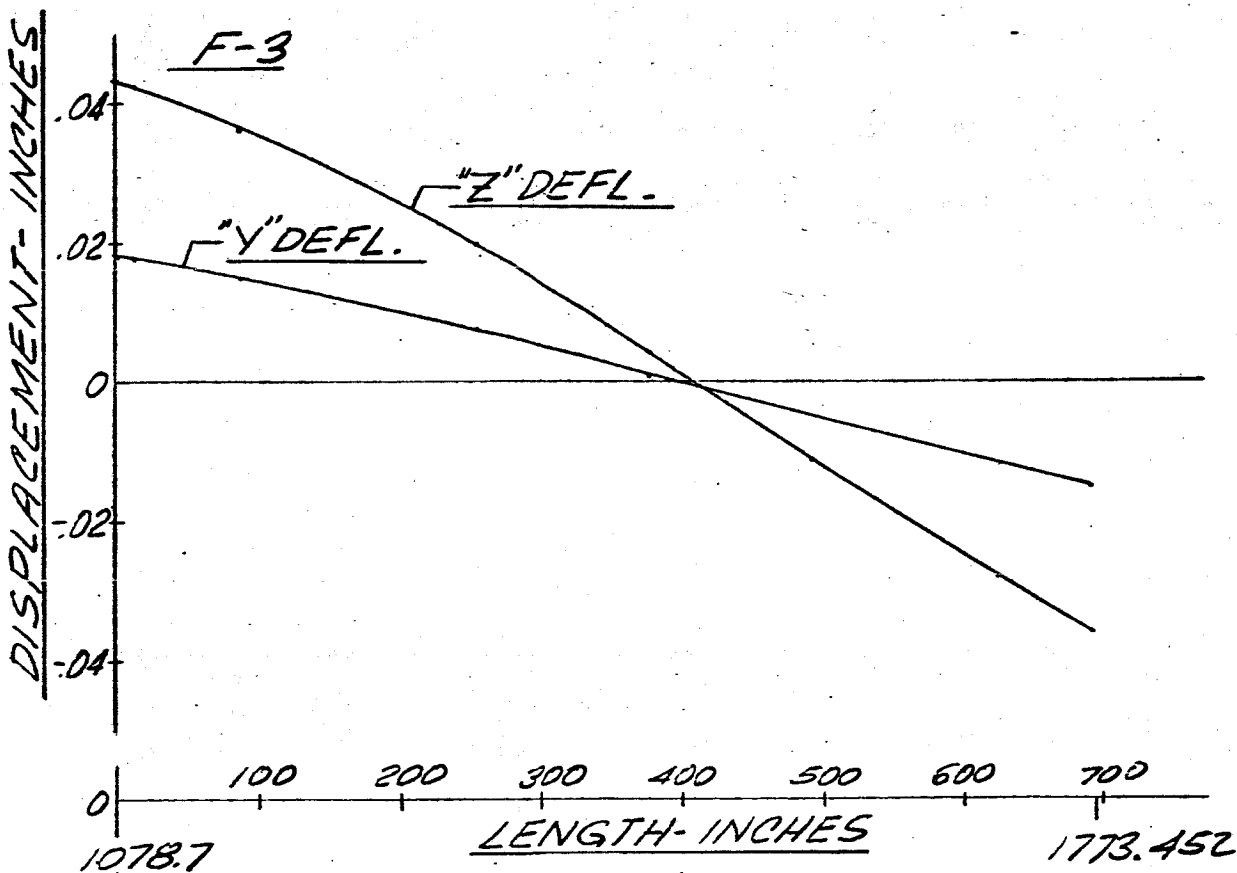


FIG. 84 DISPLACEMENT VS LENGTH SATURN SA-DI

FREQUENCY=2.80 CPS.  
MAIN TANK & UPPER STAGES

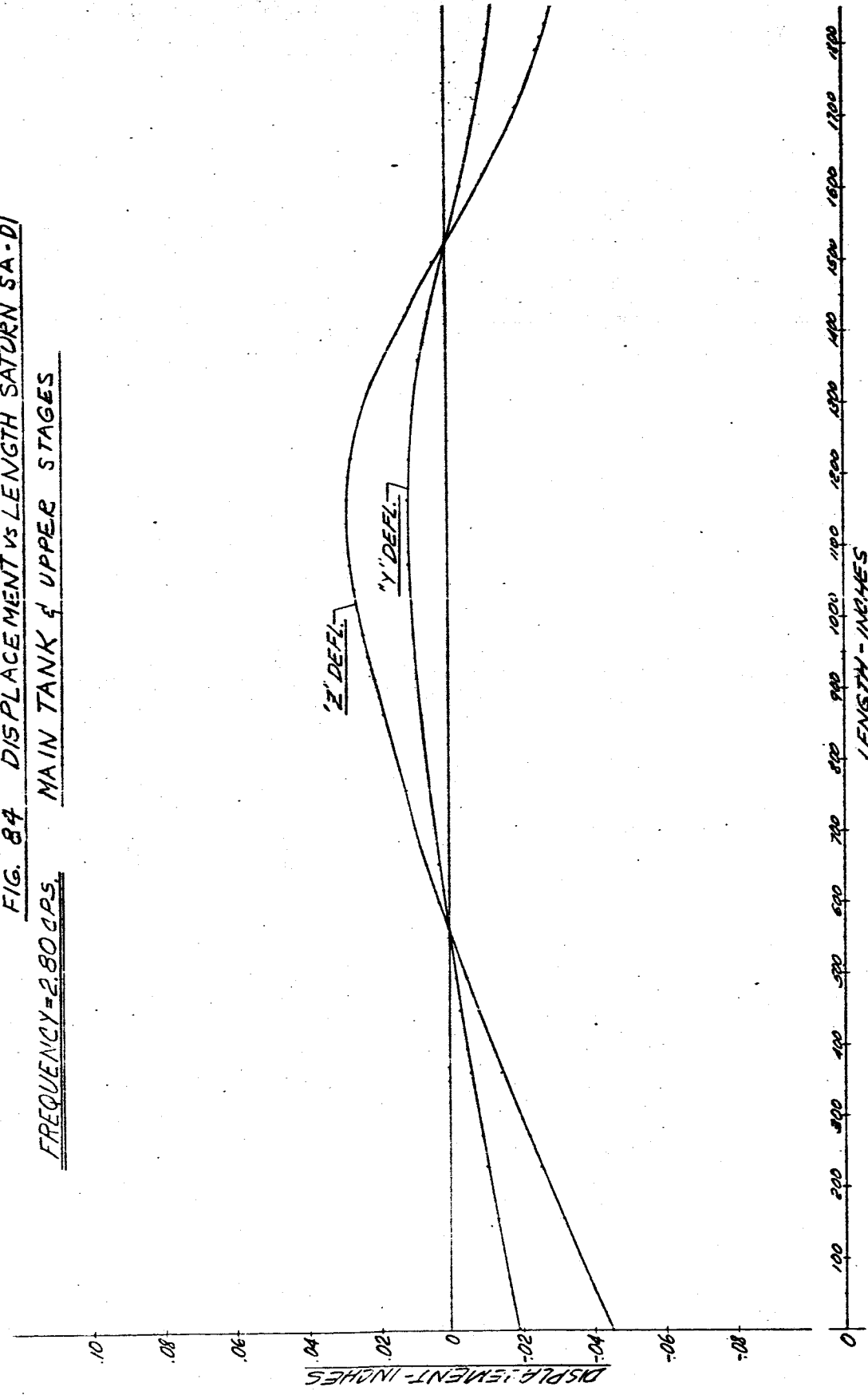


FIG B5 DISPLACEMENT VS LENGTH SATURN SA-D1

FREQUENCY = 2.80 CPS

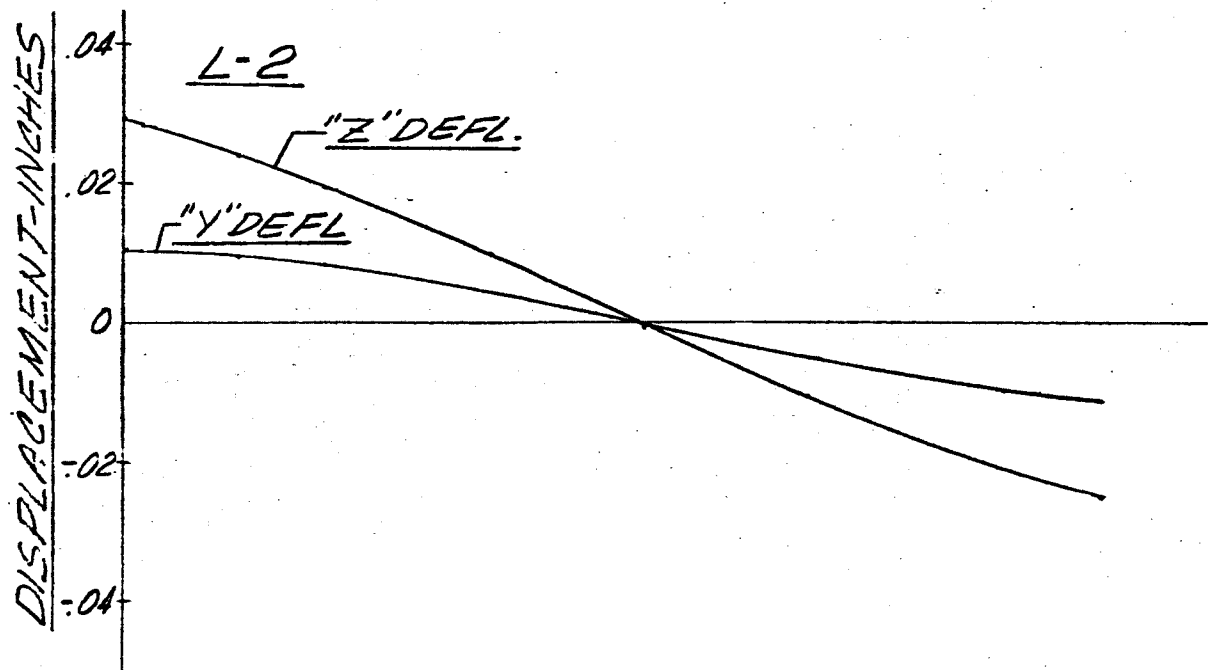
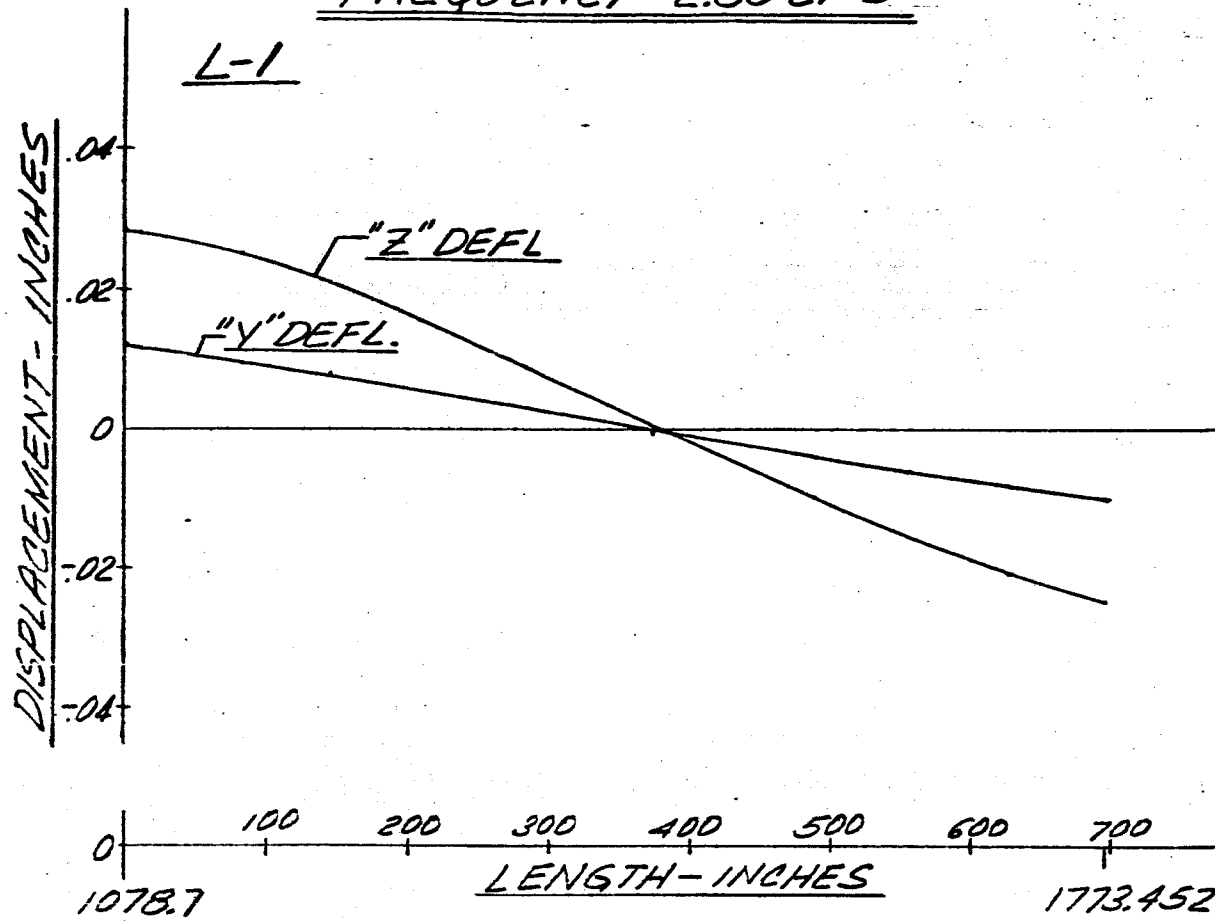
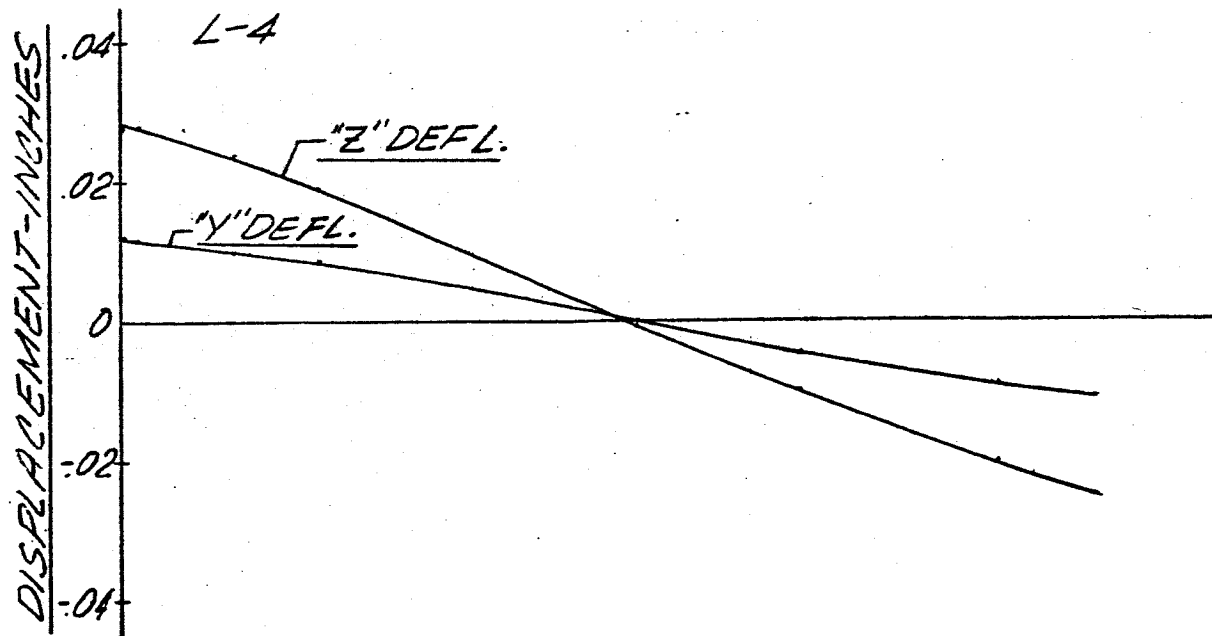
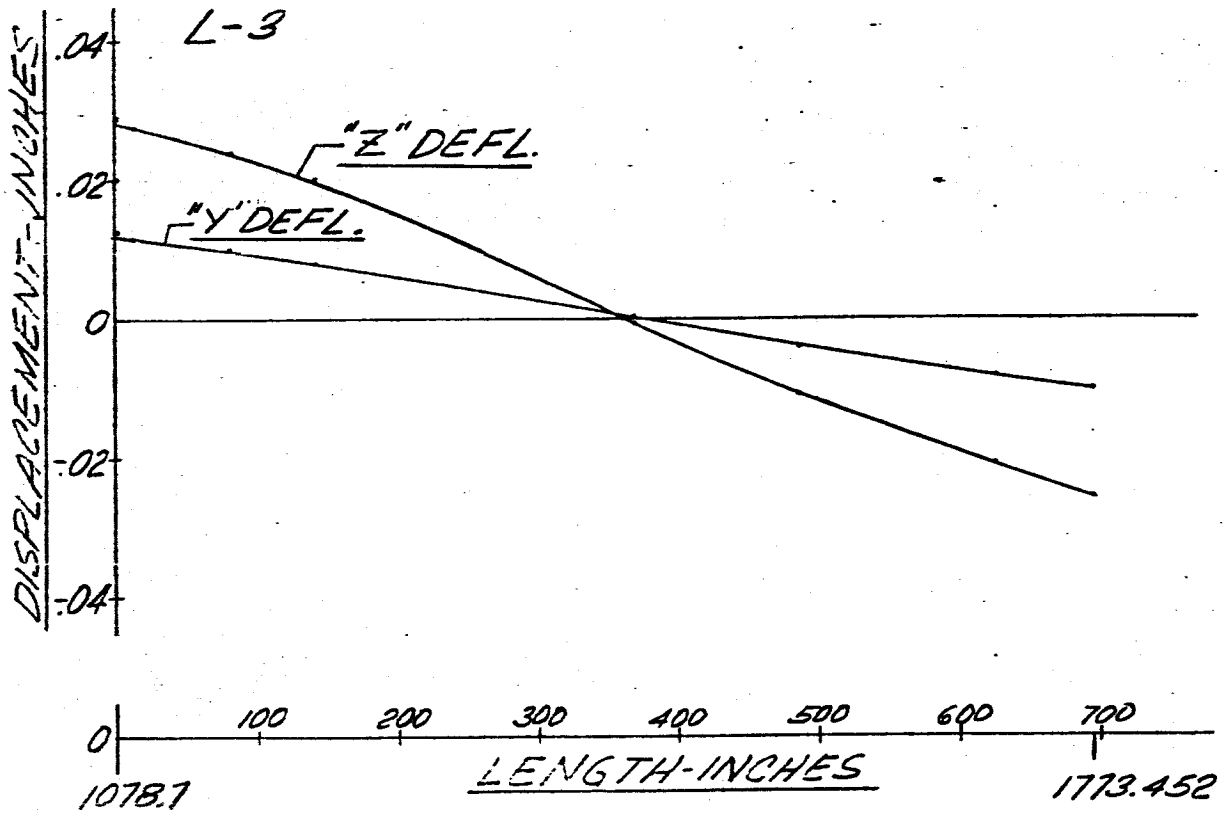


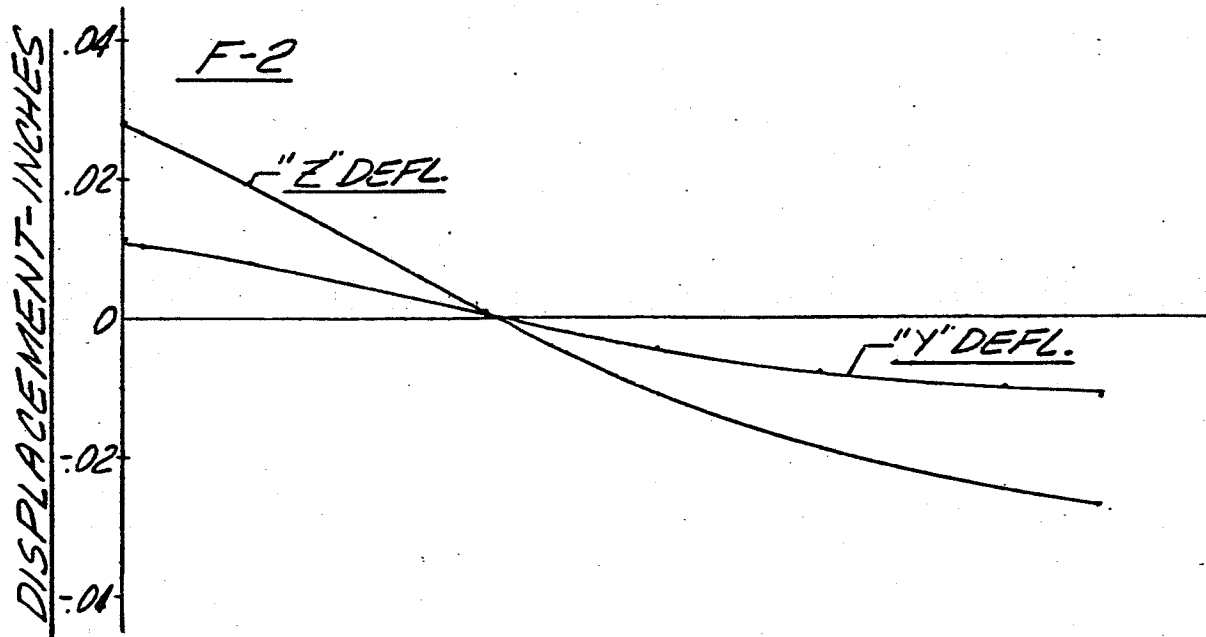
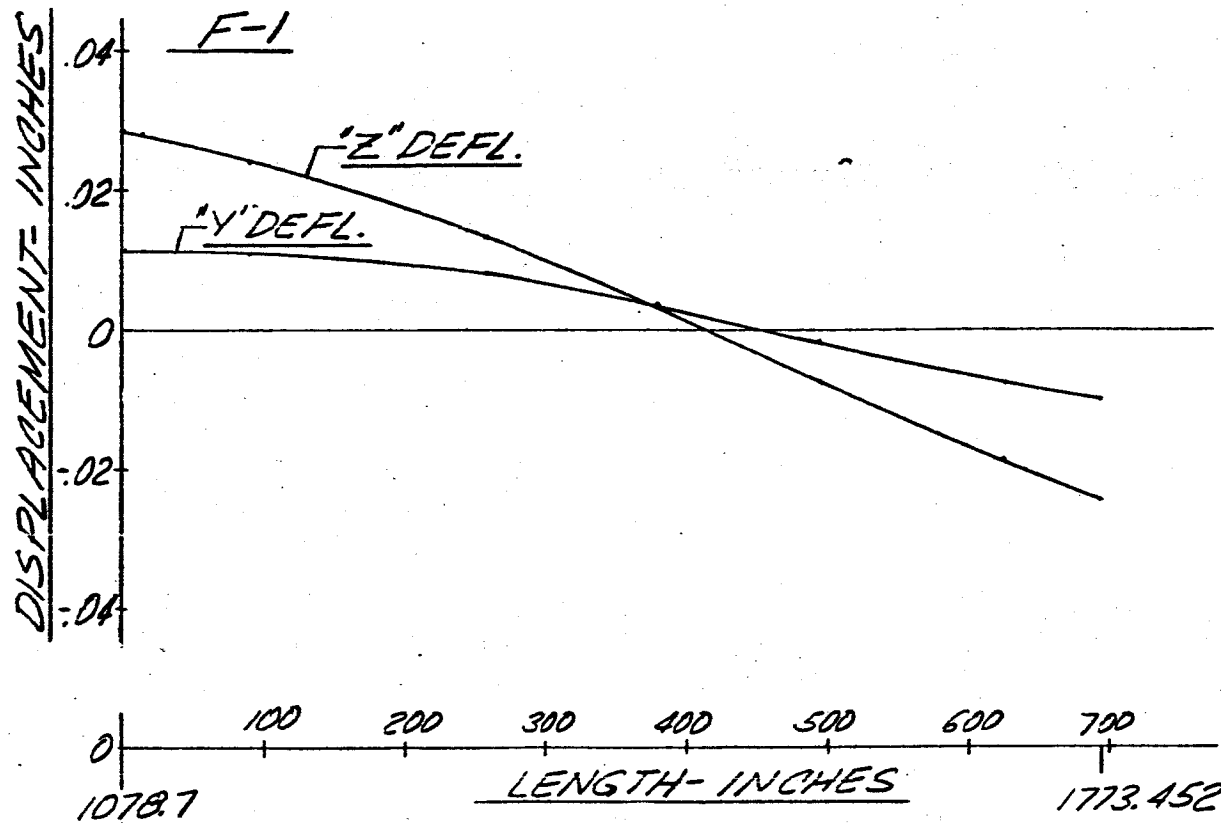
FIG 86 DISPLACEMENT VS LENGTH SATURN SA-D1  
FREQUENCY=2.80 CPS



-169-

FIG 87 DISPLACEMENT VS LENGTH SATURN SA-DI

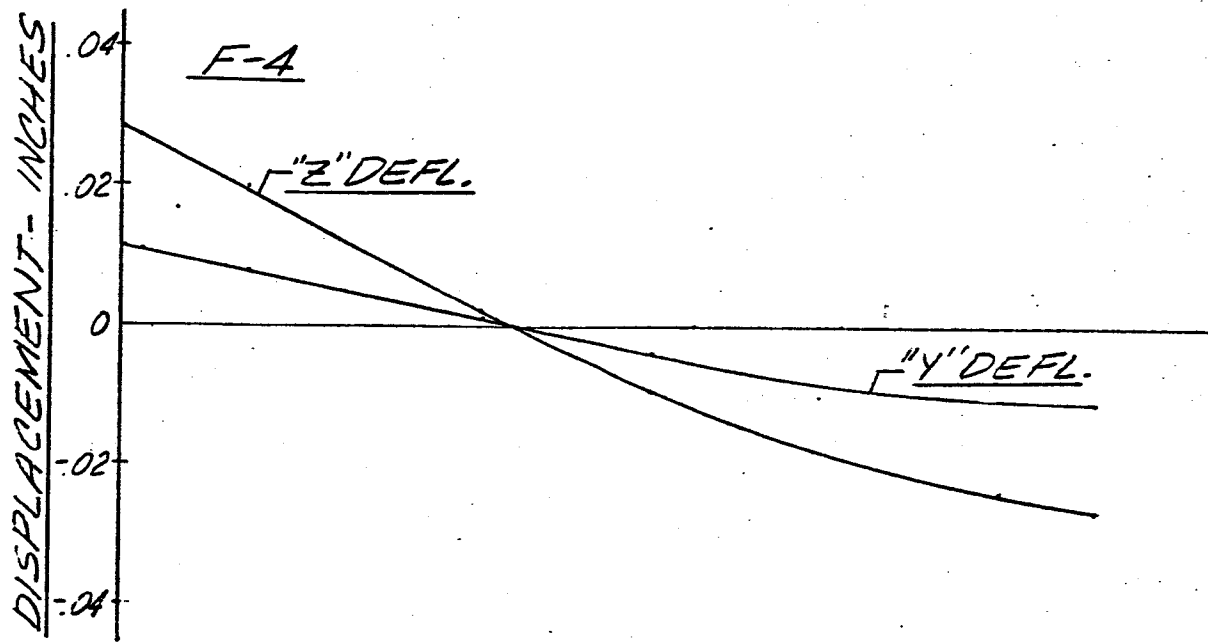
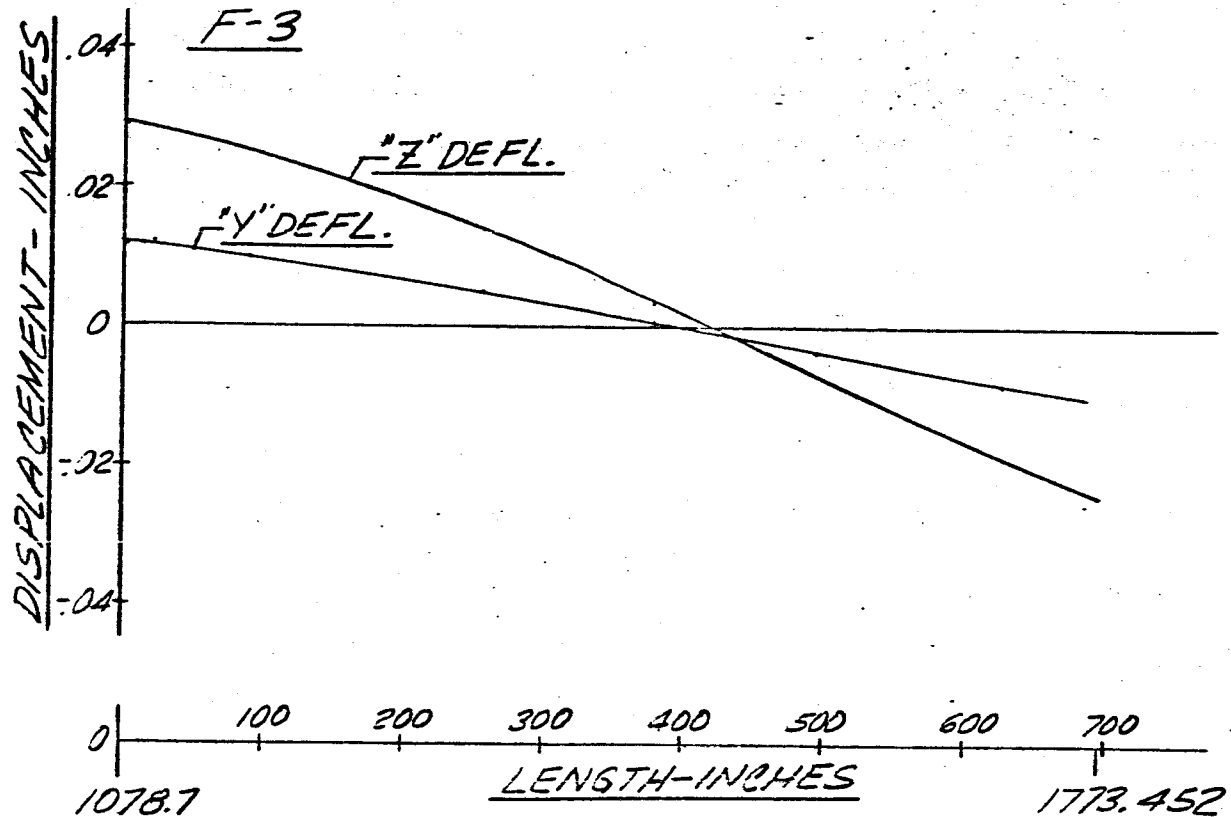
FREQUENCY = 2.80 CPS



-170-

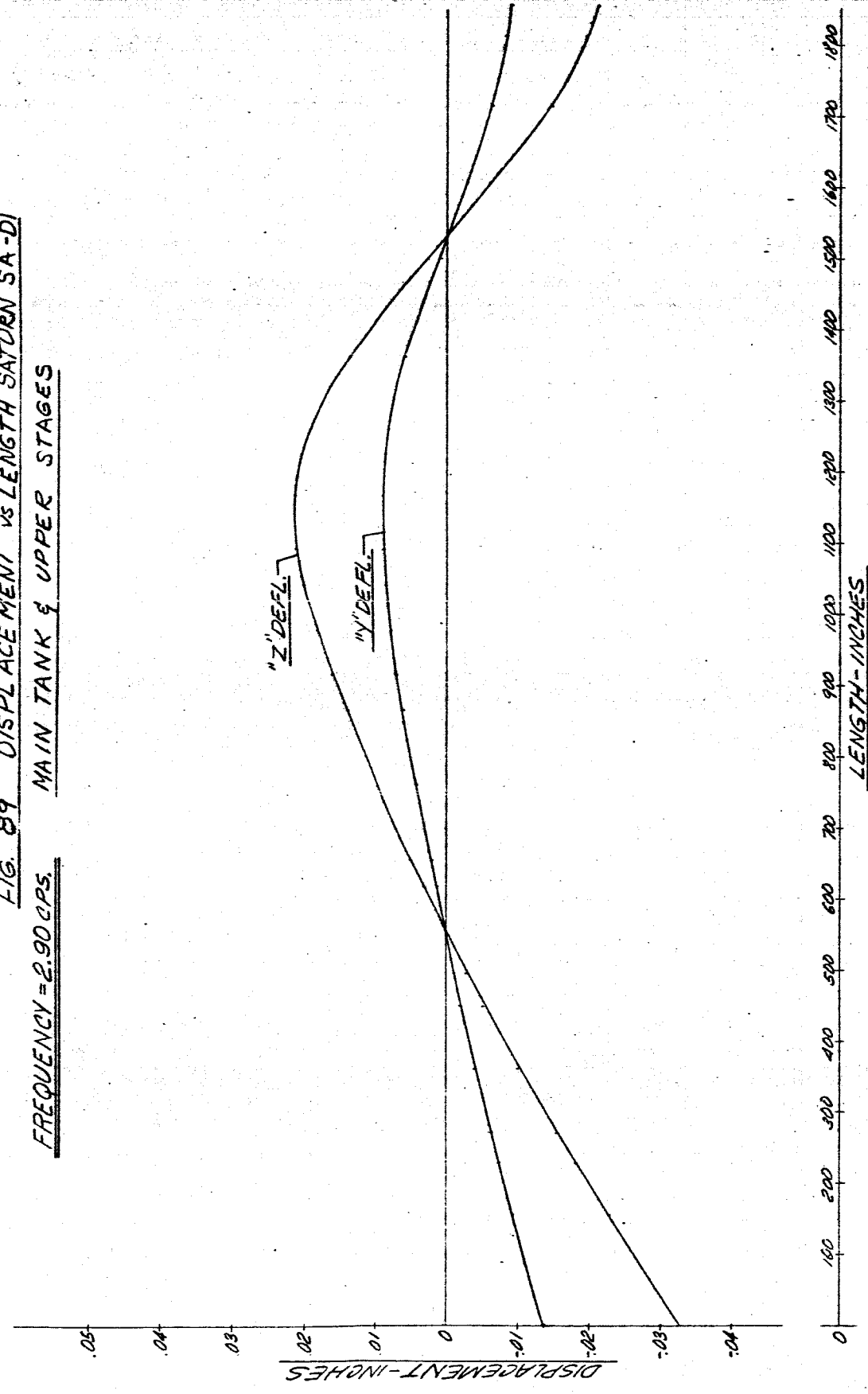
FIG 88 DISPLACEMENT IS LENGTH SATURN SA-DI

FREQUENCY=2.80 CPS.



-171-

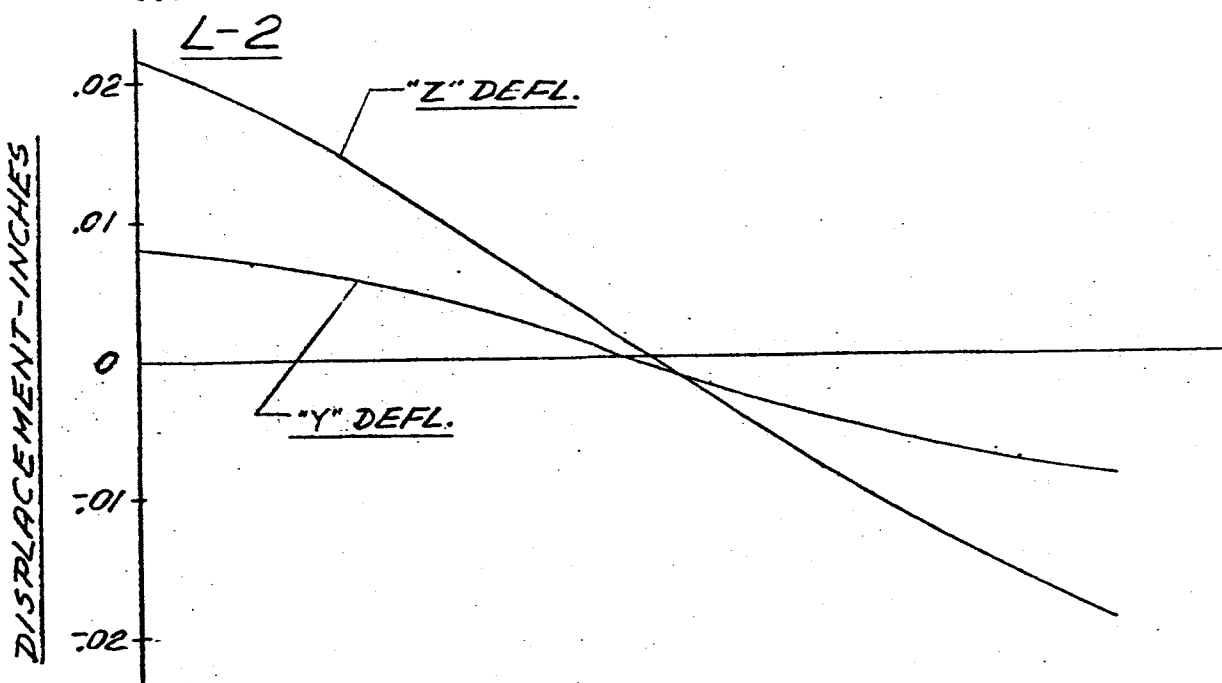
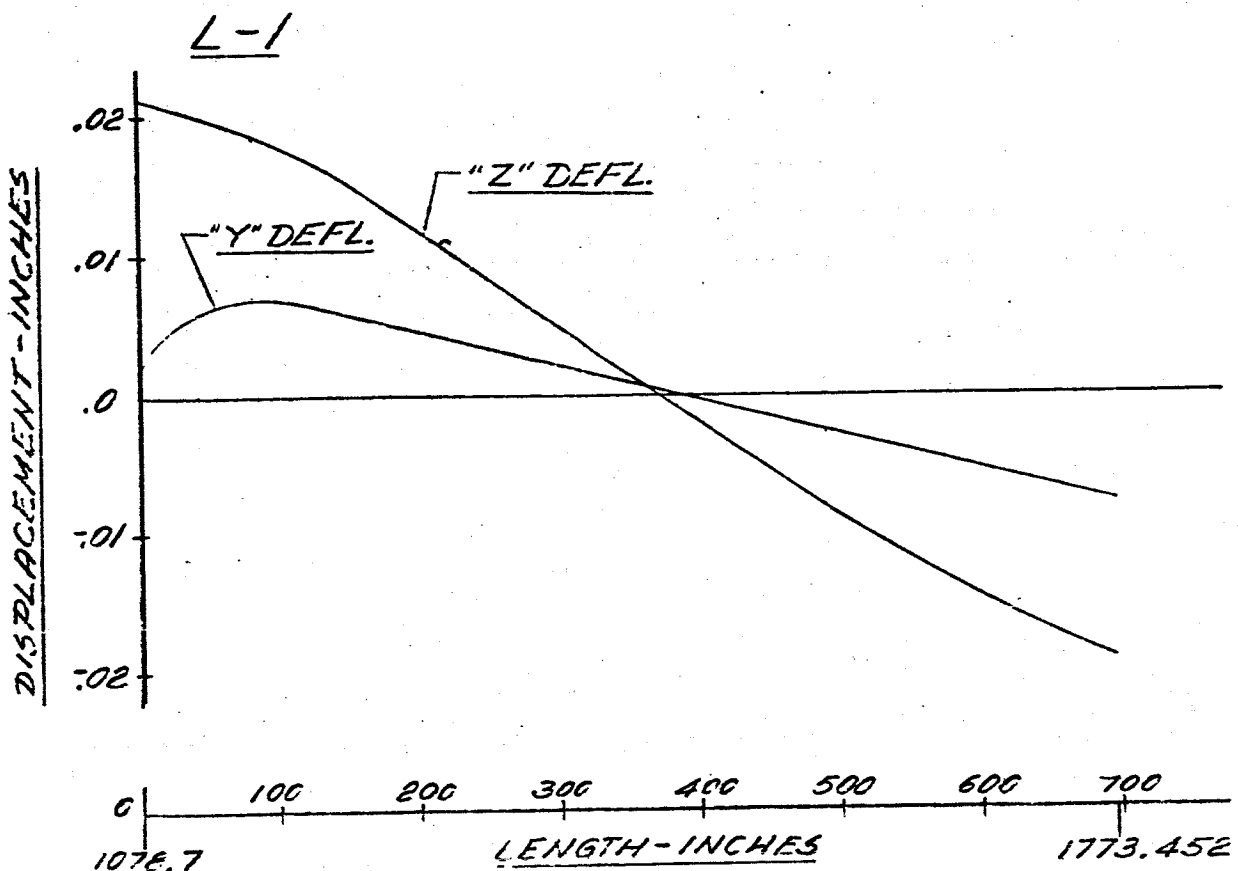
FIG. 89 DISPLACEMENT vs LENGTH SATURN SA-DI  
MAIN TANK & UPPER STAGES  
FREQUENCY = 2.90 CPS.



-172-

FIG 90 DISPLACEMENT VC LENGTH SATURN SA-D1

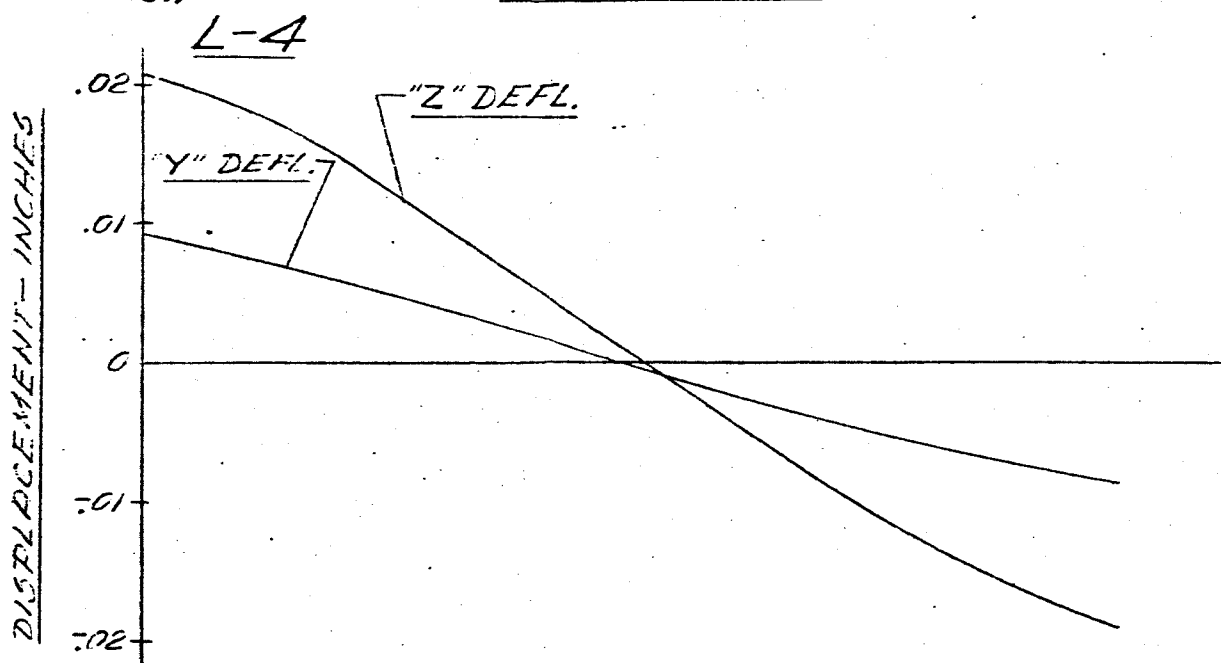
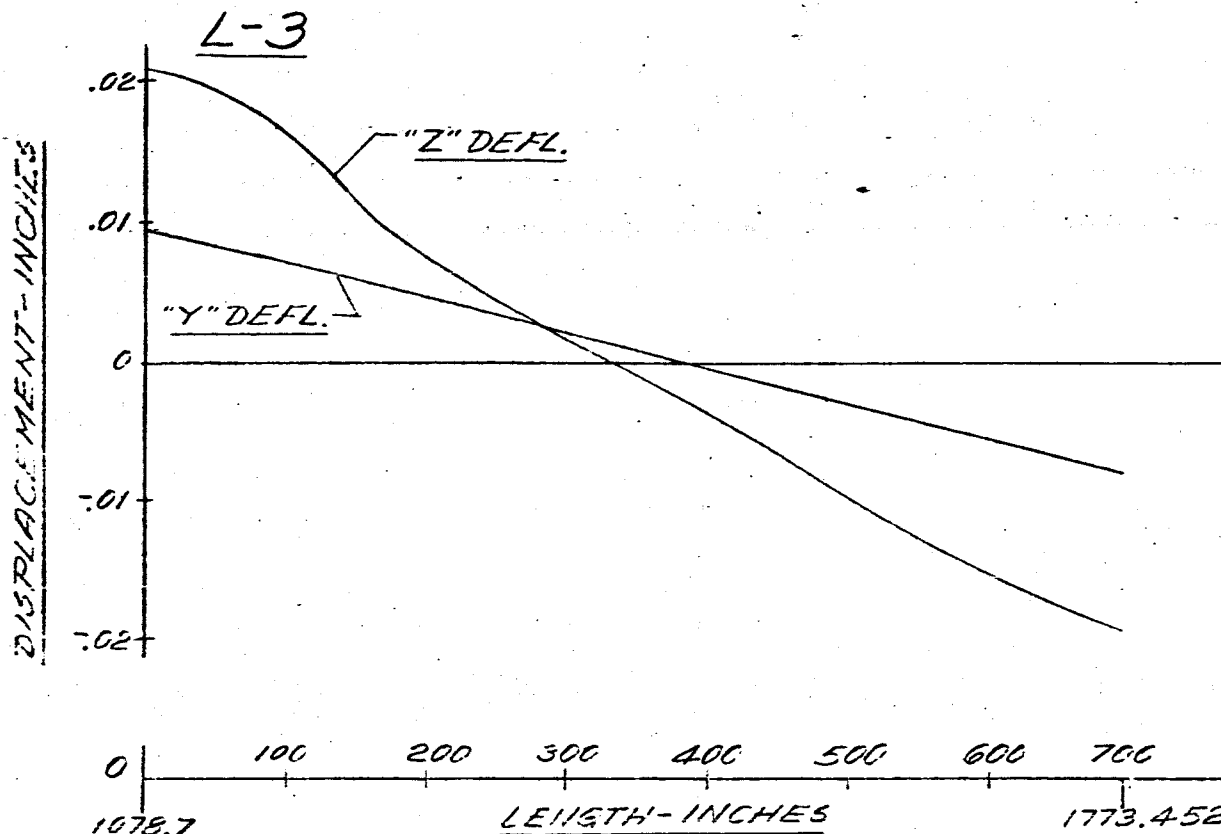
FREQUENCY = 2.90 CPS



-173-

FIG 91 DISPLACEMENT VS LENGTH SATURN SA-D1

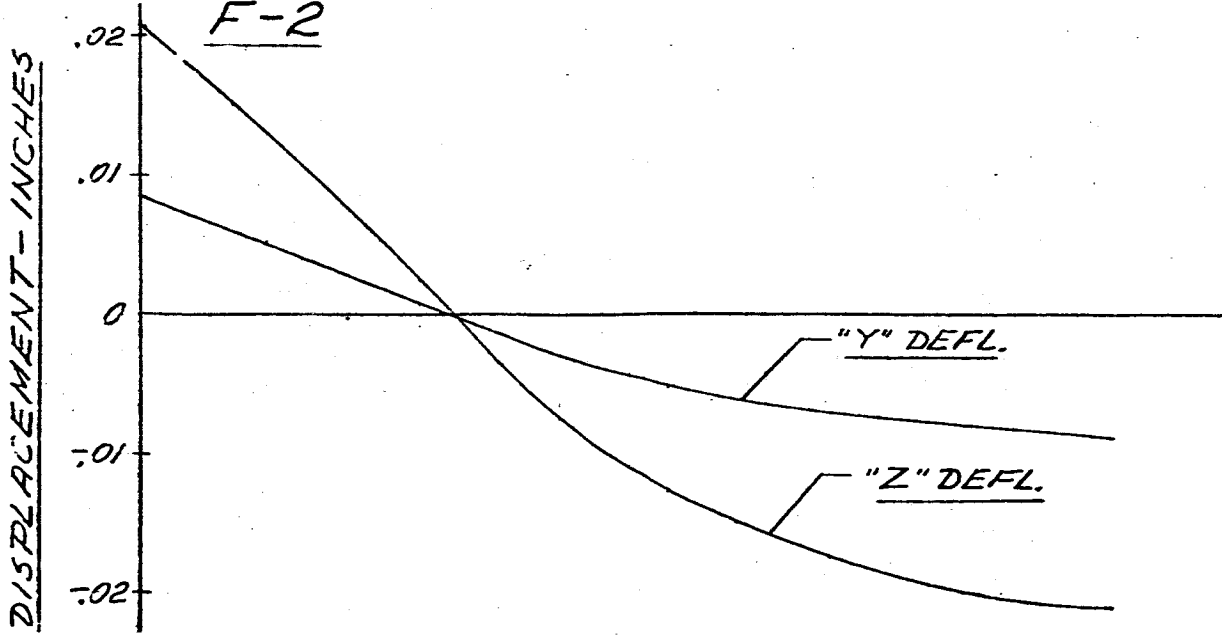
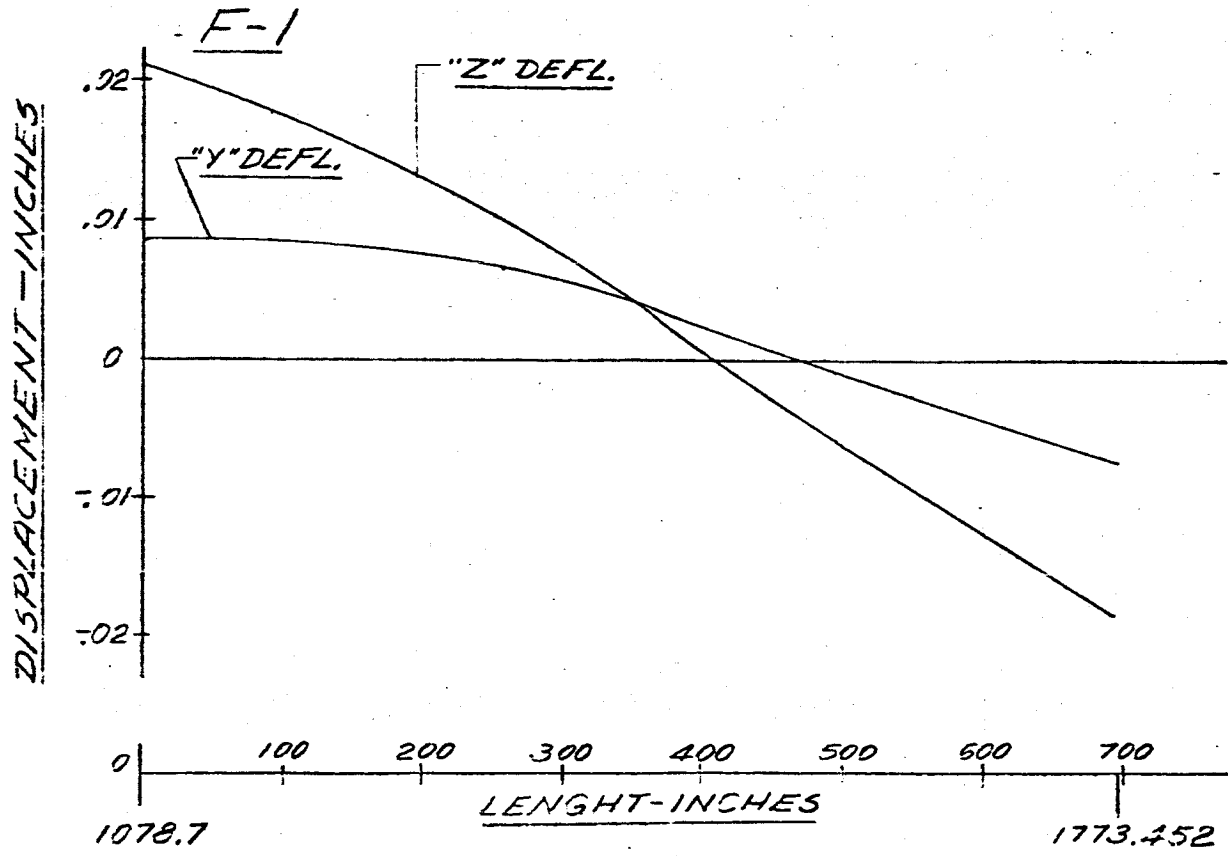
FREQUENCY = 2.90 CPS



- 174 -

FIG 92 DISPLACEMENT VS LENGTH FOR TURN SA-DI

FREQUENCY = 2.90 CPS



-175-

FIG 93 DISPLACEMENT VS LENGTH SATURN SA-DI

FREQUENCY = 2.90 CPS

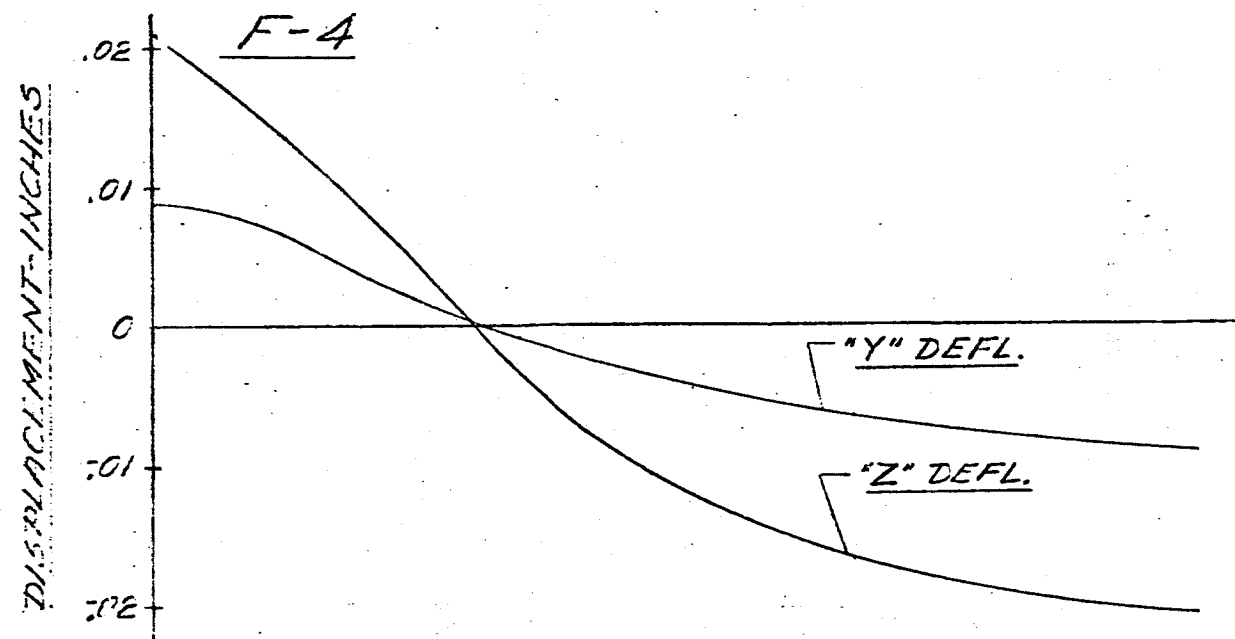
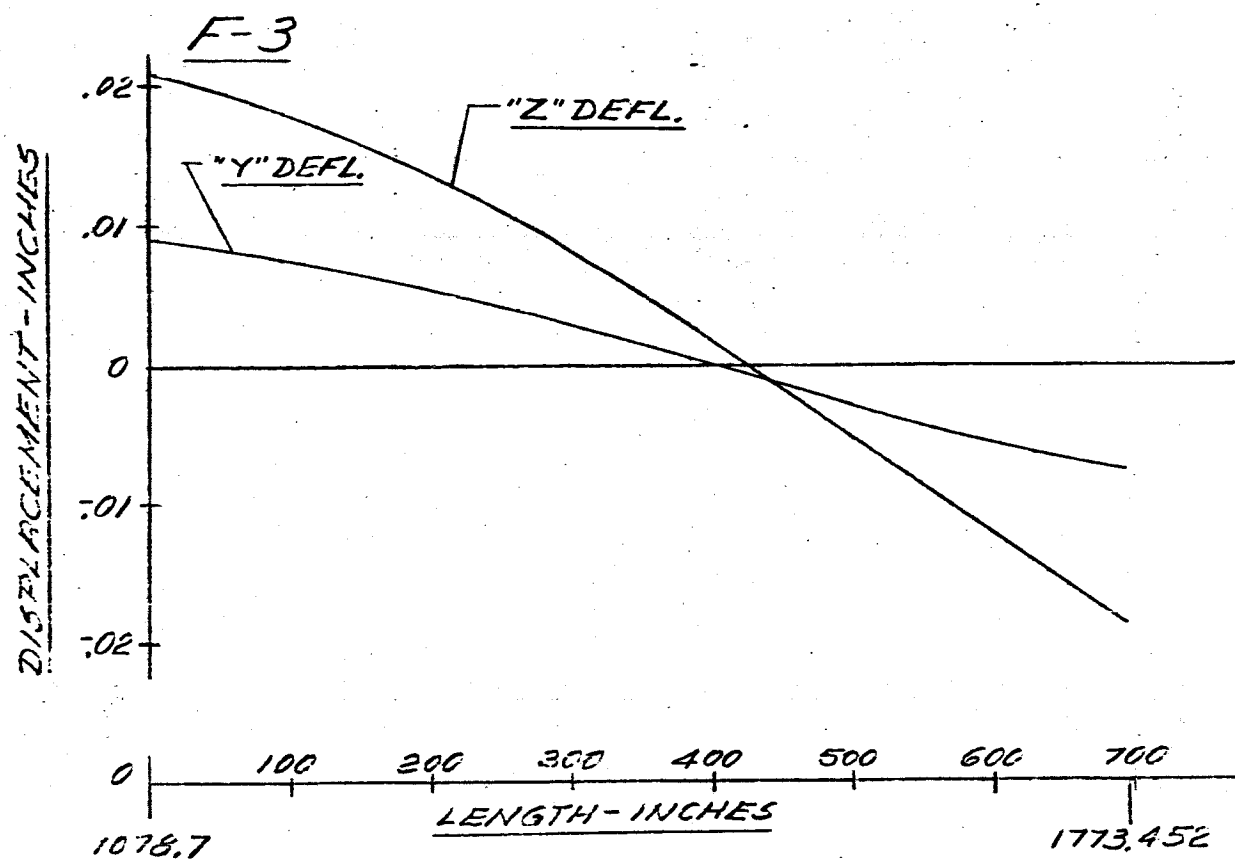
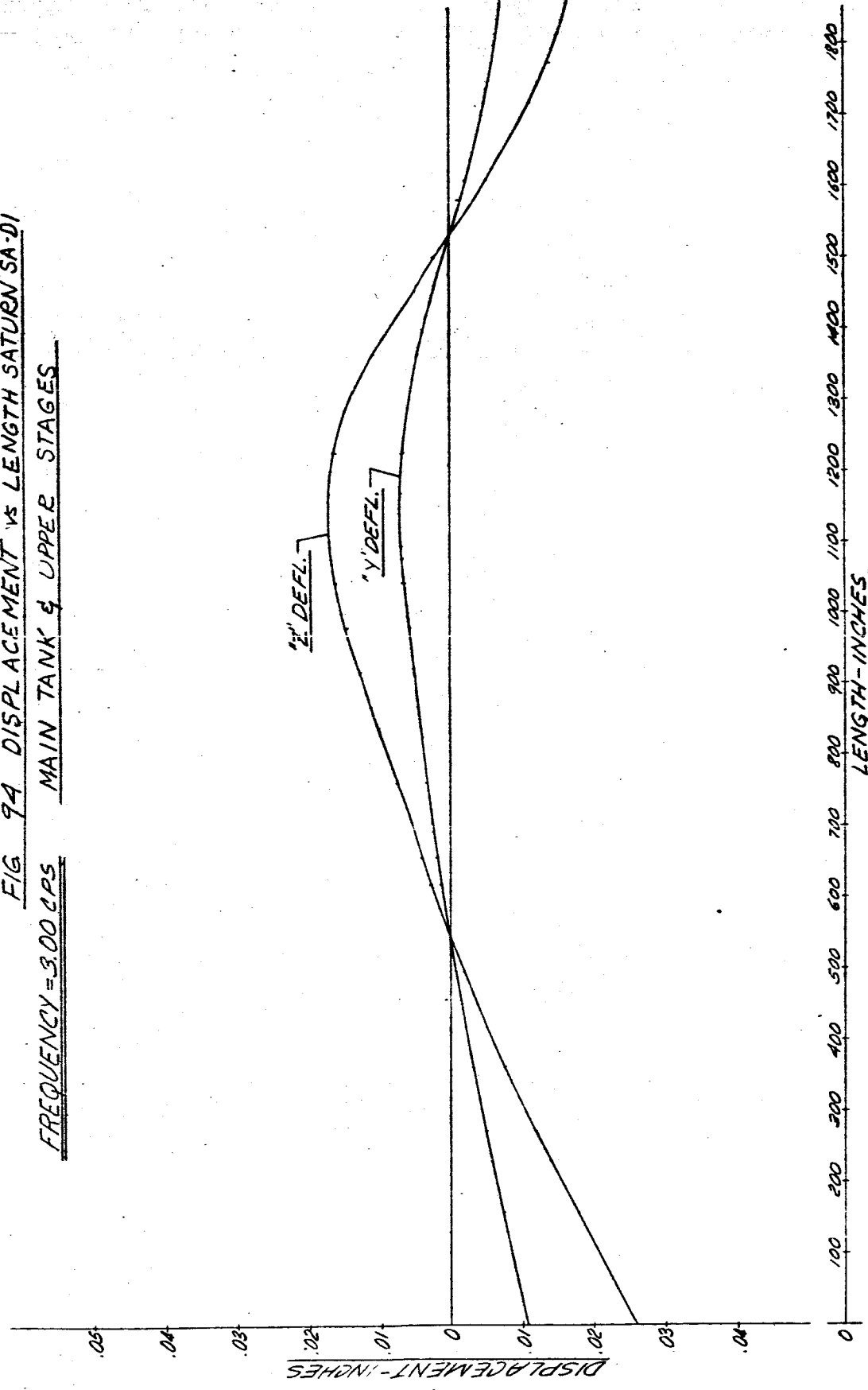


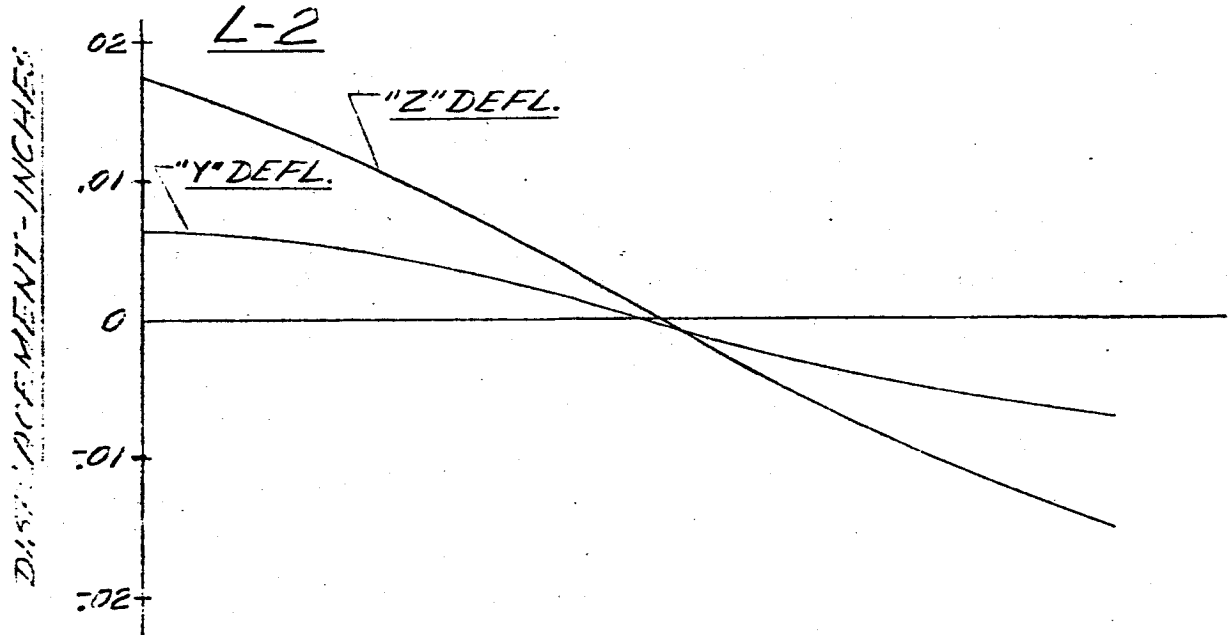
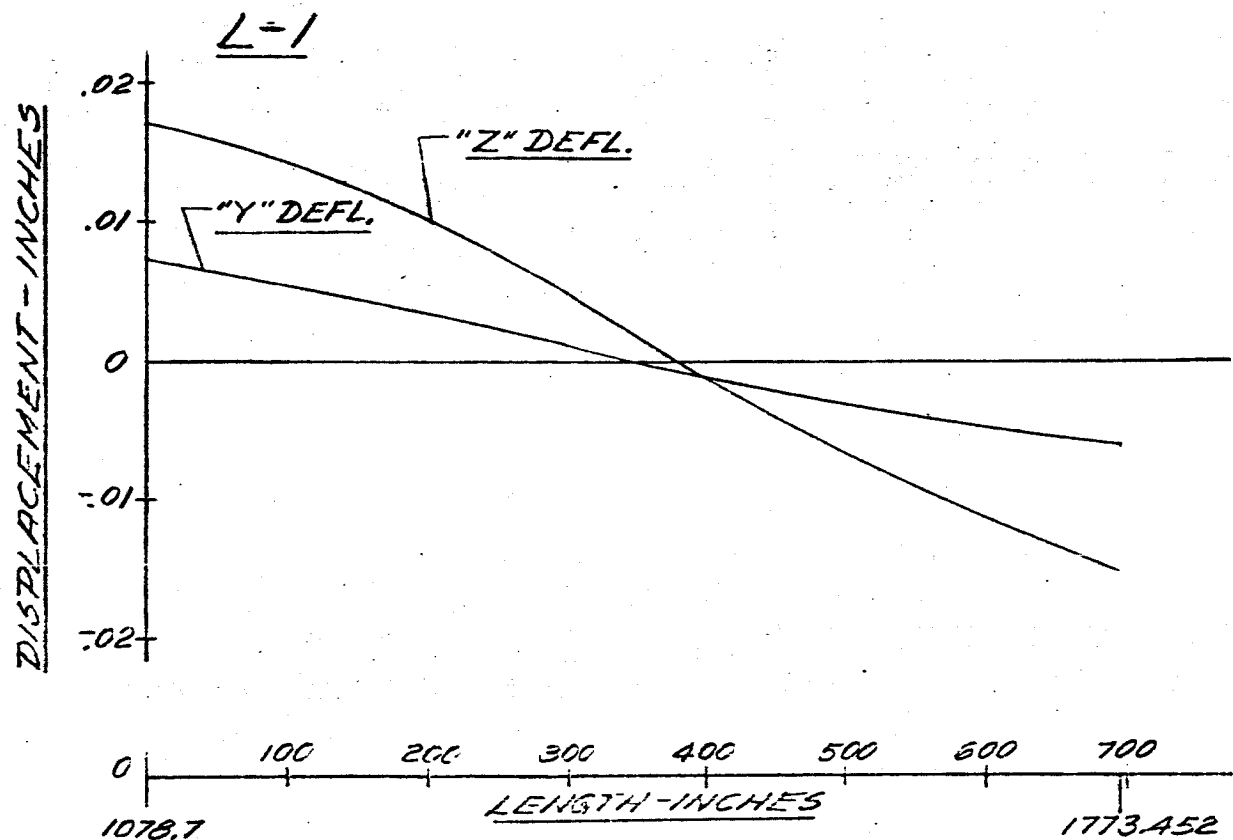
FIG 9A DISPLACEMENT vs LENGTH SATURN SA-D1  
MAIN TANK & UPPER STAGES  
FREQUENCY = 3.00 CPS



-177-

FIG 95 DISPLACEMENT VS LENGTH SATURN SA-DI

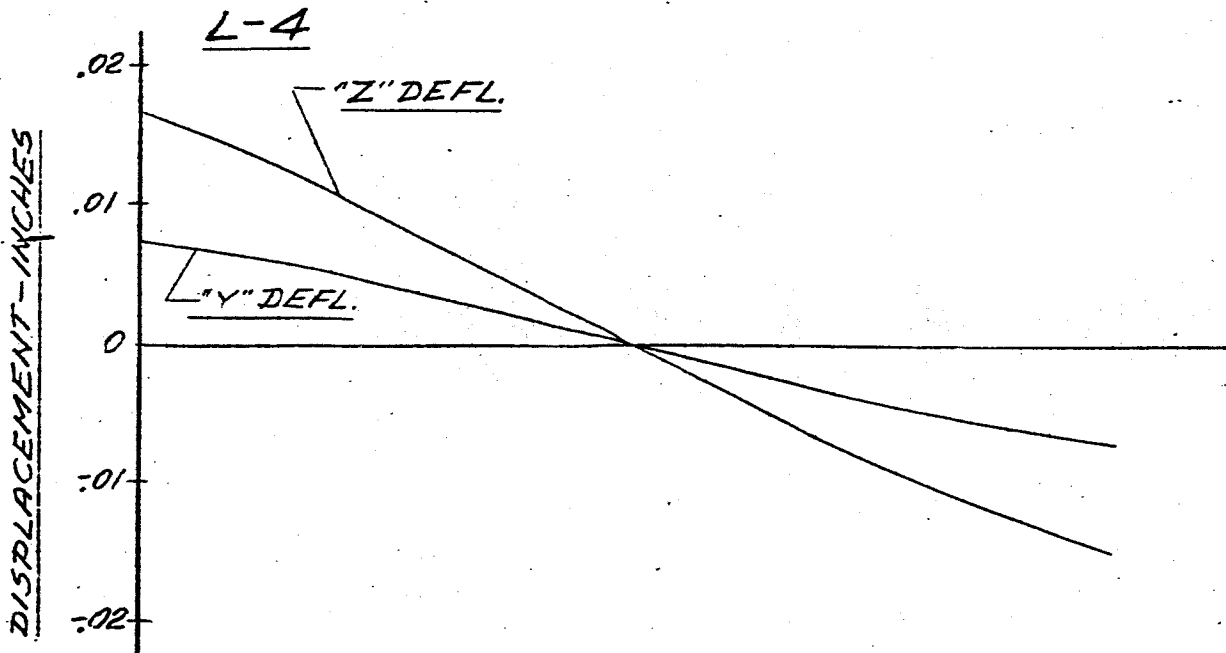
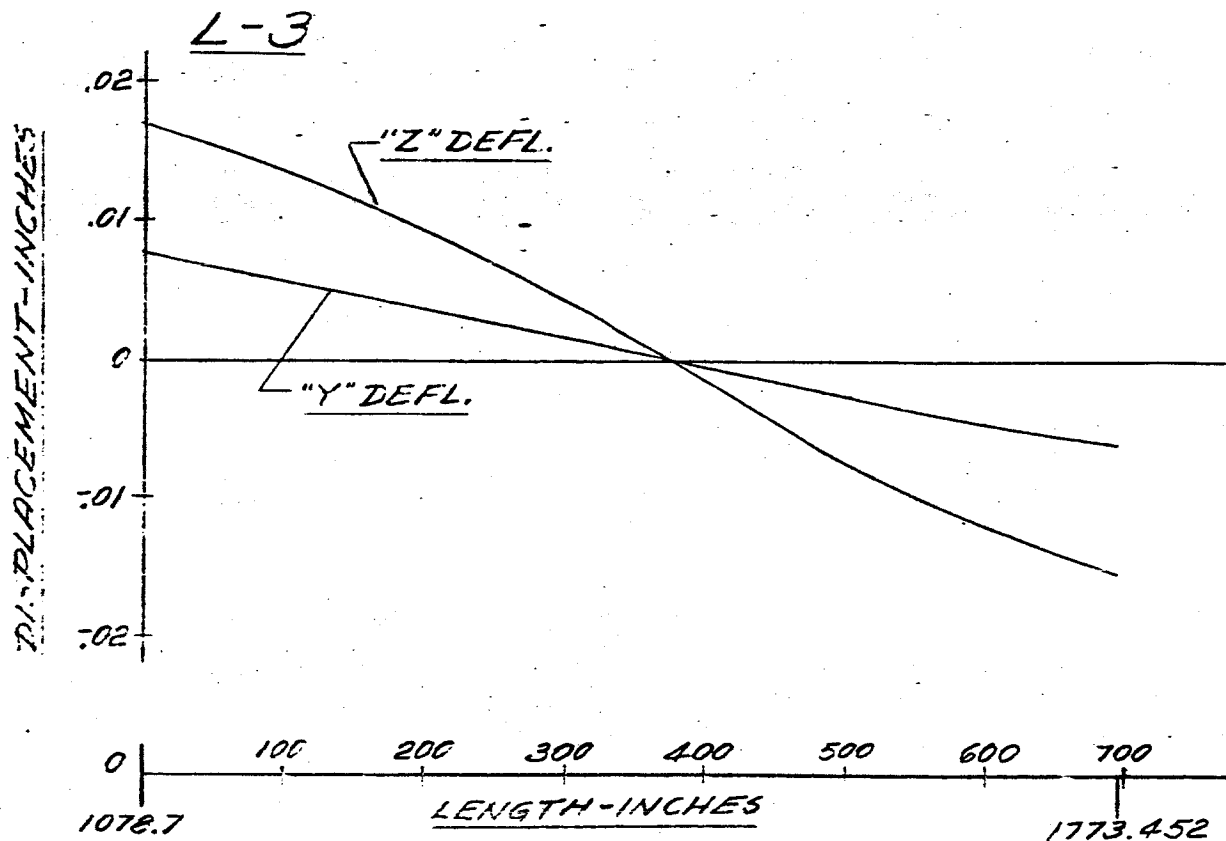
FREQUENCY = 3.00 CPS



-178-

FIG 96 DISPLACEMENT VS LENGTH SATURN SA-DI

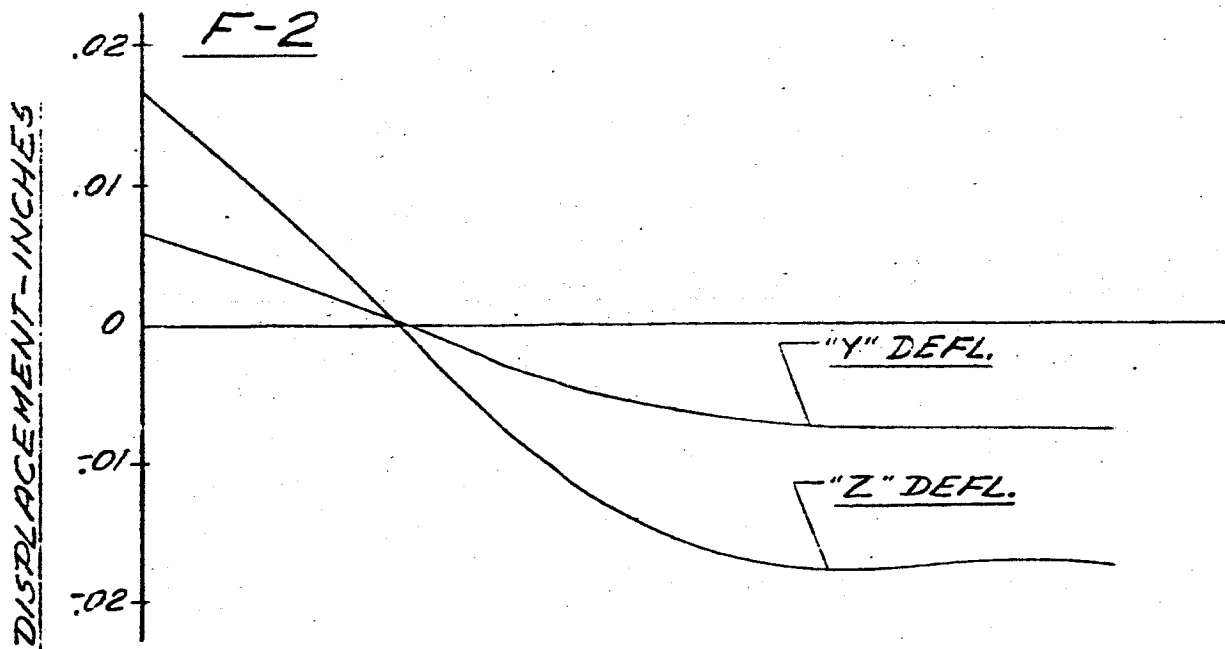
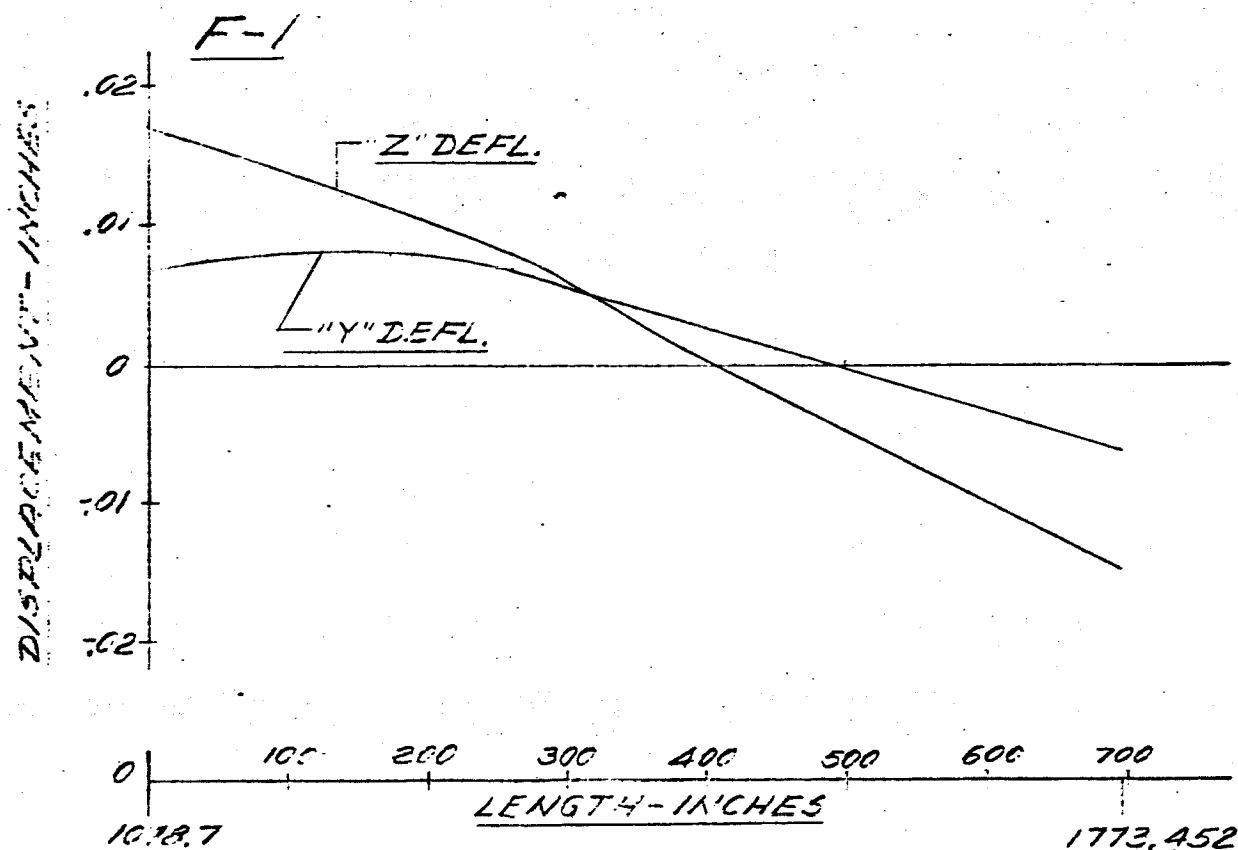
FREQUENCY = 3.00 CPS



-179-

FIG 9<sup>o</sup> DISPLACEMENT IS LENGTH SATURN SA-D1

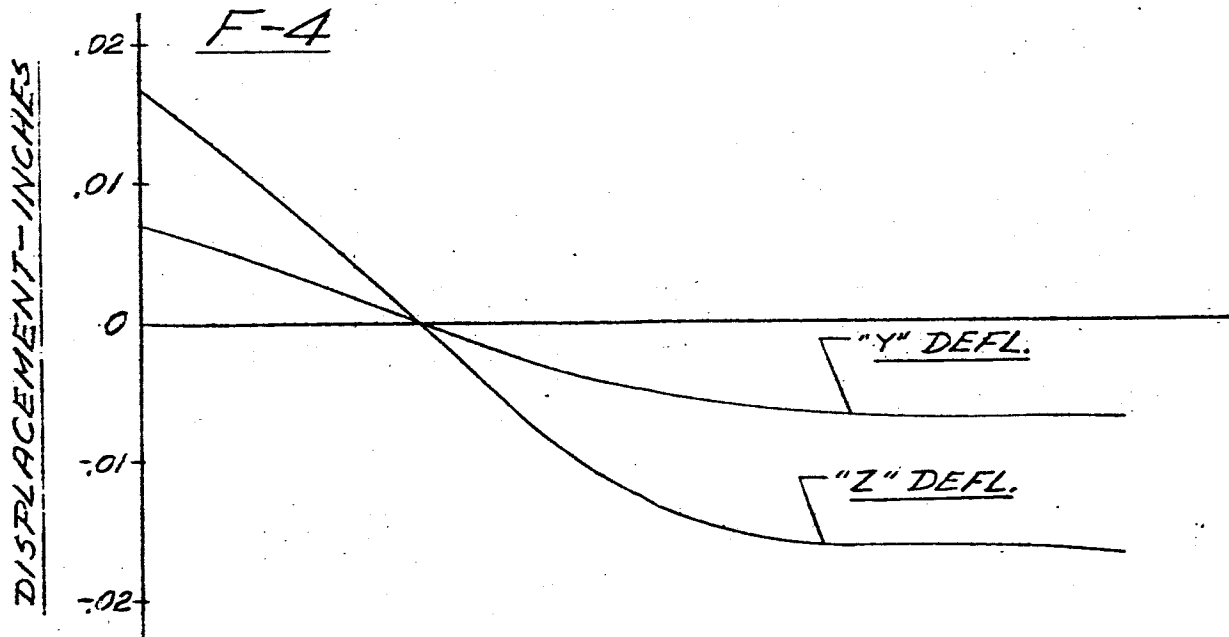
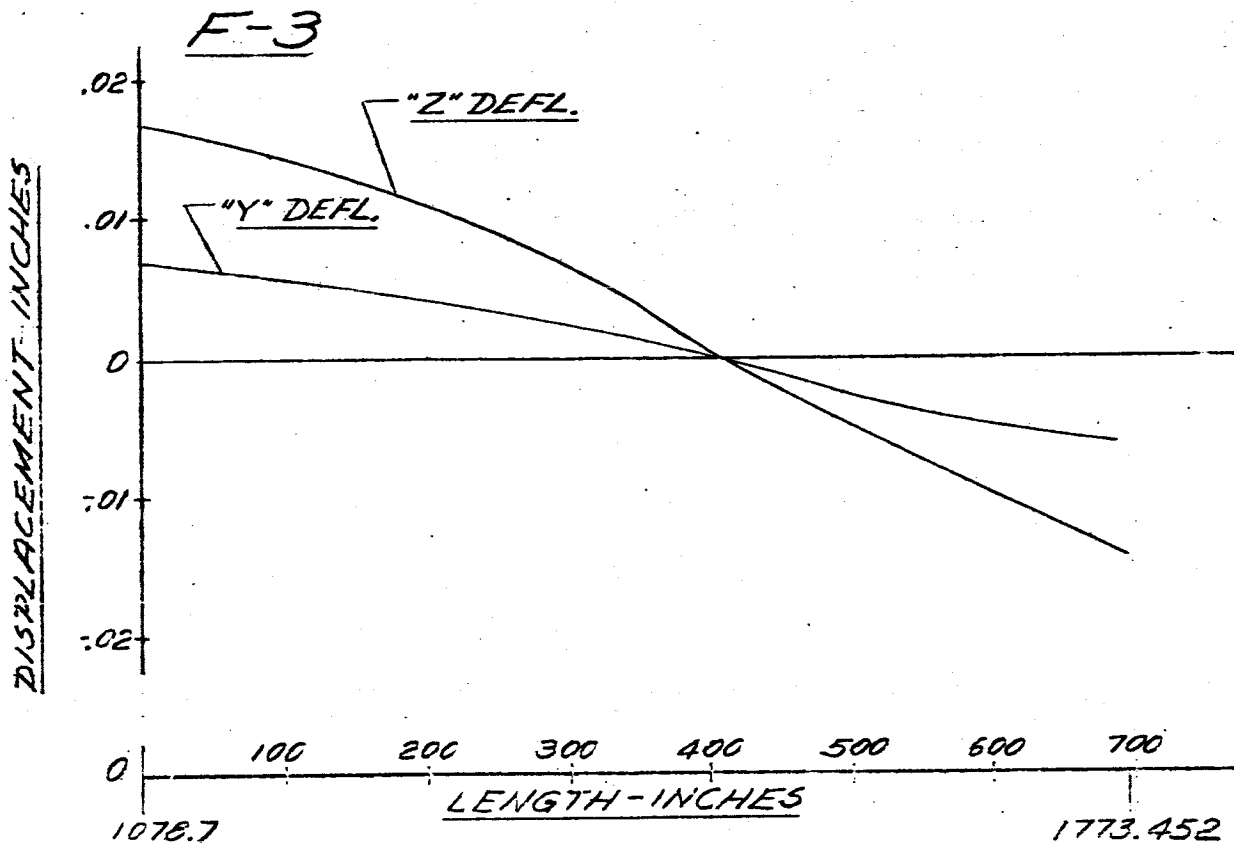
FREQUENCY = 3.00 CPS



-180-

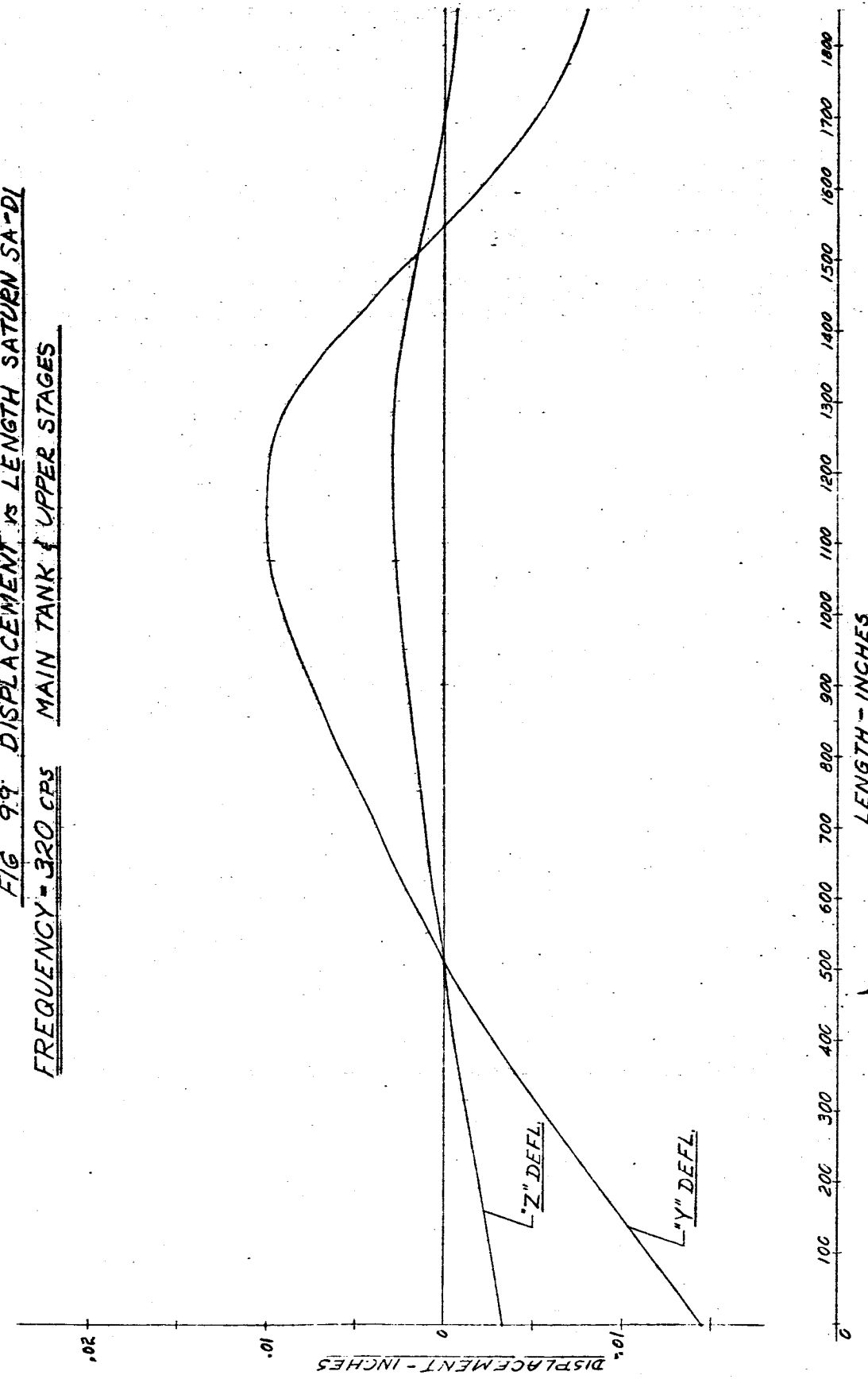
FIG 9B DISPLACEMENT VS LENGTH SATURN SA-DI

FREQUENCY = 3.00 CPS



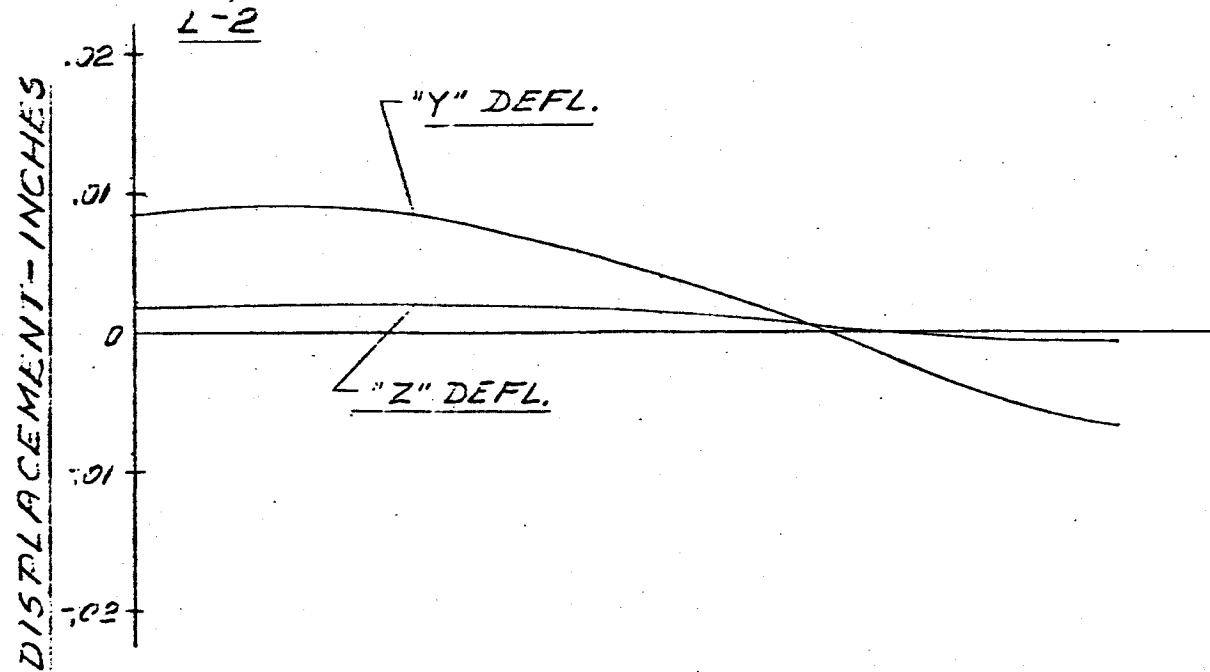
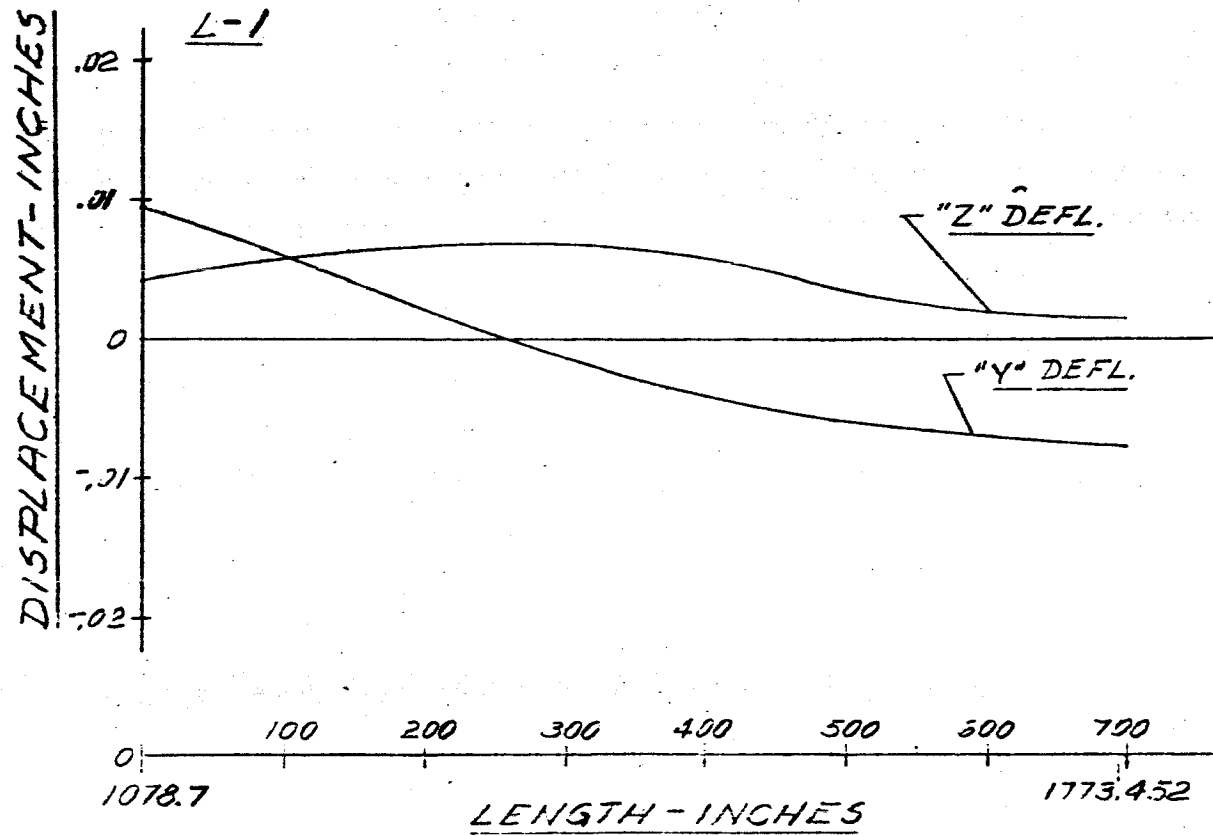
-181-

FIG 9.9. DISPLACEMENT vs LENGTH SATURN SA-DI  
FREQUENCY = 320 CPS MAIN TANK & UPPER STAGES



-182-

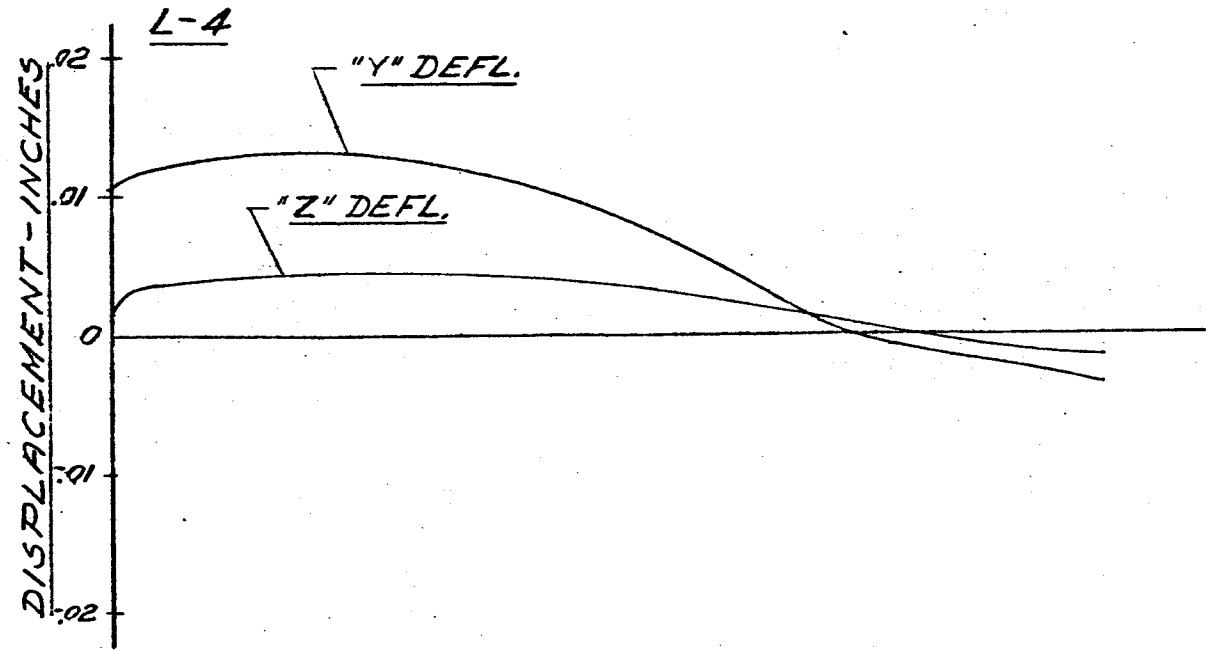
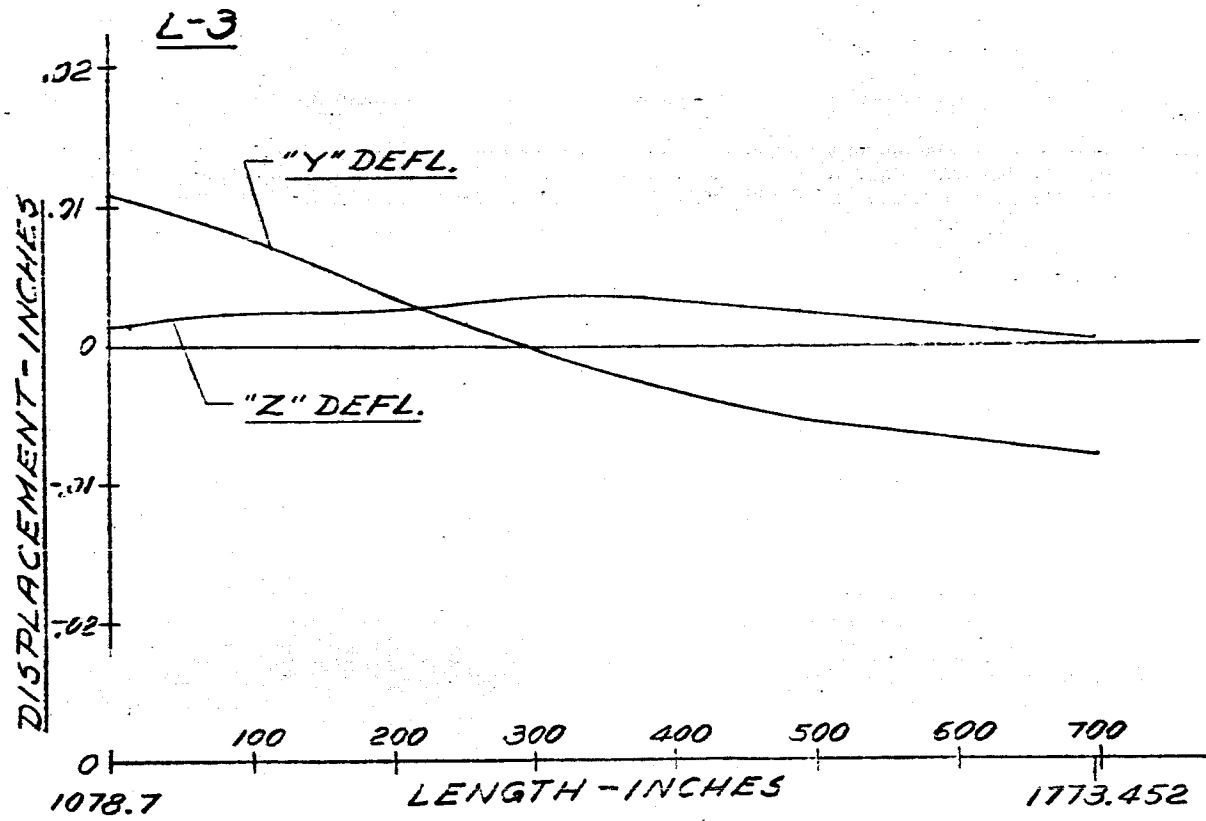
FIG 100 DISPLACEMENT VS LENGTH SATURN SA-DI  
FREQUENCY = 3.20 CPS



-183-

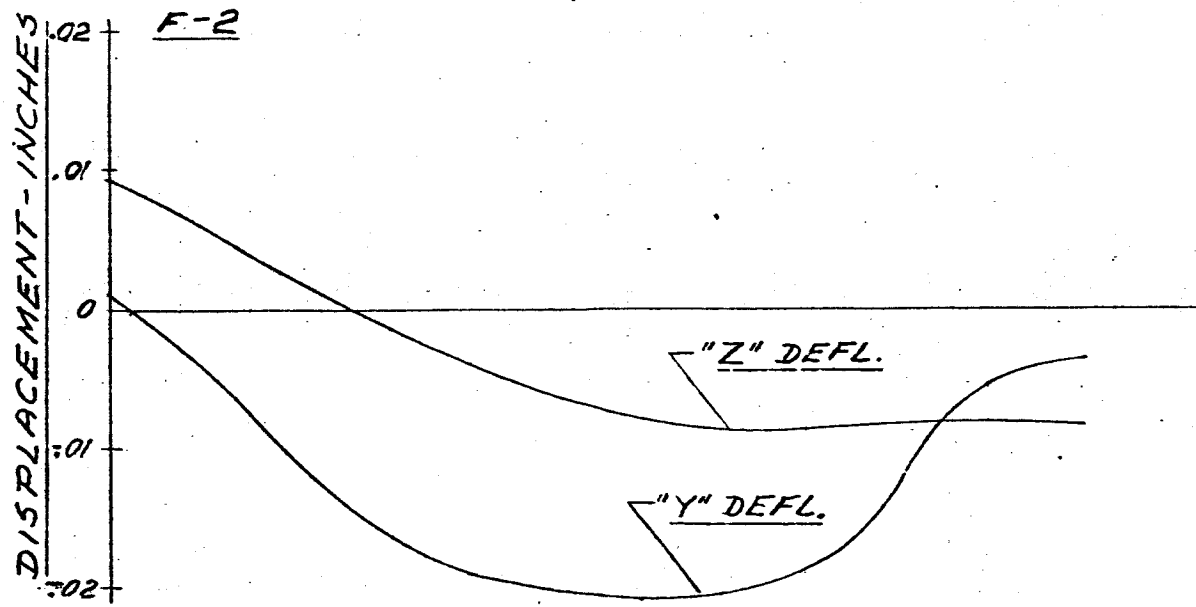
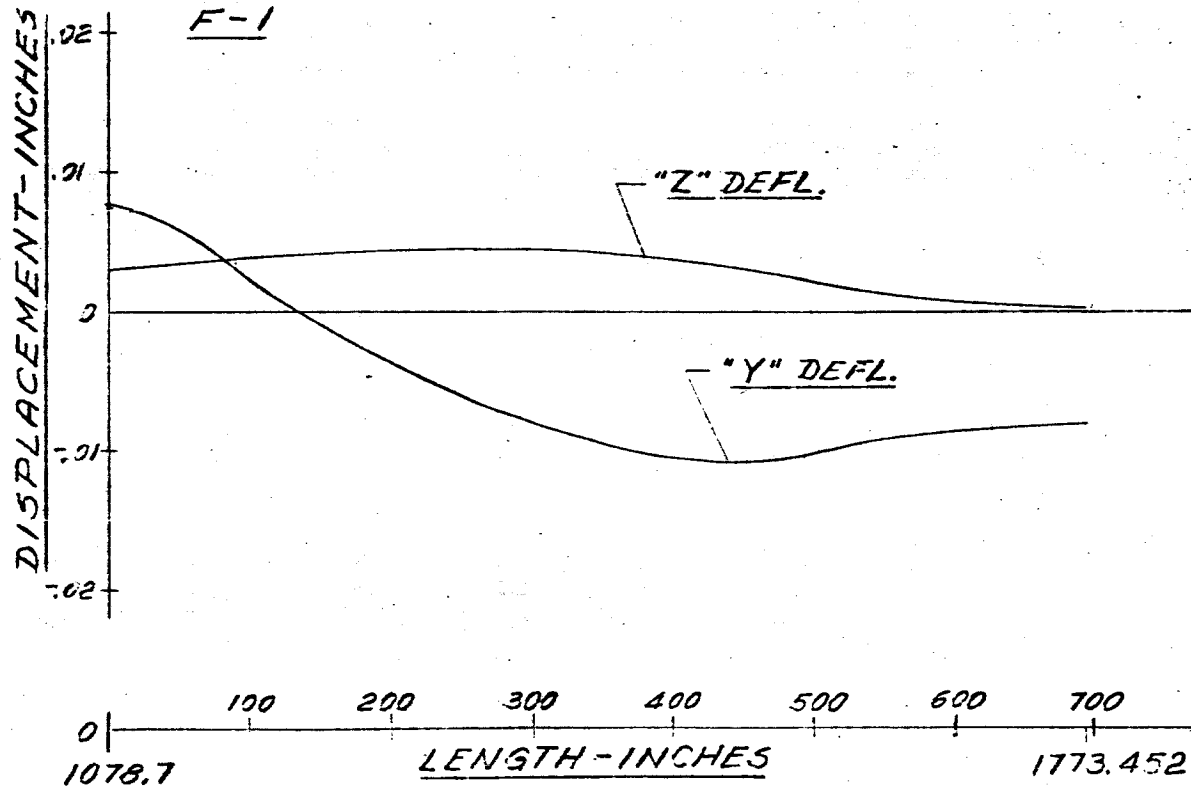
FIG 101 DISPLACEMENT VS LENGTH SATURN SA-D

FREQUENCY = 3.20 CPS.



-184-

FIG. 102 DISPLACEMENT VS LENGTH SATURN SA-DI  
FREQUENCY = 3.20 CPS



-185-

FIG. 103 DISPLACEMENT VS LENGTH SATURN SA-DI  
FREQUENCY = 3.20 CPS

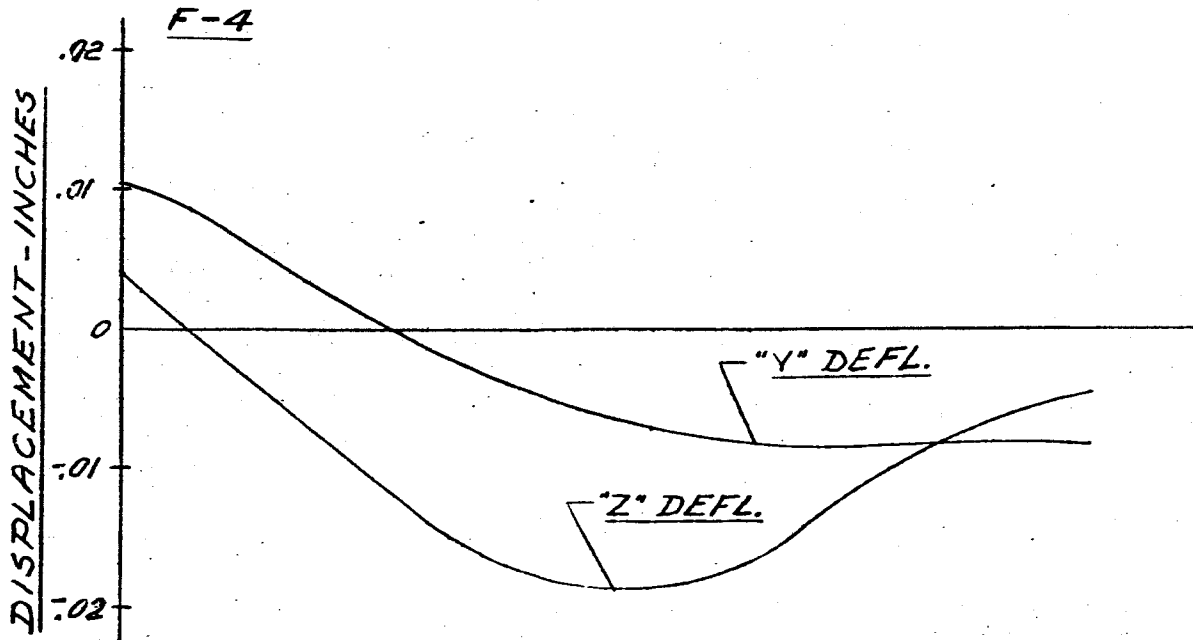
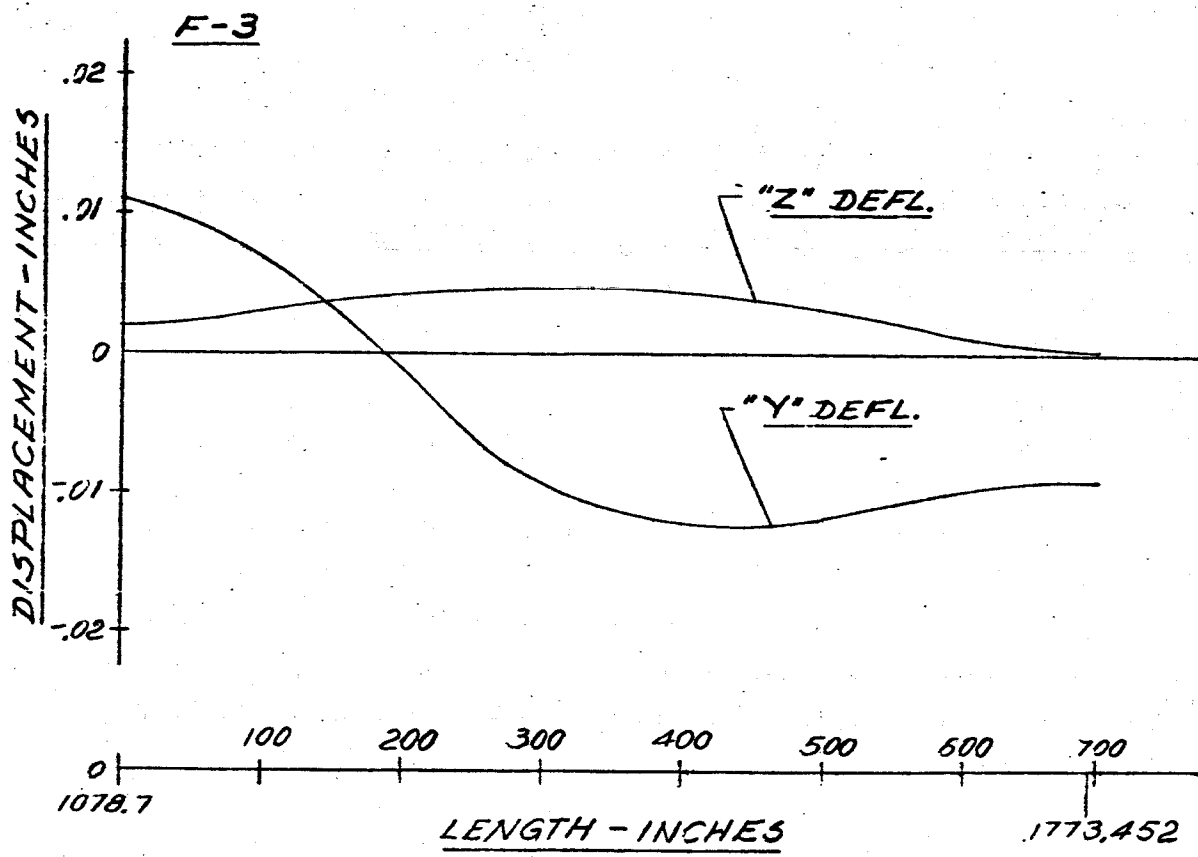


FIG 104 DISPLACEMENT VS LENGTH SATURN SA-01  
MAIN TANK & UPPER STAGES  
FREQUENCY = 3.25 cps

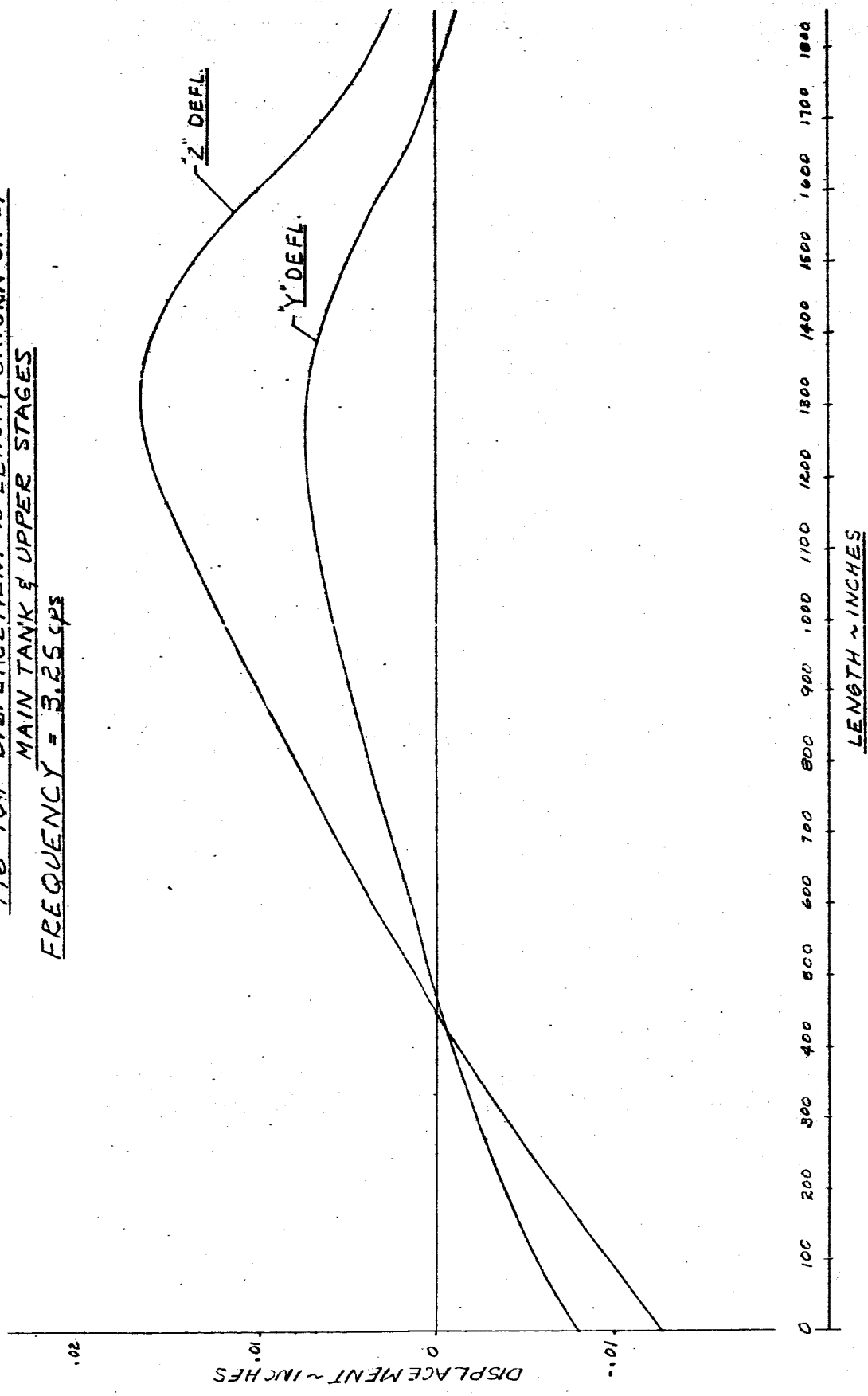
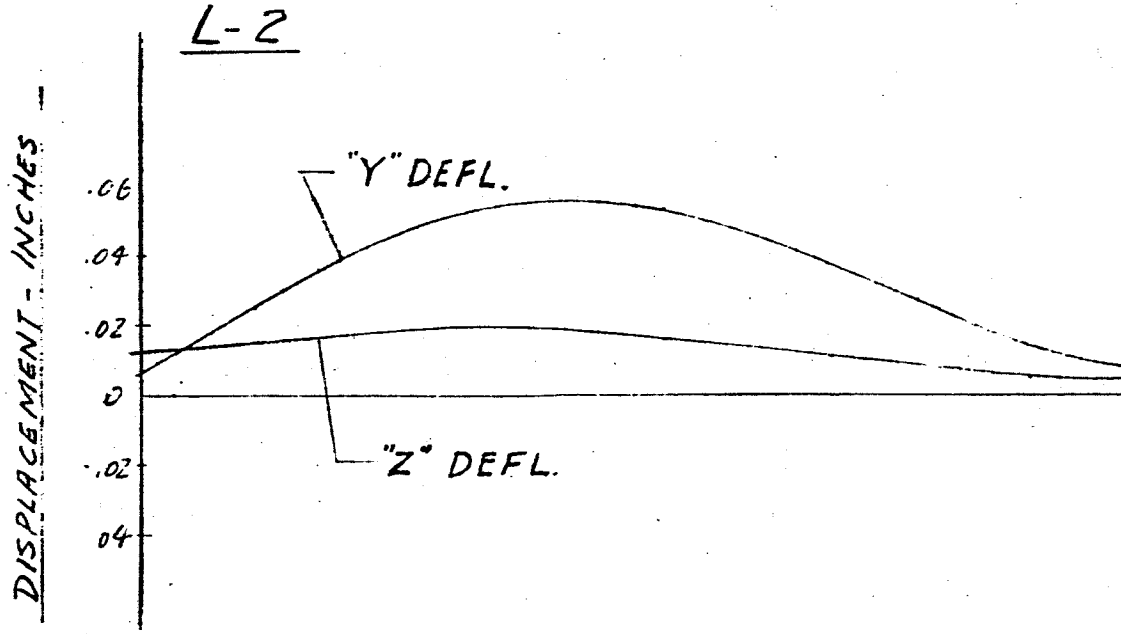
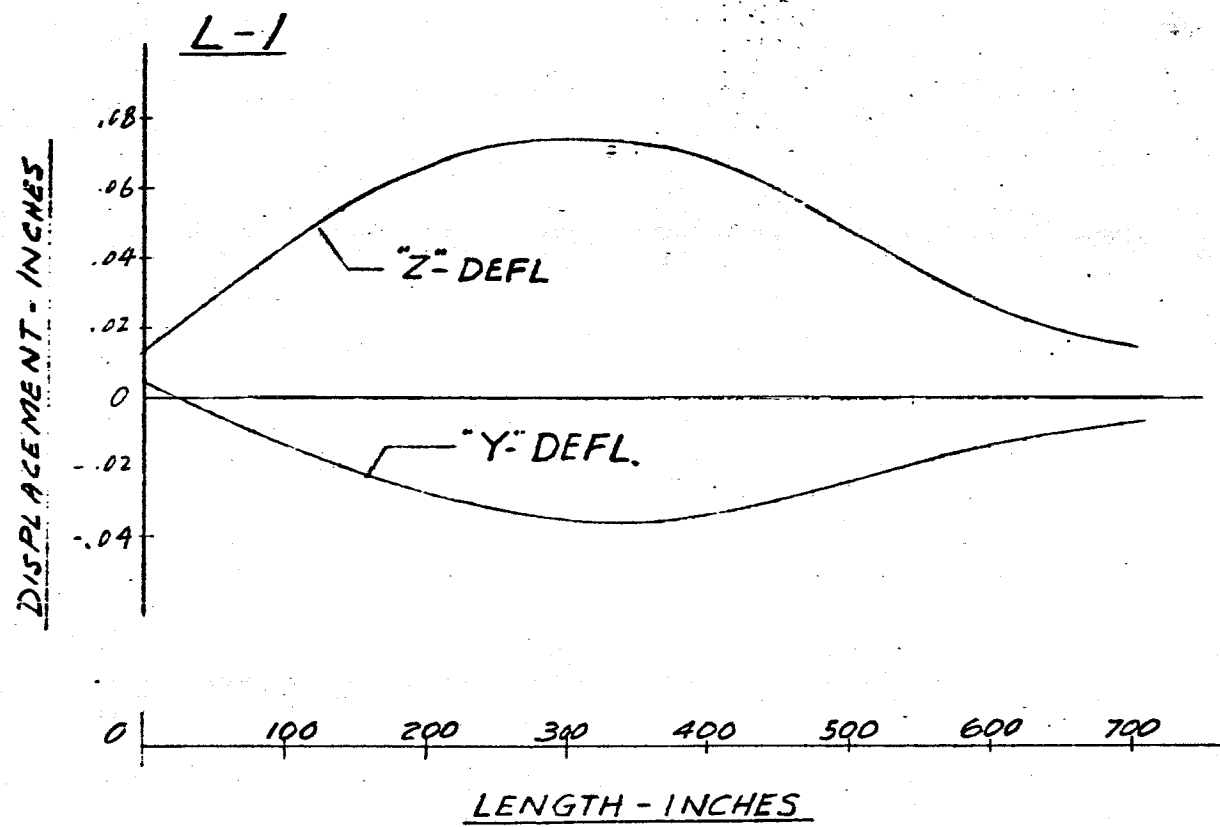


FIG. 105 DISPLACEMENT VS LENGTH SATURN SA-01

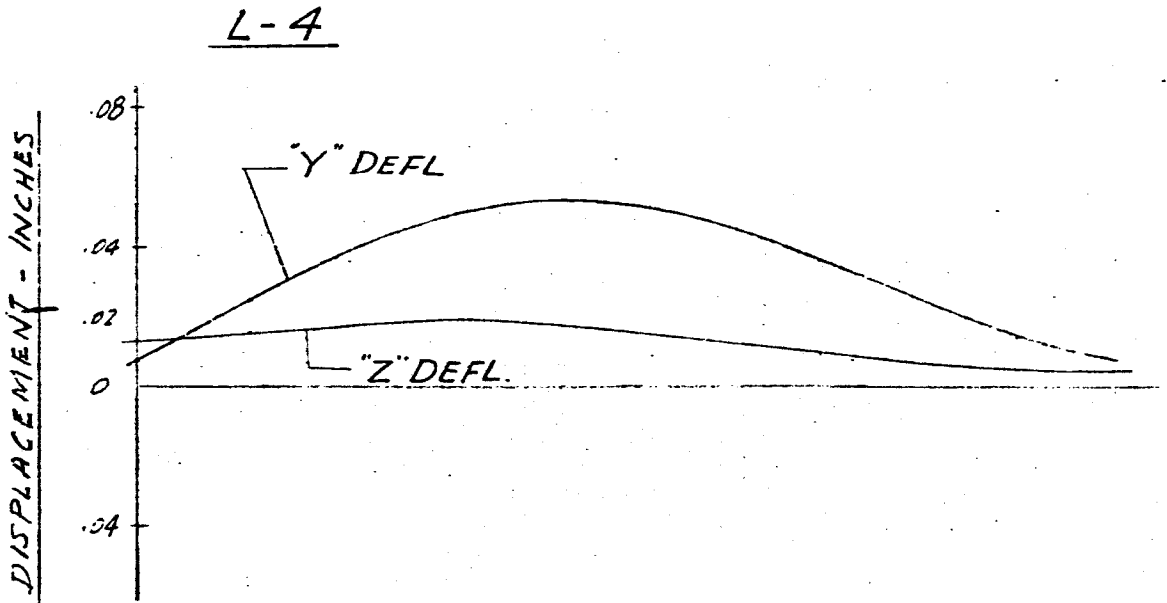
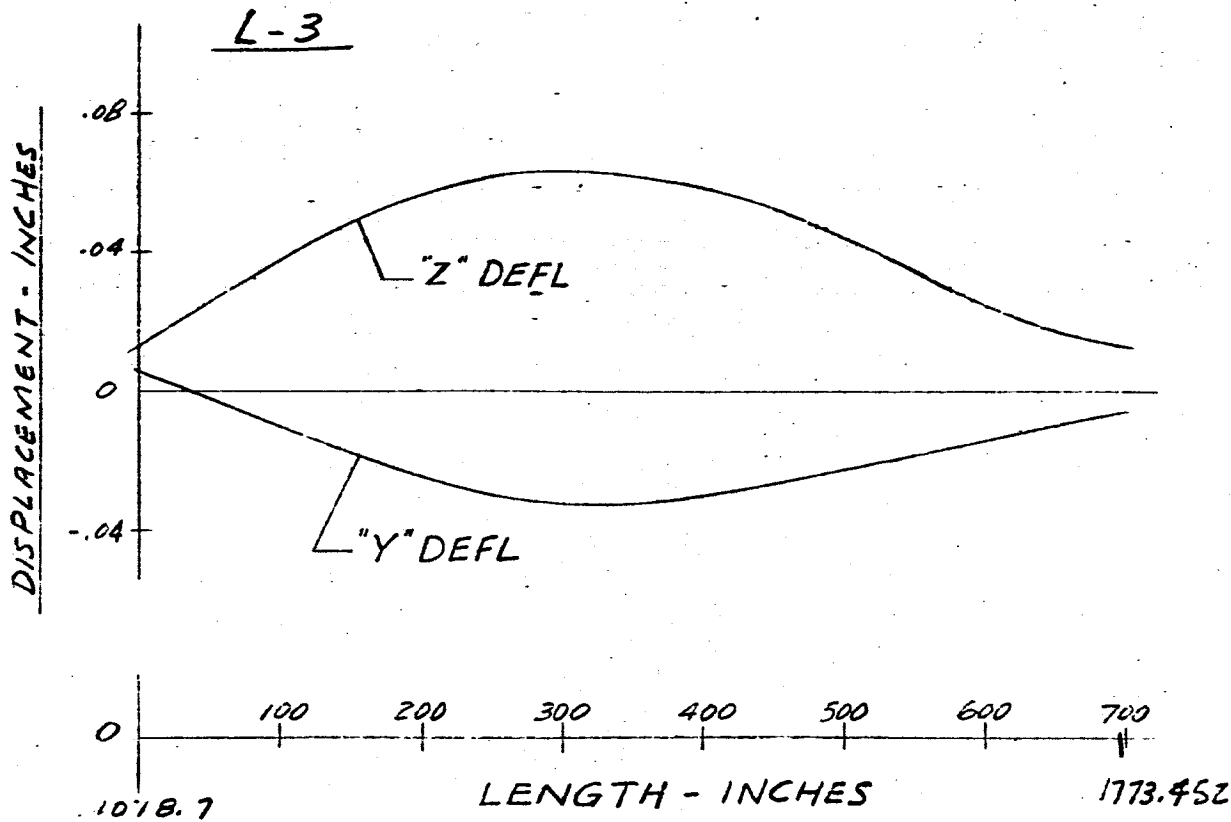
FREQUENCY = 3.25 CPS



-188-

FIG. 106 DISPLACEMENT VS LENGTH SATURN SA-DI

FREQUENCY Y = 3.25 CPS.



-189-

FIG. 107 DISPLACEMENT VS LENGTH SATURN SA-D1

FREQUENCY = 3.25 cps

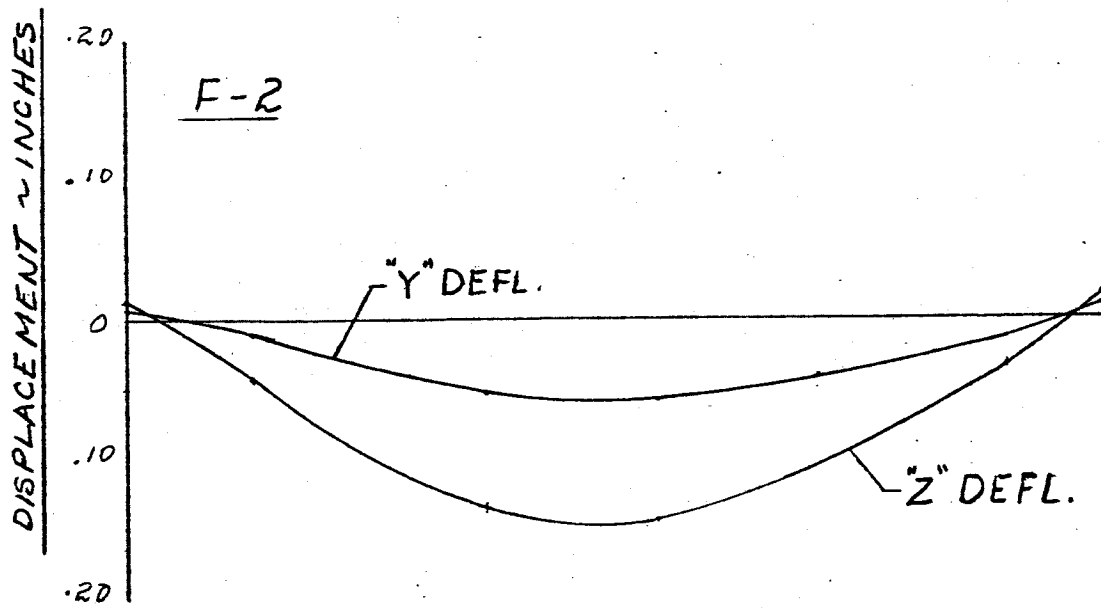
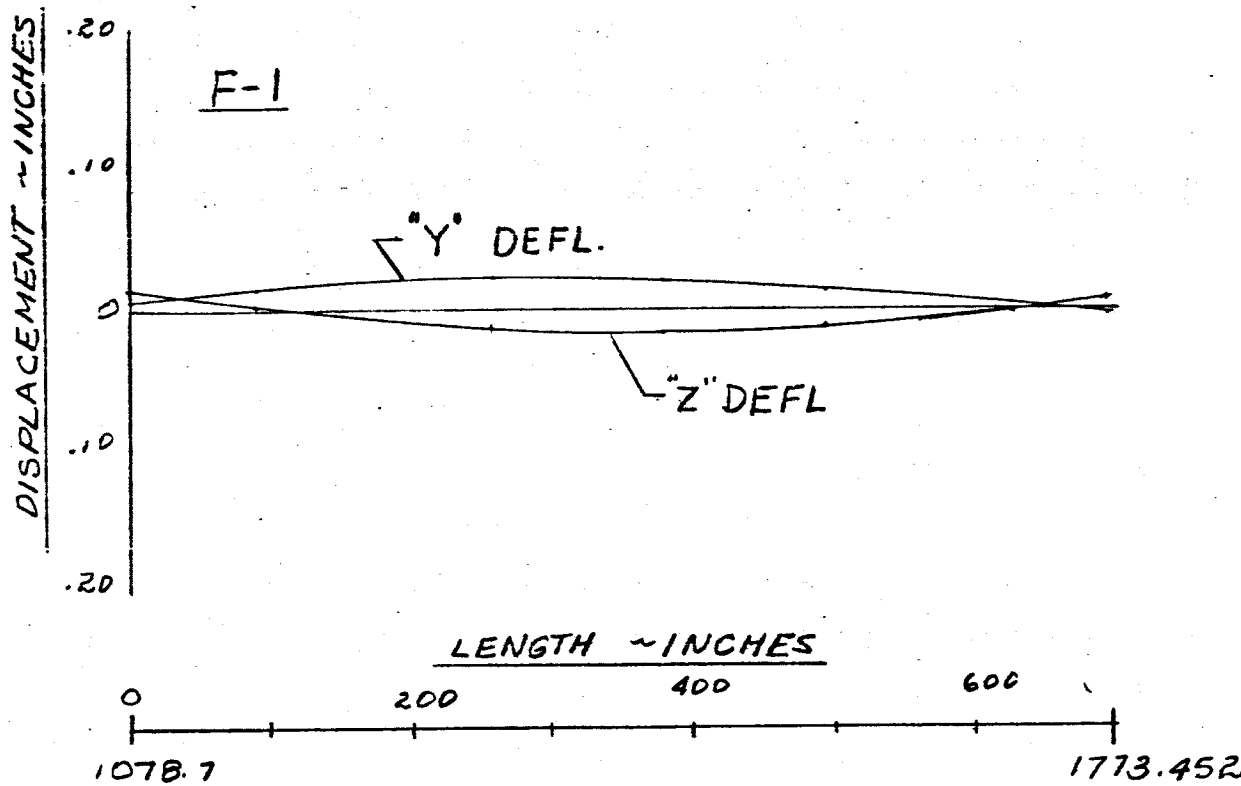
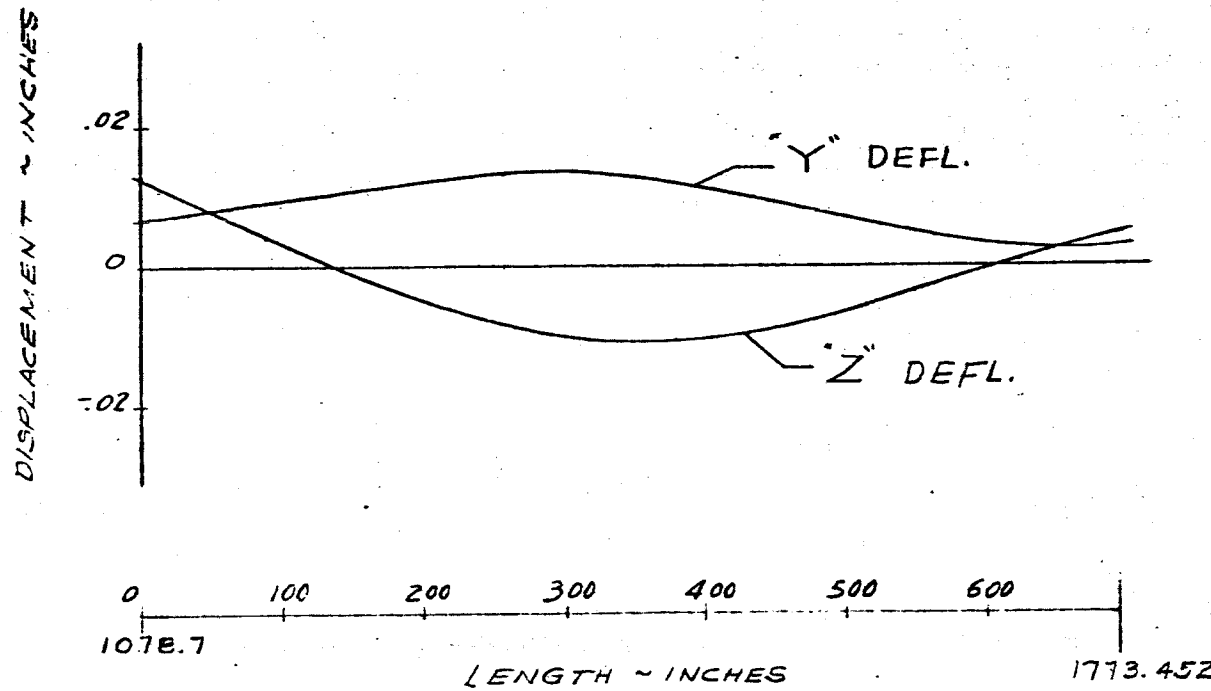


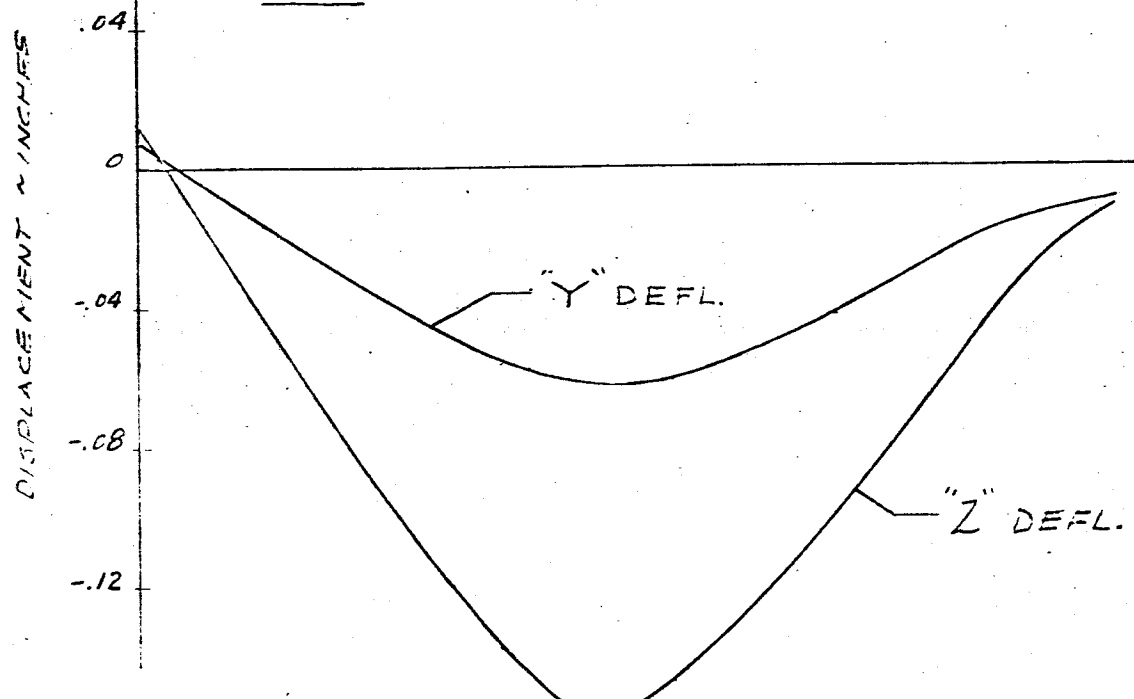
FIG 108 DISPLACEMENT VS LENGTH - SATURN SA-DI

FREQUENCY = 3.25 C.P.S.

F-3

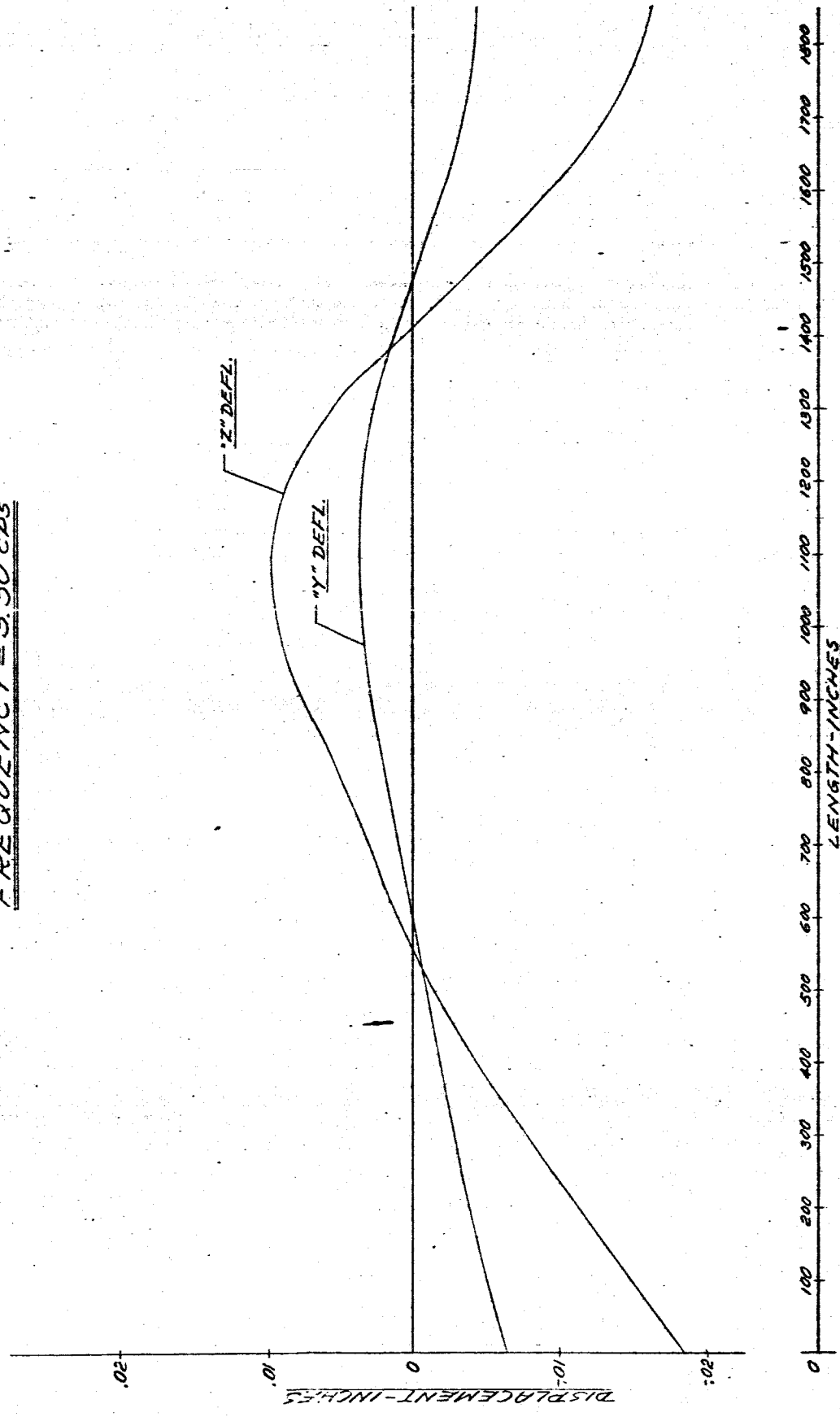


F-4



- 191 -

FIG 109 DISPLACEMENT vs LENGTH SATURN S-AD-1  
MAIN TANK & UPPER STAGES  
FREQUENCY = 3.30 CPS

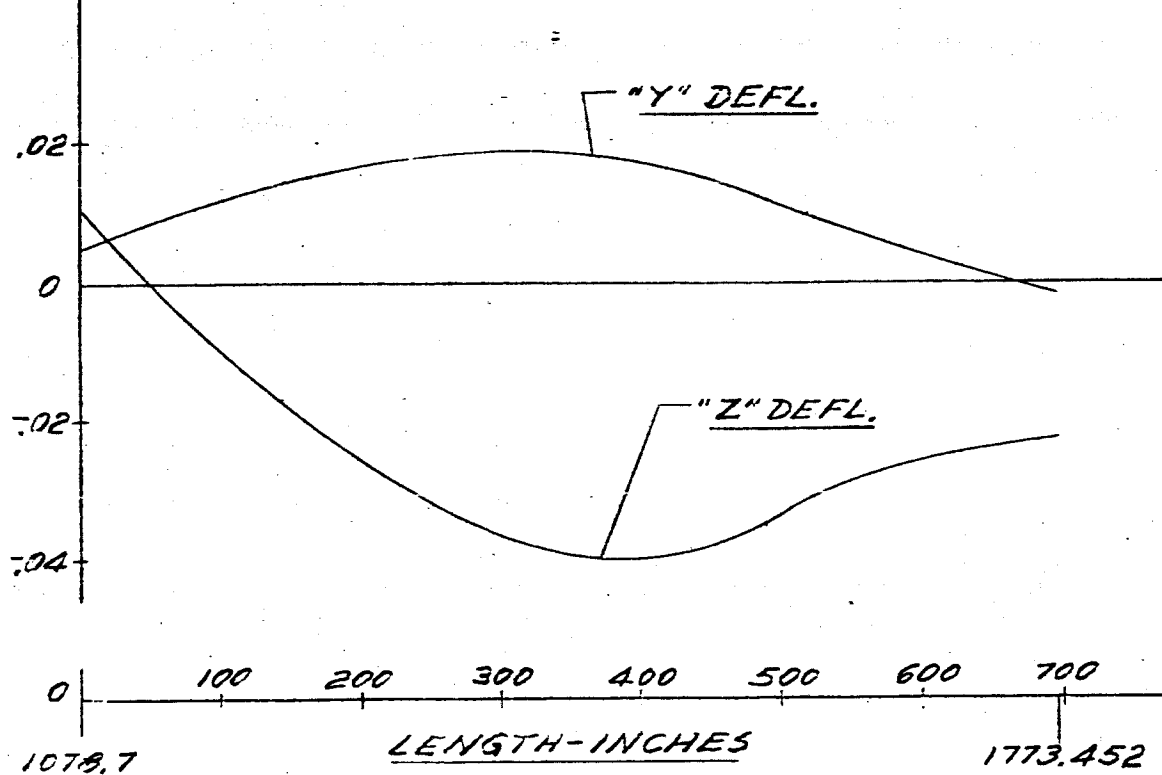


-192-

FIG. 110 DISPLACEMENT VS LENGTH SATURN SA-DI  
FREQUENCY = 3.30 CPS

L-1

DISPLACEMENT-INCHES



L-2

DISPLACEMENT-INCHES

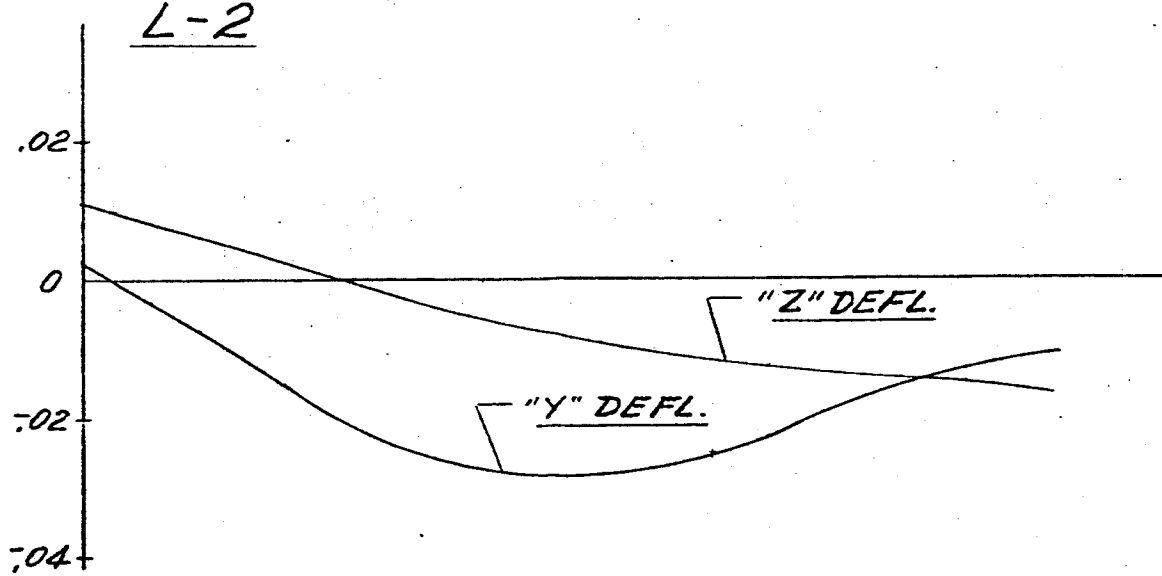


FIG. III DISPLACEMENT vs LENGTH SATURN SA-DI  
FREQUENCY = 3.30 CPS

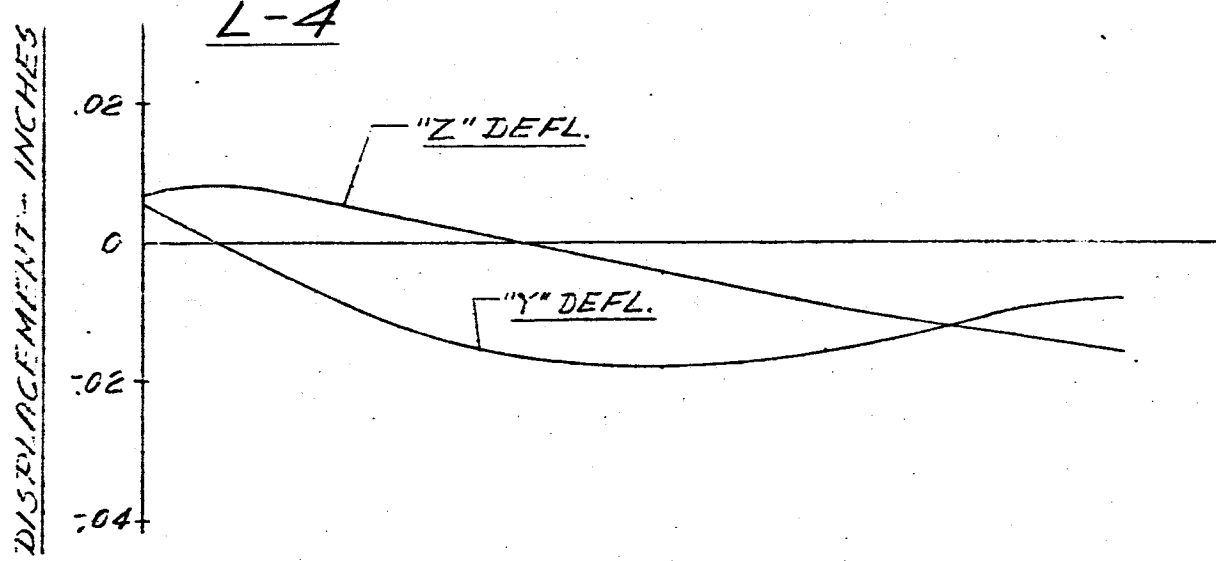
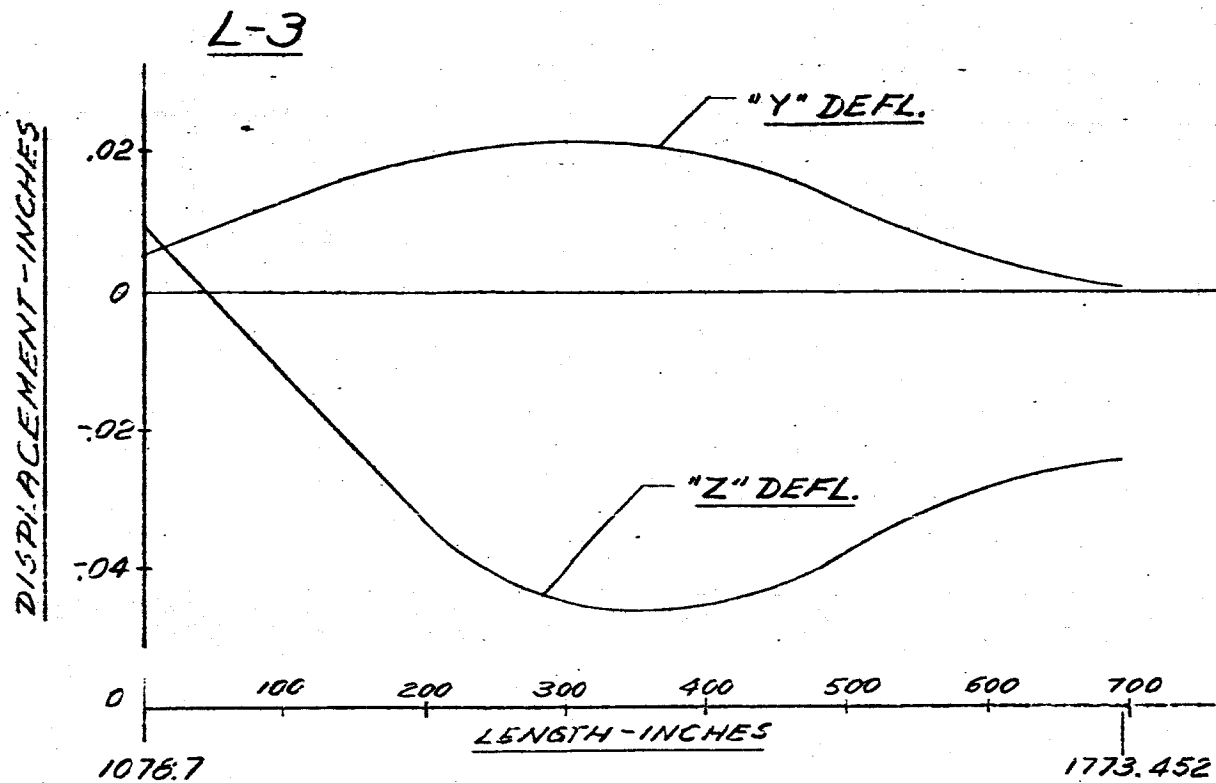
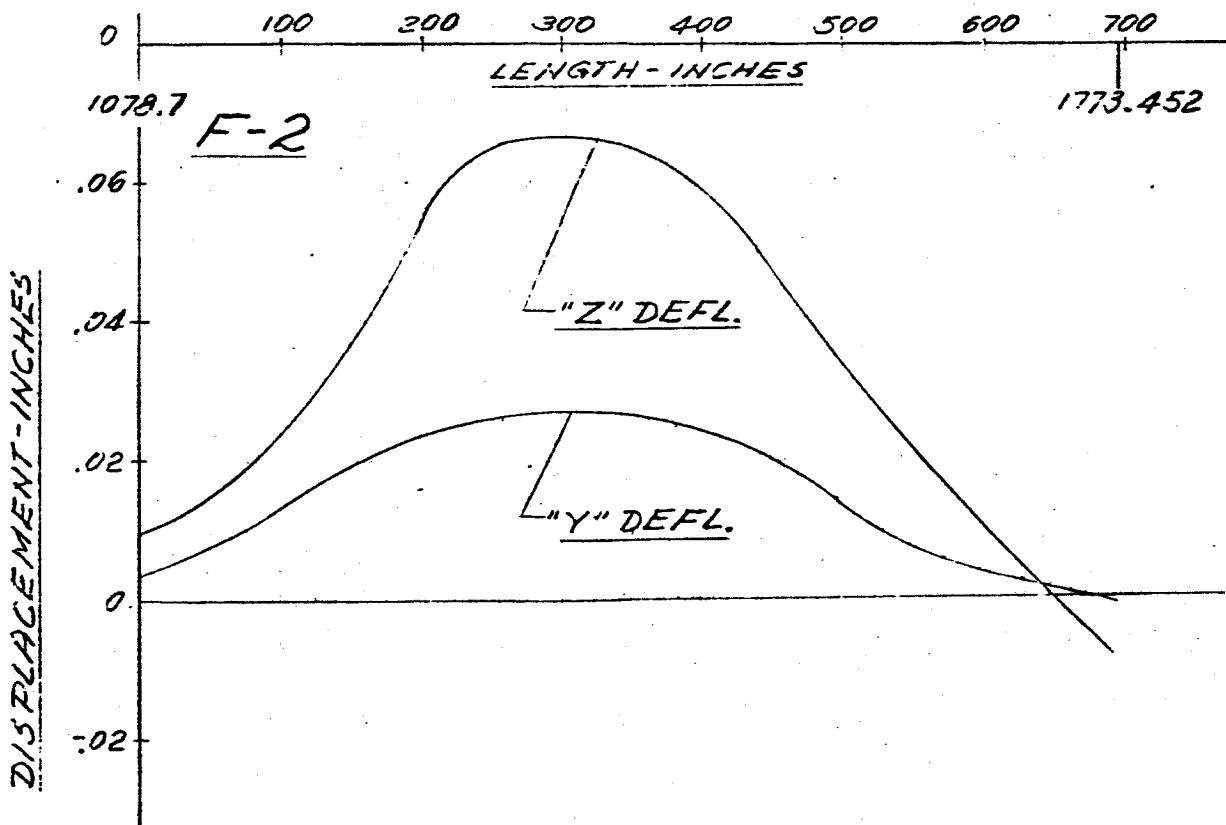
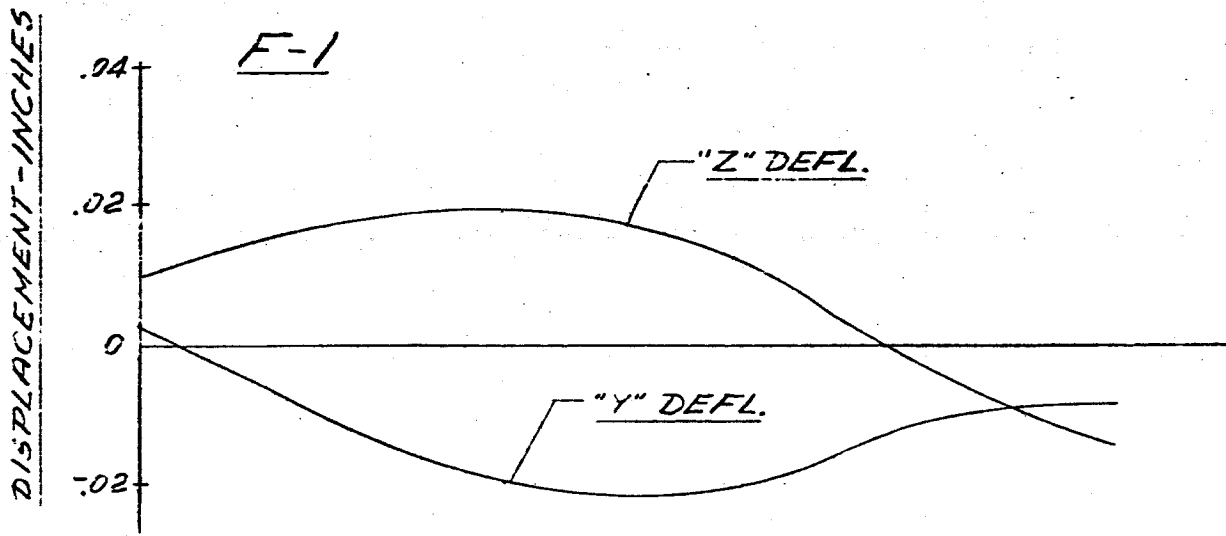


FIG. 112 DISPLACEMENT VS LENGTH SATURN SA-DI

FREQUENCY = 3.30 CPS



-195-

FIG. 113 DISPLACEMENT VS LENGTH SATURN SA-D1  
FREQUENCY = 3.30 CPS

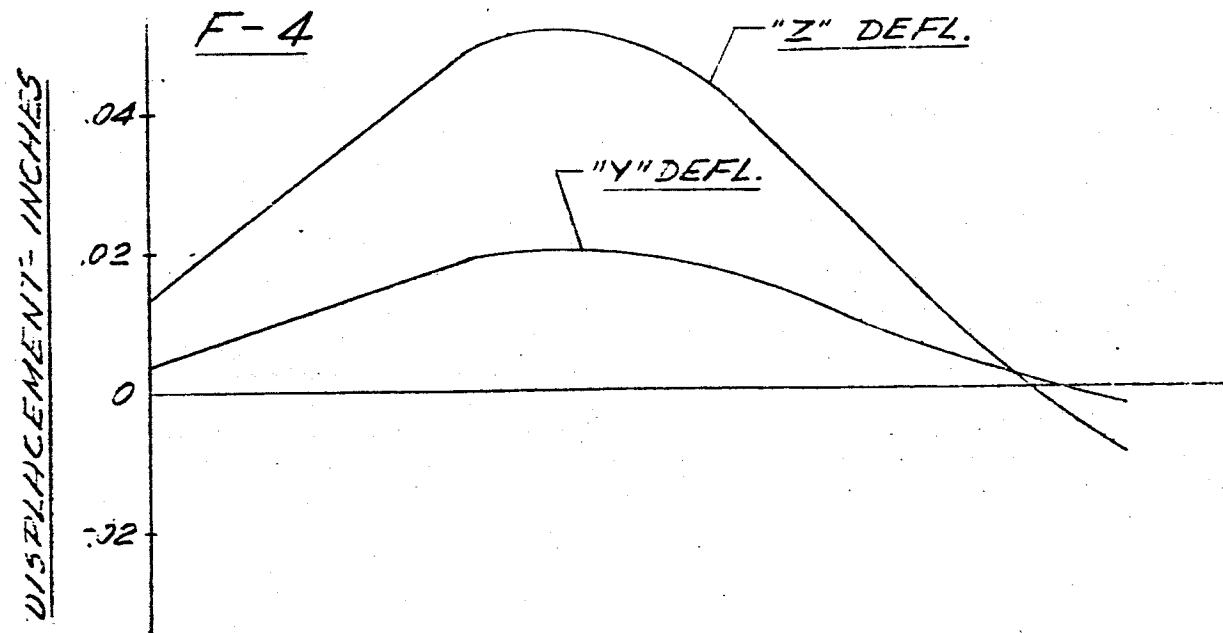
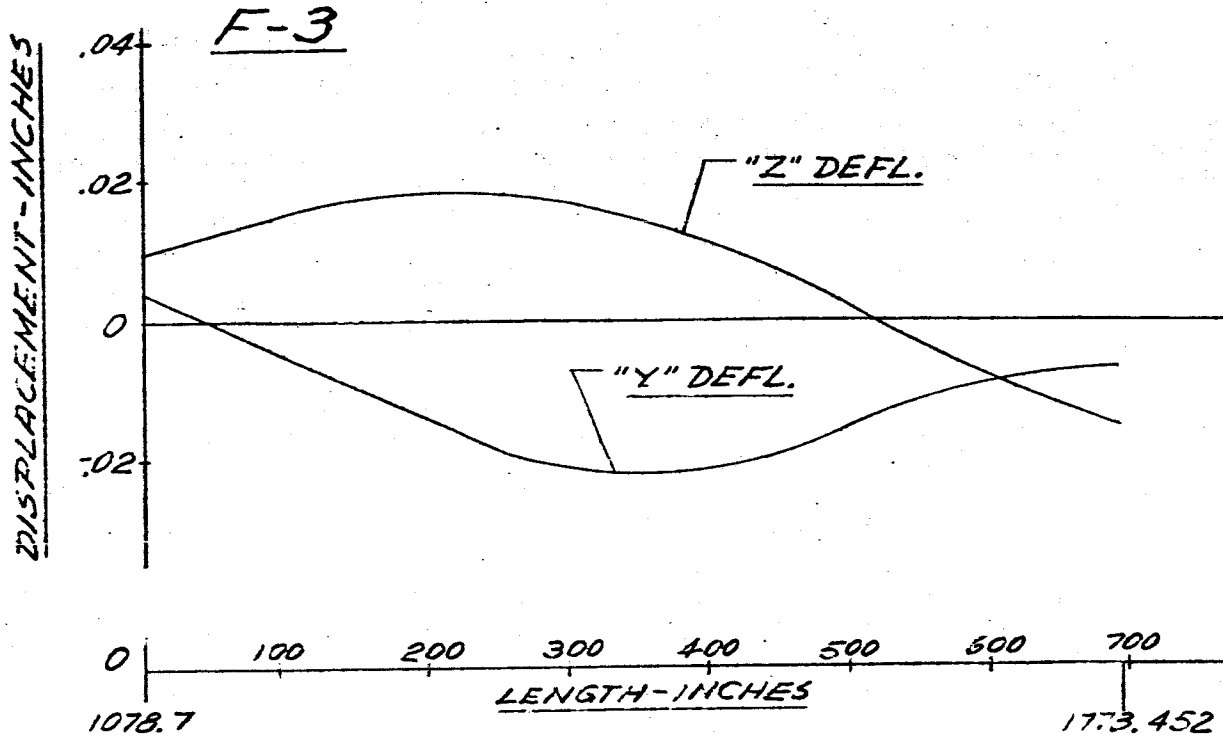
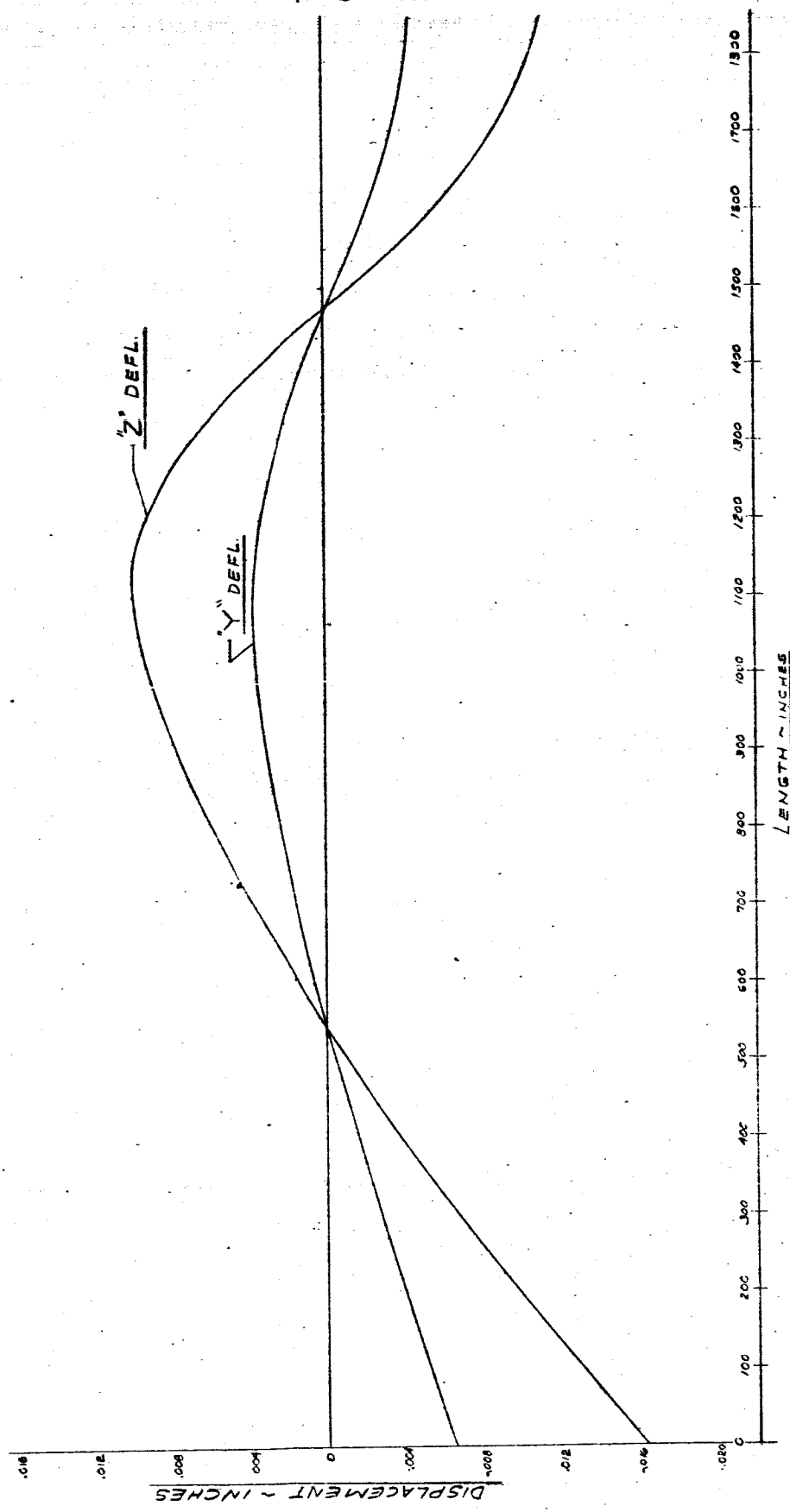


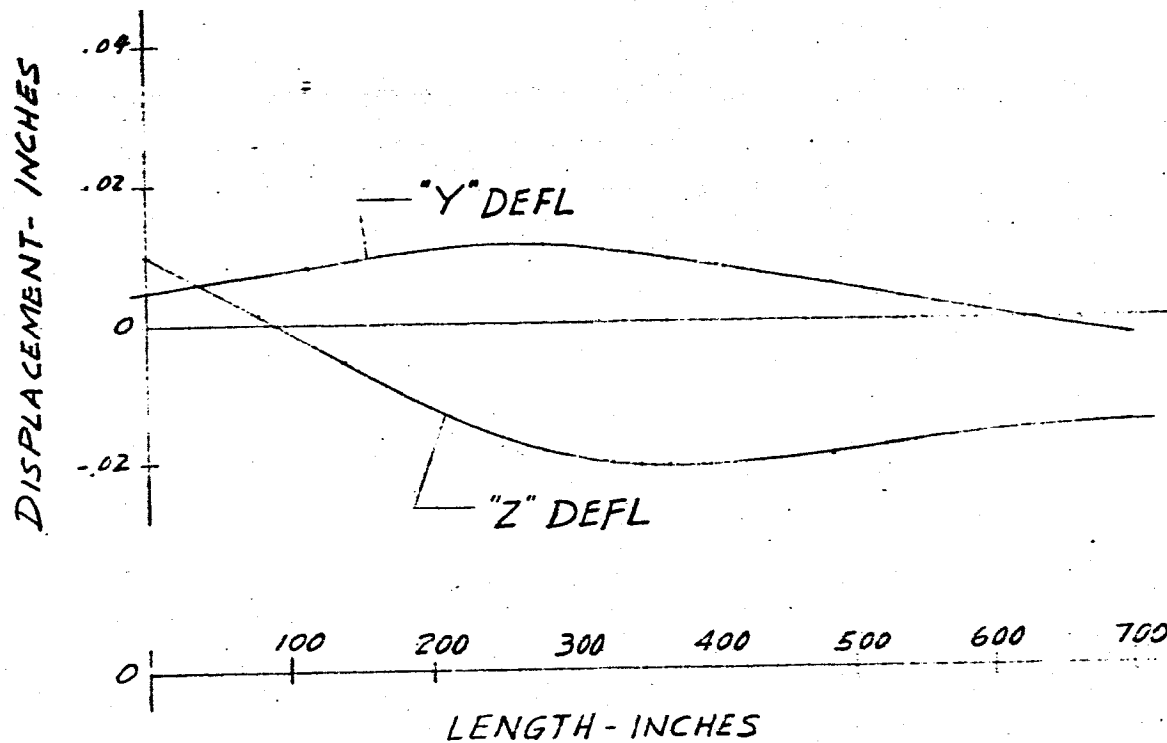
FIG. 114 DISPLACEMENT vs LENGTH SATURN SA-D1  
MAIN TANK & UPPER STAGES  
FREQUENCY = 3.35 cps



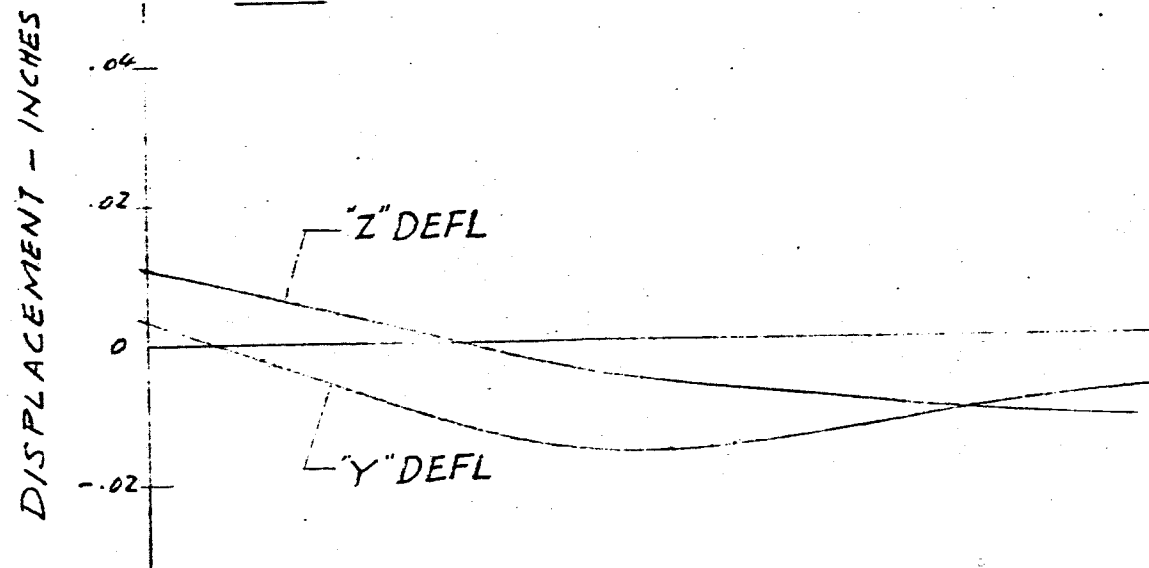
-197-

FIG. 115 DISPLACEMENT VS LENGTH SATURN SA-D1  
FREQUENCY = 3.35 CPS

L-1



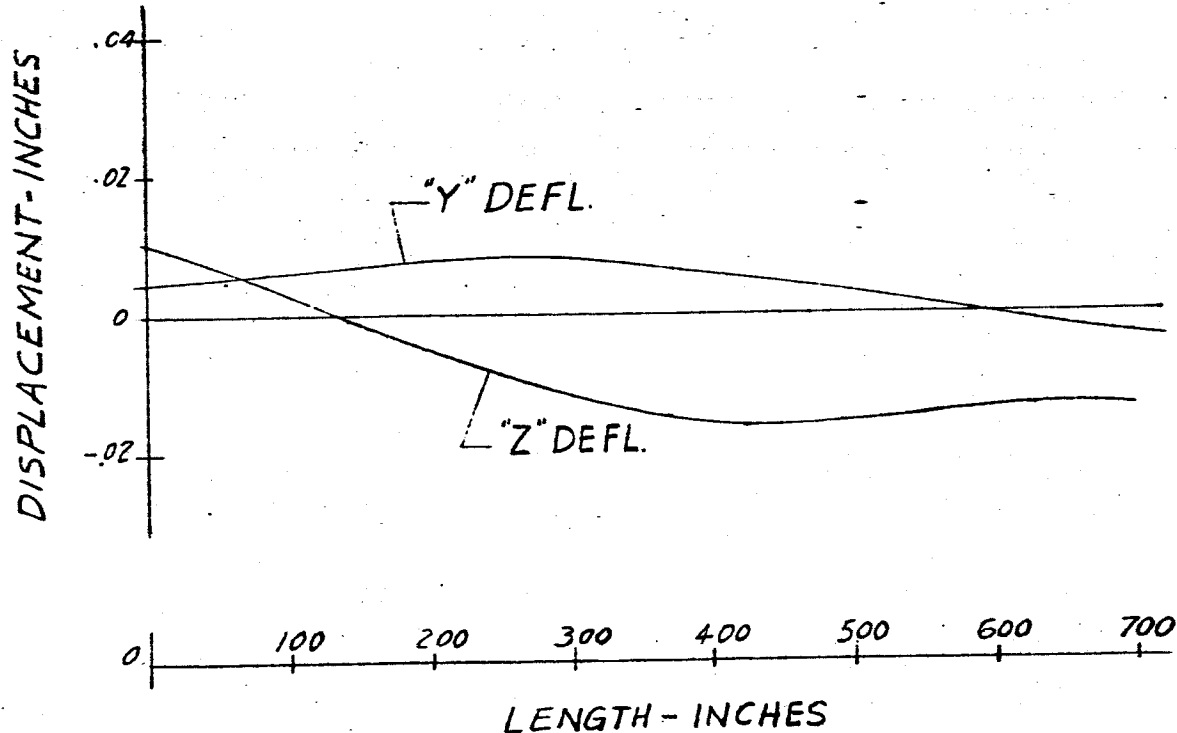
L-2



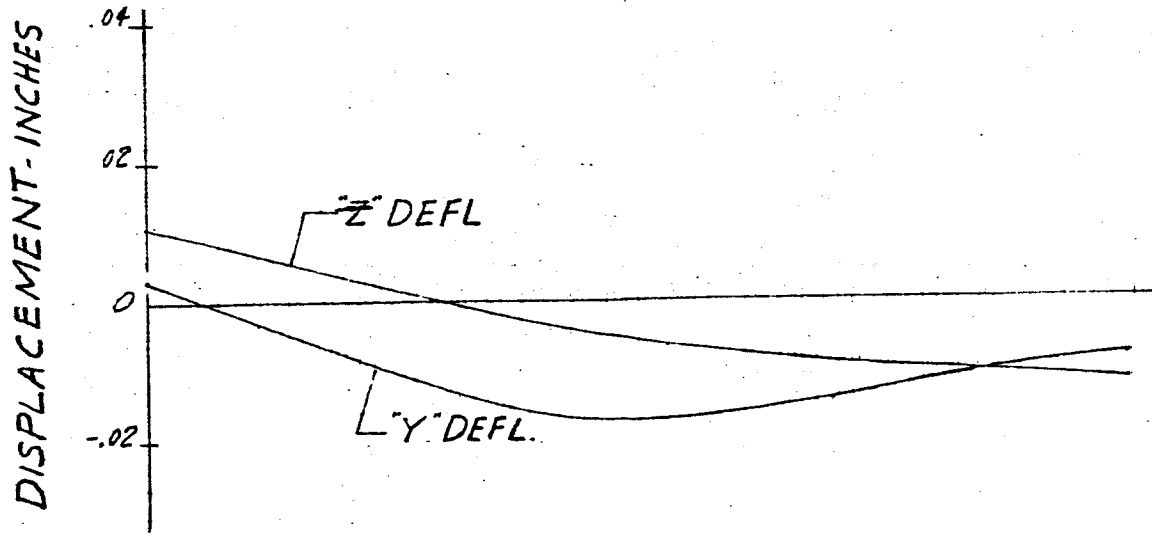
-198-

FIG. 116 DISPLACEMENT vs LENGTH SATURN SA-DI  
FREQUENCY = 3.35 CPS

L-3



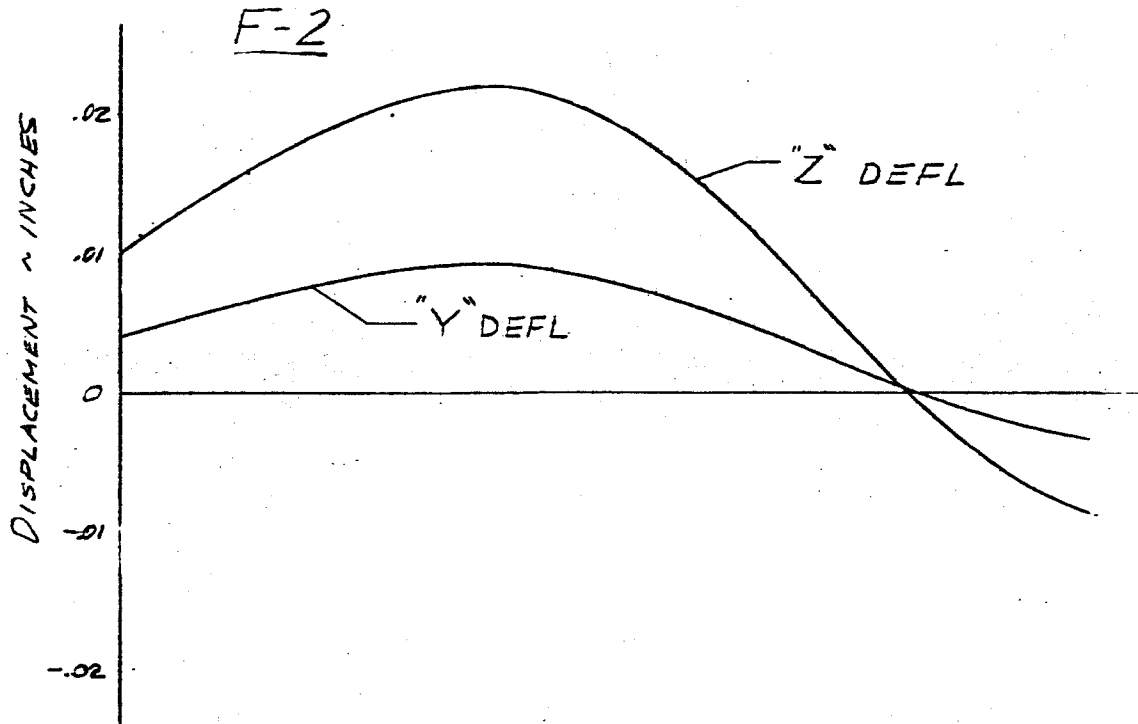
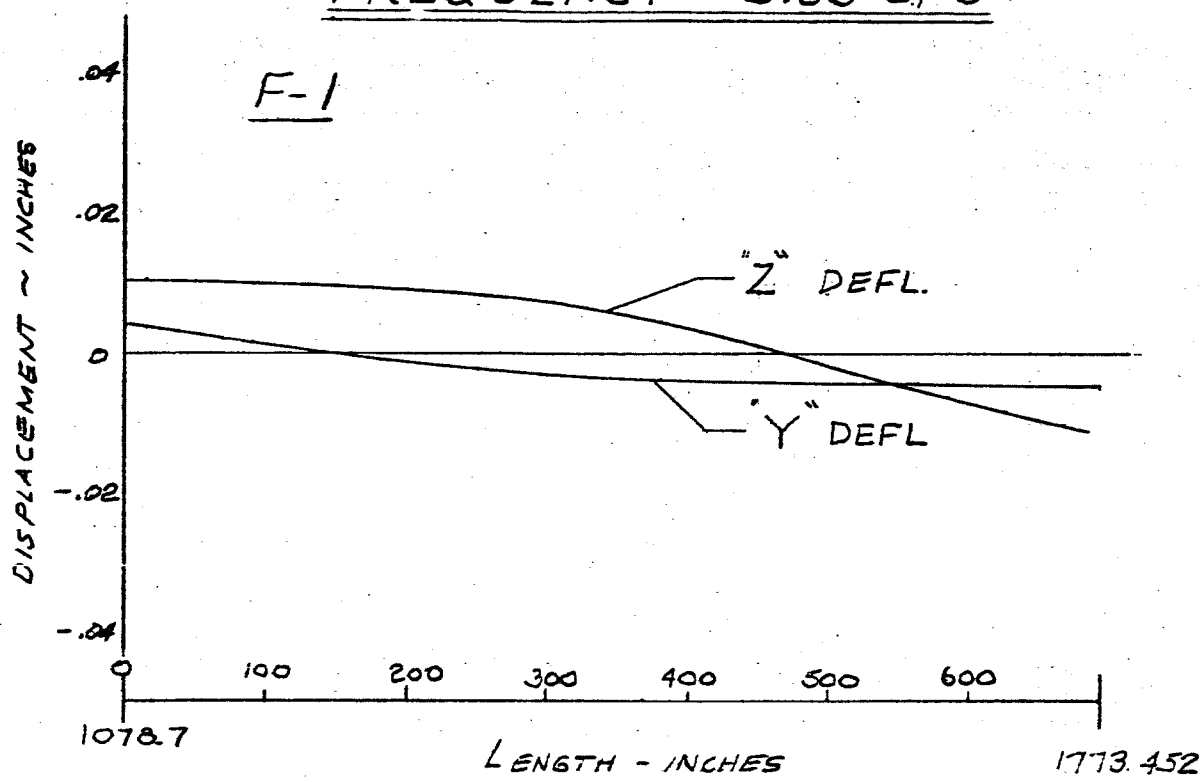
L-4



-199-

FIG 117 DISPLACEMENT VS LENGTH SATURN SA-D1

FREQUENCY = 3.35 CPS



-200-

FIG 118 DISPLACEMENT VS LENGTH SATURN SA-D1

FREQUENCY = 3.35 CPS.

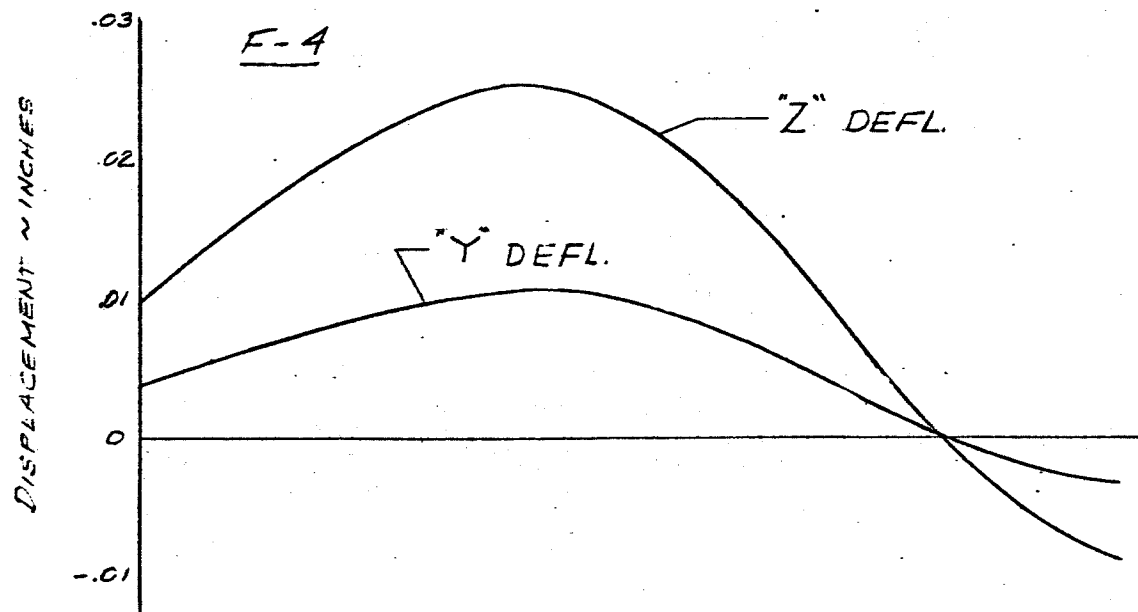
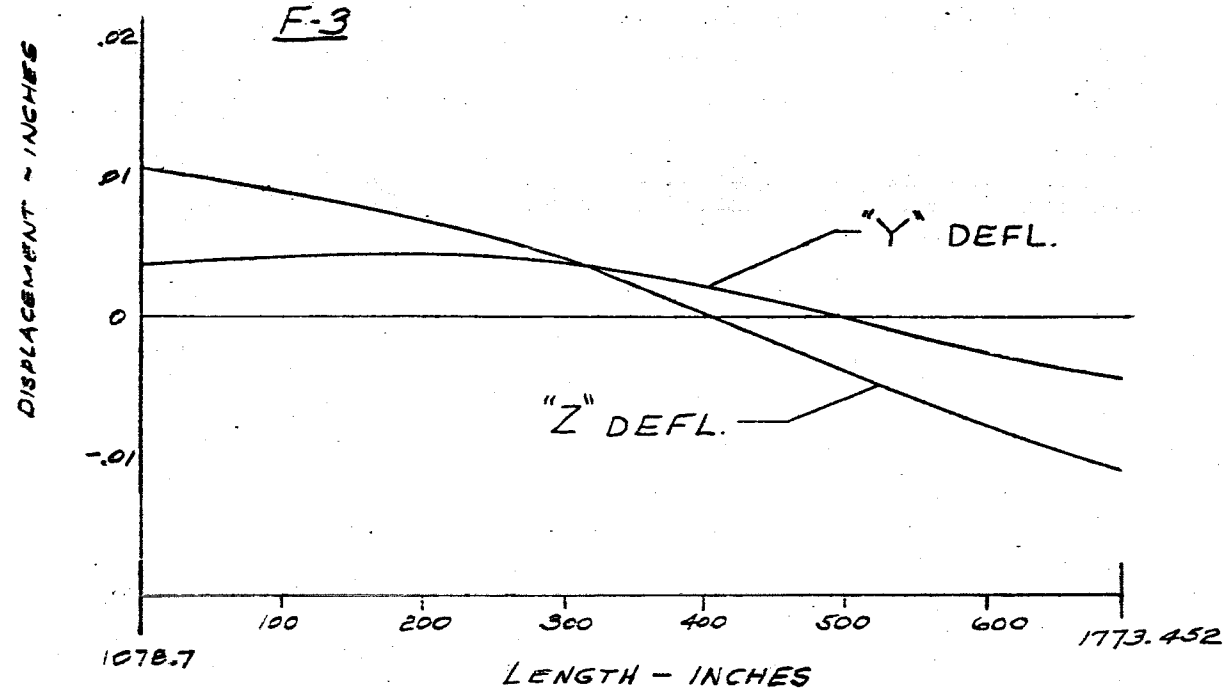
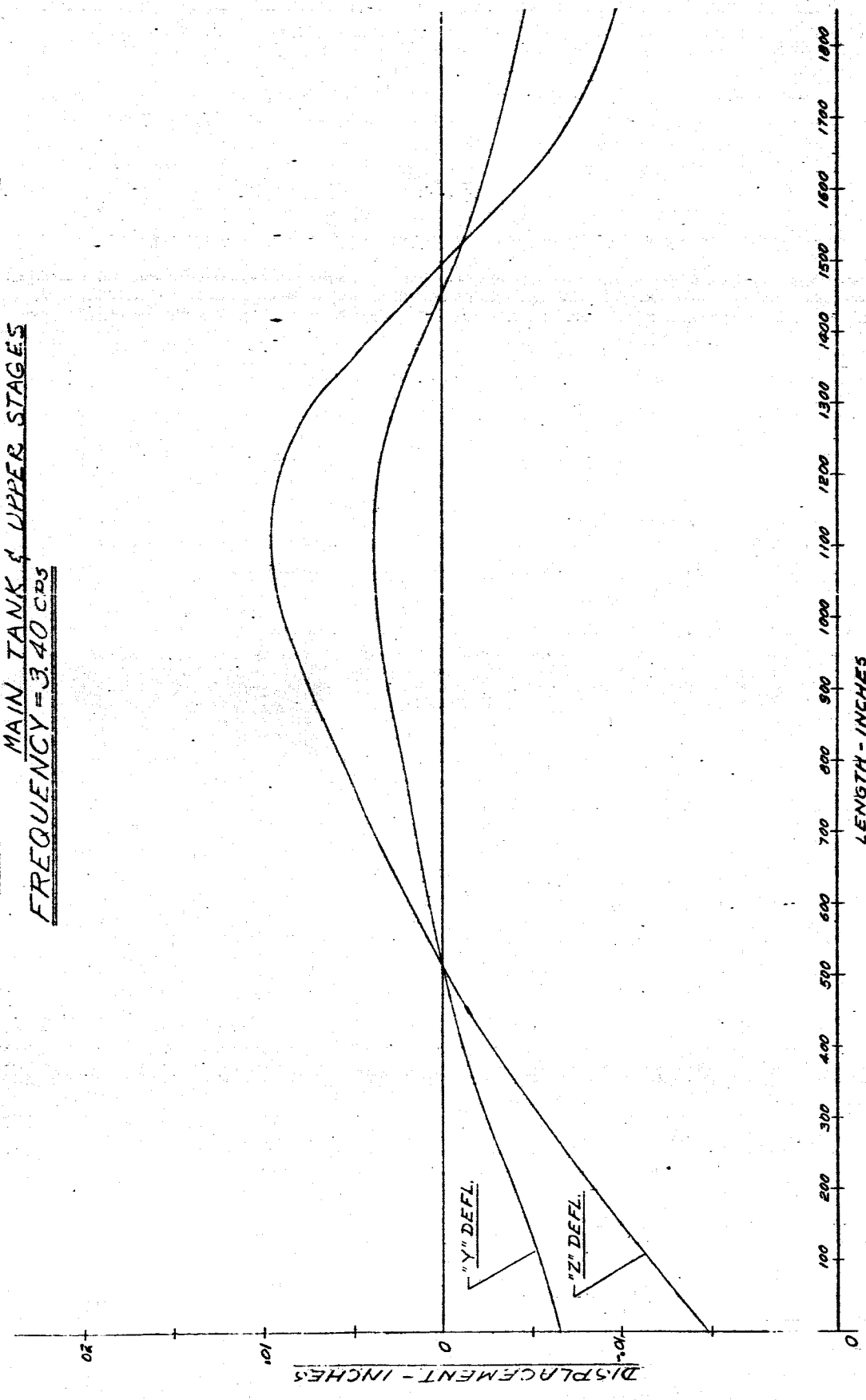


FIG. 119 DISPLACEMENT VS LENGTH SATURN SA-DI  
MAIN TANK & UPPER STAGES  
FREQUENCY = 3.40 CPS



-202-

FIG. 120 DISPLACEMENT VS LENGTH SATURN SA-DI  
FREQUENCY = 3.40 CPS

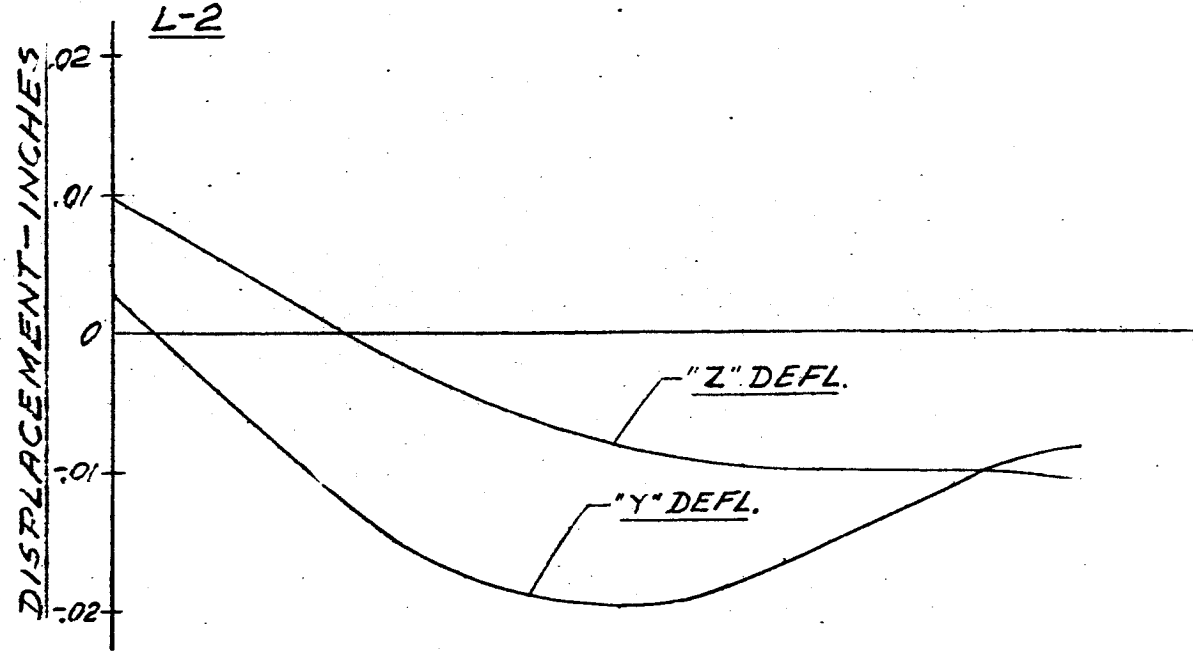
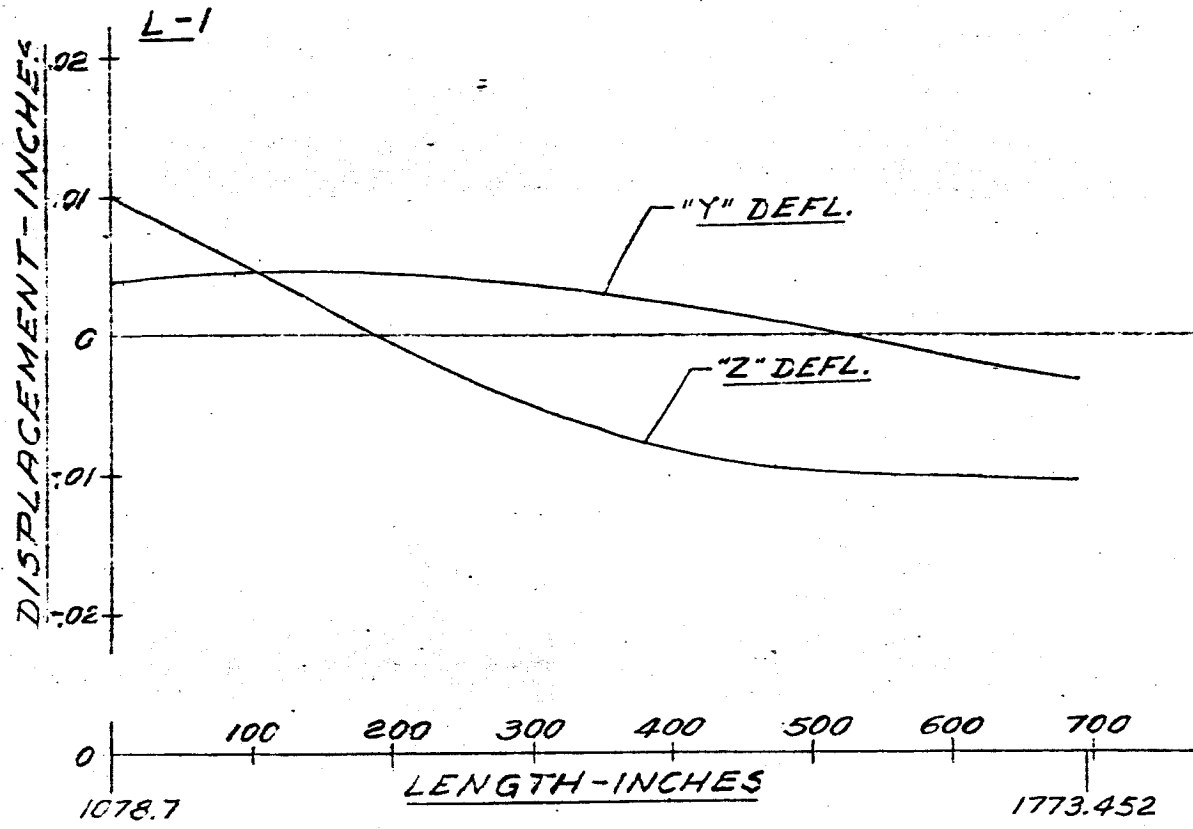


FIG. 121 DISPLACEMENT VS LENGTH SATURN SA -D1  
FREQUENCY = 3.40 CPS

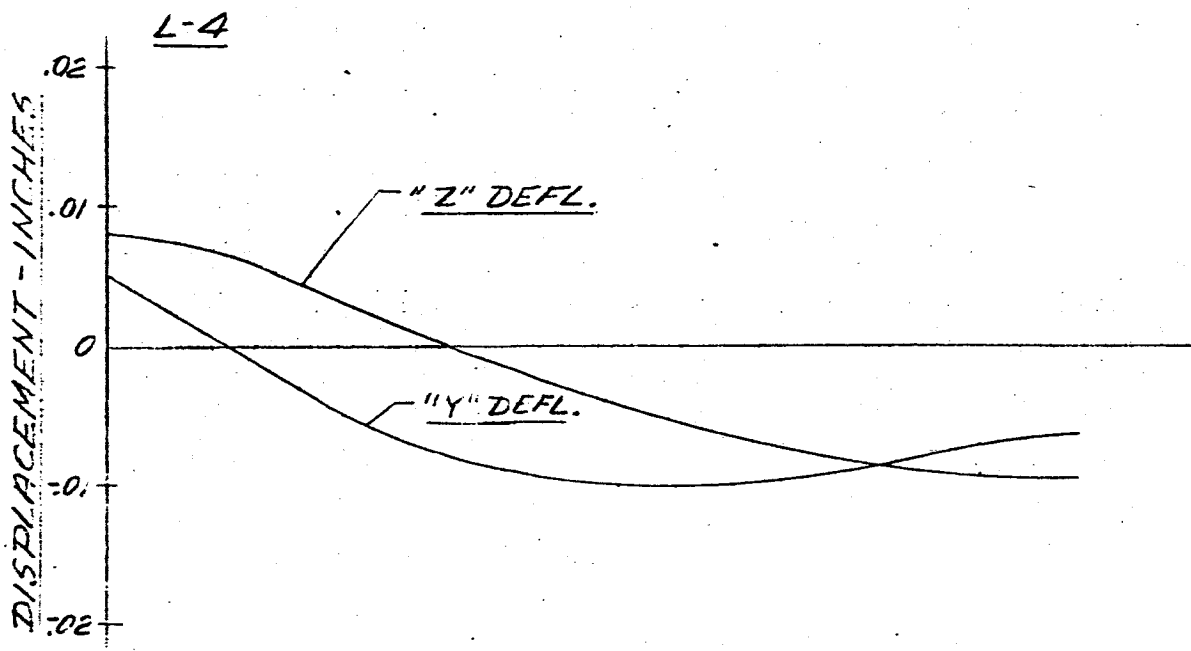
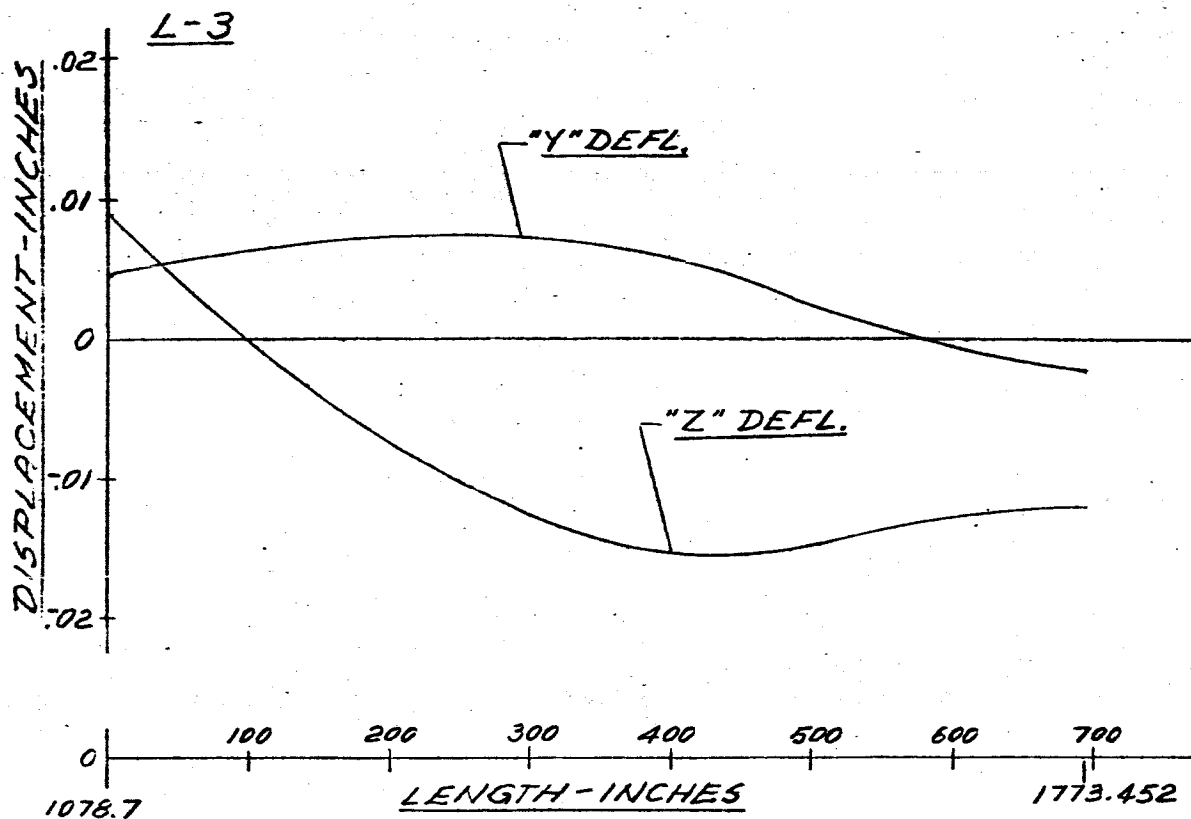
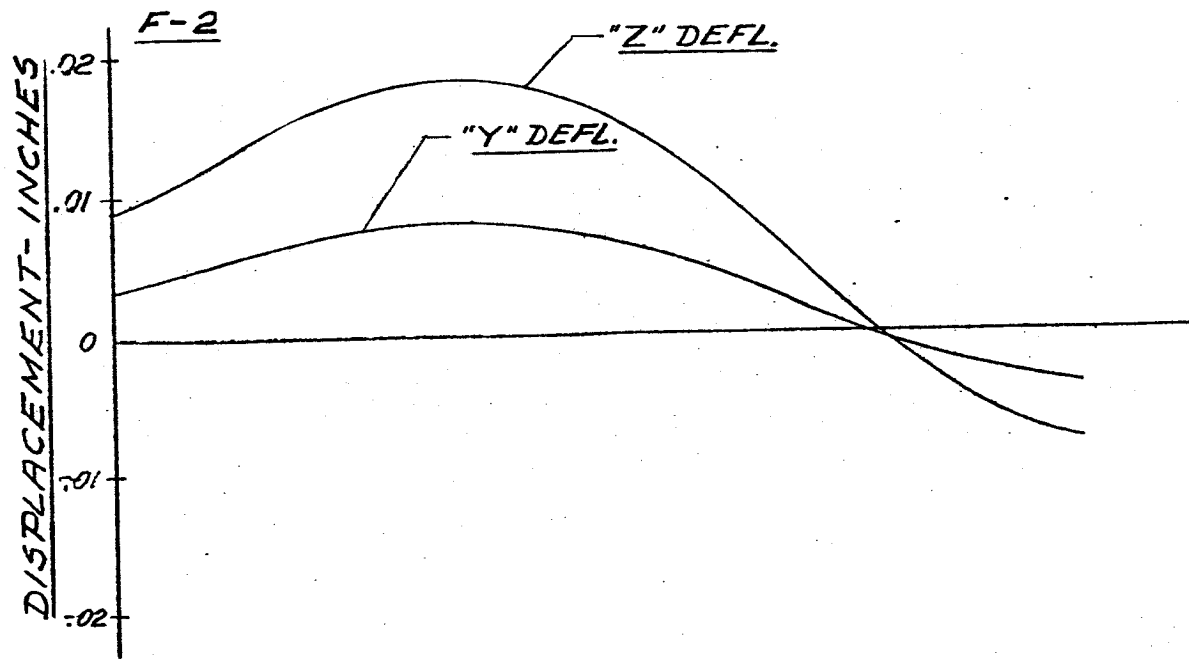
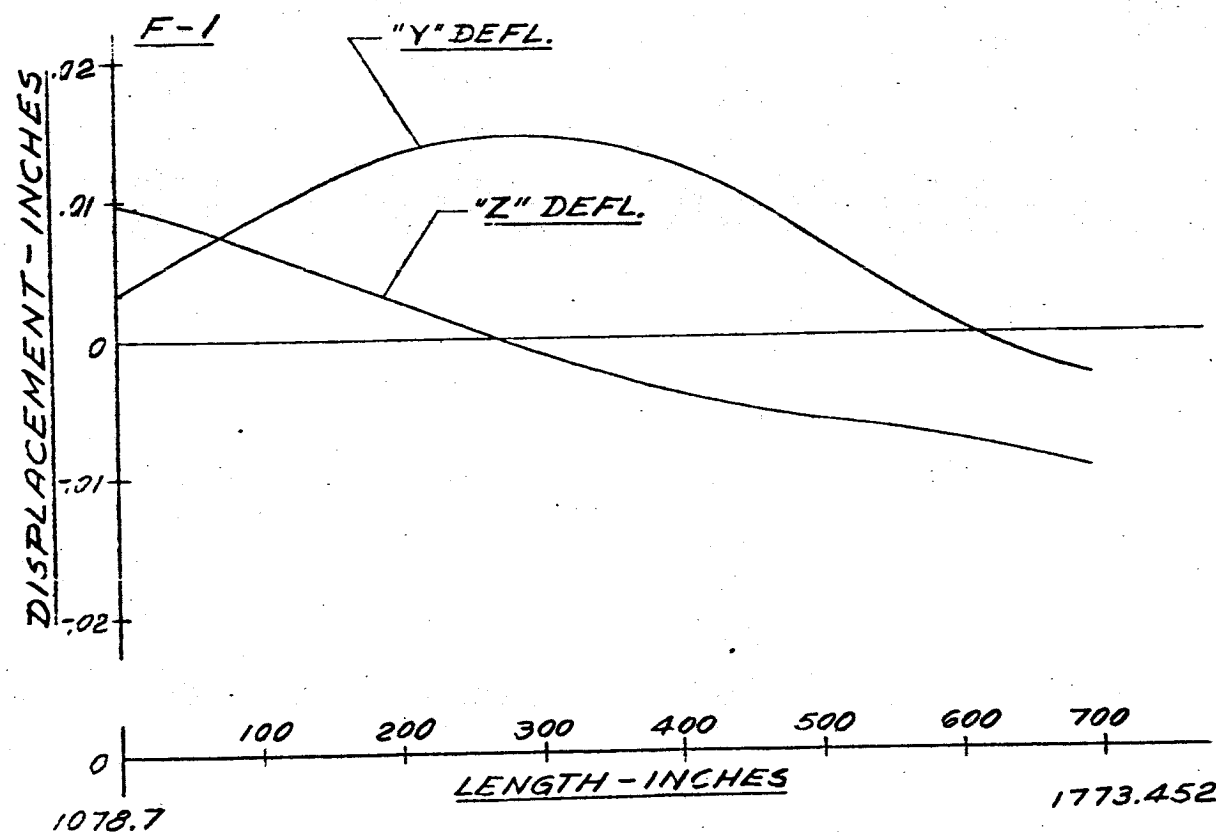


FIG. 122 DISPLACEMENT VS LENGTH SATURIS SA  
FREQUENCY = 3.40 CPS



-205-

FIG. 123 DISPLACEMENT VS LENGTH SATURN SA-01  
FREQUENCY = 3.40 CPS

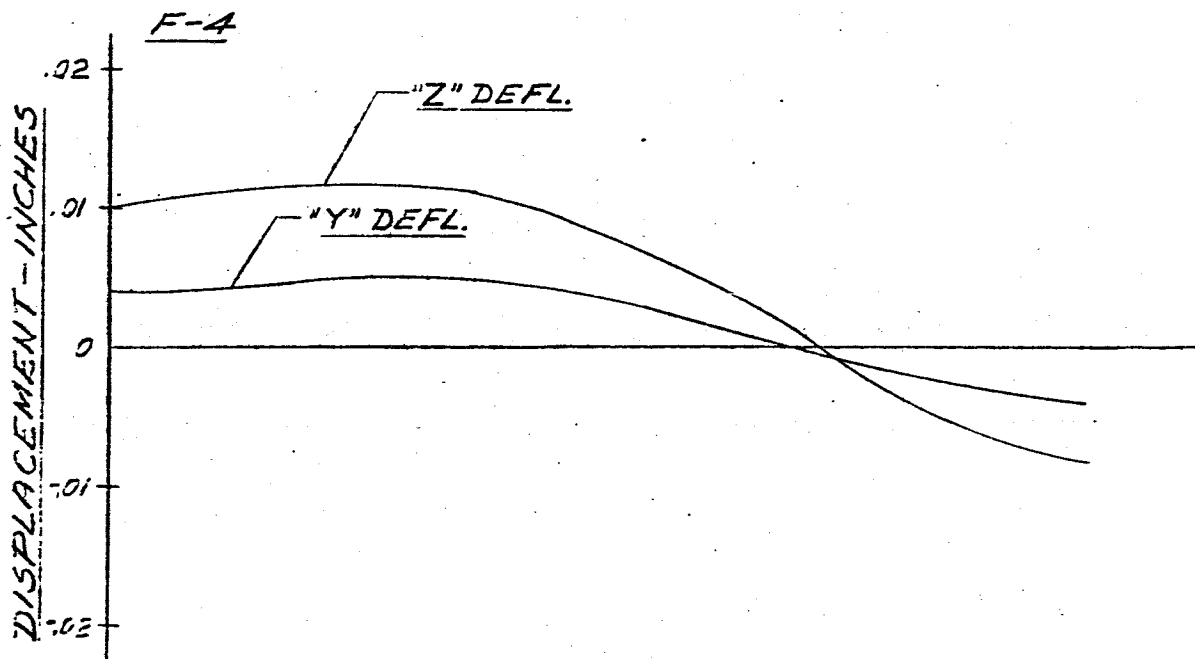
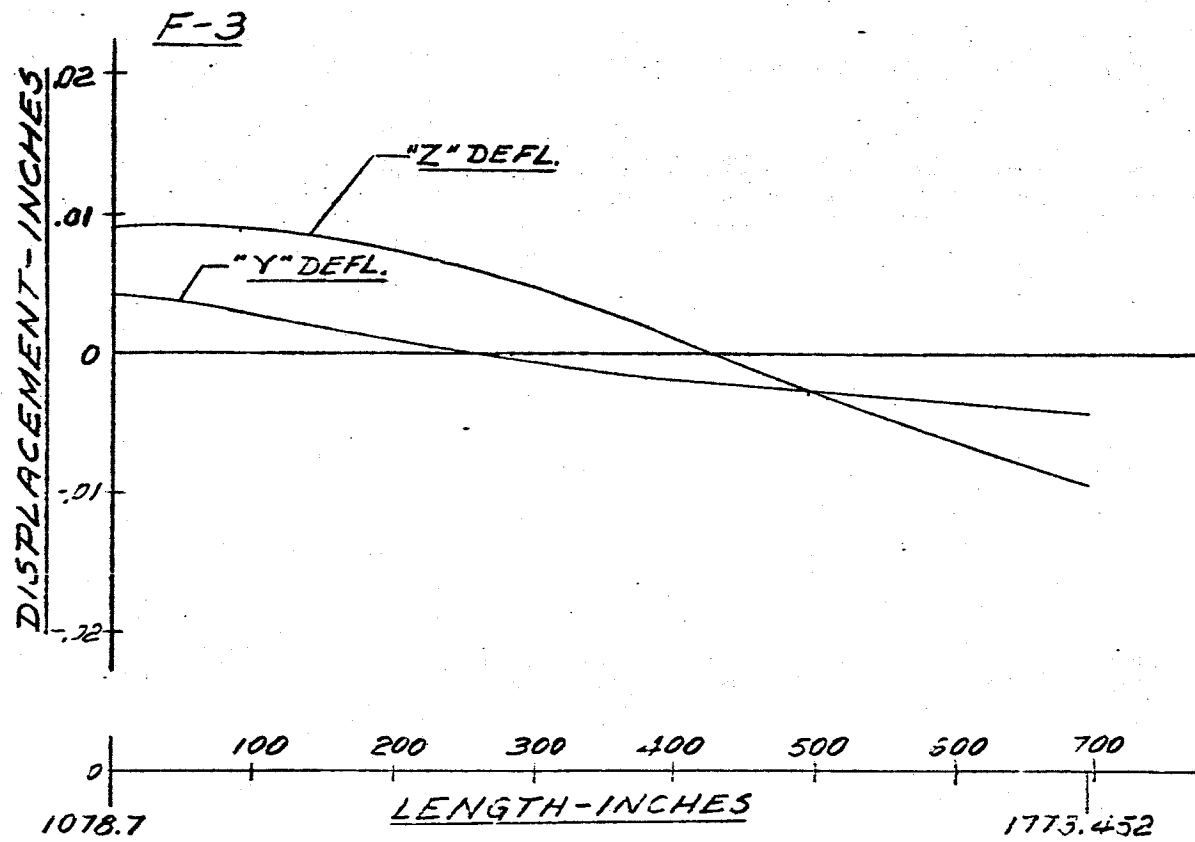
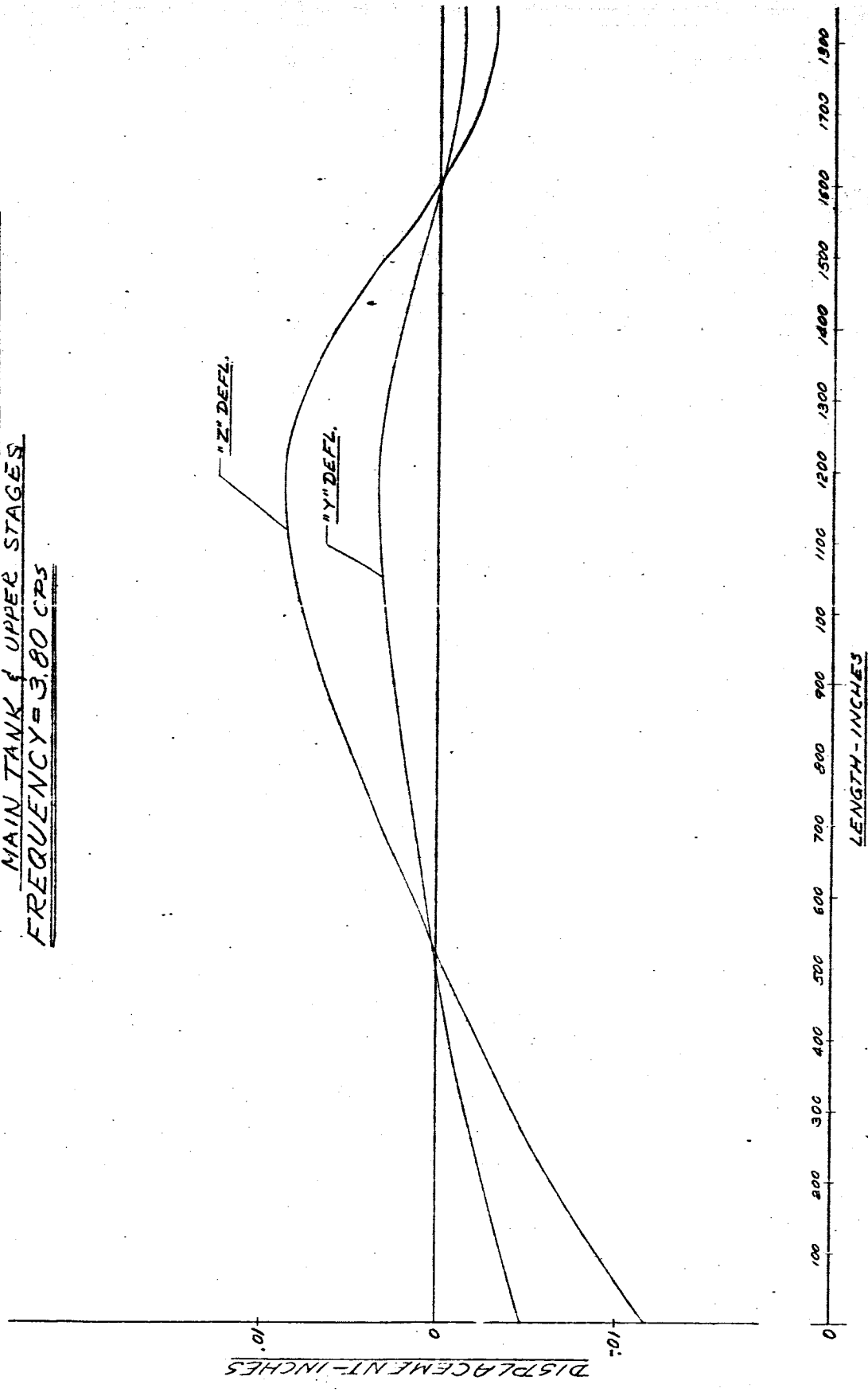
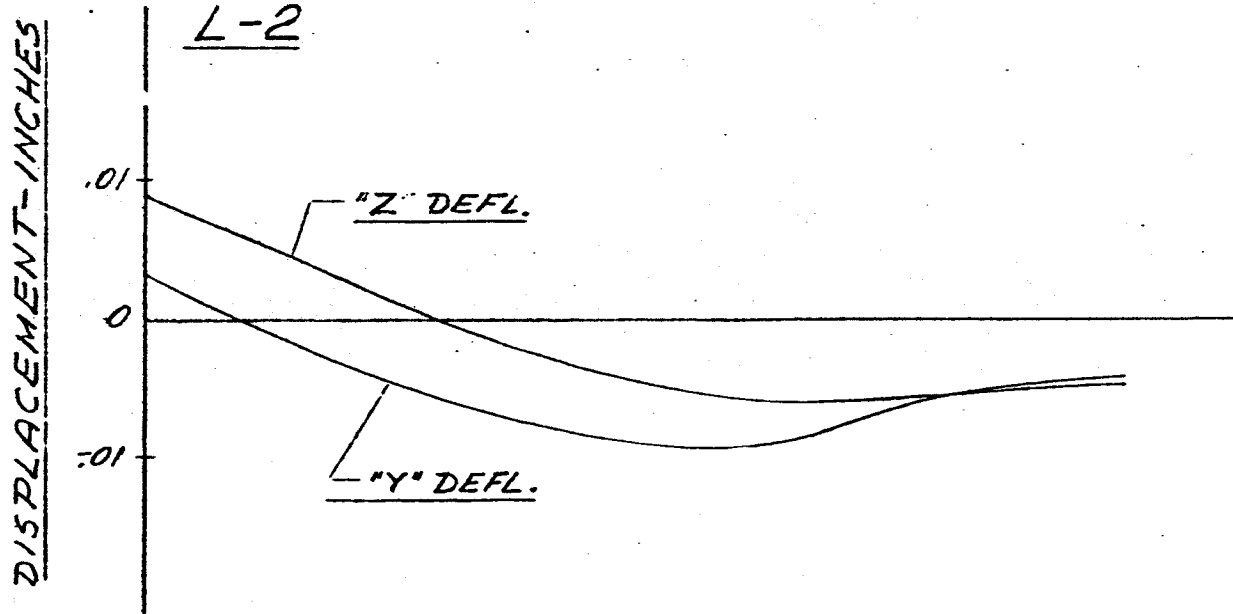
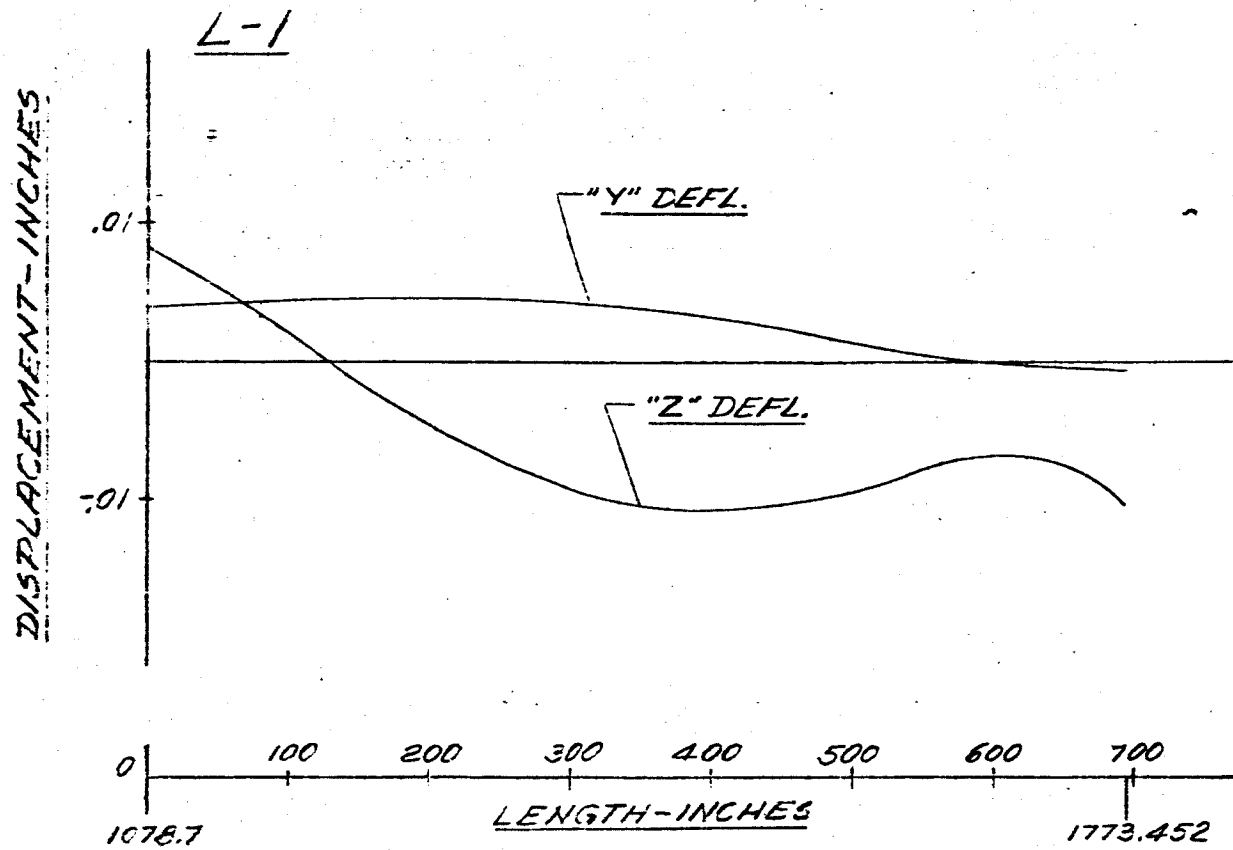


FIG. 12.4 DISPLACEMENT vs LENGTH SATURN SA-DI  
MAIN TANK & UPPER STAGES  
FREQUENCY = 3.80 CPS



-207-

FIG. 125 DISPLACEMENT vs LENGTH SATURN SA-DI  
FREQUENCY = 3.80 CPS



-208-

FIG. 126 DISPLACEMENT vs LENGTH SATURN SA-DI  
FREQUENCY = 3.80 CPS

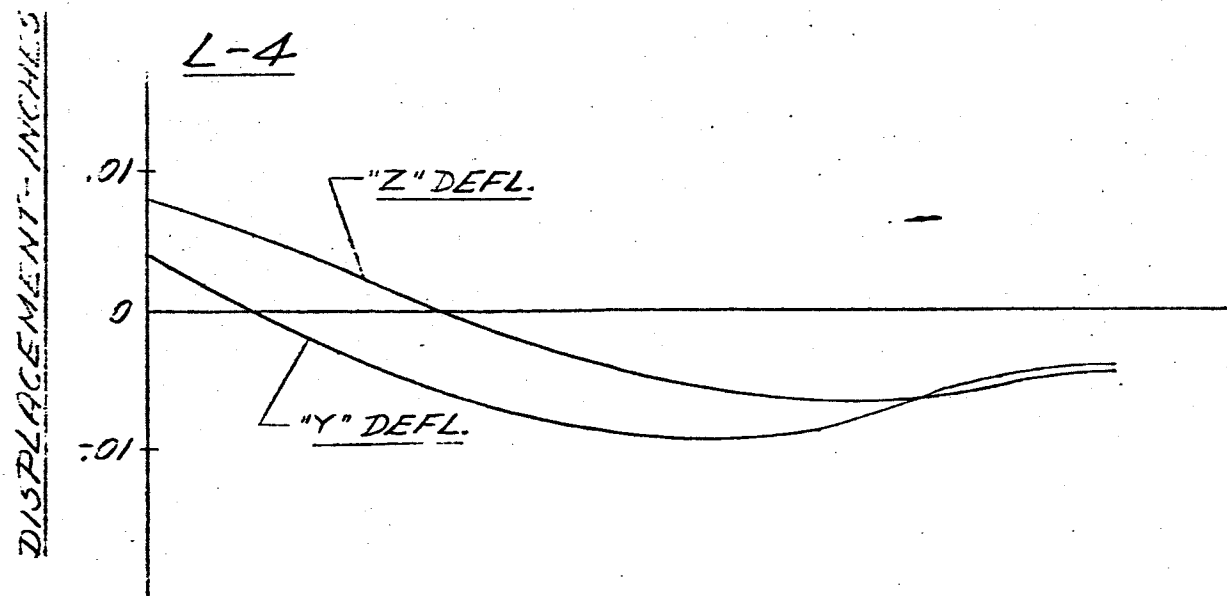
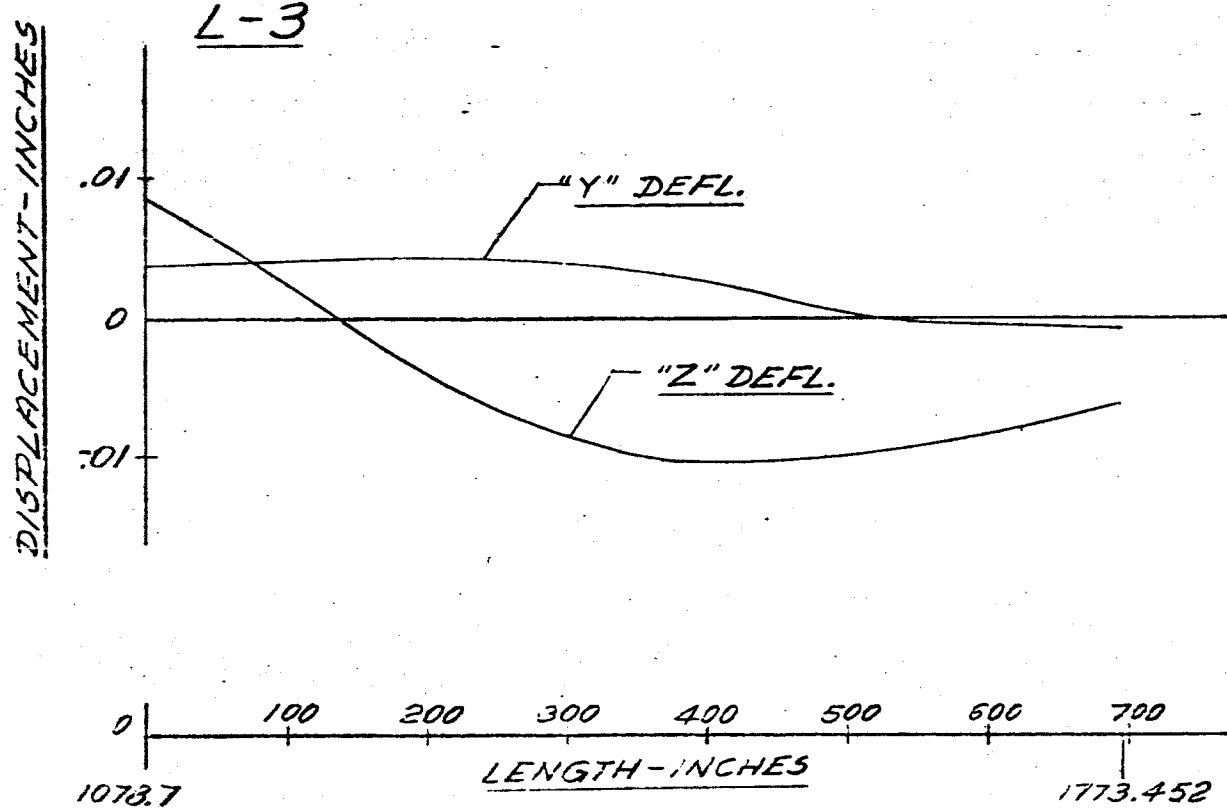
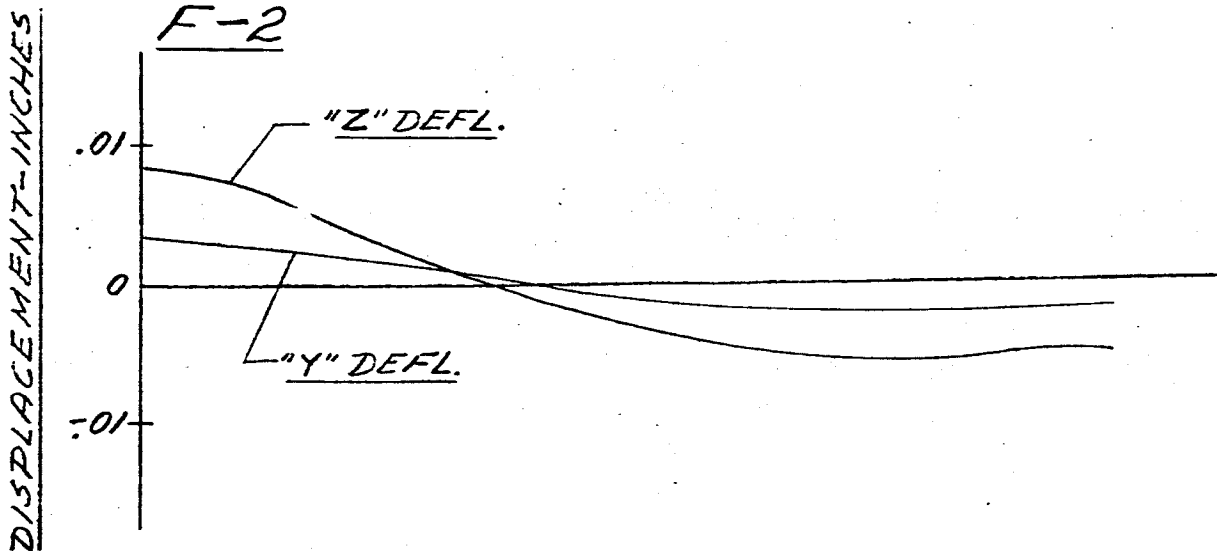
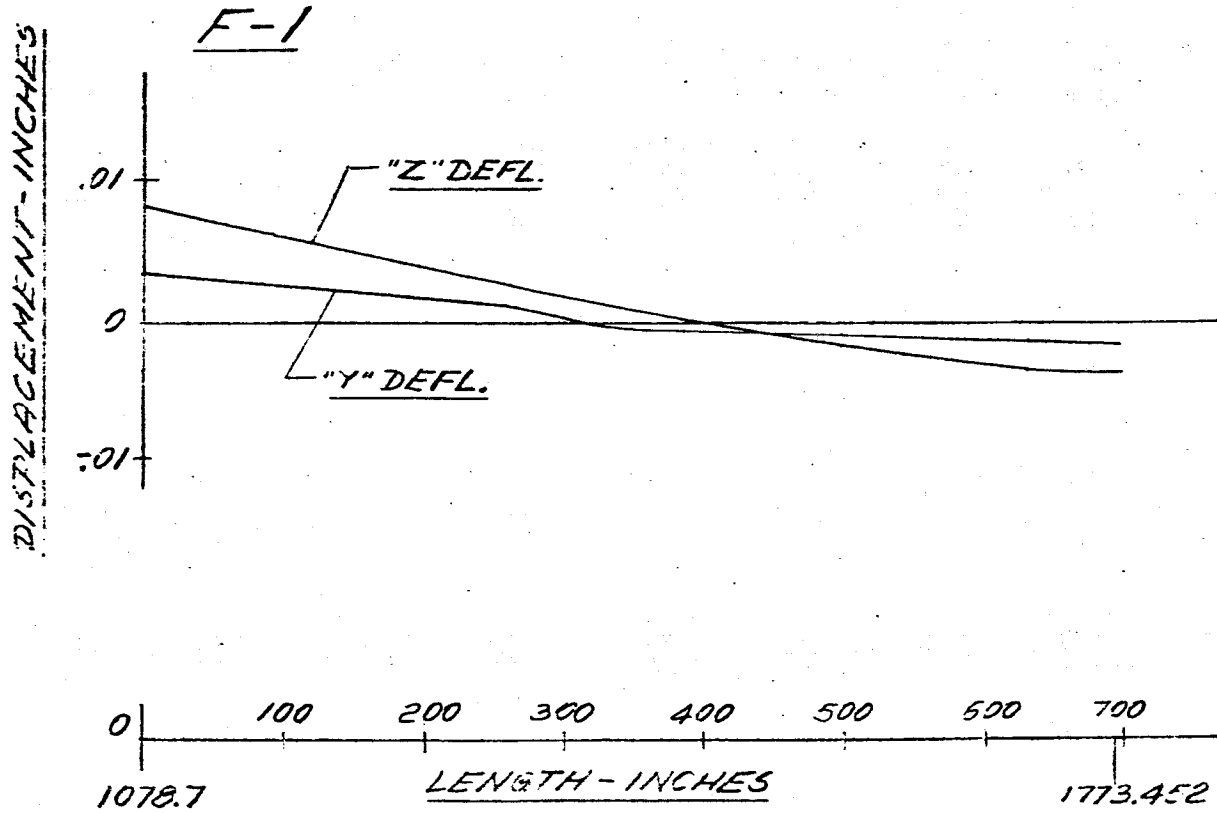


FIG. 127 DISPLACEMENT VS LENGTH SATURN SA-D1

FREQUENCY = 3.80 CPS



-210-

FIG. 12B DISPLACEMENT VS LENGTH SATURN SA-01

FREQUENCY = 3.80 CPS

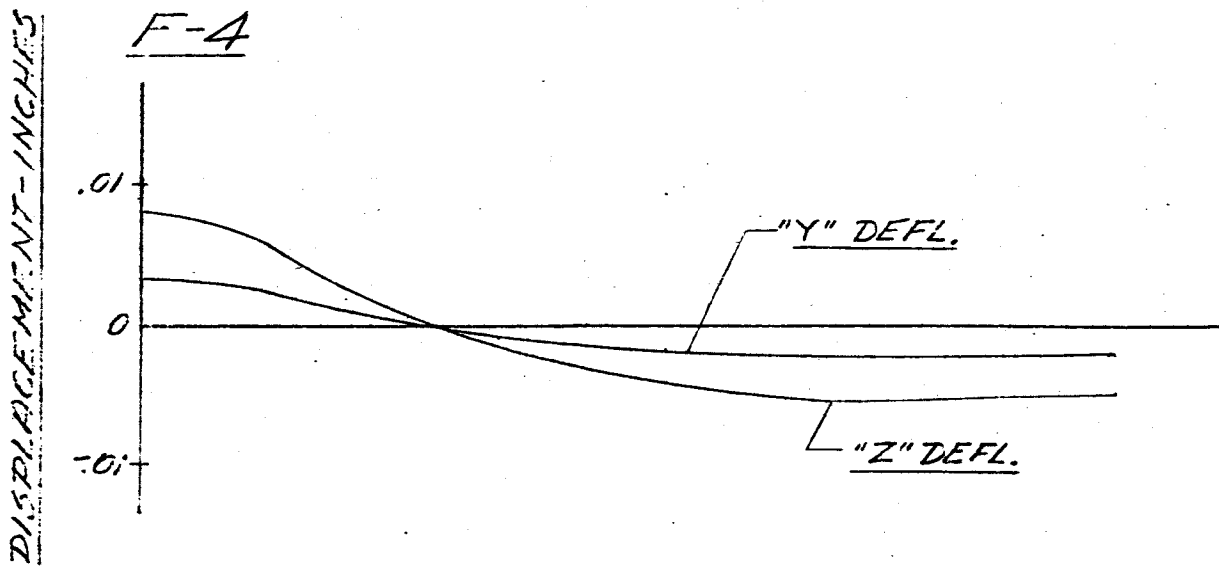
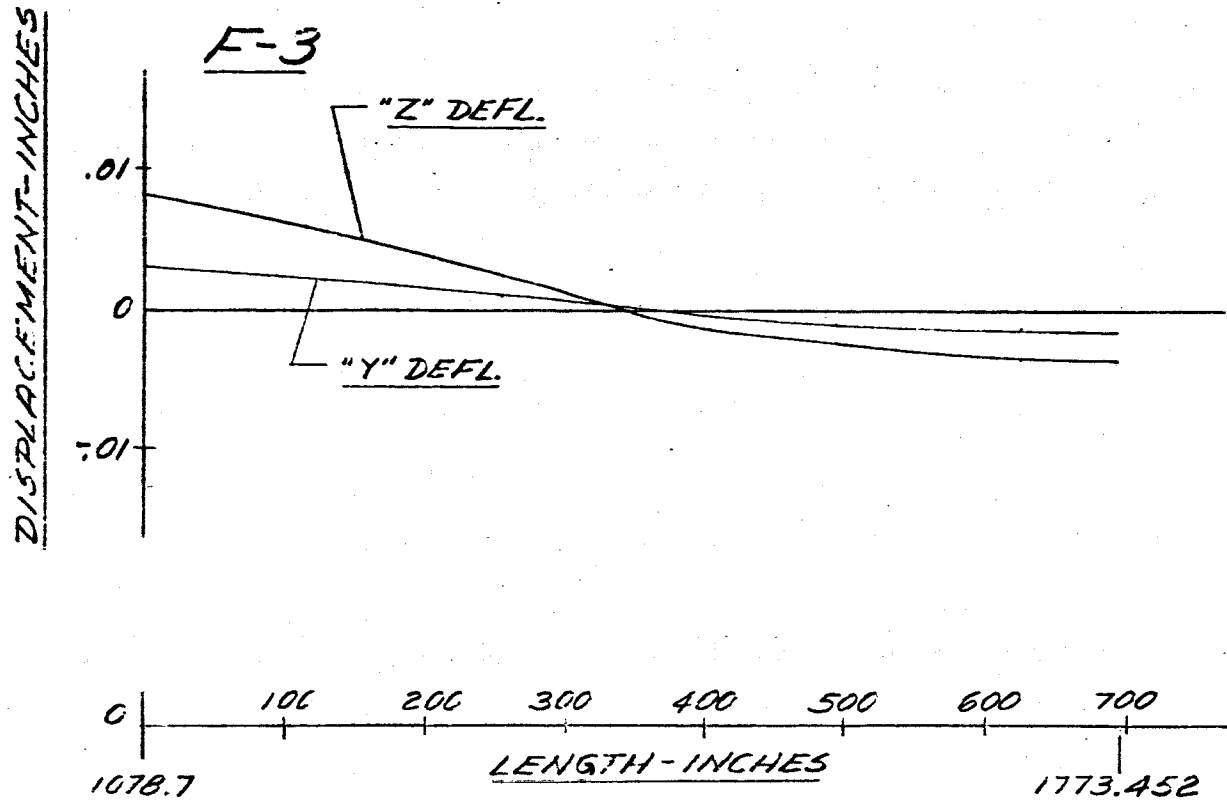
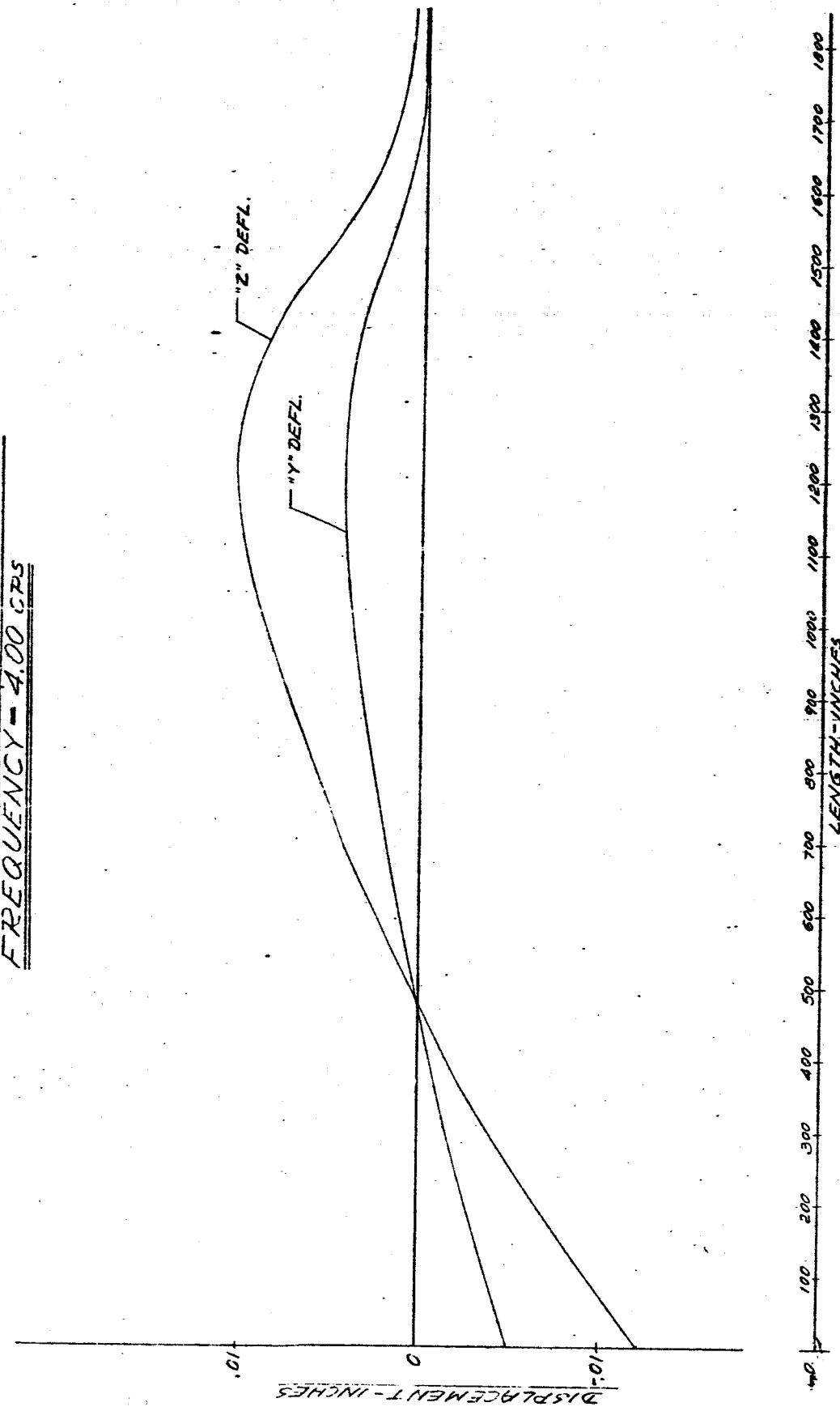


FIG. 129 DISPLACEMENT VS LENGTH SATURN SA-01  
MAIN TANK & UPPER STAGES  
FREQUENCY - 4.00 CPS

- 211 -



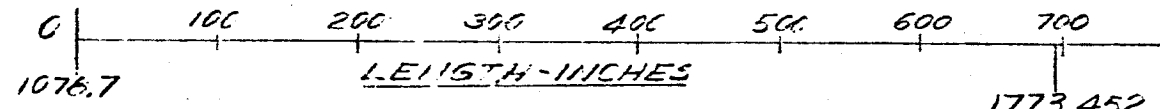
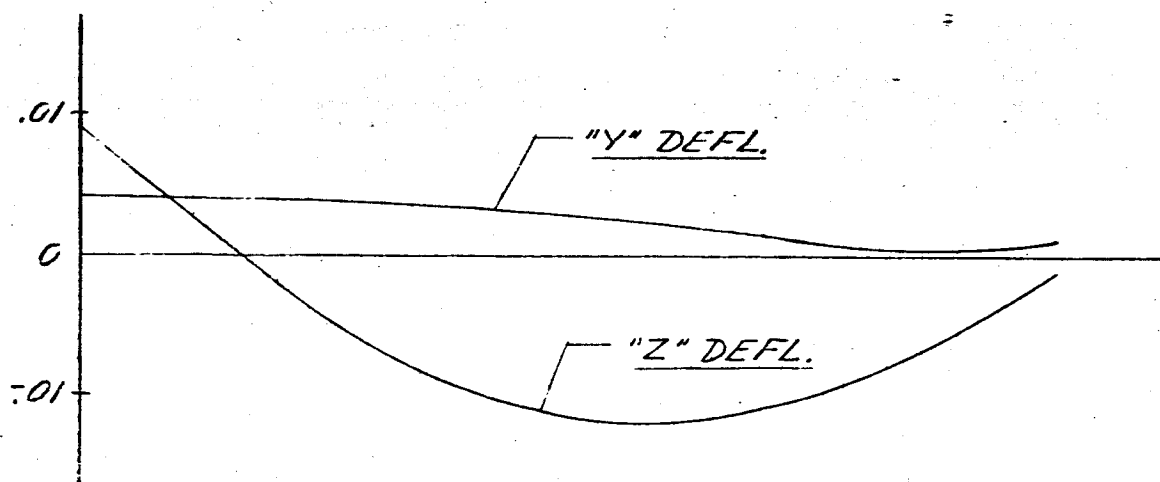
-212-

FIG. 130 DISPLACEMENT VS LENGTH SATURN SA-D1

FREQUENCY = 4.00 CPS

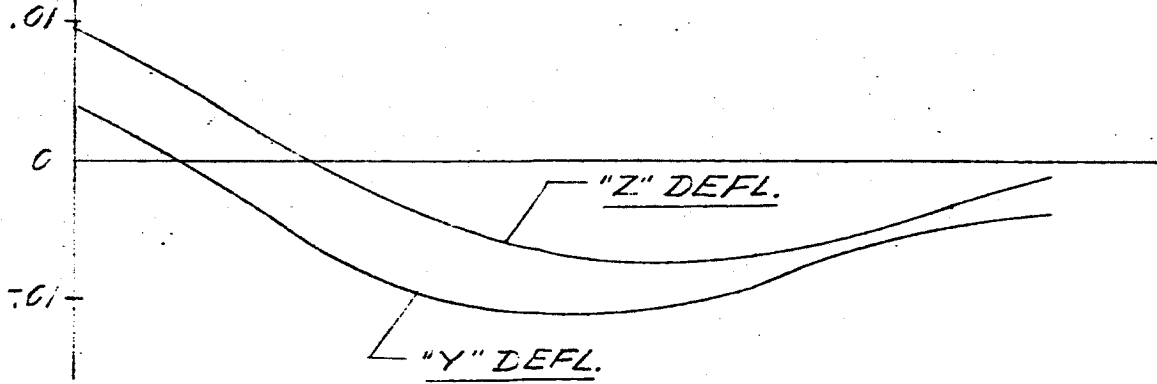
DISPLACEMENT - INCHES

L-1



DISPLACEMENT - INCHES

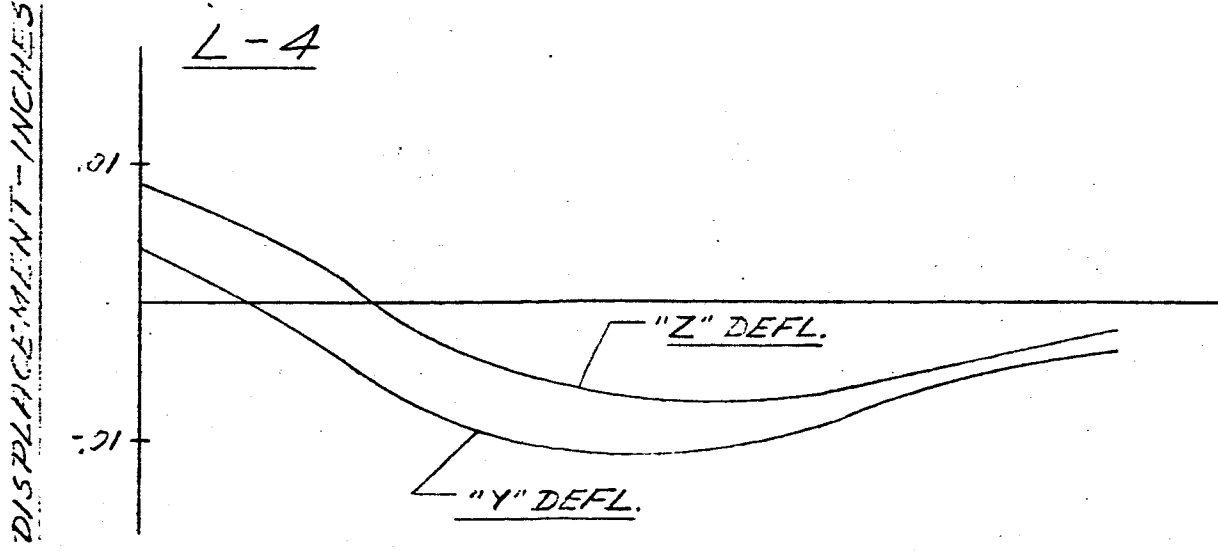
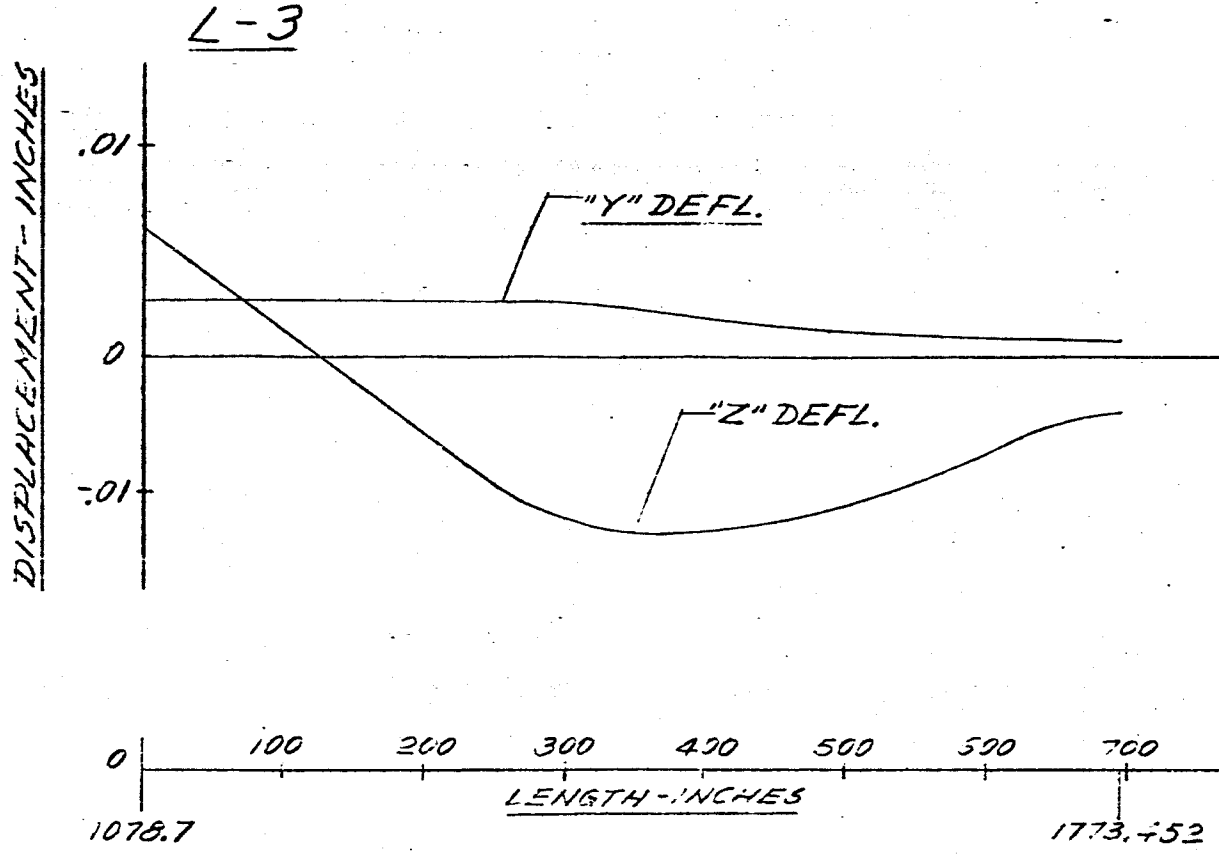
L-2



-213-

FIG. 131 DISPLACEMENT vs LENGTH SATURN SA-DI

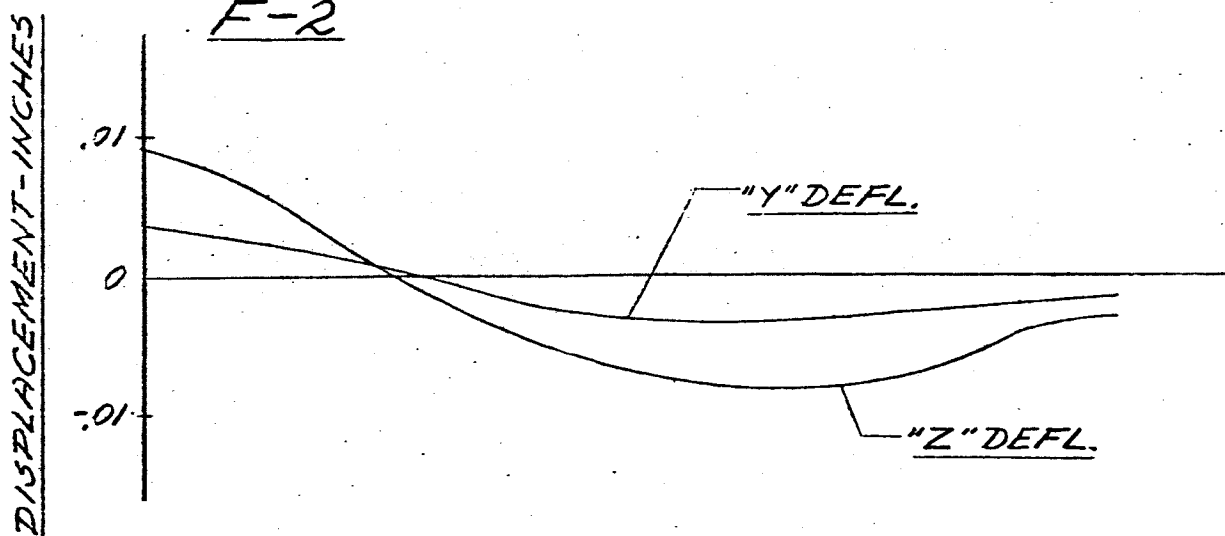
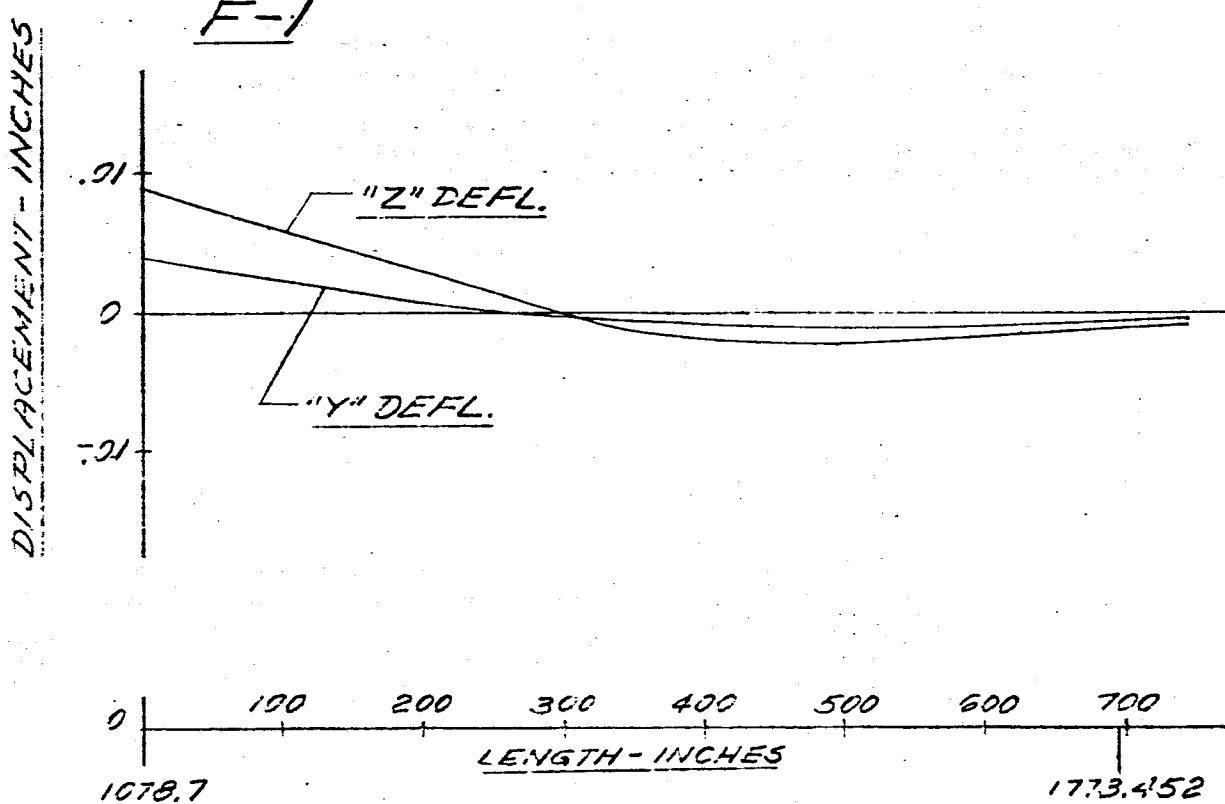
FREQUENCY = 4.00 CPS



-214-

FIG. 132 DISPLACEMENT VS LENGTH SATURN SA-D1

FREQUENCY = 4.70 CPS



-215-

FIG. 133 DISPLACEMENT VS LENGTH SATURN SA-DI

FREQUENCY = 4.00 CPS

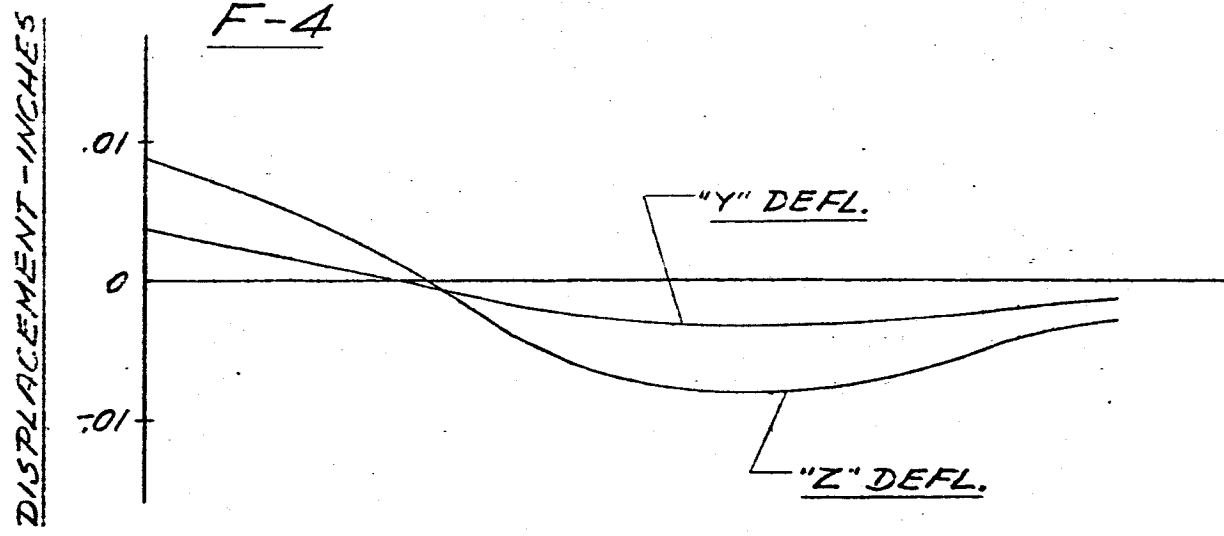
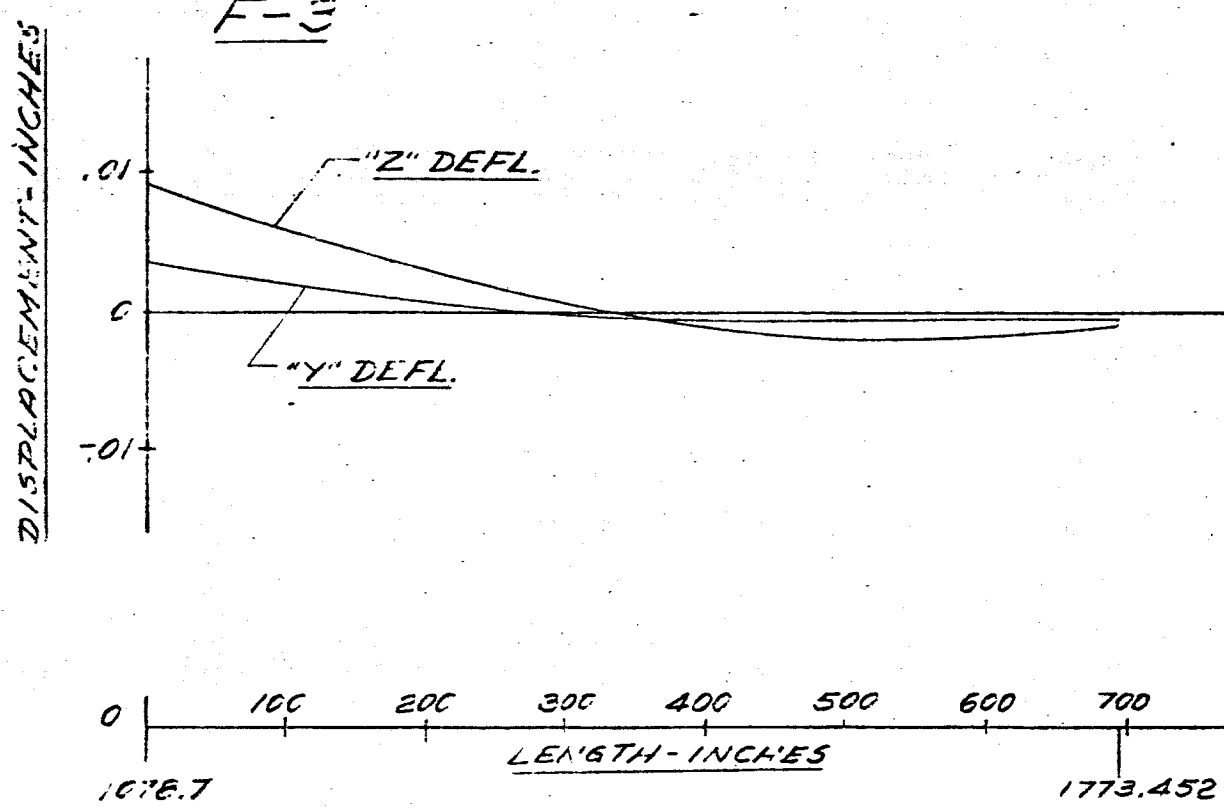
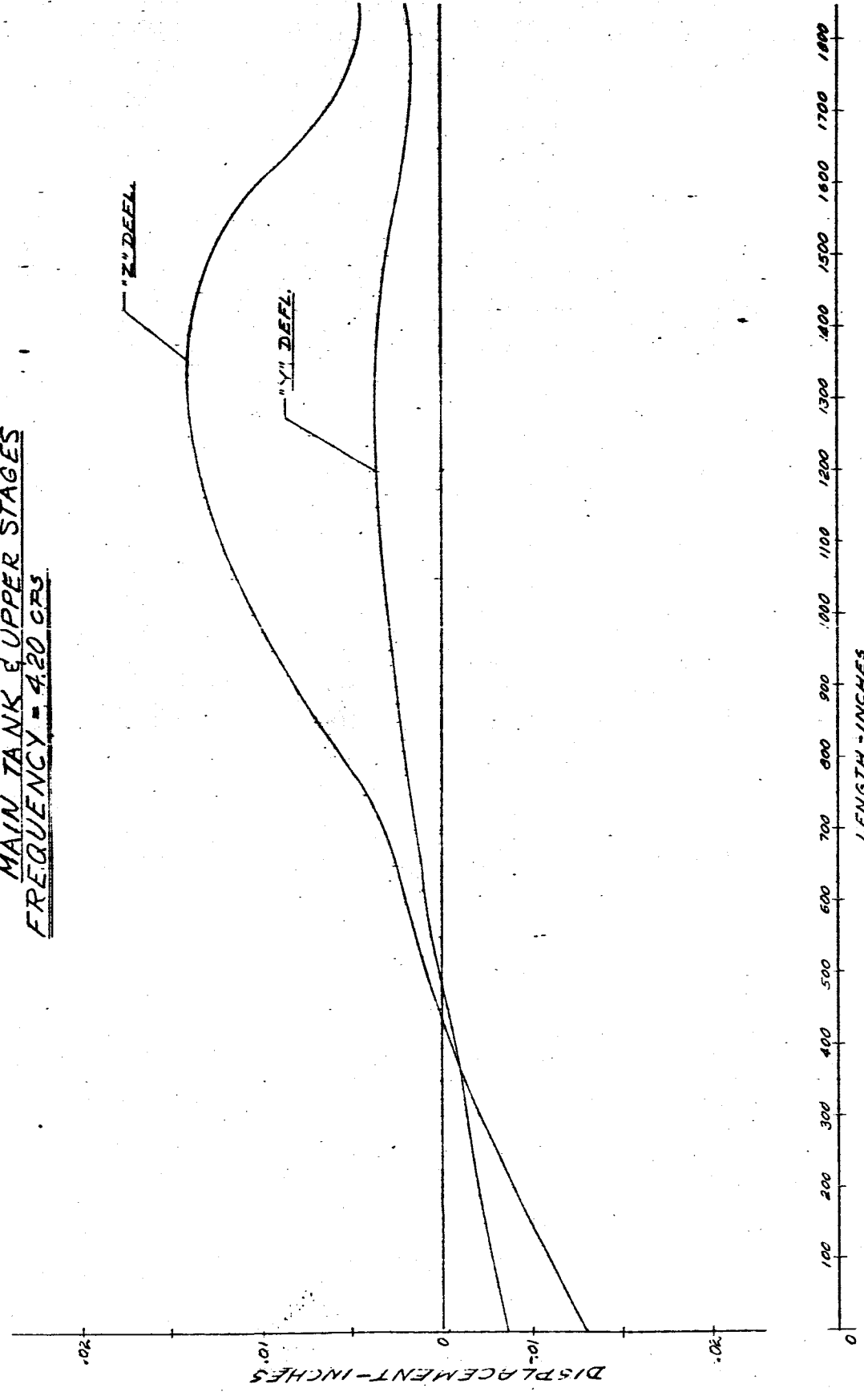


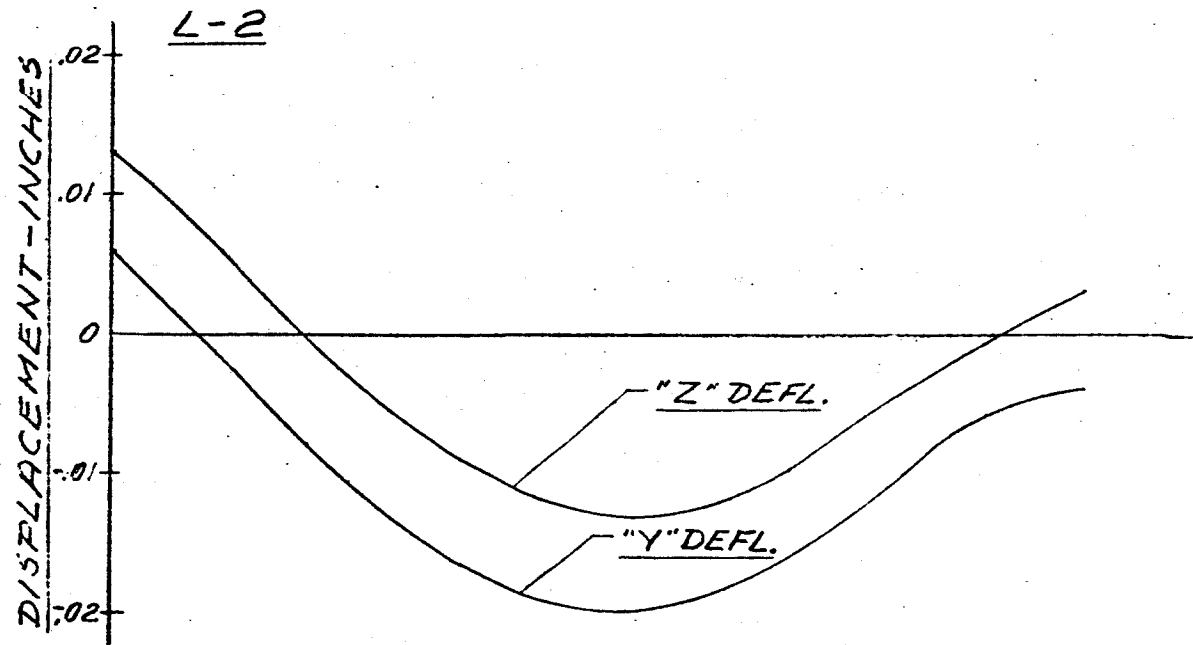
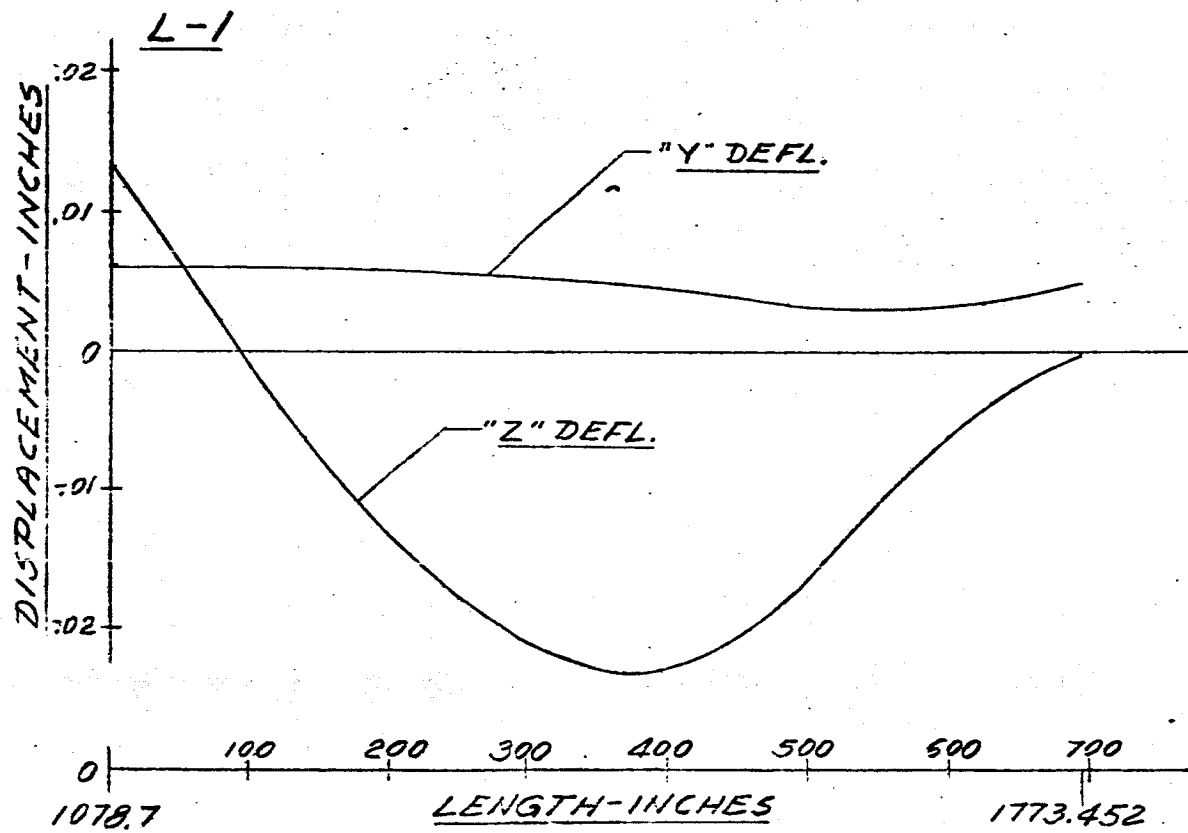
FIG. 134 DISPLACEMENT vs LENGTH SATURN SA-D  
MAIN TANK & UPPER STAGES  
FREQUENCY = 4.20 CPS



-217-

FIG. 135 DISPLACEMENT VS LENGTH SATURN SA-DI

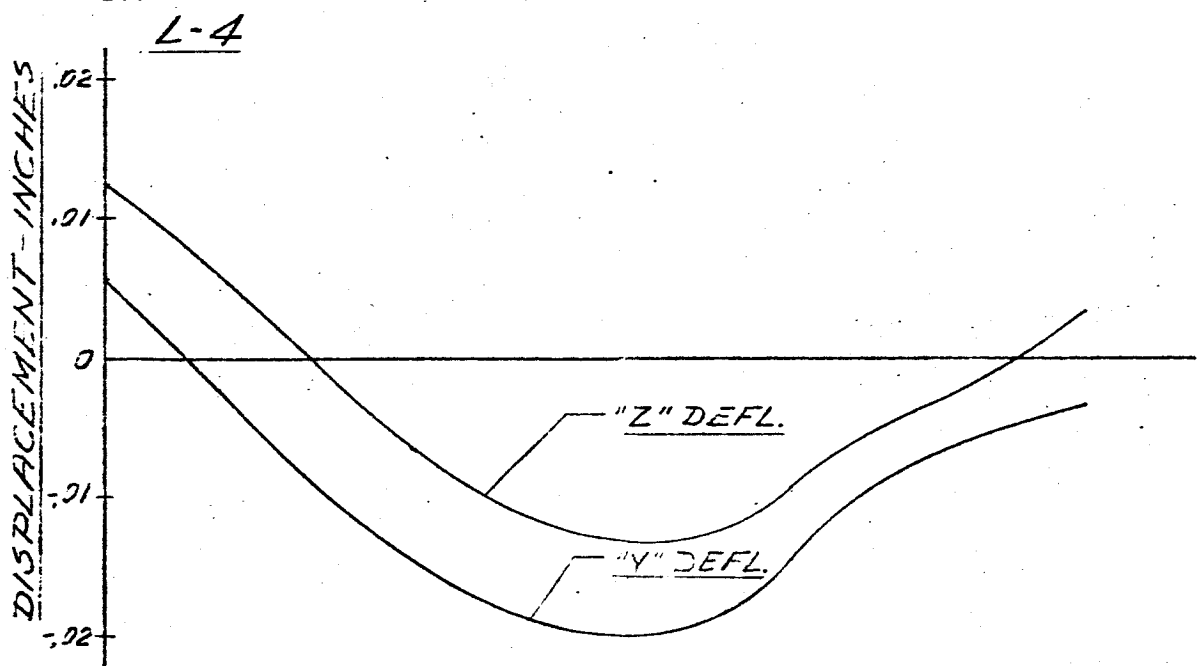
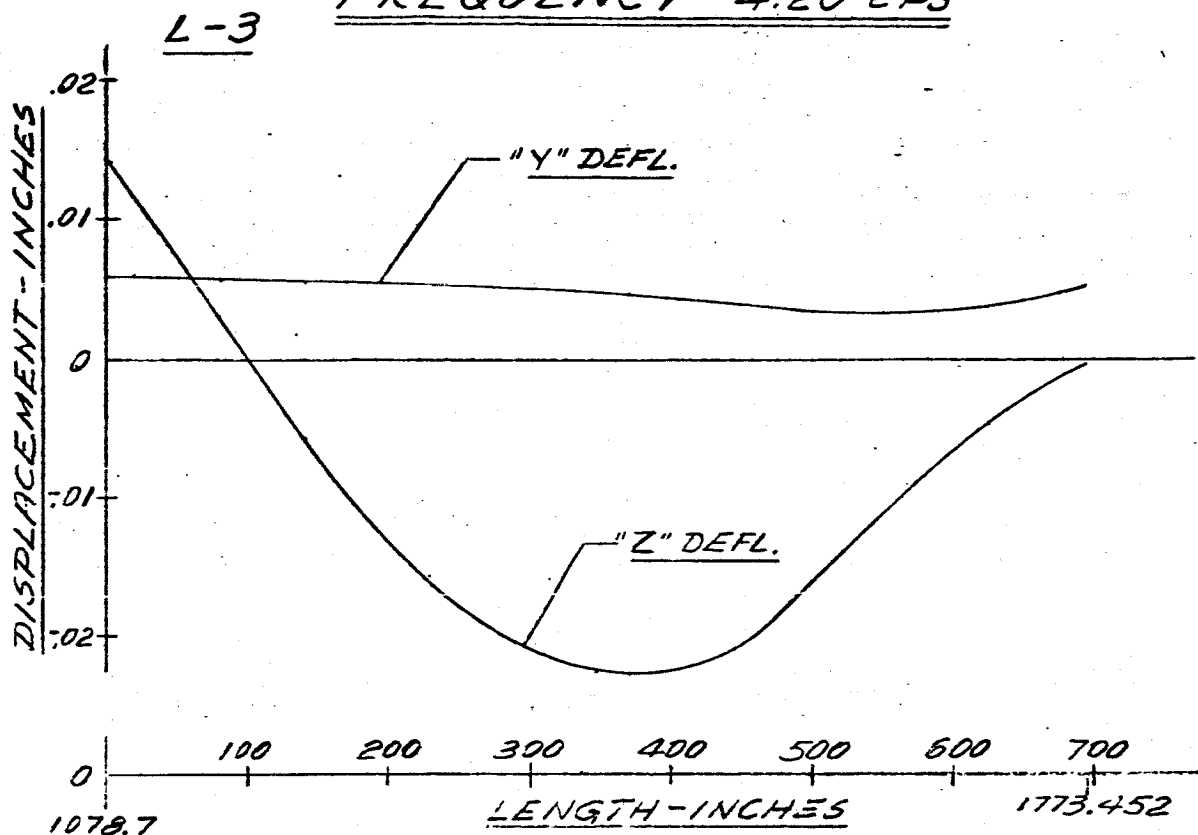
FREQUENCY = 4.20 CPS



-218-

FIG. 136 DISPLACEMENT vs LENGTH SATURN SA-DI

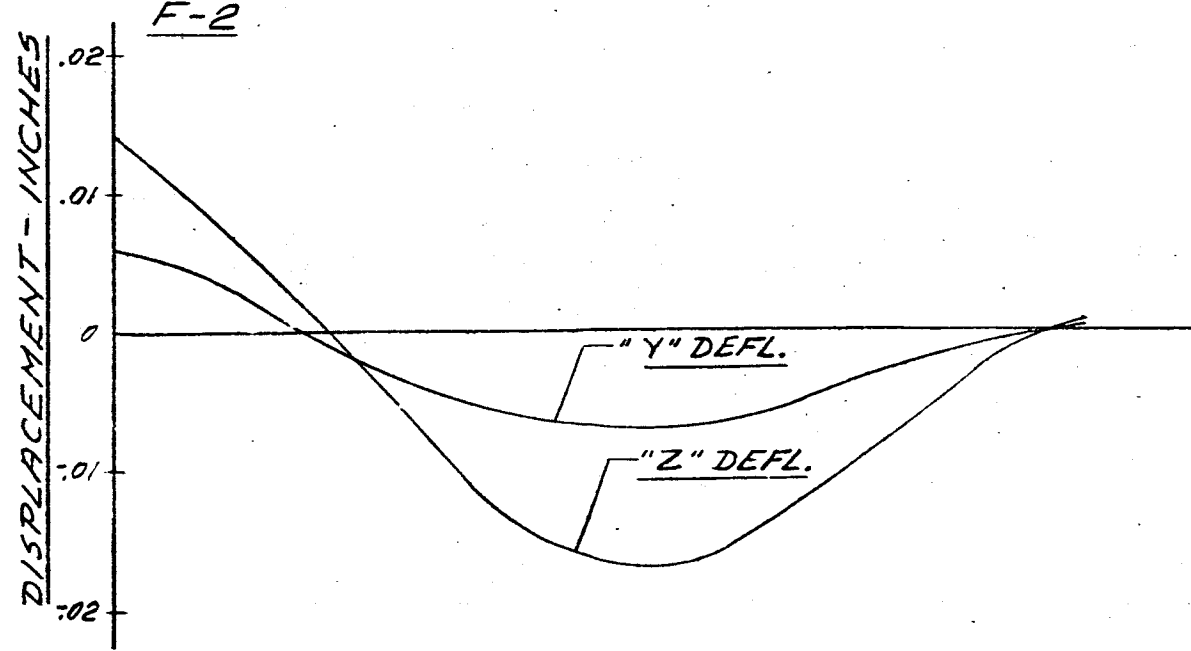
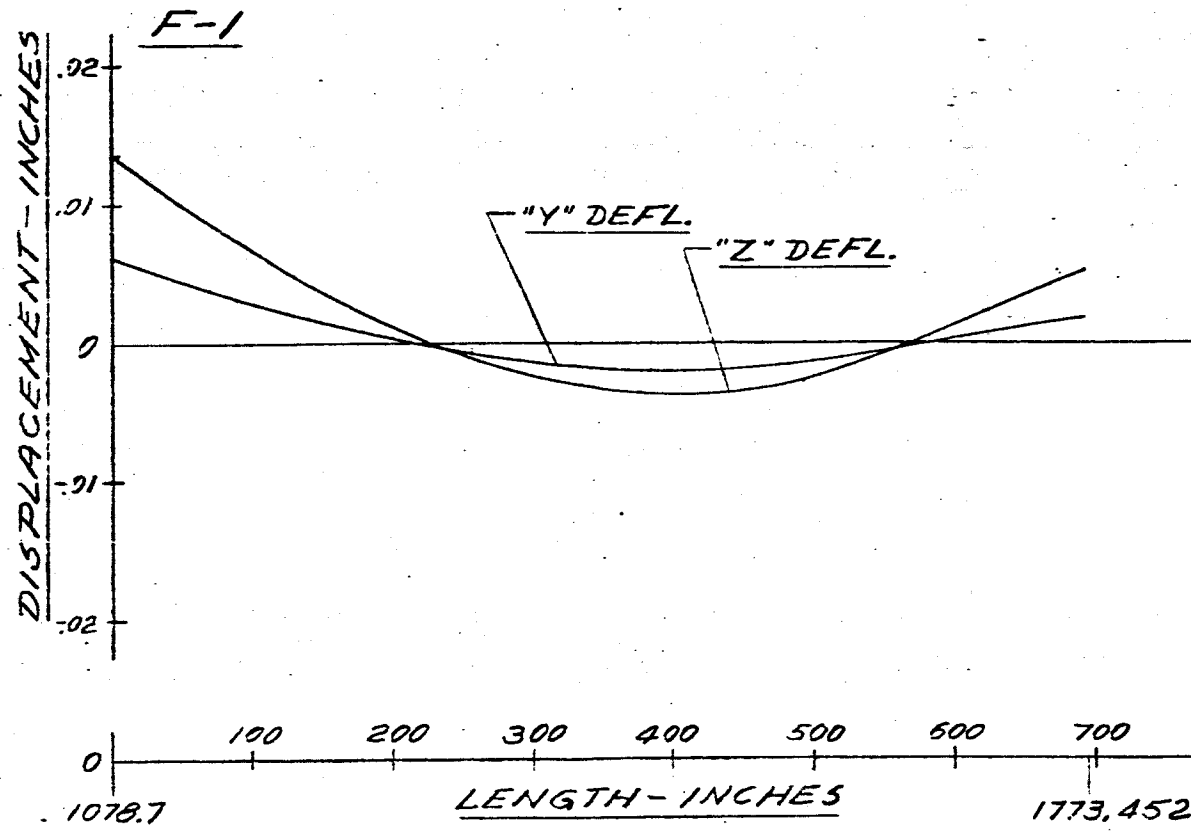
FREQUENCY = 4.20 CPS



-219-

FIG. 137 DISPLACEMENT VS LENGTH SATURN SA-61

FREQUENCY = 4.20 CPS



-220-

FIG. 13B DISPLACEMENT vs LENGTH SATURN SA-DI

FREQUENCY = 4.20 CPS

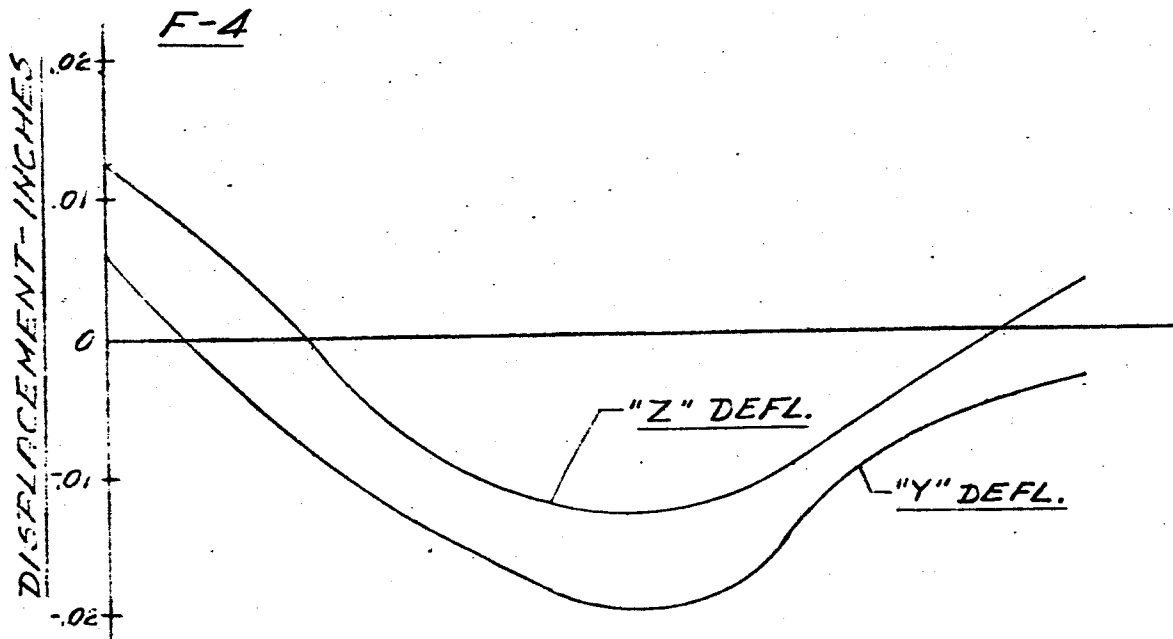
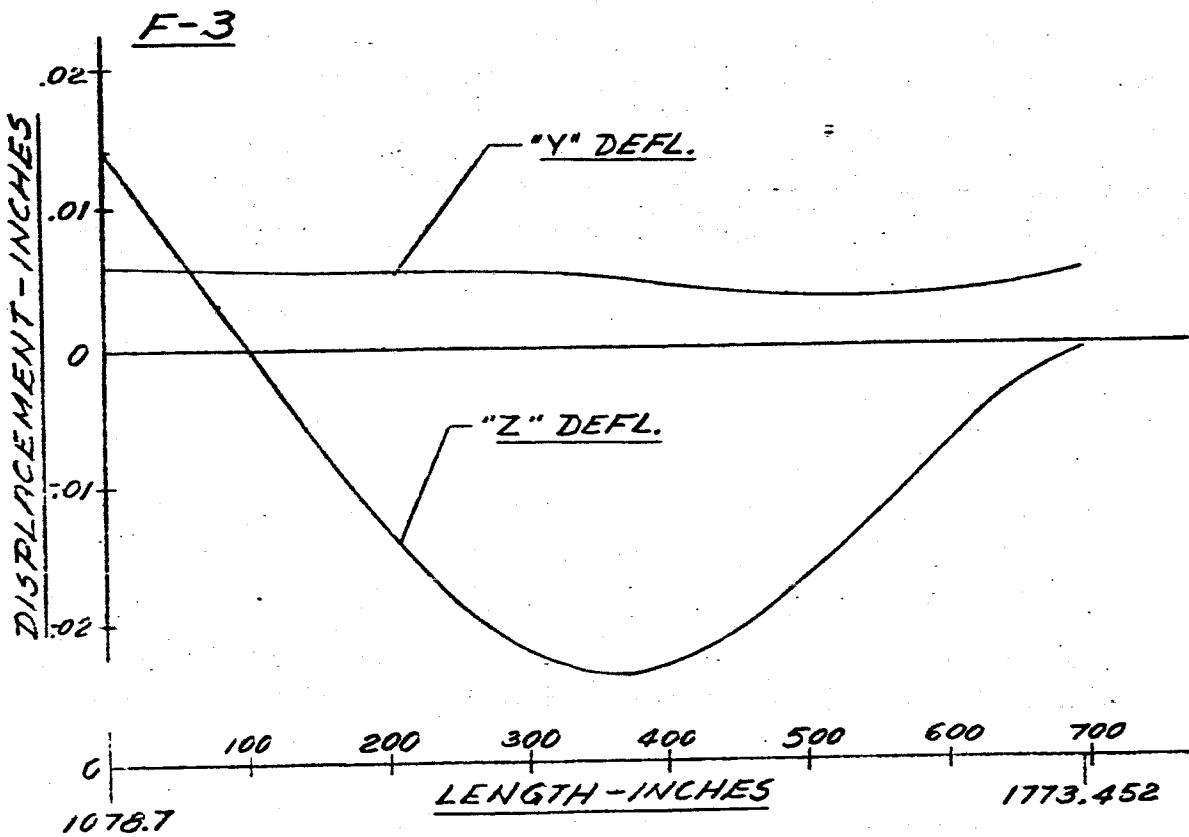
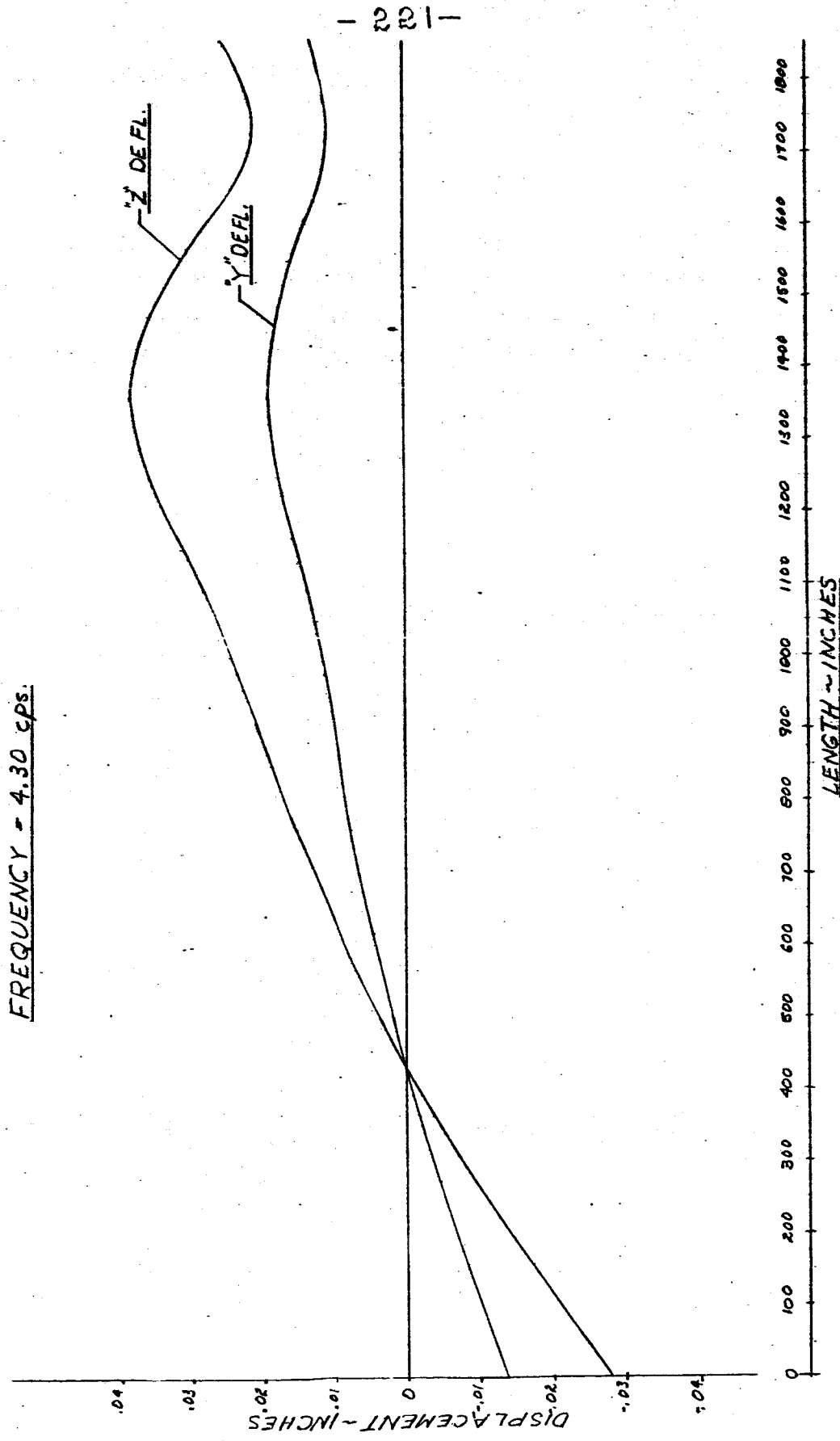


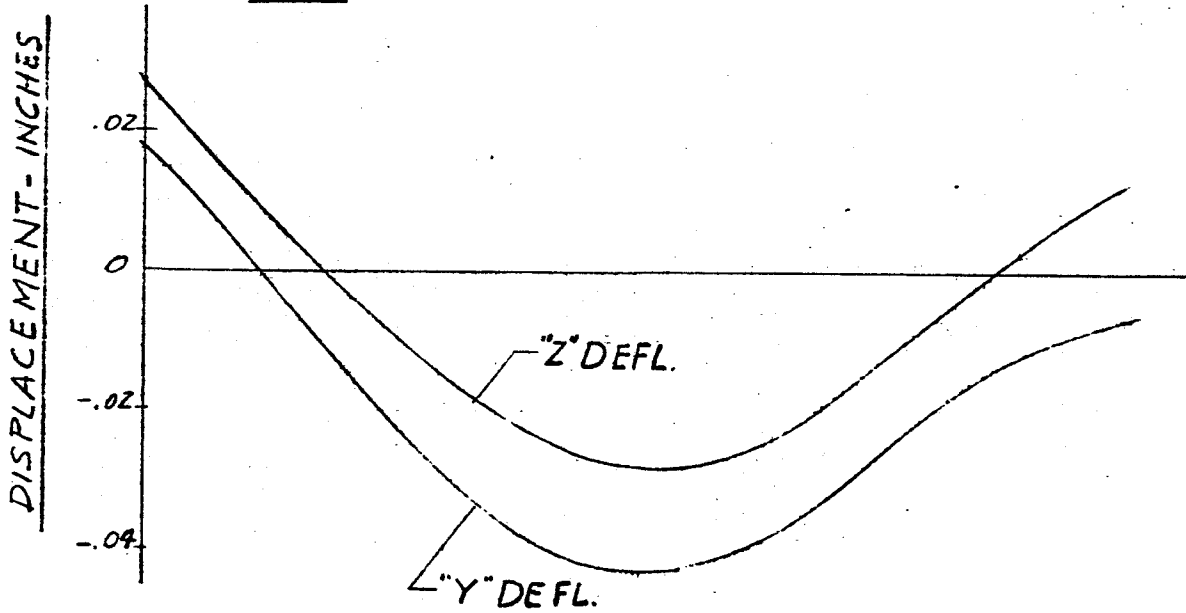
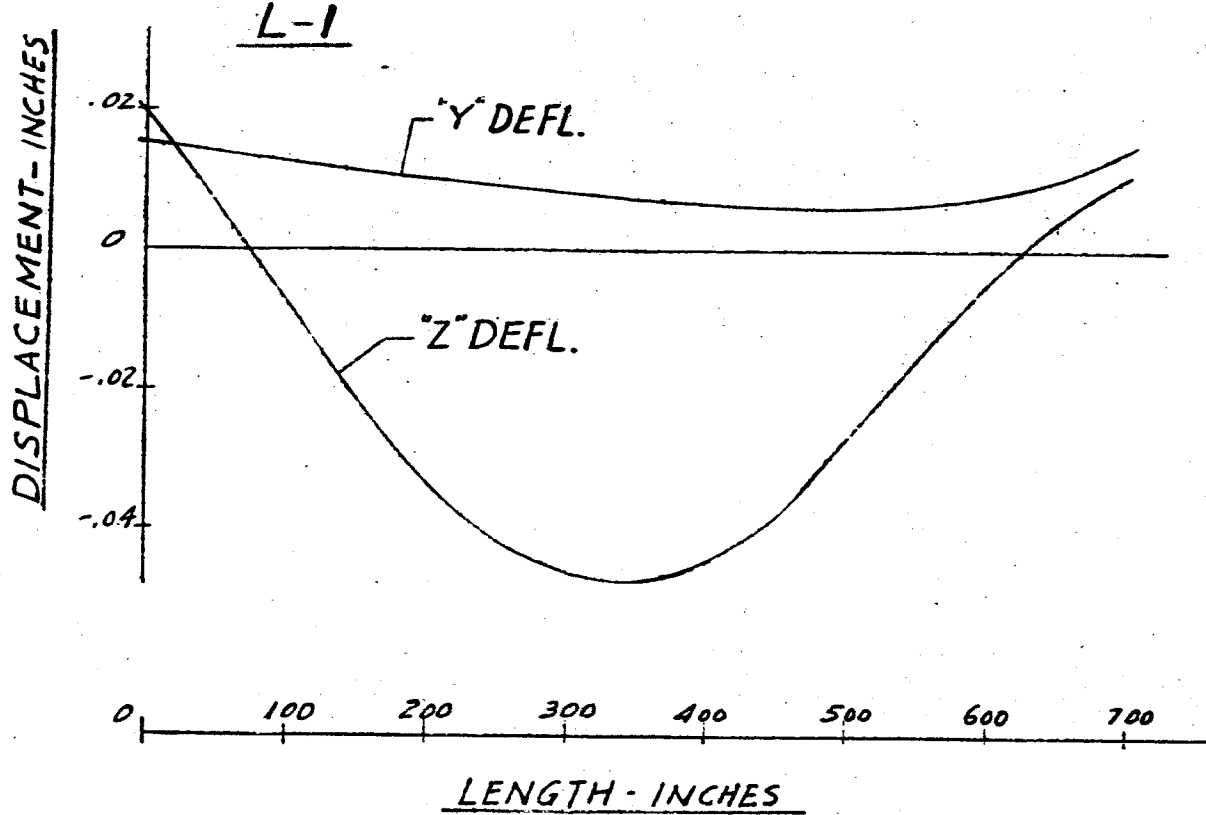
FIG. 139 DISPLACEMENT vs LENGTH SATURN SA-DI  
MAIN TANK & UPPER STAGES  
FREQUENCY = 4.30 cps.



- 222 -

FIG. 140 DISPLACEMENT VS LENGTH SATURN SA-DI

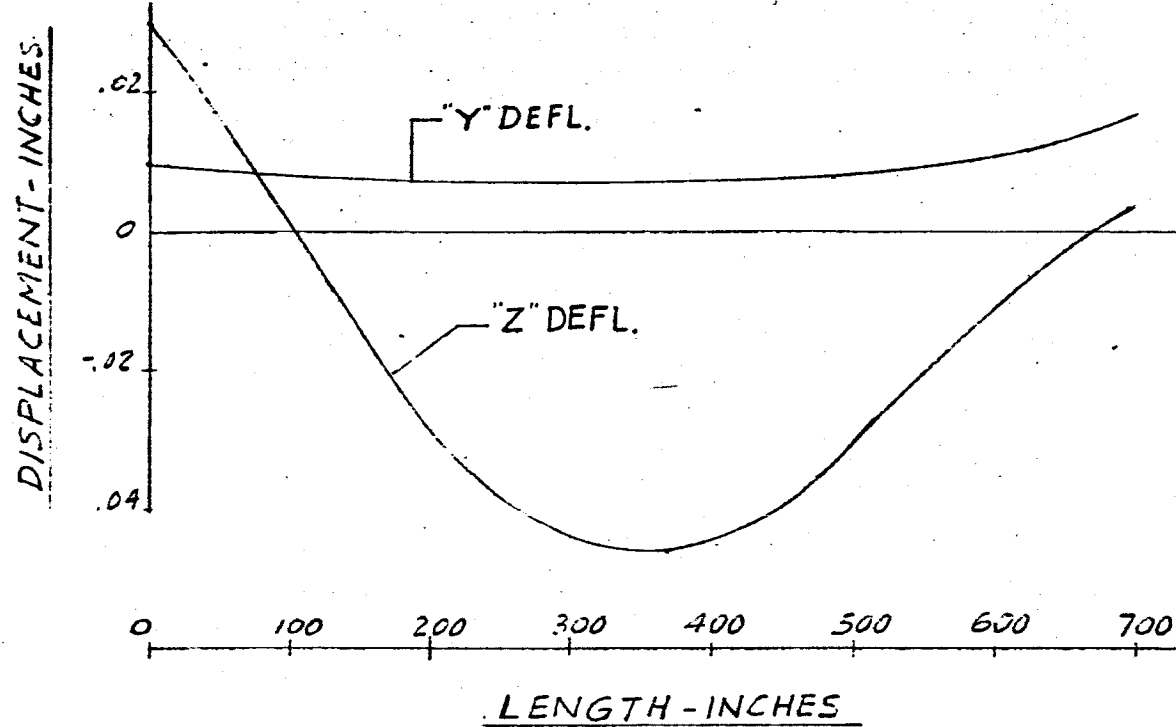
FREQUENCY = 4.30 CPS



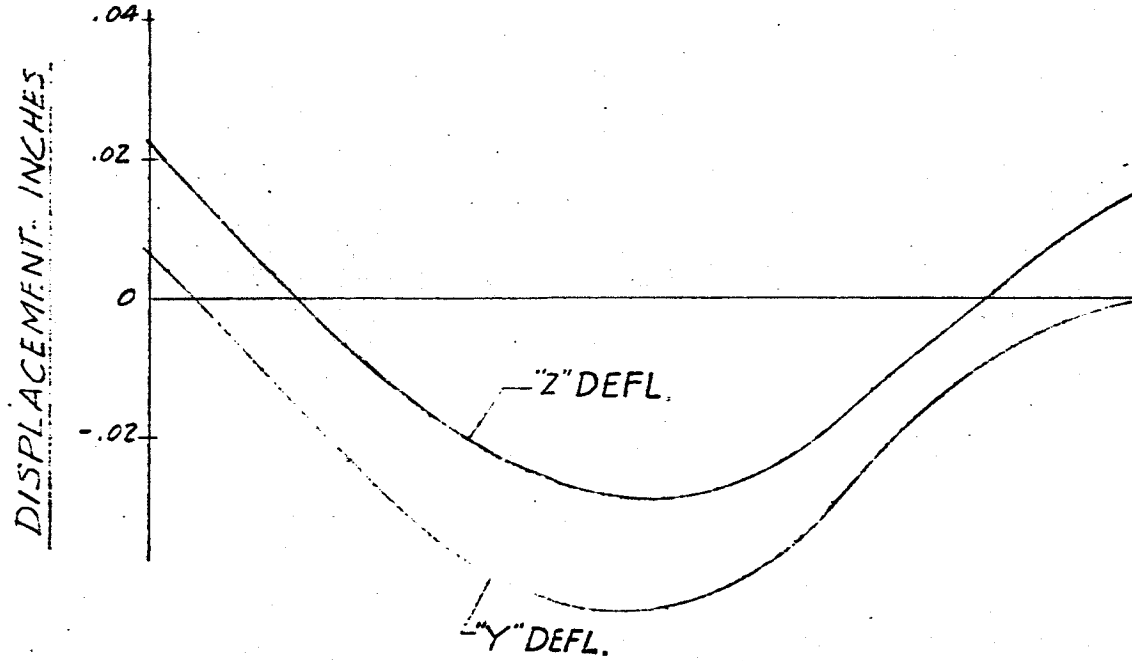
- 223 -

FIG. 141 DISPLACEMENT VS LENGTH SATURN SA-D1  
FREQUENCY = 4.30 CPS

L-3



L-4



- 224 -

FIG. 142. DISPLACEMENT VS LENGTH SATURN SA-41

FREQUENCY = 4.30 cps

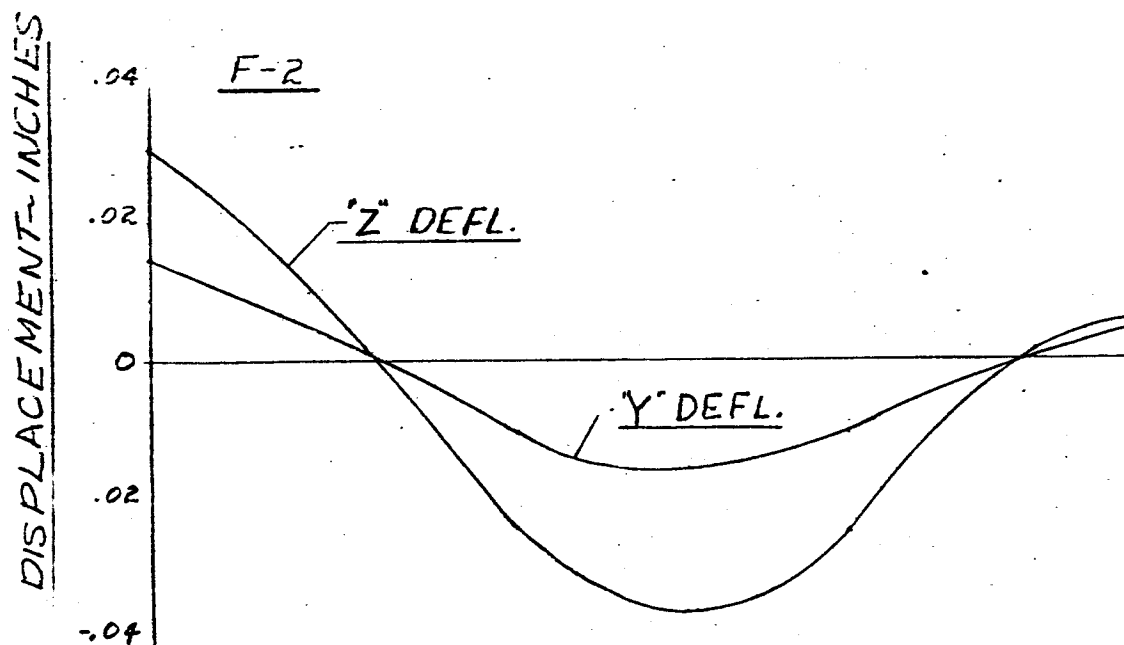
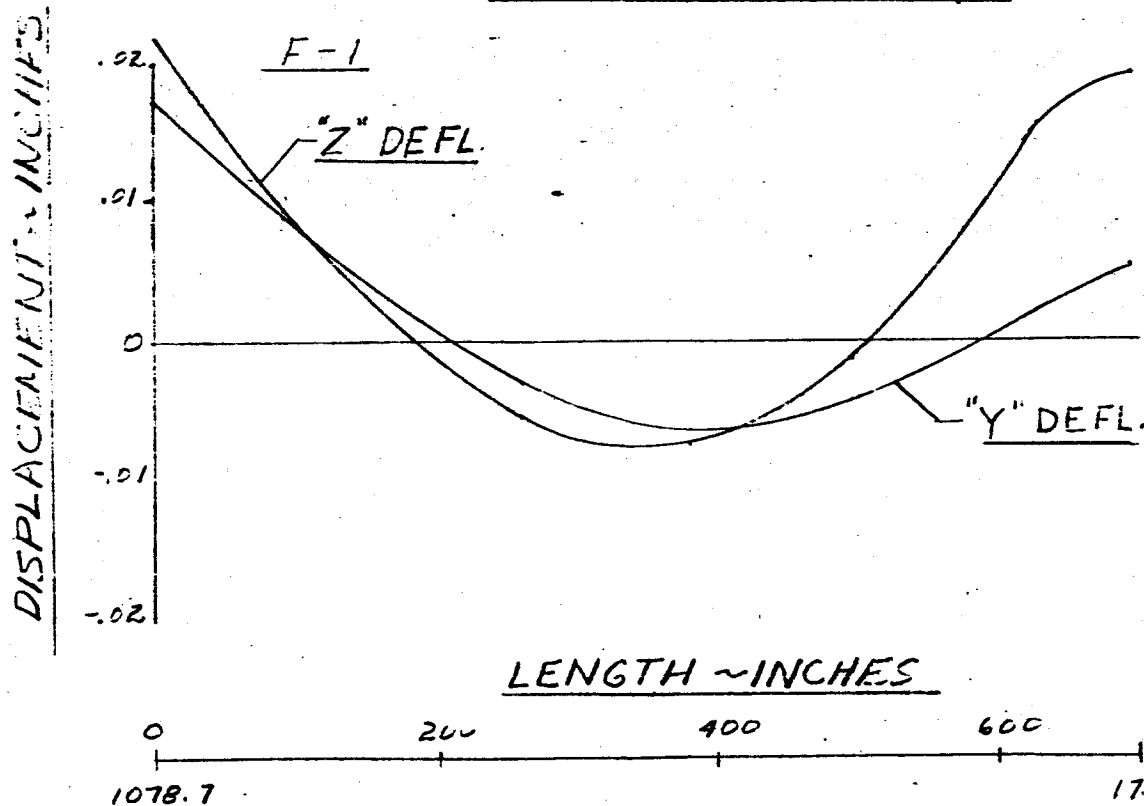
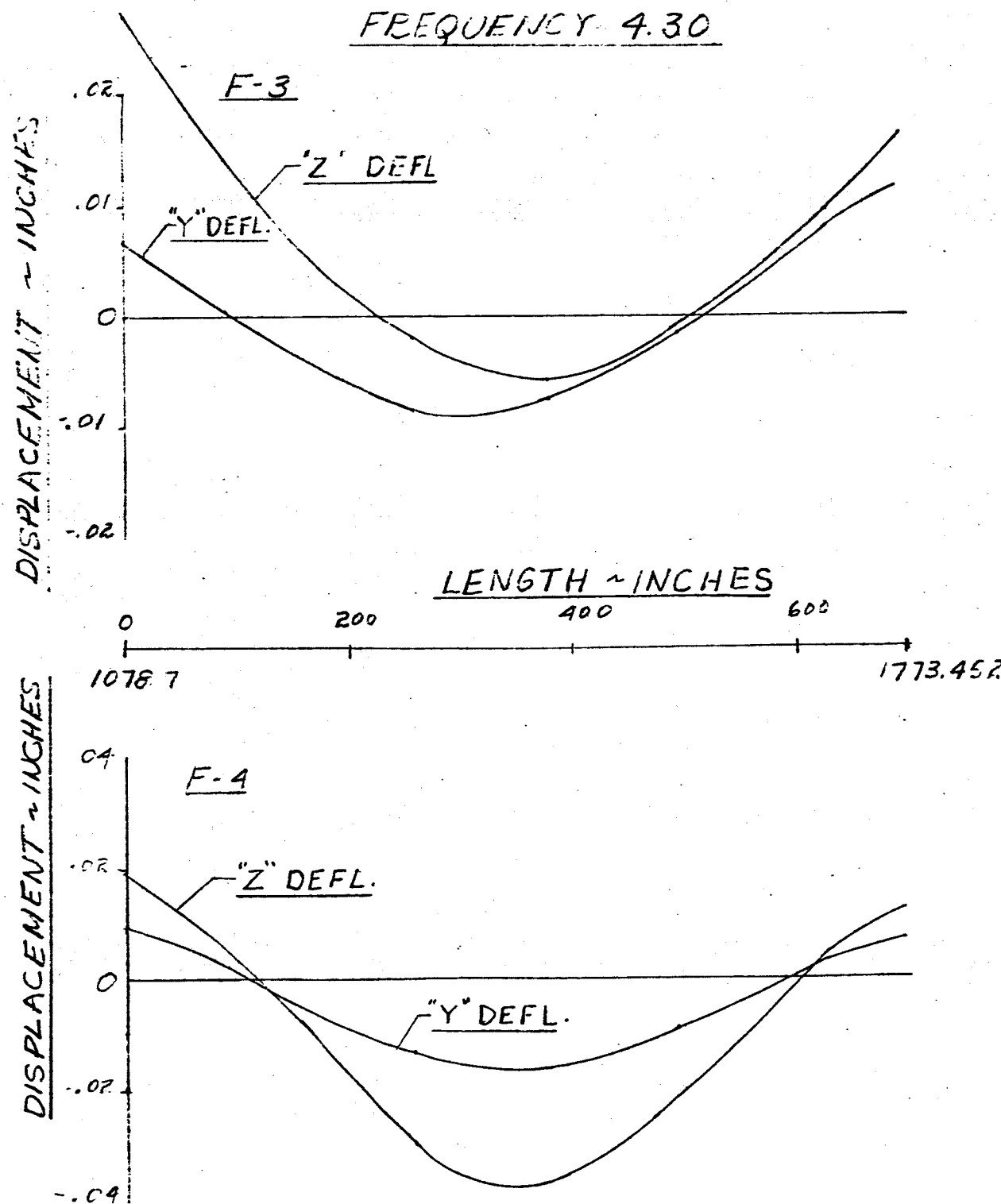


FIG. 14E DISPLACEMENT VS LENGTH SATURN SA-DI



-226-

FIG. 144 DISPLACEMENT VS LENGTH SATURN SA-DL  
MAIN TANK & UPPER STAGES  
FREQUENCY = 4.40 cps

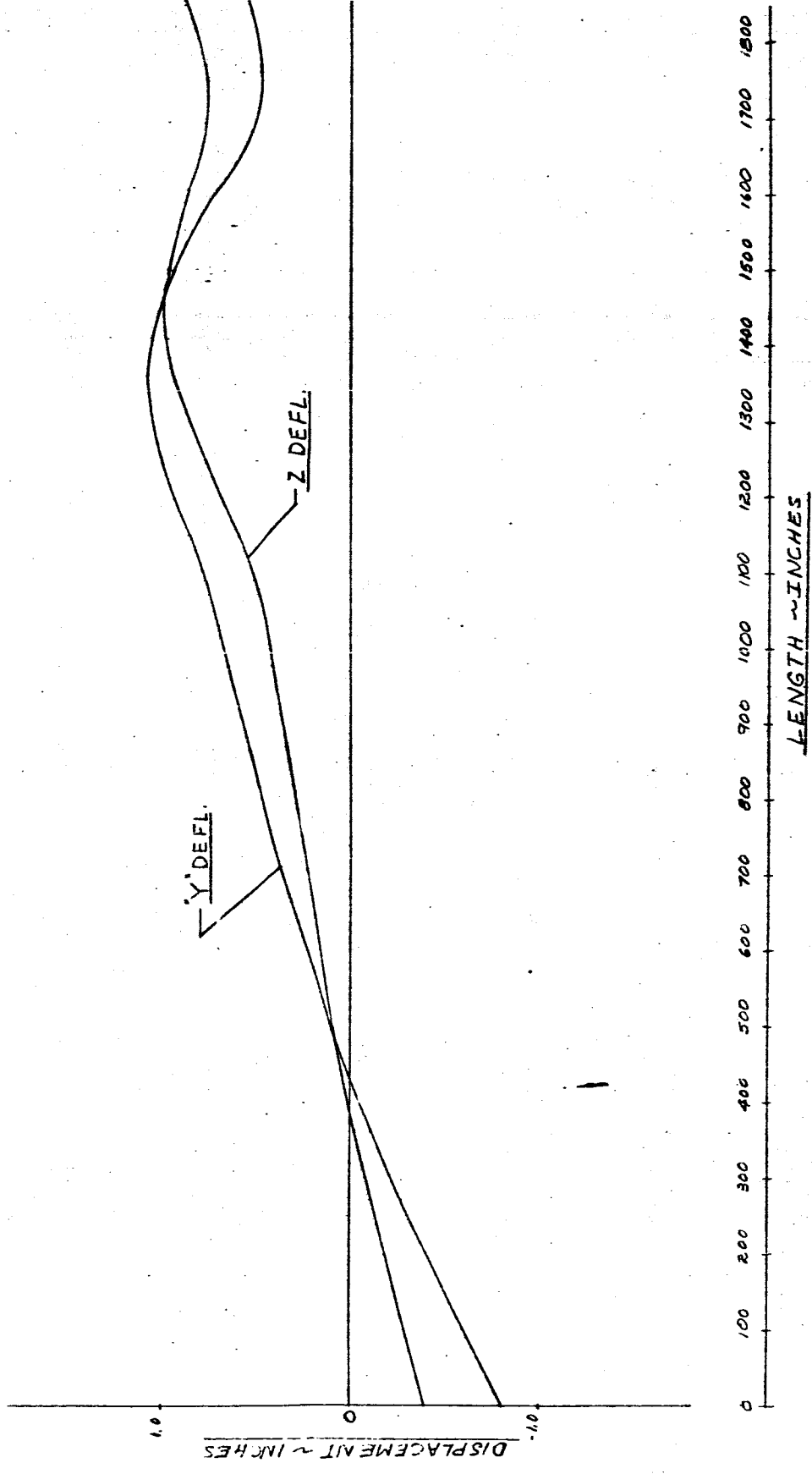
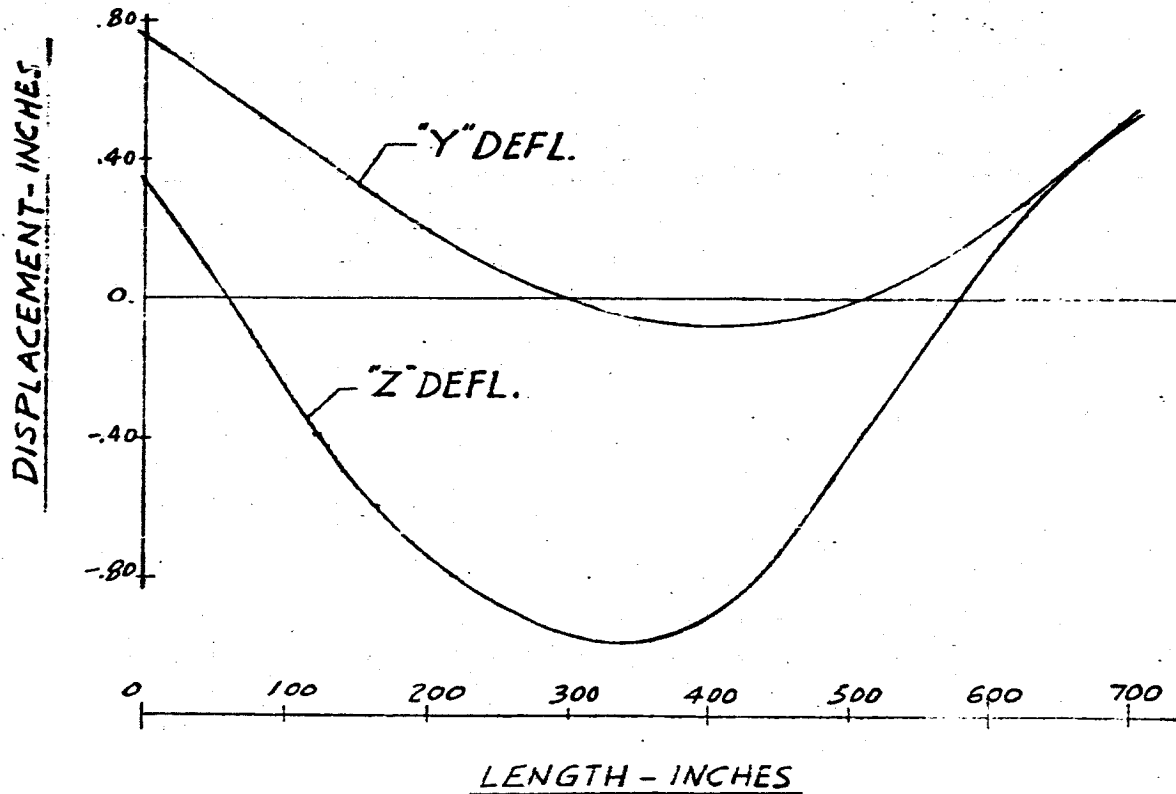
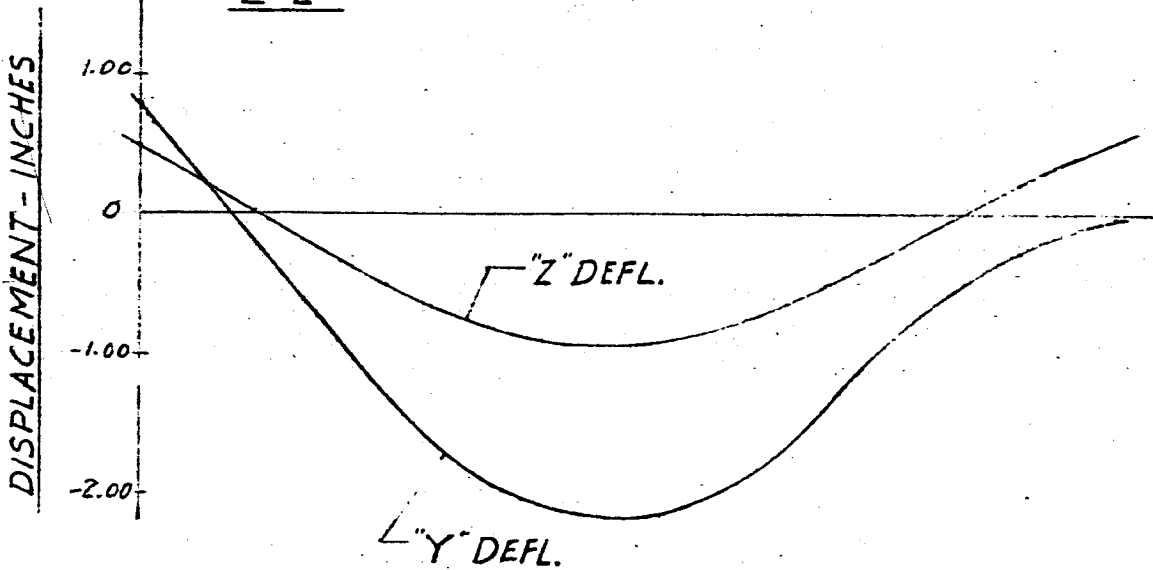


FIG. 145 DISPLACEMENT vs LENGTH SATURN SA-01  
FREQUENCY = 4.40 CPS

L-1



L-2

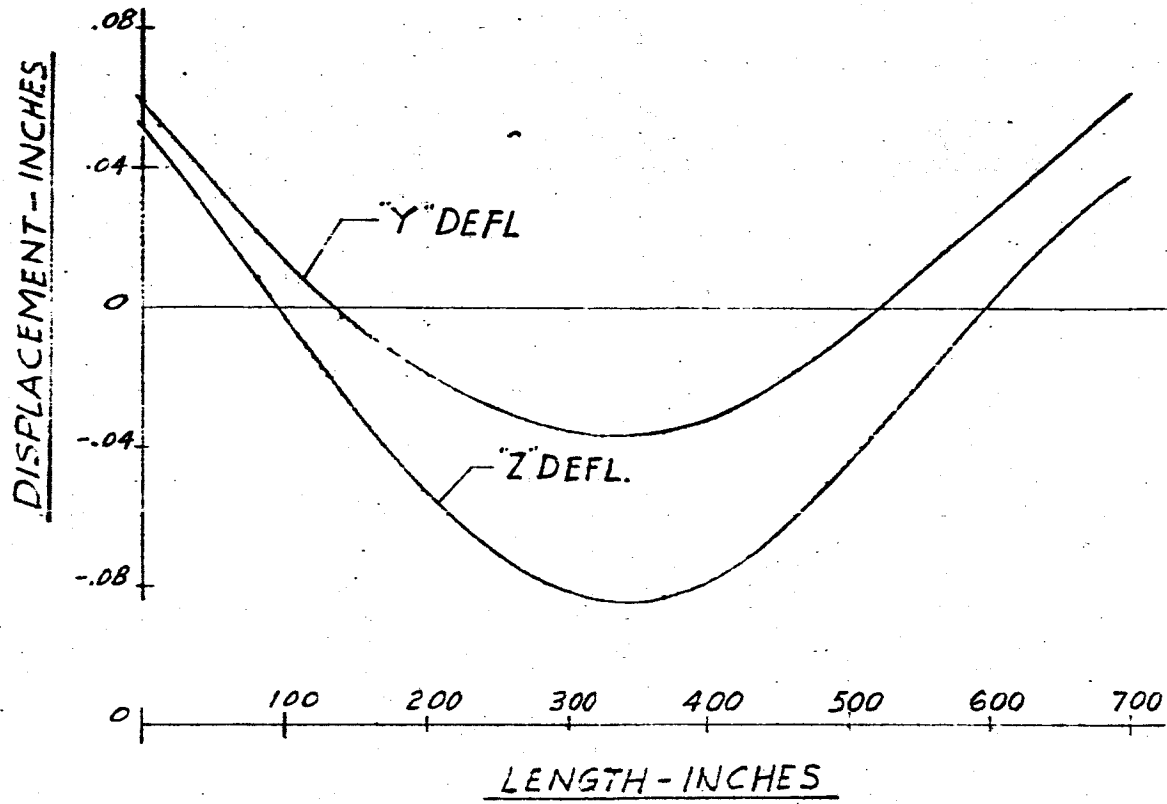


-228-

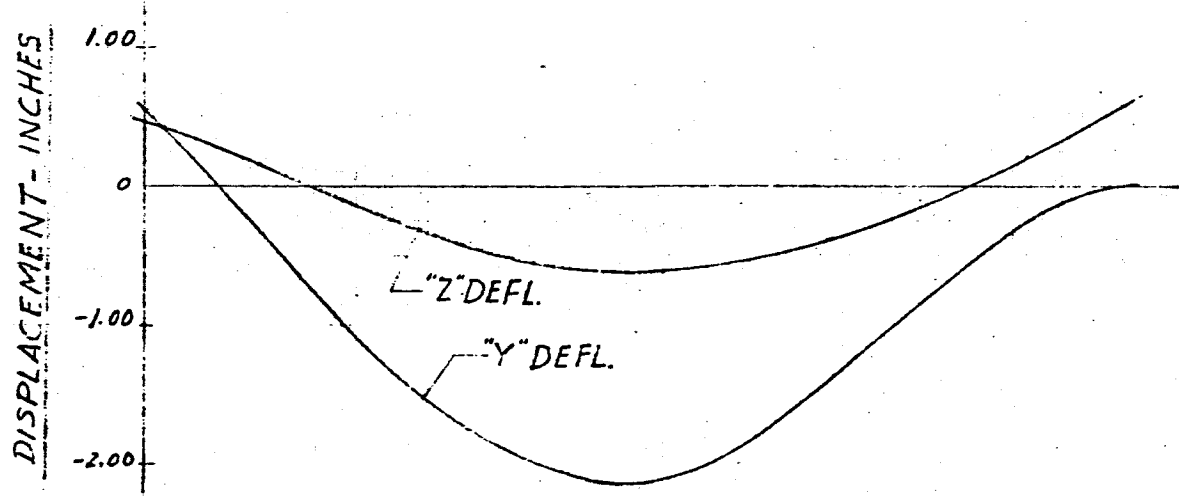
FIG. 146 DISPLACEMENT VS LENGTH SATURN SA-D1

FREQUENCY = 4.40 CPS

L-3



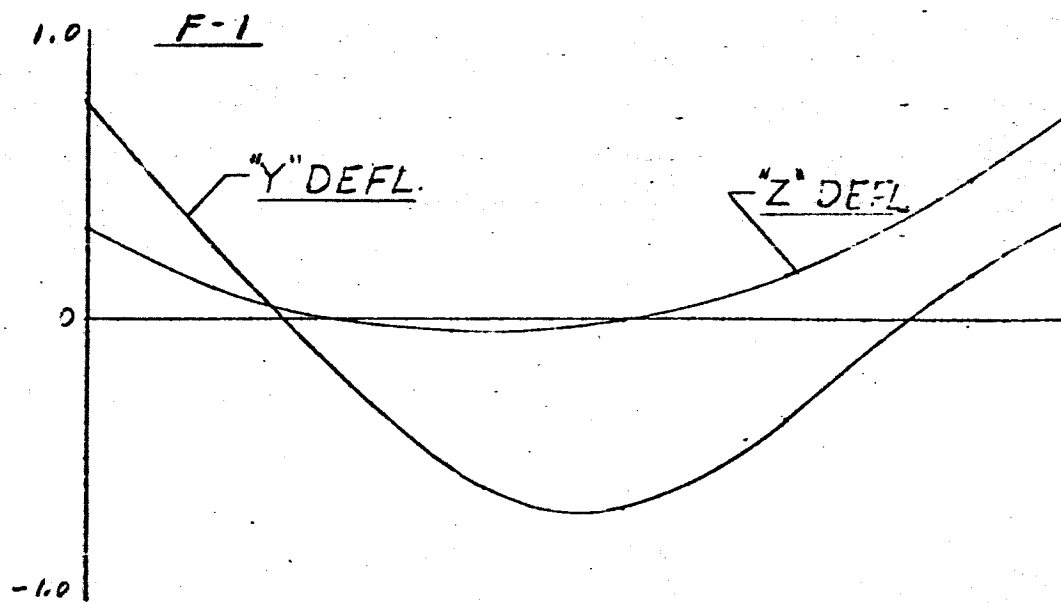
L-4



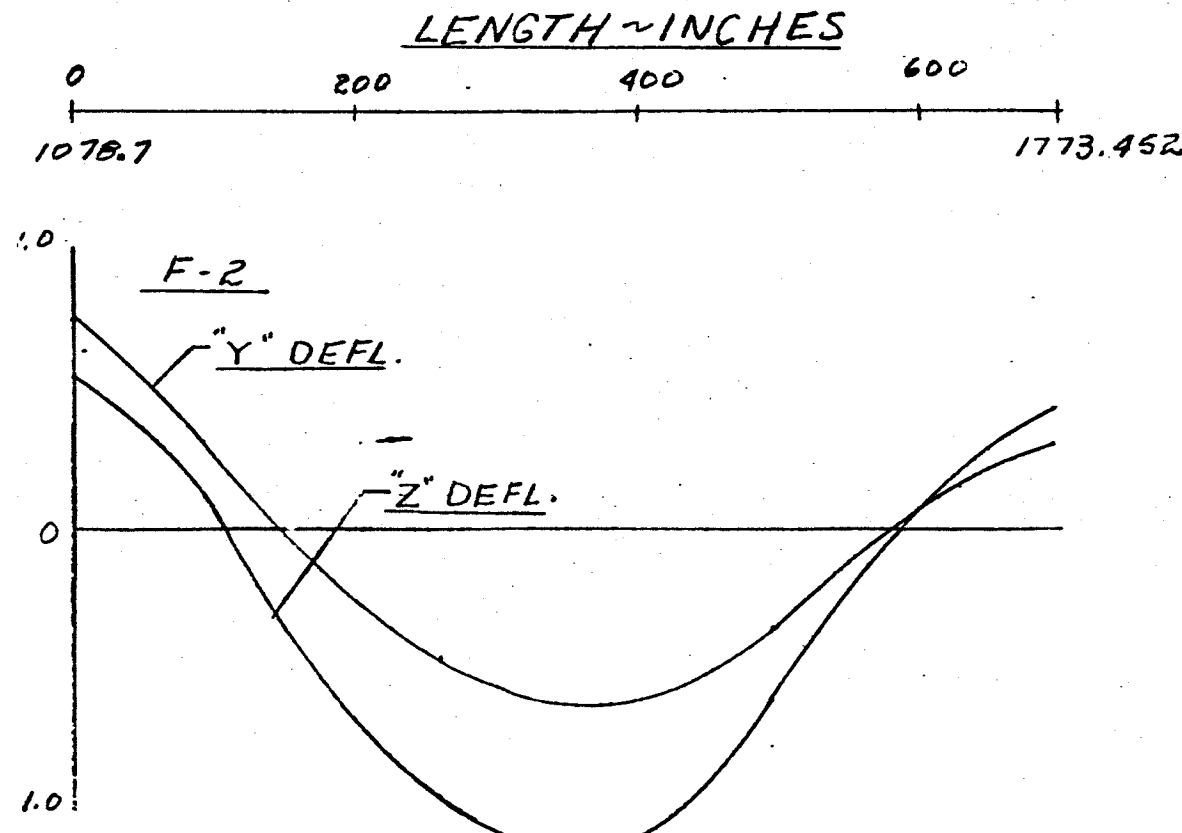
- 229 -

FIG. 147 DISPLACEMENT VS LENGTH SATURN SA-D1

DISPLACEMENT ~ INCHES



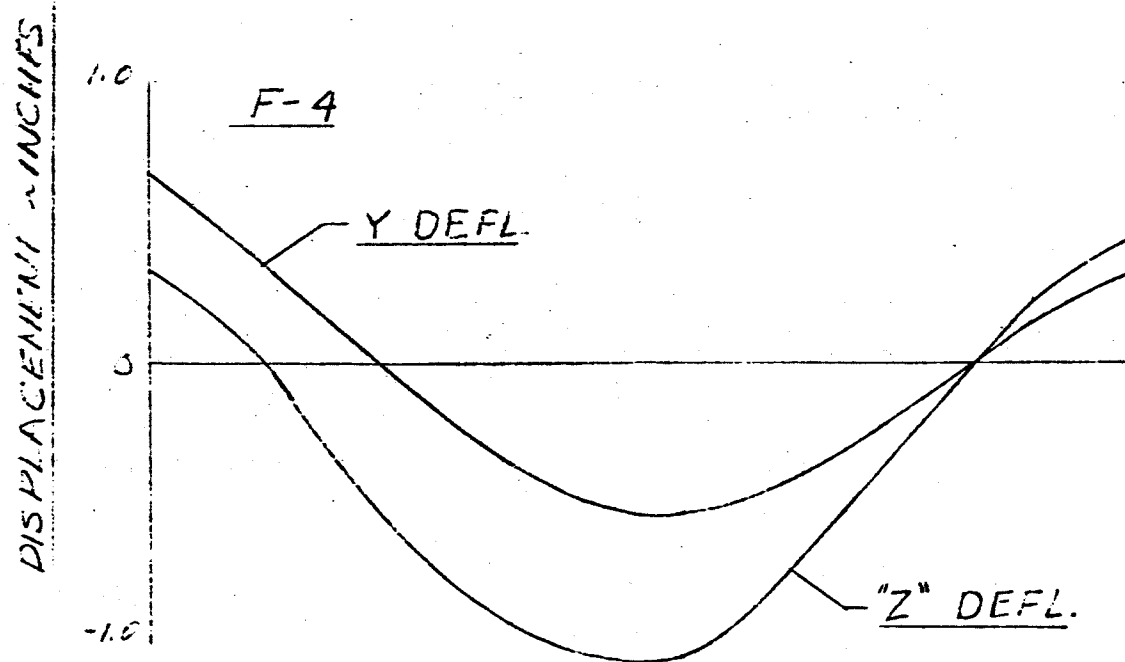
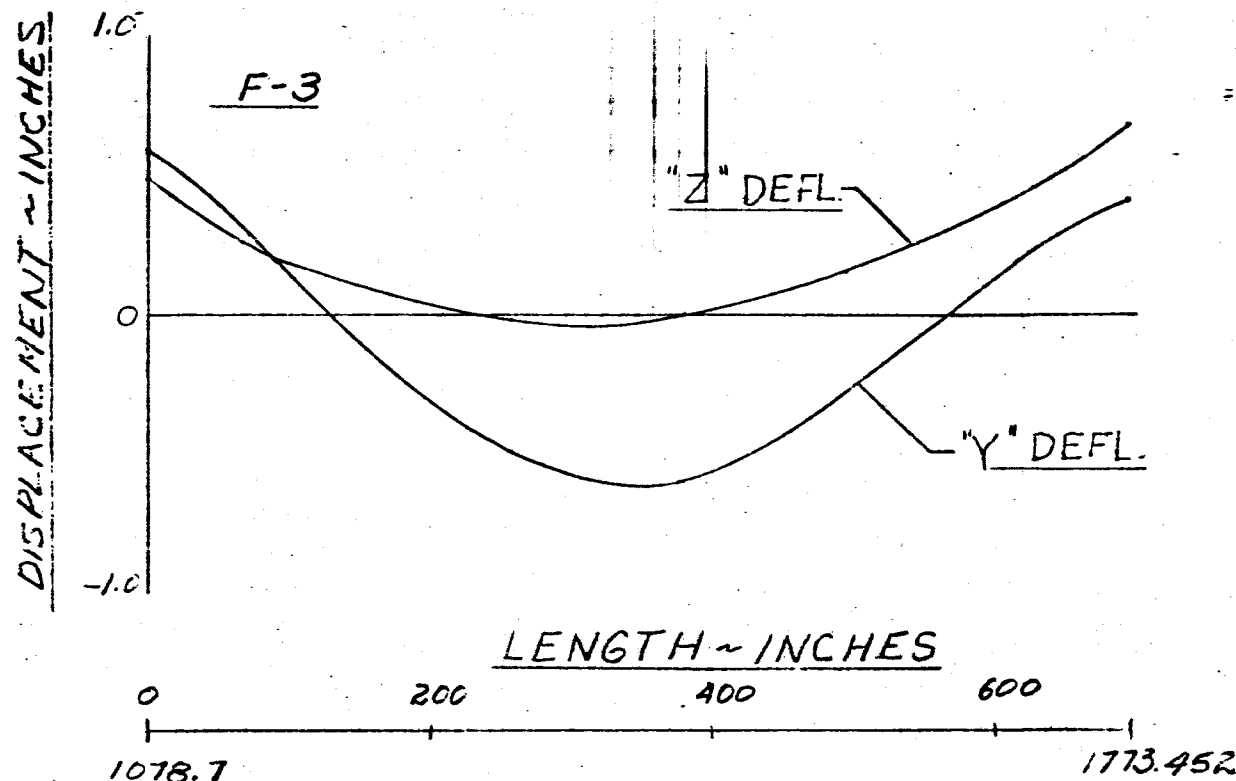
DISPLACEMENT ~ INCHES



-230-

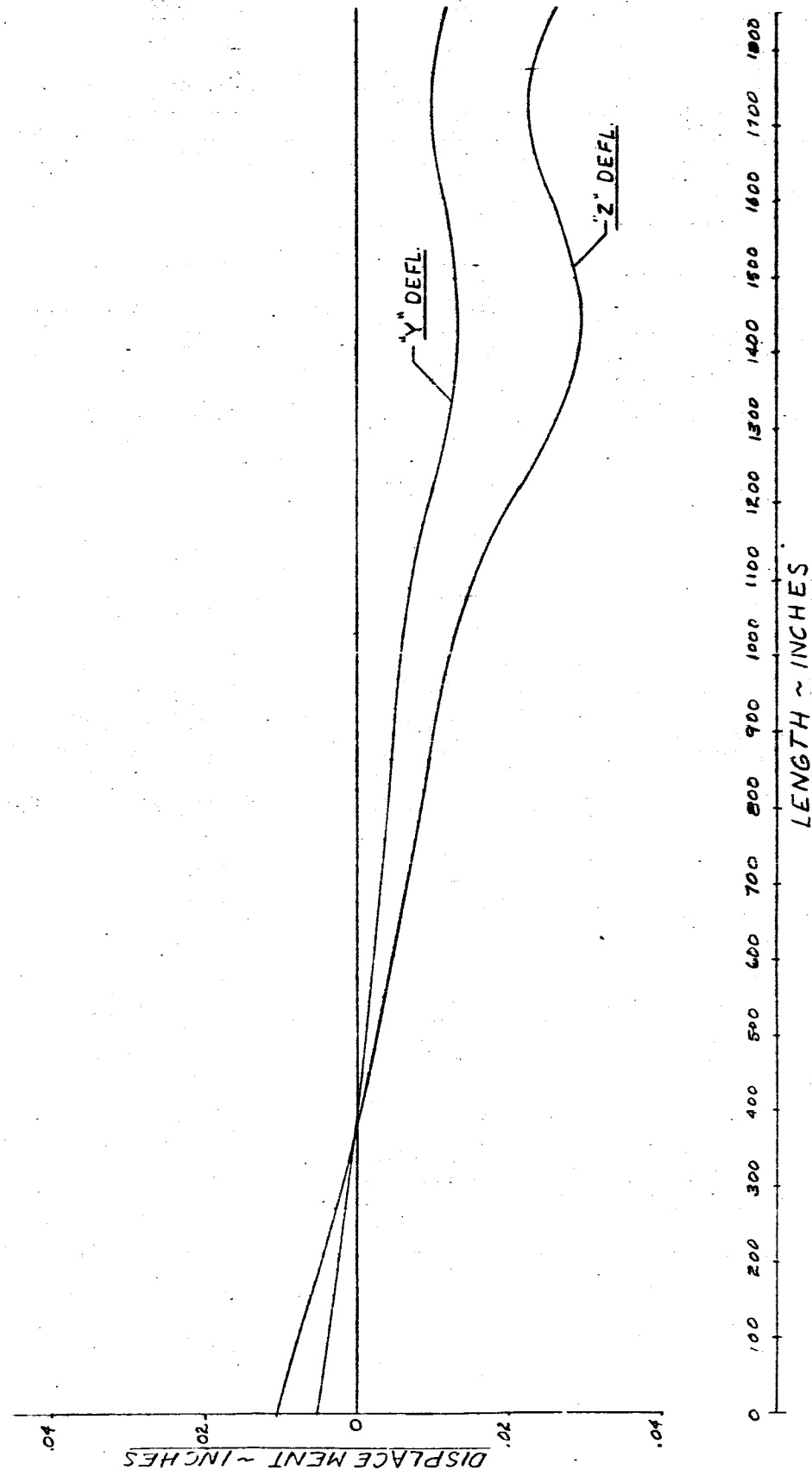
FIG. 148 DISPLACEMENT vs LENGTH SATURN SA-DI

FREQUENCY = 4.40 cps.



- 23 -

FIG. 149 DISPLACEMENT VS LENGTH SATURN SA-01  
MAIN TANK & UPPER STAGES  
FREQUENCY = 4.50 cps.

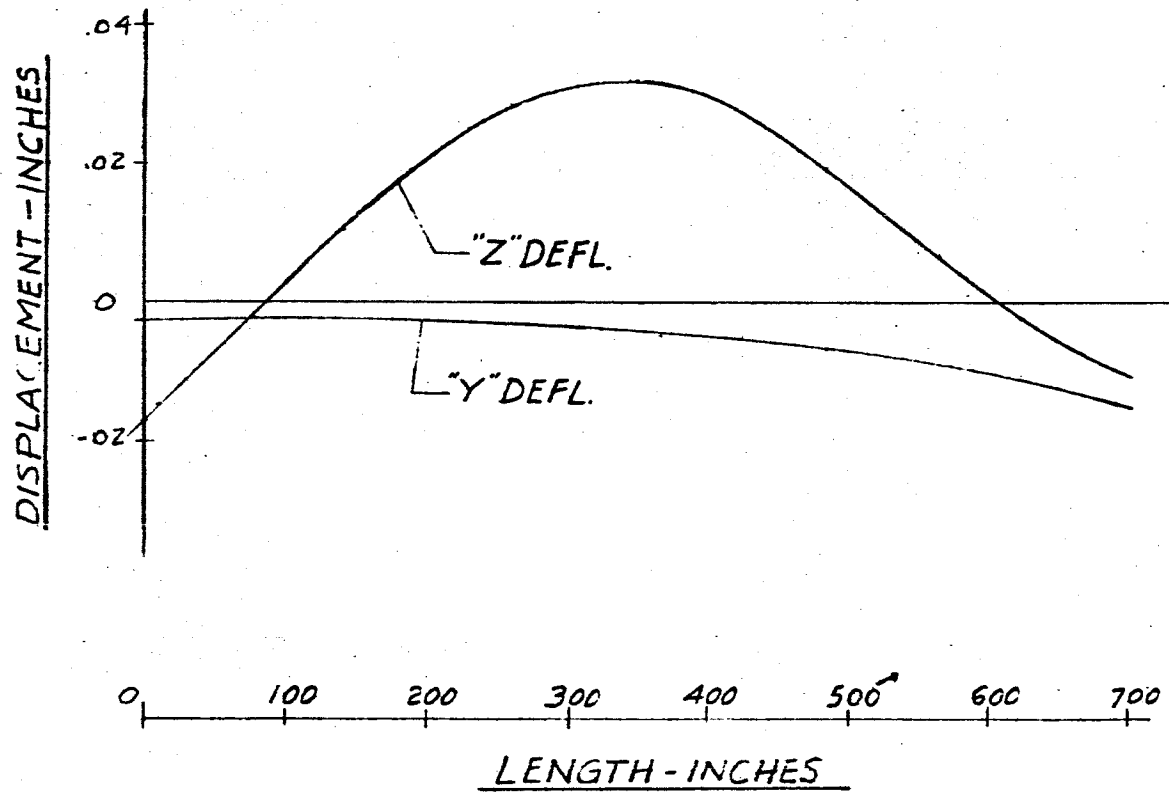


-232-

FIG. 150 DISPLACEMENT vs LENGTH SATURN SA-D1

FREQUENCY = 4.50 CPS

L-1



L-2

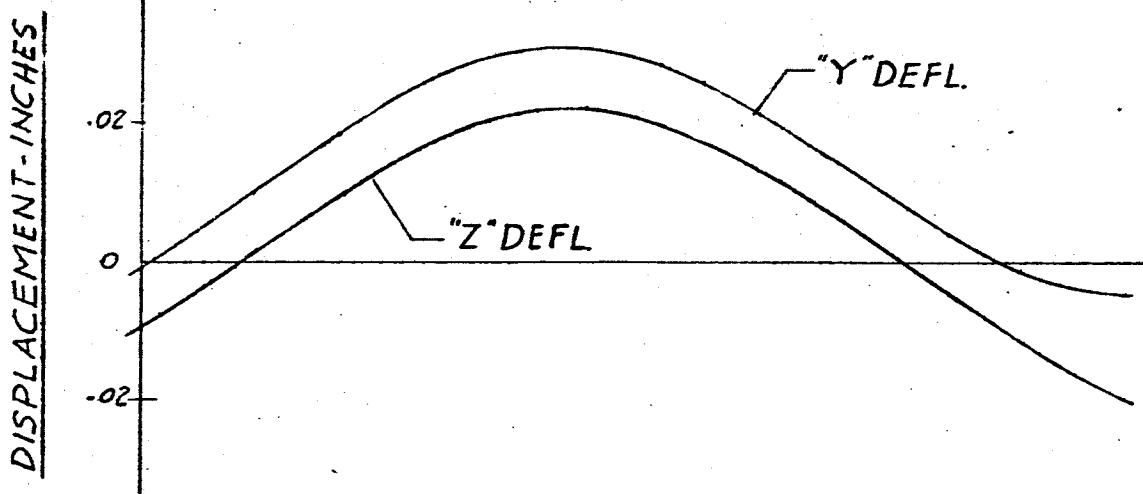
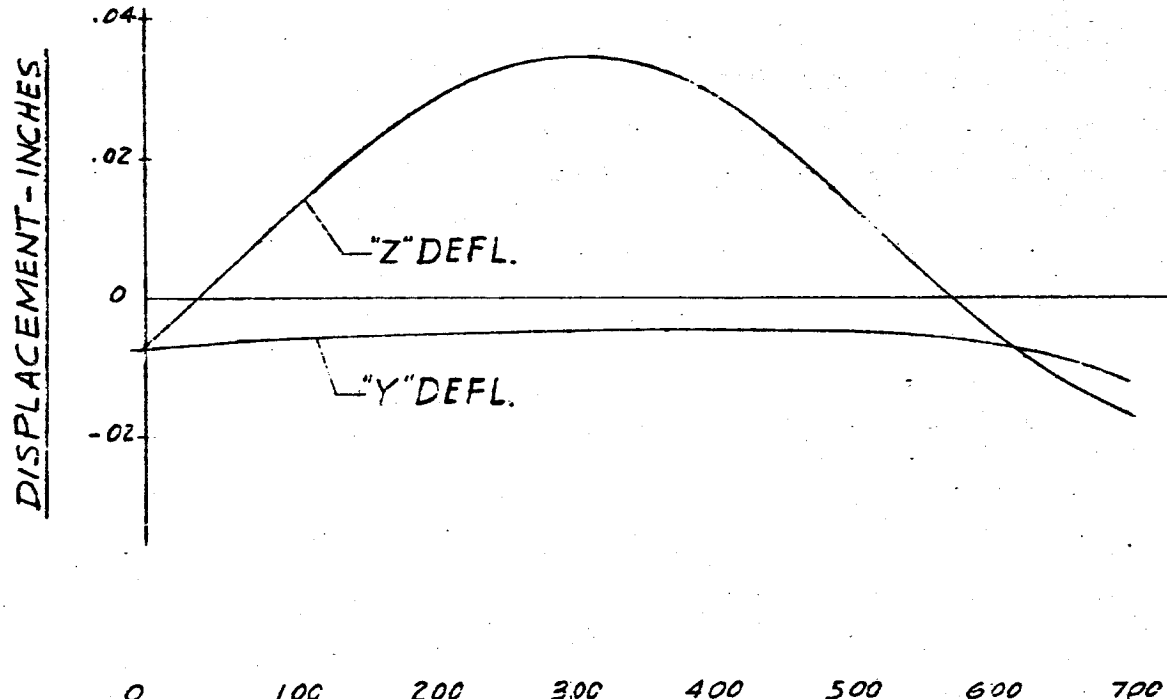


FIG. 151 DISPLACEMENT VS LENGTH SATURN SA-DI  
FREQUENCY = 4.50 CPS

L-3



LENGTH - INCHES

L-4

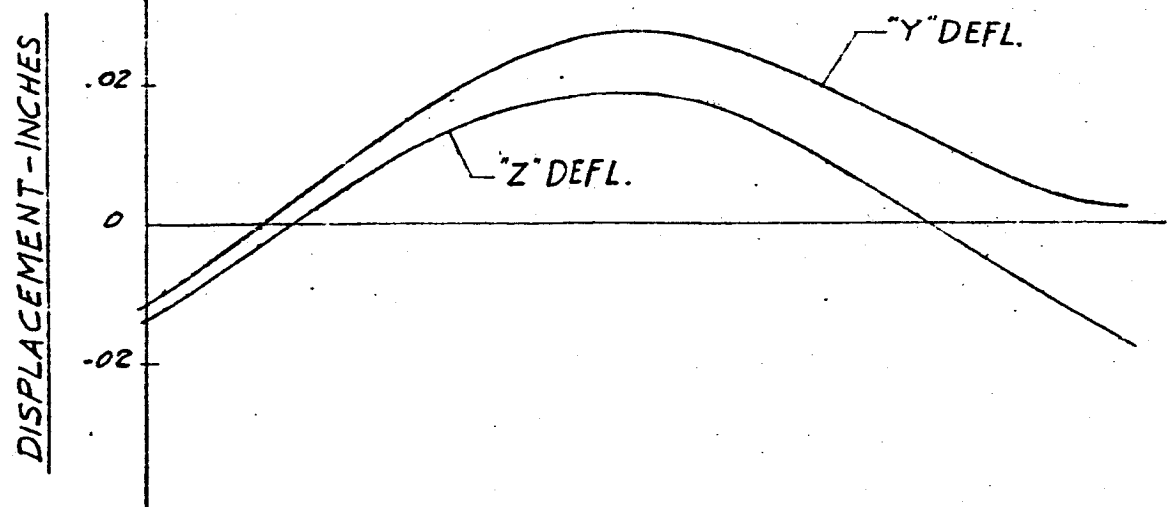
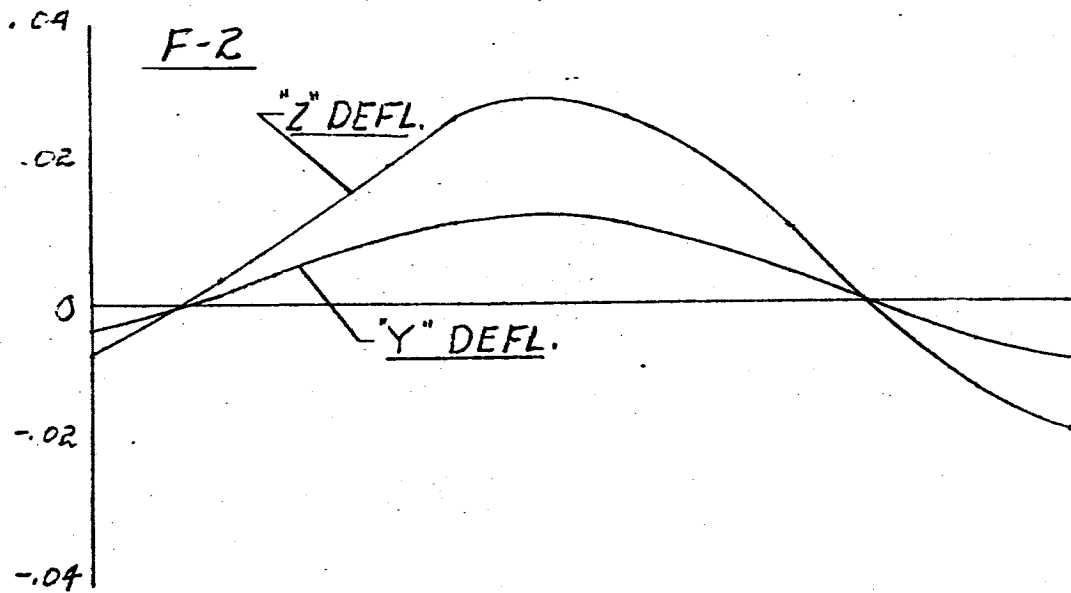
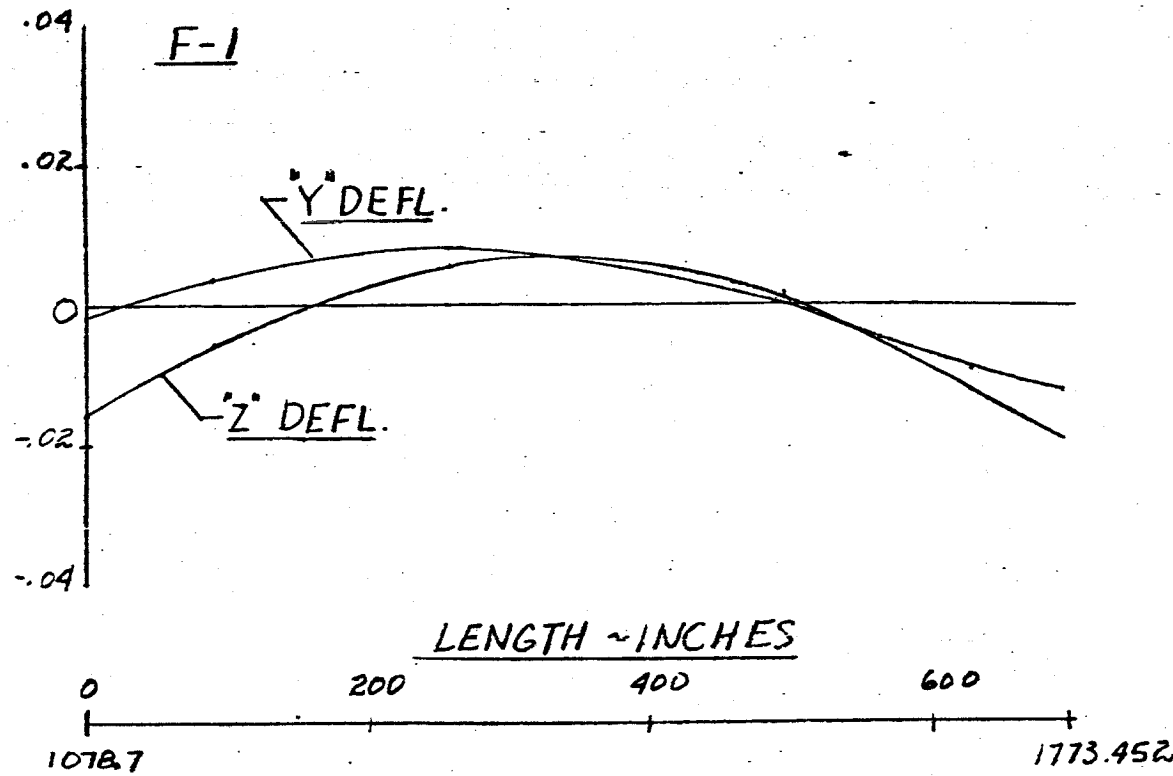


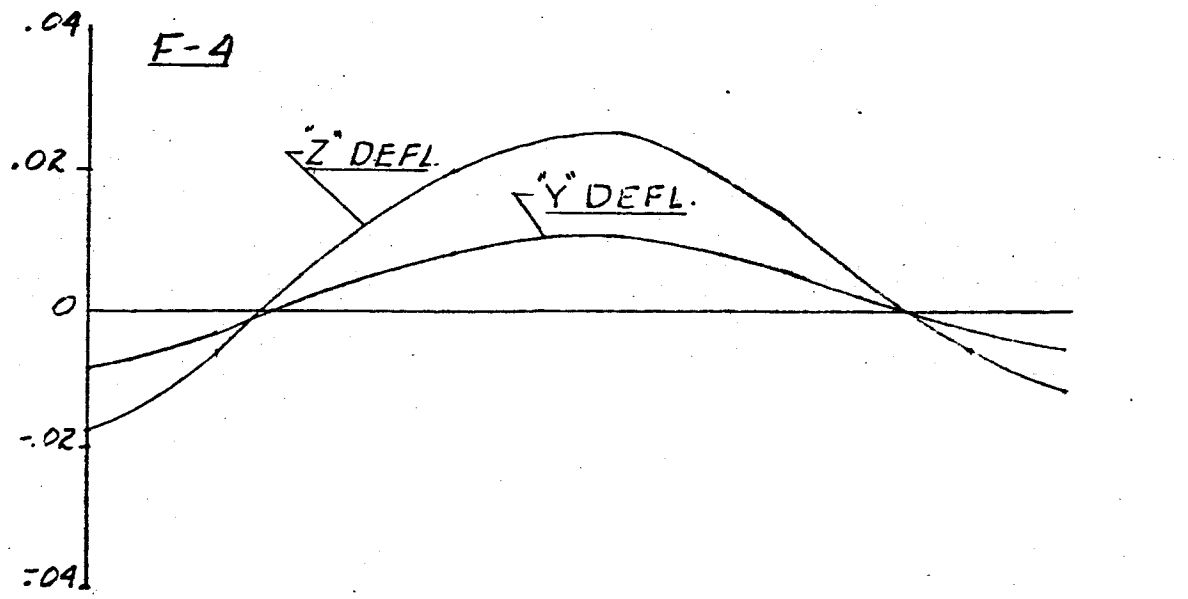
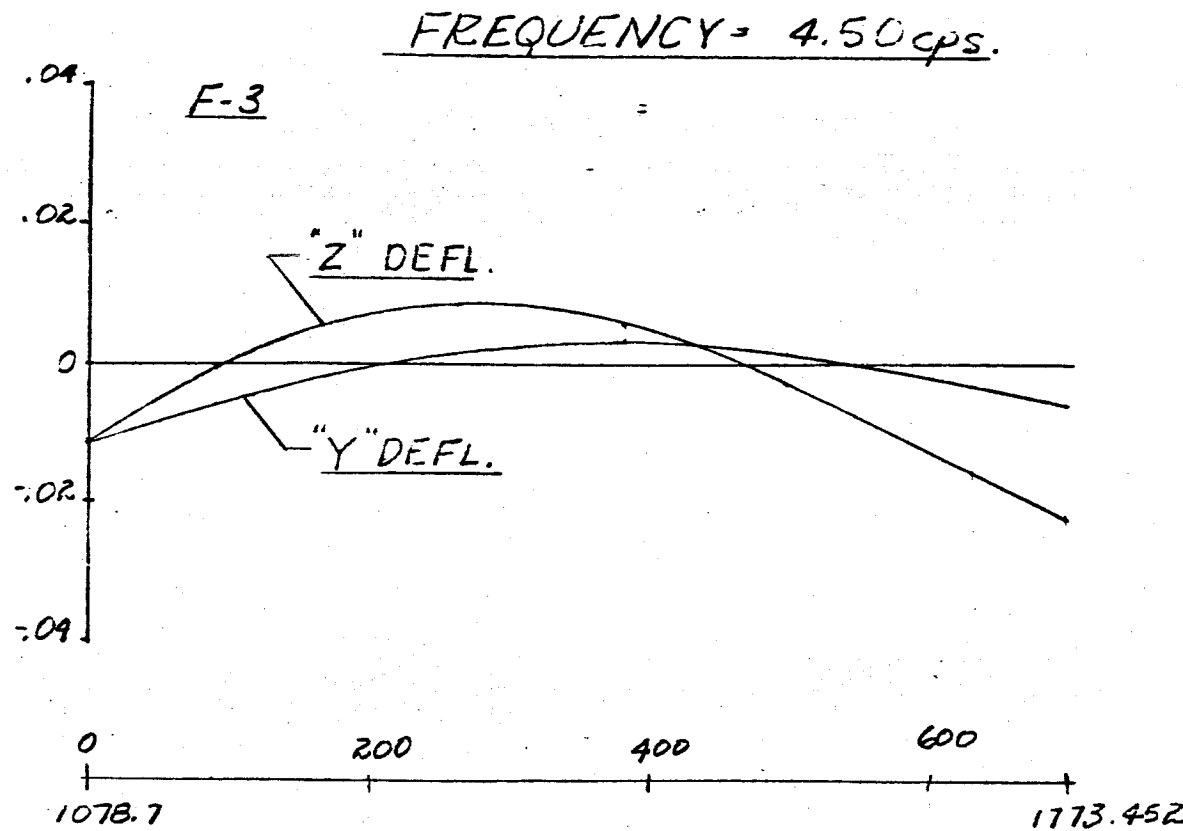
FIG 152 DISPLACEMENT VS LENGTH. SATURN SA-DI

FREQUENCY = 4.50 cps



- 235 -

FIG. 153 DISPLACEMENT VS LENGTH SATURN SA-01



- 2.36 -

FIG. 154 DISPLACEMENT vs LENGTH SATURN SA-DI  
MAIN TANK & UPPER STAGES  
FREQUENCY = 4.60 CPS

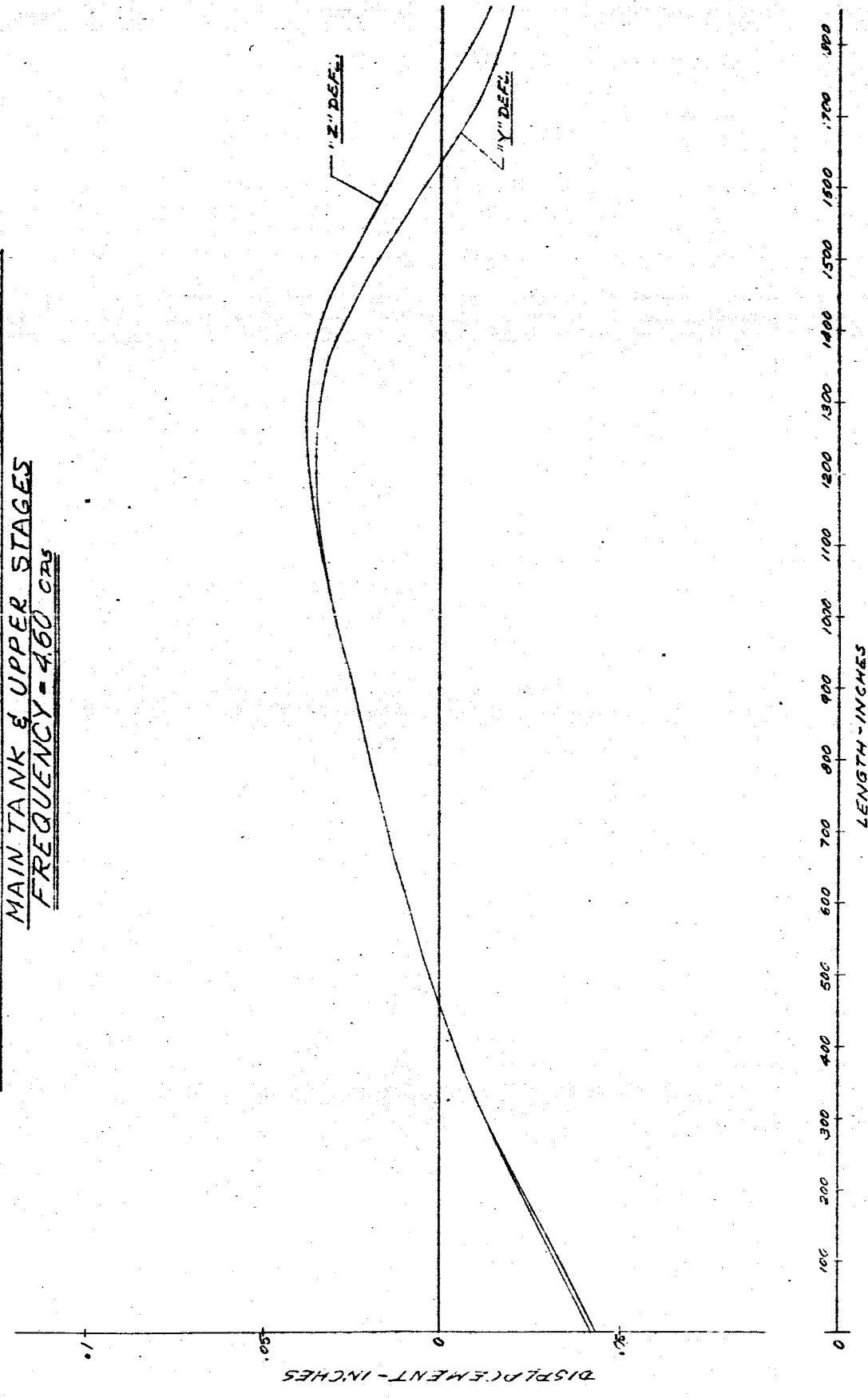
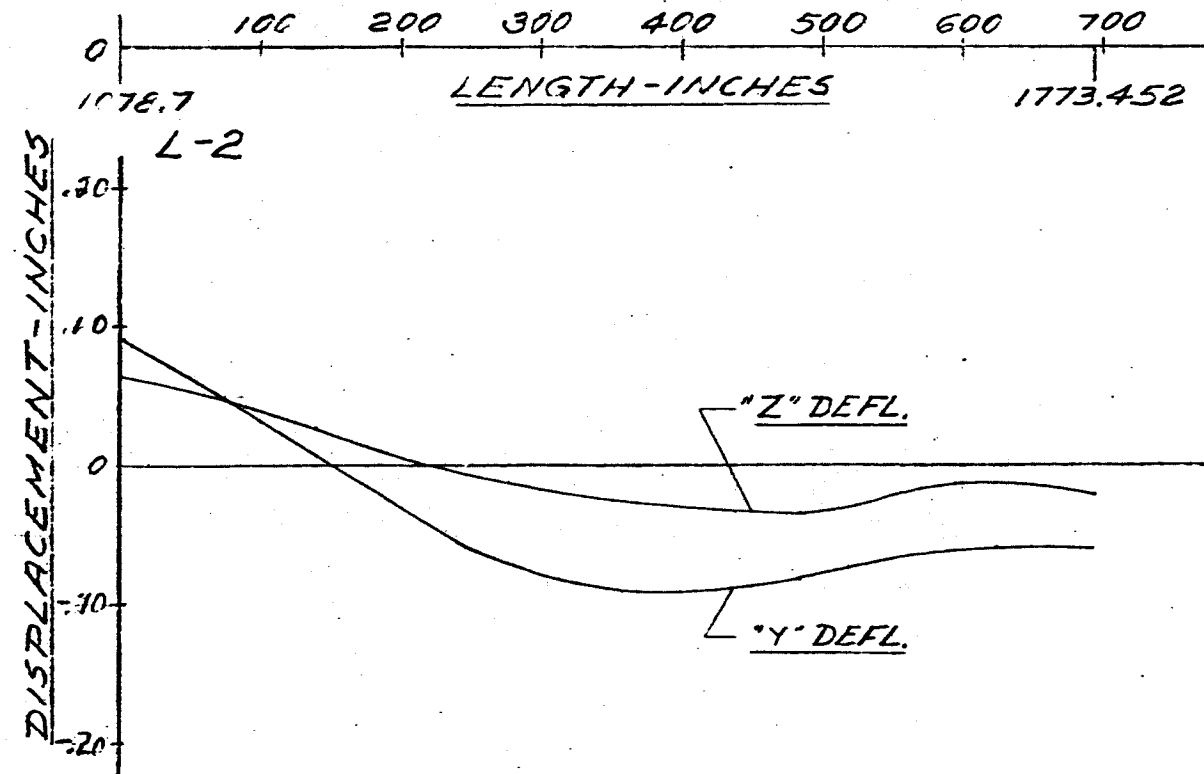
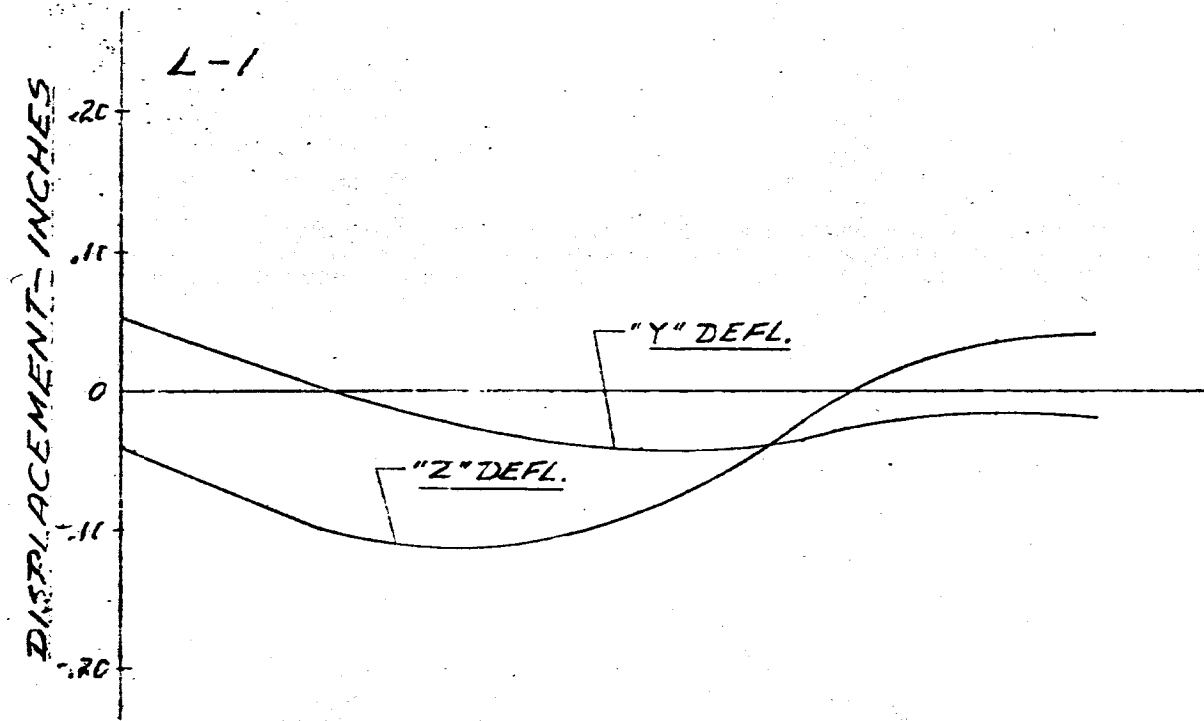


FIG. 155 DISPLACEMENT VS LENGTH SATURN SA-DI  
FREQUENCY = 4.60 CPS

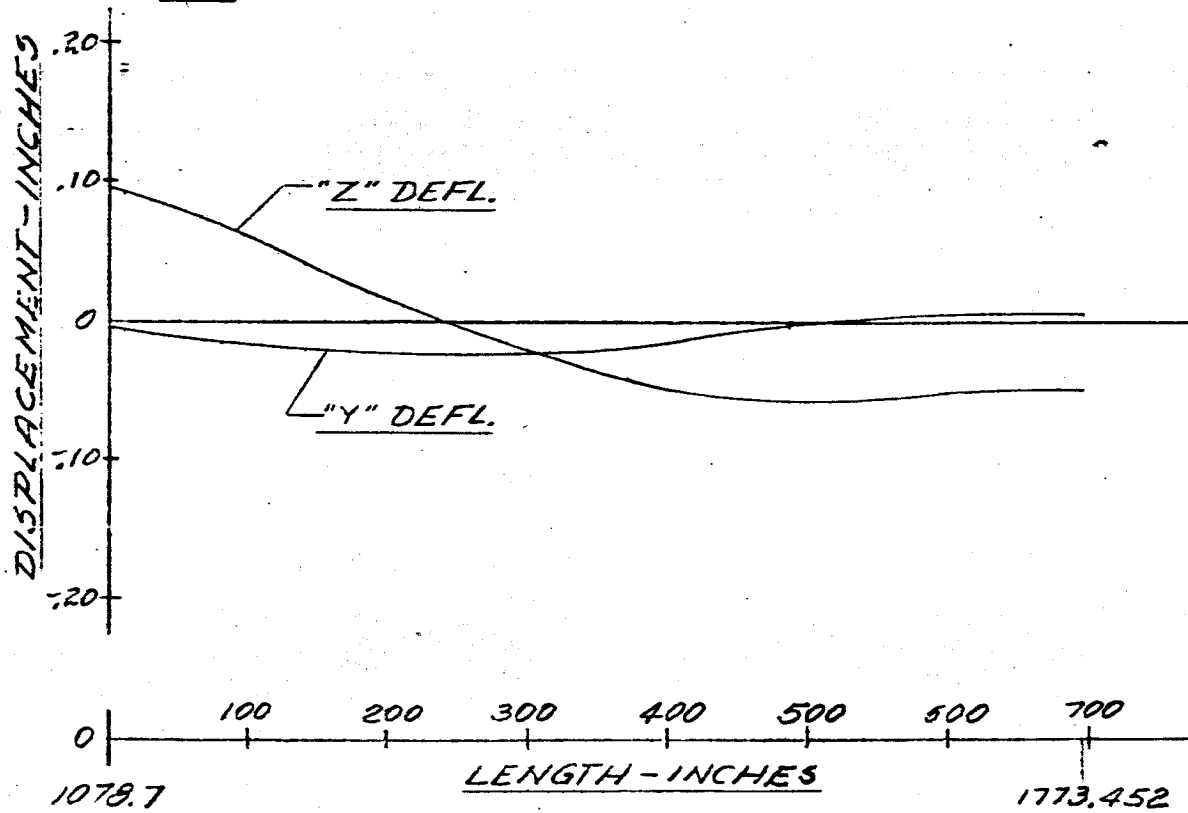


- 238 -

FIG. 156 DISPLACEMENT VS LENGTH SATURN SA-DI

FREQUENCY = 4.60 CPS

L-3



L-4

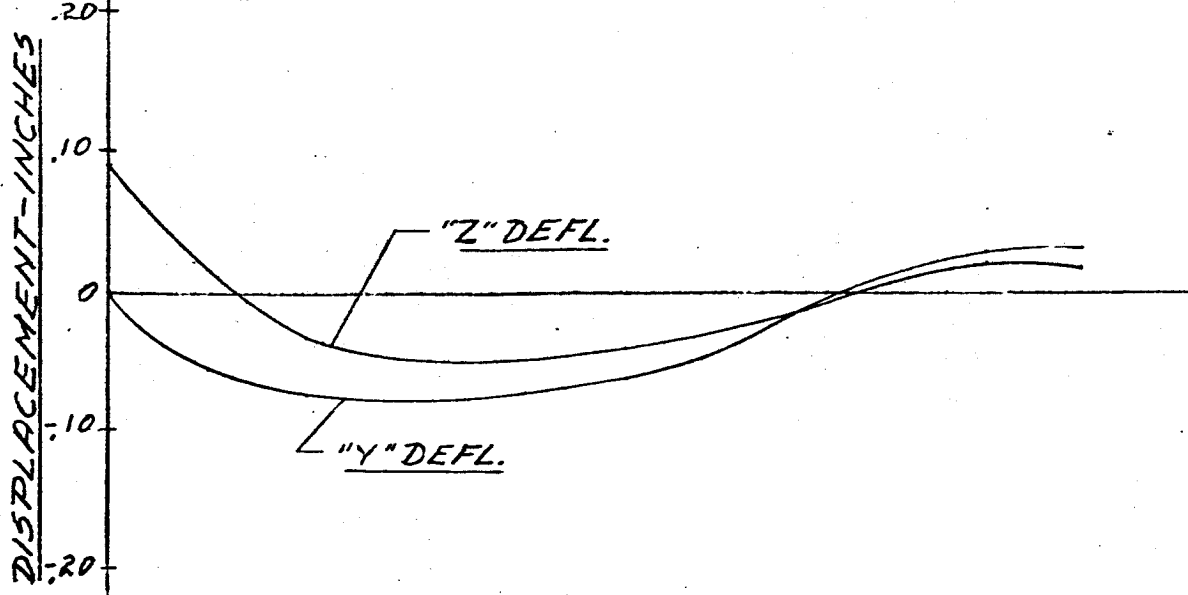


FIG. 157 DISPLACEMENT vs LENGTH SATURN SA-CI  
FREQUENCY = 4.60 CPS

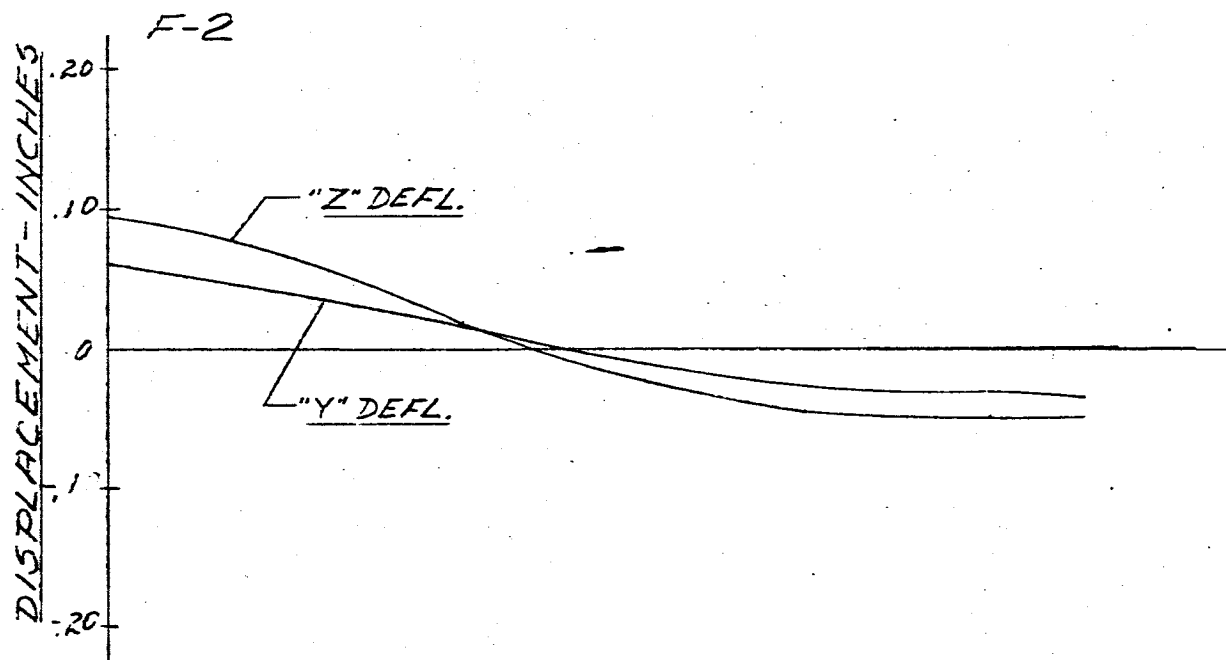
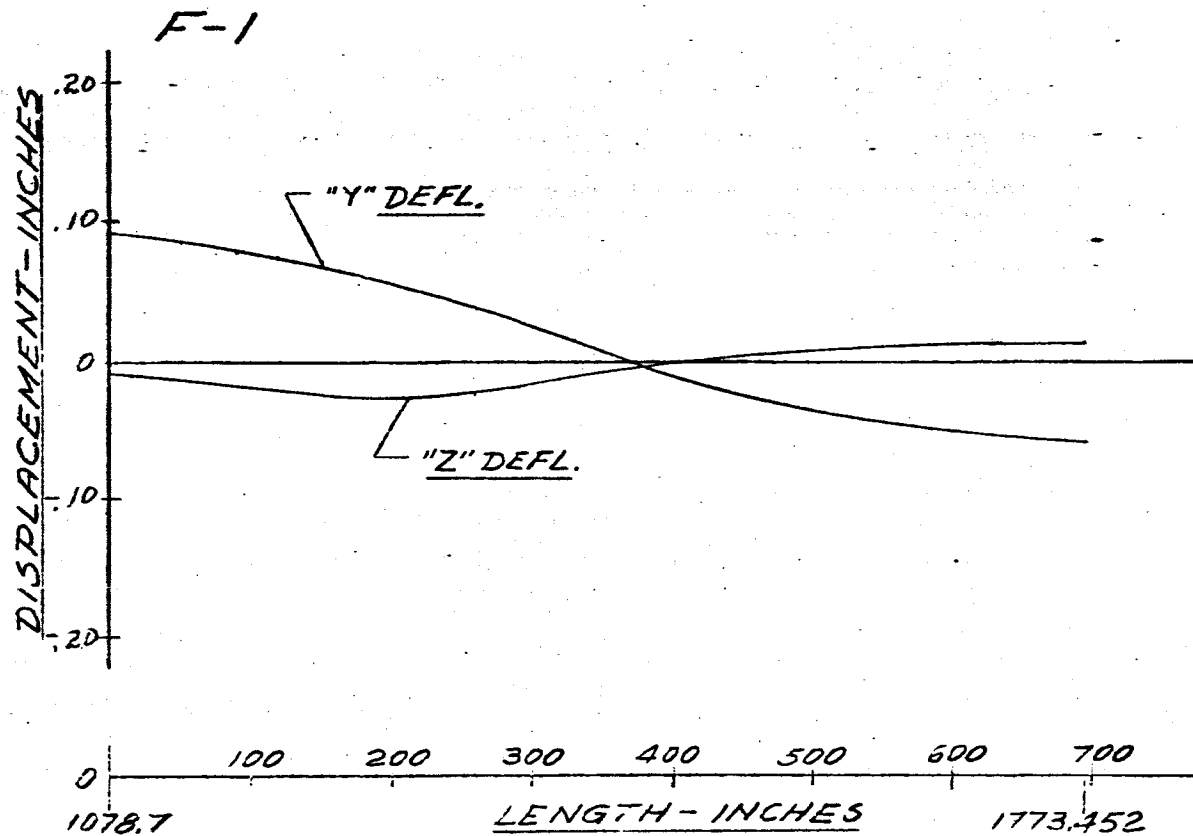
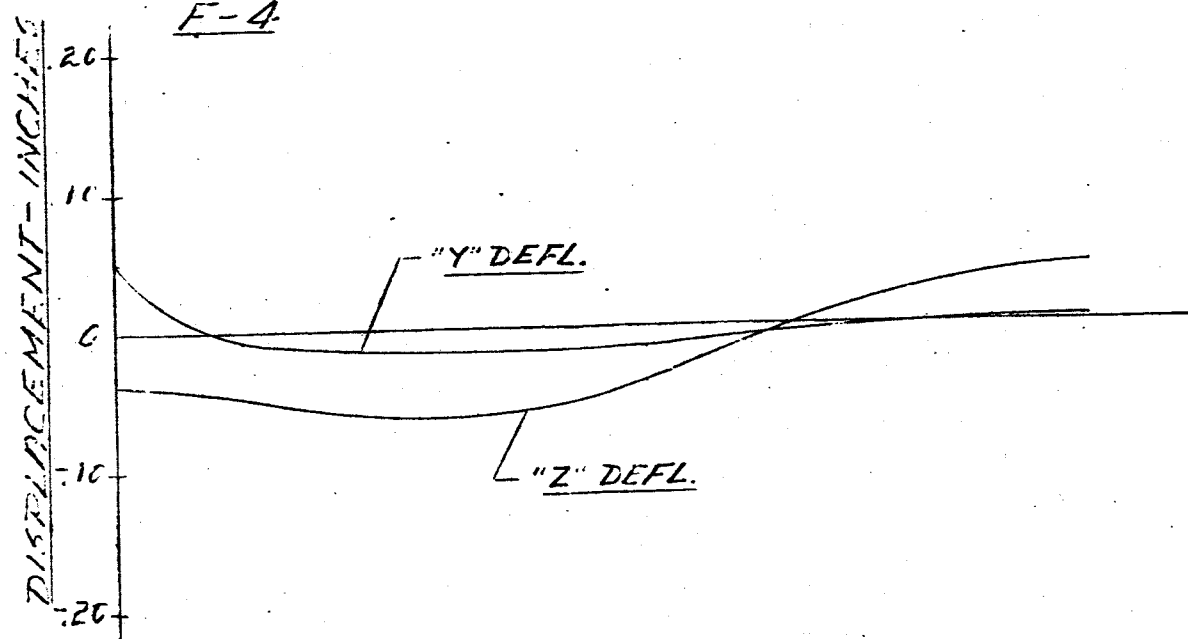
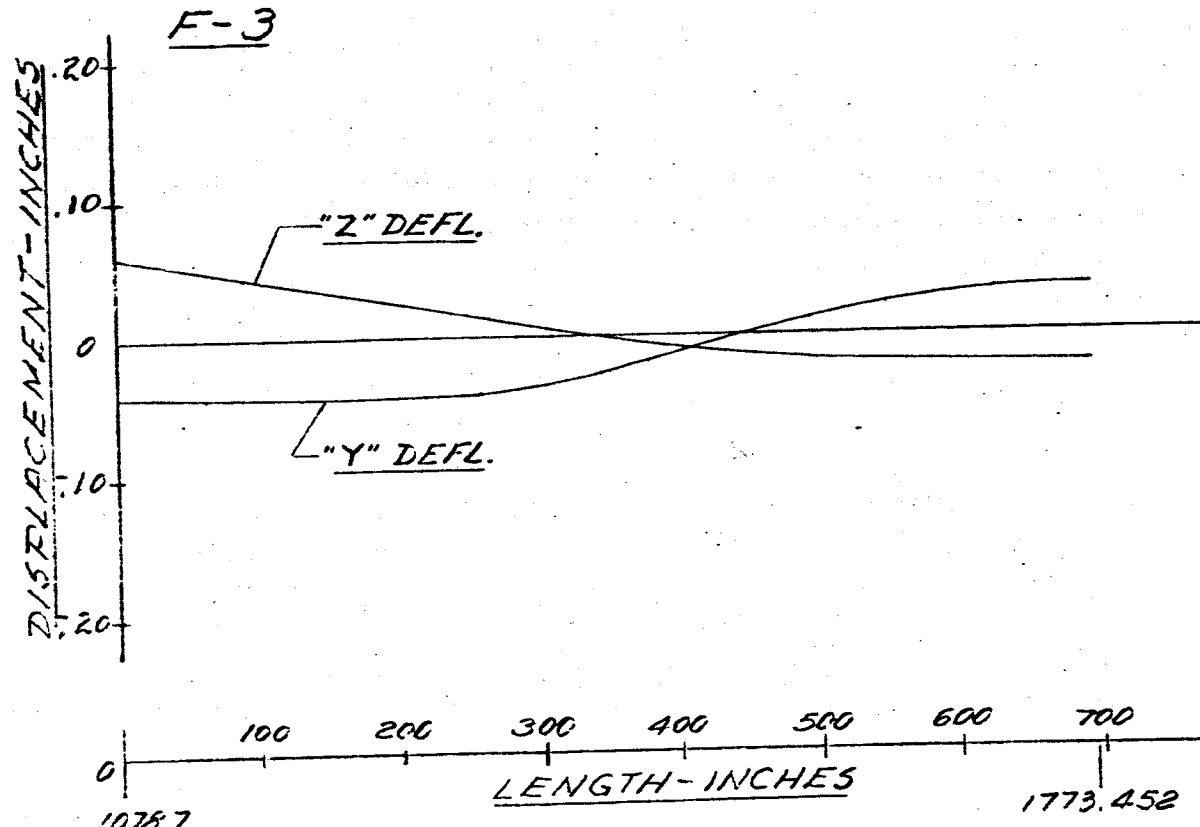
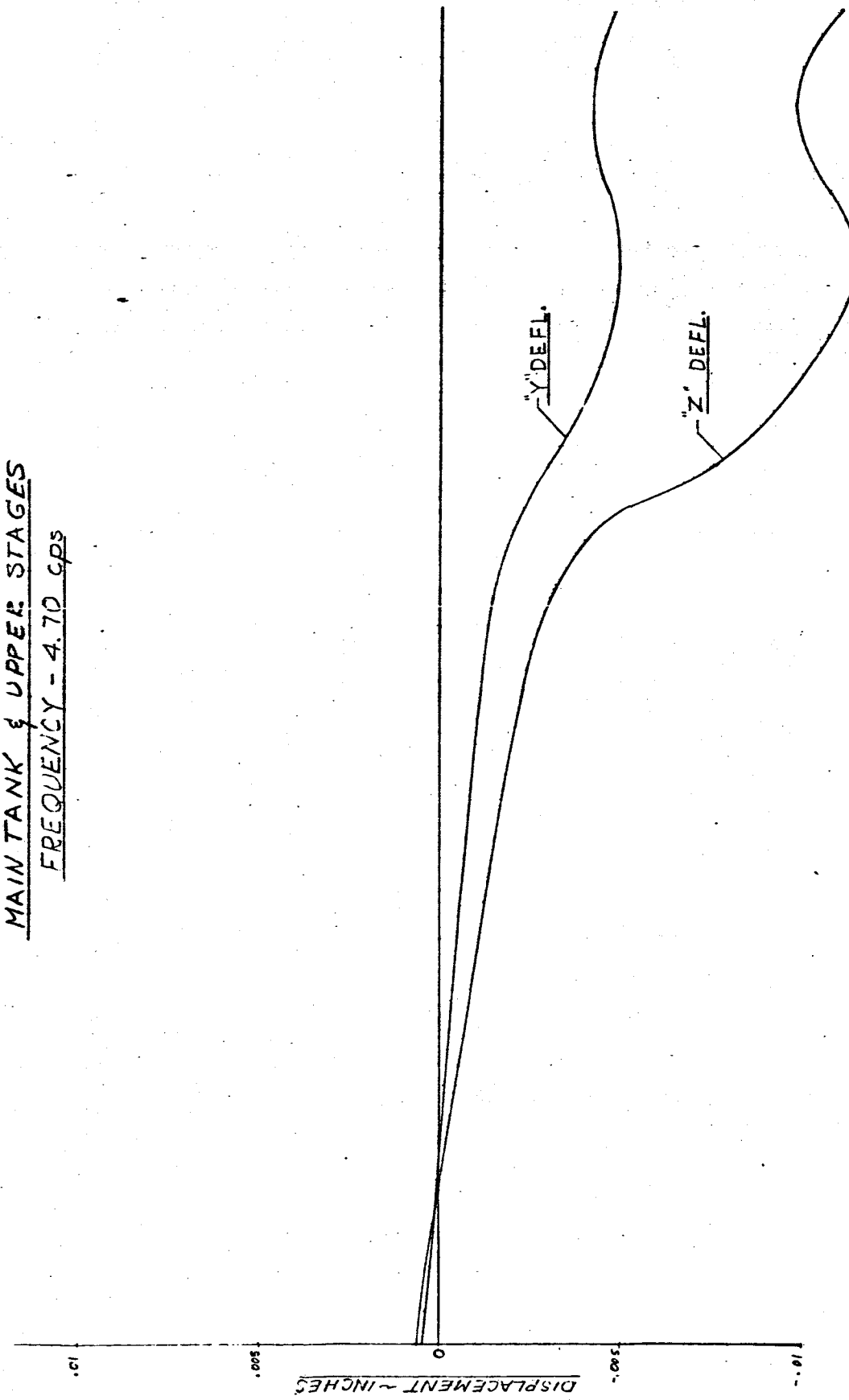


FIG. 158 DISPLACEMENT vs LENGTH SATURN SA-D1  
FREQUENCY = 4.60 CPS



-241-

FIG. 159 DISPLACEMENT VS LENGTH SATURN SA-DI  
MAIN TANK & UPPER STAGES  
FREQUENCY - 4.70 cps



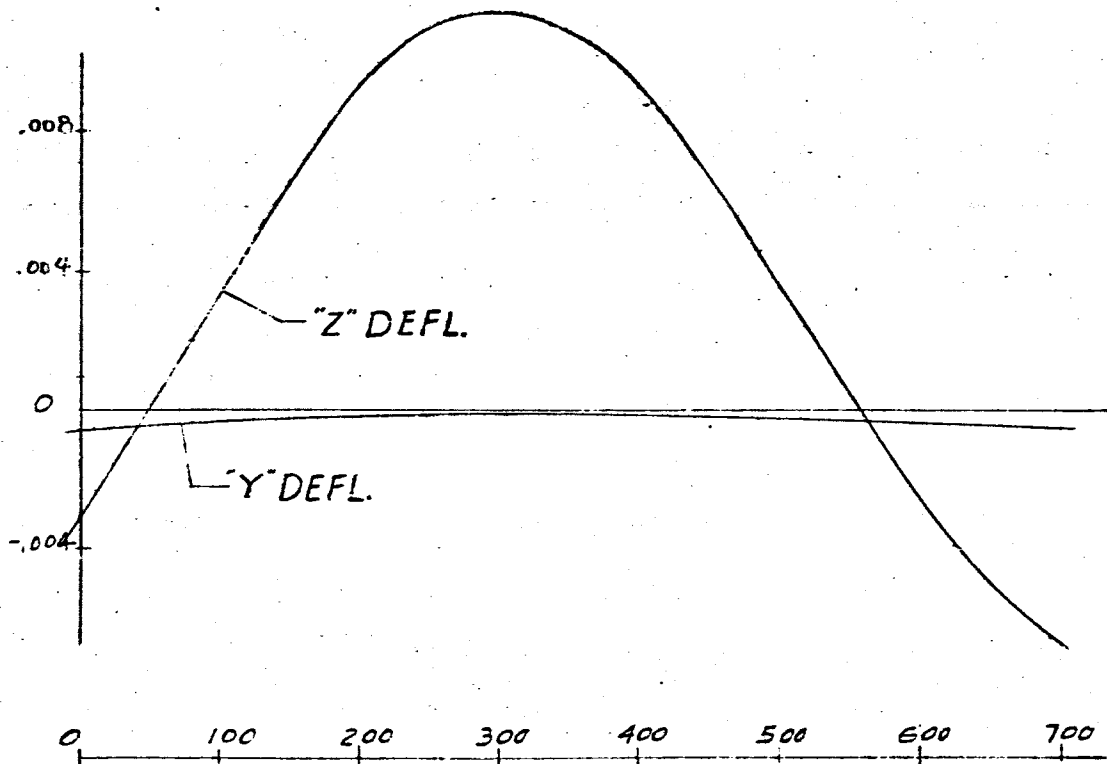
- 242 -

FIG. 160 DISPLACEMENT VS LENGTH SATURN SA-11

FREQUENCY = 4.70 CPS

L-1

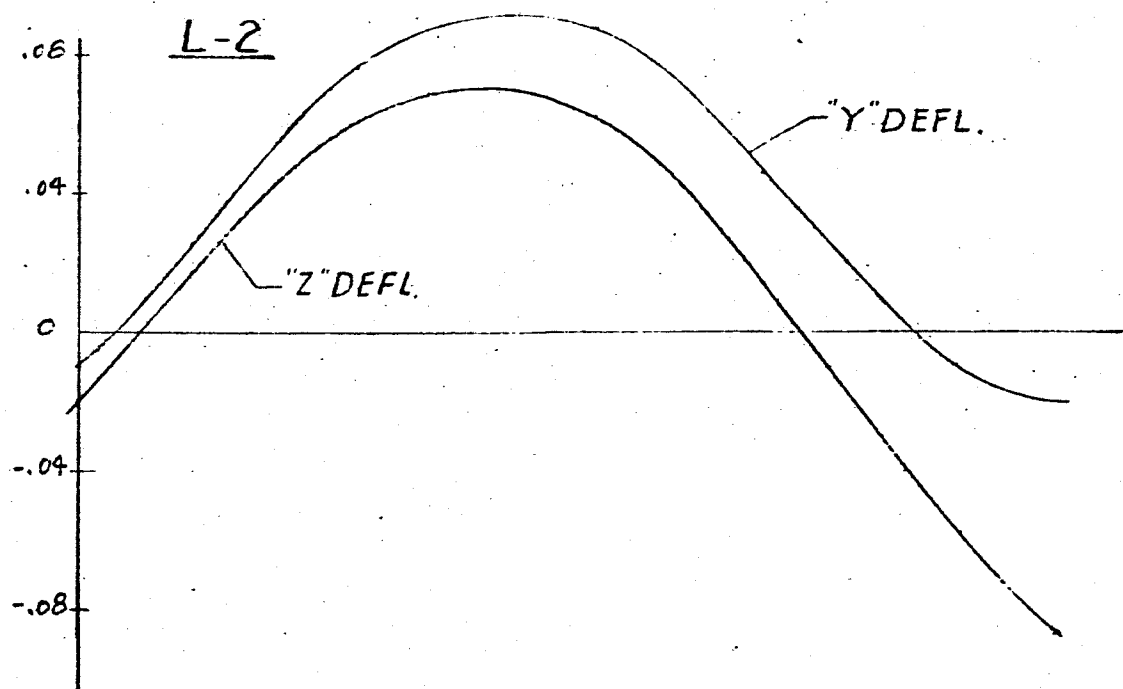
DISPLACEMENT - INCHES



LENGTH - INCHES

L-2

DISPLACEMENT - INCHES



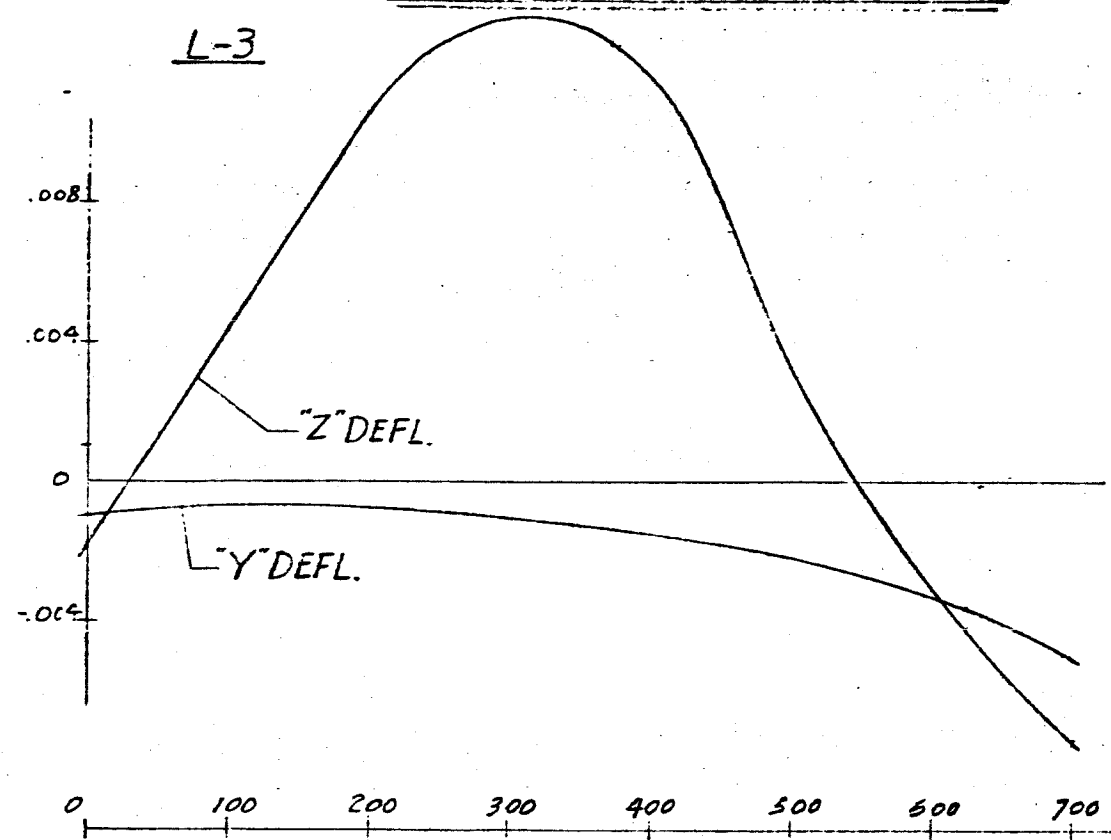
- 243 -

FIG. 161 DISPLACEMENT VS LENGTH SATURN SA-01

FREQUENCY = 4.70 C.P.S.

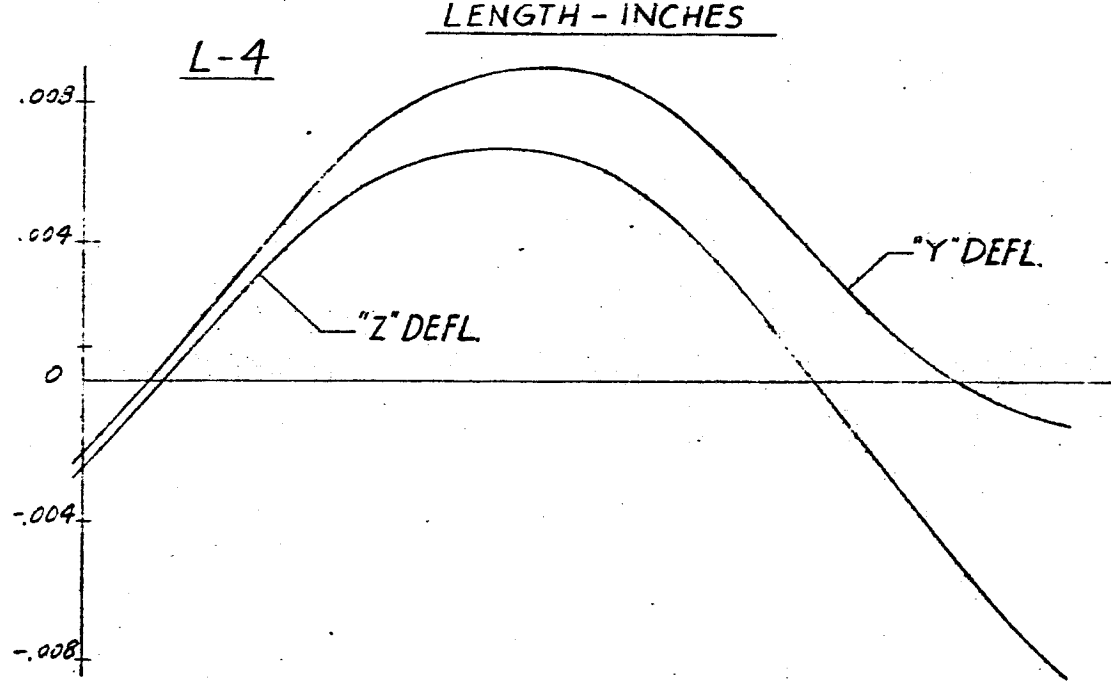
L-3

DISPLACEMENT - INCHES



L-4

DISPLACEMENT - INCHES

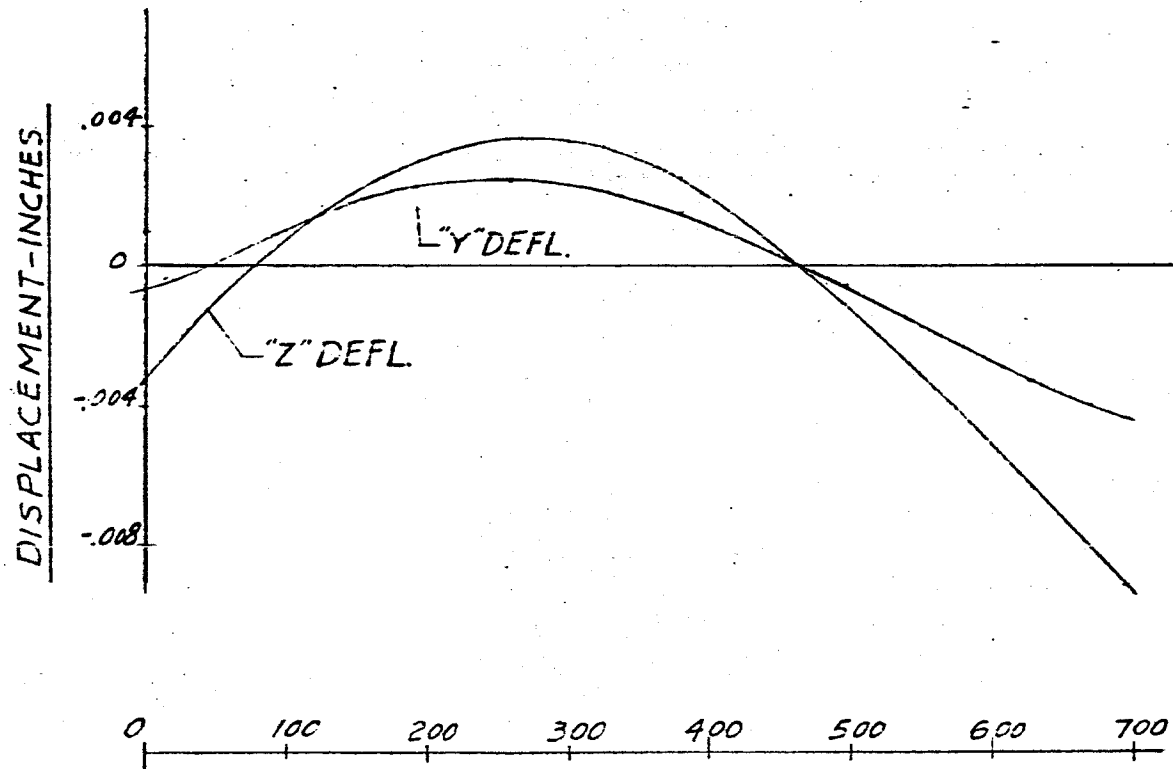


-244-

FIG. 162 DISPLACEMENT vs LENGTH SATURN SA-DI

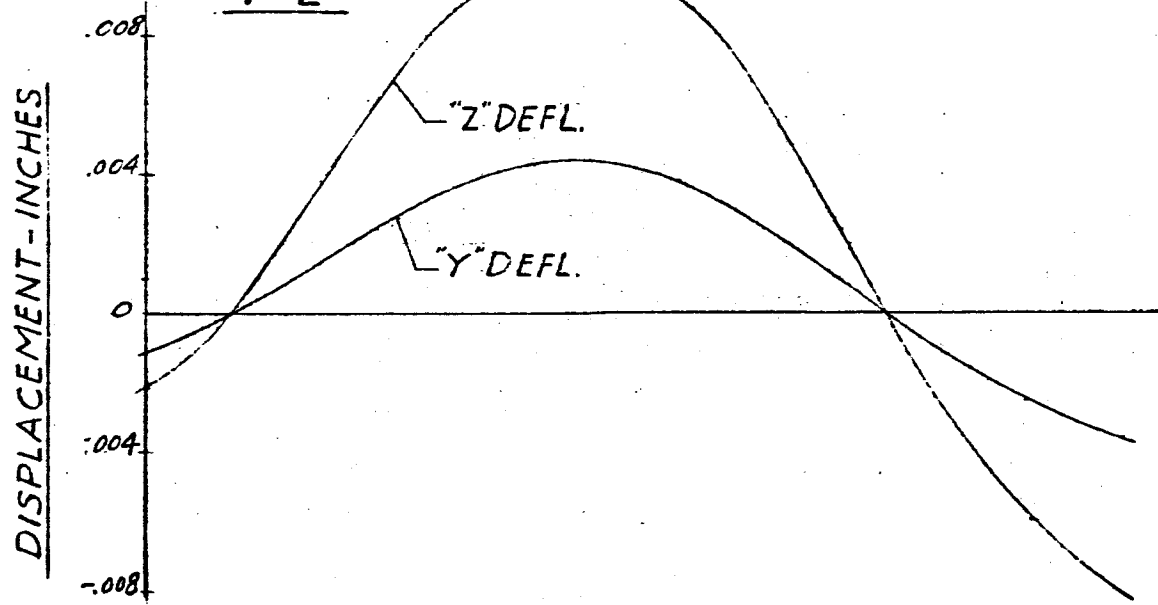
FREQUENCY = 4.70 CPS

F-1



LENGTH - INCHES

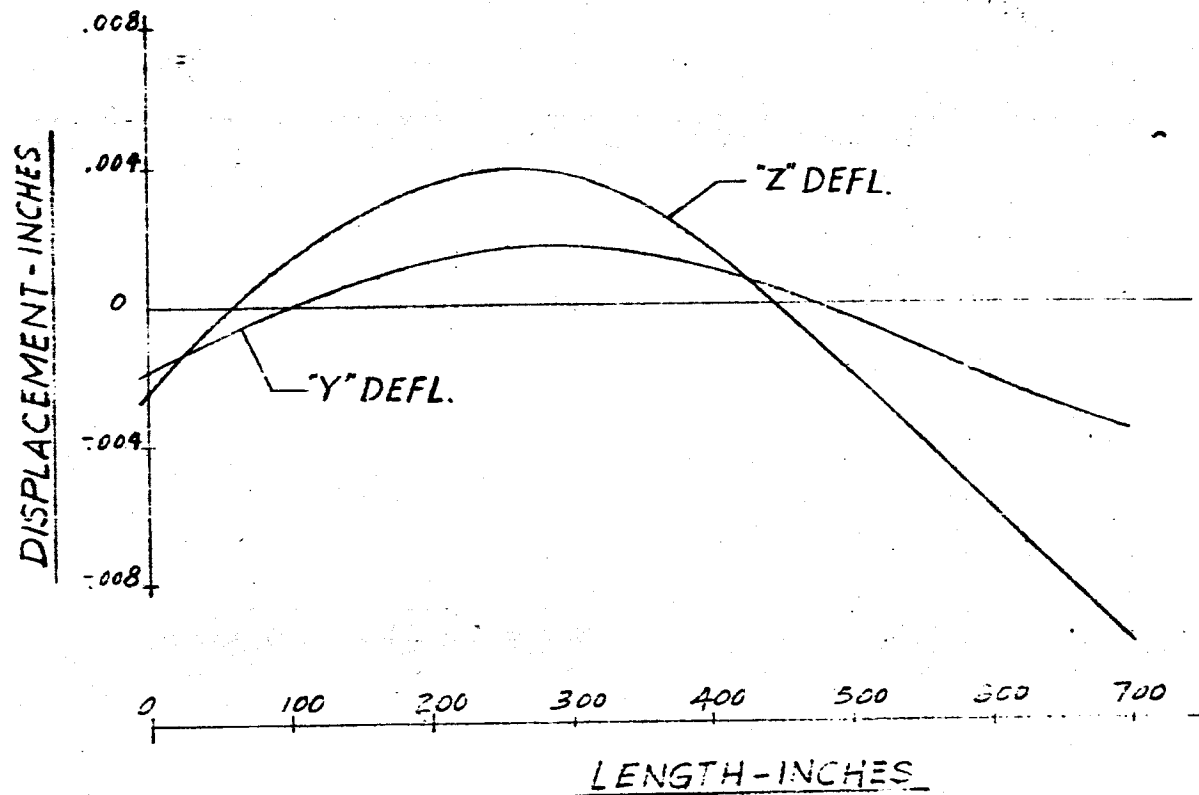
F-2



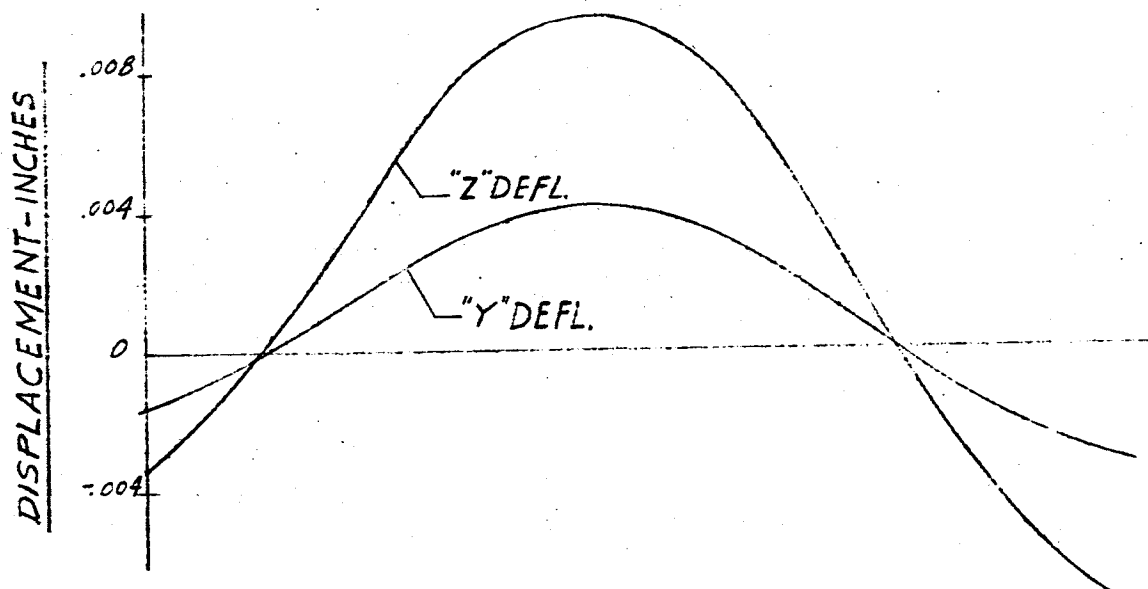
-245-

FIG. 163 DISPLACEMENT VS LENGTH SATURN SA-01  
FREQUENCY Y = 4.70 CPS

F-3

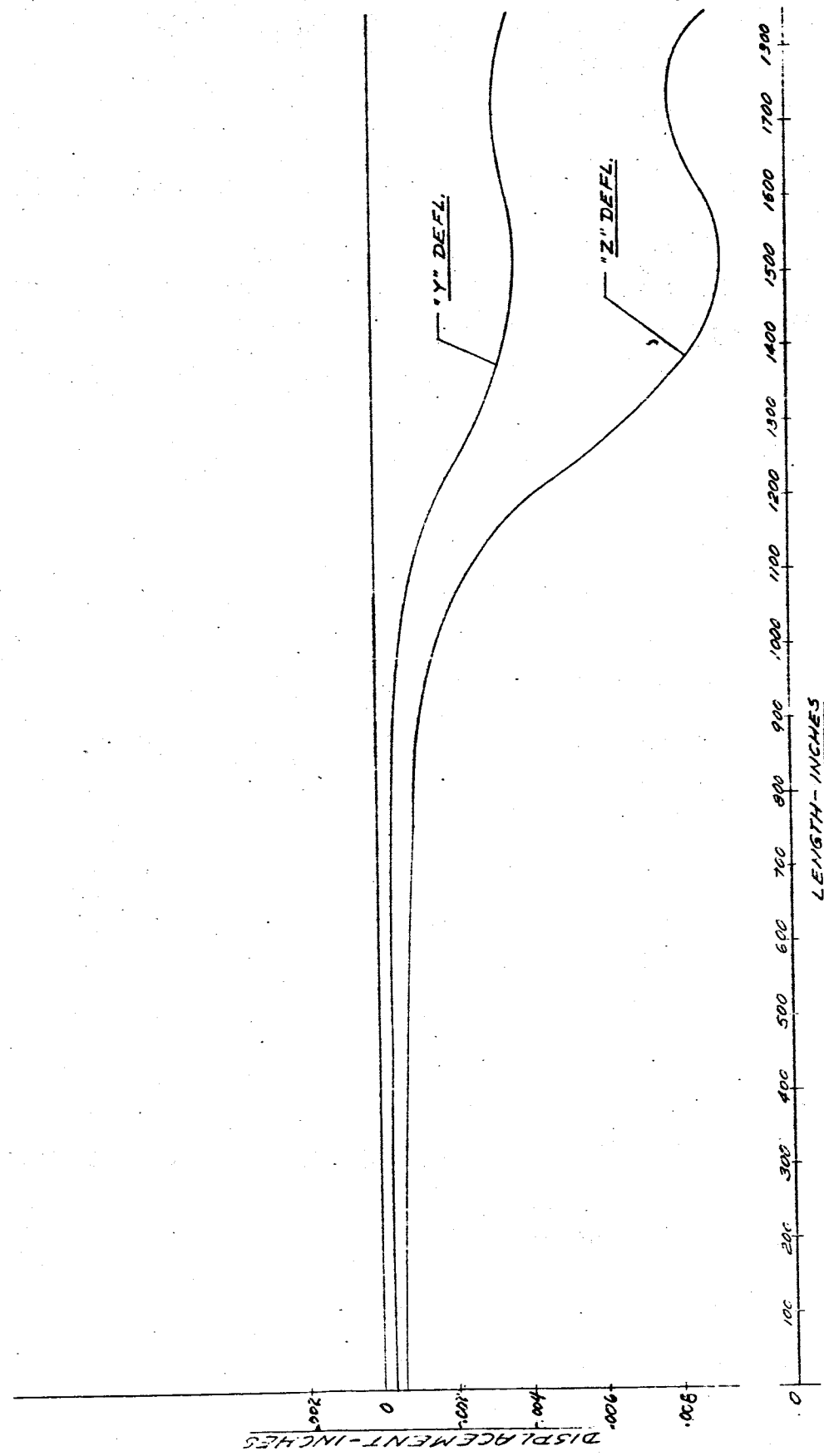


F-4



- 246 -

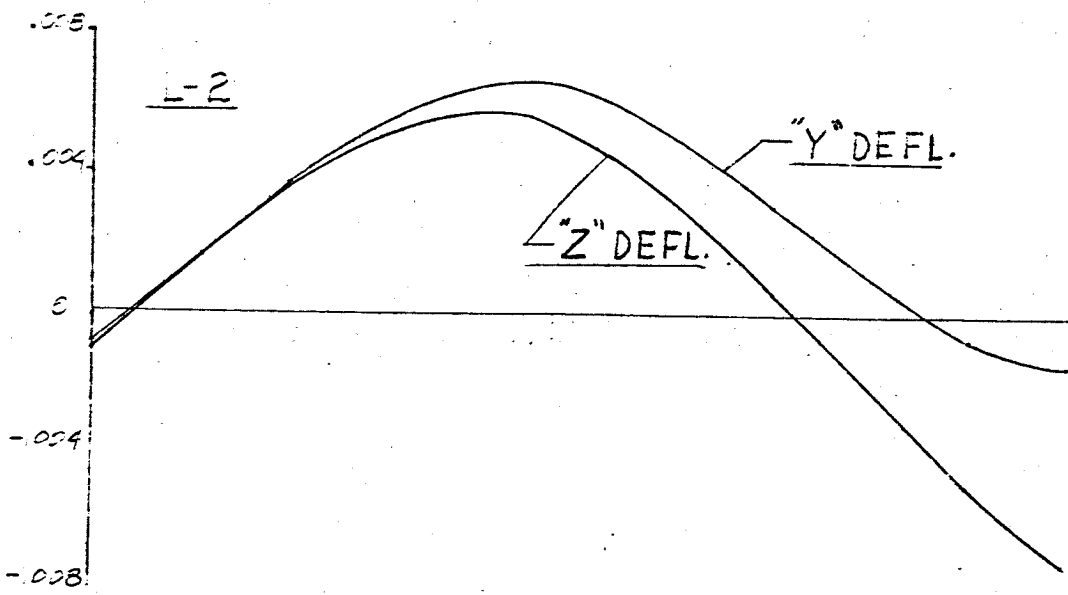
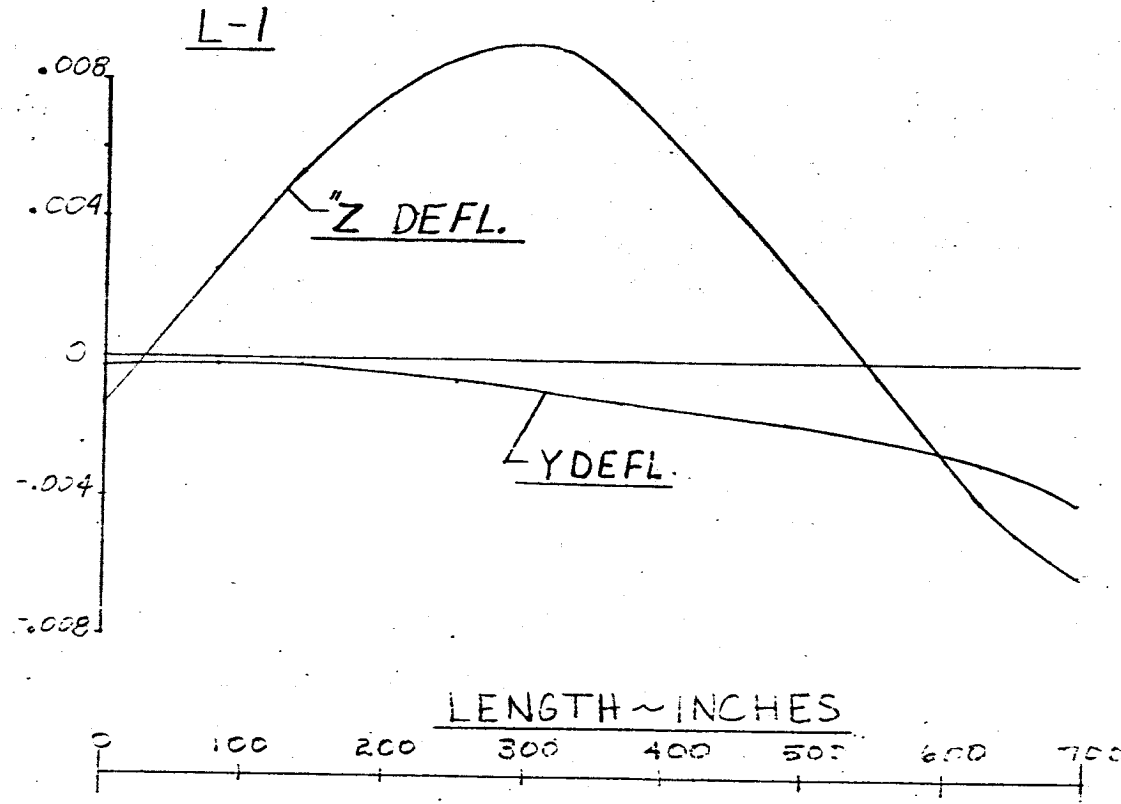
FIG. 164 DISPLACEMENT VS LENGTH SATURN SA-DI  
MAIN TANK & UPPER STAGES  
FREQUENCY = 4.80 cps



-247-

FIG. 165 DISPLACEMENT VS LENGTH SATURN SA-DI

FREQUENCY - 4.80 cps.



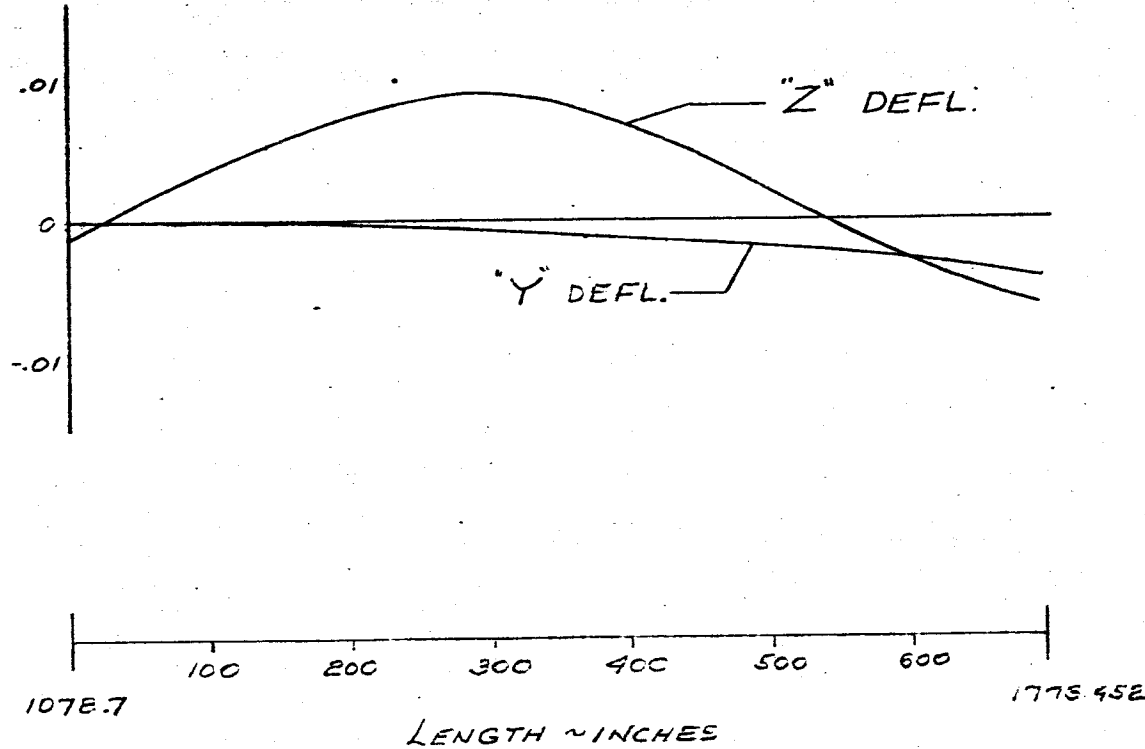
-248-

FIG 166 DISPLACEMENT VS LENGTH SATURN SA-DI

FREQUENCY = 4.80 CPS

DISPLACEMENT ~ INCHES

L-3

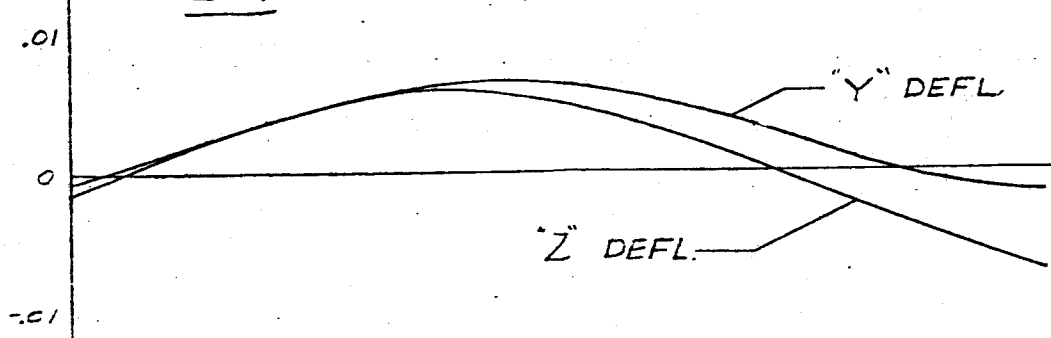


1078.7 1775.452

LENGTH ~ INCHES

DISPLACEMENT ~ INCHES

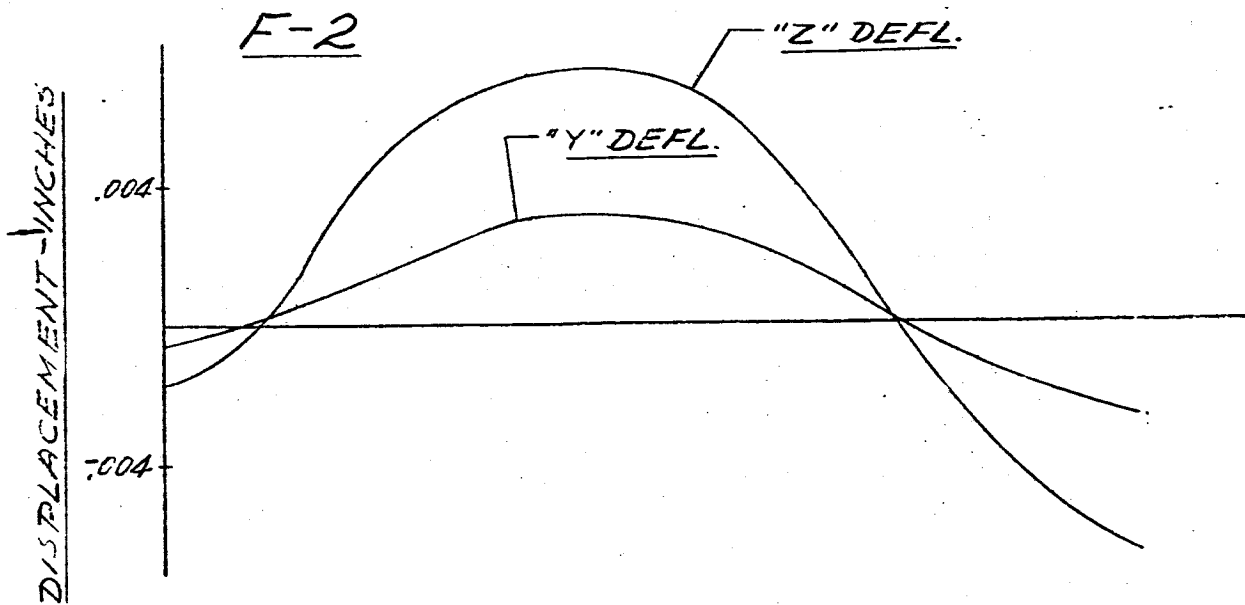
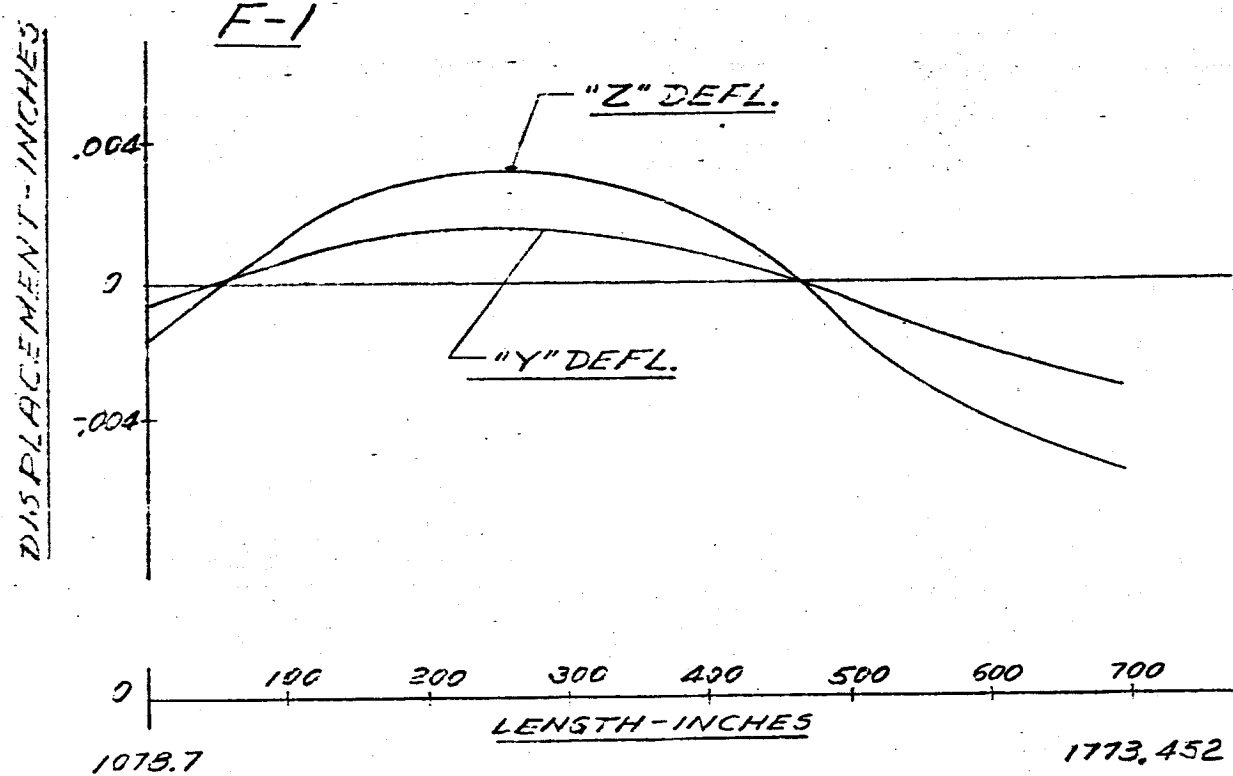
L-4



-249-

FIG 167 DISPLACEMENT VS LENGTH SATURN SA-DI

FREQUENCY = 4.90 CPS



-250-

FIG. 168 DISPLACEMENT vs LENGTH SATURN SA-01

FREQUENCY = 4.80 cps

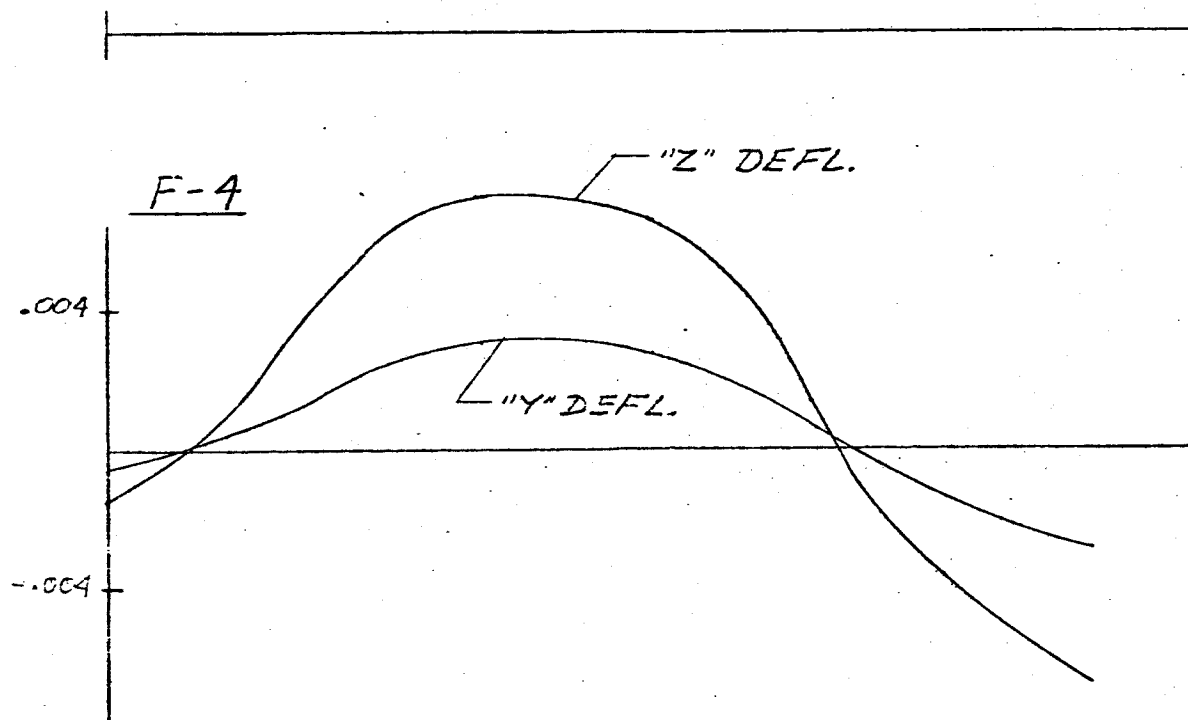
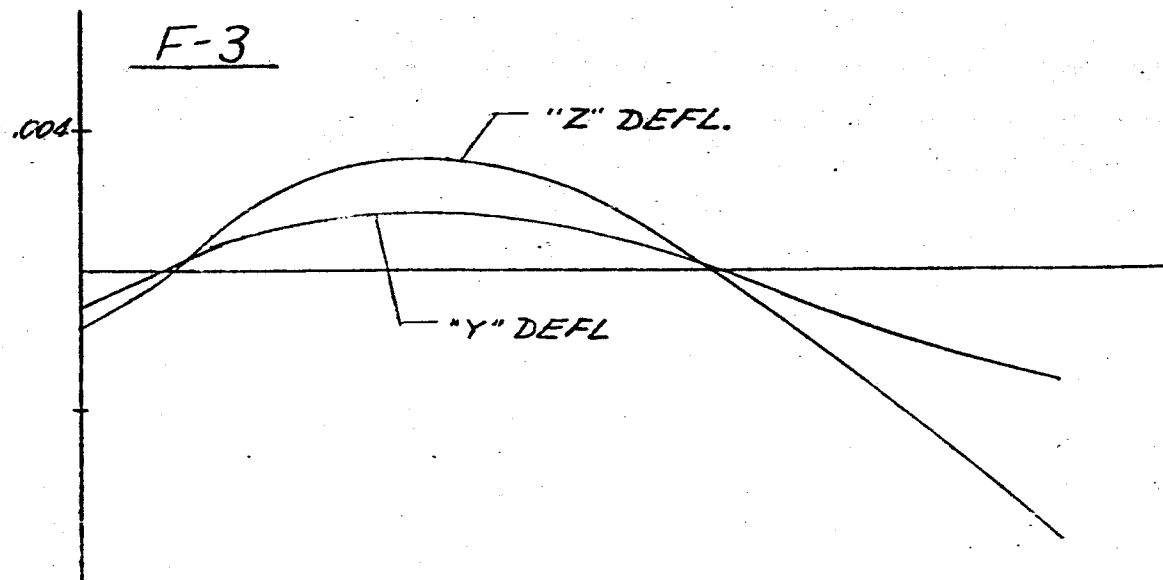
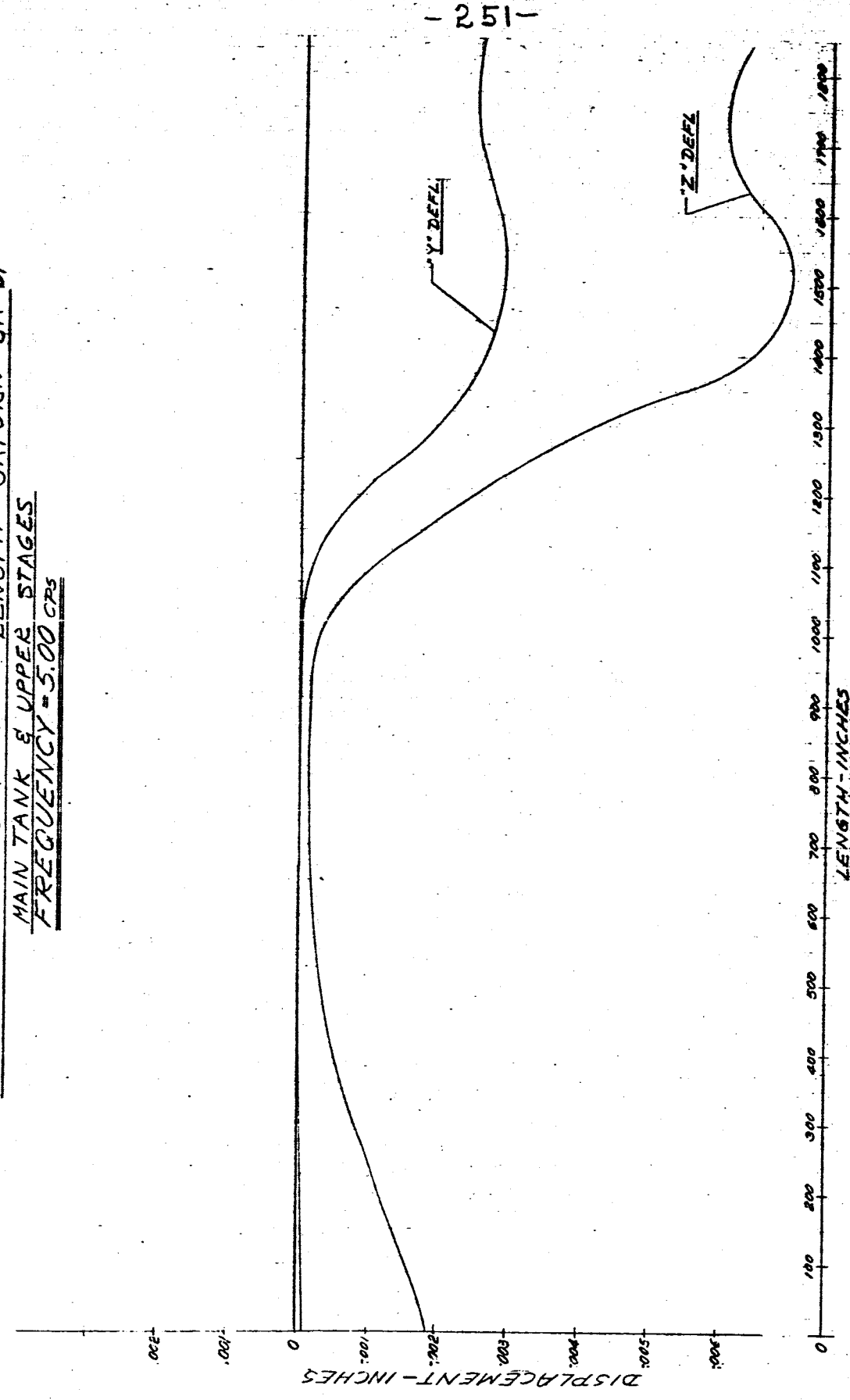


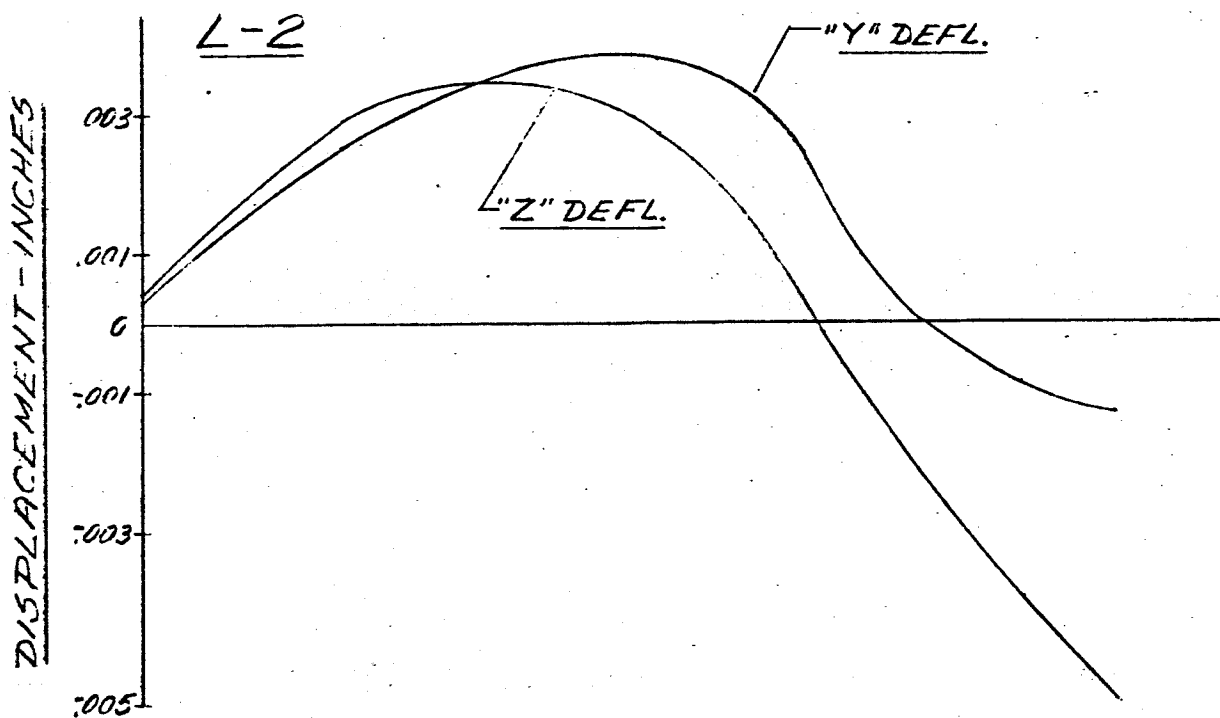
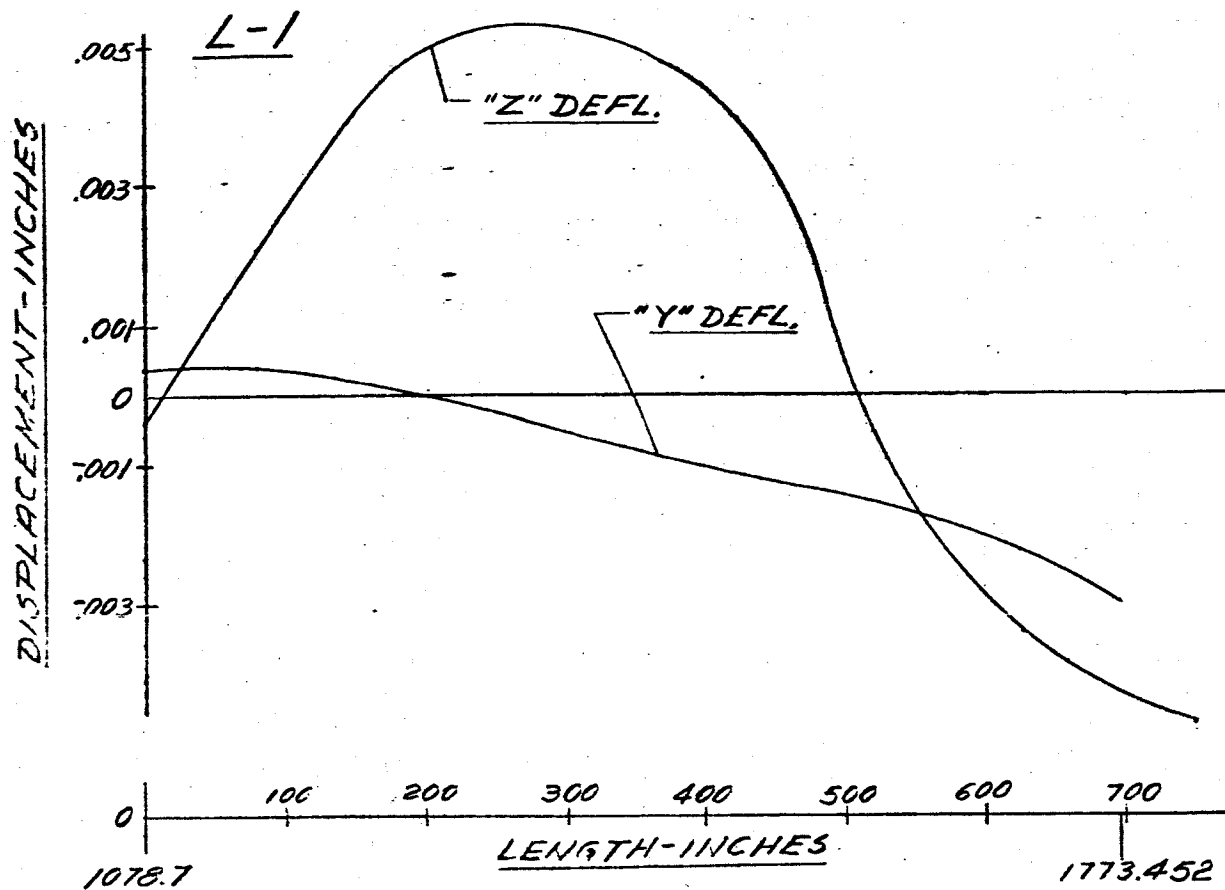
FIG. 169 DISPLACEMENT vs LENGTH SATURN SA-DI  
MAIN TANK & UPPER STAGES  
FREQUENCY = 5.00 CPS



-252-

FIG. 170 DISPLACEMENT VS LENGTH SATURN SA-DI

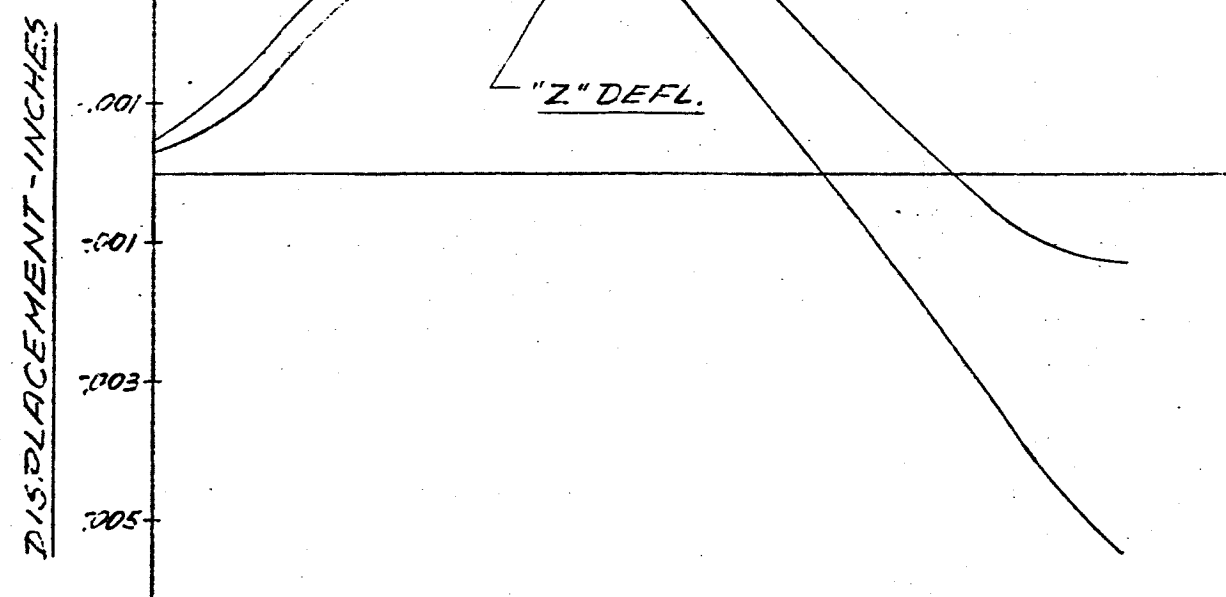
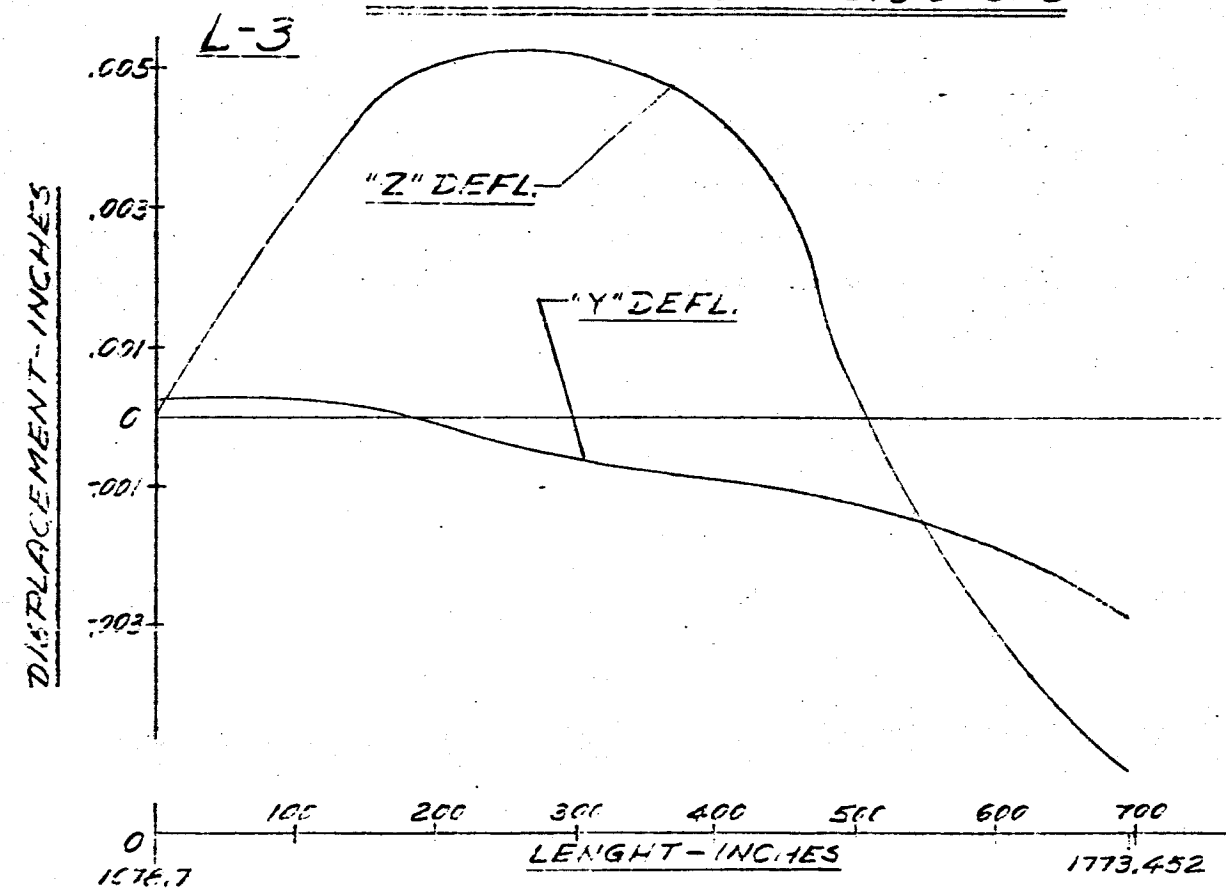
FREQUENCY = 5.00 CPS



-253-

FIG. 171 DISPLACEMENT VS LENGTH SATURN SA-DI

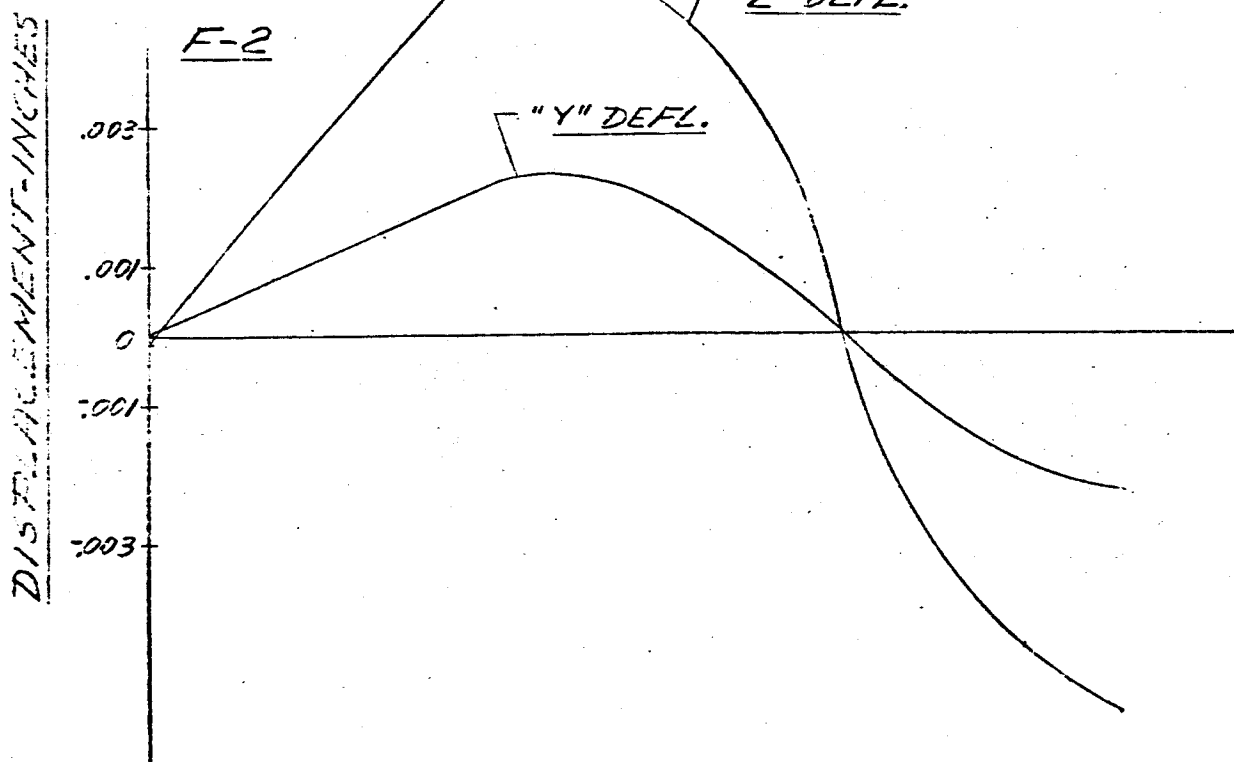
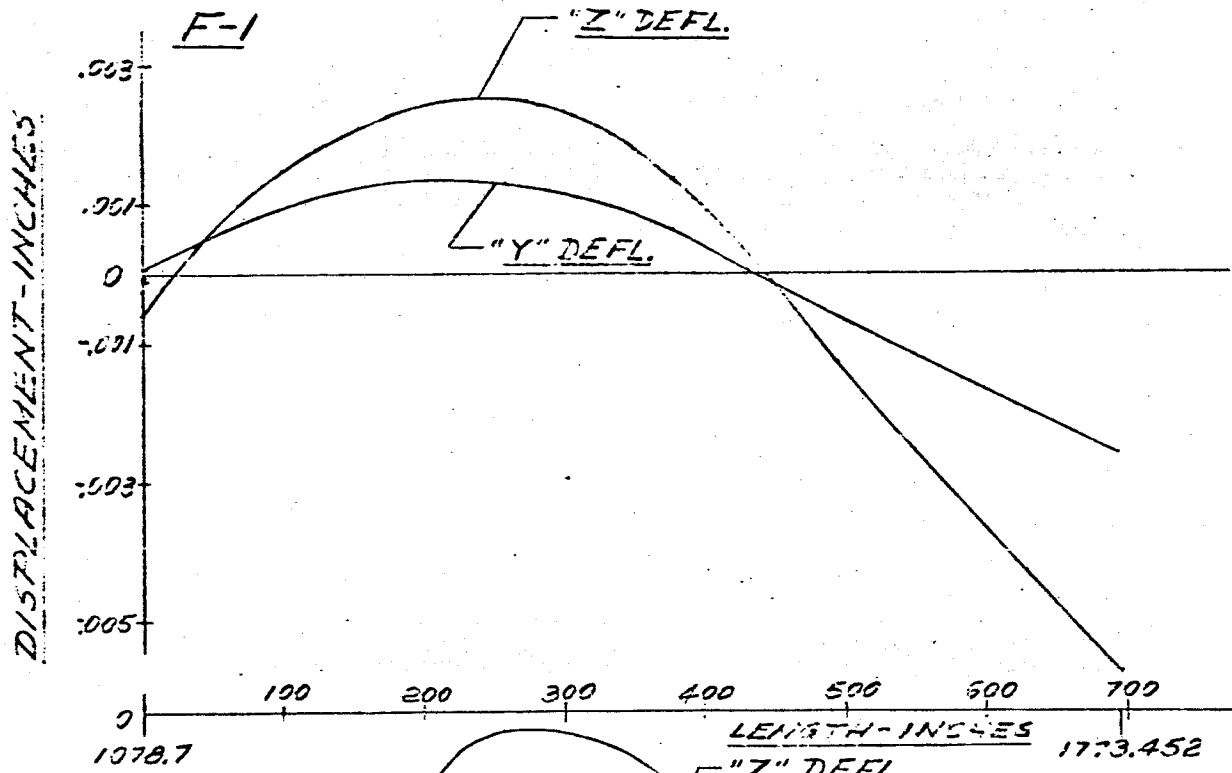
FREQUENCY = 5.00 CPS



-254-

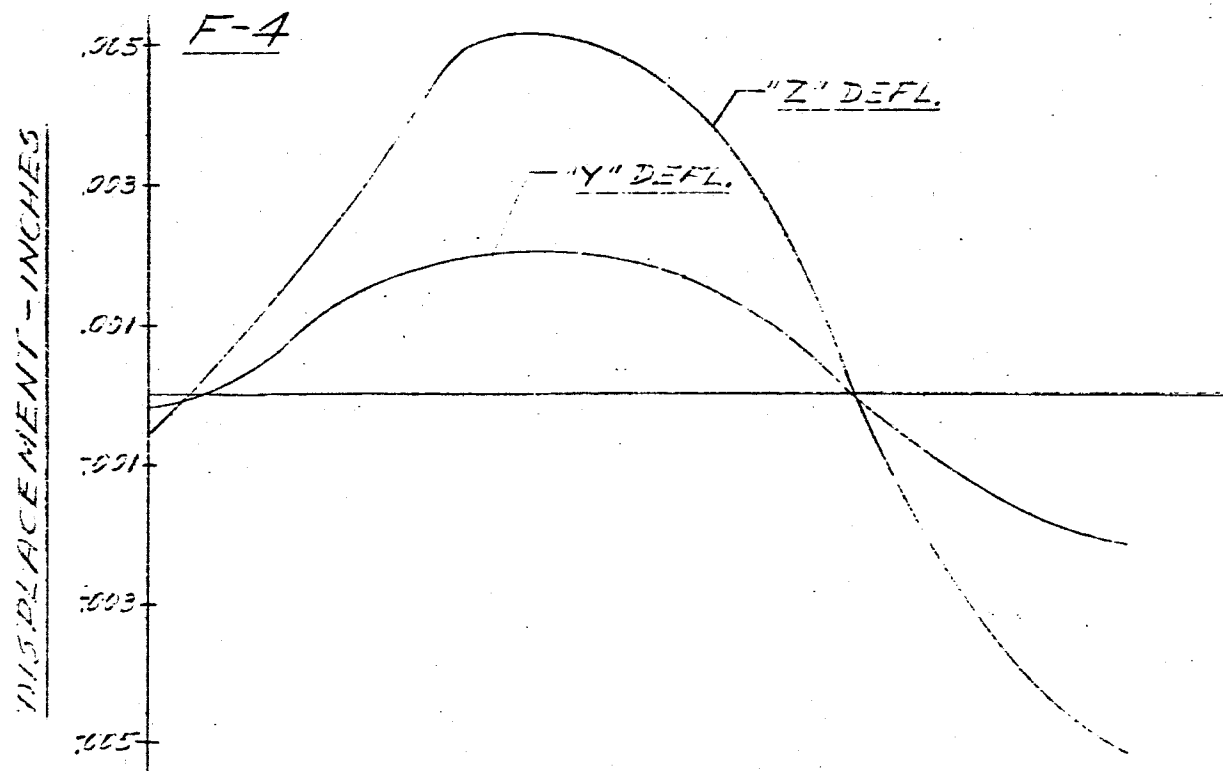
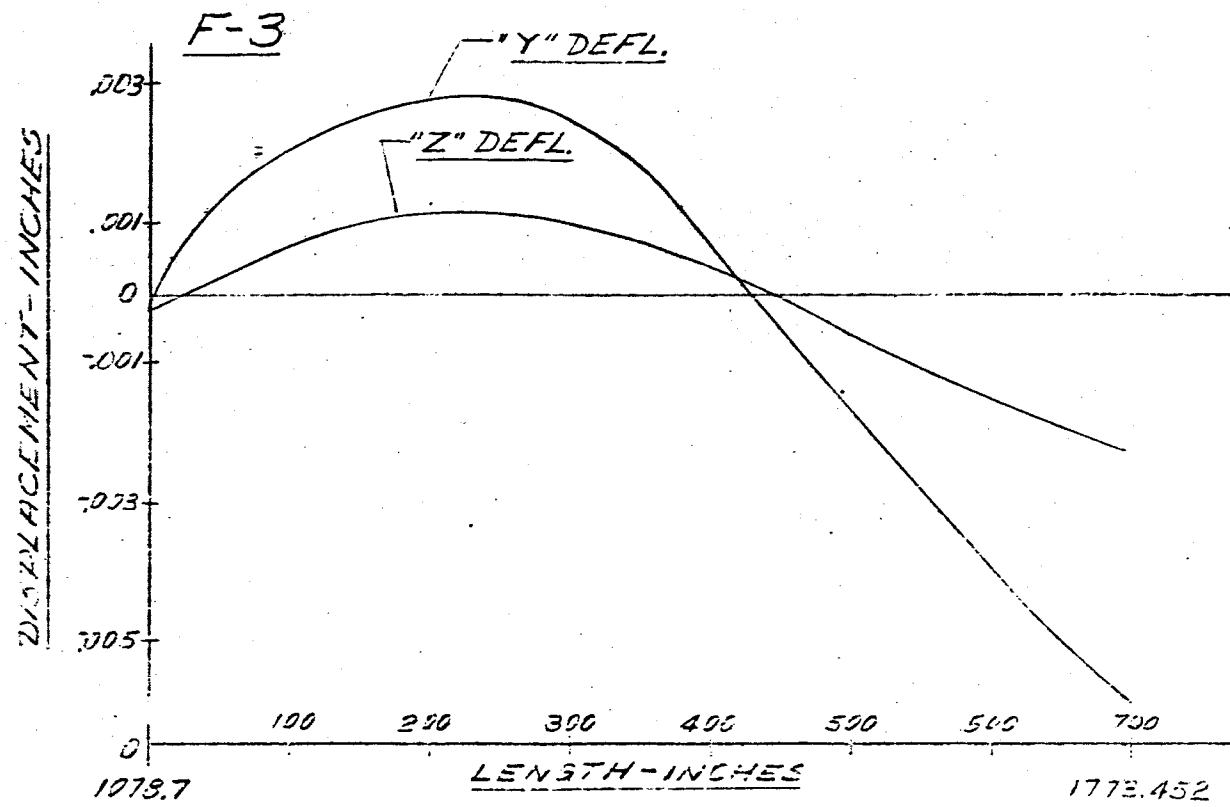
FIG 172. DISPLACEMENT VS LENGTH SHTURIS SA-51

FREQUENCY = 5.00 CPS



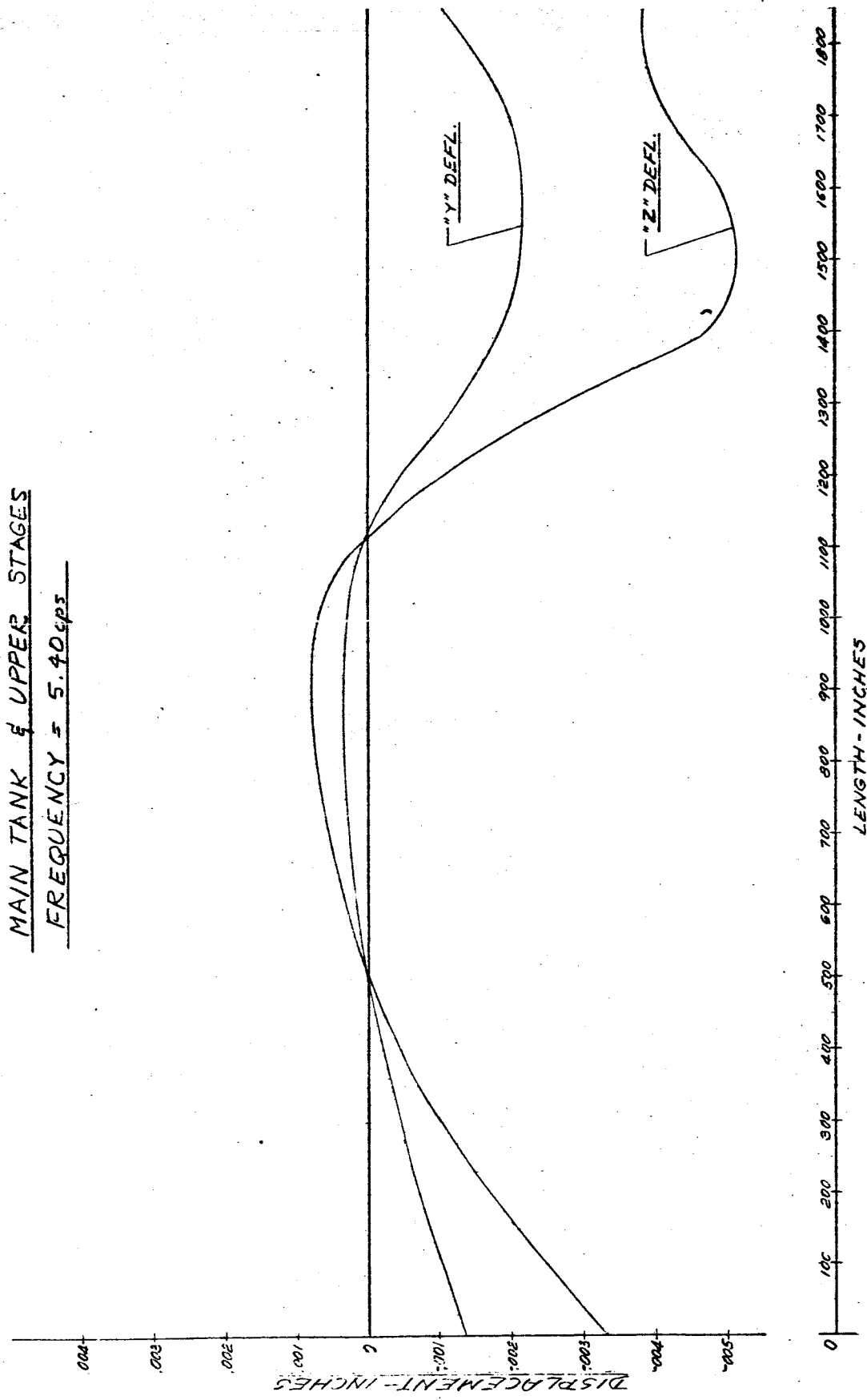
-255-

FIG 173 DISPLACEMENT VS LENGTH SATURN SA-DI  
FREQUENCY = 5.00 CPS



- 256 -

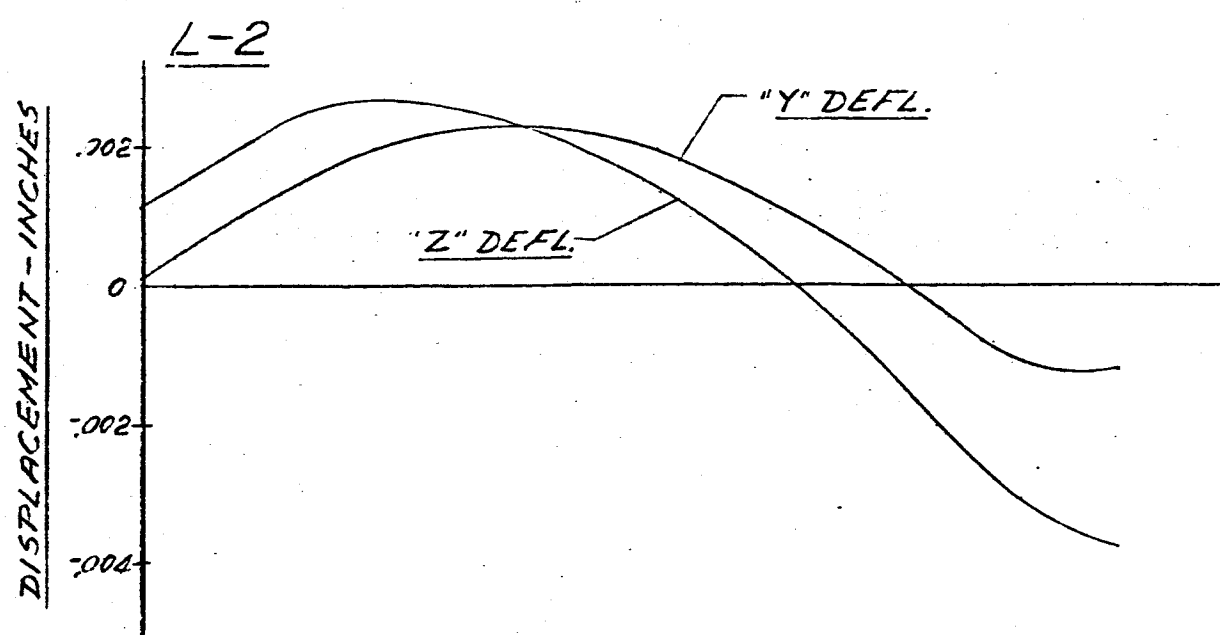
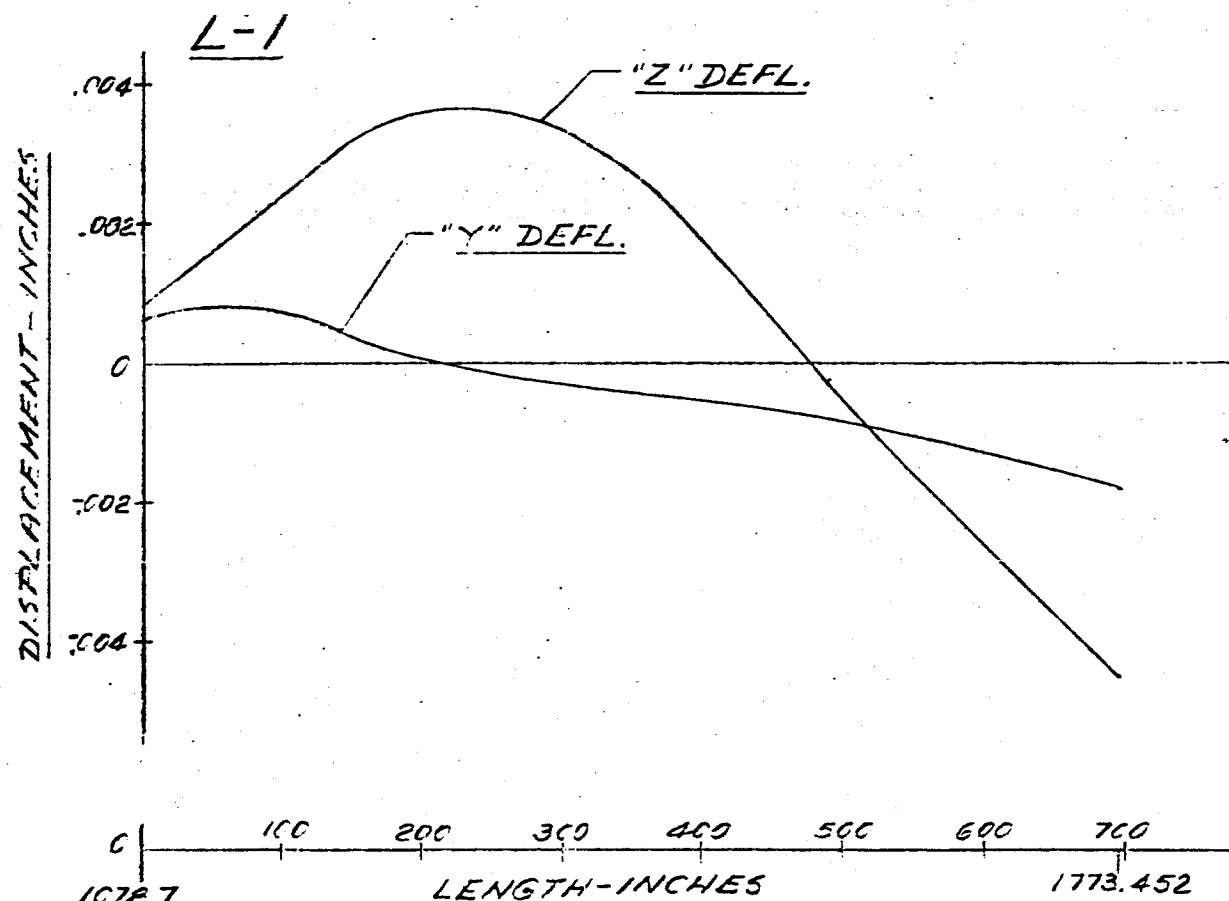
FIG. 174 DISPLACEMENT vs LENGTH SATURN SA-D1  
MAIN TANK & UPPER STAGES  
FREQUENCY = 5.40 cps



-257-

FIG 175 DISPLACEMENT VS LENGTH SATURN SA-DI

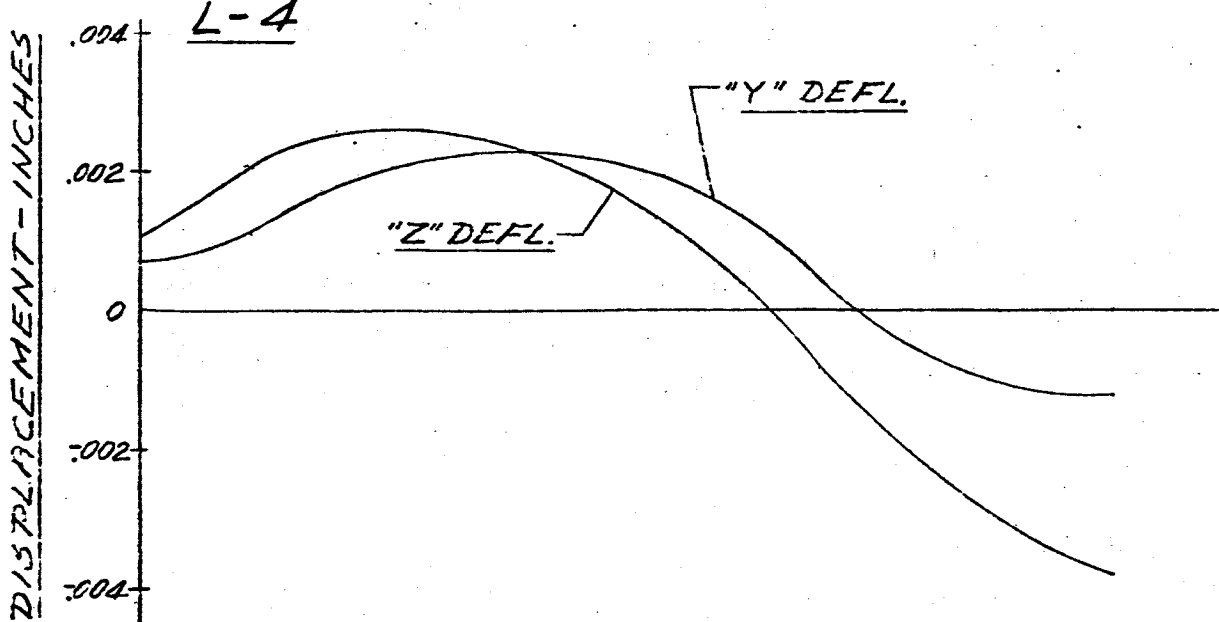
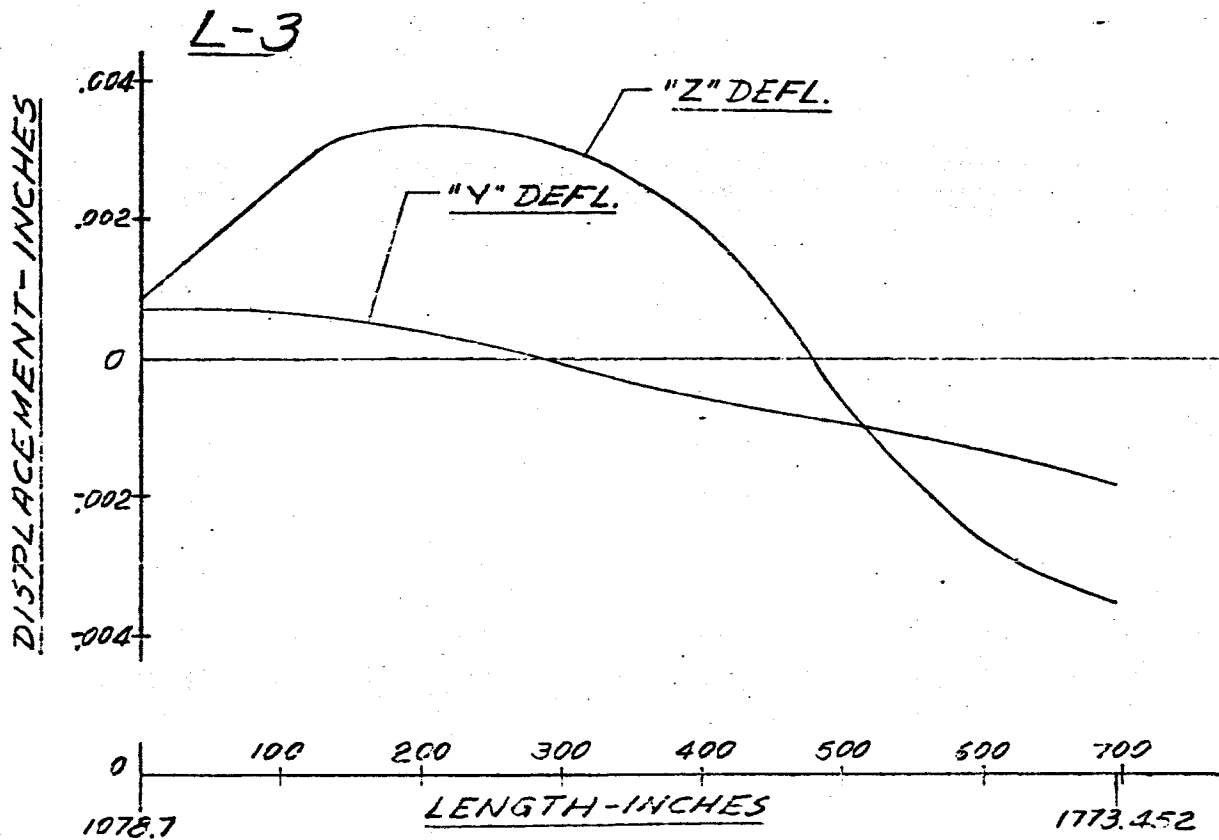
FREQUENCY = 5.40 CPS



-258-

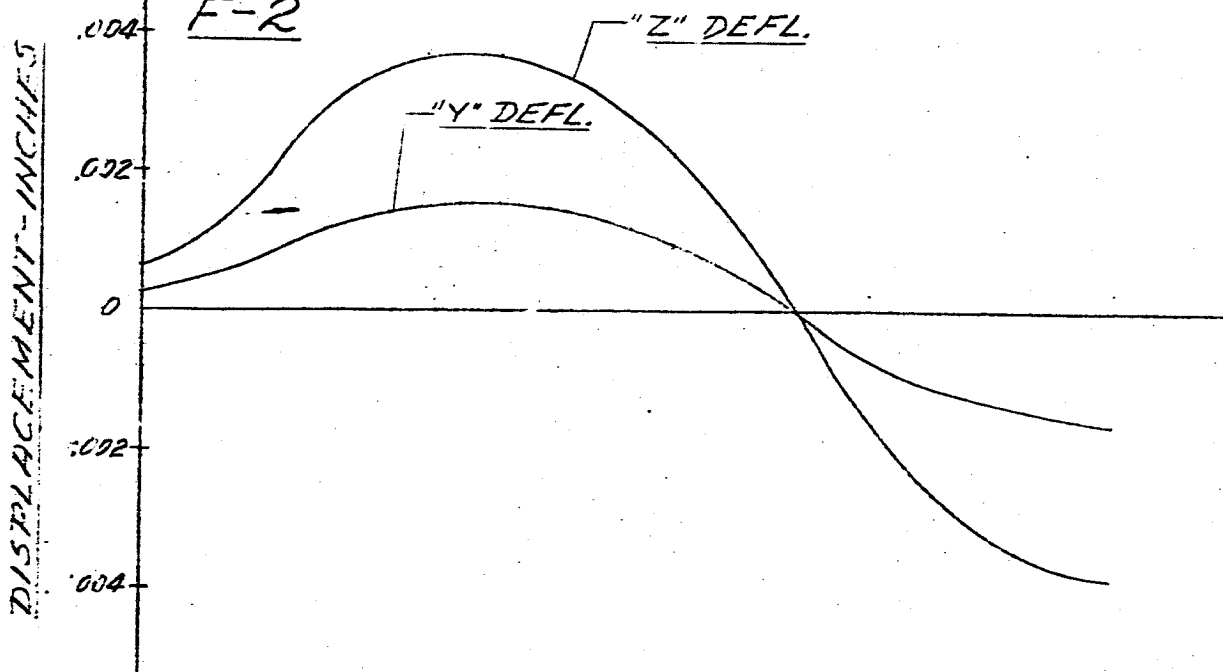
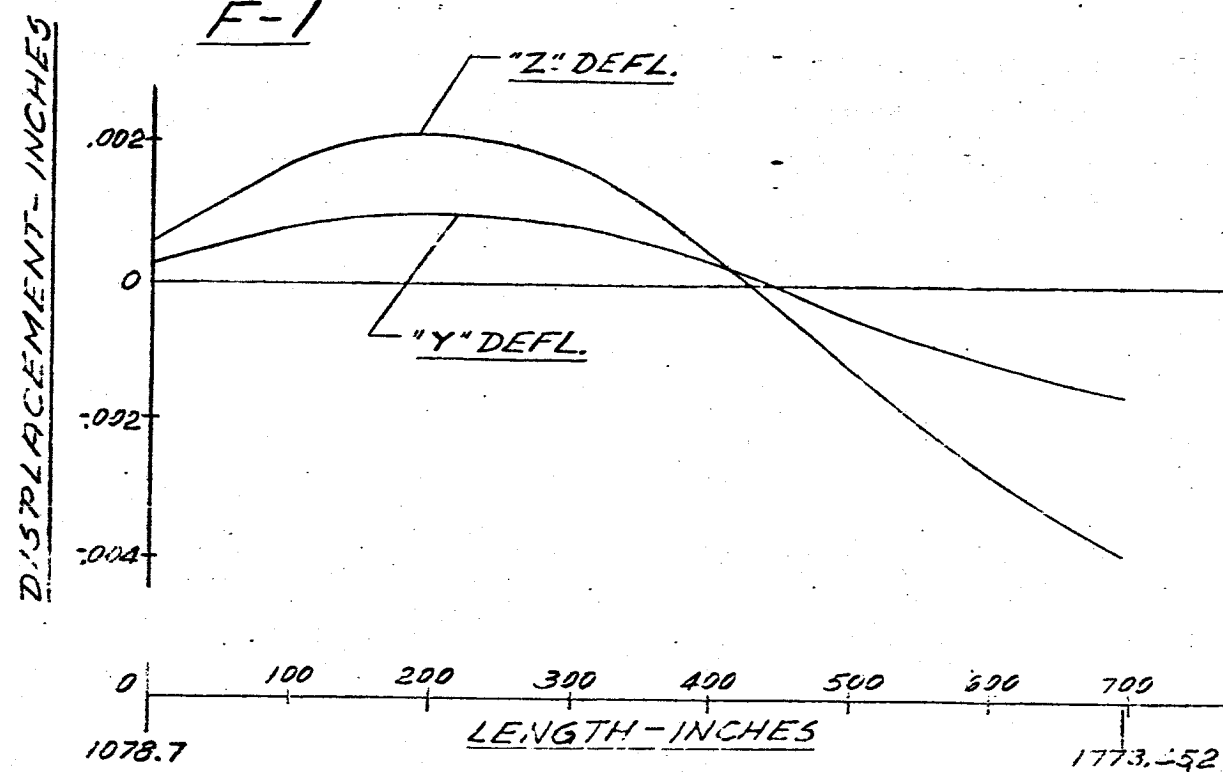
FIG. 176 DISPLACEMENT VS LENGTH SATURN SA-DI

FREQUENCY = 5.40 CPS



-259-

FIG. 177 DISPLACEMENT VS LENGTH SATURN SA-DI  
FREQUENCY = 5.40 CPS



-260-

FIG 178 DISPLACEMENT VS LENGTH SATURN SA DI  
FREQUENCY = 5.40 CPS

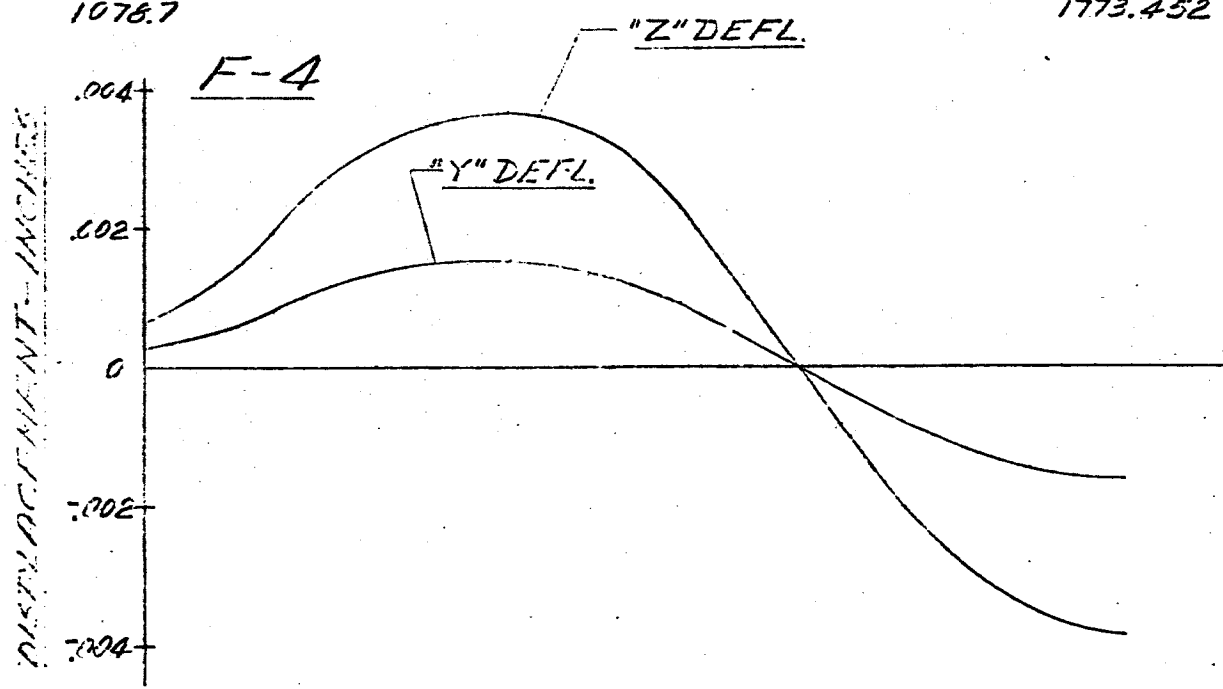
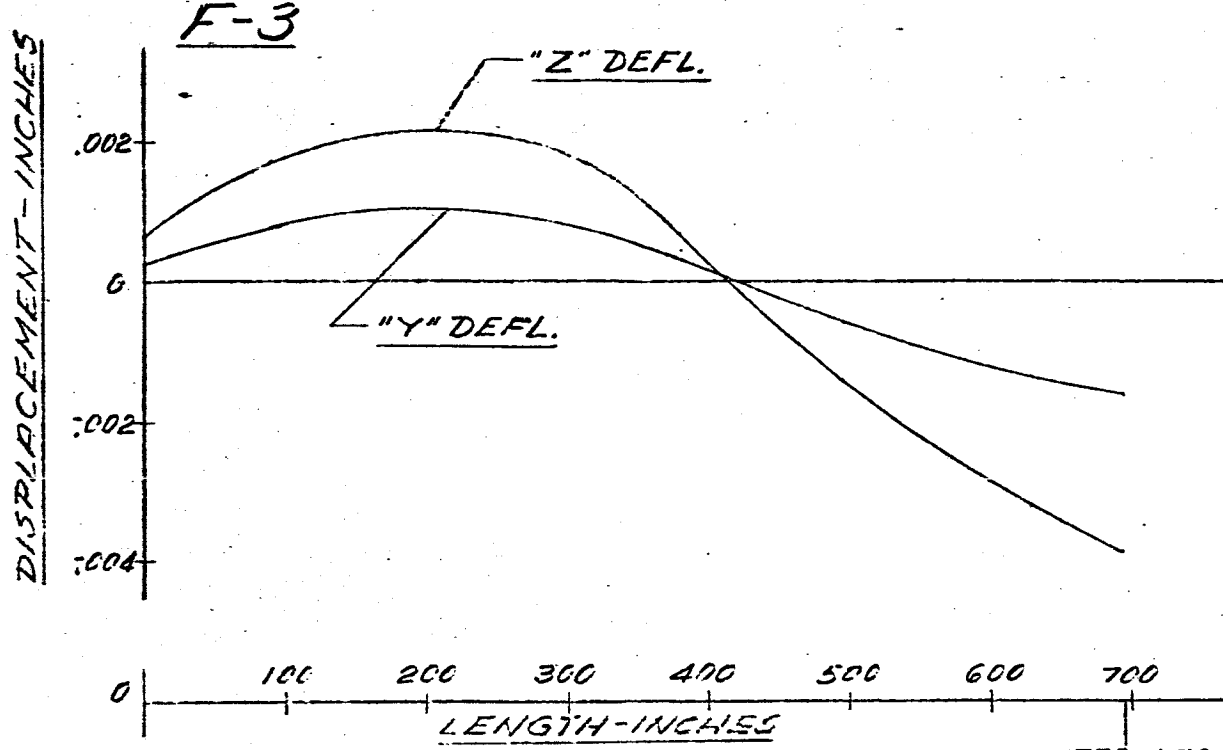
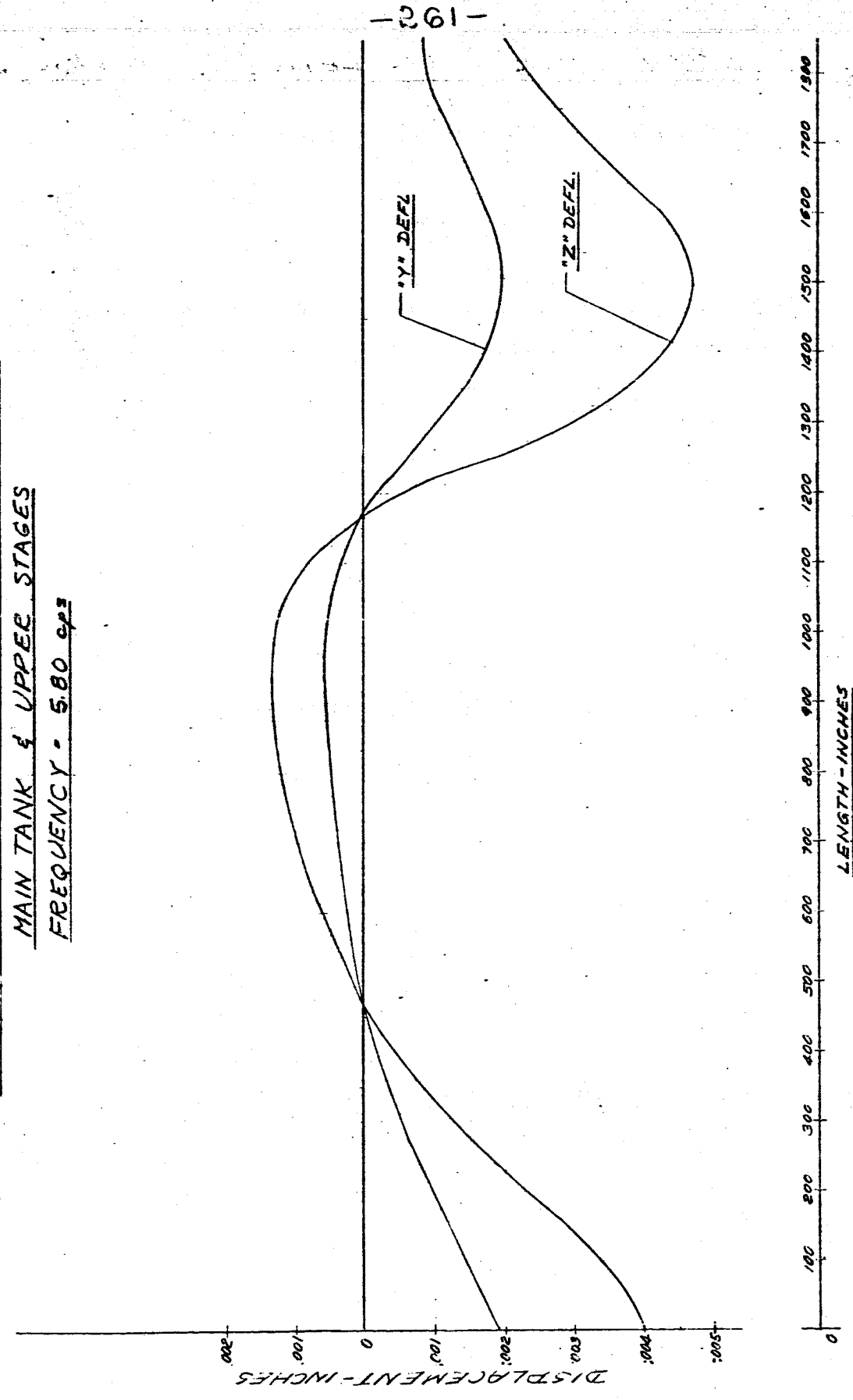


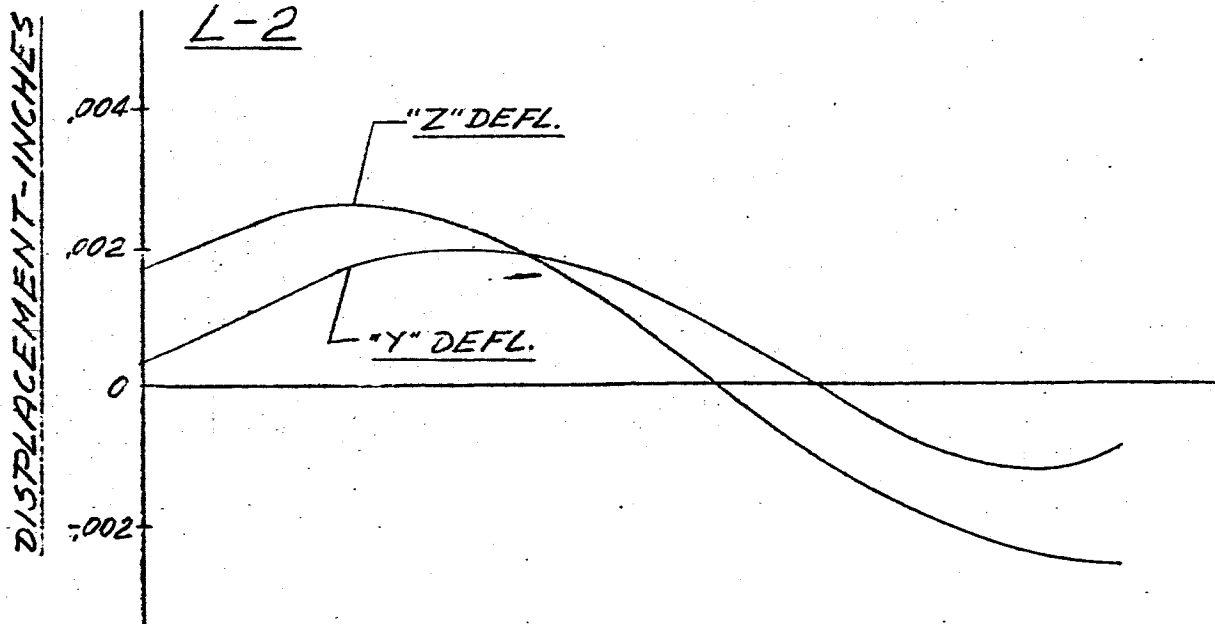
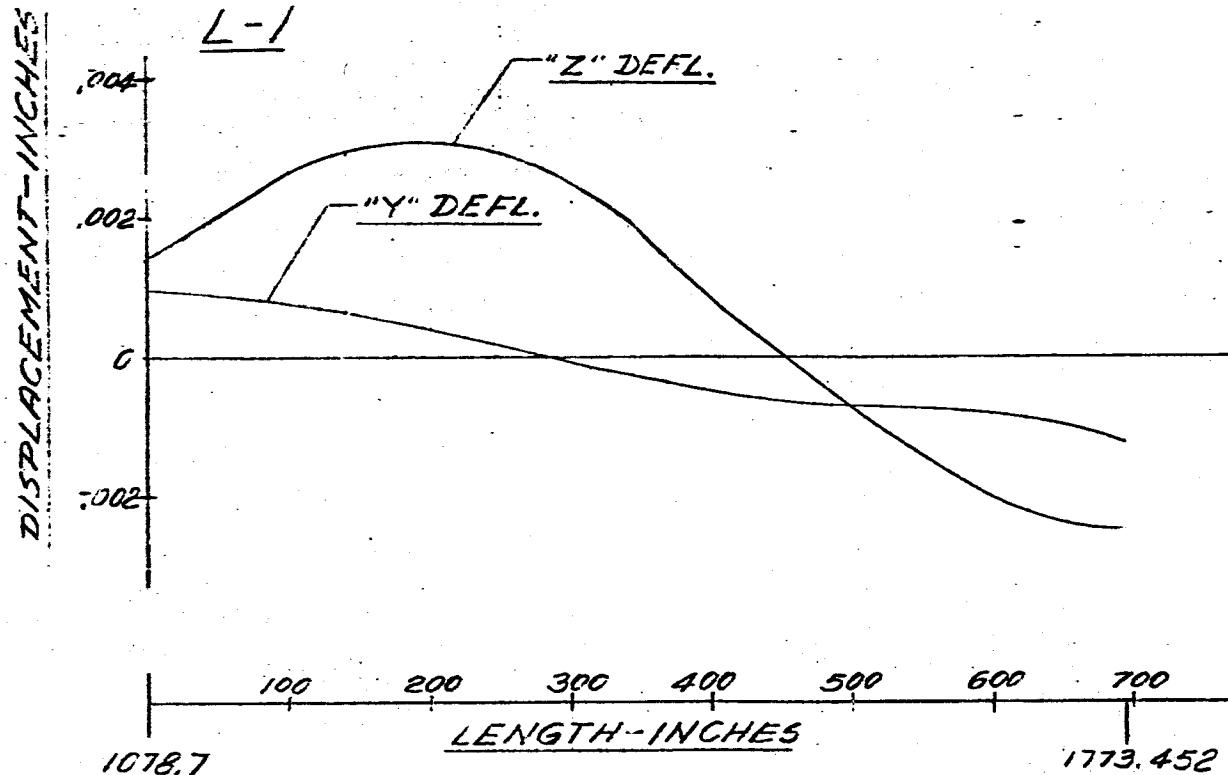
FIG. 179 DISPLACEMENT vs LENGTH SATURN SA-DI  
MAIN TANK & UPPER STAGES  
FREQUENCY - 5.80 cps



-262-

FIG. 18C DISPLACEMENT VS LENGTH SATURN SA-DI

FREQUENCY = 5.80 CPS

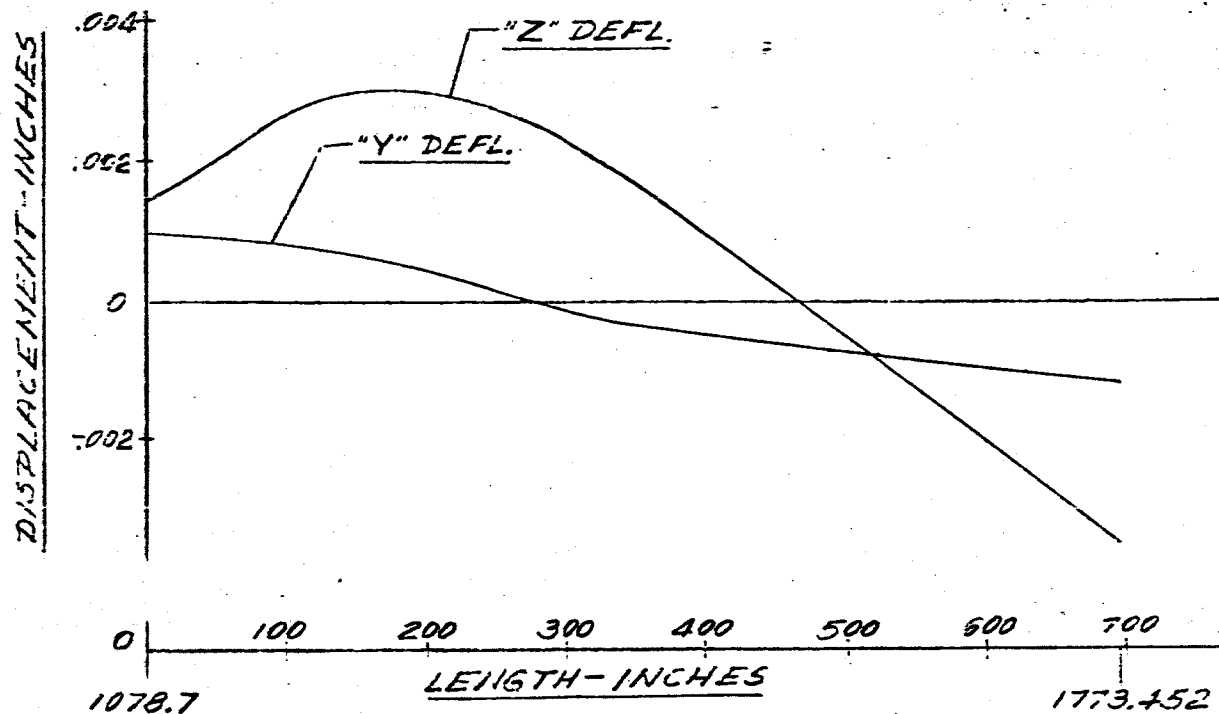


-263-

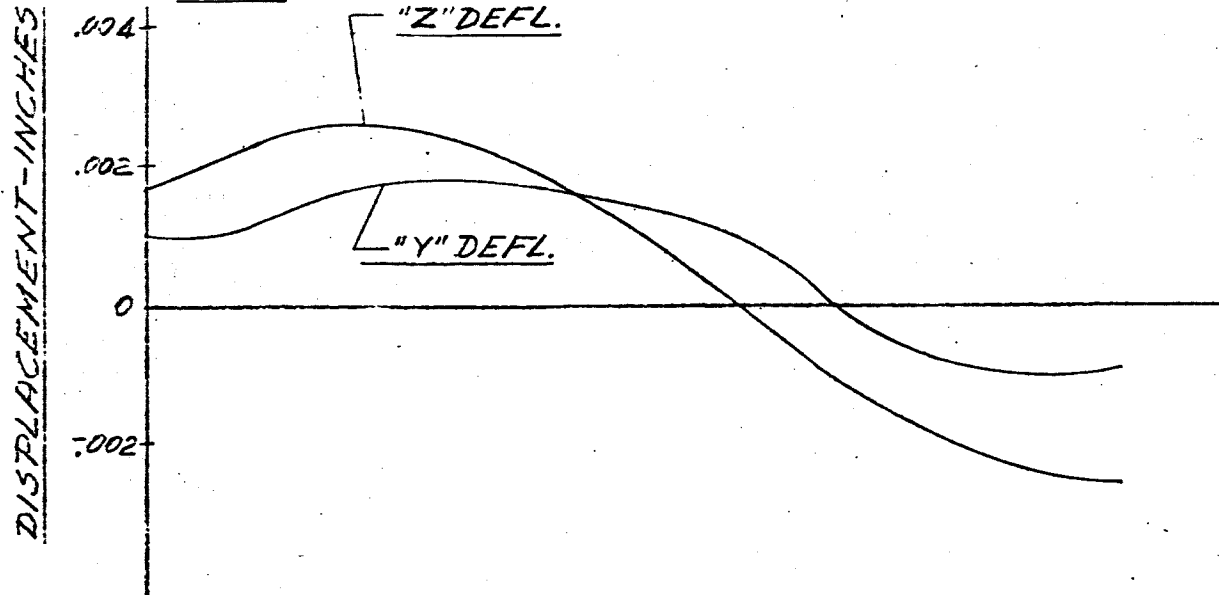
FIG. 1B1. DISPLACEMENT VS LENGTH SATURN SA-D1

FREQUENCY = .50 CPS

L-3



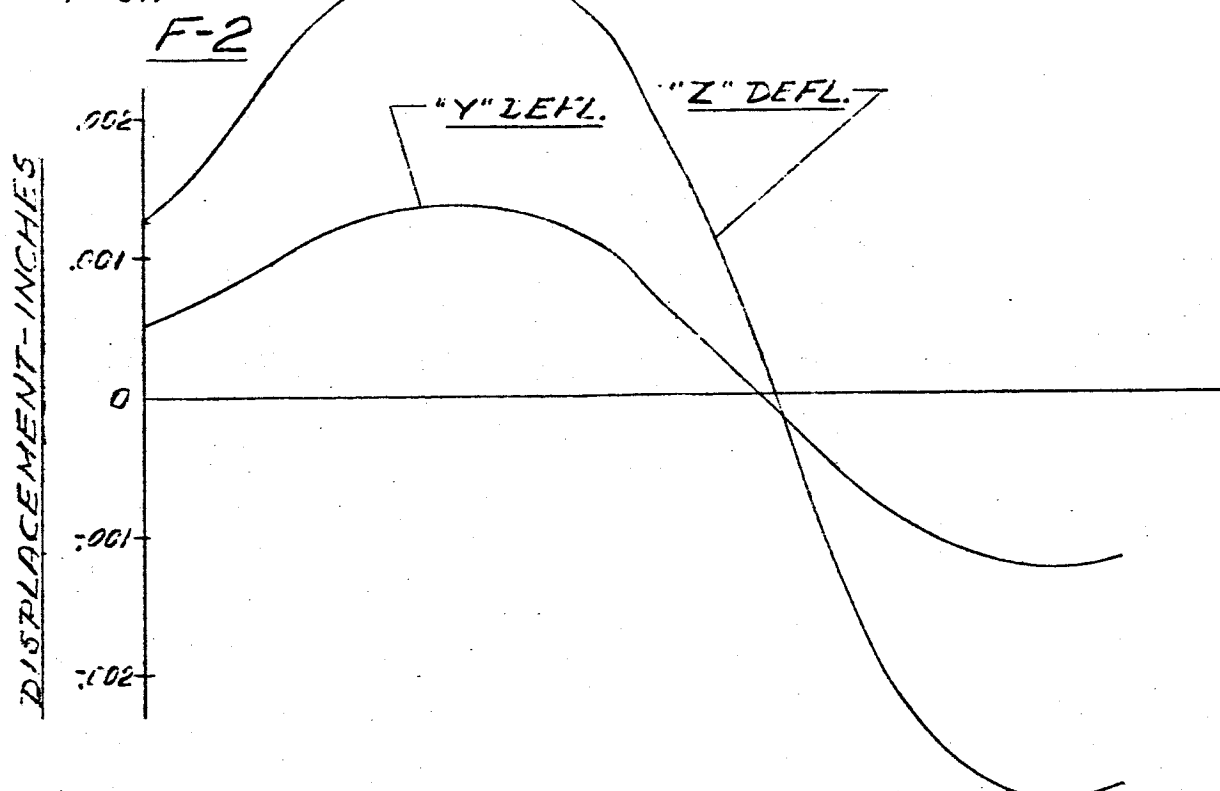
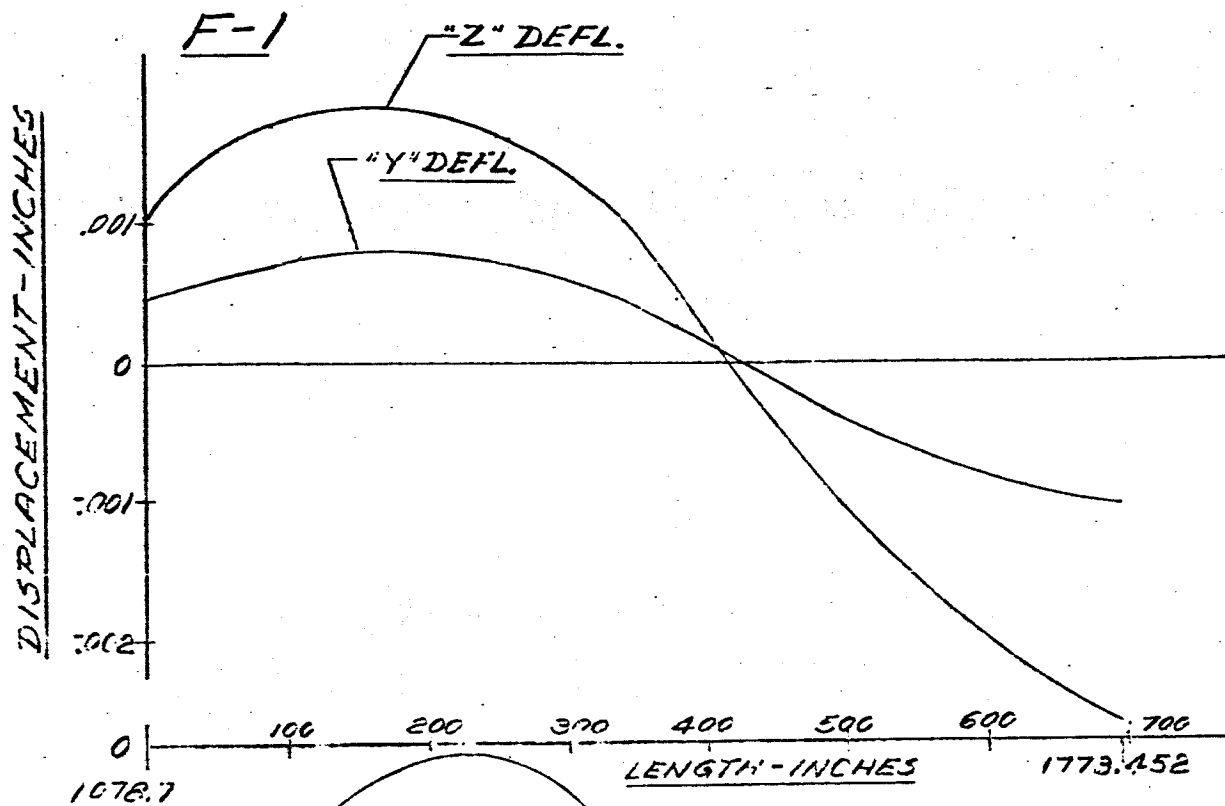
L-4



-264-

FIG. 1B2 DISPLACEMENT VS LENGTH SATURN SA-DI

FREQUENCY = 5.80 CPS



-265-

FIG. 183 DISPLACEMENT VS LENGTH SATURN SA-DI

FREQUENCY = 5.80 CPS

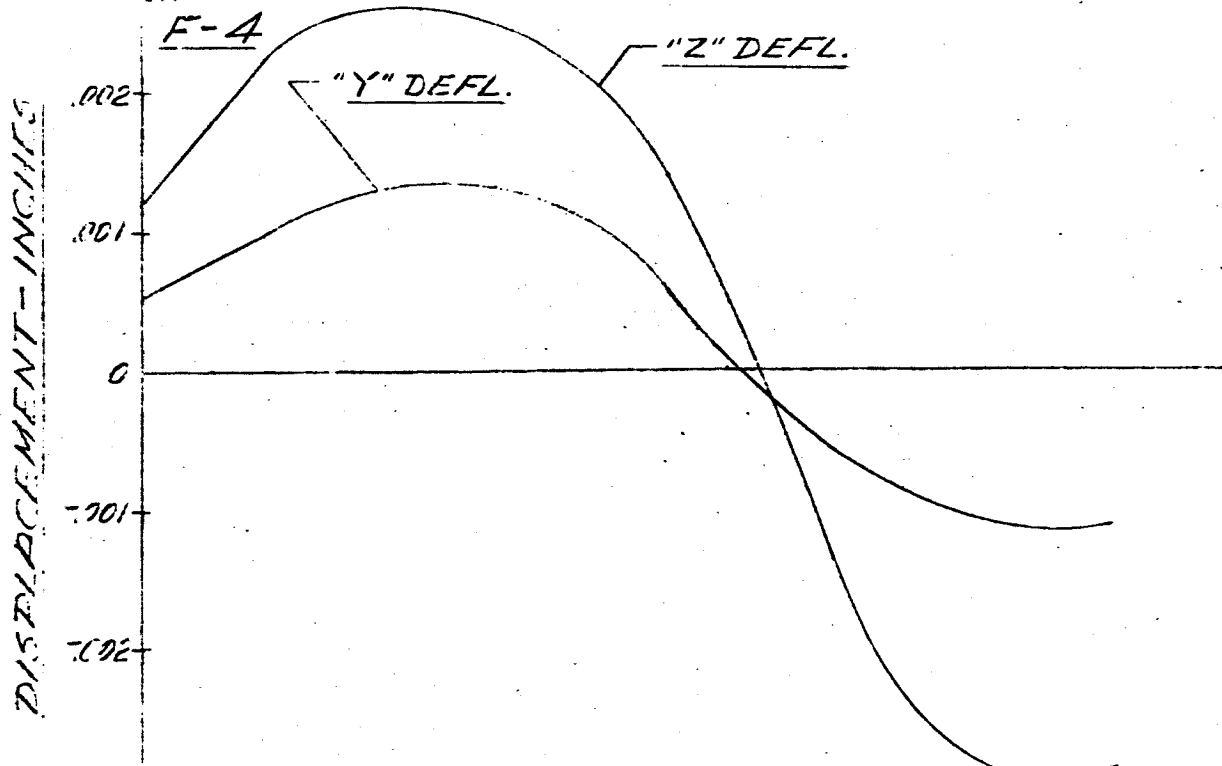
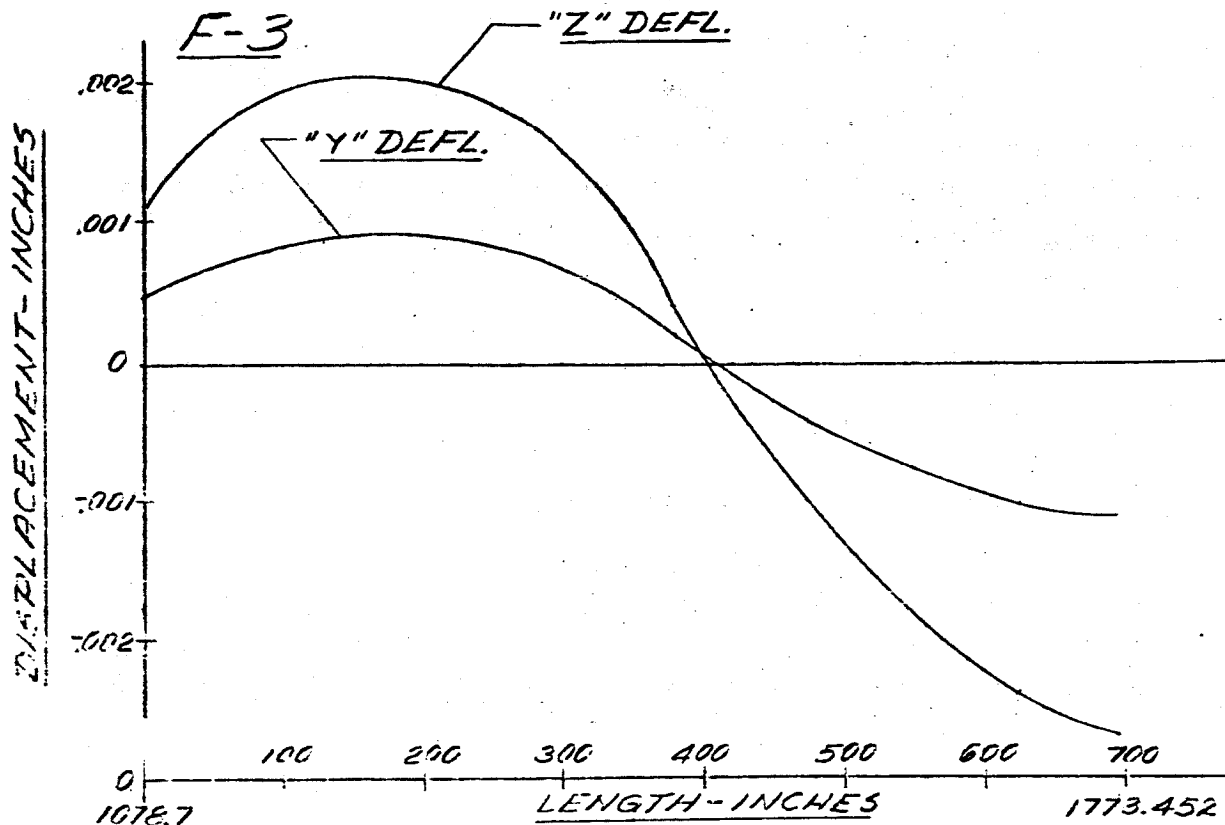
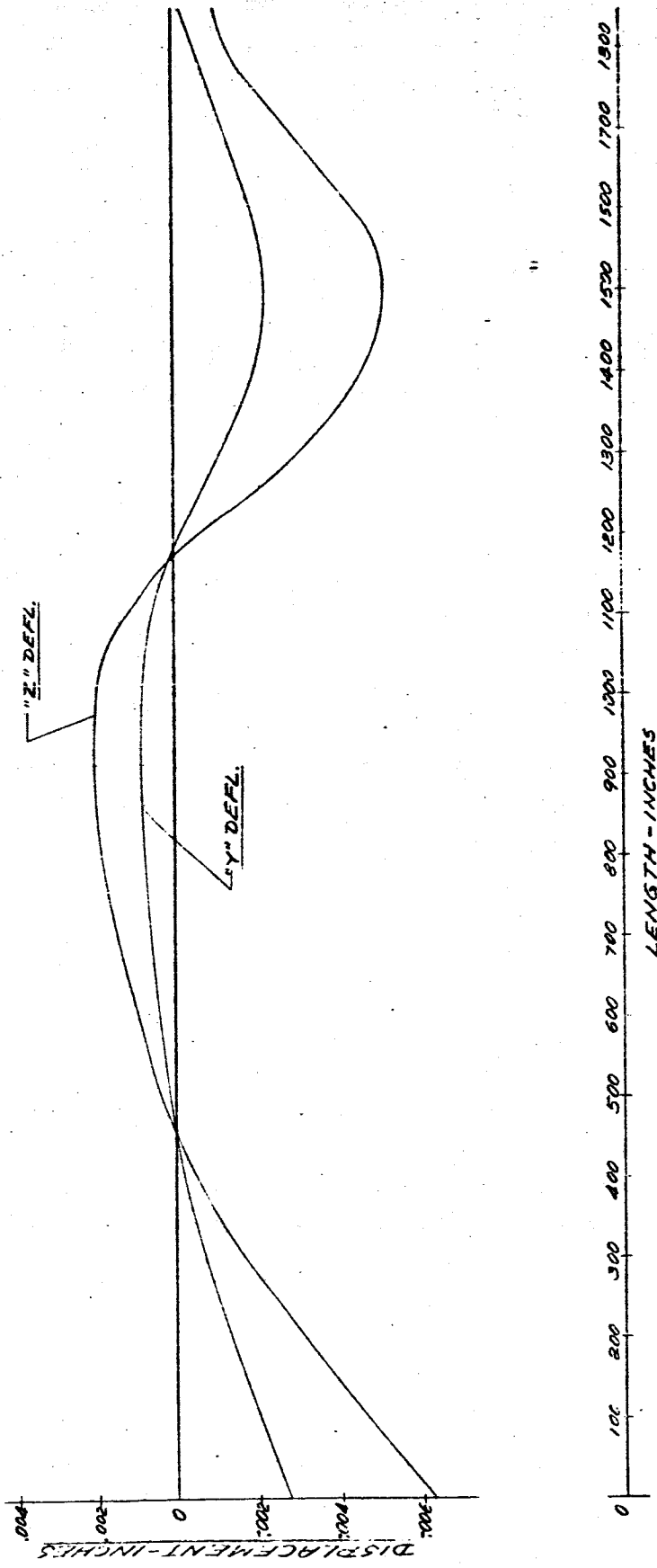


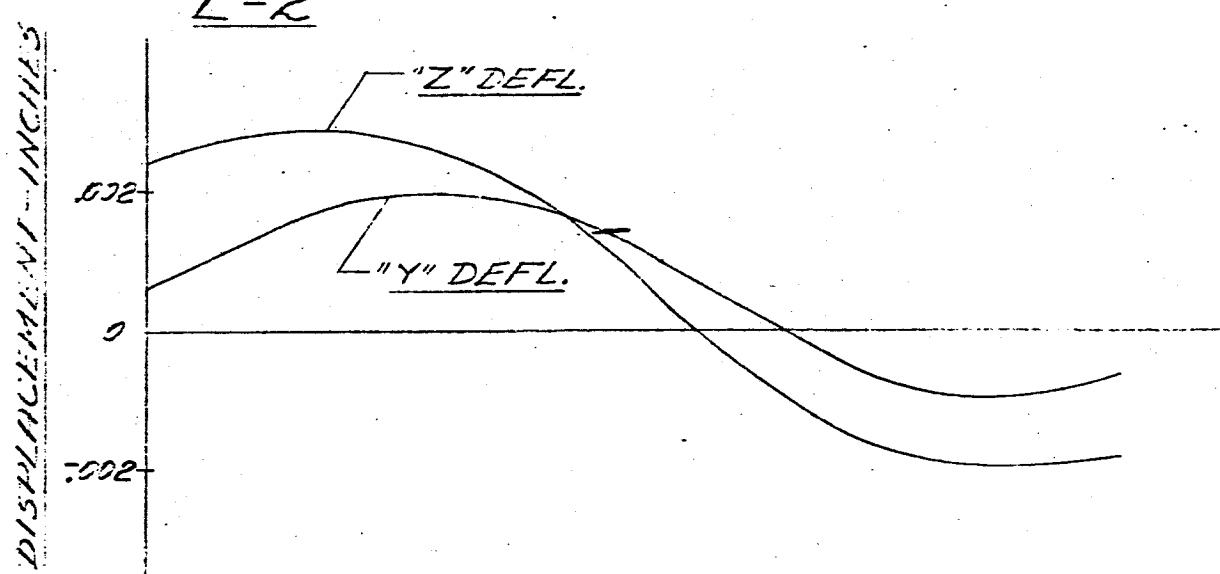
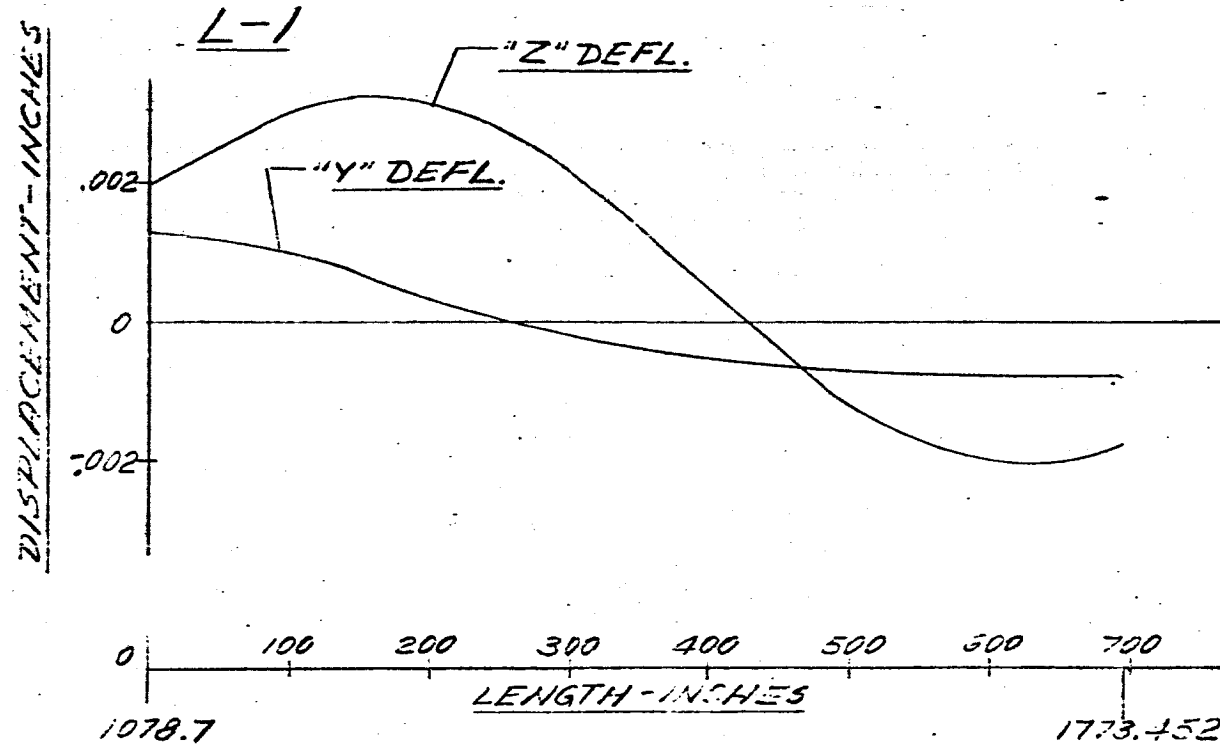
FIG 184 DISPLACEMENT vs LENGTH SATURN SA-DI  
MAIN TANK & UPPER STAGES  
FREQUENCY = 6.10 cps.



- 267 -

FIG 185 DISPLACEMENT VS LENGTH SATURN SA-DI

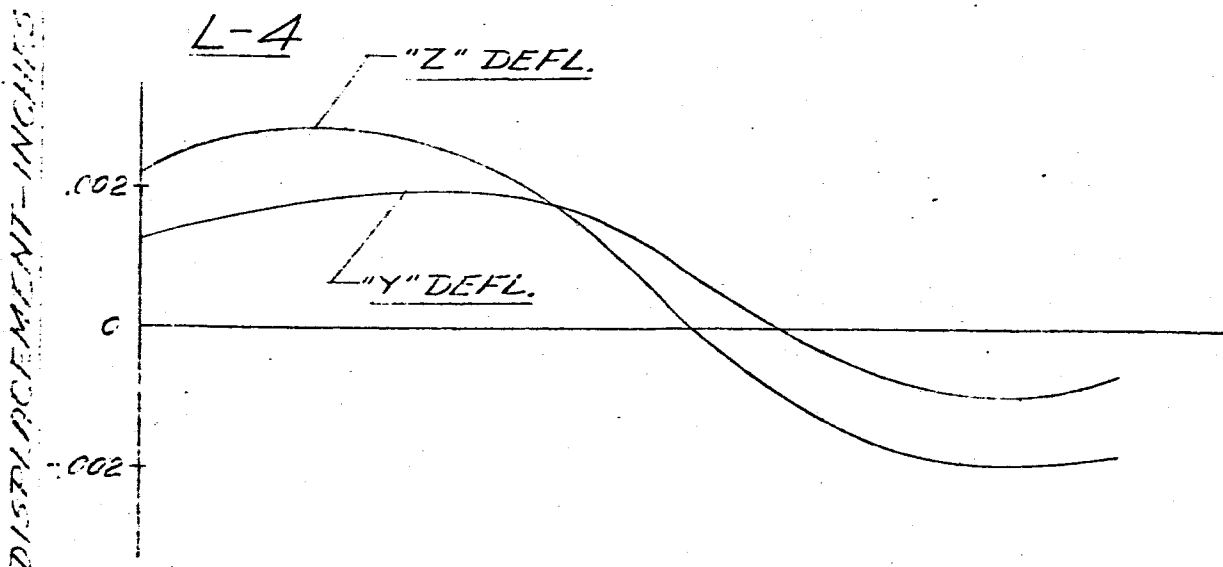
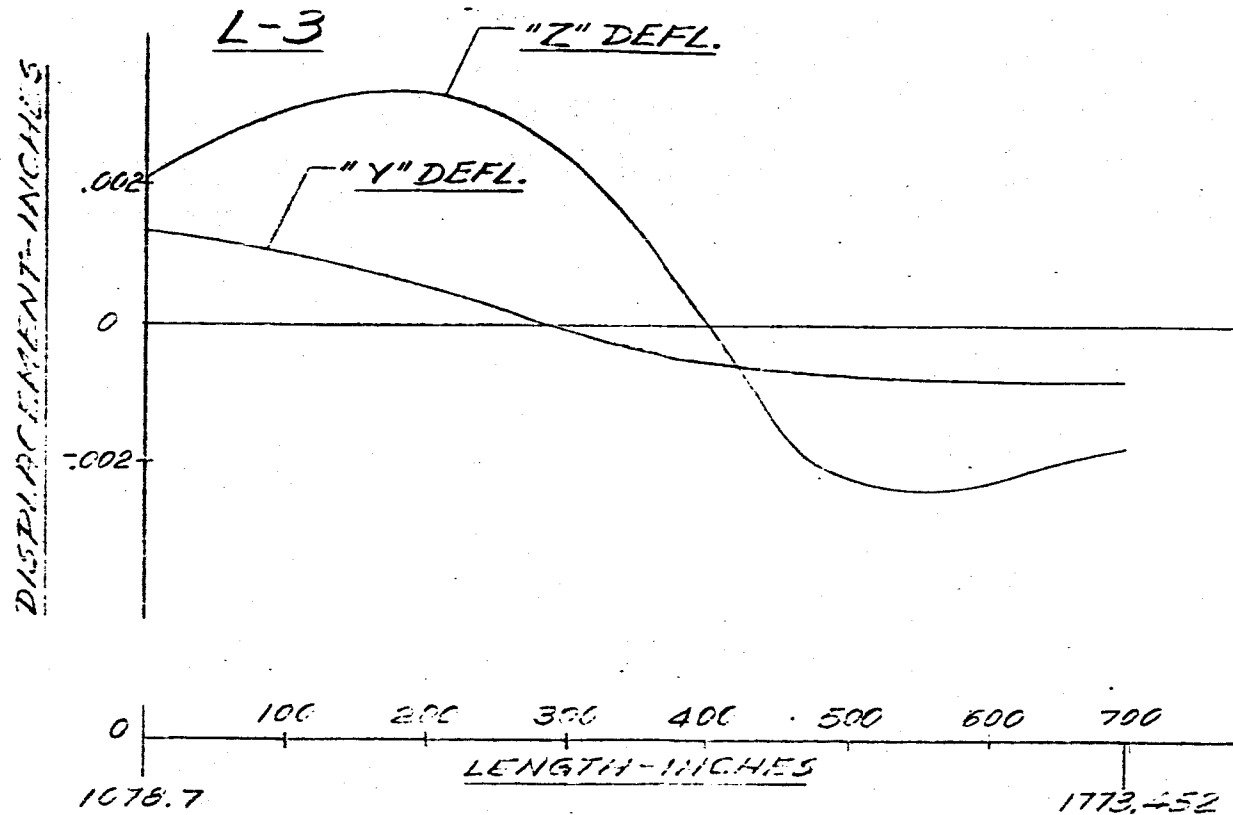
FREQUENCY = 6.10 CPS



-268-

FIG 186 DISPLACEMENT VS LENGTH SATURN SA-01

FREQUENCY = 6.10 CPS

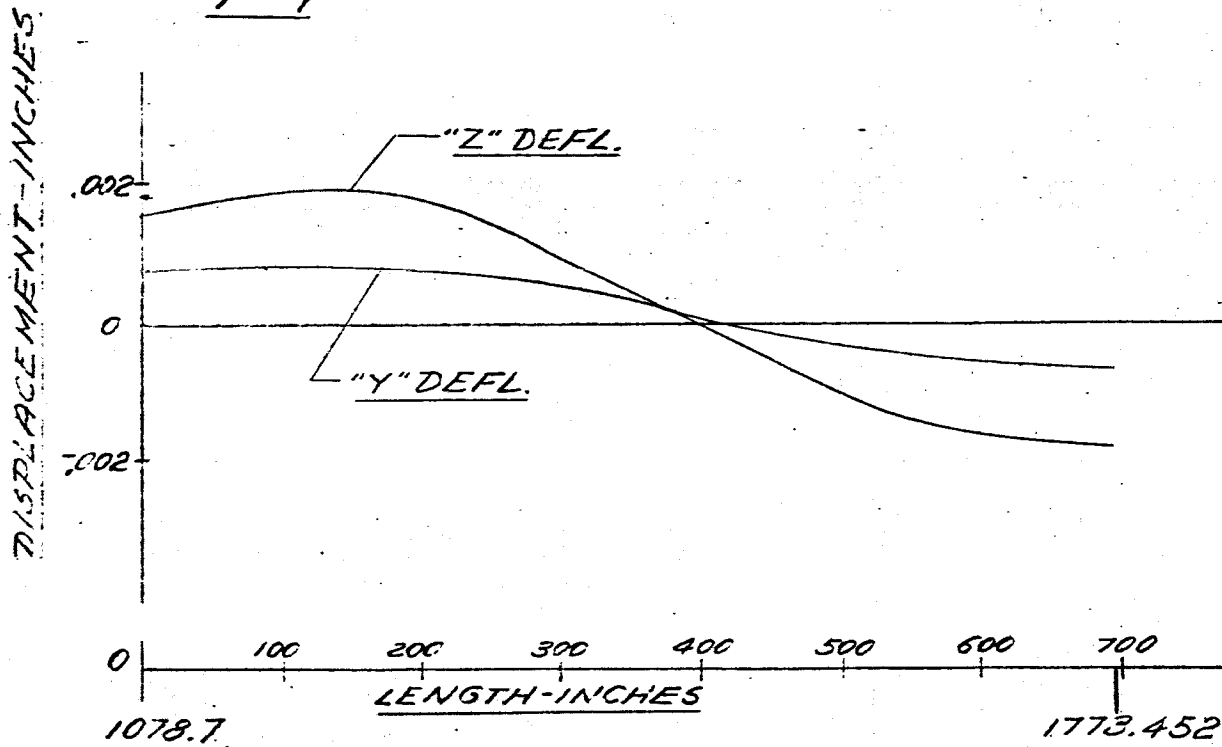


-269-

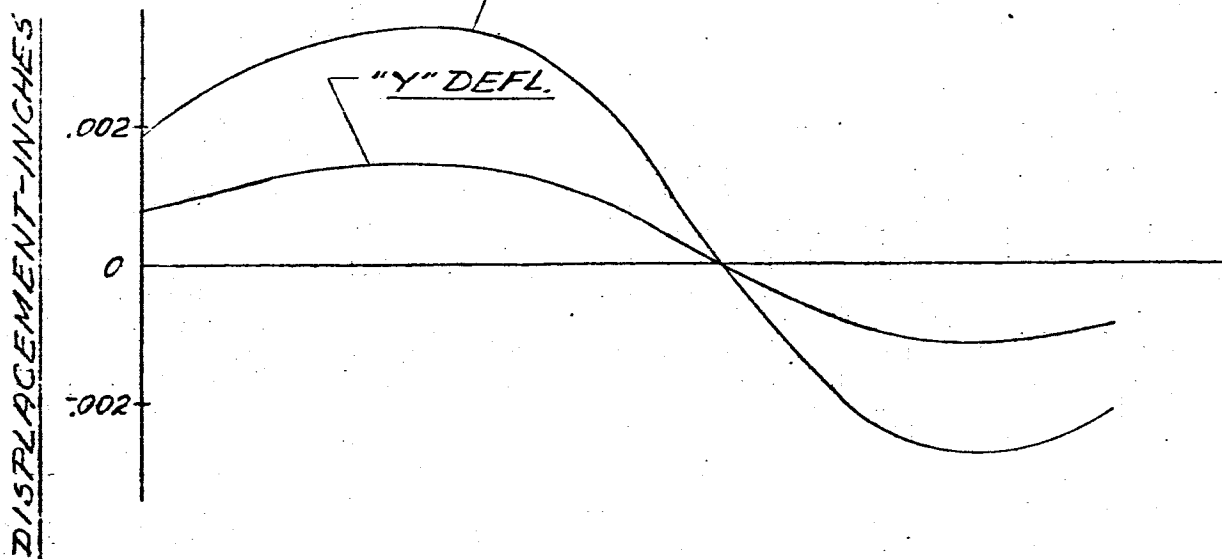
FIG 187 DISPLACEMENT vs LENGTH SATURN SA-DI

FREQUENCY = 6.10 CPS

F-1



F-2



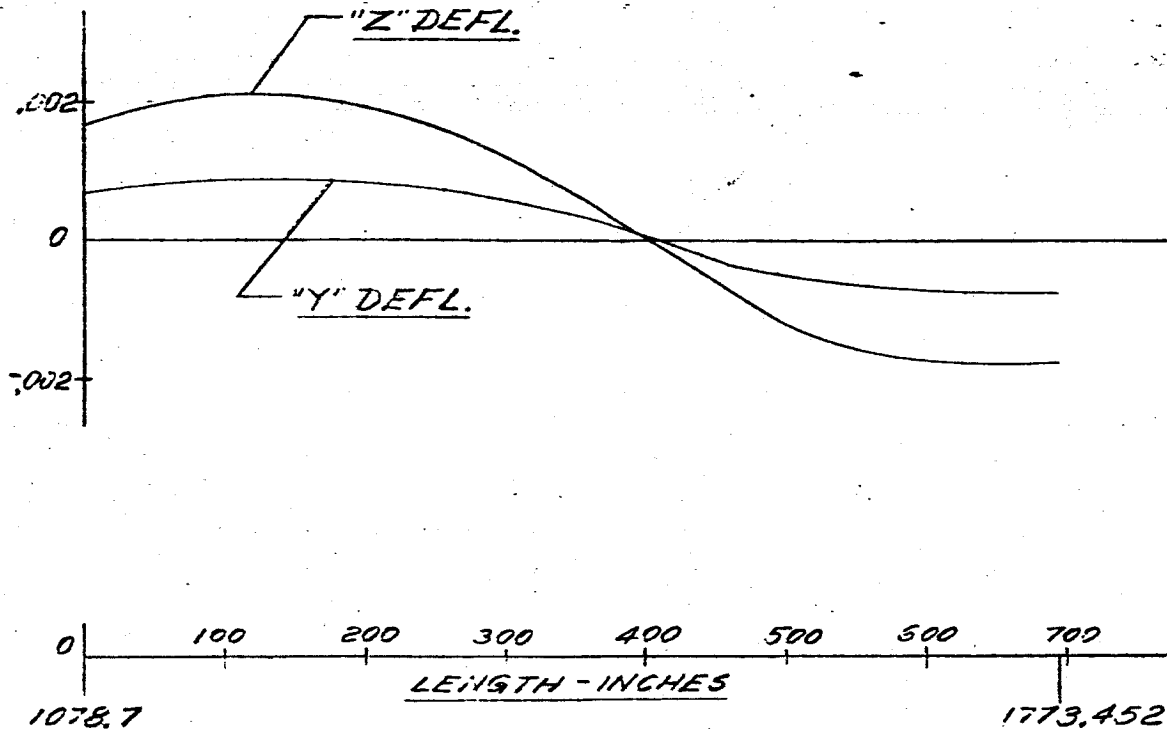
-270-

FIG 188 DISPLACEMENT vs LENGTH SATURN SA-DI

FREQUENCY = 6.10 CPS.

DISPLACEMENT - INCHES

F-3



F-4

DISPLACEMENT - INCHES

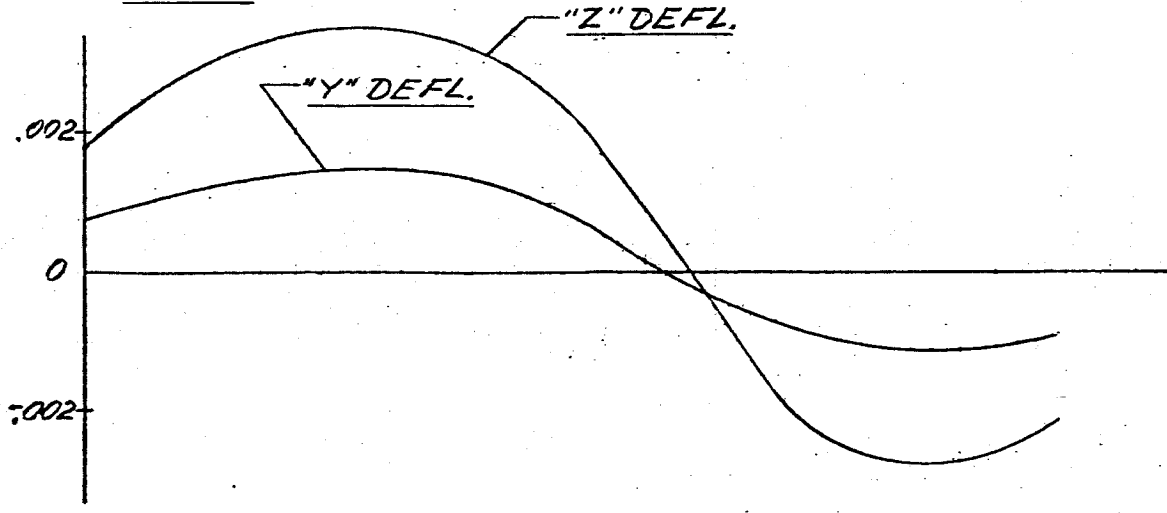
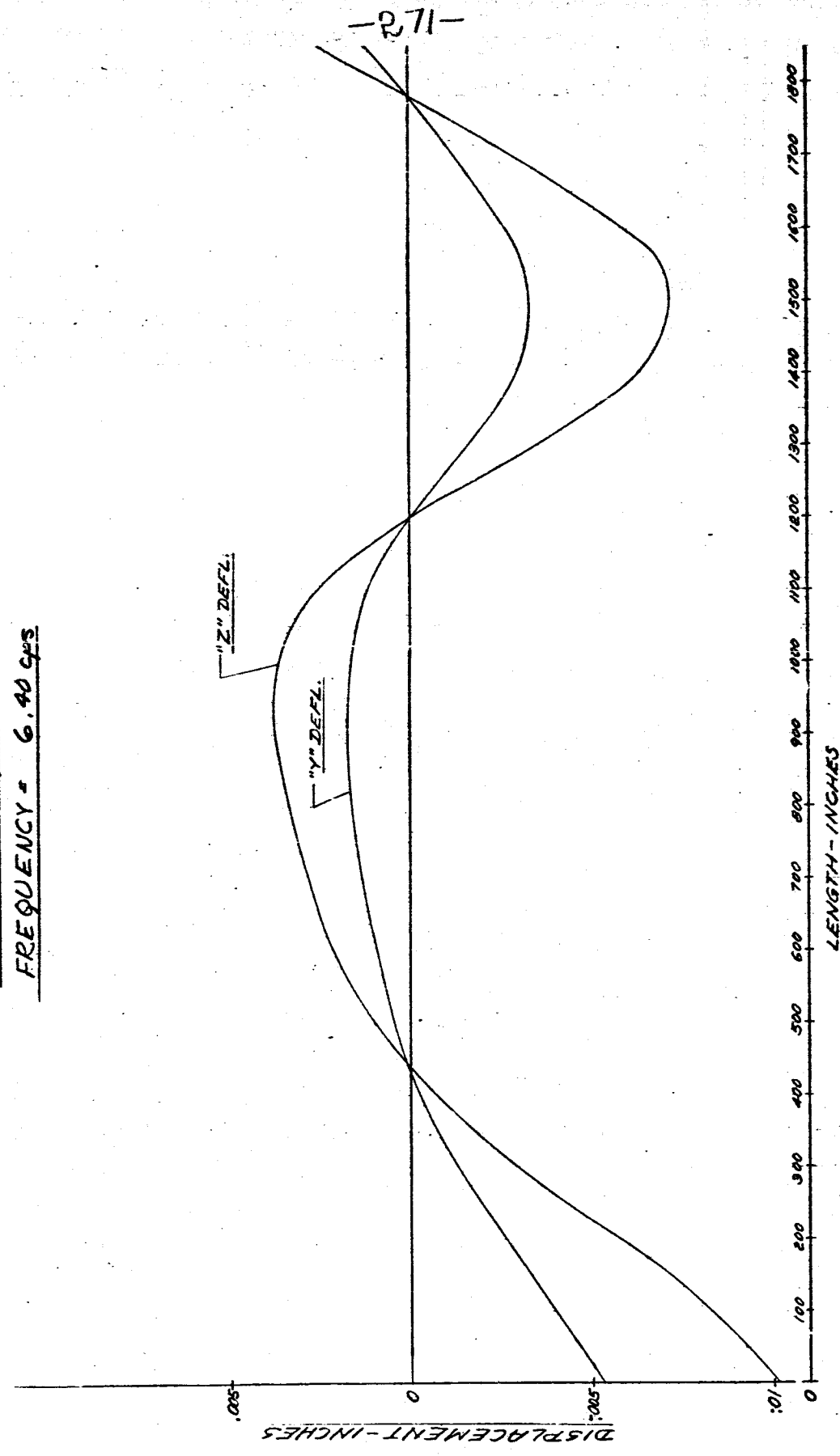


FIG. 189 DISPLACEMENT VS LENGTH SATURN SA-01  
MAIN TANK & UPPER STAGES  
FREQUENCY = 6.40 cps

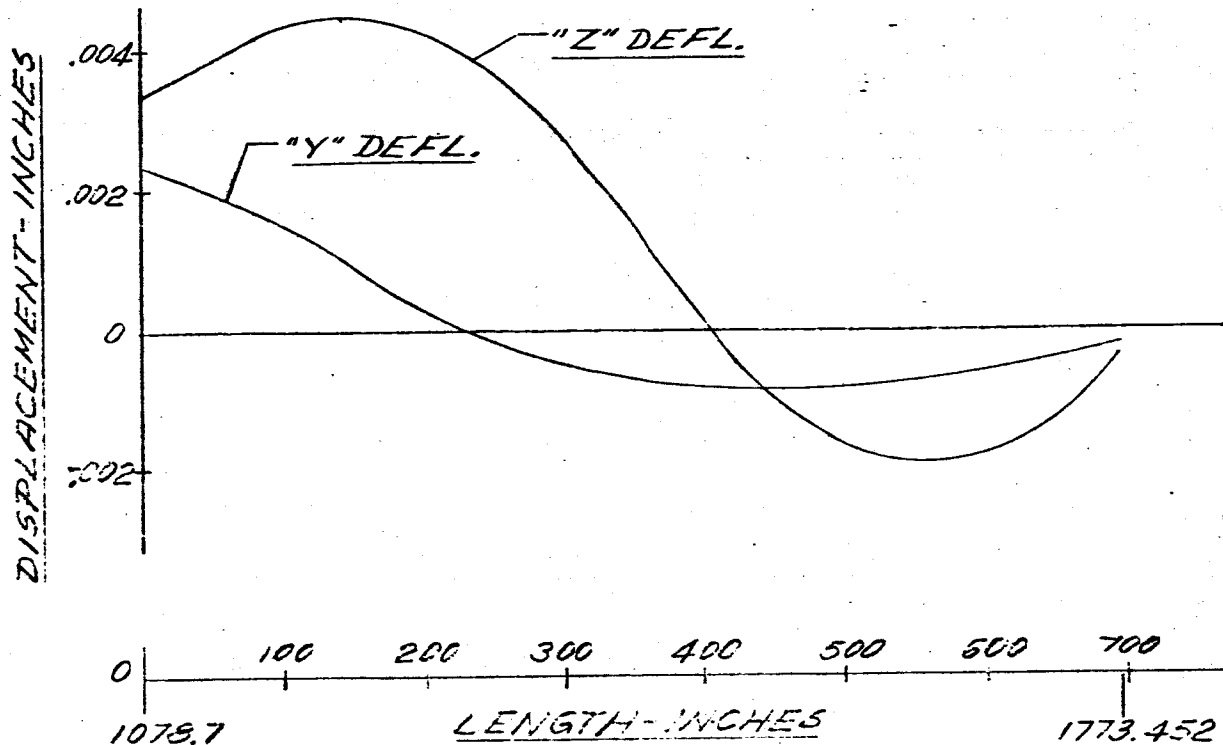


-272-

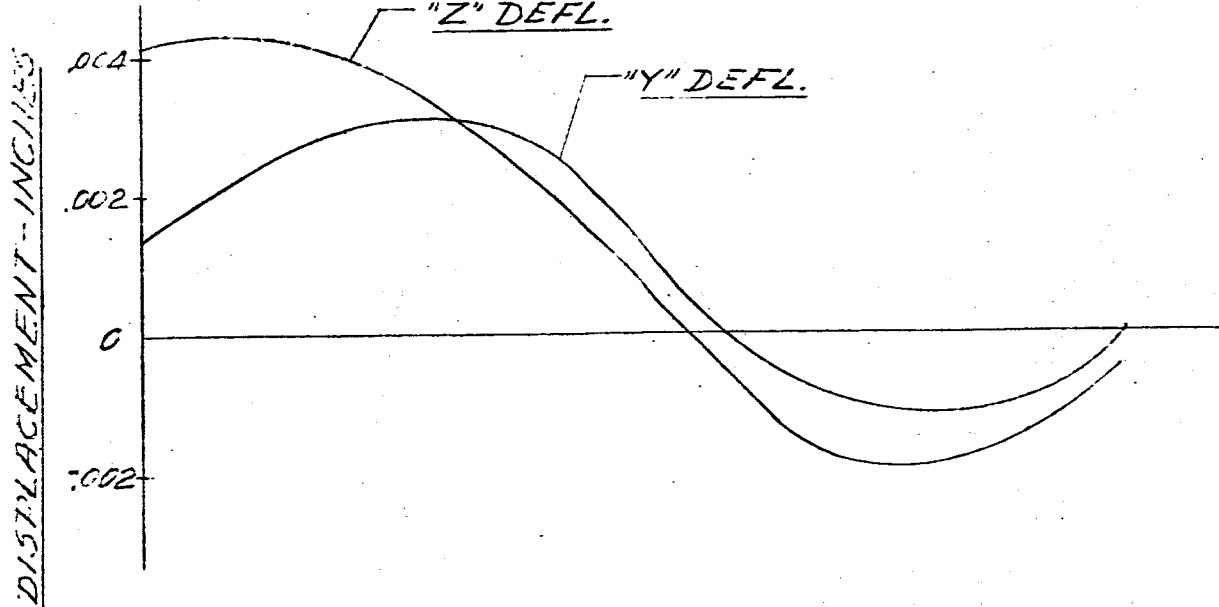
FIG. 190 DISPLACEMENT vs LENGTH SATURN SA-DI

FREQUENCY = 6.40 CPS

L-1



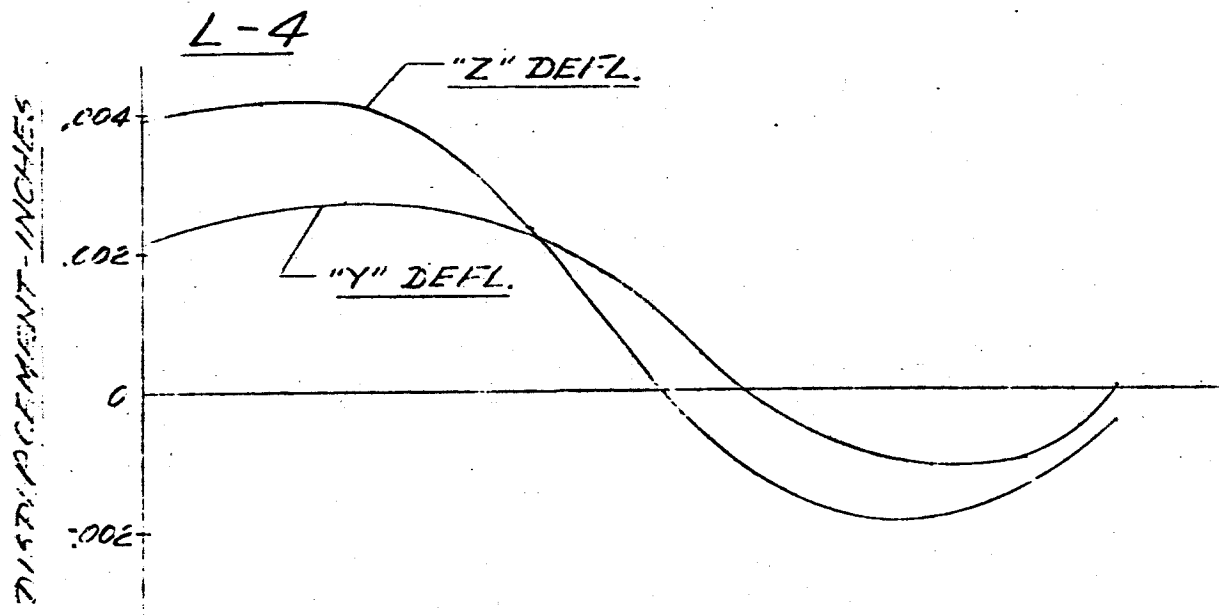
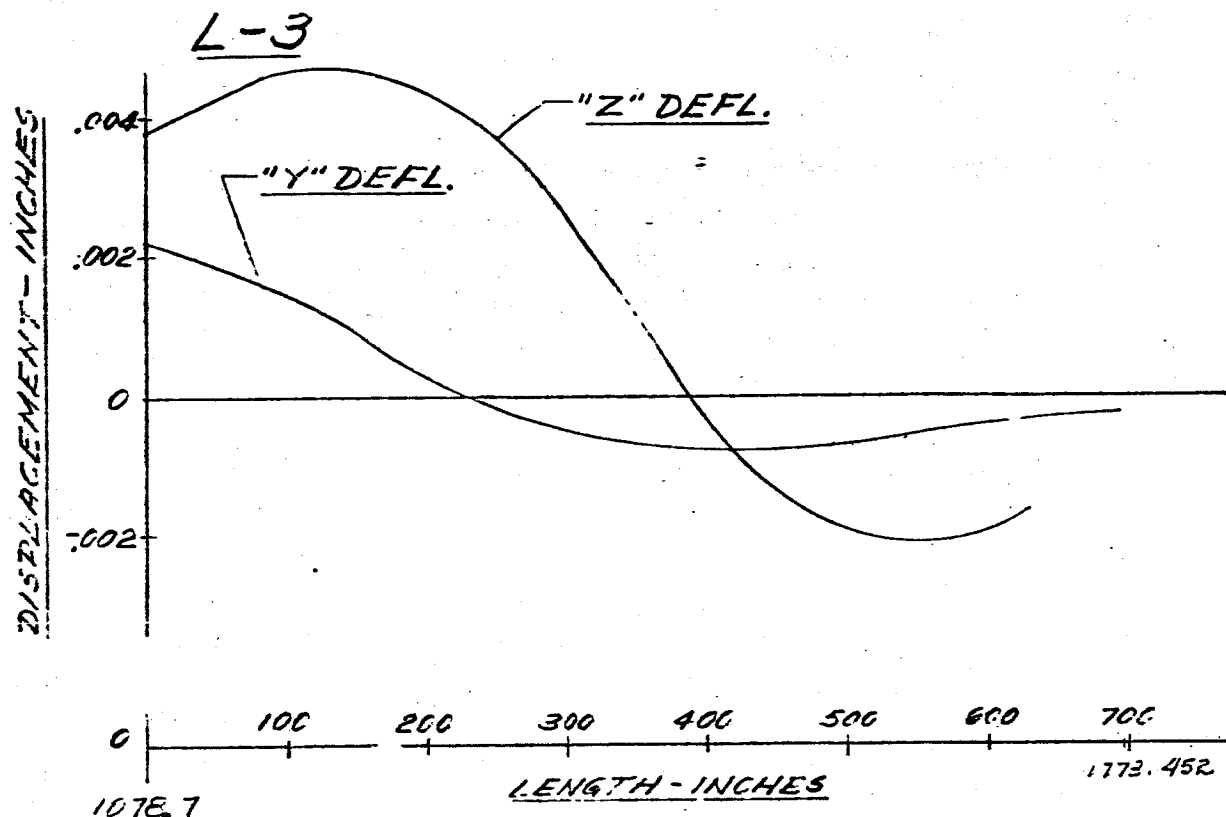
L-2



-273-

FIG. 191 DISPLACEMENT VS LENGTH SATURN SA-DI

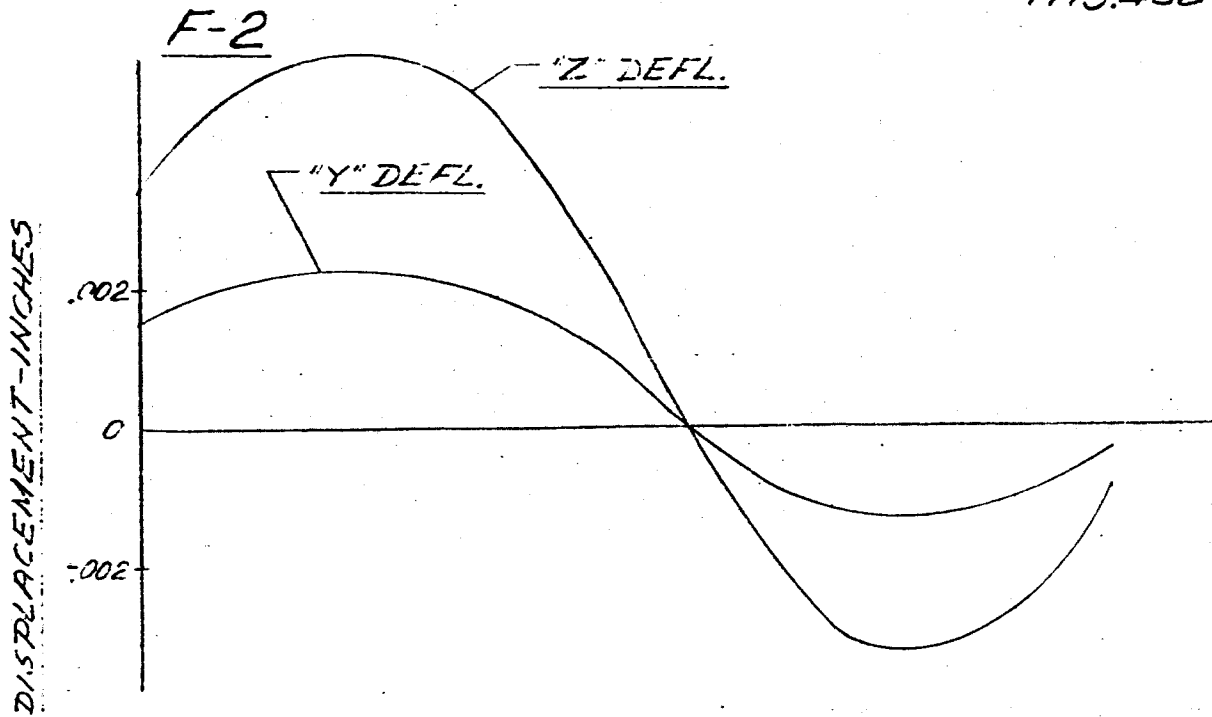
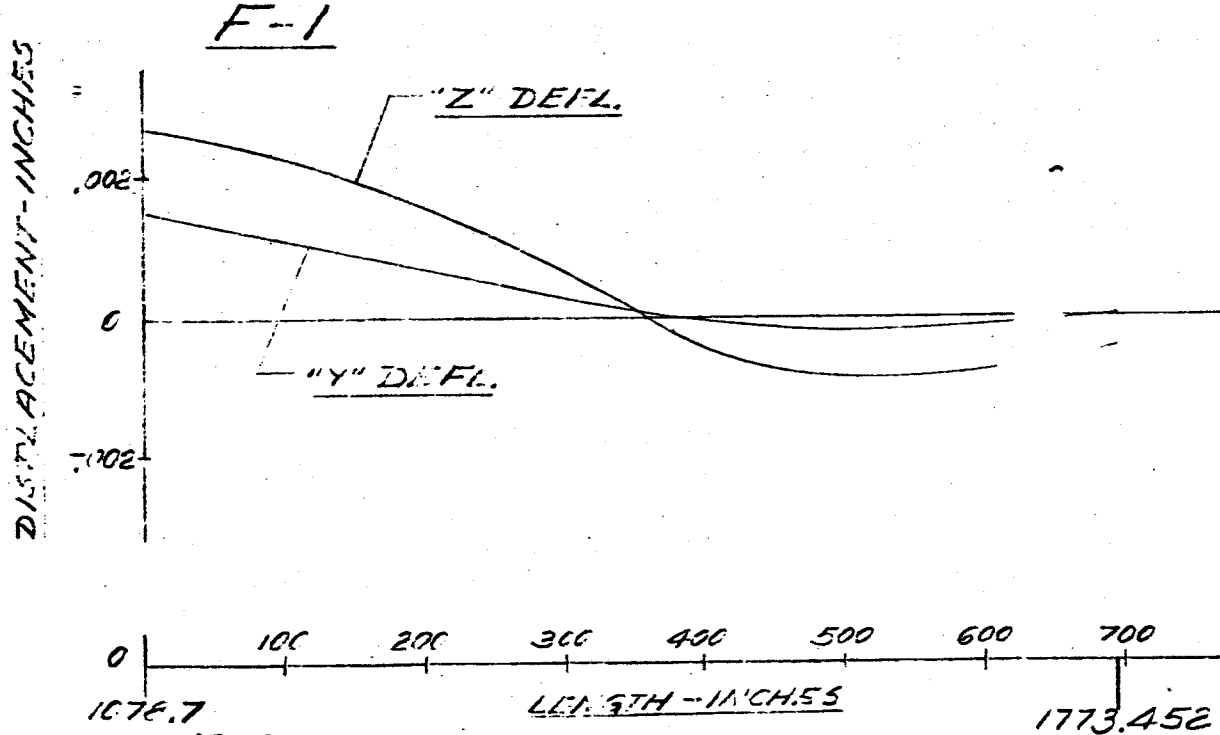
FREQUENCY = 6.40 CPS



-274-

FIG. 192 DISPLACEMENT VS LENGTH SATURN SA-DI

FREQUENCY = 6.40 CPS



-275-

FIG. 193 DISPLACEMENT vs LENGTH SATURN SA-01

FREQUENCY = 6.40 CPS

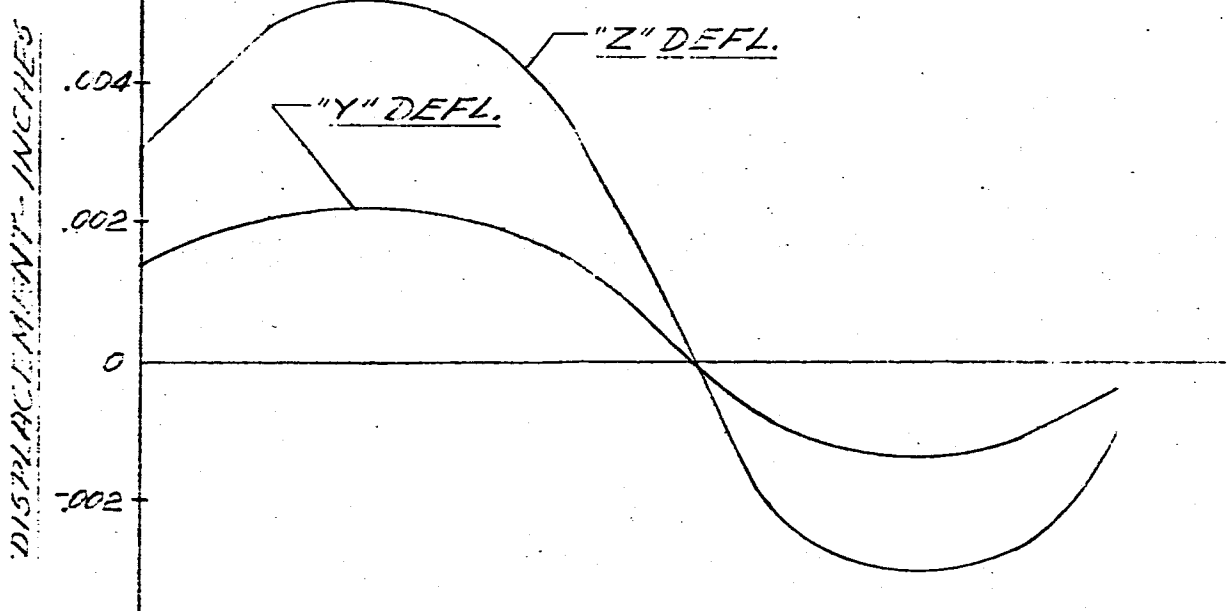
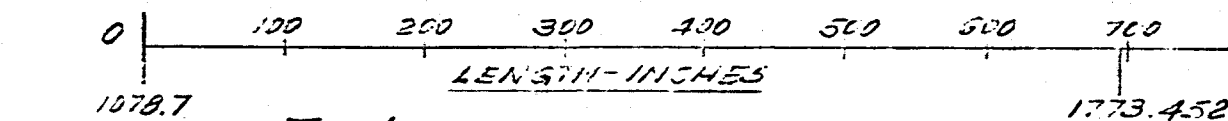
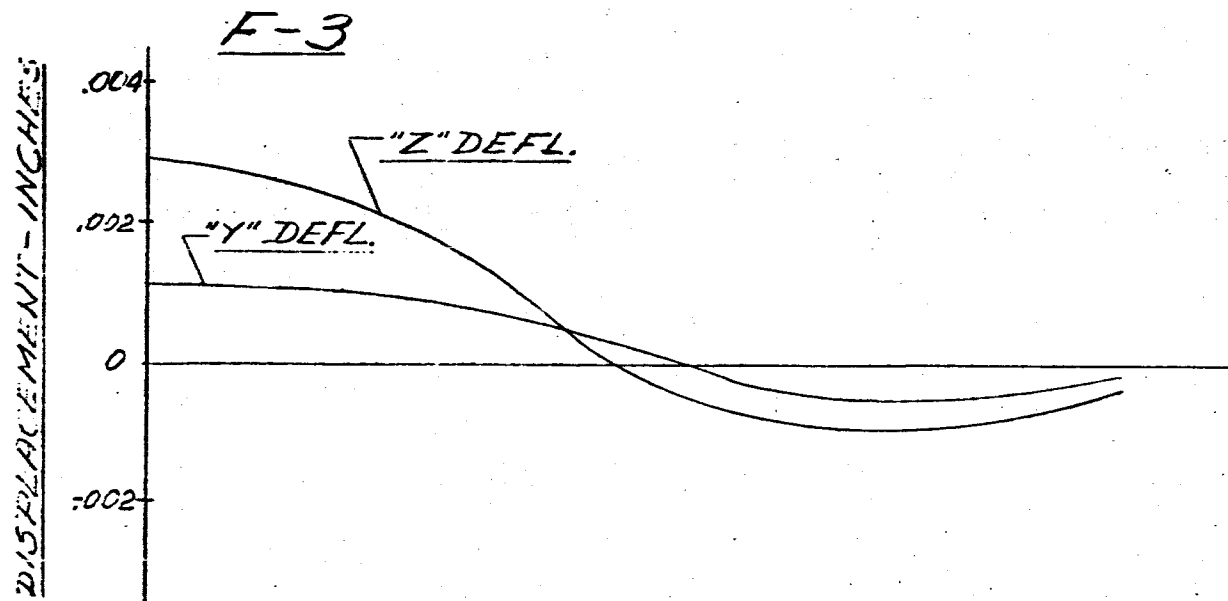
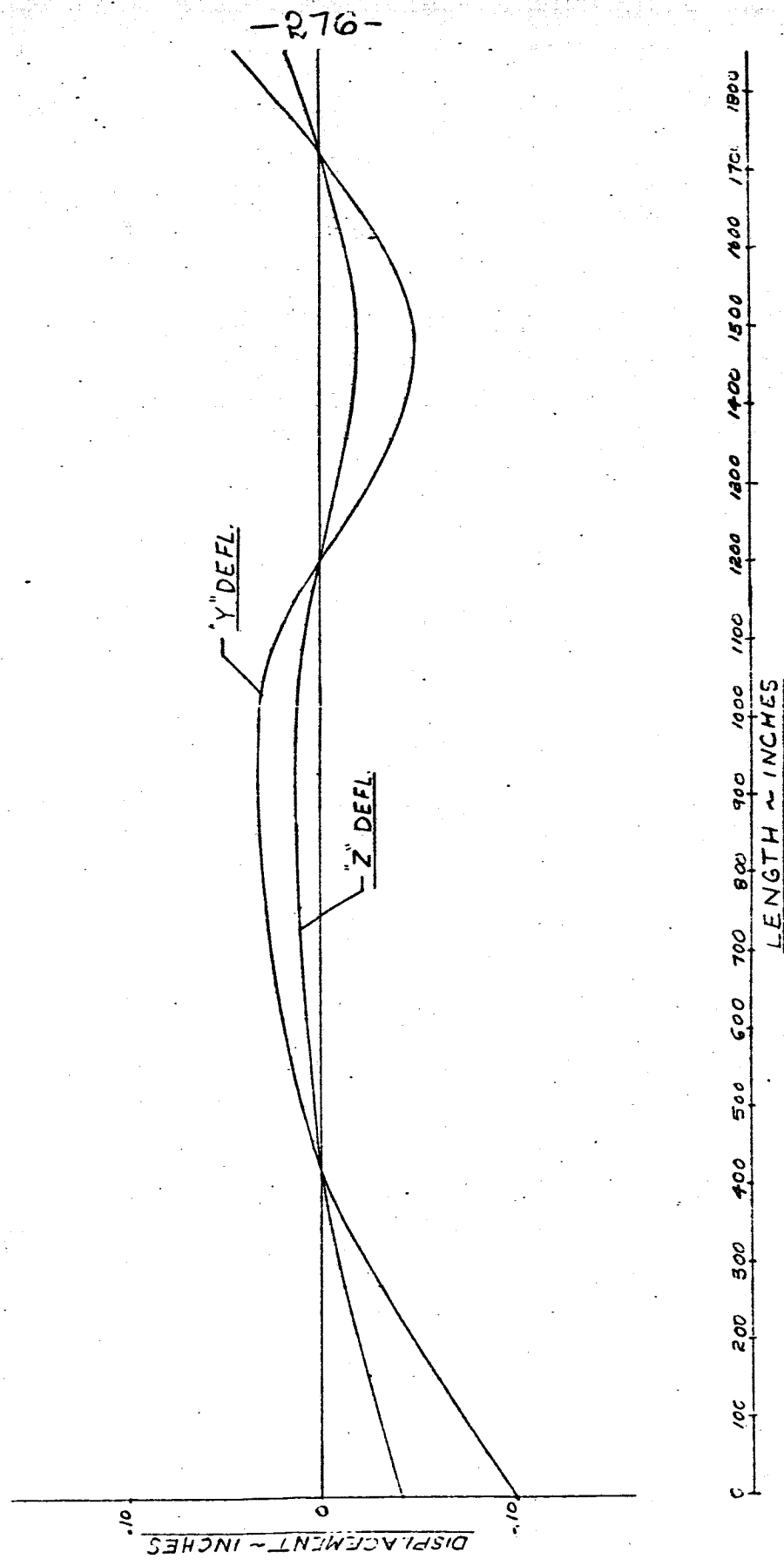


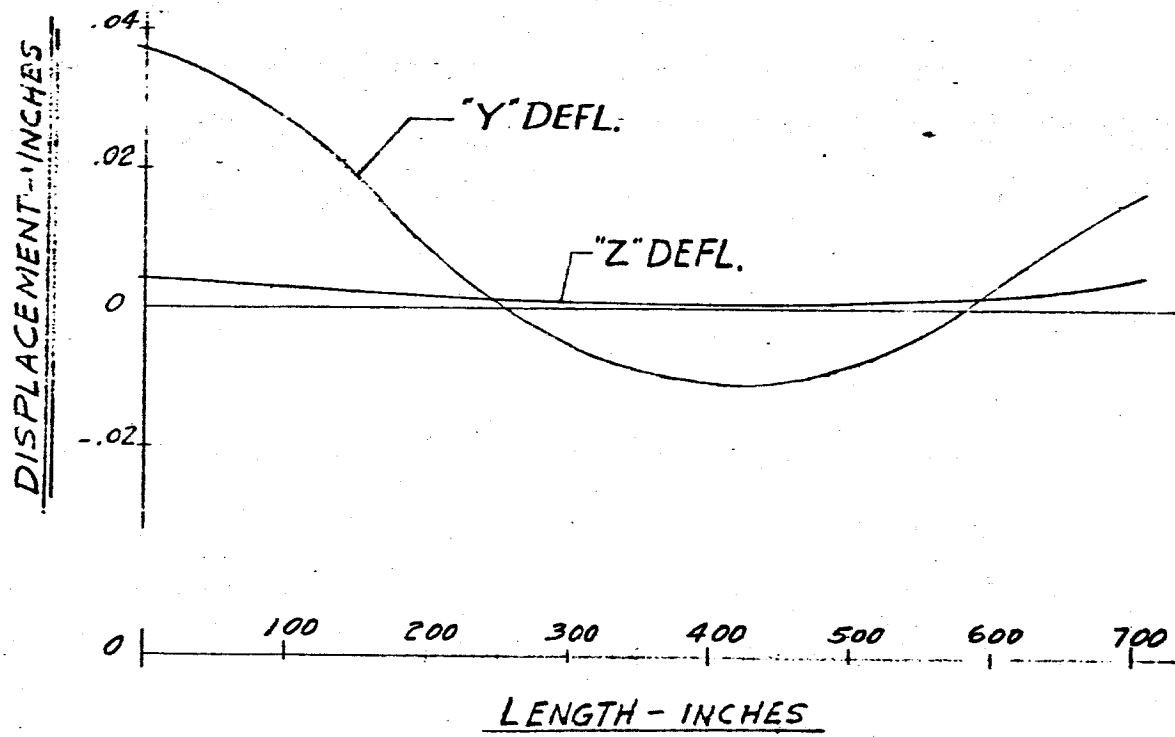
FIG. 194 DISPLACEMENT vs LENGTH SATURN SA-DI  
MAIN TANK & UPPER STAGES  
FREQUENCY = 6.65 cps.



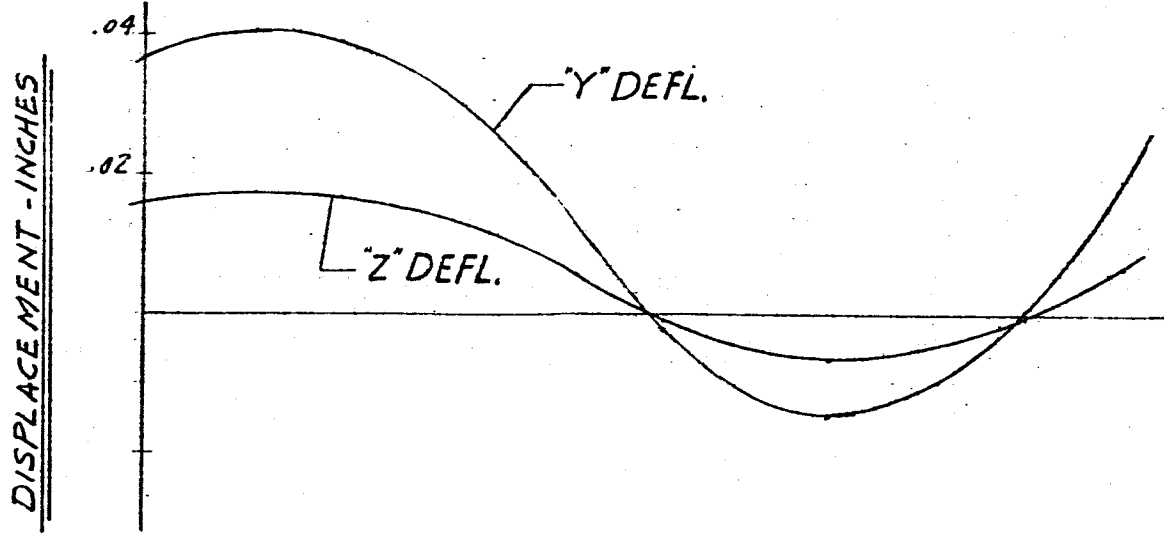
-277-

FIG. 195 DISPLACEMENT vs LENGTH SATURN SA-DI  
FREQUENCY = 6.65 CPS

L-1



L-2

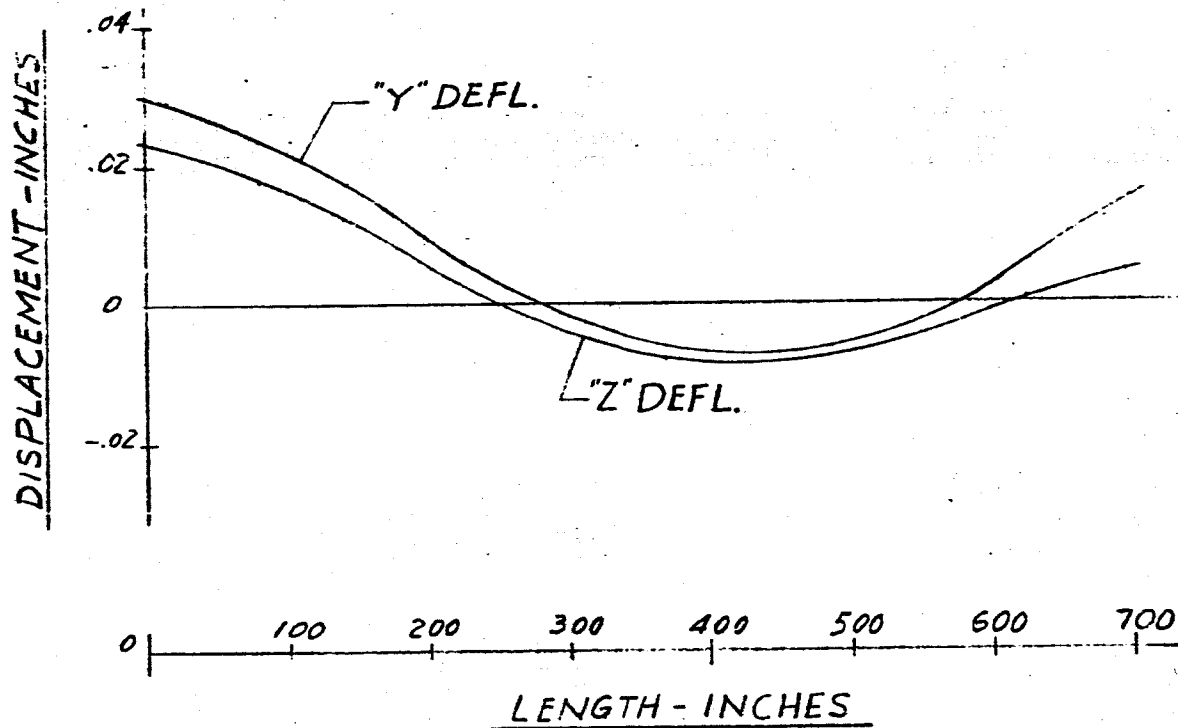


-278-

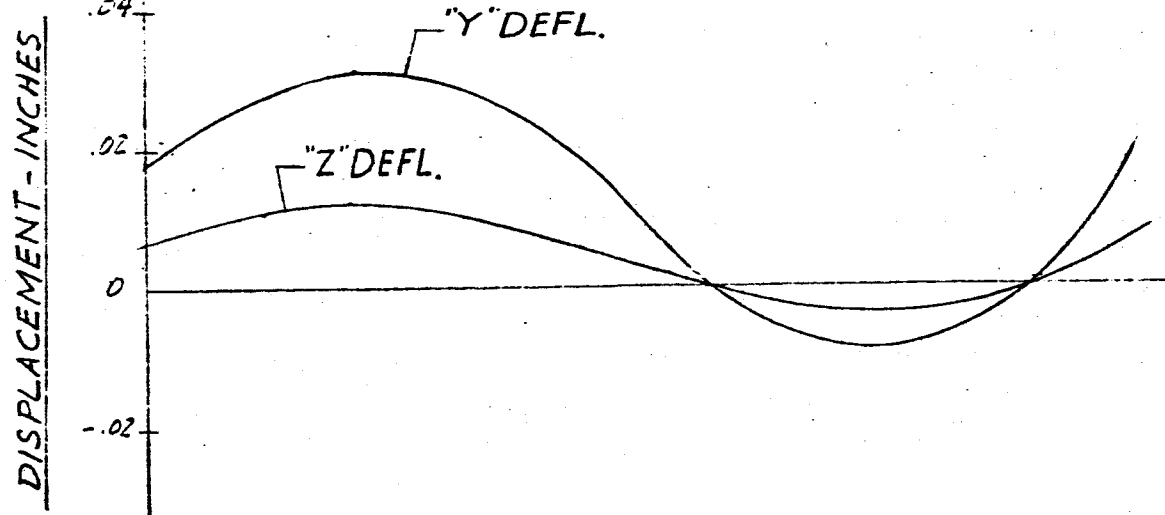
FIG 196 DISPLACEMENT vs LENGTH SATURN SA-DI

FREQUENCY = 6.65 CPS

L-3



L-4

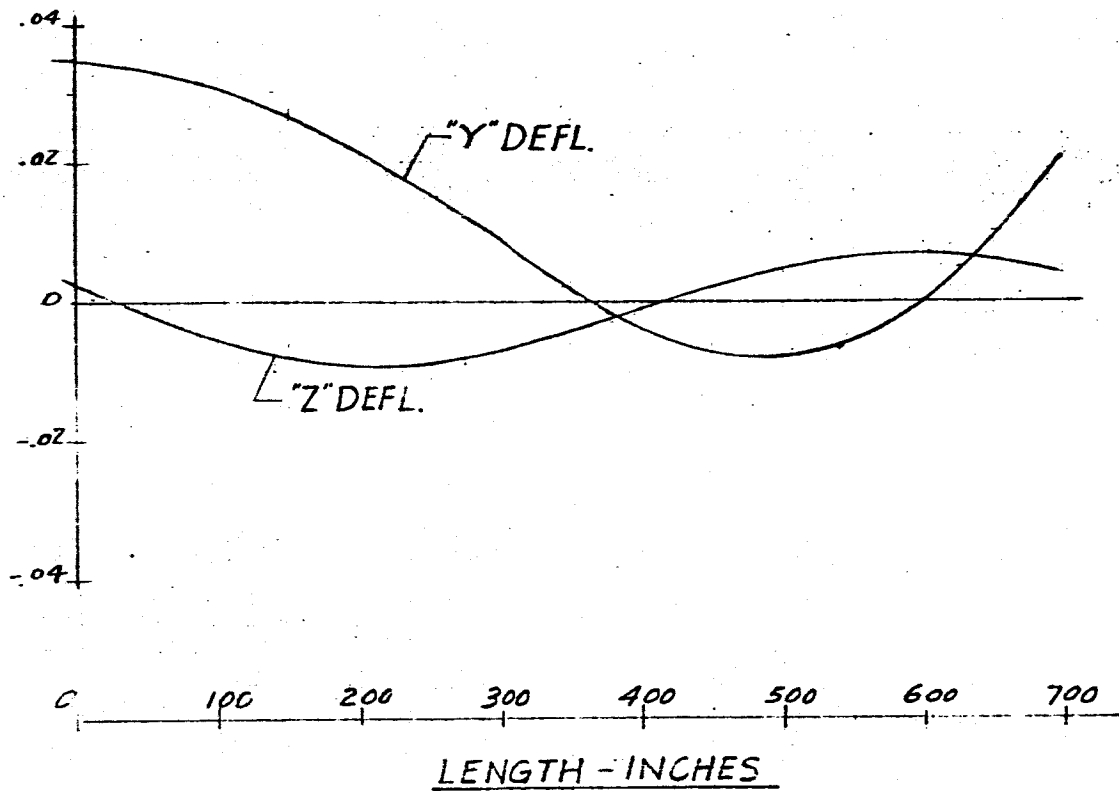


-279-

FIG. 197 DISPLACEMENT VS LENGTH SATURN SA-DI  
FREQUENCY = 6.65 CPS

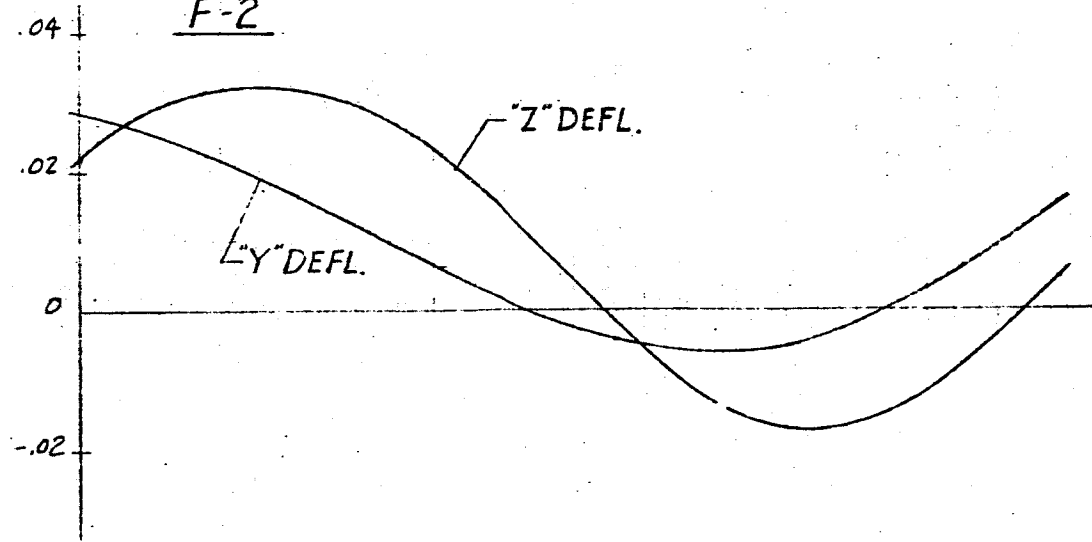
F-1

DISPLACEMENT - INCHES



F-2

DISPLACEMENT - INCHES

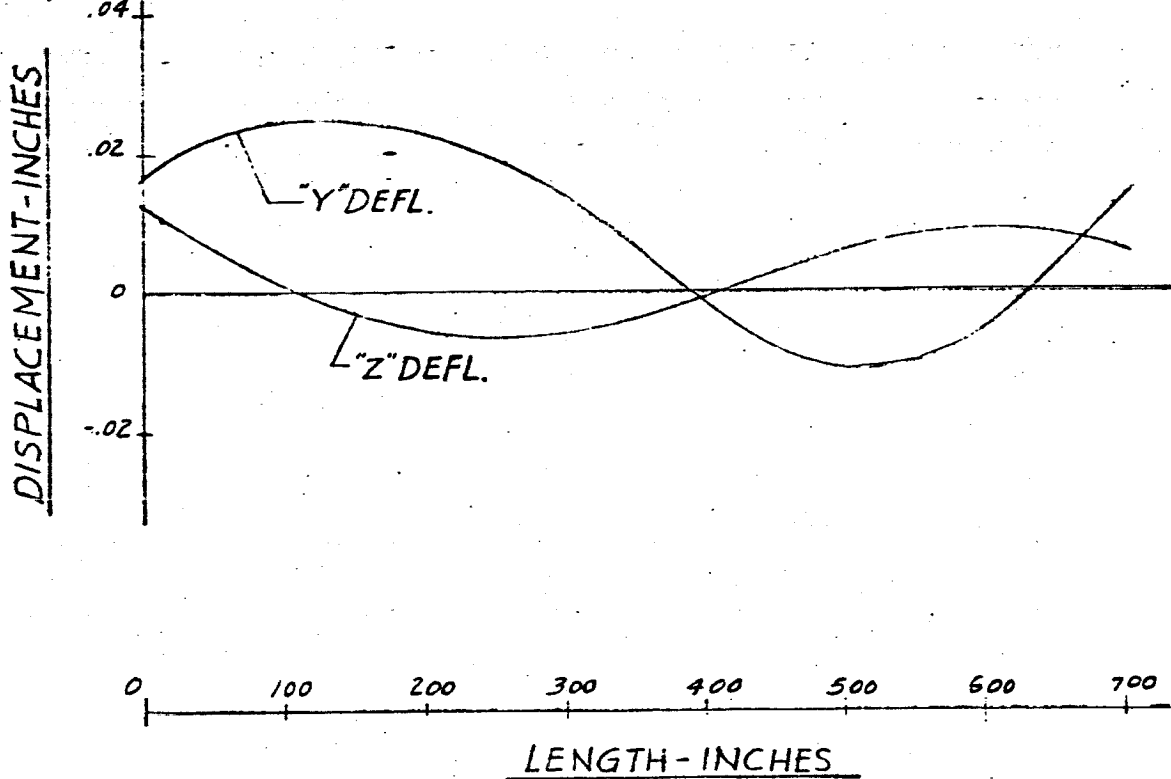


- 280 -

FIG 198 DISPLACEMENT VS LENGTH SATURN SA-DI

FREQUENCY = 6.65 CPS.

F-3



F-4

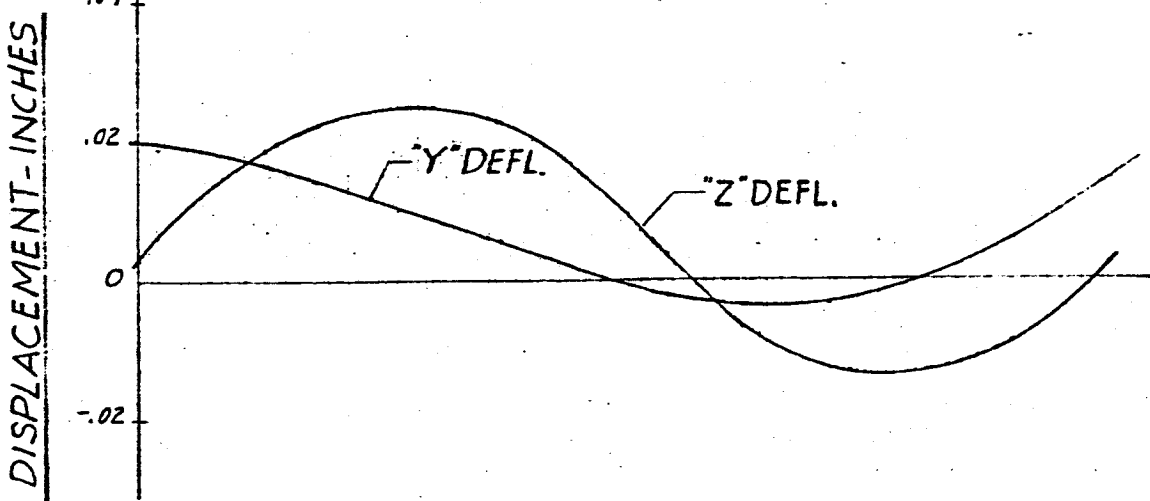
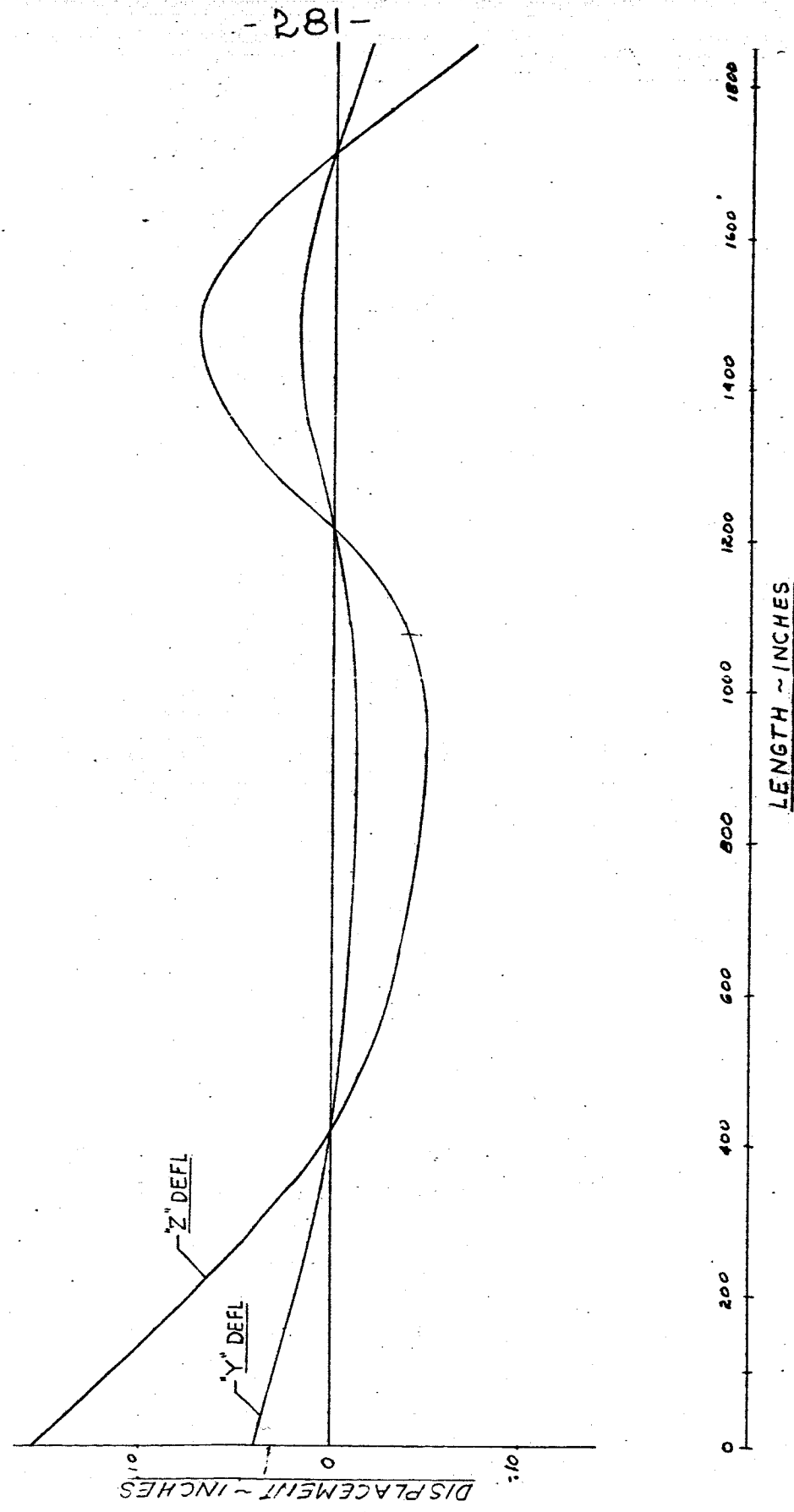


FIG. 199 DISPLACEMENT vs LENGTH SATURN SA-DI  
MAIN TANK & UPPER STAGES  
FREQUENCY = 6.75 cps.

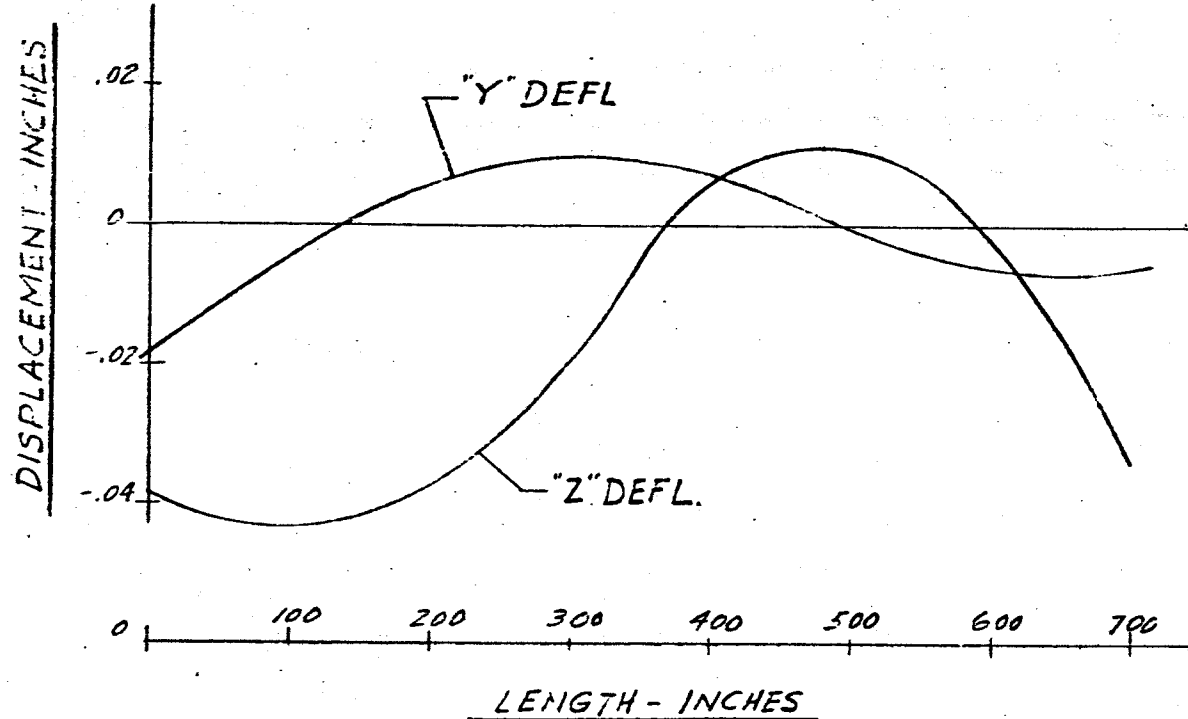


-282-

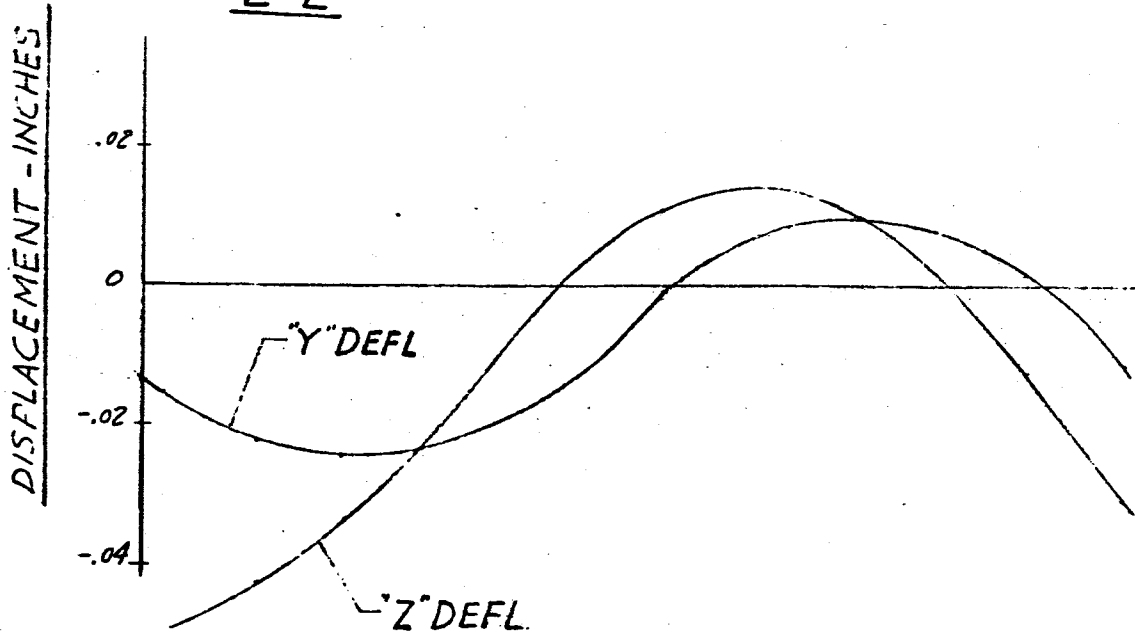
FIG. 200 DISPLACEMENT vs LENGTH SATURN SA-DI

FREQUENCY = 6.75 CPS

L-1



L-2

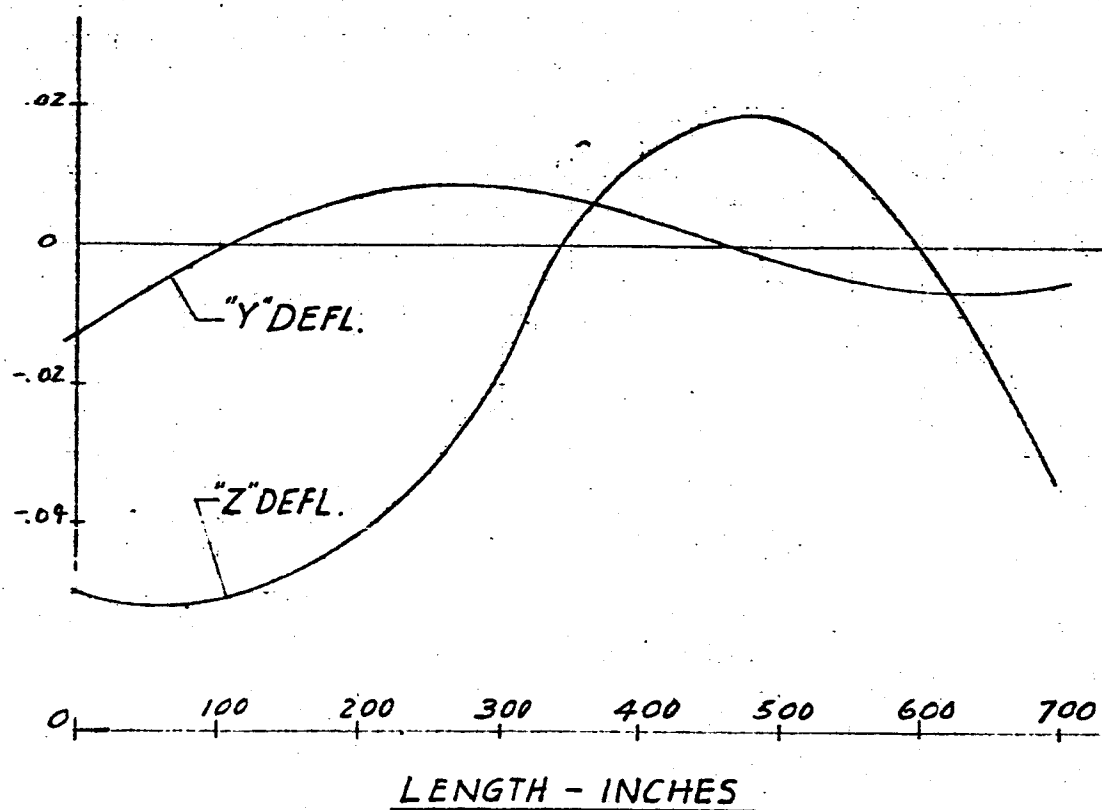


-283-

FIG. 201 DISPLACEMENT VS LENGTH SATURN SA-DI  
FREQUENCY = 6.75 CPS.

L-3

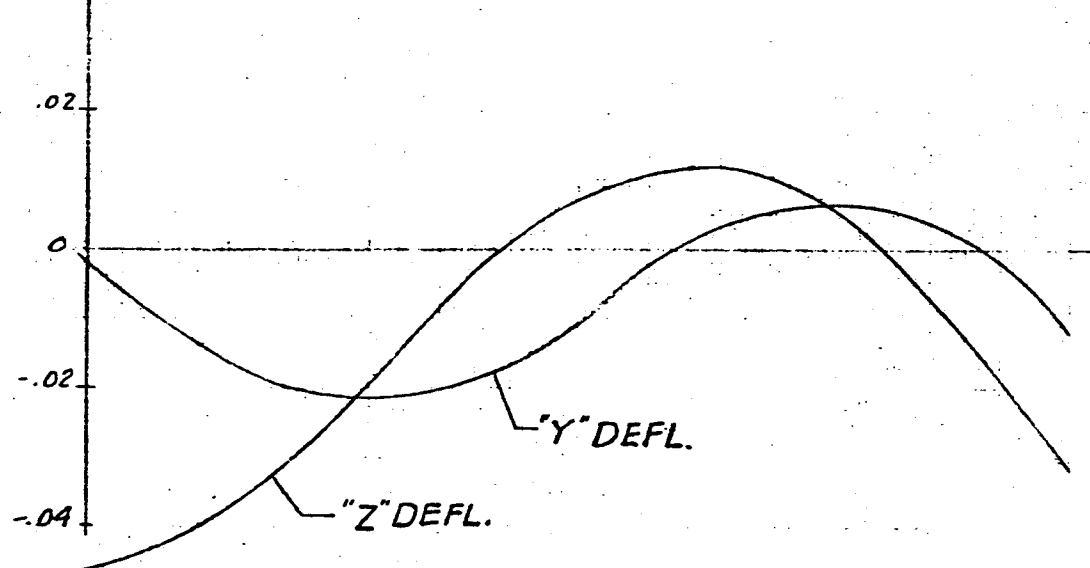
DISPLACEMENT - INCHES



LENGTH - INCHES

L-4

DISPLACEMENT - INCHES

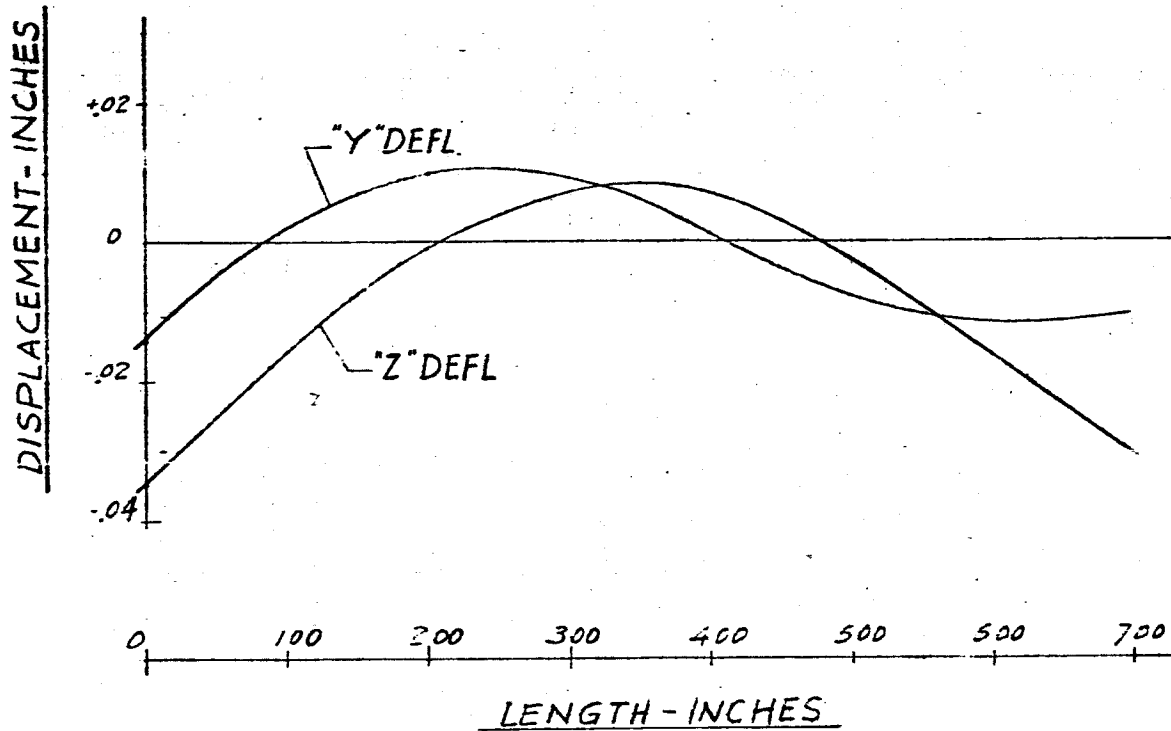


-284-

FIG 202 DISPLACEMENT VS LENGTH SATURN SA-DI

FREQUENCY = 6.75 CPS

F-1



F-2

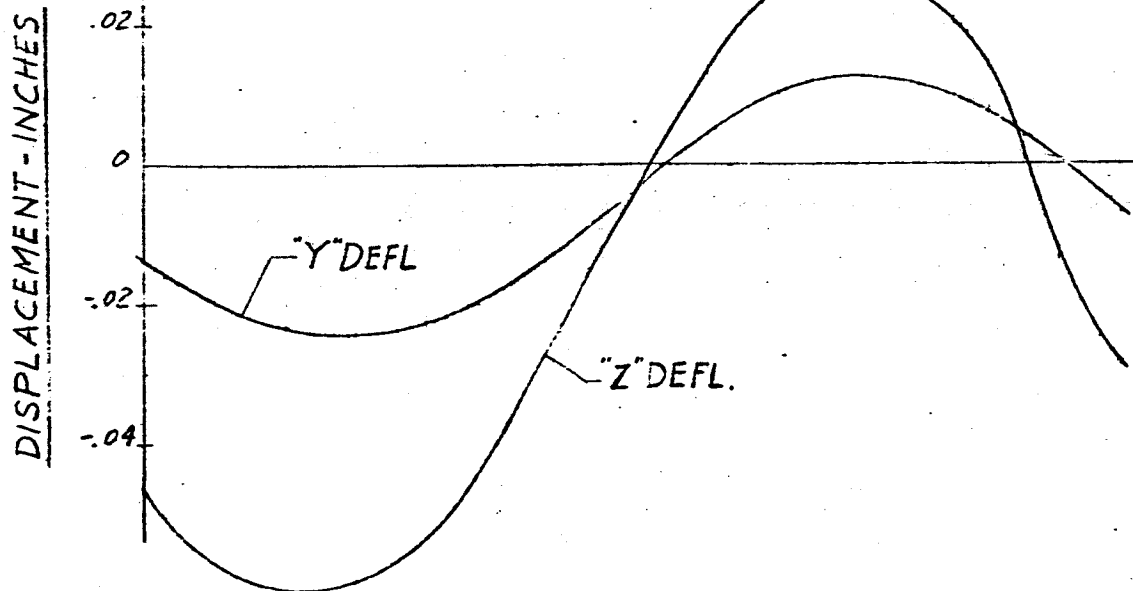
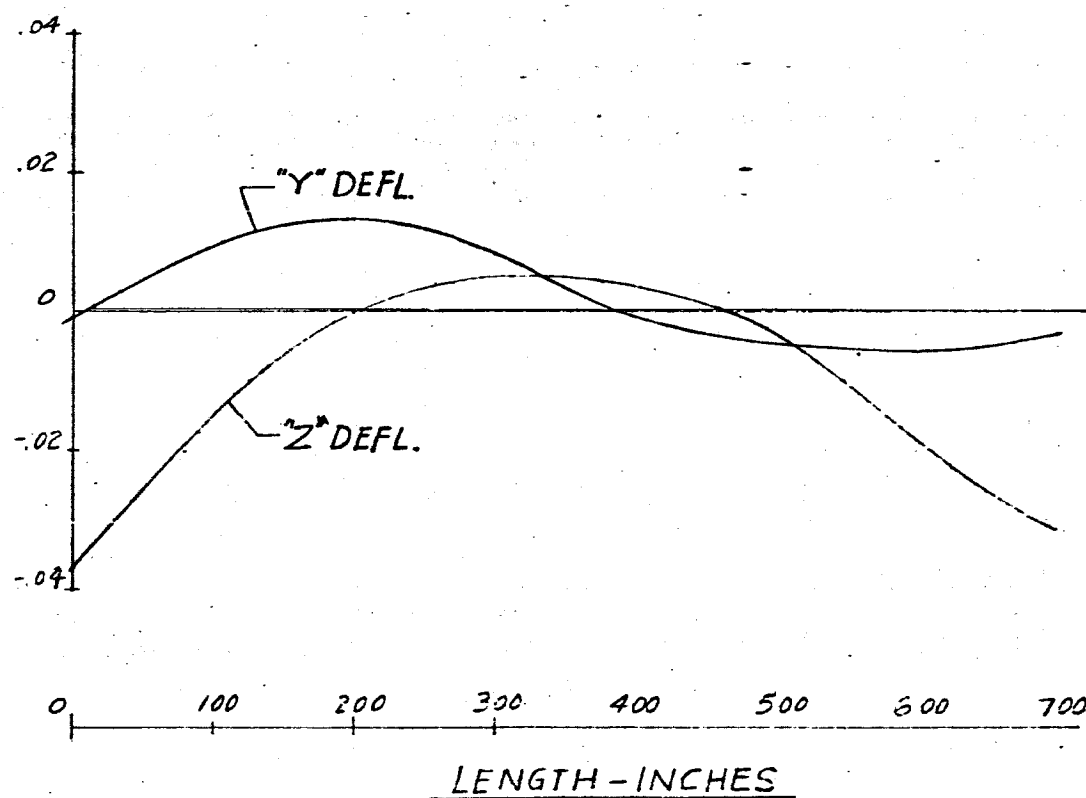


FIG. 203 DISPLACEMENT vs LENGTH SATURN SA-DI

FREQUENCY = 6.75 CPS

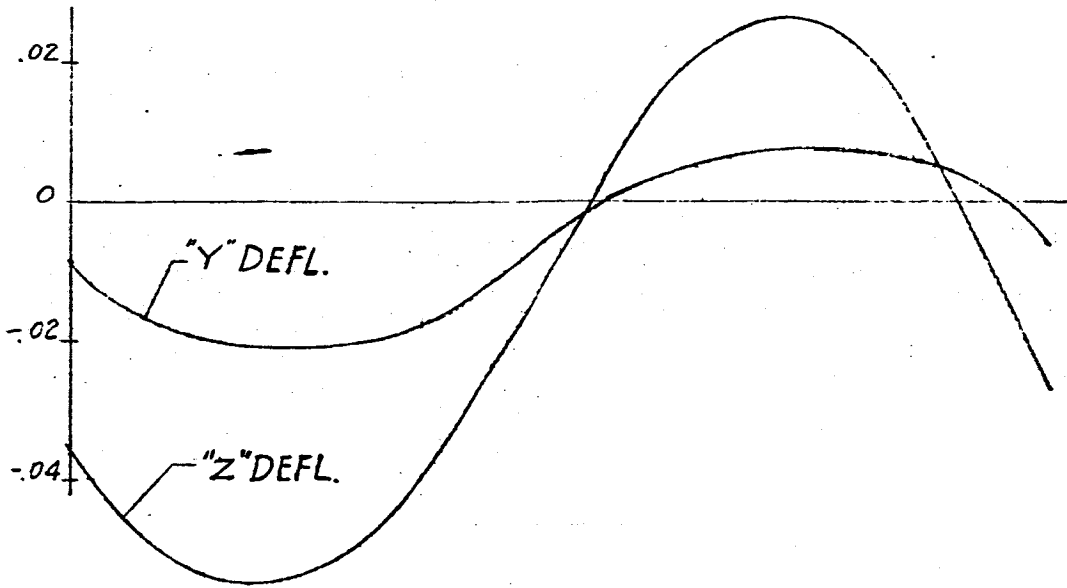
F-3

DISPLACEMENT - INCHES



F-4

DISPLACEMENT - INCHES



-286-

FIG. 204 DISPLACEMENT VS LENGTH SATURN SA-DI  
MAIN TANK & UPPER STAGES  
FREQUENCY = 6.80 cps

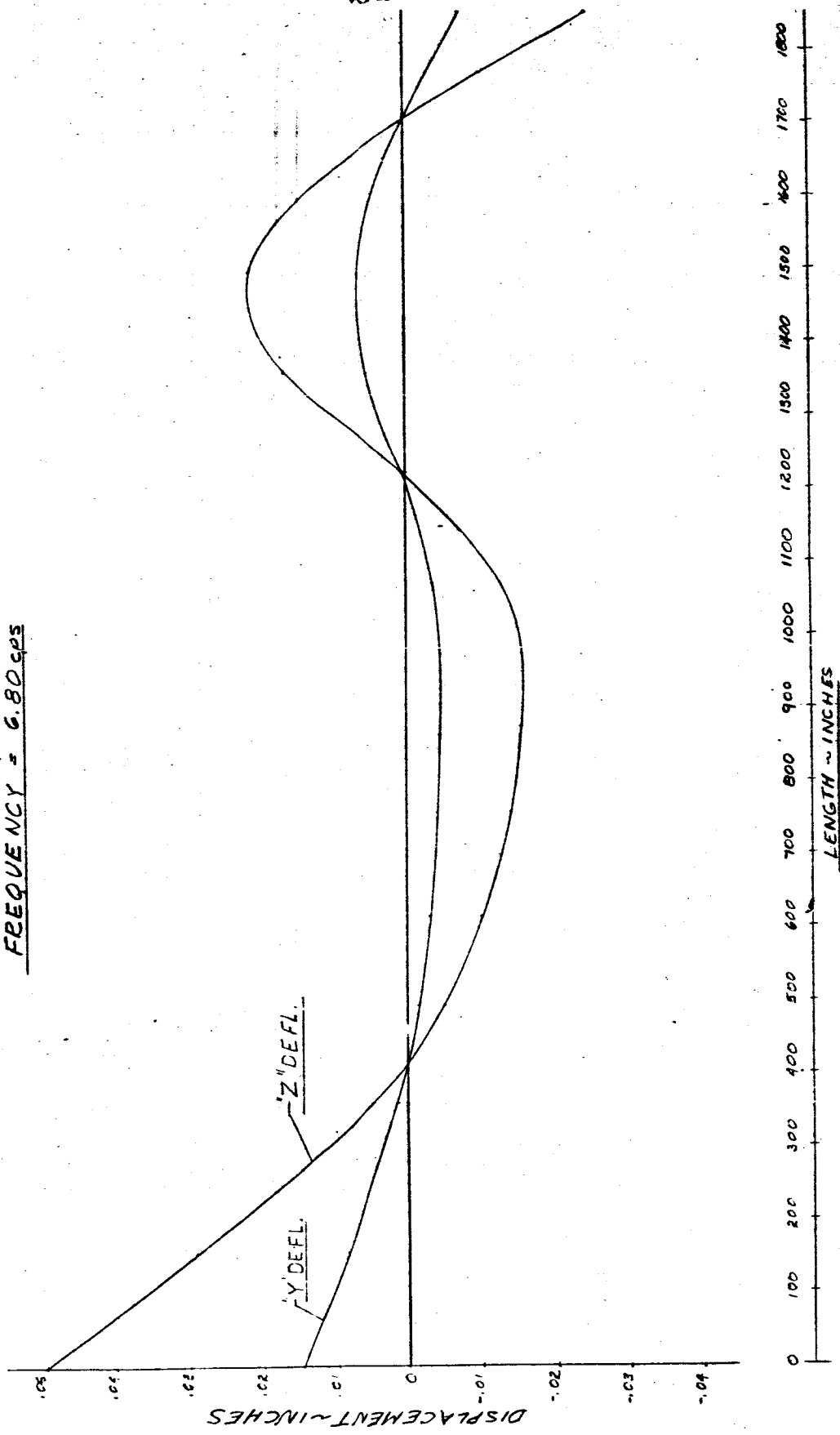


FIG. 205 DISPLACEMENT & LENGTH SATURN SA-DI  
MAIN TANK & UPPER STAGES

FREQUENCY = 7.20 cps

- 287 -

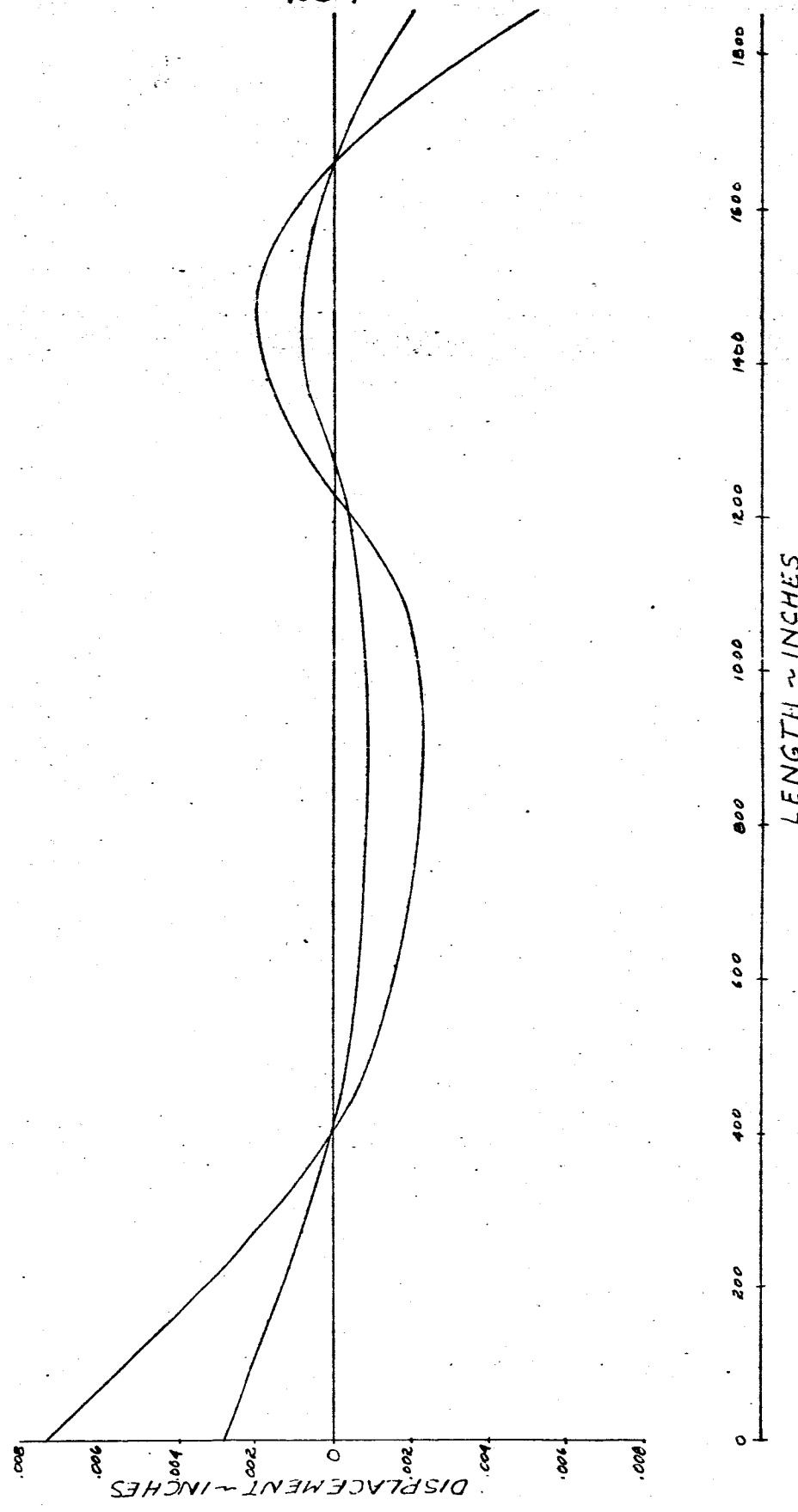
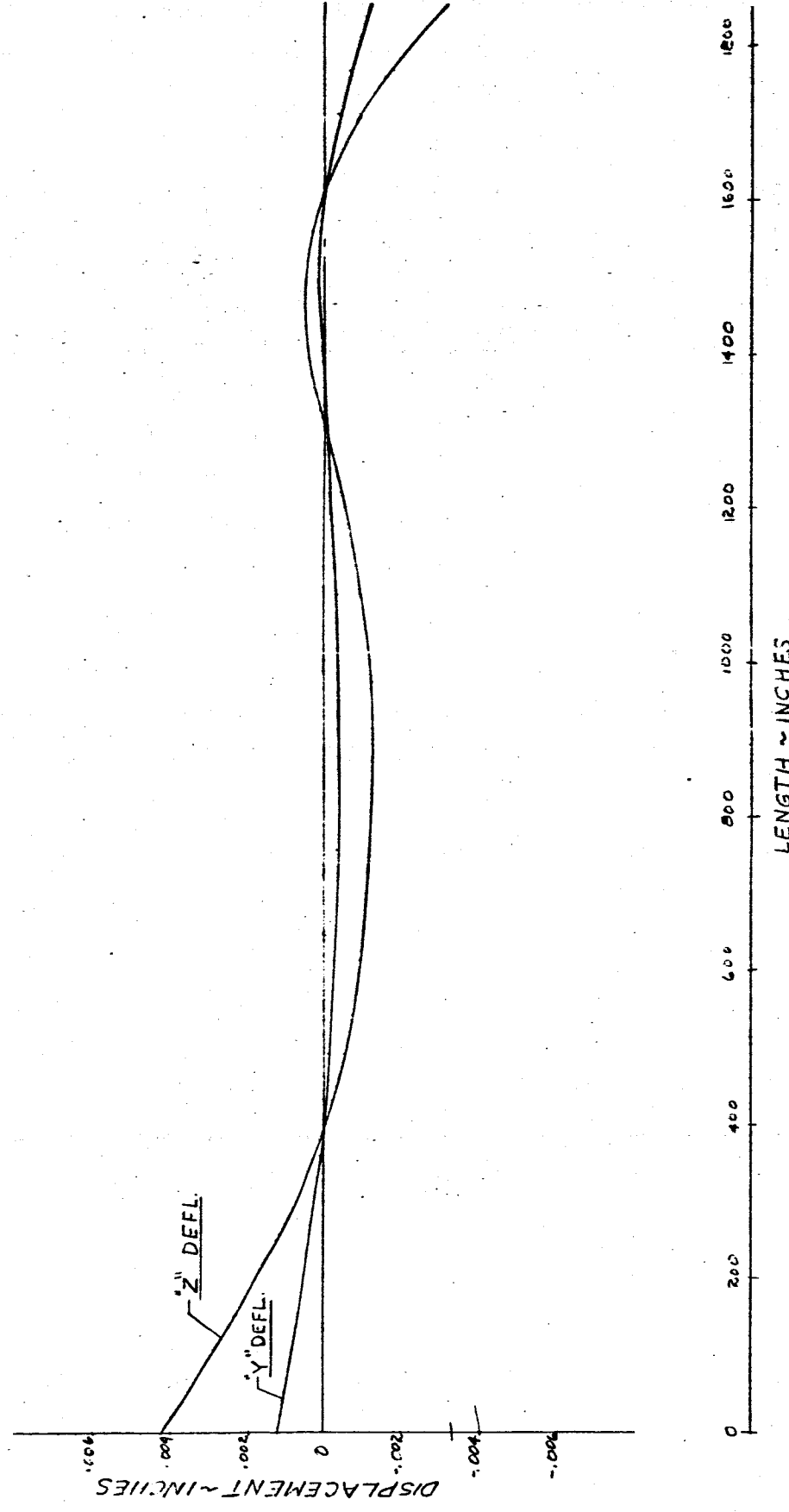


FIG 206 DISPLACEMENT vs LENGTH SATURN SA-DI  
MAIN TANK & UPPER STAGES

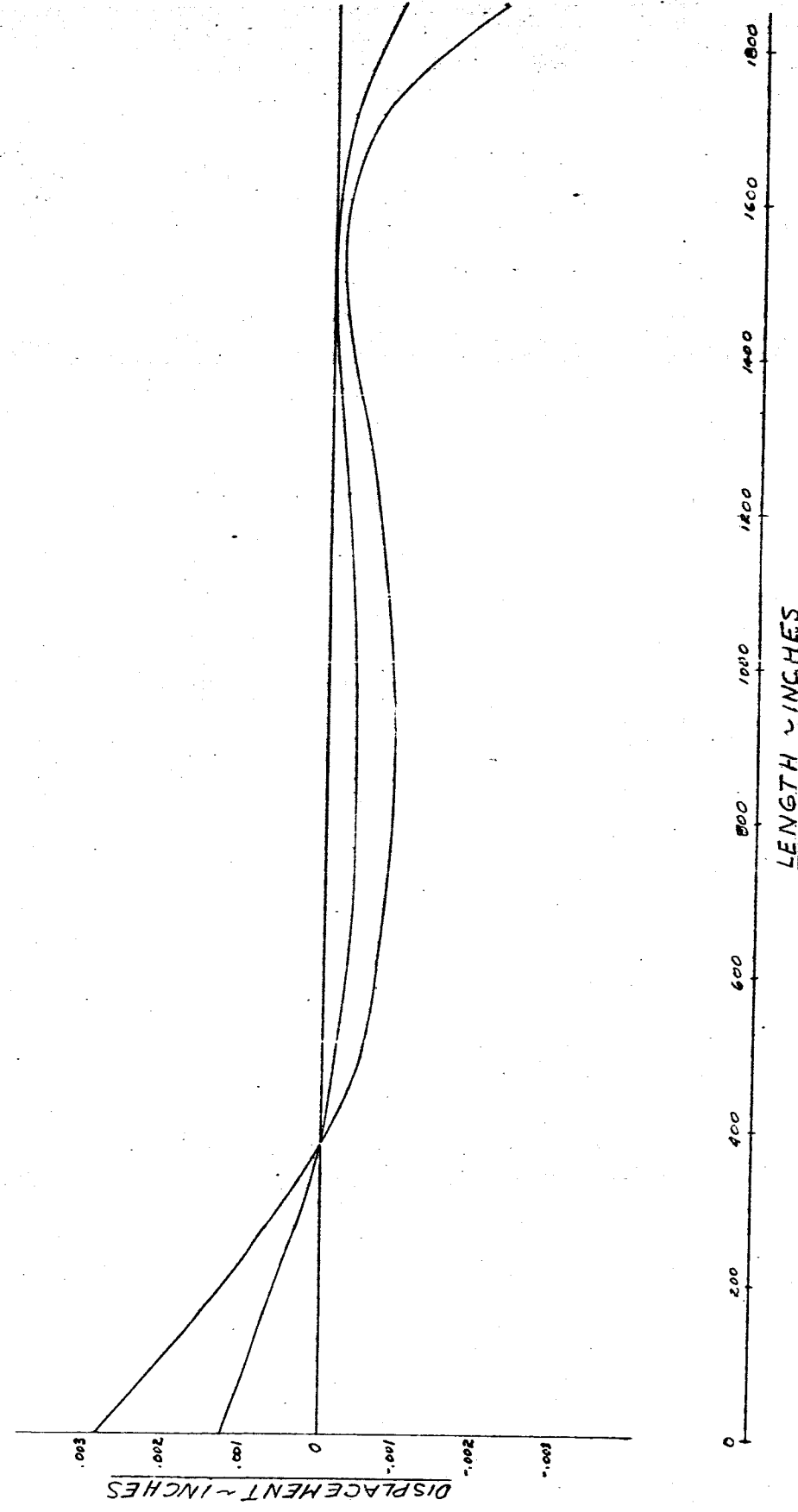
FREQUENCY = 7.60 cps.

-2 89-



- 289 -

FIG. 207 DISPLACEMENT vs LENGTH SATURN SA-DI  
MAIN TANK & UPPER STAGES  
FREQUENCY = 8.00 cps.



- 290 -

FIG. 203 FREQUENCY vs. RESPONSE  
- PAYLOAD PT. NO. 1 -

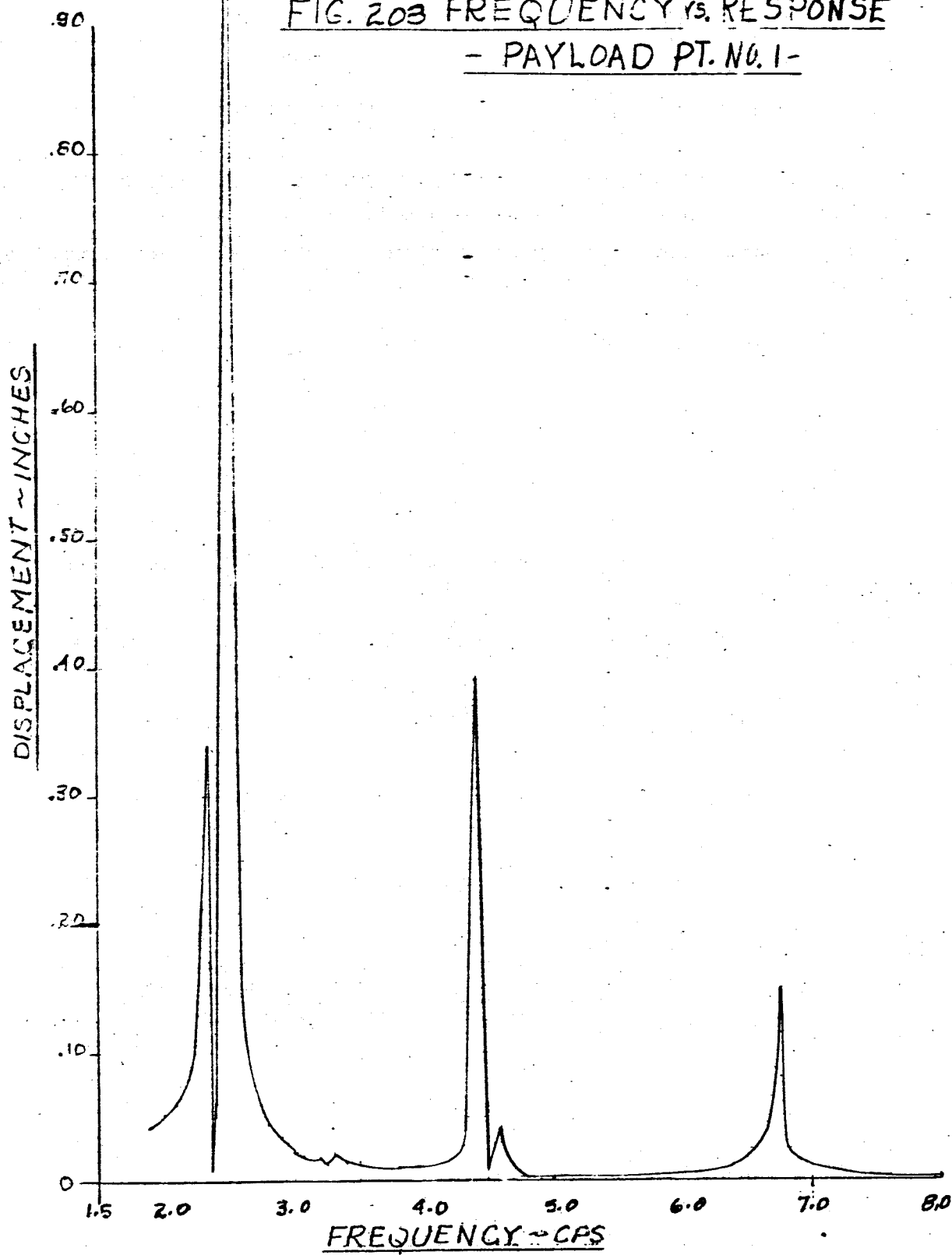
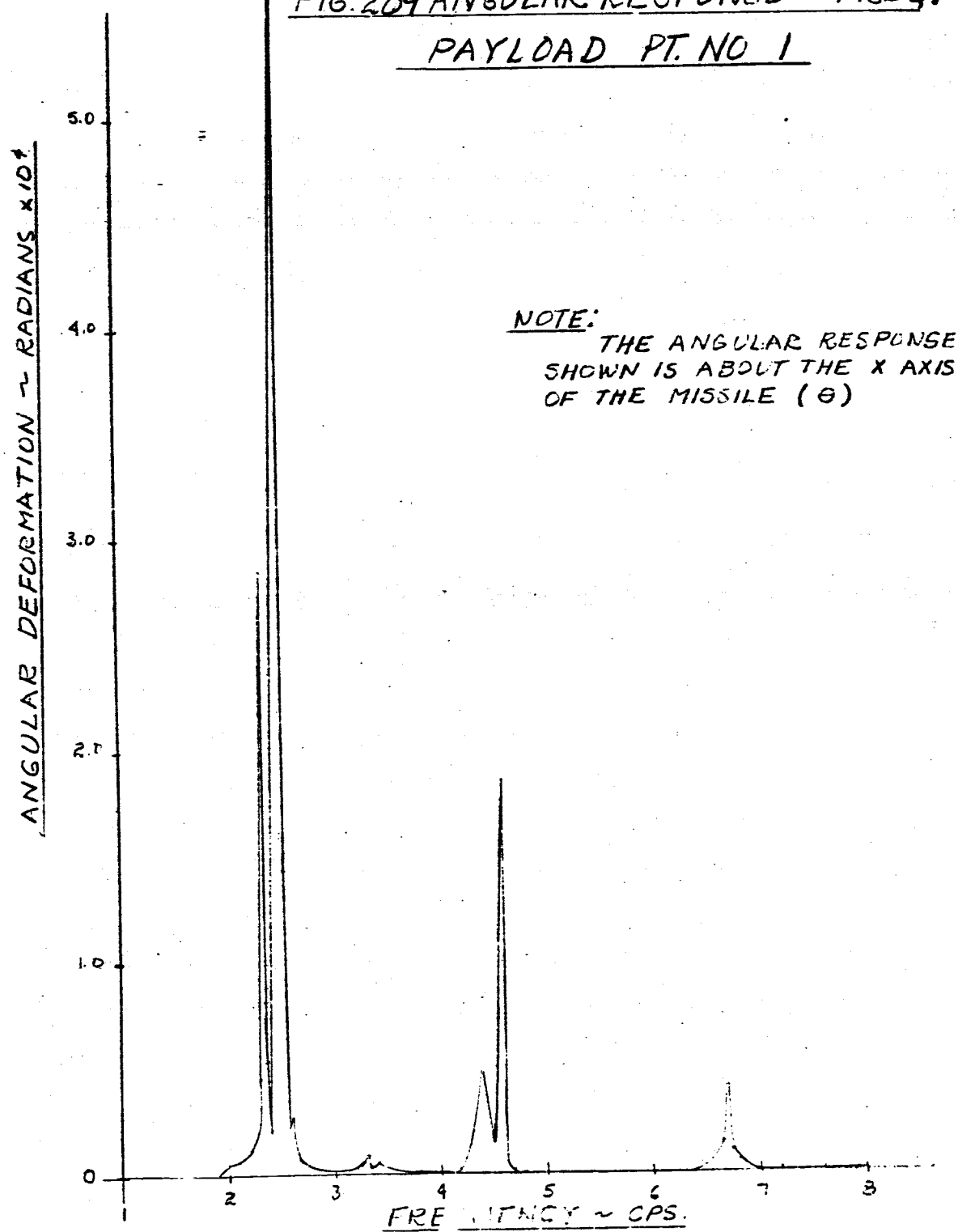


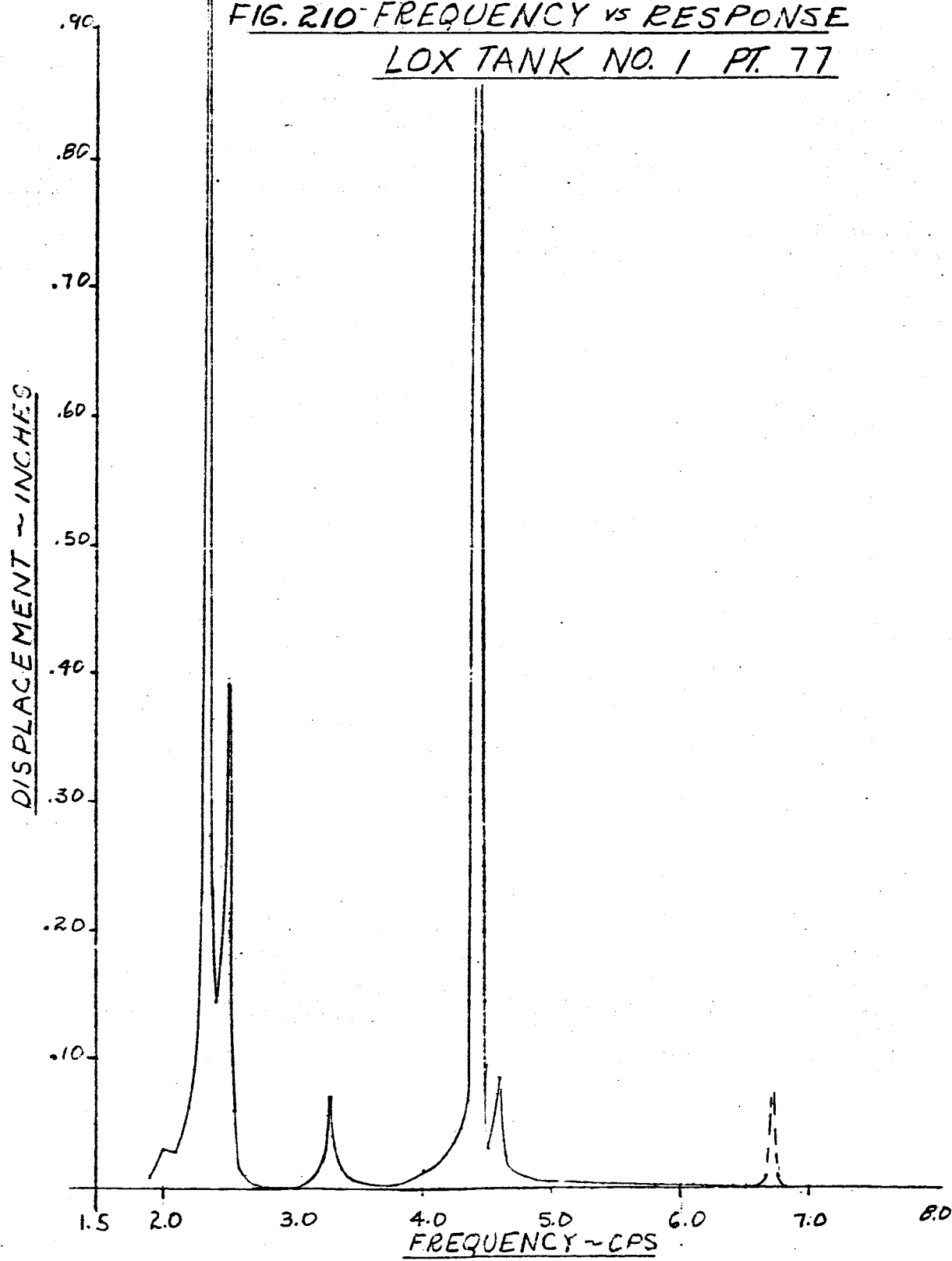
FIG. 209 ANGULAR RESPONSE vs FREQ.

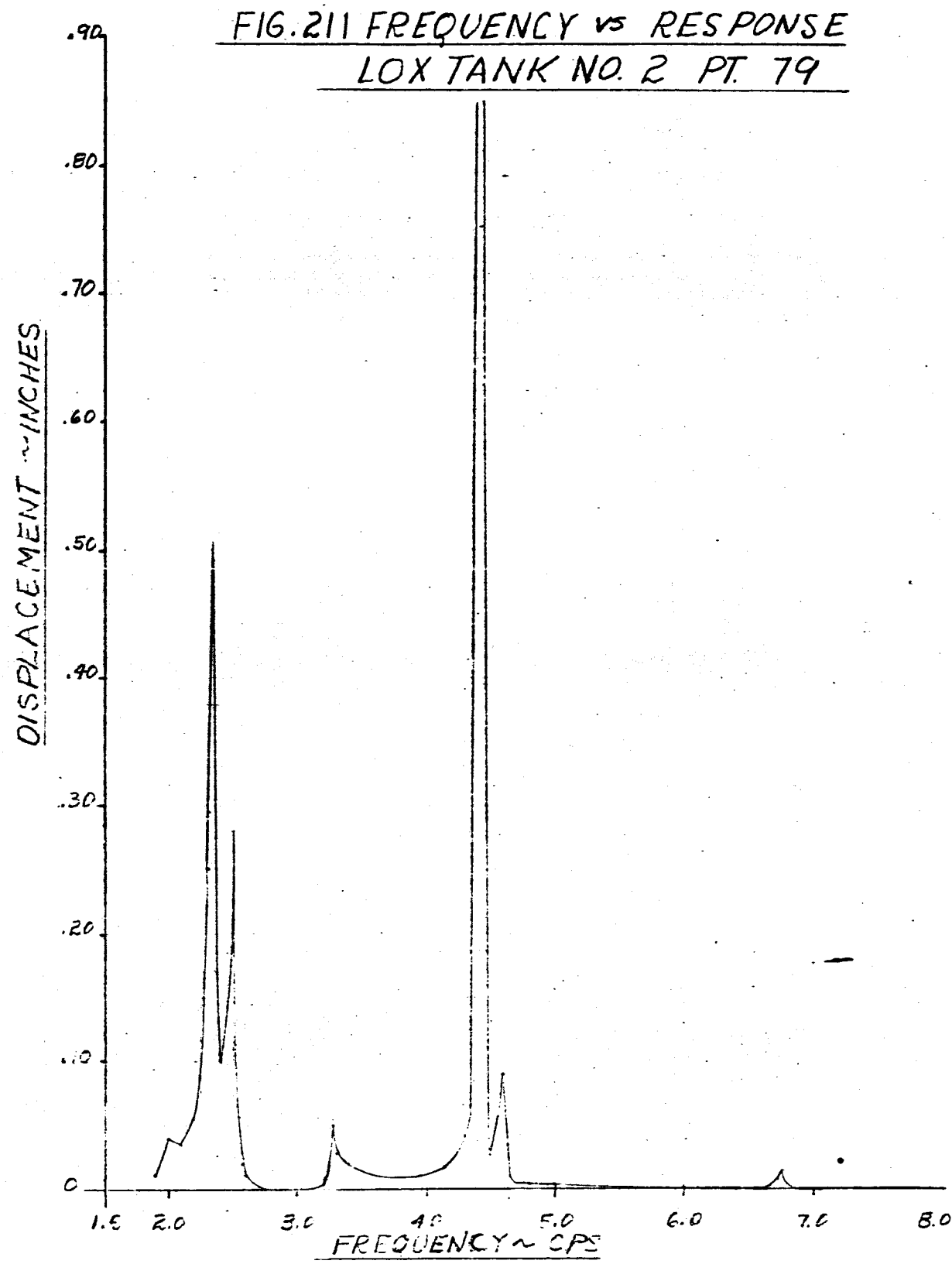
PAYOUT PT. NO 1



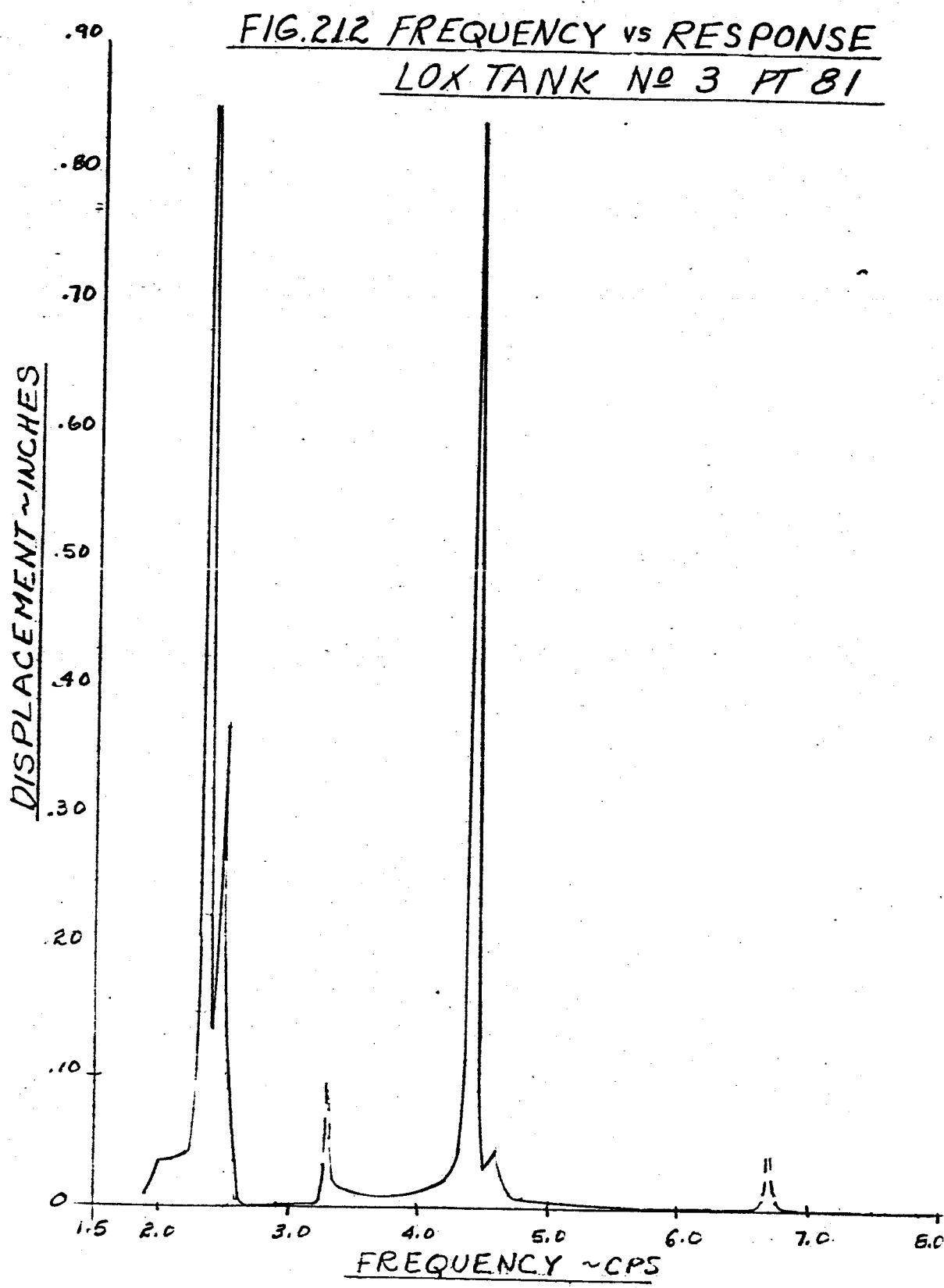
-292-

FIG. 210 - FREQUENCY vs RESPONSE  
LOX TANK NO. 1 PT. 77





- 294 -



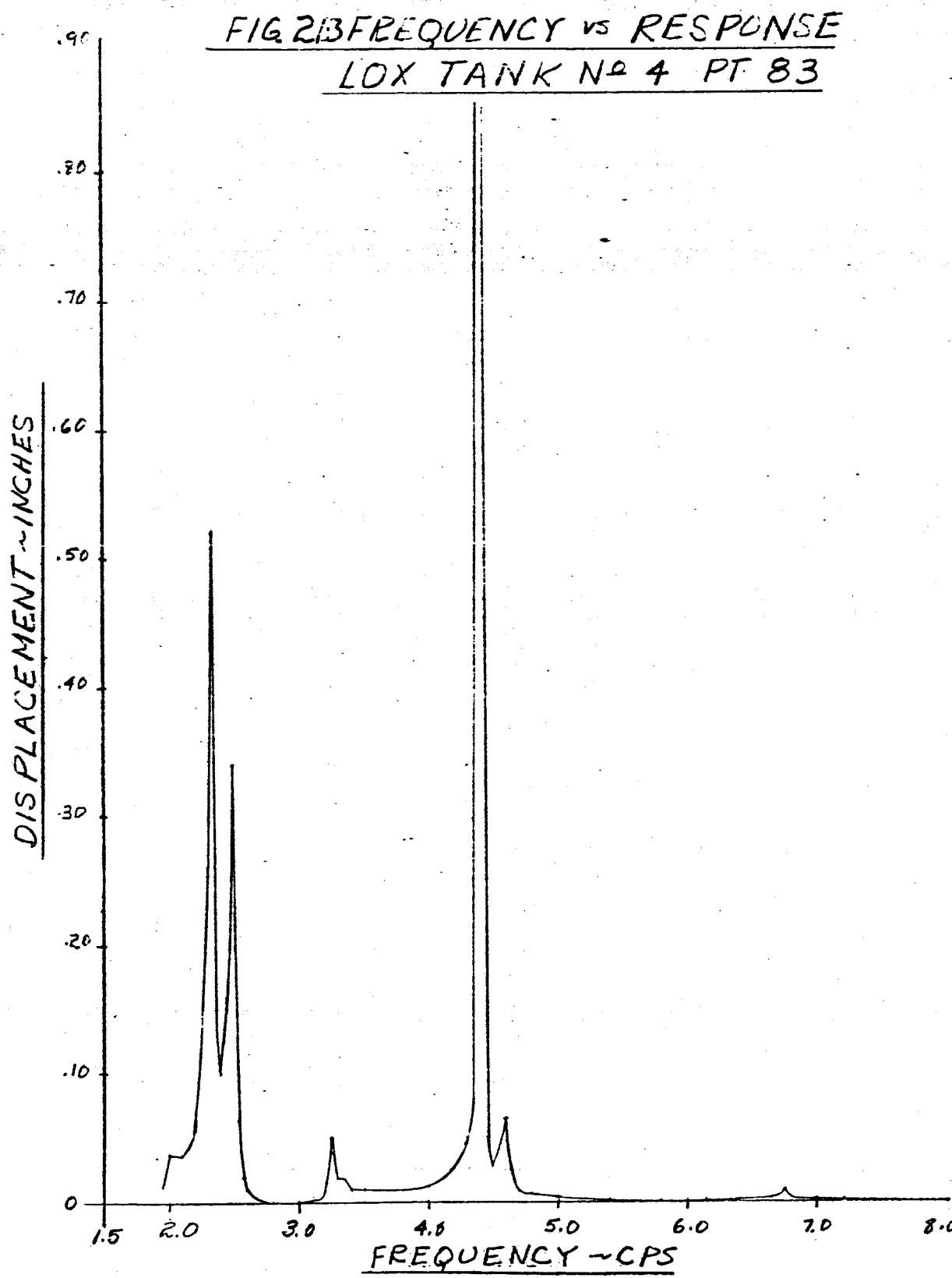


FIG. 214 FREQUENCY vs RESPONSE  
FUEL TANK NO. 1 PT. 78

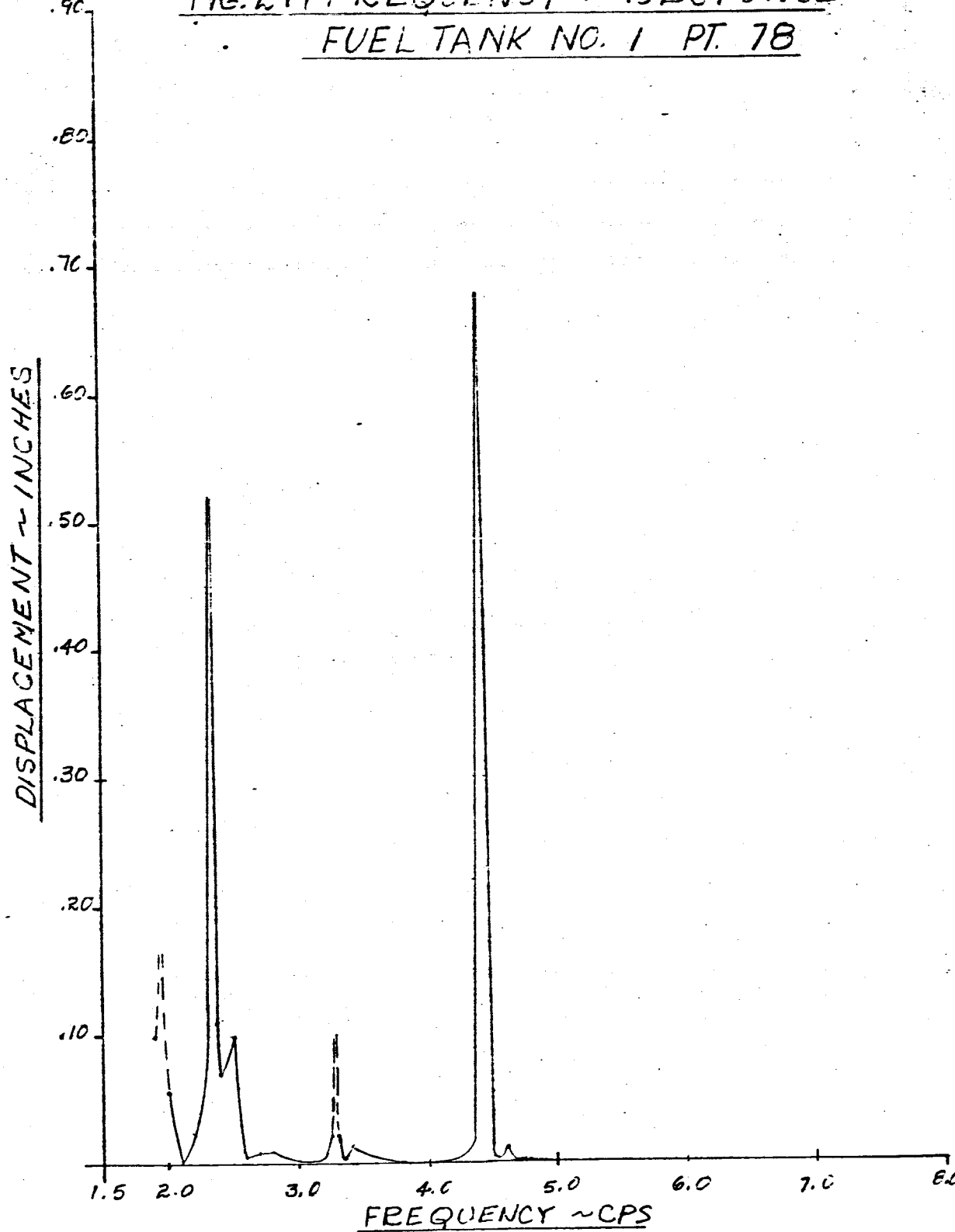
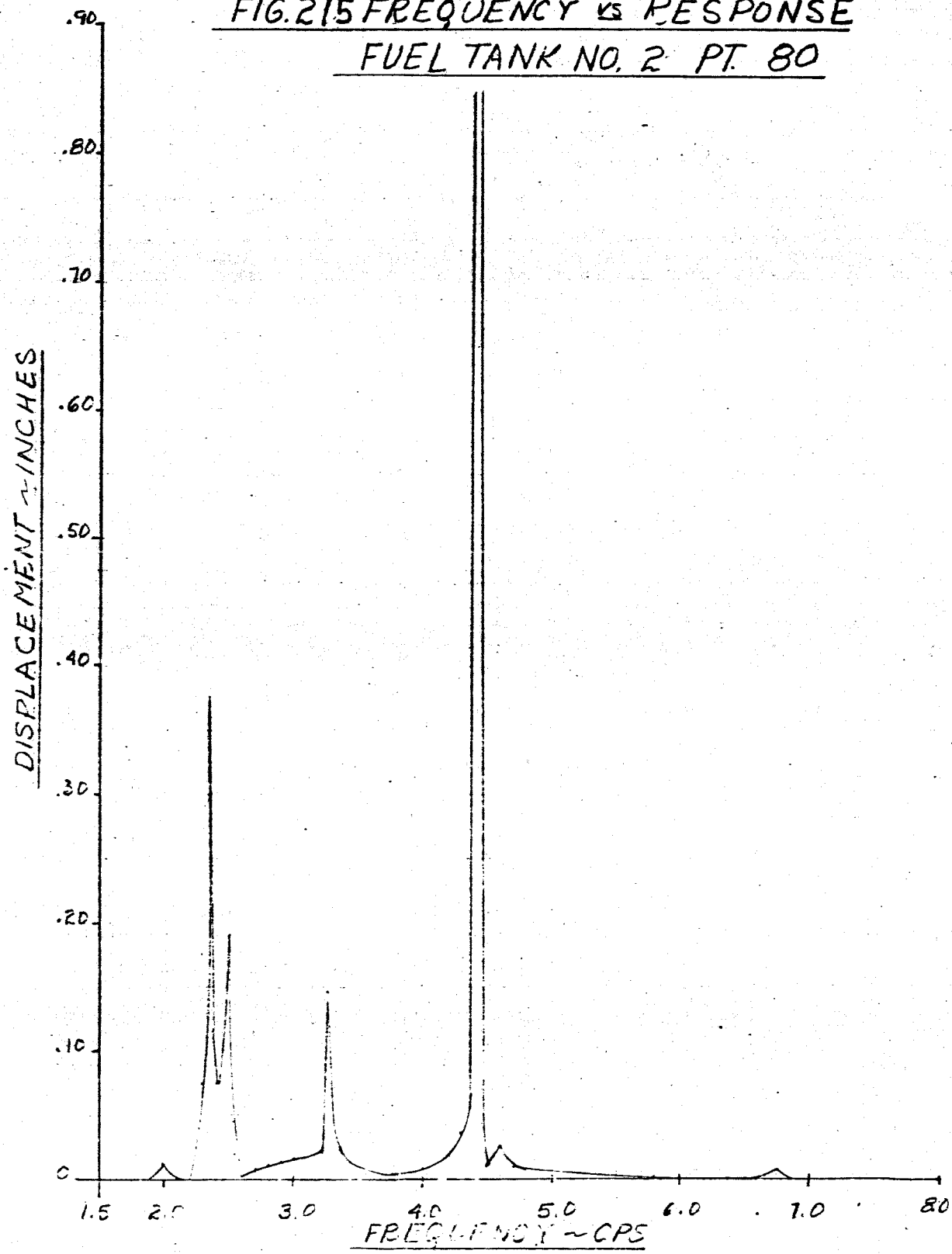
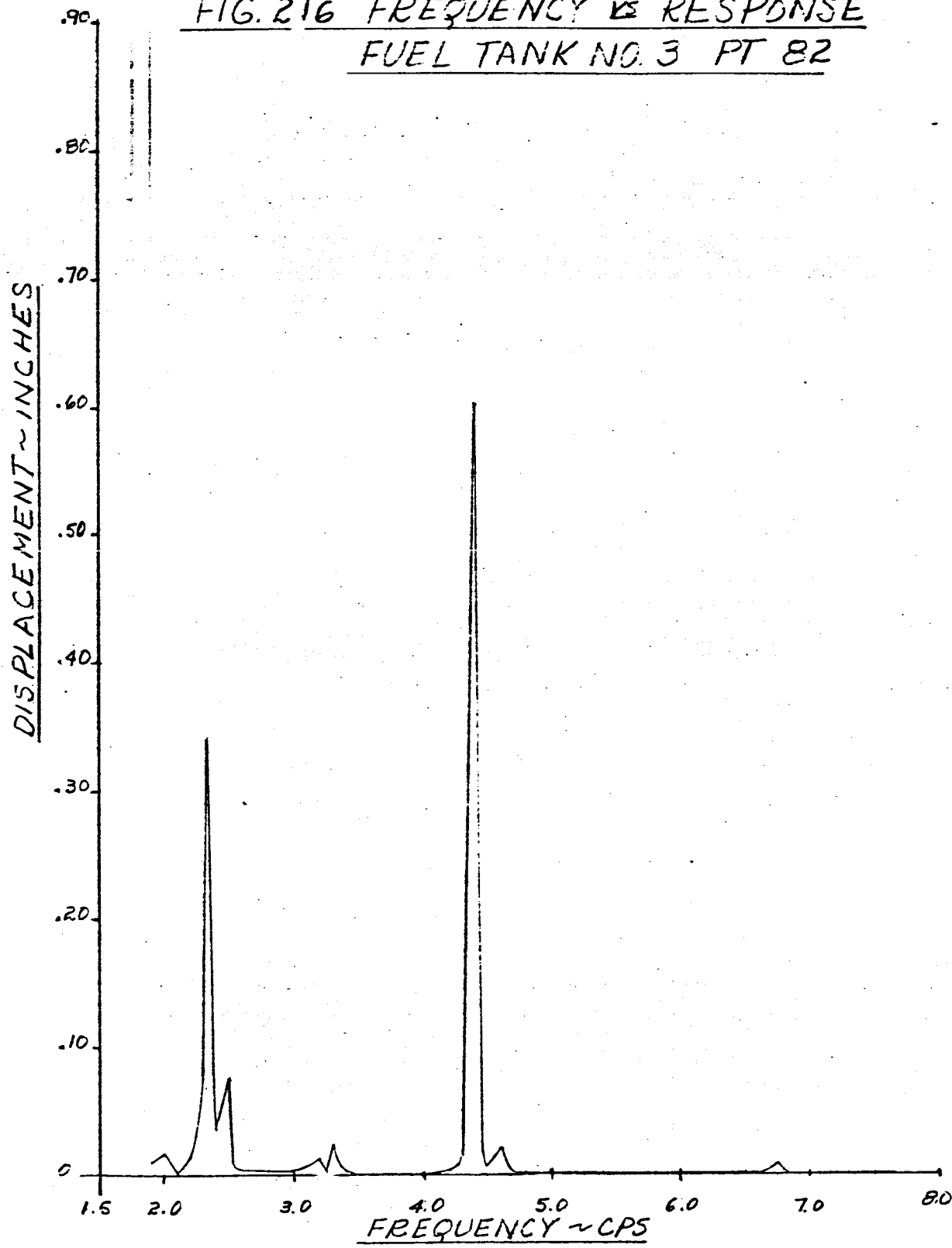


FIG. 215 FREQUENCY VS RESPONSE  
FUEL TANK NO. 2 PT. 80



-298-

FIG. 216 FREQUENCY VS RESPONSE  
FUEL TANK NO. 3 PT 82



- 299 -

FIG. 217 FREQUENCY VS RESPONSE  
FUEL TANK NO. 4 PT. 76

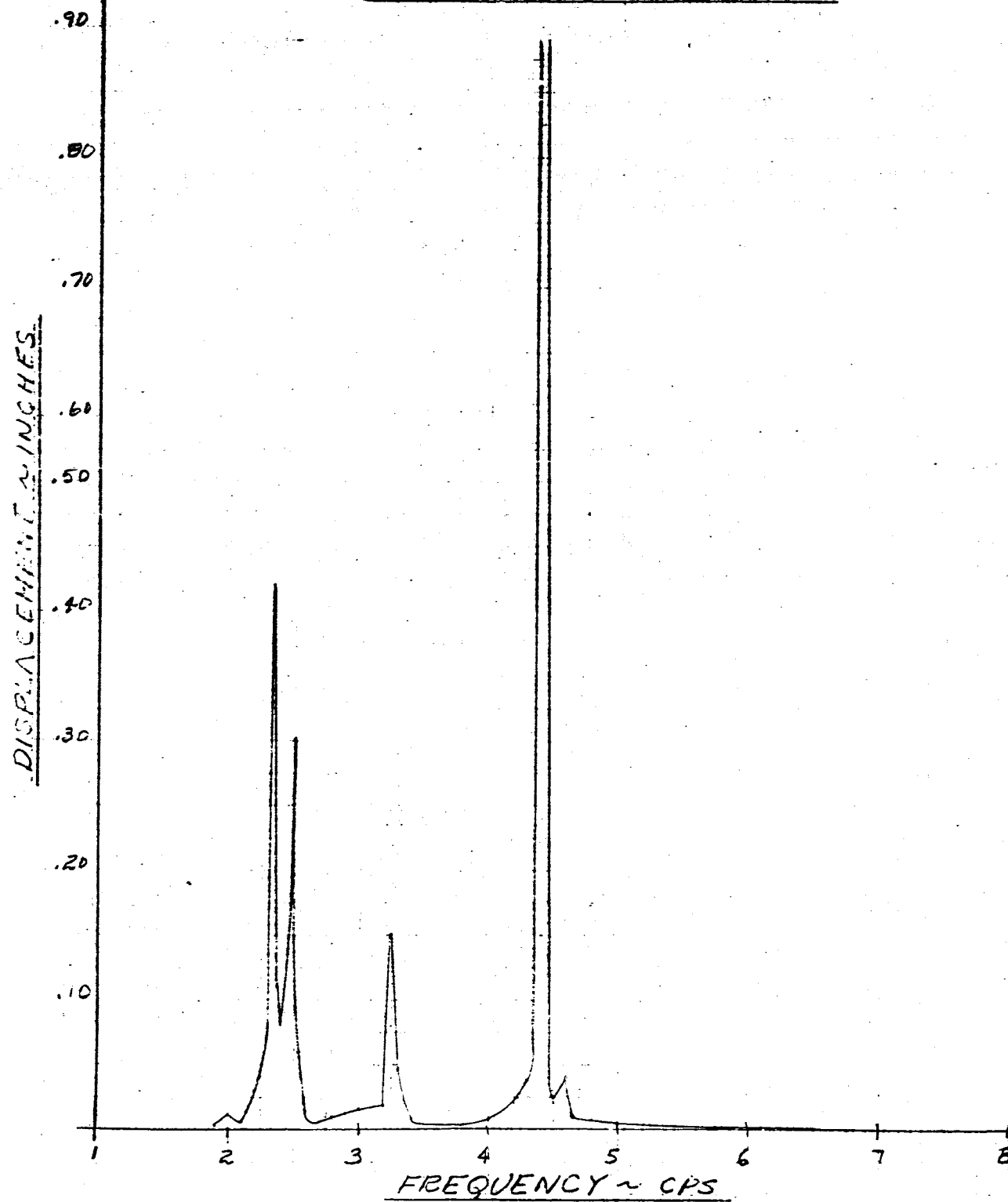
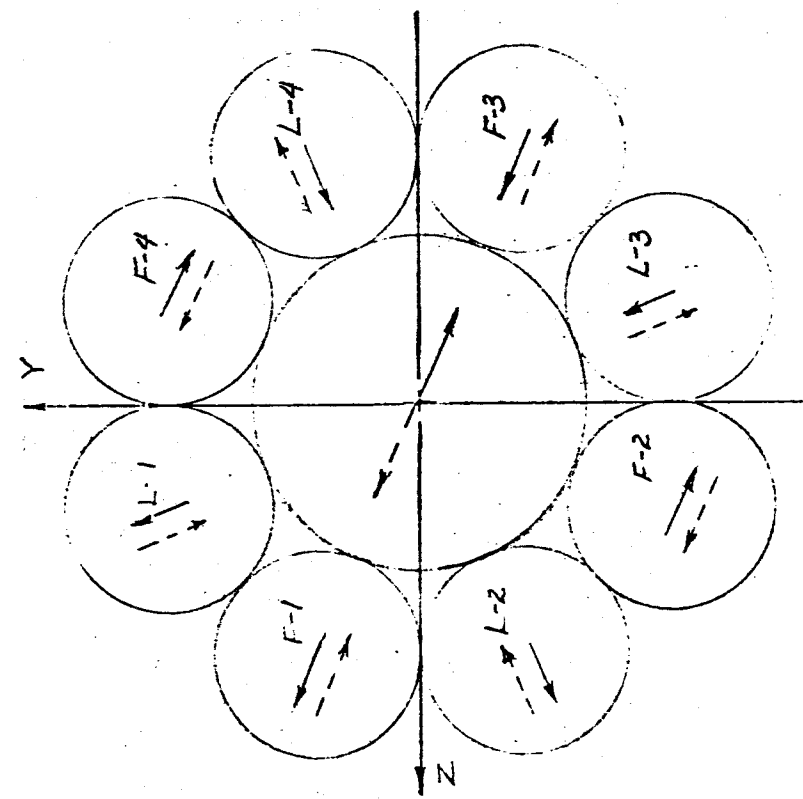
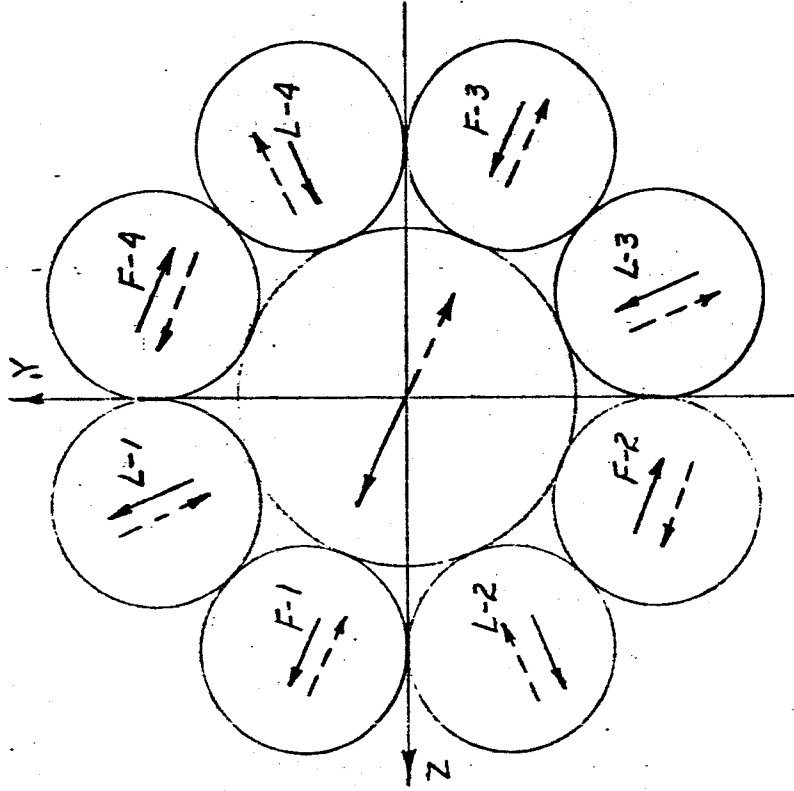


FIG. 218 QUALITATIVE VECTOR RESPONSE  
OF THE SATURN SA-DI

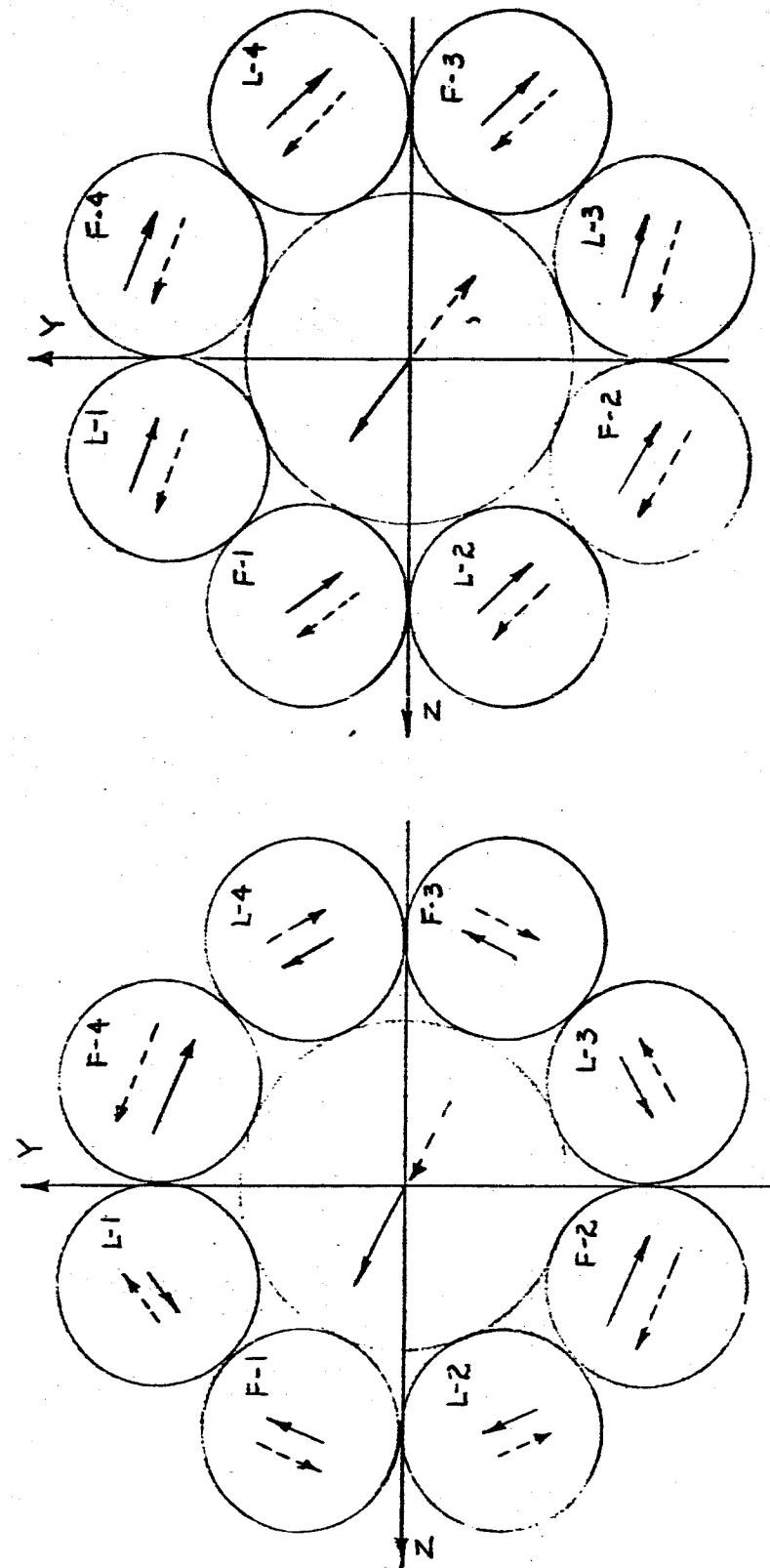


2.30 cps →  
2.34 cps →



2.50 cps →  
2.54 cps →

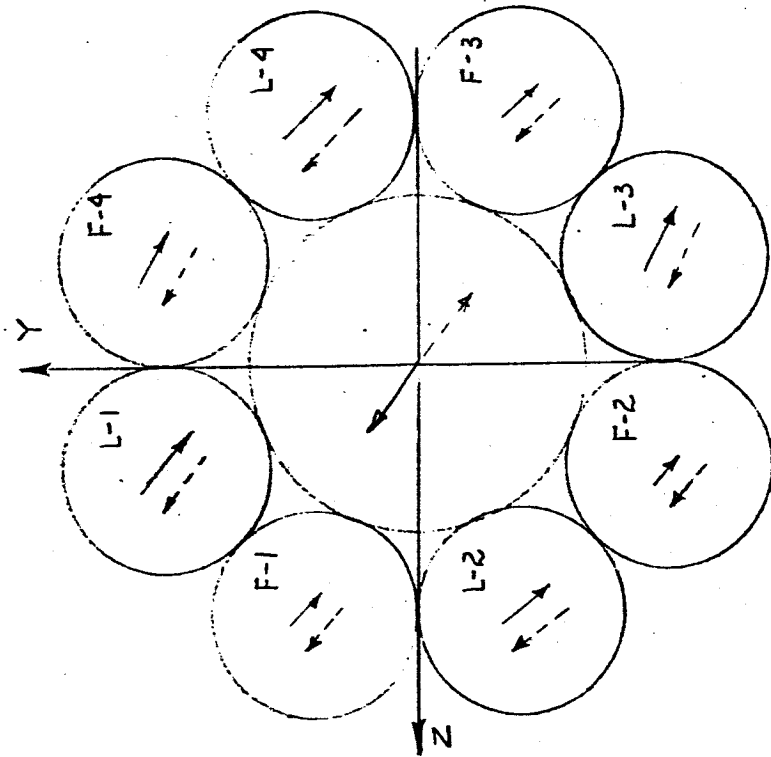
FIG. 219 QUALITATIVE VECTOR RESPONSE  
OF THE SATURN SA-DI



(a) FUEL TANK MODE ( $F\cdot 2 \neq F\cdot 4$ )  
(b) SECOND CLUSTER MODE

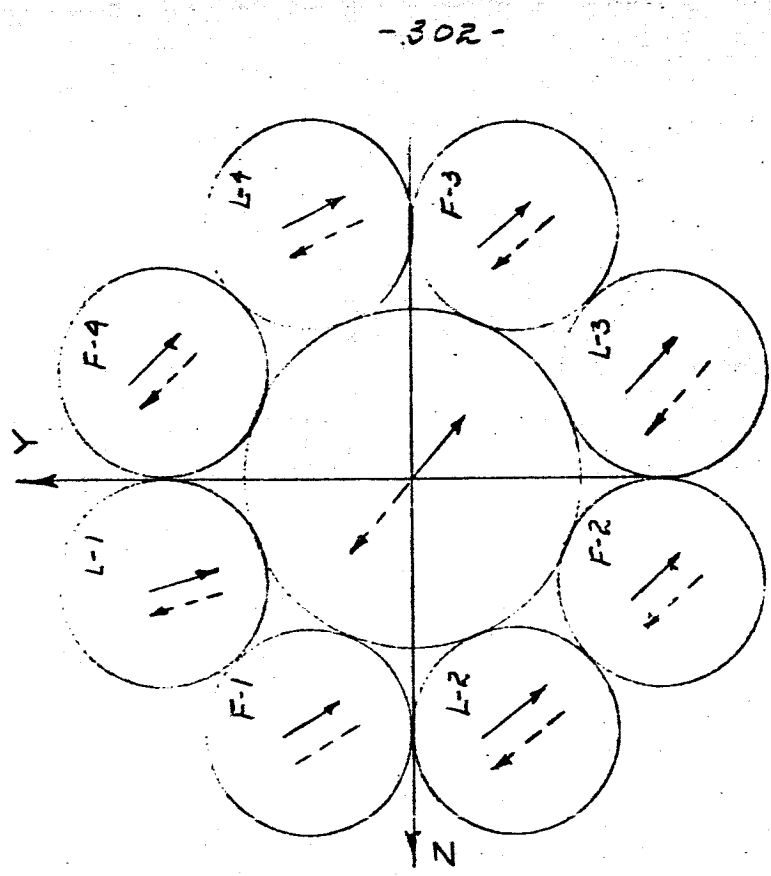
4.90 cps →  
4.50 cps →  
4.25 cps →  
3.30 cps →  
3.25 cps →

FIG. 220 QUALITATIVE VECTOR RESPONSES  
OF THE SATURN SA-D1



(a) LOX TANK MODE

4. 60 cps →  
4.70 cps →



NOTE: THE OUTER TANKS HAVE A 2 UP HOUR SHARE.  
6.65 cps →  
6.75 cps →

(b) SECOND BENDING MODE

-302-

## DISTRIBUTION LIST

Missile Division

	<u>Dept. No.</u>
H.F. McKenney, General Manager, Missile Division	1000
M. von Braun, Director, Research and Engineering	1007
R.P. Erickson, Chief Engineer, Advanced Development	7130
R.F. May, Chief Engineer, Systems	7110
E.F. Dunford, Asst. Chief Engineer, Preliminary Design	7131
R.A. Horvath, Manager, Mechanics	7132
F.A. Reid, Manager, Gas Dynamics	7133
L. Tomich, Manager, Aeroballistics	7135
A.H. Albert, Manager, Computation Laboratory	7160
J.H. Hunter, Manager, Analytical & Data Processing Systems	7160
E.E. Heibeck, Managing Engineer, Structural Design	7432
C. Rydz, Group Supervisor, Structural Dynamics	7132
G.A. Socks, Group Supervisor, Flight Dynamics	7132
J.D. O'Rourke, Structural Dynamics (2)	7132
G. Marcopoulos, Structural Dynamics	7132
R.J. Thompson, Structural Dynamics	7132
S. Manuel, Computation Laboratory	7160
 Technical Files (5)	 2743

Space Division

C.C. Gage, Chief Engineer, Propulsion and Vehicle Engineering	2730
T.R. Cotter, Vehicle Engineering Section	2731
J.H. Landon, Structural Engineering Section	2733

External - Marshall Space Flight Center  
Redstone Arsenal, Alabama

Helmut Bauer, Chief, Flutter and Vibration  
 Dynamic Analysis Branch  
 Aeroballistics Division (3 copies)

H. Horn, Branch Chief,  
 Dynamic Analysis Branch  
 (M-AERO-B, Bldg. 4484) (1 copy)

R. Hunt, Assistant to the Branch Chief  
 Structures Branch  
 Propulsion and Vehicle Engineering Division  
 (M-PNVE-S, HIC Bldg.) (2 copies)

Director (10 copies)  
 George C. Marshall Space Flight Center  
 National Aeronautics and Space Administration  
 Huntsville, Alabama  
 ATTN: M-P&C-CA